

UNITED STATES AIR FORCE
SUMMER RESEARCH PROGRAM -- 1997
SUMMER RESEARCH EXTENSION PROGRAM FINAL REPORTS

VOLUME 1
PROGRAM MANAGEMENT REPORT

ARMSTRONG LABORATORY

RESEARCH & DEVELOPMENT LABORATORIES

5800 Uplander Way

Culver City, CA 90230-6608

Program Director, RDL
Gary Moore

Program Manager, AFOSR
Major Linda Steel-Goodwin

Program Manager, RDL
Scott Licoscas

Program Administrator, RDL
Johnetta Thompson

Program Administrator, RDL
Rebecca Kelly-Clemmons

Submitted to:

AIR FORCE OFFICE OF SCIENTIFIC RESEARCH

Bolling Air Force Base

Washington, D.C.

December 1997

20010319 040

AQM01-06-1201

PREFACE

This volume is part of a five-volume set that summarizes the research of participants in the 1997 AFOSR Summer Research Extension Program (SREP.) The current volume, Volume 1 of 5, presents the final reports of SREP participants at Armstrong Laboratory. Volume 1 also includes the Management Report.

Reports presented in this volume are arranged alphabetically by author and are numbered consecutively – e.g., 1-1, 1-2, 1-3; 2-1, 2-2, 2-3, with each series of reports preceded by a 35 page management summary. Reports in the five-volume set are organized as follows:

VOLUME	TITLE
1	Armstrong Laboratory
2	Phillips Laboratory
3	Rome Laboratory
4A	Wright Laboratory
4B	Wright Laboratory
5	Arnold Engineering Development Center Air Logistics Centers United States Air Force Academy Wilford Hall Medical Center

REPORT DOCUMENTATION PAGE

Public reporting burden for this collection of information is estimated to average 1 hour per response, including the time for reviewing instructions, searching existing data sources, gathering the required information, reviewing and collecting the information, and completing and reviewing the collection of information. Send comments regarding this burden estimate or any other aspect of this collection of information, including suggestions for reducing the burden, to Washington Headquarters Services, Directorate for Information Operations and Reports, 1215 Jefferson Davis Highway, Suite 1204, Arlington, VA 22202-4302, and to the Office of Management and Budget, Paperwork Project, Washington, DC 20503.

AFRL-SR-BL-TR-00-

0708

1. AGENCY USE ONLY (Leave blank)		2. REPORT DATE December, 1997		3. REPORT	
4. TITLE AND SUBTITLE 1997 Summer Research Program (SRP), Summer Research Extension Program (SREP), Final Report, Volume 1, Armstrong Laboratory and Program Management				5. FUNDING NUMBERS F49620-93-C-0063	
6. AUTHOR(S) Gary Moore					
7. PERFORMING ORGANIZATION NAME(S) AND ADDRESS(ES) Research & Development Laboratories (RDL) 5800 Uplander Way Culver City, CA 90230-6608				8. PERFORMING ORGANIZATION REPORT NUMBER	
9. SPONSORING/MONITORING AGENCY NAME(S) AND ADDRESS(ES) Air Force Office of Scientific Research (AFOSR) 801 N. Randolph St. Arlington, VA 22203-1977				10. SPONSORING/MONITORING AGENCY REPORT NUMBER	
11. SUPPLEMENTARY NOTES					
12a. DISTRIBUTION AVAILABILITY STATEMENT Approved for Public Release				12b. DISTRIBUTION CODE	
13. ABSTRACT (Maximum 200 words) The United States Air Force Summer Research Program (SRP) is designed to introduce university, college, and technical institute faculty members to Air Force research. This is accomplished by the faculty members, graduate students, and high school students being selected on a nationally advertised competitive basis during the summer intersession period to perform research at Air Force Research Laboratory (AFRL) Technical Directorates and Air Force Air Logistics Centers (ALC). AFOSR also offers its research associates (faculty only) an opportunity, under the Summer Research Extension Program (SREP), to continue their AFOSR-sponsored research at their home institutions through the award of research grants. This volume consists of the SREP program background, management information, statistics, a listing of the participants, and the technical report for each participant of the SREP working at the AF Armstrong Laboratory.					
14. SUBJECT TERMS Air Force Research, Air Force, Engineering, Laboratories, Reports, Summer, Universities, Faculty, Graduate Student, High School Student				15. NUMBER OF PAGES	
				16. PRICE CODE	
17. SECURITY CLASSIFICATION OF REPORT Unclassified		18. SECURITY CLASSIFICATION OF THIS PAGE Unclassified		19. SECURITY CLASSIFICATION OF ABSTRACT Unclassified	
				20. LIMITATION OF ABSTRACT UL	

GENERAL INSTRUCTIONS FOR COMPLETING SF 298

The Report Documentation Page (RDP) is used in announcing and cataloging reports. It is important that this information be consistent with the rest of the report, particularly the cover and title page. Instructions for filling in each block of the form follow. It is important to *stay within the lines* to meet *optical scanning requirements*.

Block 1. Agency Use Only (Leave blank).

Block 2. Report Date. Full publication date including day, month, and year, if available
(e.g. 1 Jan 88). Must cite at least the year.

Block 3. Type of Report and Dates Covered. State whether report is interim, final, etc. If applicable, enter inclusive report dates (e.g. 10 Jun 87 - 30 Jun 88).

Block 4. Title and Subtitle. A title is taken from the part of the report that provides the most meaningful and complete information. When a report is prepared in more than one volume, repeat the primary title, add volume number, and include subtitle for the specific volume. On classified documents enter the title classification in parentheses.

Block 5. Funding Numbers. To include contract and grant numbers; may include program element number(s), project number(s), task number(s), and work unit number(s). Use the following labels:

C - Contract	PR - Project
G - Grant	TA - Task
PE - Program	WU - Work Unit
Element	Accession No.

Block 6. Author(s). Name(s) of person(s) responsible for writing the report, performing the research, or credited with the content of the report. If editor or compiler, this should follow the name(s).

Block 7. Performing Organization Name(s) and Address(es).
Self-explanatory.

Block 8. Performing Organization Report Number. Enter the unique alphanumeric report number(s) assigned by the organization performing the report.

Block 9. Sponsoring/Monitoring Agency Name(s) and Address(es).
Self-explanatory.

Block 10. Sponsoring/Monitoring Agency Report Number. (If known)

Block 11. Supplementary Notes. Enter information not included elsewhere such as: Prepared in cooperation with....; Trans. of....; To be published in.... When a report is revised, include a statement whether the new report supersedes or supplements the older report.

Block 12a. Distribution/Availability Statement. Denotes public availability or limitations. Cite any availability to the public. Enter additional limitations or special markings in all capitals (e.g. NOFORN, REL, ITAR).

DOD - See DoDD 5230.24, "Distribution Statements on Technical Documents."

DOE - See authorities.

NASA - See Handbook NHB 2200.2.

NTIS - Leave blank.

Block 12b. Distribution Code.

DOD - Leave blank.

DOE - Enter DOE distribution categories from the Standard Distribution for Unclassified Scientific and Technical Reports.
Leave blank.

NASA - Leave blank.

NTIS -

Block 13. Abstract. Include a brief (*Maximum 200 words*) factual summary of the most significant information contained in the report.

Block 14. Subject Terms. Keywords or phrases identifying major subjects in the report.

Block 15. Number of Pages. Enter the total number of pages.

Block 16. Price Code. Enter appropriate price code (*NTIS only*).

Blocks 17. - 19. Security Classifications. Self-explanatory. Enter U.S. Security Classification in accordance with U.S. Security Regulations (i.e., UNCLASSIFIED). If form contains classified information, stamp classification on the top and bottom of the page.

Block 20. Limitation of Abstract. This block must be completed to assign a limitation to the abstract. Enter either UL (unlimited) or SAR (same as report). An entry in this block is necessary if the abstract is to be limited. If blank, the abstract is assumed to be unlimited.

1997 SREP Final Technical Report Table of Contents

Armstrong Laboratory

Volume 1

	Principle Investigator	Report Title University/Institution	Laboratory & Directorate
1	Dr. Richelle M. Allen-King	Trans-1,2-Dichloroethene Transformation Rate in a Metallic Iron/Water System: Effects of Concentration and Temperature Washington State University	AL/EQC
2	Dr. Anthony R. Andrews	Development of Multianalyte Electrochemiluminescence Sensors & Biosensors Ohio University	AL/EQC
3	Dr. Jer-Sen Chen	Development of Perception Based Video Compression Algorithms Using Reconfigurable Hardware Wright State University	AL/CFHV
4	Dr. Cheng Cheng	Investigation & Eval of Optimization Algorithms Guiding the Assignment of Recruits to Training School Seats John Hopkins University	AL/HRM
5	Dr. Randolph D. Glickman	Optical Detection of Intracellular Photooxidative Reactions University of Texas Health Science Center	AL/OEO
6	Dr. Nandini Kannan	Predicting Altitude Decompression sickness Using Survival Models University of Texas at San Antonio	AL/CFTS
7	Dr. Antti J. Koivo	Skill Improvements Via Reflected Force Feedback Purdue Research Foundation	AL/CFBA
8	Dr. Suk B. Kong	Degradation & Toxicology Studies of JP-8 Fuel in Air, Soil & Drinking Water Incarnate Word College	AL/OEA
9	Dr. Audrey D. Levine	Biogeochemical Assessment of Natl Attenuation of JP-4 Contaminated Ground in the Presence of Fluorinated Surfactants Utah State University	AL/EQC
10	Dr. Robert G. Main	The Effect of Video Image Size & Screen Refresher Rate On Mess Retention Cal State University, Chico	AL/HRT
11	Dr. Phillip H. Marshall	On the Resilience of Time-to-Contact Judgements: The Determination of Inhibitory and Facilitory Influences, and Factor Structure Texas Tech University	AL/HRM
12	Dr. Bruce V. Mutter	Environmental cost Analysis: Calculating Return on Investment for Emerging Technologies Bluefield State College	AL/EQP

1997 SREP Final Technical Report Table of Contents

Armstrong Laboratory

Volume 1 (cont.)

	Principle Investigator	Report Title University/Institution	Laboratory & Directorate
13	Dr. Sundaram Narayanan	Java-Based Interactive Simulation Architecture for Airbase Logistics Modeling Wright State University	AL/HRT
14	Dr. Barth F. Smets	Coupling of 2, 4-&2, 6-Dinitrotoluene Mineralization W/NO ₂ Removal by University of Cincinnati	AL/EQC
15	Dr. Mary Alice Smith	In Vitro Detection of Apoptosis in Differentiating Mesenchymal Cells Using Immunohistochemistry and Image Analysis University of Georgia	AL/OET
16	Dr. William A. Stock	Application of Meta-Analysis to Research on Pilot Training: Extensions to Flight Simulator Visual System Research Arizona State University	AL/HRA
17	Dr. Nancy J. Stone	Evaluation of a Scale Designed to Measure the Underlying Constructs of Engagement, Involvement, & Self-Regulated Learning Creighton University	AL/HRT
18	Dr. Mariusz Ziejewski	Characterization of Human Head/Neck Response in Z-Direction in Terms of Significant Anthropomorphic Parameters, Gender, Helmet Weight and Helmet Center North Dakota State University	AL/CFBV
19	Dr. Kevin M. Lambert	Magnetic Effects on the Deposition & Dissolution of Calcium Carbonate Scale Brigham Young University	AL/EQS
20	Dr. Jacqueline C. Shin	Coordination of Cognitive & Perceptual-Motor Activities Pennsylvania State University	AL/HRM
21	Dr. Travis C. Tubre	The Development of a General Measure of Performance Texas A&M University-College Station	AL/HRT
22	Dr. Robert B. Trelease	Development of Qualitative Process Modeling Systems for Cytokines, Cell Adhesion Molecules, and Gene Regulation University of California – Los Angeles	AL/AOH

1997 SREP Final Technical Report Table of Contents

Phillips Laboratory

Volume 2

	Principle Investigator	Report Title University/Institution	Laboratory & Directorate
1	Dr. Graham R. Allan	Temporal & Spatial Characterization of a Synchronously-Pumped New Mexico Highlands University	PL/LIDN
2	Dr. Joseph M. Calo	Transient Studies of the Effects of Fire Suppressants in a Well-Stirred Combustor Brown University	PL/GPID
3	Dr. James J. Carroll	Examination of Critical Issues in the Triggering of Gamma Rays from 178Hf ^{m2} Youngstown State University	PL/WSQ
4	Dr. Soyoung S. Cha	Gradient-Data Tomography for Hartman Sensor Application to Aero-Optical Field Reconstruction University of Illinois at Chicago	PL/LIMS
5	Dr. Judith E. Dayhoff	Dynamic Neural Networks: Towards Control of Optical Air Flow Distortions University of Maryland	PL/LIMS
6	Dr. Ronald R. DeLyser	Computational Evaluation of Optical Sensors University of Denver	PL/WSTS
7	Dr. Andrew G. Detwiler	Analysis & Interpretation of Contrail Formation Theory & Observations South Dakota School of Mines – Technology	PL/GPAB
8	Dr. Itzhak Dotan	Measurements of Ion-Molecule Reactions at Very High Temperature The Open University of Israel	PL/GPID
9	Dr. George W. Hanson	Electromagnetic Modeling of Complex Dielectric/Metallic Mines In A Layered University of Wisconsin – Milwaukee	PL/WSQ
10	Dr. Mayer Humi	Optical & Clear Air Turbulence Worcester Polytechnic Inst.	PL/GPAA
11	Dr. Christopher H. Jenkins	Shape Control of an Inflated Circular Disk Experimental Investigation South Dakota School of Mines – Technology	PL/VT
12	Dr. Dikshitulu K. Kalluri	Numerical Simulation of Electromagnetic Wave Transformation in a Dynamic Magnetized Plasma University of Lowell	PL/GPIA
13	Dr. Aravinda Kar	Improved Chemical Oxygen-Iodine Laser (COIL) Cutting Models to Optimize Laser Parameters University of Central Florida	PL/LIDB

1997 SREP Final Technical Report Table of Contents

Phillips Laboratory

Volume 2 (cont.)

	Principle Investigator	Report Title University/Institution	Laboratory & Directorate
14	Dr. Andre Y. Lee	Characterization of Thermoplastic Inorganic-Organic Hybrid Polymers Michigan State University	PL/RKS
15	Dr. Feng-Bao Lin	Improvement in Fracture Propagation Modeling for Structural Ballistic Risk Assessment Polytechnic University of New York	PL/RKEM
16	Dr. Ronald A. Madler	Cross Sectional Area Estimation of Orbital Debris Embry-Riddle Aeronautical University	PL/WSAT
17	Dr. Carlos A. Ordonez	Incorporation of Boundary condition Models into the AF Computer Simulation University of North Texas	PL/WSQA
18	Dr. James M. Stiles	Wide Swath, High Resolution, Low Ambiguity SAR Using Digital Beamforming Arrays University of Kansas	PL/VTRA
19	Dr. Charles M. Swenson	Balloon Retromodulator Experiment Post- flight Analysis Utah State University	PL/VTRA
20	Dr. Miguel Velez-Reyes	Development of Algorithms for Linear & Nonlinear Retrieval Problems in Atmospheric Remote Sensing University of Puerto Rico	PL/GPAS
21	Dr. John D. Holtzclaw	Experimental Investigation of Ipinging Jets University of Cincinnati	PL/RKS
22	Dr. Jeffrey W. Nicholson	Radar Waves with Optical Carriers University of New Mexico	PL/LIDB

1997 SREP Final Technical Report Table of Contents

Rome Laboratory

Volume 3

Principle Investigator	Report Title University/Institution	Laboratory & Directorate
1 Dr. A. F. Anwar	Deep Quantum Well Channels for Ultra Low Noise HEMTs for Millimeter and Sub-millimeter Wave Applications University of Connecticut	AFRL/SNH
2 Dr. Ahmed E. Barbour	Investigating the Algorithmic Nature of the Proof Structure of ORA Larch/VHDL Georgia Southern University	RL/ERDD
3 Dr. Milica Barjaktarovic	Specification & Verification of MISSI Architecture Using SPIN Wilkes University	RL/C3AB
4 Dr. Daniel C. Bukofzer	Analysis, Performance Evaluations, & Computer Simulations of Receivers Processing Low Probability of Intercept Signals Cal State Univ. Fresno	RL/C3BA
5 Dr. Xuesheng Chen	Non-Destructive Optical Characterization of Composition & Its Uniformity in Multilayer Ternary Semiconductor Stacks Wheaton College	RL/ERX
6 Dr. Jun Chen	Amplitude Modulation Using Feedback Sustained Pulsation as Sub-Carrier in Rochester Inst of Technol	RL/OCPA
7 Dr. Everett E. Crisman	Development of Anti-Reflection Thin Films for Improved Coupling of Laser Energy into Light Activated, Semiconductor Re-Configurable, Microwave Source/Antenna Brown University	RL/ERAC
8 Dr. Digendra K. Das	Development of a Stimulation Model for Determining the Precision Of Reliability SUNYIT	RL/ERSR
9 Dr. Matthew E. Edwards	An Application of PROFILER for Modeling the Diffusion of Of Aluminum-Copper on a Silicon Substrate Spelman College	RL/ERDR
10 Dr. Kaliappan Gopalan	Analysis of Stressed Speech Using Cepstral Domain Features Purdue University – Calumet	RL/IRAA
11 Dr. James P. LeBlanc	Multichannel Autoregressive Modeling & Multichannel Innovations Based New Mexico State University	RL/OCSS
12 Dr. Hrshukesh N. Mhaskar	Multi-Source Direction Finding Cal State University, Los Angeles	RL/ERAA
13 Dr. Ronald W. Noel	An Evolutionary Sys for Machine Recognition of Software Source Code Rensselaer Polytechnic Inst	RL/C3CA

1997 SREP Final Technical Report Table of Contents

Rome Laboratory

Volume 3 (cont.)

Principle Investigator	Report Title University/Institution	Laboratory & Directorate
14 Dr. Glenn E. Prescott	Rapid Prototyping of Software Radio Sys Using Field Programmable Gate Arrays University of Kansas Center for Research	RL/C3BB
15 Dr. Mysore R. Rao	Wavelet Transform Techniques for Isolation, Detection & Classification of Concealed Objects in Images Rochester Institute of Technology	RL/OCSM
16 Dr. Scott E. Spetka	IPL HTML Interface Performance Evaluation SUNY of Tech Utica	RL/IRD
17 Dr. Gang Sun	Investigation of Si/ZnS Near Infrared Intersubband Lasers University of Massachusetts-Boston	RL/EROOC
18 Mr. Parker E. Bradley	Development of a User-Friendly Computer Environment for Blind Source Syracuse University	RL/C3BB

1997 SREP Final Technical Report Table of Contents

Wright Laboratory

Volume 4A

Principle Investigator	Report Title University/Institution	Laboratory & Directorate
1 Dr. Mohammad S. Alam	Infrared Image Registration & High Resolution Reconstruction Using Rotationally Translated Video Sequences* Purdue University	WL/AAJT
2 Dr. Pnina Ari-Gur	Optimizing Microstructure, Texture & Orientation Image Microscopy of Hot Rolled Ti-6Al-4V Western Michigan University	WL/MLLN
3 Dr. James D. Baldwin	Multi-Site & Widespread Fatigue Damage in Aircraft Structure in the Presence of Prior Corrosion University of Oklahoma	WL/FIB
4 Dr. Armando R. Barreto	Deconvolution of the Space-Time Radar Spectrum Florida International University	WL/AAMR
5 Dr. Marc M. Cahay	Improved Modeling of Space-Charge Effects in a New Cold Cathode Emitter University of Cincinnati	WL/AADM
6 Dr. Reaz A. Chaudhuri	Interfacing of Local Asymptotic Singular & Global Axisymmetric Micromechanical University of Utah	WL/MLBM
7 Dr. Robert J. DeAngelis	Texture Formation During the Thermo-Mechanical Processing of Copper Plate University of Nebraska - Lincoln	WL/MNMW
8 Dr. Gregory S. Elliott	The Study of a Transverse Jet in a Supersonic Cross-Flow Using Advanced Laser Rutgers: State University of New Jersey	WL/POPT
9 Dr. Altan M. Ferendeci	Development of Multiple Metal-Dielectric Layers for 3-D MMIC University of Cincinnati	WL/AADI
10 Dr. Allen G. Greenwood	Development of a Prototype to Test & Demonstrate the MODDCE Framework Mississippi State University	WL/MTI
11 Dr. Michael A. Grinfeld	Mismatch Stresses & Lamellar Microstructure of TiAl-Alloys Rutgers University- Piscataway	WL/MLLM
12 Dr. Michael C. Larson	Interfacial Sliding in Brittle Fibrous Composites Tulane University	WL/MLLM
13 Dr. Douglas A. Lawrence	Tools for the Analysis & Design of Gain Scheduled Missile Autopilots Ohio University	WL/MNAG

1997 SREP Final Technical Report Table of Contents

Wright Laboratory (cont.)

Volume 4A

	Principle Investigator	Report Title University/Institution	Laboratory & Directorate
14	Dr. Junghsen Lieh	Determination of 3D Deformations, Forces & Moments of Aircraft Wright State University	WL/FIVM
15	Dr. Zongli Lin	Control of Linear Sys w/Rate Limited Actuators & Its Applications to Flight Control Systems SUNY Stony Brook	WL/FI
16	Dr. Paul Marshall	Experimental & Computational Investigations of Bromine & Iodine Chemistry in Flame Suppression University of North Texas	WL/MLBT
17	Dr. Hui Meng	Development of Holographic Visualization & Holographic Velocimetry Techniques Kansas State University	WL/POSC
18	Dr. Douglas J. Miller	Band Gap Calculations on Squarate-Containing Conjugated Oligomers for the Prediction of Conductive and Non-Linear Optical Properties of Polymeric Materials Cedarville College	WL/MLBP
19	Dr. Timothy S. Newman	Classification & Visualization of Tissue in Multiple Modalities of Brain MR University of Alabama at Huntsville	WL/AACR
20	Dr. Mohammed Y. Niamat	FPGA Implementation of the Xpatch Ray Tracer University of Toledo	WL/AAST
21	Dr. Anthony C. Okafor	Development of Optimum Drilling Process for Advanced Composites University of Missouri – Rolla	WL/MTI
22	Dr. George A. Petersson	Absolute Rates for Chemical Reactions Wesleyan University	WL/MLBT
23	Dr. Mohamed N. Rahaman	Process Modeling of the Densification of Granular Ceramics Interaction Between Densification and Creep University of Missouri – Rolla	WL/MLLN

1997 SREP Final Technical Report Table of Contents

Wright Laboratory (cont.)

Volume 4B

	Principle Investigator	Report Title University/Institution	Laboratory & Directorate
24	Dr. Martin Schwartz	Quantum Mechanical Modeling of the Thermochemistry of Halogenated Fire Suppressants University of North Texas	WL/MLBT
25	Dr. Marek Skowronski	Investigation of Slip Boundaries in 4H-SiC Crystals Carnegie Melon University	WL/MLPO
26	Dr. Yong D. Song	Guidance & Control of Missile Sys Under Uncertain Flight Conditions North Carolina A&T State University	WL/MNAG
27	Dr. Raghavan Srinivasan	Models for Microstructural Evolution During Dynamic Recovery Wright State University	WL/MLIM
28	Dr. Scott K. Thomas	The Effects of Transient Acceleration Loadings on the Performance of a Copper-Ethanol Heat Pipe with Spiral Grooves Wright State University	WL/POOS
29	Dr. James P. Thomas	The Effect of Temperature on Fatigue Crack Growth of TI-6AL-4V in the Ripple University of Notre Dame	WL/MLLN
30	Dr. Karen A. Tomko	Scalable Parallel Solution of the 3D Navier-Stokes Equations Wright State University	WL/FIM
31	Dr. J. M. Wolff	Off Design Inviscid/Viscous Forced Response Prediction Model for High Cycle Wright State University	WL/POTF
32	Mr. Todd C. Hathaway	Experiments on Consolidation of Aluminum Powders Using Simple Shear University of North Texas	WL/MLLN
33	Ms. Diana M. Hayes	Error Correction & Compensation for Mueller Matrices Accounting for Imperfect Polarizers University of North Texas	WL/MNGA

1997 SREP Final Technical Report Table of Contents

Volume 5

	Principle Investigator	Report Title University/Institution	Laboratory & Directorate
Arnold Engineering Development Center			
1	Dr. Frank G. Collins	Development of Laser Vapor Screen Flow Visualization Sys Tennessee University Space Institute	AEDC
United States Air Force Academy			
2	Mr. Derek E. Lang	Experimental Investigation of Liquid Crystal Applications for Boundary Layer Characterization University of Washington	USAF/DFA
Air Logistics Centers			
3	Dr. Sandra A. Ashford	Development of Jet Engine Test Facility Vibration Signature & Diagnostic System University of Detroit Mercy	OCALC/TIE
4	Dr. Roger G. Ford	Use of Statistical Process Control in a Repair/Refurbish/ Remanufactureg Environment St. Mary's University	SAALC
Wilford Hall Medical Center			
5	Dr. Stedra L. Stillmana	Metabolite Profile Following the Administration of Fenproporex University of Alabama at Birmingham	WHMC

1997 SUMMER RESEARCH EXTENSION PROGRAM (SREP) MANAGEMENT REPORT

1.0 BACKGROUND

Under the provisions of Air Force Office of Scientific Research (AFOSR) contract F49620-90-C-0076, September 1990, Research & Development Laboratories (RDL), an 8(a) contractor in Culver City, CA, manages AFOSR's Summer Research Program. This report is issued in partial fulfillment of that contract (CLIN 0003AC).

The Summer Research Extension Program (SREP) is one of four programs AFOSR manages under the Summer Research Program. The Summer Faculty Research Program (SFRP) and the Graduate Student Research Program (GSRP) place college-level research associates in Air Force research laboratories around the United States for 8 to 12 weeks of research with Air Force scientists. The High School Apprenticeship Program (HSAP) is the fourth element of the Summer Research Program, allowing promising mathematics and science students to spend two months of their summer vacations working at Air Force laboratories within commuting distance from their homes.

SFRP associates and exceptional GSRP associates are encouraged, at the end of their summer tours, to write proposals to extend their summer research during the following calendar year at their home institutions. AFOSR provides funds adequate to pay for 100 SREP subcontracts. In addition, AFOSR has traditionally provided further funding, when available, to pay for additional SREP proposals, including those submitted by associates from Historically Black Colleges and Universities (HBCUs) and Minority Institutions (MIs). Finally, laboratories may transfer internal funds to AFOSR to fund additional SREPs. Ultimately the laboratories inform RDL of their SREP choices, RDL gets AFOSR approval, and RDL forwards a subcontract to the institution where the SREP associate is employed. The subcontract (see Appendix 1 for a sample) cites the SREP associate as the principal investigator and requires submission of a report at the end of the subcontract period.

Institutions are encouraged to share costs of the SREP research, and many do so. The most common cost-sharing arrangement is reduction in the overhead, fringes, or administrative charges institutions would normally add on to the principal investigator's or research associate's labor. Some institutions also provide other support (e.g., computer run time, administrative assistance, facilities and equipment or research assistants) at reduced or no cost.

When RDL receives the signed subcontract, we fund the effort initially by providing 90% of the subcontract amount to the institution (normally \$18,000 for a \$20,000 SREP). When we receive the end-of-research report, we evaluate it administratively and send a copy to the laboratory for a technical evaluation. When the laboratory notifies us the SREP report is acceptable, we release the remaining funds to the institution.

2.0 THE 1997 SREP PROGRAM

SELECTION DATA: A total of 572 faculty members (SFRP Associates) and 235 graduate students (GSRP associates) applied to participate in the 1996 Summer Research Program. From these applicants 188 SFRPs and 109 GSRPs were selected. The education level of those selected was as follows:

1996 SRP Associates, by Degree			
SFRP		GSRP	
PHD	MS	MS	BS
182	4	45	49

Of the participants in the 1997 Summer Research Program 90 percent of SFRPs and 11 percent of GSRPs submitted proposals for the SREP. Ninety proposals from SFRPs and ten from GSRPs were selected for funding, which equates to a selection rate of 54% of the SFRP proposals and of 34% for GSRP proposals.

1997 SREP: Proposals Submitted vs. Proposals Selected			
	Summer 1996 Participants	Submitted SREP Proposals	SREPs Funded
SFRP	188	142	90
GSRP	109	17	10
TOTAL	297	159	100

The funding was provided as follows:

Contractual slots funded by AFOSR	99
Laboratory funded	<u>1</u>
Total	100

Twenty-two HBCU/MI associates from the 1996 summer program submitted SREP proposals; eleven were selected (none were lab-funded; all were funded by additional AFOSR funds).

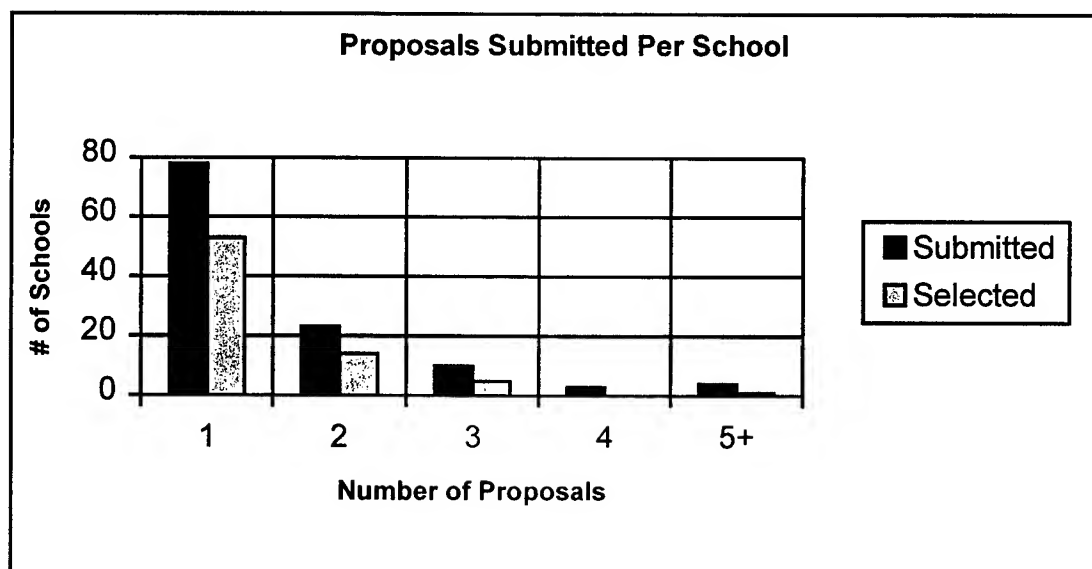
Proposals Submitted and Selected, by Laboratory		
	Applied	Selected
United States Air Force Academy	2	1
Air Logistics Centers	7	2
Armstrong Laboratory	38	21
Arnold Engineering Development Center	1	1
Phillips Laboratory	31	22
Rome Laboratory	18	18
Wilford Hall Medical Center	1	1
Wright Laboratory	63	34
TOTAL	161	100

Note: Wright Laboratory funded 1.

The 306 1996 Summer Research Program participants represented 135 institutions.

Institutions Represented on the 1996 SRP and 1997 SREP		
Number of schools represented in the Summer 92 Program	Number of schools represented in submitted proposals	Number of schools represented in Funded Proposals
135	118	73

Forty schools had more than one participant submitting proposals.



The selection rate for the 78 schools submitting 1 proposal (68%) was better than those submitting 2 proposals (61%), 3 proposals (50%), 4 proposals (0%) or 5+ proposals (25%). The 4 schools that submitted 5+ proposals accounted for 30 (15%) of the 196 proposals submitted.

Of the 196 proposals submitted, 159 offered institution cost sharing. Of the funded proposals which offered cost sharing, the minimum cost share was \$1000.00, the maximum was \$68,000.00 with an average cost share of \$12,016.00.

Proposals and Institution Cost Sharing		
	Proposals Submitted	Proposals Funded
With cost sharing	159	82
Without cost sharing	37	18
Total	196	100

The SREP participants were residents of 41 different states. Number of states represented at each laboratory were:

States Represented, by Proposals Submitted/Selected per Laboratory		
	Proposals Submitted	Proposals Funded
Air Logistics Centers	7	2
Armstrong Laboratory	38	22
Arnold Engineering Development Center	1	1
Phillips Laboratory	31	22
Rome Laboratory	18	18
United States Air Force Academy	2	1
Wilford Hall Medical Center	1	1
Wright Laboratory	63	33

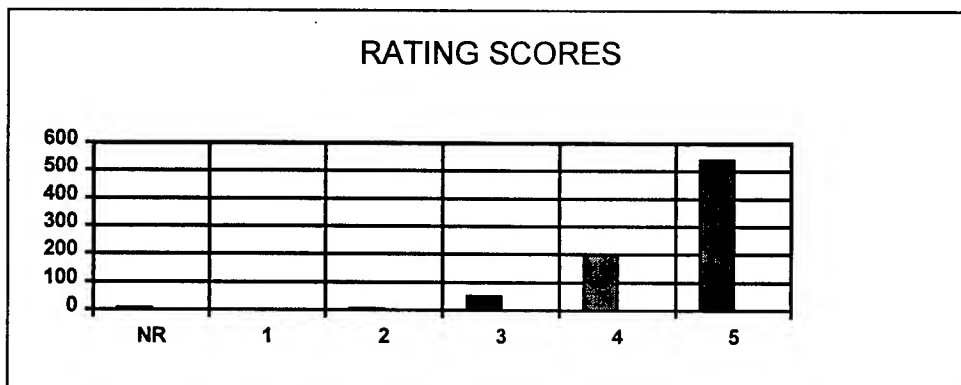
ADMINISTRATIVE EVALUATION: The administrative quality of the SREP associates' final reports was satisfactory. Most complied with the formatting and other instructions provided to them by RDL. Ninety seven final reports and two interim reports have been received and are included in this report. The subcontracts were funded by \$2,469,573.00 of Air Force money. Institution cost sharing totaled \$3,458,667.00.

TECHNICAL EVALUATION: The form used for the technical evaluation is provided as Appendix 2. ninety-two evaluation reports were received. Participants by laboratory versus evaluations submitted is shown below:

	Participants	Evaluations	Percent
Air Logistics Centers	7	7	100
Armstrong Laboratory	38 ¹	20	95.2
Arnold Engineering Development Center	1	1	100
United States Air Force Academy	1	1	100
Phillips Laboratory	31	31	100
Rome Laboratory	18	18	100
Wilford Hall Medical Center	1	1	100
Wright Laboratory	63	57	91.9
Total	100 ³	93	95.9

The number of evaluations submitted for the 1997 SREP (95.9%) shows a marked improvement over the 1996 SREP submittals (65%).

PROGRAM EVALUATION: Each laboratory focal point evaluated ten areas (see Appendix 2) with a rating from one (lowest) to five (highest). The distribution of ratings was as follows:

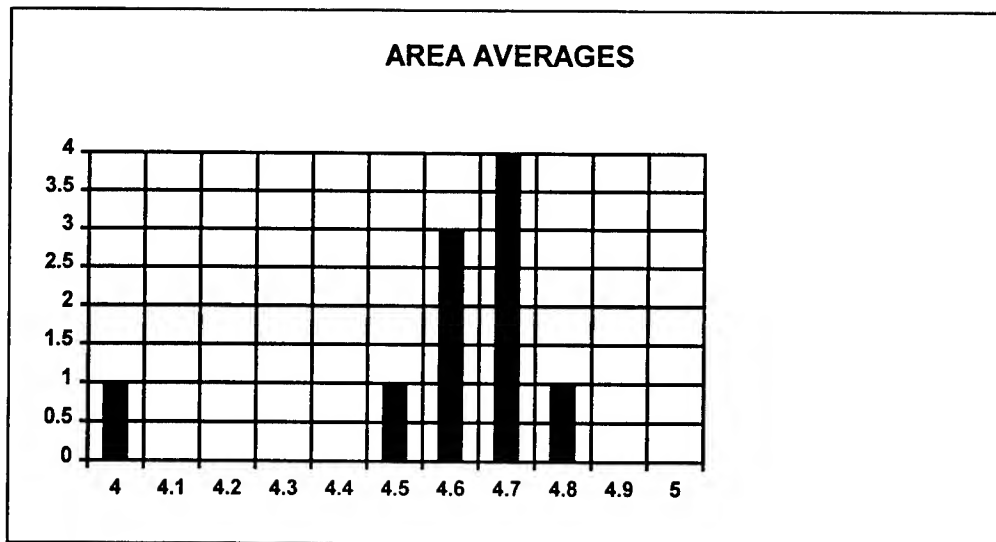


Rating	Not Rated	1	2	3	4	5
# Responses	7	1	7	62 (6%)	226 (25%)	617 (67%)

The 8 low ratings (one 1 and seven 2's) were for question 5 (one 2) "The USAF should continue to pursue the research in this SREP report" and question 10 (one 1 and six 2's) "The one-year period for complete SREP research is about right", in addition over 30% of the threes (20 of 62) were for question ten. The average rating by question was:

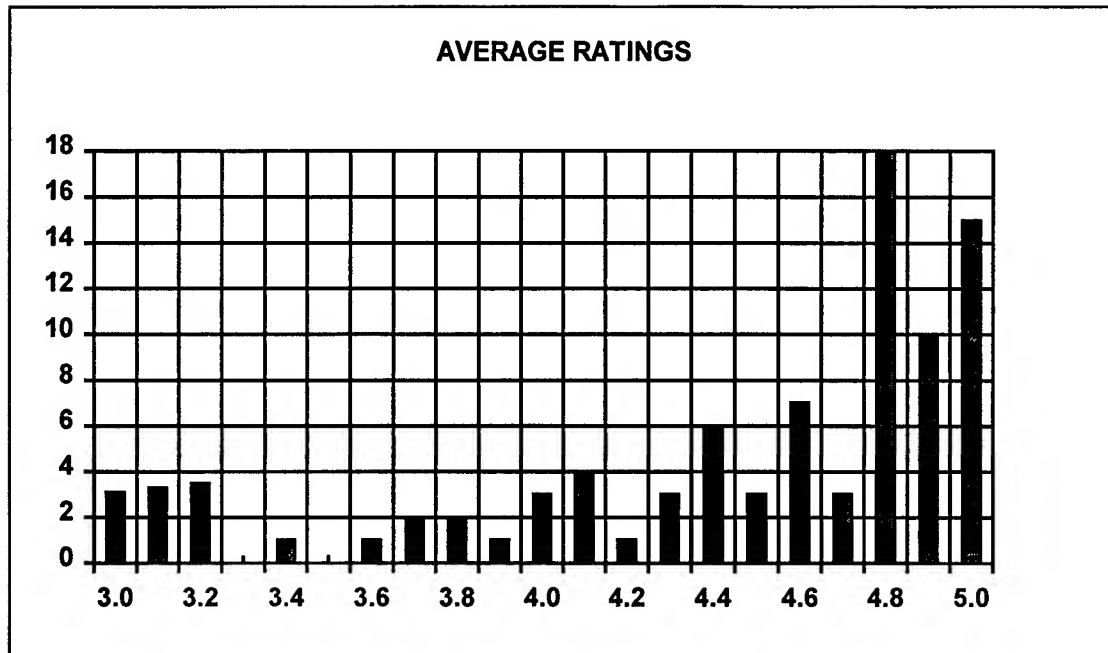
Question	1	2	3	4	5	6	7	8	9	10
Average	4.6	4.6	4.7	4.7	4.6	4.7	4.8	4.5	4.6	4.0

The distribution of the averages was:



Area 10 “the one-year period for complete SREP research is about right” had the lowest average rating (4.1). The overall average across all factors was 4.6 with a small sample standard deviation of 0.2. The average rating for area 10 (4.1) is approximately three sigma lower than the overall average (4.6) indicating that a significant number of the evaluators feel that a period of other than one year should be available for complete SREP research.

The average ratings ranged from 3.4 to 5.0. The overall average for those reports that were evaluated was 4.6. Since the distribution of the ratings is not a normal distribution the average of 4.6 is misleading. In fact over half of the reports received an average rating of 4.8 or higher. The distribution of the average report ratings is as shown:



It is clear from the high ratings that the laboratories place a high value on AFOSR's Summer Research Extension Programs.

3.0 SUBCONTRACTS SUMMARY

Table 1 provides a summary of the SREP subcontracts. The individual reports are published in volumes as shown:

<u>Laboratory</u>	<u>Volume</u>
Air Logistics Centers	5
Armstrong Laboratory	1
Arnold Engineering Development Center	5
Phillips Laboratory	2
Rome Laboratory	3
United States Air Force Academy	5
Wilford Hall Medical Center	5
Wright Laboratory	4A, 4B

SREP SUB-CONTRACT DATA

Report Author Author's University	Author's Degree	Sponsoring Lab	Performance Period	Contract Amount	Univ. Cost Share
Allen-King , Richelle Earth Sciences Washington State University, Pullman, WA	PhD 97-0833	AL/EQ	01/01/97 12/31/97	\$24999.00	\$4969.00
		trans-1,2-Dichloroethene Transformation Rate in a Metallic Iron/Water Sys			
Andrews , Anthony Analytical Chemistry Ohio University, Athens, OH	PhD 97-0831	AL/EQ	01/01/97 12/31/97	\$25000.00	\$18137.00
		Development of Multianalyte Electrochemiluminescence Sensors & Biosensors			
Chen , Jer-Sen Electrical Engineering Wright State University, Dayton, OH	PhD 97-0801	AL/CF	01/01/97 12/31/97	\$25000.00	\$6304.00
		Development of Perception Based Video Compression Algorithms using Reconfigurabl			
Cheng , Cheng Statistics Johns Hopkins University, Baltimore, MD	PhD 97-0837	AL/HR	01/01/97 12/31/97	\$25000.00	\$0.00
		Investigation & Eval of Optimization Algorithms Guiding the Assignment of Recrui			
Glickman , Randolph Zoology Univ of Texas Health Science Center, San	PhD 97-0836	AL/OE	01/01/97 12/31/97	\$23827.00	\$338.00
		Optical Detection of Intracellular Photooxidative Reactions			
Kannan , Nandini Statistics Univ of Texas at San Antonio, San Antonio, TX	PhD 97-0829	AL/CF	01/16/97 07/31/97	\$19000.00	\$3854.00
		Predicting Altitude Decompression Sickness Using Survival Models			
Koivo , Antti Automatic Controls Purdue Research Foundation, West Lafayette, IN		AL/CF	01/01/97 08/31/97	\$25000.00	\$0.00
	97-0828	Skill Improvements Via Reflected Force Feedback			
Kong , Suk Organic Chemistry Incarnate Word College, San Antonio, TX	PhD 97-0835	AL/OE	01/01/97 12/31/97	\$23900.00	\$11393.00
		Degradation & Toxicology Studies of JP-8 Fuel in Air, Soil & Drinking Water			
Levine , Audrey Environmental Engineering Utah State University, Logan, UT	PhD 97-0830	AL/EQ	01/01/97 12/31/97	\$24857.00	\$8705.00
		Biogeochemical Assessment of Natl Attenuation of JP-4 Contaminated Ground Water			
Main , Robert Educational Technology Cal State Univ, Chico, Chico, CA	PhD 97-0873	AL/HR	01/01/97 08/31/97	\$25000.00	\$12716.00
		The Effect of Video Image Size & Screen Refresher Rate on Mess Retention			
Marshall , Phillip Psychology Texas Tech University, Lubbock, TX	PhD 97-0870	AL/HR	01/01/97 12/31/97	\$25000.00	\$17886.00
		On the Resilience of Time-to-Contact Judgements:The Determination of Inhibitory			
Mutter , Bruce Architecture Bluefield State College, Bluefield, WV	MS 97-0834	AL/EQ	01/01/97 12/31/97	\$25000.00	\$6780.00
		Environmental Cost Analysis:Calculating Return on Investment for Emerging Tech			
Narayanan , Sundaram Industrial & Systems Engineering Wright State University, Dayton, OH	PhD 97-0838	AL/HR	01/01/97 12/31/97	\$25000.00	\$6304.00
		Java-Based Interactive Simulation Architecture for Airbase Logistics Modeling			
Smets , Barth Environmental Engineering University of Connecticut, Storrs, CT	PhD 97-0832	AL/EQ	01/01/97 12/31/97	\$25000.00	\$28363.00
		Coupling of 2,4-&2,6-Dinitrotoluene Mineralization w/NO2 Removal by Denitrificat			
Smith , Mary Alice toxicology University of Georgia, Athens, GA	PhD 97-0901	AL/OE	01/01/97 12/31/97	\$25000.00	\$8640.00
		In Vitro Detection of Apoptosis in Differentiating Mesenchymal Cells Using Immun			

SREP SUB-CONTRACT DATA

Report Author Author's University	Author's Degree	Sponsoring Lab	Performance Period		Contract Amount	Univ. Cost Share
Stock , William Experimental Psychology Arizona State University, Tempe, AZ	PhD 97-0839	AL/HR	01/01/97	12/13/97	\$24916.00	\$19199.00
		Application of Meta-Analysis to Res on Pilot Training: Ext to Flight Simulator				
Stone , Nancy Industrial-Organizational Psychology Creighton University, Omaha, NE	PhD 97-0871	AL/HR	01/01/97	12/31/97	\$24994.00	\$31255.00
		Evaluation of Engagement, Involvement, & Self-Regulated Learning Scales & Their				
Ziejewski , Mariusz Mechanical Engineering North Dakota State University, Fargo, ND	PhD 97-0827	AL/CF	01/01/97	12/31/97	\$25000.00	\$25294.00
		Characterization of Human Head/Neck Response in Z-Direction in Terms of Signific				
Lambert , Kevin Mechanical Engineering Brigham Young University, Provo, UT	MA 97-0898	AL/EQ	01/01/97	12/31/97	\$19800.00	\$9504.00
		Magnetic Effects on the Deposition & Dissolution of Calcium Carbonate Scale				
Shin , Jacqueline Psychology Pennsylvania State University, University Park,	MS 97-0874	AL/HR	01/01/97	12/31/97	\$24939.00	\$4500.00
		Coordinatin of Cognitive & Perceptual-Motor Activities				
Tubre , Travis Psychology Texas A & M Univ-College Station, College	BS 97-0840	AL/HR	01/01/97	12/31/97	\$24923.00	\$16844.00
		The Development of a General Measure of Performance				
Collins , Frank Mechanical Engineering Tennessee Univ Space Institute, Tullahoma, TN	PhD 97-0853	AEDC/E	01/01/97	12/31/97	\$25000.00	\$24671.00
		Development of Laser Vapor Screen Flow Visualization Sys for 16T at AEDC				
Lang , Derek Aerodynamics University of Washington, Seattle, WA	BS 97-0865	FJSRL/F	01/01/97	06/30/97	\$24963.00	\$5970.00
		Experimental Investigation of Liquid Crystal Applications for Boundary Layer				
Ashford , Sandra Aerospace Engineering University of Detroit Mercy, Detroit, MI	PhD 97-0841	ALC/OC	01/01/97	12/31/97	\$25000.00	\$2077.00
		Development of Jet Engine Test Facility Vibration Signature & Diagnostic Sys				
Allan , Graham Physics New Mexico Highlands University, Las Vegas, NM	PhD 97-0879	PL/LI	01/01/97	12/31/97	\$25000.00	\$6000.00
		Temporal & SpatialCharacterisation of a Synchronously-Pumped Periodically-Poled				
Calo , Joseph Chemical Engineering Brown University, Providence, RI	PhD 97-0875	PL/GP	01/01/97	12/31/97	\$25000.00	\$14221.00
		Transient Studies of the Effects of Fire Suppressants in a Well-Stirred Combusto				
Carroll , James Nuclear Physics Youngstown State University, Youngstown, OH	PhD 97-0881	PL/WS	01/01/97	12/31/97	\$25000.00	\$4500.00
		Examination of Critical Issues in the Triggering of Gamma Rays from 178Hfm2				
Cha , Soyoung Mechanical Engineering Univ of Illinois at Chicago, Chicago, IL	PhD 97-0876	PL/LI	01/01/97	12/31/97	\$25000.00	\$5000.00
		Gradient-Data Tomography for Hartmann Sensor Application to Aero-Optical Field				
Dayhoff , Judith Biophysics Univ of Maryland, College Park, MD	PhD 97-0850	PL/LI	01/01/97	12/31/97	\$25000.00	\$0.00
		Dynamic Neural Networks:Towards Control of Optical Air Flow Distortions				
DeLyser , Ronald Electrical Engineering University of Denver, Denver, CO	PhD 97-0851	PL/WS	01/01/97	12/31/97	\$24801.00	\$0.00
		Computational Evaluation of Optical Sensors				

SREP SUB-CONTRACT DATA

Report Author Author's University	Author's Degree	Sponsoring Lab	Performance Period	Contract Amount	Univ. Cost Share
Detwiler , Andrew Atmospheric Sciences S Dakota School of Mines/Tech, Rapid City, SD	PhD 97-0848	PL/GP Analysis & Interpretation of Contrail Formation Theory & Observations	01/01/97 12/31/97	\$25000.00	\$2500.00
Dotan , Itzhak Chemistry The Open University of Israel, Tel-Aviv Israel,	PhD 97-0882	PL/GP Measurements of Ion-Molecule Reactions at Very High Temperatures	01/01/97 12/31/97	\$25000.00	\$25210.00
Hanson , George Electrical Engineering Univ of Wisconsin - Milwaukee, Milwaukee, WI	PhD 97-0877	PL/WS Electromagnetic Modeling of Complex Dielectric/Metallic Mines In a Layered Earth	01/01/97 12/31/97	\$25000.00	\$23347.00
Humi , Mayer Applied Mathematics Worcester Polytechnic Inst, Worcester, MA	PhD 97-0883	PL/GP Optical & Clear Air Turbulence	01/01/97 12/31/97	\$25000.00	\$0.00
Jenkins , Christopher Mechanical Engineering S Dakota School of Mines/Tech, Rapid City, SD	PhD 97-0846	PL/VT Shape Control of an Inflated Circular Disk:Experimental Inves	01/01/97 12/31/97	\$25000.00	\$3803.00
Kalluri , Dikshitulu Electrical Engineering University of Lowell, Lowell, MA	PhD 97-0847	PL/GP Numerical Simulation of Electromagnetic Wave Transformation in a Dynamic Magneti	01/01/97 12/31/97	\$25000.00	\$7307.00
Kar , Aravinda Engineering University of Central Florida, Orlando, FL	PhD 97-0849	PL/LI Improved Chem. Oxygen-Iodine Laser (COIL)Cutting Model to Optimize Laser Paramet	01/01/97 12/31/97	\$25000.00	\$5292.00
Lee , Andre Physics Michigan State University, East Lansing, MI	PhD 97-0843	PL/RK Characterization of Thermoplastic Inorganic-Organic Hybrid Polymers	01/01/97 12/31/97	\$24623.00	\$10239.00
Lin , Feng-Bao Structural Mechanics Polytechnic Inst of New York, Brooklyn, NY	PhD 97-0842	PL/RK Improvement in Fracture Propagation Modeling for Structural Ballistic Risk	01/01/97 12/31/97	\$25000.00	\$11577.00
Madler , Ronald Aerospace Engineering Embry-Riddle Aeronautical University, Prescott,	PhD 97-0878	PL/WS Cross Sectional Area Estimation of Orbital Debris	01/01/97 12/31/97	\$25000.00	\$5339.00
Ordonez , Carlos Physics University of North Texas, Denton, TX	PhD 97-0852	PL/WS Incorporation of Boundary Condition Models into the AF Computer Simulation Prog,	01/01/97 12/31/97	\$25000.00	\$11401.00
Stiles , James Electrical Engineering University of Kansas, Lawrence, KS	PhD 97-0880	PL/VT Wide Swath, High Resolution, Low Ambiguity SAR Using Digital Beamforming Arrays	01/01/97 12/31/97	\$25000.00	\$4968.00
Swenson , Charles Electrical Engineering Utah State University, Logan, UT	PhD 97-0845	PL/VT Balloon Retromodulator Experiment Post-flight Analysis	01/01/97 12/31/97	\$25000.00	\$0.00
Velez-Reyes , Miguel Electrical Engineering University of Puerto Rico, Mayaguez, PR	PhD 97-0868	PL/GP Development of Algorithms for Linear & Nonlinear Retrieval Problems in Atmospher	02/01/97 12/31/97	\$25000.00	\$14386.00
Holtzclaw , John Aeronautical Engineering University of Cincinnati, Cincinnati, OH	BS 97-0844	PL/RK Experimental Investigation of Ipinging Jets	01/01/97 12/31/97	\$25000.00	\$17950.00

SREP SUB-CONTRACT DATA

Report Author Author's University	Author's Degree	Sponsoring Lab	Performance Period	Contract Amount	Univ. Cost Share
Nicholson , Jeffrey Physics University of New Mexico, Albuquerque, NM	BS 97-0869	PL/LI	01/01/97 12/31/97 Radar Waves With Optical Carriers	\$24982.00	\$0.00
Anwar , A. Electrical Engineering University of Connecticut, Storrs, CT	PhD 97-0860	RL/ER	01/01/97 12/31/97 Deep Quantum Well Channels for Ultra Low Noise HEMTs	\$24995.00	\$9313.00
Barbour , Ahmed Computer Science Georgia Southern University, Statesboro, GA	PhD 97-0859	RL/ER	01/01/97 12/31/97 Investigating the Algorithmic Nature of the Proof Structure of ORA Larch/VHDL	\$25000.00	\$28890.00
Barjaktarovic , Milica Electrical Engineering Wilkes University, Wilkes Barre, PA	PhD 97-0858	RL/C3	01/15/97 05/30/97 Specification & Verification of MISSI Architecture Using SPIN	\$24958.00	\$3168.00
Bukofzer , Daniel Electrical Engineering Cal State Univ, Fresno, Fresno, CA	PhD 97-0888	RL/C3	01/01/97 12/31/97 Analysis, Performance Evaluations, & Computer Simulations of Rec Processing	\$25000.00	\$4999.00
Chen , Xuesheng Physics Wheaton College, Norton, MA	PhD 97-0887	RL/ER	01/01/97 12/31/97 Non-Destructive Optical Characterization of Composition & its Uniformity in Mult	\$25000.00	\$0.00
Chen , Jun Physics Rochester Inst of Technol, Rochester, NY	PhD 97-0862	RL/OC	01/01/97 12/31/97 Amplitude Modulation Using Feedback Sustained Pulsation as Sub-Carrier in Multi-	\$25000.00	\$6250.00
Crisman , Everett Electrical Sciences Brown University, Providence, RI	PhD 97-0855	RL/ER	01/01/97 12/31/97 Development of Anti-Reflection Thin Films for Improved Coupling of Laser Energy	\$25000.00	\$5100.00
Das , Digendra Mechanical Engineering SUNYIT, Utica, NY	PhD 97-0891	RL/ER	01/01/97 12/31/97 Development of a Simulation Model for Determining the Precision of Reliability	\$24999.00	\$10811.00
Edwards , Matthew Physics Program Spelman College, Atlanta, GA	PhD 97-0885	RL/ER	01/01/97 12/31/97 An Application of PROFILER for Modeling the Diffusion of Aluminum-Copper	\$25000.00	\$800.00
Gopalan , Kaliappan Electrical Engineering Purdue University - Calumet, Hammond, IN	PhD 97-0861	RL/IR	01/01/97 12/31/97 Analysis of Stressed Speech Using Cepstral Domain Features	\$25000.00	\$30987.00
LeBlanc , James Klipsch School of Elec & Comp Eng New Mexico State University, Las Cruces, NM	PhD 97-0856	RL/OC	01/01/97 12/31/97 Multichannel Autoregressive Modeling & Multichannel Innovations Based Detection	\$25000.00	\$36317.00
Mhaskar , Hrushikesh Mathematics Cal State Univ, Los Angeles, Los Angeles, CA	PhD 97-0889	RL/ER	01/01/97 12/31/97 Multi-Source Direction Finding	\$25000.00	\$0.00
Noel , Ronald Engineering Psychology Rensselaer Polytechnic Instit, Troy, NY	PhD 97-0884	RL/C3	01/01/97 12/31/97 An Evolutionary Sys for Machine Recognition of Software Source Code	\$25000.00	\$0.00
Prescott , Glenn Electrical Engineering University of Kansas Center for Research,	PhD 97-0854	RL/C3	01/01/97 12/31/97 Rapid Prototyping of Software Radio Sys Using Field Programmable Gate Arrays	\$25000.00	\$6000.00

SREP SUB-CONTRACT DATA

Report Author Author's University	Author's Degree	Sponsoring Lab	Performance Period		Contract Amount	Univ. Cost Share
Rao , Mysore Electrical Engineering Rochester Inst of Technol, Rochester, NY	PhD 97-0886	RL/OC	01/01/97	12/31/97	\$25000.00	\$6250.00
		Wavelet Transform Techniques for Isolation, Detection & Classification of Conceal				
Spetka , Scott Computer Science SUNY OF Tech Utica, Utica, NY	PhD 97-0857	RL/IR	01/01/97	12/31/97	\$24998.00	\$11753.00
		IPL HTML Interface Performance Evaluation				
Sun , Gang Electrical Engineering University of Massachusetts-Boston, Boston, MA	PhD 97-0890	RL/ER	01/01/97	12/31/97	\$25000.00	\$9866.00
		Investigation of Si/ZnS Near Infrared Intersubband Lasers				
Bradley , Parker Physics Syracuse University, Syracuse, NY	BS 97-0863	RL/C3	01/01/97	12/31/97	\$25000.00	\$0.00
		Development of a User-Friendly Computer Environment for Blind Source Separation				
Ford , Roger Industrial Engineering St. Mary's Univ of San Antonio, San Antonio, TX	PhD 97-0864	ALC/SA	01/01/97	12/31/97	\$19200.00	\$3816.00
		Use of Statistical Process Control in a Repair/Refurbish/Remfg Environme				
Stillman , Stedra Chemistry Univ of Alabama at Birmingham, Birmingham,	BS 97-0903	WHMC/	05/01/97	12/31/97	\$25000.00	\$0.00
		Metabolite Profile Following the Administration of Fenproporex				
Alam , Mohammad Electrical Engineering Purdue University, Fort Wayne, IN	PhD 97-0892	WL/AA	01/01/97	12/31/97	\$24988.00	\$0.00
		Infrared Image Registration & High Resolution Reconstruction Using Rotationally				
Ari-Gur , Pnina Materials Engineering Western Michigan University, Kalamazoo, MI	PhD 97-0819	WL/ML	01/01/97	12/31/97	\$25000.00	\$14740.00
		Optimizing Microstructure, Texture & Orientation Image Microscopy of Hot Rolled				
Baldwin , James Mechanical Engineering University of Oklahoma, Norman, OK	PhD 97-0807	WL/FI	01/01/97	12/31/97	\$24991.00	\$13869.00
		Multi-Site & Widespread Fatigue Damage in Aircraft Structure in the Presence of				
Barreto , Armando Electrical Engineering Florida International Univ, Miami, FL	PhD 97-0803	WL/AA	01/01/97	12/31/97	\$24833.00	\$20291.00
		Deconvoluton of the Space-Time Radar Spectrum				
Cahay , Marc Electrical Engineering University of Cincinnati, Cincinnati, OH	PhD 97-0902	WL/AA	01/01/97	12/31/97	\$25000.00	\$10383.00
		Improved Modeling of Space-Charge Effects in a New Cold Cathode Emitter				
Chaudhuri , Reaz Structural Mechanics University of Utah, Salt Lake City, UT	PhD 97-0820	WL/ML	01/01/97	12/31/97	\$25000.00	\$4000.00
		Interfacing of Local Asyptotic Singular & Global Axisymmetric Micromechanical				
DeAngelis , Robert Materials Science Univ of Nebraska - Lincoln, Lincoln, NE	PhD 97-0825	WL/MN	01/01/97	12/31/97	\$25000.00	\$19821.00
		Texture Formation During the Thermo-Mechanical Processing of Copper Plate				
Elliott , Gregory Mechanical Engineering Rutgers:State Univ of New Jersey, Piscataway, NJ	PhD 97-0897	WL/PO	01/01/97	12/31/97	\$25000.00	\$7550.00
		The Study of a Transverse jet in a Supersonic Cross-Flow Using Advanced Laser				
Ferendeci , Altan Electrical Engineering University of Cincinnati, Cincinnati, OH	PhD 97-0804	WL/AA	01/01/97	12/31/97	\$25000.00	\$17940.00
		Development of Multiple Metal-Dielectric Layers for 3-D MMIC				

SREP SUB-CONTRACT DATA

Report Author Author's University	Author's Degree	Sponsoring Lab	Performance Period	Contract Amount	Univ. Cost Share
Greenwood , Allen Management Science Mississippi State University, Mississippi Sta, MS	PhD 97-0815	WL/MT Development of a Prototype to Test & Demonstrate the MODDCE Framework	01/01/97 12/31/97	\$24975.00	\$8020.00
Grinfeld , Michael Mechanical Engineering Rutgers University, Piscataway, Piscataway, NJ	PhD 97-0812	WL/ML Mismatch Stresses & Lamellar Microstructure of TiAl-Alloys	01/01/97 03/31/97	\$25000.00	\$5646.00
Larson , Michael Applied Mechanics Tulane University, New Orleans, LA	PhD 97-0900	WL/ML Interfacial Sliding in Brittle fibrous Composites	01/01/97 11/30/97	\$25000.00	\$5000.00
Lawrence , Douglas Electrical ENgineering Ohio University, Athens, OH	PhD 97-0813	WL/MN Tools for the Analysis & Design of Gain Scheduled Missile Autopilots	01/01/97 12/31/97	\$24999.00	\$23273.00
Lieh , Junghsen Mechanical Engineering Wright State University, Dayton, OH	PhD 97-0894	WL/FI Determination of 3D Deformations, Forces & Moments of Aircraft Tires w/a Synchro	01/01/97 12/31/97	\$25000.00	\$6304.00
Lin , Zongli Electrical Engineering SUNY Stony Brook, Stony Brook, NY	PhD 97-0806	WL/FI Control of Linear Sys w/Rate Limited Actuators & Its Applications	01/01/97 12/31/97	\$25000.00	\$11100.00
Marshall , Paul Chemistry University of North Texas, Denton, TX	PhD 97-0821	WL/ML Experimental & Computational Investigations of Bromine & Iodine Chemistry in	01/01/97 12/31/97	\$25000.00	\$26714.00
Meng , Hui Mechanical Engineering Kansas State University, Manhattan, KS	PhD 97-0817	WL/PO Development of Holographic Visualization & Holographic Velocimetry Techniques	01/01/97 12/31/97	\$25000.00	\$0.00
Miller , Douglas Chemistry Cedarville College, Cedarville, OH	PhD 97-0808	WL/ML Band Gap Calculations on Squarate-Containing Conjugated Oligomers for the Predic	01/01/97 12/31/97	\$25000.00	\$0.00
Newman , Timothy Computer Science Univ of Alabama at Huntsville, Huntsville, AL	PhD 97-0893	WL/AA Classification & Visualization of Tissue in Multiple Modalities of Brain MR	01/01/97 12/31/97	\$25000.00	\$0.00
Niamat , Mohammed Electrical Engineering University of Toledo, Toledo, OH	PhD 97-0802	WL/AA FPGA Implementation of the Xpatch Ray Tracer	01/01/97 12/31/97	\$25000.00	\$13620.00
Okafor , Anthony Mechanical Engineering University of Missouri - Rolla, Rolla, MO	PhD 97-0896	WL/MT Development of Optimum Drilling Process for Advanced Composites	01/01/97 12/31/97	\$25000.00	\$39643.00
Petersson , George Chemistry Wesleyan University, Middletown, CT	PhD 97-0823	WL/ML Absolute Rates for Chemical Reactions	01/01/97 12/31/97	\$25000.00	\$6200.00
Rahaman , Mohamed Materials Science University of Missouri - Rolla, Rolla, MO	PhD 97-0822	WL/ML Process Modeling of the Densification of Granular Ceramics	01/01/97 12/31/97	\$25000.00	\$24928.00
Schwartz , Martin Physical Chemistry University of North Texas, Denton, TX	PhD 97-0895	WL/ML Quantum Mechanical Modeling of the Thermochemistry of Halogenated Fire Suppresan	01/01/97 12/31/97	\$25000.00	\$29641.00

SREP SUB-CONTRACT DATA

Report Author Author's University	Author's Degree	Sponsoring Lab	Performance Period		Contract Amount	Univ. Cost Share
Skowronski, Marek Solid State Physics Carnegie Melon University, Pittsburgh, PA	PhD 97-0811	WL/ML	01/01/97	12/31/97	\$25000.00	\$0.00
Investigation of Slip Boundaries in 4H-SiC Crystals						
Song, Yong Electrical Engineering North Carolina A&T State University,	PhD 97-0814	WL/MN	01/01/97	12/31/97	\$25000.00	\$0.00
Guidance & Control of Missile Sys Under Uncertain Flight Conditions						
Srinivasan, Raghavan Materials Science & Engineering Wright State University, Dayton, OH	PhD 97-0809	WL/ML	01/01/97	12/31/97	\$25000.00	\$6304.00
Models for Microstructural Evolution during Dynamic Recovery & Dynamic Recrystal						
Thomas, Scott Mechanical Engineering Wright State University, Dayton, OH	PhD 97-0818	WL/PO	01/01/97	12/31/97	\$25000.00	\$6304.00
The Effects of Transient Acceleration Loadings on the Performance of a Copper-Et						
Thomas, James Applied Mechanics University of Notre Dame, Notre Dame, IN	PhD 97-0810	WL/ML	01/01/97	12/31/97	\$25000.00	\$0.00
The Effect of Temperature on Fatigue Crack Growth of TI-6AL-4V in the Ripple Loa						
Tomko, Karen Computer Engineering Wright State University, Dayton, OH	PhD 97-0805	WL/FI	01/01/97	12/31/97	\$25000.00	\$6304.00
Scabable Parallel Solution of the 3D Navier-Stokes Equations						
Trelease, Robert Anatomy Univ of Calif, Los Angeles, Los Angeles, CA	PhD 97-0866	AL/MD	01/01/97	12/31/97	\$25000.00	\$0.00
Development of Qualitative Process Modeling Sys for Cytokines, Cell Adhesion Mol						
Wolff, J Mechanical Engineering Wright State University, Dayton, OH	PhD 97-0816	WL/PO	01/01/97	12/31/97	\$25000.00	\$13592.00
Off Design Inviscid/Viscous Forced Response Prediction Model for High Cycle Fati						
Hathaway, Todd Metallurgical Engineering Univ of Texas A&M, College Station, TX	BS 97-0824	PL/RK	01/01/97	12/31/97	\$25000.00	\$23040.00
Experiments on Consolidation of Aluminum Powders Using Simple Shear						
Hayes, Diana Mathematics University of North Texas, Denton, TX	MS 97-0826	WL/MN	01/16/97	08/31/97	\$15113.00	\$3804.00
Error Correction & Compensation for Mueller Matrices						

APPENDIX 1:

SAMPLE SREP SUBCONTRACT

**AIR FORCE OFFICE OF SCIENTIFIC RESEARCH
1996 SUMMER RESEARCH EXTENSION PROGRAM
SUBCONTRACT 96-0881**

BETWEEN

Research & Development Laboratories
5800 Uplander Way
Culver City, CA 90230-6608

AND

Wright State University
Research and Sponsored Programs
Dayton, OH 45435

REFERENCE: Summer Research Extension Program Proposal 95-0117
Start Date: 01/01/96 End Date: 12/31/96
Proposal Amount: \$25,000
Proposal Title: "HELPR: A Hybrid Evolutionary Learning System For Pattern
Recognition

(1) PRINCIPAL INVESTIGATOR:

Dr. Mateen M. Rizki
Dept. of Computer Science & Engineering
Wright State University
Dayton, OH 45435

(2) UNITED STATES AFOSR CONTRACT NUMBER: F49620-93-C-0063

**(3) CATALOG OF FEDERAL DOMESTIC ASSISTANCE NUMBER (CFDA): 12.800
PROJECT TITLE: AIR FORCE DEFENSE RESEARCH SOURCES PROGRAM**

(4) ATTACHMENTS

- 1 REPORT OF INVENTIONS AND SUBCONTRACT**
- 2 CONTRACT CLAUSES**
- 3 FINAL REPORT INSTRUCTIONS**

*****SIGN SREP SUBCONTRACT AND RETURN TO RDL*****

1. BACKGROUND: Research & Development Laboratories (RDL) is under contract (F49620-93-C-0063) to the United States Air Force to administer the Summer Research Program (SRP), sponsored by the Air Force Office of Scientific Research (AFOSR), Bolling Air Force Base, D.C. Under the SRP, a selected number of college faculty members and graduate students spend part of the summer conducting research in Air Force laboratories. After completion of the summer tour participants may submit, through their home institutions, proposals for follow-on research. The follow-on research is known as the Summer Research Extension Program (SREP). Approximately 61 SREP proposals annually will be selected by the Air Force for funding of up to \$25,000; shared funding by the academic institution is encouraged. SREP efforts selected for funding are administered by RDL through subcontracts with the institutions. This subcontract represents an agreement between RDL and the institution herein designated in Section 5 below.
2. RDL PAYMENTS: RDL will provide the following payments to SREP institutions:
 - 80 percent of the negotiated SREP dollar amount at the start of the SREP research period.
 - The remainder of the funds within 30 days after receipt at RDL of the acceptable written final report for the SREP research.
3. INSTITUTION'S RESPONSIBILITIES: As a subcontractor to RDL, the institution designated on the title page will:

- a. Assure that the research performed and the resources utilized adhere to those defined in the SREP proposal.
- b. Provide the level and amounts of institutional support specified in the SREP proposal..
- c. Notify RDL as soon as possible, but not later than 30 days, of any changes in 3a or 3b above, or any change to the assignment or amount of participation of the Principal Investigator designated on the title page.
- d. Assure that the research is completed and the final report is delivered to RDL not later than twelve months from the effective date of this subcontract, but no later than December 31, 1999. The effective date of the subcontract is one week after the date that the institution's contracting representative signs this subcontract, but no later than January 15, 1999.
- e. Assure that the final report is submitted in accordance with Attachment 3.
- f. Agree that any release of information relating to this subcontract (news releases, articles, manuscripts, brochures, advertisements, still and motion pictures, speeches, trade associations meetings, symposia, etc.) will include a statement that the project or effort depicted was or is sponsored by: Air Force Office of Scientific Research, Bolling AFB, D.C.
- g. Notify RDL of inventions or patents claimed as the result of this research as specified in Attachment 1.
- h. RDL is required by the prime contract to flow down patent rights and technical data requirements to this subcontract. Attachment 2 to this

subcontract contains a list of contract clauses incorporated by reference in the prime contract.

4. All notices to RDL shall be addressed to:

RDL AFOSR Program Office
5800 Uplander Way
Culver City, CA 90230-6609

5. By their signatures below, the parties agree to provisions of this subcontract.

Abe Sopher
RDL Contracts Manager

Signature of Institution Contracting Official

Typed/Printed Name

Date

Title

Institution

Date/Phone

ATTACHMENT 1
REPORT OF INVENTIONS AND SUBCONTRACT, DD FORM 882

Research associates will complete a DD Form 882, “**REPORT OF INVENTIONS AND SUBCONTRACT**” in accordance with the instructions on the back of the form. The completed form should be forwarded along with the final report.

block 1a: Your name (subcontractor)

block 1c: Your subcontract number

block 2a: RDL

block 2c: F49620-93-C-0063

Call for other information if necessary

This form is used only if you created an invention resulting from work done under the Summer Research Program. If you have no such inventions to report, just write a small note stating:

*“I have no inventions to report as a result of my work on the
AFOSR 1999 Summer Research Extension Program”*

*Signature, date
Type/Print Name
Associate Number*

ATTACHMENT 2
CONTRACT CLAUSES

This contract incorporates by reference the following clauses of the Federal Acquisition Regulations (FAR), with the same force and effect as if they were given in full text. Upon request, the Contracting Officer or RDL will make their full text available (FAR 52.252-2).

FAR CLAUSES

TITLE AND DATE

52.202-1	DEFINITIONS
52.203-3	GRATUITIES
52.203-5	COVENANT AGAINST CONTINGENT FEES
52.203-6	RESTRICTIONS ON SUBCONTRACTOR SALES TO THE GOVERNMENT
52.203-7	ANTI-KICKBACK PROCEDURES
52.203-8	CANCELLATION, RECISSION, AND RECOVERY OF FUNDS FOR ILLEGAL OR IMPROPER ACTIVITY
52.203-10	PRICE OR FEE ADJUSTMENT FOR ILLEGAL OR IMPROPER ACTIVITY
52.203-12	LIMITATION ON PAYMENTS TO INFLUENCE CERTAIN FEDERAL TRANSACTIONS
52.204-2	SECURITY REQUIREMENTS
52.209-6	PROTECTING THE GOVERNMENT'S INTEREST WHEN SUBCONTRACTING WITH CONTRACTORS DEBARRED, SUSPENDED, OR PROPOSED FOR DEBARMENT
52.215-2	AUDIT AND RECORDS - NEGOTIATION
52.215-10	PRICE REDUCTION FOR DEFECTIVE COST OR PRICING DATA

52.215-12	SUBCONTRACTOR COST OR PRICING DATA
52.215-14	INTEGRITY OF UNIT PRICES
52.215-8	ORDER OF PRECEDENCE
52.215-18	REVERSION OR ADJUSTMENT OF PLANS FOR POSTRETIREMENT BENEFITS OTHER THAN PENSIONS
52.222-3	CONVICT LABOR
52.222-26	EQUAL OPPORTUNITY
52.222-35	AFFIRMATIVE ACTION FOR SPECIAL DISABLED AND VIETNAM ERA VETERANS
52.222-36	AFFIRMATIVE ACTION FOR HANDICAPPED WORKERS
52.222-37	EMPLOYMENT REPORTS ON SPECIAL DISABLED VETERAN AND VETERANS OF THE VIETNAM ERA
52.223-2	CLEAN AIR AND WATER
52.223-6	DRUG-FREE WORKPLACE
52.224-1	PRIVACY ACT NOTIFICATION
52.224-2	PRIVACY ACT
52.227-1	ALT. I - AUTHORIZATION AND CONSENT
52.227-2	NOTICE AND ASSISTANCE REGARDING PATIENT AND COPYRIGHT INFRINGEMENT
52.227-10	FILING OF PATENT APPLICATIONS - CLASSIFIED SUBJECT MATTER
52.227-11	PATENT RIGHTS - RETENTION BY THE CONTRACTOR (SHORT FORM)
52.228-7	INSURANCE - LIABILITY TO THIRD PERSONS

52.230-5	COST ACCOUNTING STANDARDS - EDUCATIONAL INSTRUCTIONS
52.232-23	ALT. I - ASSIGNMENT OF CLAIMS
52.233-1	DISPUTES
52.233-3	ALT. I - PROTEST AFTER AWARD
52.237-3	CONTINUITY OF SERVICES
52.246-25	LIMITATION OF LIABILITY - SERVICES
52.247-63	PREFERENCE FOR U.S. - FLAG AIR CARRIERS
52.249-5	TERMINATION FOR CONVENIENCE OF THE GOVERNMENT (EDUCATIONAL AND OTHER NONPROFIT INSTITUTIONS)
52.249-14	EXCUSABLE DELAYS
52.251-1	GOVERNMENT SUPPLY SOURCES

DOD FAR CLAUSES**DESCRIPTION**

252.203-7001	SPECIAL PROHIBITION ON EMPLOYMENT
252.215-7000	PRICING ADJUSTMENTS
252.223-7004	DRUG FREE WORKFORCE (APPLIES TO SUBCONTRACTS WHERE THERE IS ACCESS TO CLASSIFIED INFORMATION)
252.225-7001	BUY AMERICAN ACT AND BALANCE OF PAYMENTS PROGRAM
252.225-7002	QUALIFYING COUNTRY SOURCES AS SUBCONTRACTS
252.227-7013	RIGHTS IN TECHNICAL DATA - NONCOMMERCIAL ITEMS
252.227-7030	TECHNICAL DATA - WITHOLDING PAYMENT
252.227-7037	VALIDATION OF RESTRICTIVE MARKINGS ON TECHNICAL DATA
252.231-7000	SUPPLEMENTAL COST PRINCIPLES
252.232-7006	REDUCTIONS OR SUSPENSION OF CONTRACT PAYMENTS UPON FINDING OF FRAUD

ATTACHMENT 3
Final Report Instructions for 1997 Summer Research Extension Program (SREP)

You must submit a final research extension report and a DD Form 882 "Report of Inventions and Subcontract". The final 20 percent of your proposal award will be awarded when RDL has received your report and DD Form 882 in acceptable format.

Send one original and one copy of the final research report to RDL no later than 12 months after the effective date of the SREP subcontract, but no later than December 31, 1997.

Each final report will be copied and bound with other reports in multiple volumes published by RDL for AFOSR. PLEASE comply with the formatted instructions below. RDL will return reports that don't comply.

For the 1997 summer research extension report, the following procedures pertain:

1. Use black print, as close to letter quality as possible, on white 8 1/2 in. by 11 in. paper.
2. Use a 10-point font that is 12 characters per inch. Use 1 1/2 or double-spacing between lines of text.
3. Allow a minimum of one inch wide margin at top and bottom and left and right sides, or else material may be covered up in binding. The page number (see also 8 below) should therefore be centered one inch from the bottom. The one-inch margin all sides applies to every page, whether text, appendices, figures, tables, printouts, graphs, copies of other materials, or any other content.
4. Maximum page count is restricted to 40 pages.
5. **Please Do Not submit:**
 - Pages printed on both sides.
 - Color illustrations; original photos (use reproducible halftones integrated on the page); foldouts; pasted-up pages.
 - Special covers or binders causing pages to be punched, stapled, or perforated.
6. On the title page, type the following in single-spaced clusters:
 - Report title (capital letters);
 - Name(s) of investigator(s), title and department;
 - University including mailing address;
 - "Final Report for:
Summer Research Extension Program
 - Acknowledgment of Air Force Office of Scientific Research, Bolling AFB,
Washington DC sponsorship (plus the institution sponsorship of the institution has shared in costs);
 - Month and year of publication
7. The next page after the title page will be the abstract. Type the title (single-spaced between lines), double space below the last line of the title, then type the author(s) name, title, department and institution. Enter two double spaces, center the word "Abstract", double-space, and type the abstract text, maximum one page.

8. Begin the first page of text by repeating the title and author at the top. The content should follow that of a standard research paper; introduction, discussion of problem, methodology, results, conclusion, and reference.
9. Number all pages of your report consecutively 1-40, starting with the title page.
10. The next three pages show examples of:
 - Title page
 - Abstract
 - First page of text

APPENDIX 2:

SAMPLE SREP SUBCONTRACT

**SUMMER RESEARCH EXTENSION PROGRAM
TECHNICAL EVALUATION**

SREP No: 97-0852

Principal Investigator: DR Carlos Ordonez
University of North Texas

Circle the rating level number, 1 (low) through 5 (high),
you feel best evaluate each statement and return the
completed form to RDL by fax or mail to:

RDL
Attn: SREP Tech Evals
5800 Uplander Way
Culver City, CA 90230-6608
(310) 216-5940 or (800) 677-1363

-
- | | |
|--|-----------|
| 1. This SREP report has a high level of technical merit. | 1 2 3 4 5 |
| 2. The SREP program is important to accomplishing the lab's mission. | 1 2 3 4 5 |
| 3. This SREP report accomplished what the associate's proposal promised. | 1 2 3 4 5 |
| 4. This SREP report addresses area(s) important to the USAF. | 1 2 3 4 5 |
| 5. The USAF should continue to pursue the research in this SREP report. | 1 2 3 4 5 |
| 6. The USAF should maintain research relationships with this SREP associate. | 1 2 3 4 5 |
| 7. The money spent on this SREP effort was well worth it. | 1 2 3 4 5 |
| 8. This SREP report is well organized and well written. | 1 2 3 4 5 |
| 9. I'll be eager to be a focal point for summer and SREP associates in the future. | 1 2 3 4 5 |
| 10. The one-year period for complete SREP research is about right. | 1 2 3 4 5 |
-

11. If you could change any one thing about the SREP program, what would you change:

12. What do you definitely NOT change about the SREP program?

PLEASE USE THE BACK FOR ANY OTHER COMMENTS

Laboratory Phillips Laboratory
Lab Focal Point Dr Bob Peterkin
Office Symbol PL/WSQA

Phone: (505) 846-0259

***trans*-1,2-DICHLOROETHENE TRANSFORMATION RATE IN A
METALLIC IRON/WATER SYSTEM:
EFFECTS OF CONCENTRATION AND TEMPERATURE**

Richelle M. Allen-King, Assistant Professor
Department of Geology

P.O. Box 64-2812
Washington State University
Pullman, WA 99164-2812

Final Report for:
Summer Research Extension Program
Armstrong Laboratory

Sponsored by:
Air Force Office of Scientific Research
Bolling Air Force Base, DC

and

Armstrong Laboratory

December 1997

***trans*-1,2-DICHLOROETHENE TRANSFORMATION RATE IN A
METALLIC IRON/WATER SYSTEM:
EFFECTS OF CONCENTRATION AND TEMPERATURE**

Richelle M. Allen-King , Assistant Professor
Department of Geology
Washington State University
Pullman, WA 99164-2812

ABSTRACT

The effects of temperature and initial solute concentration on the observed pseudo-first order reduction rate constant for *trans*-1,2-dichloroethene (DCE) in a cast iron (Fe⁰)/water system were determined in batch systems. DCE was selected as the probe compound for these investigations because of its low sorption to nonreactive sites and because its reaction rate is comparable to the rates for trichloroethene and tetrachloroethene, two of the most frequently detected groundwater contaminants. The reaction occurred more rapidly at higher temperatures compared to lower temperatures. Analysis of the data collected between 12.3 and 42.6°C using a classic Arrhenius approach allowed determination of the reaction activation energy of 10.5 kcal/mol. An activation energy of this magnitude suggests that the reaction is not limited by aqueous-phase diffusion. Additionally, the reaction rate constant approximately doubles with each 10°C increase in temperature over the environmentally relevant range. A practical consequence of this finding is that reaction rates determined at room temperature will be approximately twice as large as the rate for the same solute concentration at typical groundwater temperatures. The reaction exhibited reactive site saturation behavior at high solute:Fe⁰ specific surface area ratios and a hyperbolic kinetic model was fit to the results ranging over three orders of magnitude initial solution concentration. Reactive-site limited behavior was observed primarily at ratios >~ 7 µmol/m². At ratios ranging over approximately two orders of magnitude below this value (~0.07-7 µmol/m²), the pseudo-first order rate constant varied by only 3-fold. Because the solute:Fe⁰ SSA ratios expected in most flow-through systems in the field are in this lower range, the results imply that reactive-site limited behavior is not likely to affect most flow-through treatment systems.

***trans*-1,2-DICHLOROETHENE TRANSFORMATION RATE IN A
METALLIC IRON/WATER SYSTEM:
EFFECTS OF CONCENTRATION AND TEMPERATURE**

Richelle M. Allen-King , Assistant Professor

INTRODUCTION

Background

Chlorinated solvents in groundwater are of public concern because they can have negative impacts on human health and the environment. Drinking water standards are typically in the low part-per-billion range. For example, the drinking water standards (maximum contaminant level or MCL) for trichloroethene (TCE) and perchloroethene (PCE) are 5 µg/L [US EPA, 1987; US EPA, 1991]. Chlorinated solvents are the most frequently identified organic contaminants in groundwater for several reasons: 1) these highly chlorinated compounds tend to be persistent in aerobic groundwater; 2) during the past 40-50 years, these compounds have been commonly used industrial solvents and they have been discharged to the environment by disposal, leakage and spillage, often as a dense non-aqueous phase liquid (DNAPL); 3) DNAPLs in the subsurface, distributed as both residual and pools, can provide exceptionally long-term sources of groundwater contamination that are challenging to delineate and remediate [Mackay and Cherry, 1989; Westrick, 1990; NRC, 1993; NRC, 1994; MacDonald and Kavanaugh, 1994; Vogel et al., 1987; Pankow et al., 1996].

The US Air Force (USAF) has identified at least 1100 sites contaminated with chlorinated solvents [Burris, pers. comm.]. Therefore, treatment methods for chlorinated-solvent contaminated sites are of particular interest to the USAF. The conventional approach to groundwater remediation has been to pump contaminated groundwater to the surface for treatment [US EPA, 1990]. Because of the ineffectiveness of "pump-and-treat" as a remediation method, focus has shifted to alternative *in situ* remediation methods [NRC, 1993; NRC, 1994].

Metallic iron has promise for use in both *in situ* and *ex situ* treatment of water contaminated with chlorinated solvents. The use of metallic iron in permeable *in situ* treatment barriers is being tested as an alternative remediation and containment method for chlorinated solvents in groundwater [Gillham, 1995; Wilson, 1995; NRC, 1997; among others]. Within this concept, contaminated

groundwater flows naturally through a portion of the aquifer modified to contain iron, and the contaminants are remediated by reaction with the iron. Because transformation rates are rapid relative to typical groundwater flow velocities [Gillham and O'Hannesin, 1994; Sivavec and Horney, 1995], the *in situ* method has potential to treat groundwater with a passive system that may prove cost-effective relative to the conventional method [Wilson, 1995]. *Ex situ* treatment using an above-ground reactor has been demonstrated at a superfund site as part of the US Environmental Protection Agency SITE program. In either the *in situ* or *ex situ* applications, optimization and assurance of effective treatment system design relies on an understanding of the factors controlling the transformation reactions.

Literature Review

Zero-valent or metallic iron can bring about the reduction of dissolved chlorinated solvents such as TCE and PCE [Gillham and O'Hannesin, 1994 and references reviewed therein]. The reduction reaction is coupled to iron corrosion (oxidative dissolution) [Matheson and Tratnyek, 1994].

In a recent compilation of literature, Johnson et al. [1996] report that normalized rate coefficients (k_{SA} , normalized for iron surface area to solution ratio) vary by about 1 order of magnitude for a particular compound in metallic iron/water (Fe^0/H_2O) systems. A broad range of variables are suggested as potentially important by these researchers [Johnson et al., 1996], including, concentration, treatment and handling of the iron samples, interpretation of rate constants, and a number of solution effects - such as pH, alkalinity, and dissolved oxygen, among others. The effects of variables such as concentration and temperature, controlled within a particular study, have not been widely reported. These two variables are important because they provide insights into the fundamental chemistry of the reaction.

It has also been suggested that coatings and precipitates passivate the iron surface and slow dechlorination reactions [Gillham and O'Hannesin, 1994; Sivavec and Horney, 1995], implying a diffusion-limited process. However, thermodynamic data for VC suggests that the VC reaction is not limited by aqueous-phase diffusion [Deng et al., 1997]. Few experiments have been conducted over a range of temperatures for the Fe^0/H_2O system. Hence, thermodynamic data, which will provide additional insight on the diffusion limitation issue, is generally not available for the chlorinated ethenes.

Taken together, the experiment results and considerations described above suggest a need to account for the effects of concentration and temperature in planning remediation/reactor design with metallic iron. Most of the process-based experimental work described above has been conducted with TCE or CTET and electrolytic iron [e.g. Matheson and Tratnyek, 1994; Orth and Gillham, 1995; Johnson et al., 1996]. Recognizing that the iron selected for application at field sites will likely be of a cast variety, and that the reaction products observed with cast iron differ from electrolytic [Campbell, pers. comm.], this research focussed on a cast iron/water system.

GOAL AND RESEARCH OVERVIEW

The goal of this research was to determine the kinetic form and thermodynamic data for transformation of a probe chloroethene in the $\text{Fe}^0/\text{H}_2\text{O}$ system. To accomplish this goal, experiments were conducted over a wide range of concentrations and environmentally relevant temperatures in batch systems. *Trans*-1,2-dichloroethene (DCE) was chosen as the probe compound for this study because: 1) its reaction rate constant is comparable to the rates of PCE and TCE when normalized for system geometry and when sorption to nonreactive sites is accounted for (Table 1); 2) it does not have a high sorption coefficient to nonreactive sites (Table 1); and 3) chlorinated ethenes are environmentally important. Fisher 40-mesh cast iron was used in the experiments because it is a standard and readily available iron which is similar to commercially used cast irons [Burris et al., in prep.], and it has been used extensively in research conducted previously by USAF scientists [e.g. Burris et al., 1995; Campbell and Burris, 1996].

Table 1. Reaction rate constants and sorption coefficients for PCE, TCE, and DCE (trans-1,2-dichloroethene) in batch Fe⁰/H₂O systems.

Compound [†]	ln λ _s [†]	λ _s /ρ _{Fe} [‡] [mL/g·hr]	Sorption coefficients [§]		
			K	K/b	n
DCE	-1.79 ± 1.43	0.17	0.471	- - -	0.685
TCE	-3.06 ± 0.42	0.14	18.3	0.0207	0.655
PCE	-2.89 ± 0.98	0.17	108	0.156	0.673

[†] Rate constant and sorption coefficient data for PCE and TCE from Burris et al. [1995], for DCE from Allen-King et al. [1997b]. [‡] Rate coefficient defined from mass loss in the total system in terms of solution concentration. These are the λ_s reported in the manuscripts. [§] Normalized coefficients estimated by the author where ρ_{Fe} is the iron concentration (g/mL) in the batch system. The ρ_{Fe} used for the calculations are: 5 g Fe per 15 mL water for TCE and PCE, 1 g Fe per 1 mL water for DCE. [¶] Freundlich isotherm for DCE: C_s = KC_wⁿ, where C_s and C_w are sorbed and solution concentrations in nmol/g and nmol/mL respectively. Generalized Langmuir isotherm for TCE and PCE:

$$C_s = \frac{KC_w^n}{1 + (K/b) C_w^n} \quad (1)$$

METHODS AND MATERIALS

Batch experiments

The batch systems were prepared in approximately 161 ml vials containing 5.000 ± 0.005 g pre-cleaned cast iron (Fisher, 40 mesh), 100 ml nanopure water, and sufficient glass beads to result in a 55 ml headspace for each vial. The iron was cleaned with HCl following the procedure established by Burris et al. [1995]. The surface area of Fisher 40-mesh cast iron prepared as in the current study has been measured by others previously as $0.7\text{--}1.2$ m²/g [Burris et al., 1995; Roberts et al., 1996; Burris et al., in prep]; 1.0 m²/g is used for calculations in this study. The batch systems were prepared in a nitrogen-filled glove-bag to minimize oxygen contamination of the systems. Vials were allowed to equilibrate at 6 RPM for three days prior to addition of DCE to prevent the "unaged" surface effect observed previously by Allen-King et al. [1997a]. Each vial was amended with an appropriate volume of a 25.5 μmol DCE/ml N₂-sparged nanopure water solution to achieve the desired initial solution concentration. Volumes ranged between approximately 17 μl and 20.0 ml. (Note that vials receiving ≥ 1.00 ml DCE solution were prepared initially with an equivalent lower water volume so that the final volume in each system was 100 ml.) All vials were rotated at ~ 6 RPM in a constant temperature bath.

Experiments were conducted at 5 initial concentrations ranging over approximately three orders of magnitude: all of these experiments were conducted at $32.5 \pm 0.1^\circ\text{C}$ to increase the reaction rates compared to room temperature. Experiments were also conducted at the lowest concentration (of the five tested) at 4 temperatures ranging from 12.3 to 42.6°C . Because the Henry's law constants vary with temperature, the initial volume of DCE/water solution added to the systems designed to investigate the temperature effect was varied so that a consistent initial solution concentration of 3.5 ± 0.1 μM was achieved.

For each experiment condition, a minimum of three vials were prepared: a reaction vial containing DCE, pentane as an internal standard, and iron; an iron-free control vial; and a pentane-free control vial to ensure that the internal standard did not interfere with reaction progress. An additional replicate reaction vial was prepared for two of the experiment conditions. One vial was also prepared to test whether the addition to the batch system of a large amount of water at the time of DCE addition (which was necessary for the high concentration experiments) affected the reaction rate. For this test, 10 ml of

de-aired nanopure water was added to a replicate low concentration experiment vial (12.3°C) using the canula technique for solution transfer that was used for the high concentration experiments. Immediately following addition of the water, the DCE solution was added in the identical manner as the other reaction vials of that experiment group. The reaction rate coefficient determined was not significantly different from the other two reaction vials for this treatment.

Analytical

All analyses were conducted using headspace samples injected directly into a GC (SRI) with a GSQ-PLOT (J&W) column and flame ionization detection. The sample aliquots were 5-100 μ l, depending on the experiment concentration. Prior to sample collection, an equivalent volume of Ar was added to each vial. The GC operating parameters were as follows: temperature program, 50°C hold for 2 minutes, ramp at 25°C/min to 150°C and hold for a total time of 10.0 minutes; the carrier gas was He; the detector temperature was 150°C. Standard vials were prepared at two concentrations in duplicate for each experiment condition.

RESULTS AND DISCUSSION

Pseudo-first order kinetics

Each experiment system appeared to follow pseudo-first order kinetics for the approximately two half-lives of decay observed. The reaction concentration histories for experiments at two concentrations are shown in Figure 1 to demonstrate the behavior observed. The results also show that the pentane internal standard did not significantly affect the reaction rate; therefore, the results from pentane-free vials are treated as replicate reaction vials in the analysis.

Johnson et al. [1996] have pointed out the importance of normalizing the observed rate coefficients for the iron to water ratio in the system. Because contaminant mass is stored in both the solid (sorbed to non-reactive sites) and vapor phases in the experiment systems, the normalization procedure must account for mass stored in these phases. Following the logic of Johnson et al. [1996], observed pseudo-first order rate coefficients (k_{obs}) can be normalized to the iron surface-area concentration

$$k_{obs} = k_{SA} a_s \rho_m \quad (2)$$

where k_{SA} is defined as the "specific reaction rate constant" or the rate constant normalized for the system iron surface area concentration; a_s is the specific surface area of the iron (m^2/g); and ρ_m is the iron concentration (g/ml of solution). Because a consistent iron type is used throughout these experiments, the normalized rate coefficient (k_m) is defined based simply on the effective iron concentration,

$$k_{obs} = k_m \rho_m \quad (3)$$

Variation in temperature and concentration cause variations in the relative proportions of the DCE mass stored in either the air or solid (sorbed to nonreactive sites) phases in the experiment systems. In order to account for these differences, we use the "effective" iron concentration (ρ_m), defined as the mass of iron (m_{fe}) to a volume of water equivalent to the volume of water that would contain all of the masses in the sorbed, air and water phases in the batch system at the system concentration and temperature (V_e),

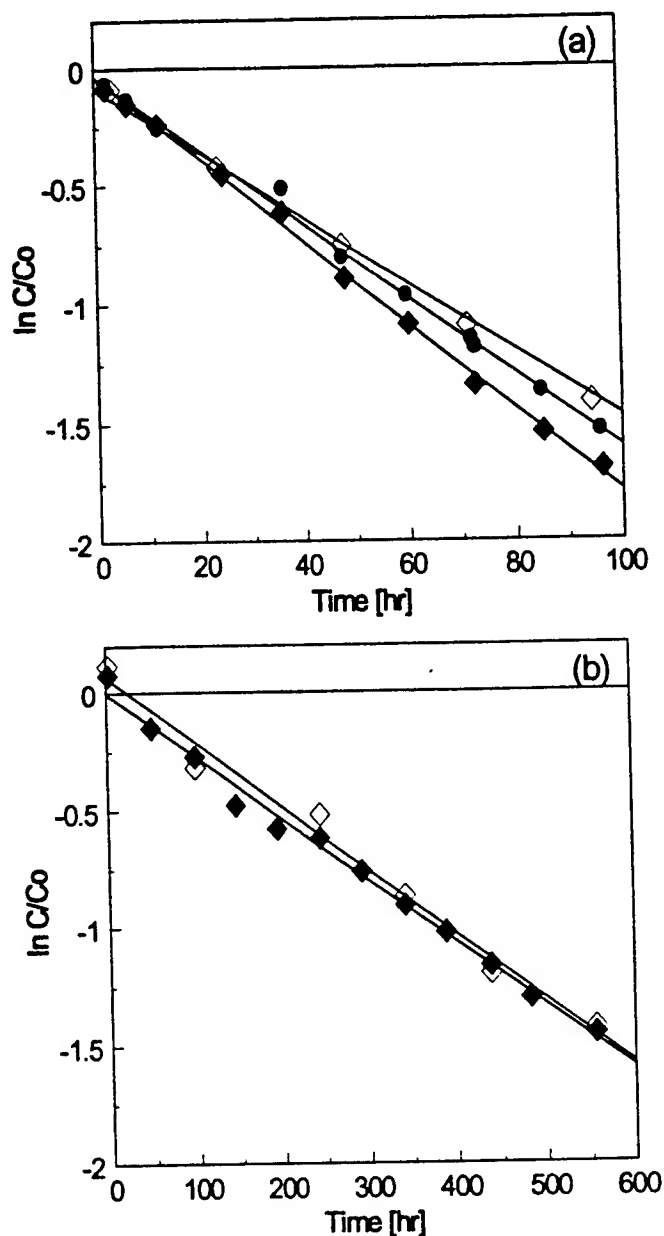


Figure 1. Pseudo-first order reaction rate determinations for experiments at two different concentrations. The initial DCE solution concentrations in the two experiments are (a) $0.0037 \mu\text{mol/ml}$, and (b) $0.92 \mu\text{mol/ml}$. Both experiments were conducted at 32.5°C . Solid symbols are for reaction vials containing internal standard. Open symbols are for reaction vials prepared without the internal standard.

$$\rho_m = \frac{m_{fe}}{V_e} \quad (4)$$

$$V_e = \frac{C_w (V_w + H_c V_a + K_F m_{fe} C_w^{n-1})}{C_w} \quad (5)$$

where C_w is the solution concentration, V_w and V_a are the volumes of water and air, respectively; H_c is the dimensionless Henry's law constant for the system temperature; and K_F and n are the Freundlich sorption coefficients. Henry's law constants at experiment temperatures were estimated from a van't Hoff-type equation and coefficients as determined by Gossett [1987]. The sorption coefficients for DCE are taken from Allen-King et al. [1997b], and were not adjusted for temperature.

The observed proportion of mass sorbed was determined from the intercept of rate-law regression, such as shown in Figure 1a. The initial proportion of the total mass sorbed to non-reactive sites determined by calculation and observation are compared in Table 2. Sorption provides an essentially negligible sink for mass at the higher concentrations. In the lower concentration experiments, the largest deviation between the estimated and observed proportions of the total mass is ~5%. This deviation may be attributable to true differences in sorption with varying temperature. Within the context of accounting for the DCE mass in the experimental system, the assumed equilibrium based method provides a reasonably good estimate (e.g. errors from the estimates in the total system are low).

Because the estimated mass sorbed to nonreactive sites varied with concentration over the course of reaction in an experiment vial, the proportion of mass sorbed used to normalize the reaction coefficient was the time-weighted average over the experiment course. For a particular experiment, the proportions of mass in each phase were relatively constant. The average proportion of the mass sorbed ranged from 9.5 to 1.1% in the lowest to highest concentration experiments, respectively (all at 32.5°C). The average proportions of mass in the headspace varied with temperature and ranged between 9.0 and 28.4% for the experiments conducted at varying temperatures.

Table 2. Comparison of the initial proportion of total system mass sorbed to nonreactive sites as determined by calculation and observation.

Initial mass DCE [μmol]	Temperature [C]	Proportion of mass sorbed [%]	
		observed	calculated
Experiments with varying temperature			
0.45	12.3	14.1	9.0
0.46	23.5	9.8	8.4
0.49	32.5	3.6	7.7
0.54	42.6	8.0	7.0
Experiments with varying concentration			
0.49	32.5	3.6	7.7
4.9	32.5	2.8	3.7
49.	32.5	nd	1.8
113	32.5	0.3	1.4
538	32.5	3.0	0.8

nd = sorption not detected

Temperature effect on reaction rate

The reaction rate followed classic Arrhenius behavior over the measured temperature range (12.3-42.6°C) (Figure 2). The activation energy (E_a) is determined as [Lasaga, 1981]:

$$E_a = -R \frac{d \ln k}{d(1/T)} \quad (6)$$

where R is the ideal gas constant and T is absolute temperature.

The activation energy determined for the reaction is 10.5 kcal/mol (95% confidence limits 6.0-15.0 kcal/mol). This value suggests that the reaction is not controlled by diffusive processes in the fluid; activation energies typical of such processes are < 5 kcal/mol [Lasaga, 1981]. The value is substantially lower than the activation energy of 40 kcal/mol which has been determined for vinyl chloride with the same cast iron as that used in this study [Deng et al., 1997].

The results of the experiments show that the reaction rate constant and the half-life approximately double with a 10°C increase in temperature over the environmental concentration range of interest. The half-life for DCE is estimated from the regression line shown in Figure 2 as

$$\ln k_{obs} = \rho_m \ln k_m = -5275 \left(\frac{1}{T} \right) + 16.4 \quad (7)$$

where an average ρ_m of 0.036 g/ml is used for the calculation; and $t_{1/2} = \ln(.5)/-k_{obs}$. Using this approach, the half-lives determined for 10 and 20°C are 187 hr and 99 hr, respectively. The reaction rate constant at 20°C is 1.9 times greater than at 10°C. An important practical implication of this result is that reaction rates and rate constants determined at room temperature (20-25°C) are likely to be about two-fold larger than those which will occur in an *in situ* treatment barrier at typical groundwater temperatures (~10°C).

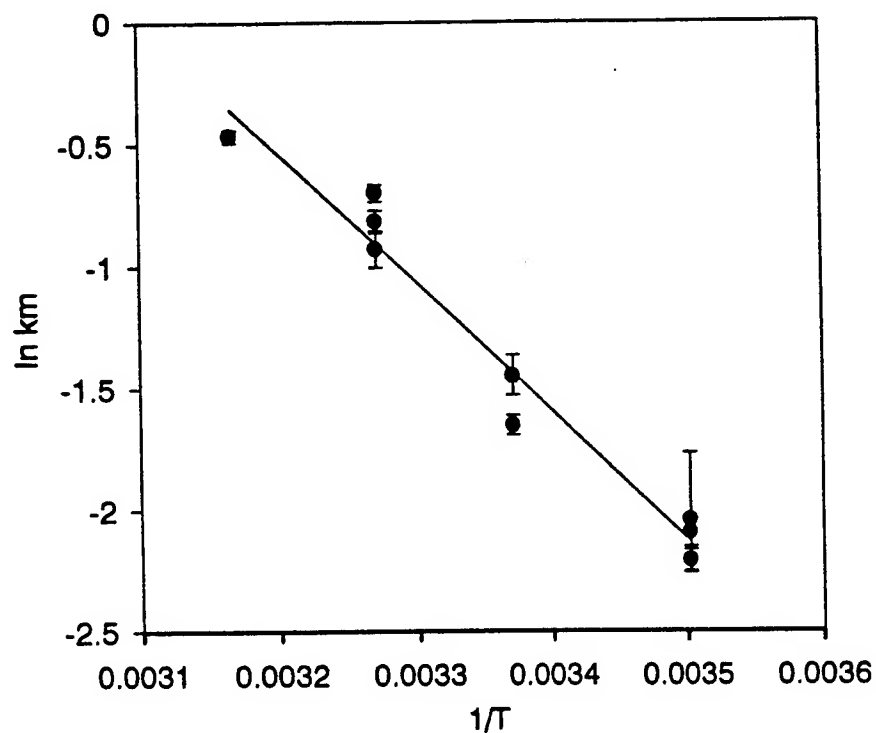


Figure 2. Arrhenius plot of temperature effect on normalized rate constant for DCE (95% confidence intervals are shown by the error bars). The temperature range investigated was 12.3 to 42.6°C. The activation energy estimated from the plot is 10.5 kcal/mol (6.0-15.0 kcal/mol are the 95% confidence intervals).

Concentration effect on reaction rate

The experiments conducted over approximately three orders of magnitude initial concentration show that the pseudo first-order rate constant is dependent on initial concentration, particularly at higher concentrations. The form of the data suggest that reactive site saturation occurs at the higher concentrations (Figure 3). The data were fit using a hyperbolic kinetic model [such as that presented by Johnson et al., 1996, among others], which accounts for surface site saturation,

$$-\frac{d[C]}{dt} = \frac{V_m[C]}{K_{1/2} + [C]} \quad (8)$$

where C is the reactant (DCE); V_m is the maximum reaction rate for the system; and $K_{1/2}$ is the half-saturation constant or solute concentration corresponding to $V_m/2$. The values determined for this experimental system by nonlinear regression of the data (Figure 3) with the residuals weighted by reciprocal rate are 0.0039 $\mu\text{mol/ml-hr}$ and 0.33 $\mu\text{mol/ml}$ for V_m and $K_{1/2}$, respectively.

The hyperbolic kinetic parameter values reported for CTET in an electrolytic iron/water system are $V_m = 0.026 \pm 0.006 \mu\text{M/s}$ and $K_{1/2} = 184 \pm 149 \mu\text{M}$ in a system with 1.02 m^2/l iron [Johnson et al., 1996]. The half-saturation constants are similar for both systems [330 μM in the present study], within the uncertainty given by the parameter fitting. Comparison of the maximum reaction rates requires normalization for the iron concentration in the two systems. The normalized values (V_m/ρ_m) are: $1.5 \times 10^{-3} \mu\text{mol/g-s}$ for CTET, $2.2 \times 10^{-5} \mu\text{mol/g-s}$ for DCE in the current study. The very large difference between these values is probably related in part to the difference in reactive surface areas for the two different irons. Although a surface site saturation effect was observed in both sets of experiments, there is not a common set of parameters which can describe both results.

Up to the current study, the literature describing whether or not concentration affects reaction rate for the chlorinated solvents in iron/water systems has not been consistent. For example, Orth and Gillham [1996] and Allen-King [1997a] have found that the trichloroethene and carbon tetrachloride (CTET) transformation can be modelled using a uniform rate constant over the concentration range tested. In these systems, the estimated solute:iron specific surface area (Fe° SSA) ratios are within the range 0.002-2.2 $\mu\text{mol/m}^2$ (Table 3).

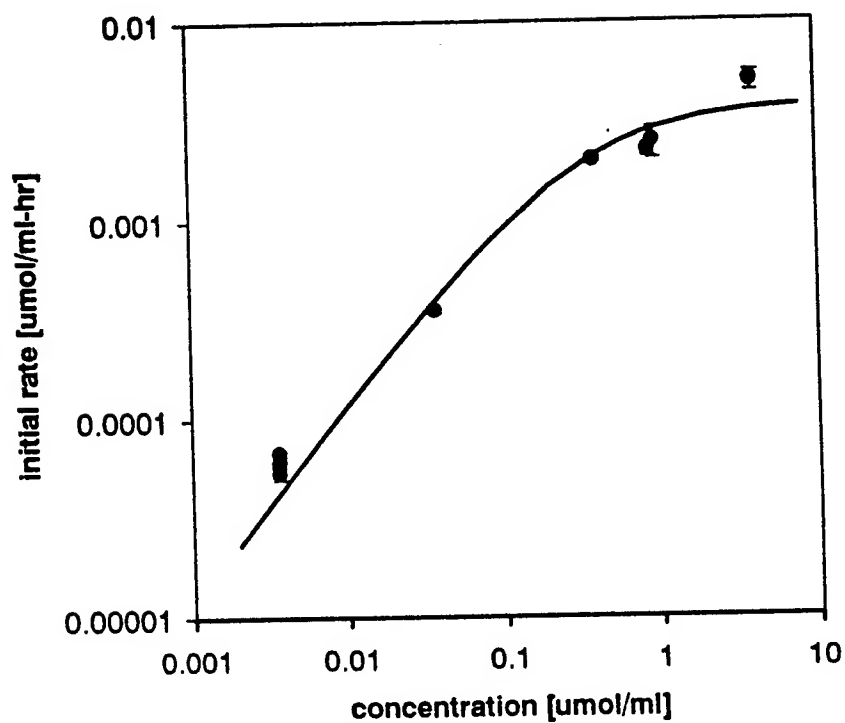


Figure 3. Variation in initial reaction rate over approximately three orders of magnitude variation in initial solute concentration. Solid symbols are observations (95% confidence intervals). The line is a the hyperbolic model fit to the data. The results suggest that reactive surface site saturation occurs at the higher concentrations.

Table 3. Solute mass: Fe⁰ surface area (Fe⁰ SA) estimated for experiments where rates were determined for a range of concentrations.

Compound	Experiment Method	Estimated Solute		Experimental Data
		Mass: Fe ⁰ SSA [*] [μmol/m ²]	Fe ⁰ SSA:H ₂ O [m ² /mL]	
CTET	Batch	20 - 780	0.001	Johnson et al., 1996
cisDCE	Batch	1.6-3.2	1	Allen-King et al., 1997b
CTET	Batch	0.002 - 0.2	0.05	Allen-King et al., 1997a
TCE	Column	0.036 - 2.2	0.21	Orth and Gillham, 1996
transDCE	Batch	1.1	1	Allen-King et al., 1997b
TCE	Batch	1.4	0.31	Burris et al., 1995
PCE	Batch	0.18	0.31	Burris et al., 1995

^{*} Estimated by the author from information provided in the referenced manuscripts.

CTET is carbon tetrachloride; cisDCE is cis-1,2-dichloroethene; transDCE is trans-1,2-dichloroethene; TCE is trichloroethene; PCE is perchloroethene.

Johnson et al. [1996] found that CTET exhibited surface site saturation in their study; the estimated solute:Fe⁰ SSA was approximately 20-780 $\mu\text{mol}/\text{m}^2$, much greater than the ratios used in experiments where no concentration effect was apparent. Allen-King et al. [1997b] also apparently observed a surface saturation effect for *cis*-1,2-dichloroethene at initial solute:Fe⁰ SSA of ~1.6-3.2 $\mu\text{mol}/\text{m}^2$.

The range of DCE:Fe⁰ SSA in the current study was approximately 0.07-80 $\mu\text{mol}/\text{g}$. Over the lower two orders of magnitude in initial solution concentration (corresponding to solute:Fe⁰ SSA of ~0.07-7 $\mu\text{mol}/\text{m}^2$), the normalized pseudo-first order rate constant declined by only 3-fold (from 0.45 to 0.14 $\text{ml}/\text{hr-g}$) with increased concentration. The studies listed in Table 3 which did not exhibit an effect of concentration on reaction rate were conducted with solute: Fe⁰ ratio less than 7 $\mu\text{mol}/\text{m}^2$.

If behavior consistent with site saturation is observed, Burris et al. [1995] reasoned that competition for reaction should occur in a co-contaminant mixture. They [Burris et al., 1995] demonstrated that competition between PCE and TCE for reaction was not observable in systems containing approximately 0.15 and 1.0 $\mu\text{mol}/\text{m}^2$ PCE and TCE respectively. Again, the concentrations selected for the competition test fall within the range which showed little effect of concentration on k_a in the current study.

In the current study, an approximately 4-fold change in k_a was observed over about 1 order of magnitude change in solution concentration at the highest concentrations tested (~7-80 $\mu\text{mol}/\text{m}^2$). This range is comparable to a portion of the solute:Fe⁰ SSA which Johnson et al. [1996] used in their study of CTET transformation, which also exhibited reactive site saturation. The solute:Fe⁰ SSA at this end of the concentration range are very high and are unlikely to occur in a flow-through treatment system. Therefore, the results of this study imply that surface site saturation is not expected to affect most flow-through treatment systems. However, if a complex mixture of contaminants, extremely high concentrations, or low Fe concentrations are used, such that solute:Fe⁰ SSA ratios are very high, surface site saturation should be considered in remediation system design.

REFERENCES

- Allen-King, R.M., D.R. Burris, and J.A. Specht. 1997a. Effect of iron "aging" on reduction kinetics in a batch metallic iron/water system. *213th ACS National Meeting, San Francisco, CA 37, 1 (April 13-17):147-149.*
- Allen-King, R. M., R. M. Halket, and D. R. Burris. 1997b. Reductive transformation and sorption of cis- and trans-1,2-dichloroethene in a metallic iron/water system. *Environ. Toxicol. Chem.* 16:424-429.
- Burris, D. R., T. J. Campbell, and V. S. Manoranjan. 1995. Sorption of trichloroethylene and tetrachloroethylene in a batch reactive metallic iron-water system. *Environ. Sci. Technol.* 29:2850-2855.
- Burris, D.R., R.M. Allen-King, V.S. Manoranjan, T.J. Campbell, G.A. Loraine, and B. Deng. In prep. Chlorinated ethene reduction by cast iron: sorption and mass transfer. In prep. for *J. Environ. Engin.*
- Deng, B., T.J. Campbell, and D.R. Burris. 1997. Kinetics of vinyl chloride reduction by metallic iron in zero-headspace systems. *213th ACS National Meeting, San Francisco, CA 37, 1 (April 13-17):81-83.*
- Campbell, T. J. and D. R. Burris. 1996. Analysis of chlorinated ethene reduction products in vapor/water phase systems by dual-column, single-detector gas chromatography. *Intern. J. Environ. Anal. Chem.* 63:119-126.
- Gillham, R. W. 1995. Resurgence in research concerning organic transformations enhanced by zero-valent metals and potential application in remediation of contaminated groundwater. *209th ACS National Meeting, Anaheim, CA 35, 1 (April 2-7):691-94.*
- Gillham, R. W., and S. F. O'Hannesin. 1994. Enhanced degradation of halogenated aliphatics by zero-valent iron. *Ground Water* 32:958-67.
- Gossett, J.M., 1987. Measurement of Henry's Law constants for C₁ and C₂ chlorinated hydrocarbons. *Environ. Sci. Technol.*, 21:202-208.

- Lasaga, A.C. 1981. Rate laws of chemical reactions. In A.C. Lasaga and R.J. Kirkpatrick (eds.), *Kinetics of Geochemical Processes (Reviews in Mineralogy, Vol. 8)*. Washington, D.C.: Mineralogical Society of America, pp. 1-68.
- Johnson, T. J., M. M. Scherer, and P. G. Tratnyek. 1996. Kinetics of halogenated organic compound degradation by iron metal. *Environ. Sci. Technol.* 30:2634-2640.
- MacDonald, J. A., and M. C. Kavanaugh. 1994. Restoring contaminated groundwater: An achievable goal? *Environ. Sci. Technol.* 28:362-68.
- Mackay, D. M., and J. A. Cherry. 1989. Groundwater contamination: Pump-and-treat remediation. *Environ. Sci. Technol.* 23, 6:630-36.
- Matheson, L. J., and P. G. Tratnyek. 1994. Reductive dechlorination of chlorinated methanes by iron metal. *Environ. Sci. Technol.* 28:2045-53.
- NRC (National Research Council). 1993. *In Situ Bioremediation: When Does it Work?* Washington, D.C.: National Academy Press.
- NRC (National Research Council). 1994. *Alternatives for Groundwater Cleanup*. Washington, D.C.: National Academy Press.
- NRC (National Research Council). 1997. *Innovations in Groundwater and Soil Cleanup*. Washington, D.C.: National Academy Press.
- Orth, W. S. and R. W. Gillham. 1996. Dechlorination of trichloroethene in aqueous solution using Fe^0 . *Environ. Sci. Technol.*, 30:66-71.
- Pankow, J. F., S. Feenstra, J. A. Cherry, and M. C. Ryan. 1996. Dense chlorinated solvents in groundwater: Background and history of the problem. In *Dense Chlorinated Solvents and Other DNAPLs in Groundwater*. J. Pankow, and J. A. Cherry (eds.), 1-52. Portland, OR: Waterloo Press.
- Roberts, A. L., L. A. Totten, W. A. Arnold, D. R. Burris, and T. J. Campbell. 1996. Reductive elimination of chlorinated ethylenes by zero-valent metals. *Environ. Sci. Technol.* 30:2654-2659.

- Sivavec, T. M., and D. P. Horney. 1995. Reductive dechlorination of chlorinated ethenes by iron metal. *209th ACS National Meeting, Anaheim, CA* 35, 1 (April 2-7):695-98.
- US EPA (Environmental Protection Agency). 1987. *Federal Register*, July 8, 1987. Washington, D.C.: U. S. Government Printing Office.
- US EPA (Environmental Protection Agency). 1990. A Guide to Pump and Treat Groundwater Remediation Technology. EPA/540/2-90/018.
- US EPA (Environmental Protection Agency). 1991. *Federal Register*, January 30, 1990. Washington, D.C.: U. S. Government Printing Office.
- Vogel, T. M., C. S. Criddle, and P. L. McCarty. 1987. Transformations of halogenated aliphatic compounds. *Environ. Sci. Technol.* 21:722-36.
- Westrick, J. J. 1990. National surveys of volatile organic compounds in ground and surface waters. In *Significance and Treatment of Volatile Organic Compounds in Water Supplies* N. M. Ram (ed.), 103-25. Chelsea, MI: Lewis.
- Wilson, E. K. 1995. Zero-valent metals provide possible solution to groundwater problems. *Chemical & Engineering News*, July 3, 19-22.

AN ELECTROCHEMILUMINESCENCE DETECTION SYSTEM FOR FLOW INJECTION
ANALYSIS OF CADMIUM

Anthony Andrews
Assistant Professor
Department of Analytical Chemistry

Ohio University
Athens, OH 45701

Final Report for:
Summer Research Extension Program
Armstrong Laboratory

Sponsored by:
Air Force Office of Scientific Research
Bolling Air Force Base
Washington, D.C.

and

Armstrong Laboratory

January 1999

**An Electrochemiluminescence Detection System for
Flow Injection Analysis of Cadmium**

Anthony Andrews
Assistant Professor
Centre for Intelligent Chemical Instrumentation
Ohio University

Abstract

A new flow injection analysis electrochemiluminescence cell has been designed, constructed and evaluated. Evaluation was undertaken by a comparison with an existing reaction from the literature. This new design has been used to generate electrochemiluminescence from cadmium and 1,10-phenanthroline in a flowing aqueous stream for the first time. An interesting ECL and voltage dependence upon pulsing from the pump in the flowing stream was seen and attempts made to eliminate the pulsing.

An Electrochemiluminescence Detection System for Flow Injection Analysis of Cadmium

Introduction

Electrochemiluminescence (ECL) is the generation of light during a chemical reaction with at least one the reagents being generated in situ at the electrode. This has the advantage of added specificity through management of the applied potential. Also, a virtually null background can be obtained by placing the electrode in a light-tight box, furnishing excellent signal-to-noise ratios. ECL reactions involving aqueous metal ions can offer an alternative method for the quantification of dissolved metals.

Our research and development of an electrochemiluminescence detection system for flow injection analysis of cadmium has shown slow yet persistent improvement over the last eighteen months. Initial work centered on improving the design of our existing ECL cell. This effort finally resulted in an overall performance improvement of three orders of magnitude by employing a unique platinum/platinum spiral cell configuration. Using this cell we have been able to replicate an existing method for ECL analysis of codeine in aqueous samples. (1) The calibration graph gave R^2 values of 0.992 for codeine in the lower ppm range when using a 100 μL flow injection loop confirmed the feasibility of the new cell design.

As we continually try new concepts in cell design, our long-term goal is using 1,10-phenanthroline as an ECL reagent for detection of aqueous cadmium ions. The hardware and interface has been developed to add a high resolution, high throughput monochromator to the battery of instrumentation currently in use. This will allow the simultaneous collection of emission spectra during the voltametric scans. Past studies for interferent ions revealed potential selectivity problems (2). The addition of the spectral information could eliminate this problem as well as help elucidate the mechanism of cadmium/1,10-phenanthroline ECL.

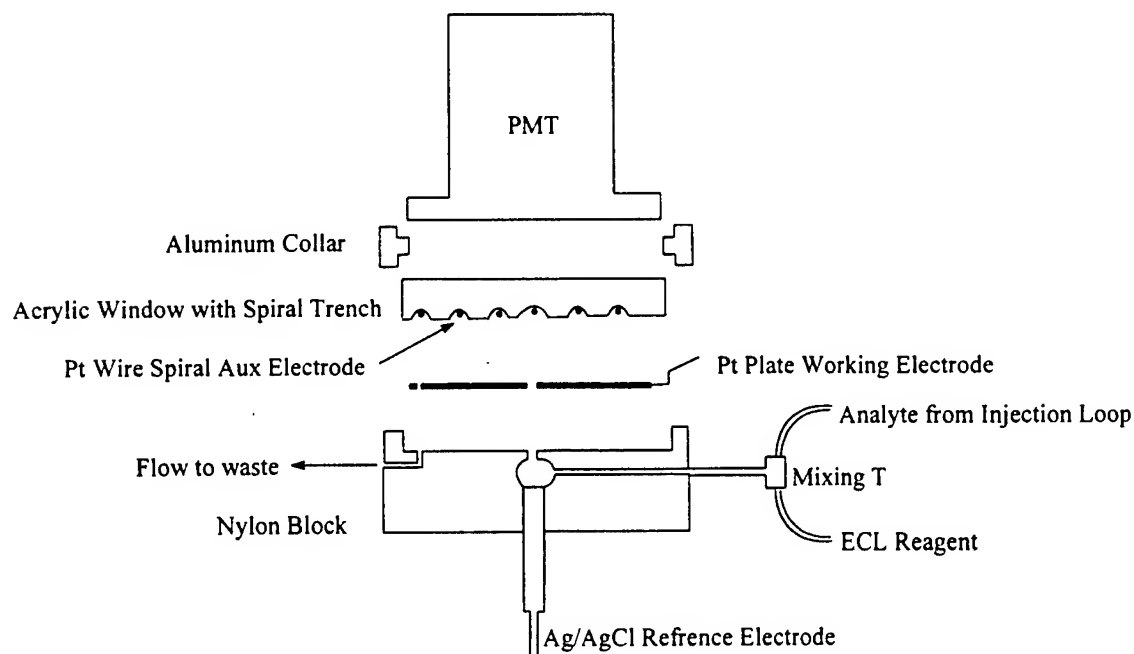
Experimental

The codeine determination developed by Greenway is a well-documented starting point for developing our ECL instrumentation. (1) Using their protocols (0.05 mol L^{-1} acetate buffer, pH 4.0) our initial work involved

improving the physical design of the ECL cell. We experimented with such variables as electrode material, relative positions of the electrodes both in reference to the detector (a Hamamatsu H5920-01 end-on photon counting PMT) and to each other, cell volume, and the shape of the spacer used to define the cell volume. By evaluating these variables one at a time we were able to make generalizations about ideal ECL cell properties. A gold working electrode provided roughly three times better measured emission than platinum for the codeine/Rubpy reaction and orders of magnitude better response than silver or glassy carbon. A platinum tube auxiliary electrode performed considerably better than stainless steel. The larger the working electrode area, the greater the ECL emissions. Smaller cell volumes performed better, but flow problems evolved when the spacer thickness dropped below 0.5 mm. The reaction is confined to the locality of the working electrode, so the working electrode must be in direct view of the PMT.

As our calibration line for codeine dropped into the low ppm range with correlation coefficients up to 0.997 we began using the cell to examine the cadmium/1,10-phenanthroline reaction for cadmium ion determination. The only major difference required was a change in working electrode material. A platinum electrode performed better for the cadmium reaction than gold.

Next, we took all the observations collected to this point and redesigned the cell. Figure 1 give a representation of the final product. The goal was to decrease the cell volume while increasing both the overall electrode areas and the working electrode area in front of the PMT. First we took the cell window material, a thick piece of acetate, and carved a spiral trench from the center out approximately 1 mm deep. Into this we inlaid a piece of platinum wire, below the surface plane of the window. Another piece of platinum was worked into a plate, 17.5 x 32 mm, and polished on one side. A hole was drilled into the cell block and through the center of the Pt plate so that when sandwiched together liquid would flow from the center of the plate outward in the spiral trench to an exit hole. The Pt wire became the auxiliary electrode, the plate the working electrode, and a Ag/AgCl reference electrode was placed in the liquid flow a few mm below the working electrode.



Overall Dimensions: 14 x 5.5 cm.

Figure 1. Design of the platinum/platinum spiral ECL cell. Not to scale.

Finally assembled, we took the new cell and repeated the codeine/Rubpy reaction. In our previous work a gold electrode had provided better responses for this reaction, so we were surprised to find equal or better results with a platinum electrode in this configuration. Figure 2 summarizes the results. The improvement can be explained by the increased working electrode area and the closer proximity of the working electrode. Also to be considered is the far greater time the solutions spend both at the electrode and in view of the PMT due to the spiral path.

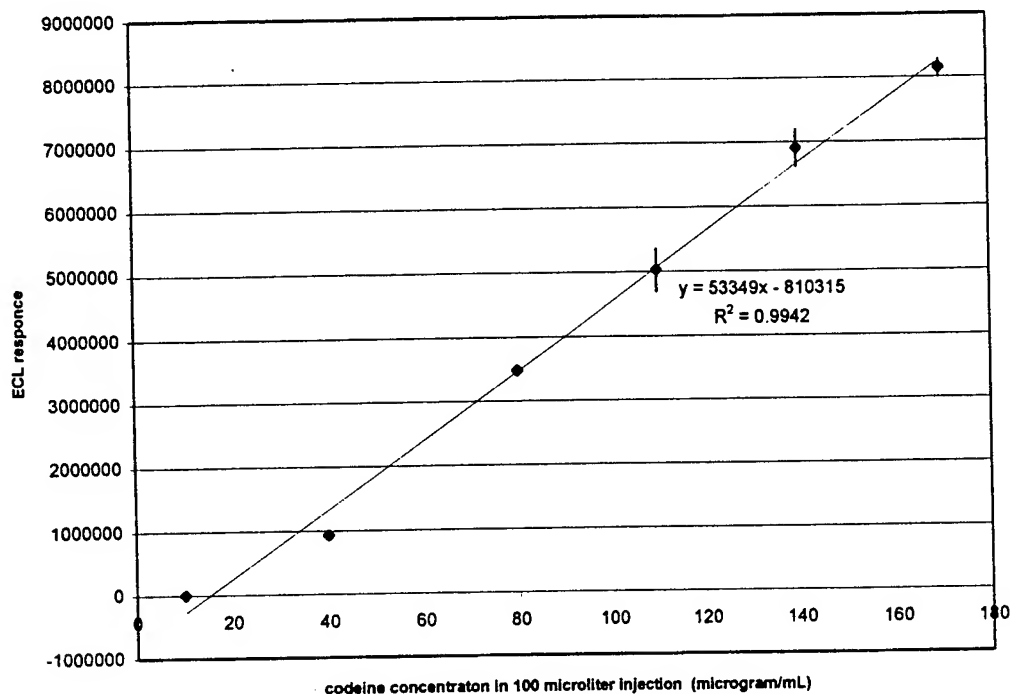


Figure 2. Calibration graph and data for codeine/Rubpy.

Chronoamperometry experiments were undertaken to estimate the effective areas of the new electrodes. This method is based on applying the Cottrell equation

$$I_t(t) = \frac{nFAD^{1/2}c}{(\pi t)^{1/2}}$$

which states that when a species with diffusion coefficient D is oxidized/reduced at an electrode. The resulting current I at time t can be used to calculate the electrode area A , where c is the bulk concentration of the electroactive species, n the number of electrons involved in the process as equivalents per mole, and F the faraday constant. Using a common electroactive material ($K_3Fe(CN)_6$ in 1 M KCl) and triplicate measurements the wire auxiliary electrode was determined to be 0.098 cm^2 and the working electrode to be 0.29 cm^2 . This is roughly ten times the working electrode area compared to the commercially available 2 mm (0.0314 cm^2 calculated, or 0.0321 cm^2 using the same chronoamperometry experiment) electrode used previously.

In the data we were obtaining from each ECL experiment we noticed a pulse consistent in both current, potential, and ECL observed. Further inspection showed that these pulses were synchronized with the roller lift-off

on the peristaltic pump that supplied the system. A simple pulse dampener consisting of a t-piece and a length of silicone tubing was added just before the ECL cell. Figure 3 shows data obtained from codeine injections with and without the pulse dampener. This greatly reduced the cycles observed while increasing the total ECL observed and reduced the deviation between injections from the sample loop.

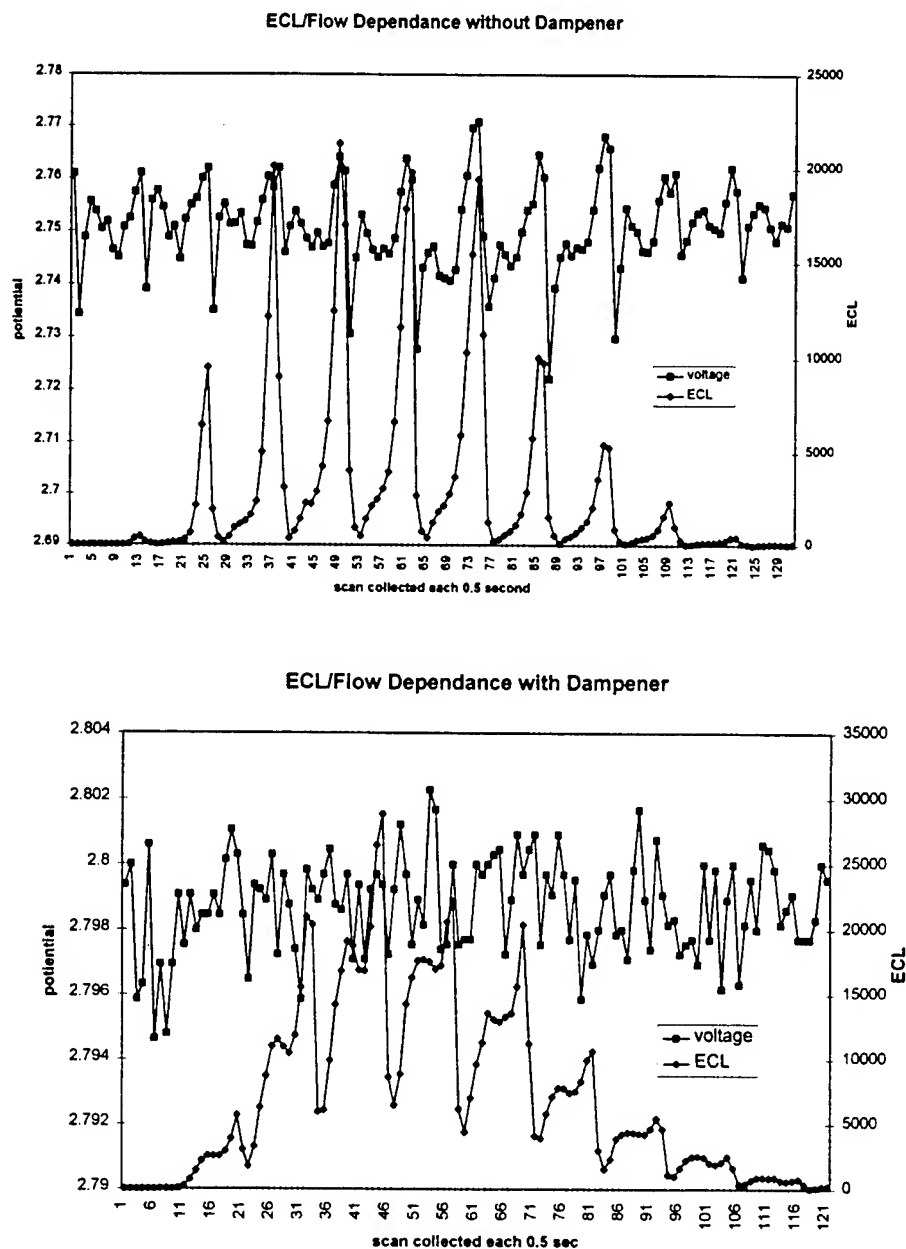


Figure 3. Comparison of pump effects with and without pulse dampener using codeine/Rubpy.

We also observed that the ECL observed is a function of the PMT sampling rate assigned to the computer. The output from the photon counting PMT goes through a National Instruments (CB-58LP) data acquisition board managed by Labview software (Version 4.1, National Instruments). The Labview program designed by our lab for ECL data acquisition includes a register that quantifies ECL emission by counting the pulses from the PMT. Labview reads this register and resets it at a user assigned rate.

We found that available computer power was limiting our detection efficiency by limiting the rate at which we could reliably read the PMT register. The 486 based computer used originally for data collection and potentiostat control struggled at a data rate of 2 sec⁻¹. This became especially problematic when the computer occasionally returned zeros as it failed to maintain the sample rate. This caused problems with quantitation.

This computer was replaced with a new Pentium II based workstation to eliminate the problem. A quick survey of data sampling rates using the new computer was undertaken by measuring the ECL from repeated injections of codeine while varying the sampling rate from 1 sec⁻¹ to 50 sec⁻¹. It was decided to use 5 sec⁻¹ as this rate appears the most efficient by providing a consistent ECL response without producing data sets of unnecessary length.

Conclusion

ECL from cadmium ions and 1,10-phenanthroline has been generated in a flow injection analysis system. A unique cell design has been created and this will open a new approach to ECL observation. The next task is applying it to the full evaluation of the cadmium ECL reactions.

Future Work

In progress is the construction of the interface between the new ECL cell and a high resolution, high throughput monochromator. Once this is completed and the unit placed under computer control we hope to collect emission spectra from the cadmium reaction. This information should prove extremely useful in deducing the reaction mechanism. The differences in the spectra produced when interfering ions are introduced will be explored.

This information could improve the selectivity of our method as well as providing additional information about the cadmium ECL mechanism and possibly other ECL mechanisms if they are shown to interfere.

Ultimately we hope to provide a solid method for determinations of aqueous cadmium that will require little to no sample preparation for sub ppm work. This method will be simple, low maintenance, and cost effective while eliminating the selectivity problems frequented in electrochemical determinations.

References

- 1) Greenway, Gillian M.; Knight, Andrew W.; Knight, Paul J. *Analyst* **1995**, *120*, 2549-2552.
- 2) Taverna, Paul J.; Mayfield, Howard; Andrews, Anthony R.J. *Anal. Chim. Acta* **1998**, *373*, 111-117.

DEVELOPMENT OF PERCEPTION BASED VIDEO COMPRESSION ALGORITHMS
USING RECONFIGURABLE HARDWARE

Jer-Sen Chen
Research Assistant Professor
Department of Computer Science

Wright State University
Dayton, OH 45435

Final Report for:
Summer Research Extension Program
Armstrong Laboratory

Sponsored by:
Air Force Office of Scientific Research
Bolling Air Force Base
Washington, D.C.

and

Armstrong Laboratory

December 1997

DEVELOPMENT OF PERCEPTION BASED VIDEO COMPRESSION ALGORITHMS USING RECONFIGURABLE HARDWARE

Jer-Sen Chen
Research Assistant Professor
Department of Computer Science and Engineering
Wright State University

Abstract

As new millennium approaches, the processor speed is breaking the one billion cycles per second clock speed. The increase in processor speed and storage capacity popularizes multimedia applications on computers. The bandwidth, however, is still a major bottleneck when delivering multimedia information. The need for data compression remains essential with all the advances of computing technologies. This report deals with lossy image/video compression, that is, information can not be recovered exactly at bit level when coded information is decoded. The goal of most multimedia compression techniques, video or audio, aims at achieving perceptual losslessness such that human eyes or ears can not distinguish the difference between the original and reconstructed data.

This report discusses rate-distortion issues in perception based video compression. It employs video streams characterized by the exponent of $1/f^e$ like noises, where e is the exponent controlling spectral distribution. The exponent e ranges from 0 for white noise, to 2 for Brownian motion. The exponent used to control spectral distribution and entropy rate is homogeneous across time and space for simplicity for analysis. Various video streams controlled by the exponent are employed for subjective rate-distortion analysis and discussion on objective measurement is also presented. The second part of the report details design and experimentation of hardware acceleration, in particular, using reconfigurable Field Programmable Gate Arrays (FPGAs). Design and experimentation using FPGAs on motion matching portion of MPEG encoder is presented. The use of FPGA provides flexibility of computing resource partition and fine grain acceleration of multiprocessing.

DEVELOPMENT OF PERCEPTION BASED VIDEO COMPRESSION ALGORITHMS USING RECONFIGURABLE HARDWARE

Jer-Sen Chen

Introduction

Advances in computing technology enable information content evolving from tradition simple text to multimedia presentation. The increase in both processing speed and data transfer rate could not overcome the greater demand of sophisticated multimedia content. The advances in processor speed and storage capacity popularizes multimedia applications on computers. The bandwidth, however, is still a major bottleneck when delivering multimedia information. The need for data compression remains essential with all the advances of computing technologies. Among different types of media, digital video consumes more storage space and communication bandwidth than other types such as text and audio. For example, a typical video stream at 640x480 pixels of resolution without any compression aid can result in more than 221 million bits per second if it runs at 30 frames per second and 24 bits per pixel true color mode. Even with current technology, especially the communication bandwidth, some form of compression is still very much in need.

A data stream consists of typically both entropy and redundancy. Entropy is the information content while redundancy is the part can be removed without loss of information. Lossless compression techniques are commonly used for text data files where exact bit level recovery is required. Lossless compression, and other compression techniques in general, are sensitive to noise and extra redundant information is needed to increase the integrity of the coding schemes during transmission.

Lossy compression techniques, usually applied to audio or video signals, can not recover exact bit level information. They are in general designed to exploit human perceptual capability such that losslessness can be achieved in terms of human perception. For example, coders and decoders are commonly designed to tolerate higher degree of distortion at frequency range where audio or video perception is much less sensitive. On the other hand, high fidelity is maintained at frequency range where perceptual sensitivity is high.

As video becomes an essential multimedia component, computers are now equipped with real time video processing capability. JPEG compression is a symmetric technique that the coder requires about same computational complexity as the decoder. MPEG compression inherits, in particular the intraframe encoding portion, substantial portion of JPEG compression components such as DCT and entropy coding. The interframe coding which employs motion compensation, however, creates asymmetry between coder and decoder.

Real time requirement for the decoder of MPEG on a personal computer with hardware acceleration on a video board is becoming popular these days. Encoding a raw video signal into a MPEG stream still requires special hardware to achieve real time performance. In other more complicated video compression techniques, even when real time can not be achieved, researchers can still take advantage of hardware acceleration to reduce time to develop research prototype or to derive experimental results.

Review of Image Compression Techniques

Image compression techniques usually explore spatial coherence of pixel data, that is, most pixels in the nearby area share common color values except at object boundaries. Redundancy occurs where individual pixel is coded among homogeneous region where pixel values are similar. To explore and remove redundancy in an image, simple spatial form of differentiation can be employed such as Adaptive Differential Pulse Code Modulation (ADPCM) or Run Length Encoding (RLE). A more sophisticated scheme can explore the coherence in the frequency domain such as Discrete Cosine Transformation (DCT) used in JPEG, or subband coding and wavelets.

JPEG

By far the most popular image compression scheme for photographs is the one proposed by Joint Photographic Expert Group (JPEG). Its algorithmic simplicity as well as its outstanding quality performance helps gain its popularity. The algorithm consists of, after decomposing the original image into eight by eight blocks, a Discrete Cosine transformation (DCT), a quantizer, and variable length encoding scheme such as Huffman codes. The decoding is exactly the reverse and

makes JPEG a highly symmetric scheme, that is, compression and decompression take approximately same amount of computational cost.

The outstanding performance of JPEG compression is measured not only objectively but also subjectively. Discrete cosine transformation has long been recognized as almost optimal as KLT. It produces very high objective measurement such as signal to noise ratio (SNR). Also because its periodicity tapers off at boundaries, the artifact of blockiness is less pronounced compared to other transformation such as Discrete Fourier Transformation (DFT). Blockiness is always the most noticeable artifact in most block based compression schemes at low bit rate.

The design of quantization matrix contributes to another degree of subjective performance improvement in JPEG compression. After transformation, each DCT coefficient is divided (quantized) by the corresponding coefficient in the 8x8 quantization matrix. Therefore the larger the quantization coefficient, the more likely the DCT coefficient is quantized to zero. The quantization matrix is designed to account for human visual perception, such as low contrast sensitivity at high spatial frequencies. The numbers in the quantization matrix therefore, in general, increase from upper left to lower right though not strictly monotonic. Many researchers have been studying the relevance of the DCT quantization coefficients to human vision [Kline92, Watson94, Solomon94].

Wavelets and Subband Coding

Another class of image compression scheme decomposes original spatial data into different frequency band and orientation. The wavelet transformation decomposes visual information by scale or resolution, where maintain the locality at each scale. Quadrature mirror filters (QMFs) are usually used in subband encoding, followed by a subsampling process. Since each frequency band takes only a fraction of the whole spectrum (within Nyquist limit), down sampling can be employed before source encoding is applied. Because human visual system appears to employ multiscale processing in nature, applying multiresolution decomposition such as wavelet transform makes sense from perceptual point of view. Efficient algorithms for computing wavelet transformation help establishing subband coding as one of the major contender in image compression. [Mallat89, Adelson87]

Similar to transform coding, wavelet image coding consists of three steps, namely transformation, quantization, and entropy encoding. As in JPEG compression, the lossy part of the processing is the quantization where quality trades off bit rate. The decoding process is also similar to JPEG, just inverses the encoding processing steps. Both encoding and decoding process in wavelet compression are symmetric, that is they require approximately same amount of computational cost.

Fractal Image Compression

Fractal geometry is usually used in describing nature. Using fractal transforms to achieve image compression can be attributed largely by Michael Barnsley [Barnsley93]. The images to be encoded are usually quite different from mathematical fractals. The self-similarities are only explored in the local sense [Fisher95], that is, from one local part of the image to another local part of the same image to be encoded.

Fractal image compression scheme, however, is highly asymmetric. That is, the coding stage is extremely computational expensive while the decoding processing costs very little. The asymmetry results from the need for exploration of self-similar structure within the image to achieve higher compression ratio. The self-similarity is usually translated into a matching or mapping process between the domain and the range, which are different partitions of the same input image.

Model and Feature Based compression

Model based coding can be best illustrated in human speech data compression. Consider at transmitting end, the human voice goes through a speech recognition engine where textual information is extracted and sent to the receiving end where a text-to-speech synthesizer can reproduce the information in human voice. The transmission of textual data instead of speech waveforms greatly reduces bandwidth or storage requirement. The idea behind the model based coding approach is to represent the scene content with a predefined model. For instance, for video telephone application, human facial models as well as animation dynamics of facial movement can be used for model based compression. Different applications may require different models.

Models can be two dimensional image based or three dimensional geometry based. For instance in the facial animation used in the video phone, two dimensional features such as contours and region can be used. Video sequences are usually encoded as contour or region change in both shape and position.

Three dimensional approaches, on the other hand, use full parameterized geometry models. The object geometry can be described using wire frame polygonal model, or parameterized using feature points of the model. Detection and recovery of model features using video camera is a very difficult problem and has been long researched in the image understanding research community. Some artificial constraints had been proposed to alleviate the difficulty in solving inverse problem, such as adding marking on the model or impose initial positional constraint on the model. These simplifications suffer the loss of naturalness in the practical operational environment.

Entropy, Perceptual Information, and Distortion

Root mean square error measure in general correlates well with human perceived difference between original image and compressed image. But counter examples can be easily devised that, in certain cases, same amount of RMSE actually translates into quite different perceived distortion [Daly93]. Alternative error measures can be utilized in designing an image compression technique to account for factors that are more closely related to factors human visual perception such as contrast sensitivity function and masking effect.

Contrast sensitivity, reciprocal of contrast threshold, is a function of spatial frequency. Noise or distortion arises from lossy image compression below the contrast threshold can be treated as visually lossless. JPEG compression takes into consideration of human visual perception in terms of non-uniform weights in DCT quantization matrix. Different coefficients in the matrix are assigned to reflect different spatial frequency component weighting. The asymmetry of the matrix also reflects different spatial responses in horizontal and vertical orientation at same spatial frequency.

Weighted error measure in the frequency or transformed domain can also be designed to account for contrast sensitivity function in other compression scheme. Improvements in image quality was reported by applying weighted DCT domain error measure to fractal compression [Chen95] though it introduced additional computational complexity to already intensive algorithm. An error measure instead of RMSE in the transformed domain, say discrete cosine transformation, is used to account for the dependency of human contrast sensitivity to spatial frequency. In particular, a weighted square error measure in the transformed domain such as DCT. The weights can be chosen as the quantization matrix recommended by JPEG committee.

Improvements can also be made in visual performance by incorporating domain knowledge [Gray93]. For instance, intensity weighted compression can be used in medical imaging such as X-ray or MRI, as well as infrared thermal imaging. In such imagery, the high intensity areas signify important events and therefore are assigned with higher weights. Manually marked area of interest can also be used to assign weights to error measure. Notice that these techniques do not depend on viewing conditions, such as pixels per degree to reflect dependency of visual perception on spatial frequency.

Rate Distortion Theory

Rate-distortion theory has long been used, for lossy compression, to quantify trade-off between bit rate and quality. The higher the bit rate or the bandwidth, we get lower distortion which translates into better quality. Other the other hand, when imposed by limited bandwidth requirement, low bit rate encoding must be employed and distortion and degradation of image and video fidelity results. Rate-distortion based video compression aims at establishing a general theory for optimal encoding.

We often here about some compressor can achieve a compression ratio of certain orders of magnitude. We then ask what is the distortion and what is the resolution of the imagery. We also question the content of the imagery. Rate-distortion in image or video compression can be commonly found when researchers compares and plots root-mean-square-error (RMSE) against bit rate in terms of bits-per-pixel. Is RMSE a good quality metric? Is bits-per-pixel general enough to account for resolution dependency?

Peak signal-to-noise ratio (PSNR) , alternatively, is defined as:

$$\text{PSNR} = 20 * \log (255 / \text{RMSE})$$

which measures the quality in terms of decibels (dB). Note that 255 is used here for brightest possible value of an 8-bit gray scale imagery. Using the above definition, it can be easily derived that each reduction of one bit per pixel, under uniform transformation, 6 dB of PSNR is reduced. This can be found in reported image or video compression literature.

The other factor in rate-distortion curve is the source information rate, or equivalently the entropy. High information content requires higher bandwidth to achieve same distortion performance, be it RMSE or PSNR. We use, in our experimentation, $1/f^e$ noise and control the information rate by varying the exponent e . When e is zero, we get white noise and the entropy is maximized. As we increase the exponent e from 0 to 2.0, the source information rate decreases in which the image appears “smoother” or not as noisy. Figure 1 shows three different $1/f^e$ noise images with exponent of 0.5, 1.0, and 1.5 respectively.

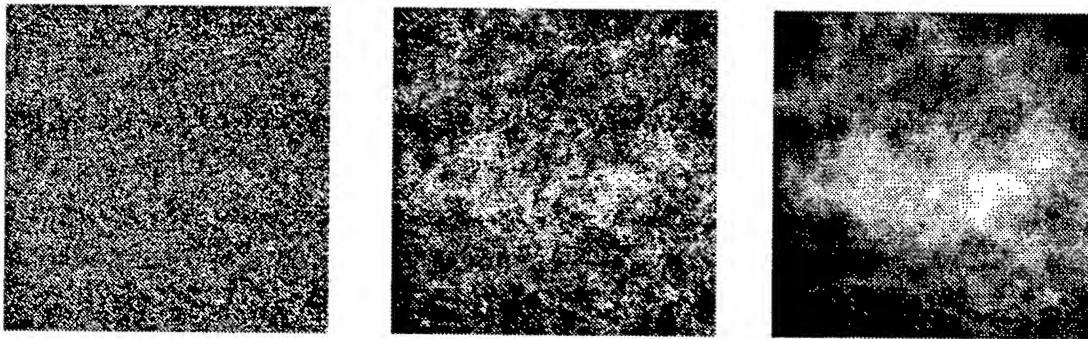


Figure 1: Various $1/f$ noises with spatial exponent of 0.5 (left), 1.0 (middle), and 1.5 (right)

High exponent translates into low information rate and require lower number of bits to achieve same PSNR or RMSE. The same principle applies to video signals. As the exponent increases, the require bandwidth, in terms of bits per second, decreases when certain performance threshold is set, be it subjectively or objectively. Figure 2 show MPEG encoding of various $1/f$ noise video streams with exponents ranging from 0.5 to 2.0. The spatial resolution of the video stream is 256x256. The x-axis is the bit rate in terms of bits per pixels and y-axis is PSNR. The exponent of the curve on the upper leftmost side of the graph is 2.0, and gradually decrease to lower right corner of exponent of 0.5. The exponent range of 0 to 0.5 was not shown on the graph because of

the curves are too close to each other. On each individual curve at a fixed value of exponent, the 6dB per bit-per-pixel rule of thumb follows. From the figure we conclude that, given source information rate of the video stream, we can predict the trade-off between the quality in terms of PSNR and the bit rate in terms of bits-per-pixel.

The spatial and temporal exponents can be set independently to account for different degrees of correlation. For simplicity, our test video streams were generated using same exponent value along both space and time. The video streams were generated using midpoint displacement algorithm generalized from [Peitgen88]. For non-uniform spatial-temporal exponent, frequency synthesis approach should be used for avoiding artifacts. Though computationally much more expensive than midpoint displacement approach. Sufficiency of characterization of video streams by the exponent of the $1/f$ noise model remains a research problem.

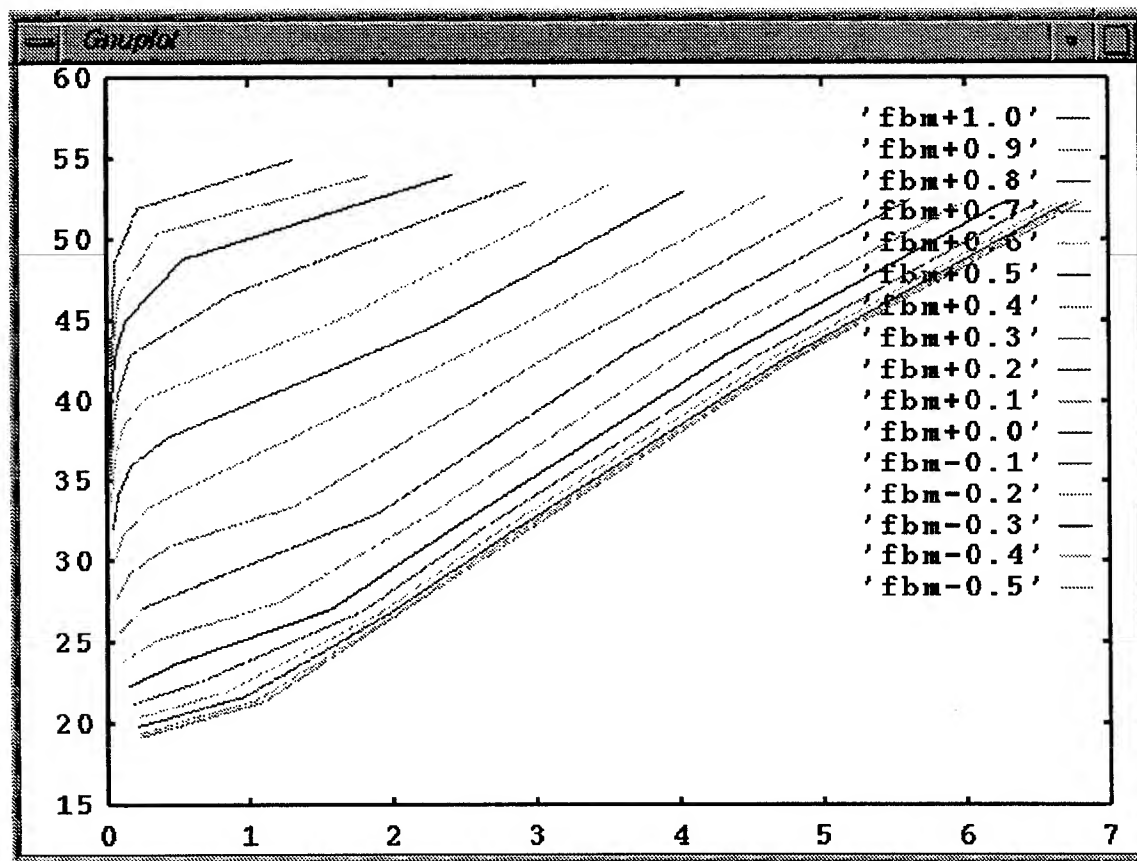


Figure 2: PSNR of $1/f$ noises with various exponents using MPEG encoding

Subjective Versus Objective Quality

Subjective quality measures, such as root-mean-square-error (RMSE) or peak-signal-to-noise-ratio (PSNR), were usually design for both practicality and analytical ease. To capture the fidelity of a compressed image or video stream, RMSE is usually used for analytical simplicity. Since image or video data is usually meant for human viewing, a good subjective quality measure that quantifies perceptual discrepancy has to been carefully designed. Unfortunately, as researchers agree that human vision is a very hard and complicated subject, so is the derivation of such objective quality measures.

RMSE and PSNR have been popularly used in image and video compression research community since, in most cased, they capture the perceptual quality of the reconstructed image or video. But researchers, especially in vision science community, have also devised various examples that illustrate the inappropriateness of RMSE measure. That is, they demonstrate in some cases that lower RMSE images could exhibit more noticeable artifacts than those with higher RMSE.

Most of the objective quality research on image and video compression has reported performance curve similar to figure3. Figure 3 shows both subjective quality measurement using PSNR on one side and some objective quality score on the other side while horizontal axis shows the bit rate in bits per pixel. Following the rule of thumb of 6 dB per bit-per-pixel, the subjective measurement exhibits almost linearly except at very low bit rate range. On the other hand, using objective score against bit-per-pixel, the curve is highly non-linear.

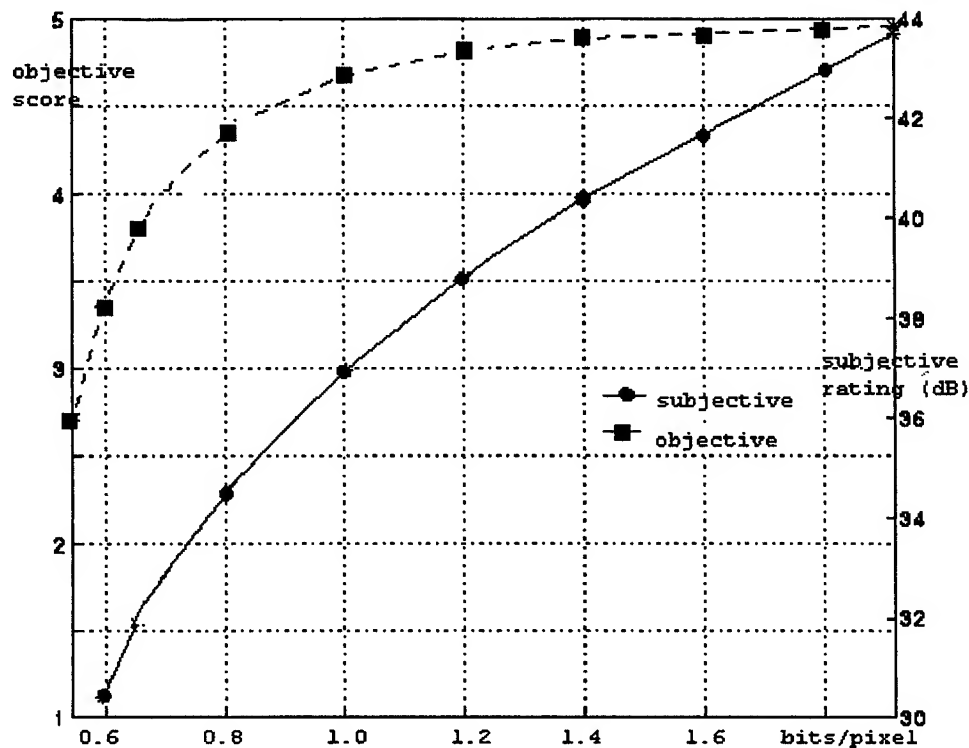


Figure 3: Subjective versus objective quality measures at different bit rates

Video Compression Techniques

The spatial acuity of human visual system depends on retinal image velocity as well as spatial frequency content of the scene. Temporal integration time of the visual system limits the temporal bandwidth. The reduction of spatial acuity in the presence of motion is usually interpreted using a rectangular "window of visibility" [Watson86] in two dimensional spatial-temporal frequency response. It has also been used to account for study of some artifacts caused by mismatch between the scene update rate and display refresh rate [Chen93].

The Nyquist sampling rate to avoid aliasing is at least twice the maximum of the signal frequency. In the temporal domain, the aliasing is usually observed in the presence of fast moving objects. A typical anti-aliasing technique involves certain degree of smoothing or averaging, either pre-sampling or post-sampling. And a typical approach for temporal anti-aliasing is using motion blur

algorithm [Potmesil83]. When a camera films a fast moving object, motion blur is generated through the integration process during the time period when the shutter is open.

Still image compression techniques discussed in the previous section can mostly be extended to compression video signals with generalization of two dimensional processing to three dimensions adding the time dimension. This extension, of course, adds great deal of computational complexity to the encoding-decoding process. To reduce the complexity so that reasonable frame rate can be achieved, one can process video signals as collection of independent images and process each frame independently. Without exploring temporal coherence in video signals, very limited compression ratio can be achieved under normal quality requirement.

Wavelet or subband coding can be directly extend to video compression, either by using a three-dimensional subband decomposition or simply by processing video sequence frame by frame individually. Adaptive bit allocation involving the additional dimension, namely the temporal dimension, is a very difficult optimization problem. Perceptual optimization presents even a greater degree of difficulty. Bit allocation can based on energy and/or motion fidelity. Adaptive exchange of spatial and temporal resolution can also be used [Podilchuk90,Podilchuk91]. Similarly, fractal compression of video signals can either be done by matching three dimensional spatial-temporal blocks, or simply by matching two dimensional spatial blocks across the video sequence. Matching directly using three dimensional blocks increases computational cost tremendously and renders itself unfeasible even with current hardware technology.

MPEG explorer temporal coherence through motion compensation [Hang95]. Current frame is first predicted or interpolated from adjacent frames to remove redundancy. Residues after interpolation requires few number of bits to encode and therefore achieve compression. MPEG is asymmetrical because, on the encoding part, it requires very high amount of computation to explore temporal redundancy through motion compensation. Current processor speed of new personal computers can achieve MPEG decoding in almost real time without addition hardware acceleration. Encoding, on the other hand, does impose additional hardware acceleration to capture video streams 30 frames per second at 640 by 480 resolution. We are exploring, in the next section, hardware acceleration using reconfigurable FPGAs on the motion compensation portion of the MPEG encoder.

Reconfigurable Hardware for Video Compression

When designing a video compression hardware, we need to take into account computing part as well as memory requirements, and the interconnection between all modules. The computing part can be improved by both algorithmic optimization and multiprocessing. Fine grain parallelism is commonly used in image or video processing. The memory requirements are influenced by the multiple access of original data and intermediate results. The interconnect network bandwidth depends on how frequent computing part communicates with memory modules.

Programmable hardware or multiprocessor systems are desirable for studying perception based video compression techniques. Digital signal processing (DSP) chips can be used to speed up well defined functionality such as DCT, wavelet transform, and even motion estimation. They can be used to facilitate human vision related study if the required processing is straightforward such as varying DCT quantization matrix to account for contrast sensitivity and masking effect. Field programmable gate array (FPGA) [Xilinx94] chips, however, can be used when greater flexibility is required for studying various types of vision based video compression performance.

Popular DSP chips such as TMS320C80 from Texas Instruments [Beinart94] consist of 4 DSP and 1 master RISC on-chip processors. With 50 MHz clock frequency that delivers over two billion RISC-like operations per second and I/O data rate of 400 million bytes per second, MPEG compression can be implemented using one or more TMS320C80 to achieve real time requirements. DSP chips provide ideal building blocks for a wide range of study in human perception based video compression techniques, including discrete cosine transformation, motion estimation, and wavelet and subband coding.

Field Programmable Gate Arrays (FPGAs)

FPGA chips, on the other hand, provide flexibility at the expense of operative sophistication. Rapid advancements in FPGA technology have already push new FPGAs with more than 40,000 gates that can run at speeds of more than 50 MHz. Mapping video compression algorithms onto hardware architecture may be too complicated or expensive to be optimized or sometimes just to

be correct. Some researchers have started applying FPGA chips in real time video compression techniques [Schoner95].

We are using a G900 printed circuit board supplied by Giga Operations [Gigaop94, Gigaop97] which is a PCI bus based board that is compatible with Pentium PCs running under Windows NT workstation. The board as shown in figure 4 is a full length card that, depending on the number of computing modules configured, can cover other expansion slots. The G900 as configured for this project uses one PCI slot and covers two additional expansion slots (1 PCI and 1 ISA). This could be a problem in systems that have many expansion boards. The G900 provides power and signal routing for the XMODS that plug directly into the G900. XMODS connect to the MCON_n sockets. The board can accommodate four XMODS. XMODS have additional sockets (HUCON/YUCON), so that a total of four XMODS may be stacked on each MCON_n socket for a maximum of sixteen XMODS configured in one G900 board.

The XMODS and onboard FPGAs are connected together by the XBUS which is a 128 bit programmable bus XBUS signals are routed to the XCON_n and YCON_n connectors and can be used for debugging or interfacing to other G900/custom interface boards. There are two onboard FPGAs. The PPGA (Xilinx XC4013E-2) controls communication between host and XMODS. The CPGA (Xilinx XC5210-5) implements clock generation, runtime configuration and power up functions. While the FPGAs can run at clock rates up to 66Mhz, the G900 board and host interface is currently limited to 16Mhz.

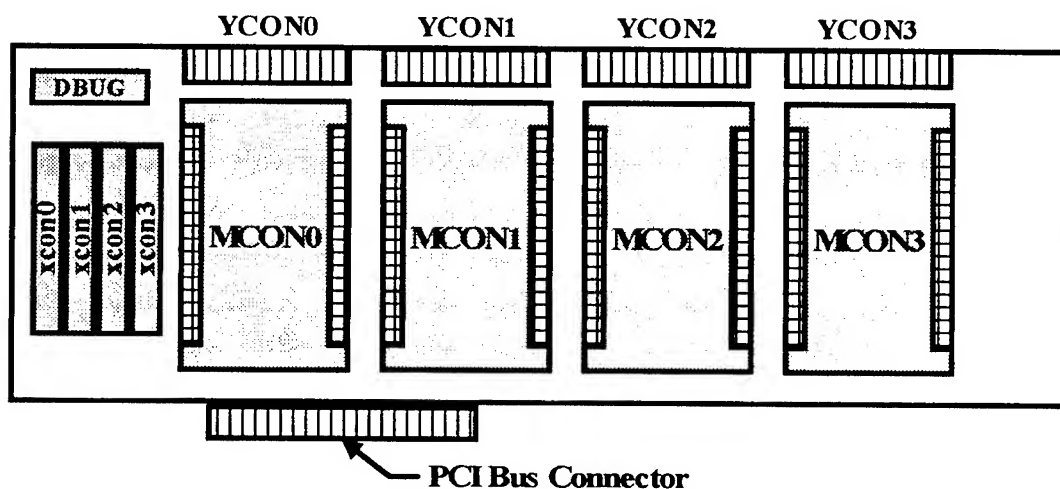


Figure 4: G900 Reconfigurable FPGA board

The MPEG2 encoder that is available from MPEG Software Simulation Group is approximately 250KB of source code. To determine function candidates for mapping into the FPGAs, the Visual C++ Profiler was run on a test video sequence named random. The test case is 27 frames (320x240 pixels) of tumbling dice shown in figure 5. The total execution time to encode random is about 46.5 seconds. Approximately 49% of the total execution time is attributed to the block difference calculation function of the motion estimation for the reduction of temporal redundancy.

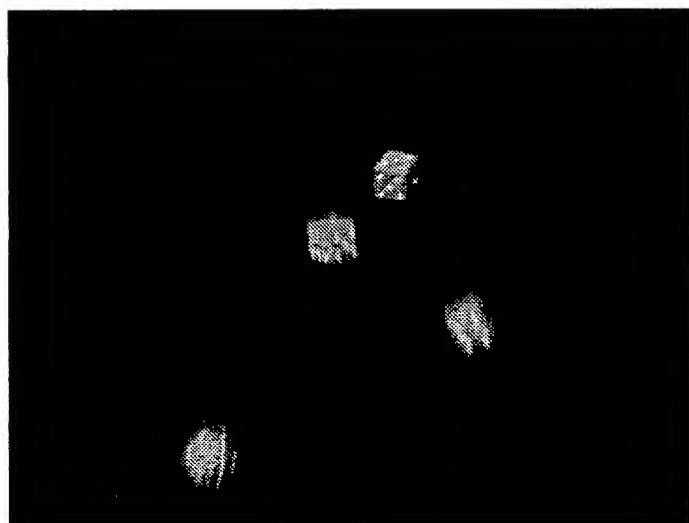


Figure 5: One frame of tumbling dice video

To encode random requires 464,565 (8×16) and 200,787 (16×16) forward macroblock calculations and also 235,015 (8×16) and 98,194 (16×16) backward macroblock calculations. This requires a total time of 9.9 seconds ($699,580 \times 8.1\text{ms} + 298,981 \times 14\text{ms}$). There is an additional 1,483,200 writes in copying the target macroblocks to the FPGAs and 1,105,920 writes to copy the forward/backward prediction frames to FPGA's SRAM. This costs another 1.0 seconds ($1.483 / 1.5$) and .7 seconds ($1.105 / 1.5$). Total I/O time is 1.7 seconds. Total execution time in the XMOD is 11.6 seconds. From design two, the Pentium requires 12.0 seconds to perform the forward calculation. Using the same analysis as in design two, the backward motion compensation prediction requires 4.4 million macroblock row calculations. This is 6.1 ($4.4 / .725$) seconds of the elapsed time. The forward and backward motion estimation requires 18.1 seconds of execution time. So the expectation was a runtime of 40.0 ($46.5 - (18.1 - 11.6)$) seconds. The actual measured runtime was 39.8 seconds.

With two XMODS running in parallel the expectation was that the computation time should be cut in half. The expected execution time was 34.2 ($46.5 - (18.1 - 5.8)$). The measured execution time was 34.5. With eight XMODS running difference calculations in parallel, execution time was reduced to 30.9 seconds which is about 34% improvement. The computation time was reduced to 2.5 seconds ($30.9 - (46.5 - 18.1)$). This is 7.2 times ($18.1 / 2.5$) improvement in the computation of the sum of the difference calculation. Again, since the calculations are performed in the same order as the original encoder the encoded files produced by this design are identical to those produced by the original encoder.

The random sequence of video frames has a background that is fairly constant. The motion estimation algorithm doesn't need to search as much as it might if the background was changing in every frame. Another video sequence called Pan (sample frame shown in figure 7) is 30 frames of 320 x 240 video with the background constantly changing. The frames were encoded using design four. The one XMOD case resulted in a large increase in execution time over the original encoder. This is caused by the fact that the original encoder can preempt the distance calculation if at the end of a macroblock row the sum of the differences exceeds the best calculation so far in the search. The XMOD based encoder can only preempt the search when the sum of the differences is zero. It must calculate the sum of the differences for the entire macroblock.

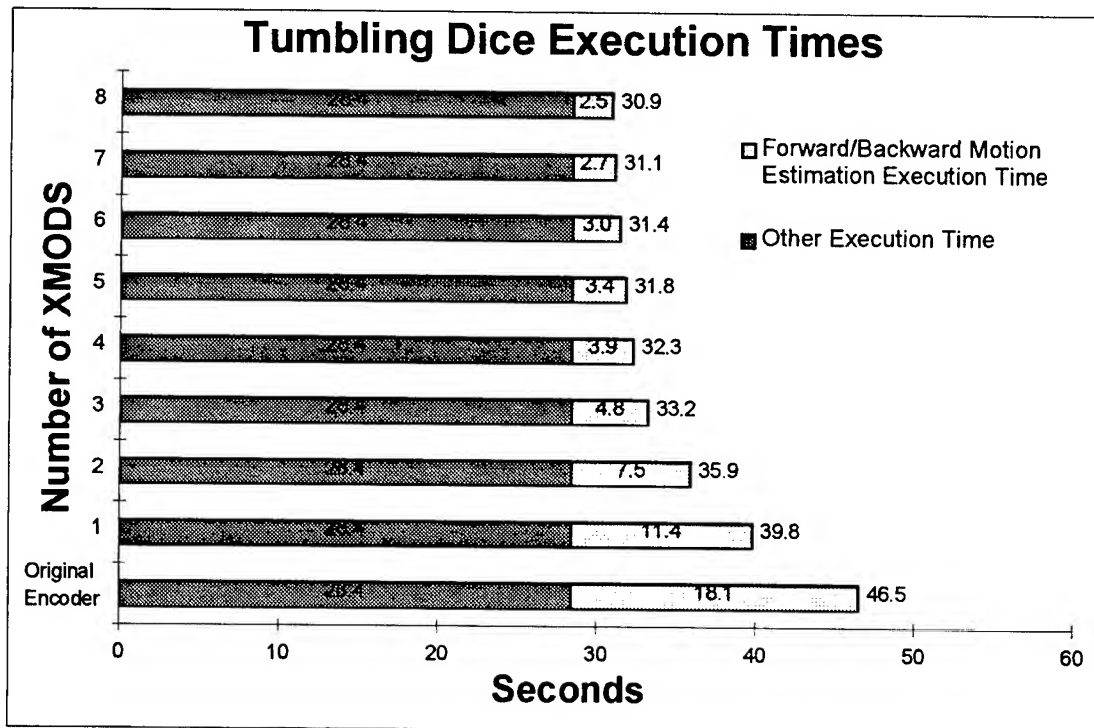


Figure 6: FPGA encoding performance of tumbling dice sequence

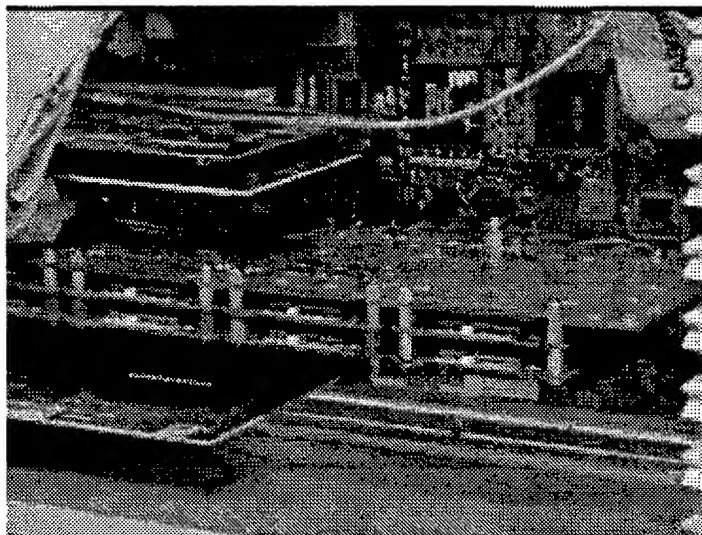


Figure 7: Sample image from Pan sequence

Measurements were collected to verify the one XMOD case. Pan requires 30.6 million macroblock row calculations for a computation time of 42.2 seconds ($30.6 / .725$). The XMOD encoder calculates 4.95 million 8×16 and 2.62 million 16×16 macroblock distances. The XMOD computation time is 76.8 seconds ($4.95M \times 8.1ms + 2.62M \times 14ms$). There is an additional 1.98 million writes in copying the target macroblocks to the FPGAs and 1.23 million writes to copy the forward/backward prediction frames to FPGA's SRAM. This costs another 1.3 seconds ($1.98 / 1.5$) and .8 seconds ($1.23 / 1.5$). Total I/O time is 2.1 seconds. Total execution time in the XMOD is 78.9 seconds. The expected execution time is 122.0 seconds ($85.3 + 78.9 - 42.2$). This is very close to the 122.6 measured elapsed time. Additional XMODS had a dramatic effect on elapsed time. With eight XMODS calculating the distances, elapsed time was 52.5 seconds which is 38.5% improvement over the original encoder. The eight XMOD case has reduced the 42.2 seconds of distance computation to 9.4 seconds ($52.5 - (85.3 - 42.2)$). This is 4.5 times improvement in computation time. Clearly encoder execution times are tied to the motion in the video frames.

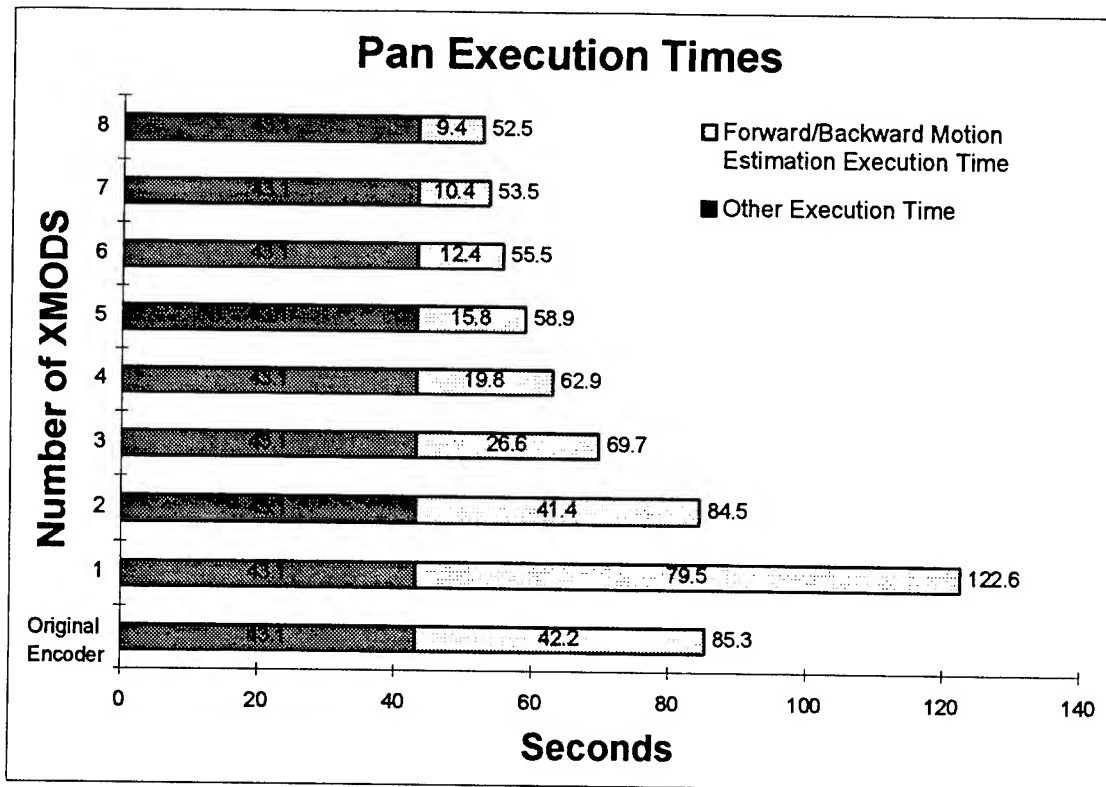


Figure 8: FPGA encoding performance of Pan sequence

Conclusions

Importance of video compression can never be overstated. While computing technology and storage capacity are evolving faster everyday, data compression provides additional dimension of breathing room for bandwidth hunger. Perceptual measurement should be carefully designed for image and video compression to provide better visual fidelity at fixed bandwidth or storage requirement. Perceptual quality depends on both source information rate as well as compression distortion or loss. We have proposed using $1/f$ video sequences with different exponents to provide examples of varying source information rate. How valid is it to characterize real and natural video streams with $1/f$ models still needs to be explored.

RMSE and PSNR have long been popularly used to quantify fidelity of lossy compression techniques. Though they correlate well with perceptual quality, counter examples have been devised by vision researchers. Robust though tractable objective quality measures are still actively explored and experimented. Quantification of video quality presents a much greater challenge

since it introduces additional degree of interaction of perceptual distortion between spatial and temporal domain.

Symmetry between coding and decoding process of video compression needs to be taken into consideration depending on the application domain. In general, complexity of encoding process is greater than the decoding one. For real-time application, such as video conferencing or surveillance, encoding speed is essential and therefore renders higher hardware cost or reduced quality performance. On the other hand, applications such as achieving does not impose real-time constraints on the symmetry of compressor/de-compressor.

We have used reconfigurable FPGAs to speed up MPEG-2 encoding. FPGAs offers flexibility that various video compression techniques can be explored and optimized for available resource. The ability to do parallel operations in hardware has the potential to speed up parts of applications by magnitudes. Tools from several different vendors were integrated into a development environment for this project. The current process is extremely burdensome. Lack of a G900 simulator is a major flaw in the design process. Testing of a design requires actually building it. The design in this project requires 45 - 60 minutes to place and route. Testing of the design requires that logic be added to the design to examine registers and other structures in the FPGA and return this information to the host (equivalent to adding printf). Nonetheless, the results were quite exciting. Mapping one component of MPEG-2 into reconfigurable computing reduced execution time 33-38%. There is still room for more tuning in the hardware design and the mapping of additional components of the MPEG-2 encoder into FGPA designs to further reduce runtimes. Reconfigurable computing currently in its infancy, has the potential to accelerate current applications with minimal source code changes and offers new applications the opportunity to fully exploit reconfigurable computing platforms.

References

[Adelson87] E. Adelson, E. Simoncelli, and R. Hingorani, "Orthogonal Pyramid Transforms for Image Coding," SPIE Visual Communication and Image Processing II, pp. 50-58, 1987.

[Barnsley93] M. Barnsley, Fractals Everywhere, 2nd edition, Academic Press, Boston, Massachusetts, 1993.

[Beinart94] J.H. Beinart, "MVP: A Multimedia Video Processor Architecture," IEEE Workshop on Visual Signal Processing and Communications, Rutgers, New Jersey, 1994.

[Chen93] Jer-Sen Chen, "A Study on the Effects of Low Update Rate Visual Displays," Proceedings of the Society of Information Display '93, Seattle, Washington, May 1993.

[Chen95] Jer-Sen Chen, "Fractal Image Compression Based on Visual Perception," Proceedings of Human Vision, Visual Perception, and Displays 1995, San Jose, California, February 1995.

[Daly93] S. Daly, "The Visible Differences Predictor: An Algorithm for the Assessment of Image Fidelity," in Digital Images and Human Vision edited by A.B. Watson, MIT Press, Cambridge, Massachusetts, 1993.

[Fisher95] Y. Fisher, Ed., Fractal Image Compression, Theory and Application, Springer-Verlag, New York, 1995.

[Gigaop97] Spectrum Reconfigurable Computing Platform RC-NTDEV-SW Documentation, Release 4.25 NT. Berkeley, California: Giga Operations, 1997.

[Gigaop94]. Taylor, Brad; and MacLeod, David. X Language Doc. Berkeley, California: Giga Operations Corporation, 1994.

[Gray93] R.M. Gray, P.C. Cosman, and K.L. Oehler, "Incorporating Visual Factors into Vector Quantizers for Image Compression," in Digital Images and Human Vision edited by A.B. Watson, MIT Press, Cambridge, Massachusetts, 1993.

[Hang95] H.M. Hang and Y.M. Chou, "Motion Estimation for Image Sequence Compression," in Handbook of Visual Communication, edited by H.M Hang and J.W. Woods, Academic Press, 1995.

[Kline92] S.A. Kline, A.D. Silverstein and T. Craney, "Relevance of human vision to JPEG-DCT compression," Human Vision, Visual Processing, and Digital Displays III, SPIE Vol. 1666, pp. 200-215, SPIE, 1992.

[Mallat89] S. Mallat, "Multi-frequency Channel De-compositions of Images and Wavelet Models," *IEEE Transactions on Acoustics, Speech, and Signal Processing*, pp. 2091-2110, 1989.

[Peitgen88] H. Peitgen and D. Saupe, Ed., The Science of Fractal Images, pp. 100-101, Springer-Verlag, New York, 1988.

[Podilchuk90] C.I. Podilchuk and N. Farvadin, "Perceptually Based Low Bit Rate Image Coding," in *Proceedings of ICASSP*, 1990.

[Podilchuk91] C.I. Podilchuk, N.S. Jayant, and P. Noll, "Sparse Code-books for Quantization of Non-dominant Sub-bands in Image Coding," in *Proceedings of ICASSP*, 1991.

[Potmesil83] M. Potmesil and I. Chakravarty, "Modeling Motion Blur in Computer-Generated Images," *Computer Graphics*, Vol. 17, No. 3, July 1983, pp. 389-399.

[Rabbani91] M. Rabbani and P.W. Jones, Digital Image Compression Techniques, SPIE Press, Bellingham, Washington, 1991.

[Schoner95] B. Schoner, J. Villasenor, S. Molloy, R. Jain, "Techniques for FPGA Implementation of Video Compression." *ACM/SIGBA International Symposium on Field-Programmable Gate Arrays*, 1995.

[Sikora97] Sikora, Thomas, "MPEG Digital Video Coding Standards." *IEEE Signal Processing Magazine* 14 (September 1997) : 82-100.

[Solomon94] J.A. Solomon, A.B. Watson, and A.J. Ahumada, Jr., "Visibility of DCT Quantization Noise: Contrast Masking," *SID 94 Digest*, 1994.

[Watkinson95] J. Watkinson, ``Compression in Video and Audio," Focal Press, an imprint of Butterworth-Heinemann Ltd., Linacre House, Jordan Hill, Oxford OX2 8DP, 1995.

[Watson86] A.B. Watson, A.J. Ahumada, Jr., and J.E. Farrell, ``Window of Visibility: a Psycho-physical Theory of Fidelity in Time-Sampled Visual Motion Displays," *Journal of Optical Society America A*, Vol. 3, No. 3, March 1986, pp. 300-307.

[Watson94] A.B. Watson, J.A. Solomon, and A.J. Ahumada, Jr., ``Visibility of DCT Quantization Noise: Effects of Display Resolution," *SID 94 Digest*, 1994.

[Xilinx96] XLINK-OS Programmer's Reference Manual. Berkeley, California: Giga Operations Corporation, 1996.

[Xilinx94] The Programmable Logic Data Book, Xilinx Inc., San Jose, California, 1994.

EVALUATION OF AN OPTIMIZATION ALGORITHM FOR
ASSIGNMENT OF RECRUITS TO TRAINING SCHOOL SEATS

Cheng Cheng
Assistant Professor

The Johns Hopkins University
3400 N. Charles Street
Baltimore, MD 21218

Final Report for:
Summer Research Extension Program
Armstrong Laboratory

Sponsored by:
Air Force Office of Scientific Research
Bolling Air Force Base, DC

and

Armstrong Laboratory

December 1997

EVALUATION OF AN OPTIMIZATION ALGORITHM FOR
ASSIGNMENT OF RECRUITS TO TRAINING SCHOOL SEATS

Cheng Cheng

Assistant Professor

Department of Mathematical Sciences

The Johns Hopkins University

Abstract

An optimization algorithm introduced by Cheng (1996) that generates cut-off scores for AF personnel classification was evaluated using a large accessions sample. The "live-data" simulation (or bootstrap resampling) method was employed to study the stability and the performance of the generated cut-off scores under two simple assignment/selection heuristics. It was found that the generated cut-off scores are reasonably stable, and may be helpful in improving the selection payoff for the Mechanical, Maintenance, and Administrative job families, at some cost of reduced payoff for the Electronics and General job families. Overall, the gains outweighs the losses.

EVALUATION OF AN OPTIMIZATION ALGORITHM FOR ASSIGNMENT OF RECRUITS TO TRAINING SCHOOL SEATS

Cheng Cheng

1. Introduction

The Armstrong Laboratory, the Army Research Institute for Behavioral Sciences, the Navy Personnel Research and Development Center, and the Center of Naval Analysis co-sponsored a project that developed a "Joint-Service Classification Research Roadmap" (Campbell & Russell, 1994). The report addressed various essential issues in personnel classification and job assignment procedures, including classification efficiency and its associated statistical measures such as the mean predicted performance (MPP). The report suggested that "Effective classification must consider many objectives and constraints to assign subjects to the job where they can perform effectively, while maintaining the efficiency of the subjecting and training system. Two major foci of recent classification research have been to develop classification methods that maximize MPP and to develop optimization methods to maximize classification objectives while satisfying constraints." This suggestion implies the need for a comprehensive sensitivity analysis of the effects of variation in critical features of a personnel management system on various assignment procedures to capture potential gain, given constraints.

For a long time there has been a need for optimization algorithms alternative to the linear programming (LP) based procedures to assign subjects to jobs or training school seats (Darby, Kyllonen & Skinner, 1996, personal communication). For various practical reasons, such as hard-to-quantify constraints on the assignment solution, the algorithms should be flexible enough to coherently incorporate qualitative constraints and the information about the qualification cut-off scores (the cut-off score profile) now used in the assignment practice. The algorithm should be able systematically adjust the cut-off scores to generate for the subjecting centers cut-off score profiles that is geared toward the optimal or a near-optimal assignment solution (Kyllonen & Darby, 1996, personal communication).

With the above considerations in mind, Cheng (1996) developed a flexible batch-sequential algorithm based on cut-off score profiles. Because of the simplicity

of its core logic, although not implemented yet, the algorithm is flexible enough to readily incorporate various constraints on the assignment solution, such as job/seat priorities, applicants' job/regional preference, Affirmative Action considerations, job qualification criteria based on multiple test scores, etc. This algorithm provides an alternative to the LP based procedures in which the above-mentioned constraints have to be incorporated into very complex payoff calculation models (Hendrix, Ward, Pina & Haney, 1979). Monte-Carlo simulation study shows that the algorithm is able to produce near-optimal assignment solutions measured by the MPP, a result qualitatively consistent with the benchmark result in Grobman, Alley & Pettit (1995), although cut-off scores, rather than decision indices, are used in the algorithm. The algorithm also contains a mechanism to systematically adjust the cut-off score profile and to generate a new cut-off profile upon producing the assignment solution.

The purpose of this study is to understand essential statistical behavior (particularly stability) of the cut-score profiles generated by the Cheng (1996) algorithm on real data, and to evaluate its performance as compared to existing assignment data. The method for investigation is "live-data" simulation, which will be detailed in the next section.

Description of the algorithm. The input to the algorithm consists of two parts: the subject file and the job description file. Each row of the subject file contains the payoff score for each job once the subject is assigned to that job. The job description file contains the number of jobs (job clusters), name of each job, a (initial) cut-off score profile giving for each job (cluster) the minimum qualifying payoff score, and quota for each job (cluster). For each subject (each row of the subject file), the algorithm goes through the following steps.

- 1° Set $j = 1$.
- 2° Take the subject's j th highest payoff score.
- 3° Is the payoff score \geq the current cut-off score for the corresponding job? If yes, go to 5°, otherwise go to 4°.
- 4° Have looked all the jobs for this subject? If yes, put the subject into the "back pool" for possible future fit-fill tradeoff (to be detailed in Section 2). If not, increase j by 1 and go to 2°.
- 5° Is the quota of the job full? If yes, go to 7°, otherwise go to 6°.

6° Assign the subject to the job. If the quota is full after assignment, set the current cut-off score for the job to the minimum payoff score (corresponding to this job) of the subjects currently assigned to this job.

7° Get the minimum payoff score (corresponding to this job) of the subjects currently assigned to this job. If the current subject's payoff score $>$ this minimum score, go to 8°, otherwise go to 4°.

8° Replace the subject having the minimum score by the current subject. Set the current cut-off score for the job to the minimum payoff score (corresponding to this job) of the subjects currently assigned to this job. Re-assign the replaced subject by the same procedure 1° – 8°.

If the initial cut-off scores are set sufficiently low so that every subject is qualified for every job initially, then upon finishing the assignments, the algorithm establishes a cut-off score profile geared toward obtaining optimal overall payoff.

Example. There are 4 jobs, with respective quota 1, 2, 2, 1. The initial cut-off scores are set to -10000 , so that every subject is qualified for every job initially. The payoff matrix of 6 subjects is given by

8	7	6	5
9	8	7	6
8	8	9	9
1	2	10	2
1	5	3	4
10	9	8	7

The steps 1° – 8° are performed for each of the 6 subjects:

Round 1: Subject 1 is assigned to Job 1.

Round 2: Subject 2 replaces Subject 1 in Job 1, and Subject 1 is re-assigned to Job 2.

Round 3: Subject 3 is assigned to Job 3.

Round 4: Subject 4 is assigned to Job 3.

Round 5: Subject 5 is assigned to Job 2.

Round 6: Subject 6 replaces Subject 2 in Job 1, Subject 2 replaces Subject 5 in Job 2, and Subject 5 is re-assigned to Job 4.

The assignment solution is: Subject 6 for Job 1, Subjects 1 & 2 for Job 2, Subjects 3 & 4 for Job 3, and Subject 5 for Job 4. The established cut-off score profile is: 10 for Job 1, 7 for Job 2, 9 for Job 3, and 4 for Job 4.

2. Data and Method

The data used in this study is the accessions sample which consists of 87801 recruits assigned to training school seats corresponding to the AFS. These are the same data used by Alley & Ree (unpublished manuscripts) to develop a new classification of the AFS, which resulted in seven job clusters. This seven-job cluster system were used in the study. The seven job clusters are Administrative (ADMIN), Elcetrical/Mechanical (EL/ME), Electronics (ELEC), General-1 (GEN-1), General-2 (GEN-2), Mechanical (MECH), and Maintainance (MAINT).

The composite scores of each of the seven job clusters were used as payoff scores to form payoff matrices. The choice of using composite scores (instead of predicted school grades) was primarily based on three reasons: (1) The basic goal of this study is to understand the statistical behavior (stability) of the cut-off score profile generated by the algorithm, rather than its performance in producing/improving MPP. (2) Ultimately, in practice, a cut-off score profile for the composites will probably be more useful than a cut-off score profile on the predicted school grades. (3) There are still some unresolved issues with predicting the school grades using multiple linear regression on the ten ASVAB subtest scores (Ree & Earles, 1997, personal communication); see Cheng & Darby (1997). Formation of the seven composite scores from the ten ASVAB subtests are displayed in Table 2.1.

Table 2.1. *Formation of the Seven Composites: 0-1-2 Weights.*

ASVAB	ADMIN	EL/ME	ELEC	GEN-1	GEN-2	MECH	MAINT
GS	0	0	1	1	2	0	1
AR	2	1	2	1	1	1	1
WK	2	2	0	1	2	0	1
PC	1	1	1	1	2	0	0
NO	0	0	0	0	0	0	0
CS	1	1	0	1	1	0	0
AS	1	2	1	1	2	2	1
MK	2	1	2	2	2	1	1
MC	0	1	0	0	0	1	1
EI	0	0	2	1	0	2	1

Informative summary statistics including mean, standard deviation (sd.), and

the five-number summary [minimum (min.), first quartile (1st q.), second quartile (2nd q.), third quartile (3rd q.), maximum (max.)], were used extensively throughout the study to describe and compare distributions and samples.

The accessions sample were divided into two halves. The first half, which consists of 43900 subjects, was used to generate the cut-off score profiles; the second half, which consists 43901 subjects, was used to evaluate and compare the job assignment solutions based on the generated cut-off score profiles. Table 2.2 shows a comparison of the two halves of the accessions sample based on the distributions of the composite scores and the percentages of each of the seven job clusters. In the first half of the table, the first one of each pair of numbers is the statistic based on the first half of the sample, and the second of each pair is the statistic based on the second half. The second half of the table contains overall statistics based on the entire sample. Clearly, for all the intended purposes here the two halves of the sample are sufficiently similar, and both are similar to the whole sample.

Table 2.2. *Comparisons of the two halves of the Accessions Sample Based on Composite Scores and Job-cluster Percentages*

	ADMIN	EL/ME	ELEC	GEN-1	GEN-2	MECH	MAINT
mean	491 493	491 495	489 491	490 492	653 657	380 384	489 494
sd.	36 36	35 35	44 44	37 37	47 47	40 39	40 40
min.	384 397	375 378	353 364	381 391	516 495	252 258	378 370
1st q.	462 464	463 468	455 458	461 463	617 620	350 355	458 464
2nd q.	488 491	489 494	487 490	487 490	651 655	380 385	488 493
3rd q.	519 521	517 522	522 525	518 520	690 693	410 414	519 524
max.	584 588	588 591	601 601	593 597	778 785	478 476	604 604
percent	18 17	20 21	11 11	15 15	20 19	6 6	10 11
overall %	17	20	12	15	20	6	10
mean	492	493	490	491	655	382	492
sd.	36	35	44	37	47	40	40
min.	384	375	353	381	495	252	370
1st q.	463	466	457	462	618	353	461
2nd q.	489	492	488	488	653	383	490
3rd q.	520	520	524	519	691	412	522
max.	588	591	601	597	785	478	604

The actual job assignment behavior reflected by the accessions sample. It is informative to first consider the actual job assignment behavior that was reflected by the accessions data. This can be accomplished by comparing the corresponding composite score distribution in the subjects assigned to each job cluster (restricted distribution) with that in the whole sample (overall distribution). If there were no selectivity for a job cluster, then the two distributions would be similar. Table 2.3 displays the statistics. The first number in each pair is the statistic for the overall distribution, and the second number is the statistic for the restricted distribution.

Table 2.3. *Comparison of the Composite Score Distributions:*

	<i>In-Job vs. Overall</i>						
	ADMIN	EL/ME	ELEC	GEN-1	GEN-2	MECH	MAINT
mean	491 485	492 494	490 525	491 497	655 646	382 394	492 496
sd.	36 37	35 33	44 34	37 39	47 45	40 32	40 34
min.	384 398	375 382	353 409	381 392	495 518	252 292	370 414
1st q.	463 456	466 470	457 502	462 466	618 612	353 371	461 470
2nd q.	489 481	492 492	488 526	488 497	653 642	383 393	490 493
3rd q.	520 513	520 517	524 551	519 528	691 678	412 417	522 520
max.	588 583	591 584	601 601	597 588	785 783	478 473	604 594

Not surprisingly, the ELEC cluster is the most selective: the restricted distribution has larger mean and quartiles, and smaller standard deviation and inter-quartile range. The three most selective jobs are ELEC, MECH and MAINT, followed by GEN-1 and EL/ME, GEN-2 and ADMIN are least selective jobs. This is a clear indication that the actual selection is not completely random, especially for the selective job clusters. The actual assignment heuristics can be very hard to model formally, due to various factors not represented by the composite scores.

The job assignment procedures. Based on the above observation, it was decided to use two simple assignment heuristics in the simulation study. The cut-off score profile based "Random Sequential" (RS) heuristic scans the subjects sequentially, and assigns a subject randomly to one of the jobs for which the subject's scores are above or equal to the corresponding cut-off scores. The cut-off score profile based "Greedy Sequential" (GS) heuristic scans the subjects sequentially, and always assigns a subject to the job for which he/she has the highest score, and that score is

above or equal to the corresponding cut-off score. The RS heuristic represents the "worst case" scenario which gives a lower bound of the MPP, and the GS heuristic represents a "near-optimal" strategy. Because the composite scores for the seven job clusters are not on the same scale (GEN-2 tends to have larger scores due to the many "2" weights in the composite, and MECH tends to have smaller scores due to fewer non-zero weights), the assignments were performed based on standardized composite scores. See the simulation method paragraph below for a description of the standardization.

Note that both heuristics are completely sequential. The replacement and the self-adjustment steps in the Cheng (1996) algorithm (see Section 1) were not used for assignments because it is unclear (unlikely) that such steps would be feasible in practice.

Fit-fill tradeoff: If after all the subjects were considered for the jobs, there are still open quota, then a "fit-fill" tradeoff is performed. To represent an "intermediate case", the unassigned subjects are scanned one-by-one and each is assigned to the open job for which he/she scores the highest, but no comparisons with the cut-off scores are made, until all jobs are filled.

The "live-data" simulation method. The live-data simulation repeatedly draws subsamples respectively from the first half and the second half of the accessions sample, generate the cut-off score profile with the Cheng (1996) algorithm based on the first subsample, then perform assignments of the subjects in the second sample to the seven job clusters using the RS and GS heuristics. One simulation run consists of the following steps:

- 1° Draw a subsample of size 200 from the first half of the accessions sample. Compute the means and standard deviations of the composite scores based on this subsample. Standardize the composite scores in the subsample using the computed means and standard deviations.

- 2° Set the quota for each job cluster according to the overall % given in the second half of Table 2.2 and the subsample size 200.

- 3° Run the cut-off score generation algorithm on the subsample to obtain a generated cut-off score profile.

- 3° Draw a subsample of size 200 from the second half of the accessions sam-

ple. Standardize the composite scores using the means and standard deviations computed in Step 1°.

4° Set the quota for each job cluster according the actual number of subjects in the second subsample assigned to each job cluster.

5° Run either the RS or the GS assignments for the second subsample, using the cut-off score profile generated in Step 3°.

6° Compute the mean payoff for each job cluster. The mean payoff for a job cluster is the sum of the composite scores (for the job cluster) of the subjects assigned to the job divided by the quota. These mean payoff scores are computed for both the assignment solution determined by Setp 5° (the *algorithm mean payoff*), and the actual assignment determined in the subsample (the *actual mean payoff*). The non-standardized scores were used for the mean payoffs.

The simulation runs were repeated 200 times independently, for RS assignment and GS assignment seperately. The primary data collected were: 200 cur-off score profiles, 200 pairs of (actual mean payoff, algorithm mean payoff) for RS assignment, and 200 pairs of (actual mean payoff, algorithm mean payoff) for GS assignment, for each job cluster. These data were used to assess the cut-off score profile generation algorithm.

3. Results

Variability of the generated cut-off score profile. Summary statistics of the 200 simulated cut-off score profiles are given in Table 3.1, where CV is the coefficient of variation defined as the absolute value of sd./mean.

Table 3.1. *Summary Statistics of the Generated Cut-score Profiles*
(in standardized scores) from 200 Simulation Runs

	ADMIN	EL/ME	ELEC	GEN-1	GEN-2	MECH	MAINT
mean	-0.23	-1.23	-0.17	-1.68	-1.92	1.04	-0.13
sd.	0.19	0.33	0.20	0.34	0.40	0.15	0.17
CV	0.83	0.27	1.17	0.20	0.21	0.15	1.39
min.	-0.83	-2.77	-0.64	-3.01	-2.85	0.62	-0.69
1st q.	-0.36	-1.34	-0.28	-1.93	-2.21	0.94	-0.22
2nd q.	-0.22	-1.16	-0.17	-1.60	-2.02	1.03	-0.12
3rd q.	-0.09	-1.03	-0.05	-1.43	-1.63	1.12	-0.02
max.	0.22	-0.60	0.41	-1.04	-0.85	1.43	0.40

Judging by the sd., CV, and inter-quartile ranges, the generated cut-off score profiles are reasonably stable for most of the job clusters. The CV for the ELEC and MAINT clusters are slightly greater than 1, indicating possible small instability. The variations may have resulted from the moderate size (200) of the subsamples used in the simulation runs.

Comparisons of mean payoff. Distributions of the algorithm mean payoff from the cut-off score based RS and GS assignment heuristics are compared with that of the actual mean payoff in Tables 3.2a and 3.2b respectively, based on the data from the 200 simulation runs. In the tables, the first number in each pair is the statistic for the actual mean payoff distribution, and the second one is the statistic for the algorithm mean payoff distribution. The larger standard deviations of the algorithm mean payoff distribution were primarily caused by the fit-fill tradeoff.

Table 3.2a. RS Assignment: *Comparisons of the Mean Payoff Distribution After Assignment for Each Job Cluster, from 200 Simulation Runs*

	ADMIN	EL/ME	ELEC	GEN-1	GEN-2	MECH	MAINT
mean	487 505	495 490	525 514	497 480	648 638	396 408	498 515
sd.	6.6 8.9	5.0 6.8	6.5 9.5	7.7 8.3	8.1 9.9	9.7 21.	7.4 8.7
min.	469 480	479 470	506 490	472 459	625 617	370 351	478 487
1st q.	482 499	492 486	521 508	491 474	643 631	389 393	492 510
2nd q.	487 505	495 490	525 515	496 481	648 638	395 407	498 515
3rd q.	491 510	499 495	530 512	502 486	654 644	403 425	503 521
max.	508 528	507 509	541 539	518 502	667 666	421 447	515 531

Table 3.2b. GS Assignment: *Comparisons of the Mean Payoff Distribution After Assignment for Each Job Cluster, from 200 Simulation Runs*

	ADMIN	EL/ME	ELEC	GEN-1	GEN-2	MECH	MAINT
mean	487 514	495 497	526 522	498 482	648 648	396 431	497 517
sd.	6.1 7.4	4.9 7.0	7.0 9.6	6.6 11.	7.1 11.	10. 14.	7.7 8.3
min.	466 493	482 481	509 489	481 449	631 621	367 377	481 490
1st q.	484 509	492 492	521 516	494 474	643 641	389 429	490 512
2nd q.	487 515	495 497	526 522	498 481	649 648	397 436	496 517
3rd q.	491 520	499 502	530 529	503 489	654 656	403 440	503 523
max.	505 534	506 513	546 542	514 512	667 679	422 454	513 542

The cut-off score based RS assignments seem to outperform the actual for the ADMIN, MECH, and MAINT clusters, but seem to be inferior to the actual for the other job clusters, especially for the ELEC and GEN-1 clusters. The cut-off score based GS assignments seem to outperform the actual for the ADMIN, MECH, MAINT and EL/ME clusters, but seem to be inferior to the actual for the other job clusters, especially for the ELEC and GEN-1 clusters, but the amount of decrement in mean payoff is smaller than that of the RS assignments. Paired T-tests for the mean payoff differences (algorithm vs actual) were computed and are given in Table 3.3. The values in paranthesis are P values.

Table 3.3. *Paired T-tests of mean payoff difference (algorithm vs actual)
for each job cluster*

	RS assignment	GS Assignment
ADMINISTR	26.63 (< 0.001)	46.08 (< 0.001)
ELEC/MECH	-9.34 (< 0.001)	+2.97 (0.002)
ELECTRON.	-13.2 (< 0.001)	-4.32 (< 0.001)
GENERAL-1	-24.4 (< 0.001)	-20.3 (< 0.001)
GENERAL-2	-11.8 (< 0.001)	-0.25 (0.4033)
MECHANICS	+7.59 (< 0.001)	29.95 (< 0.001)
MAINTAIN.	20.78 (< 0.001)	25.99 (< 0.001)

All significances at 10% level retain after the Bonferoni adjustment for 7 comparisons. For the GEN-2 cluster, the reduction in the mean payoff by the GS assignment is not significant.

Finally, the entire first half of the accessions sample were used to generate a cut-off score profile, and then RS and GS assignments were performed on the entire second half of the accessions sample, using the generated cut-off score profile. The payoff scores determined by the algorithmic assignment solutions are compared with those determined by the actual assignments in the sample. The summary statistics, together with the t statistics comparing the differences in means, are given in Tables 3.4a and 3.4b. The first number in each pair is the statistic for the actual assignment, and the second one is the statistic for the assignment by RS or GS.

Table 3.4a. RS Assignment: *Comparisons of the Payoff Distribution*
After Assignment for Each Job Cluster

	ADMIN	EL/ME	ELEC	GEN-1	GEN-2	MECH	MAINT
mean	487 503	496 491	525 518	498 481	648 636	395 405	497 518
sd.	37 32	32 30	34 27	39 35	45 48	32 45	34 25
t test	27.4	-11.1	-11.7	-26.7	-16.6	+9.25	33.17
min.	398 402	404 449	417 480	392 429	528 519	292 301	414 483
1st q.	458 484	472 467	502 494	467 453	613 600	372 361	471 497
2nd q.	483 502	494 484	527 513	498 473	645 629	396 426	494 513
3rd q.	515 525	518 511	551 538	528 505	681 669	419 440	521 534
max.	580 584	584 584	601 596	588 594	783 770	473 476	593 600

Table 3.4b. GS Assignment: *Comparisons of the Payoff Distribution*
After Assignment for Each Job Cluster

	ADMIN	EL/ME	ELEC	GEN-1	GEN-2	MECH	MAINT
mean	487 517	496 497	525 525	498 481	648 646	395 438	497 517
sd.	37 24	32 33	34 30	39 42	45 51	32 12	34 26
t test	59.48	+2.64	-1.03	-24.0	-3.31	63.07	31.45
min.	398 402	404 449	417 480	392 429	528 519	292 421	414 483
1st q.	458 498	472 468	502 500	467 449	613 610	372 427	471 496
2nd q.	483 517	494 491	527 520	498 465	645 639	396 435	494 510
3rd q.	515 536	518 521	551 548	528 510	681 684	419 446	521 532
max.	580 580	584 586	601 597	588 597	783 778	473 475	593 600

These results are fairly similar to the simulation results in Tables 3.2a and 3.2b. The major difference is that for the ELEC cluster the reduction in mean payoff by the GS assignments is not significant. However, the significance of the t tests here should be interpreted with caution: due to the large sample size (43901), a very small difference in mean will result in a significant t statistic, but the small difference may be practically negligible. Examining Table 3.4 closely, the overall gains in payoff for the MECH, MAINT, and ADMIN clusters by the cut-off score profile based GS assignment heuristic outweigh the losses.

4. Concluding Discussions

The results indicate that (1) the cut-off score profiles generated by the Cheng (1996) algorithm are reasonably stable; (2) the cut-off score profiles seem to be helpful for significantly increasing the selection payoff in the Mechanical, Maintenance, and Administrative job clusters, but with some sacrifice on the payoff in the General-1 and Electronics job clusters.

The gain and loss in mean payoff by the cut-off score profile based RS and GS assignments compared with the actual mean payoff must be carefully interpreted. The observed differences are due to many factors in the actual selection procedure. On this account, the results demonstrate that there exist heuristics in the actual selection procedure not captured by cut-off score based RS and GS heuristics. Statistical analysis more refined than Table 2.3 (such as rank correlations) can be employed to discover some characteristics of the actual selection procedure. Such a study would be useful for further investigation and evaluation of the cut-off score generation algorithm.

References.

- CAMPBELL, J. P. and RUSSELL, T. L. (1994). Building a joint-service classification research roadmap: methodological issues in selection and classification. Armstrong Laboratory, AL/HR-TP-1994-0013, Brooks AFB, TX.
- CHENG, C. and DARBY, M. M. (1997). Investigation of two statistical issues in building a classification system. Technical Paper, Armstrong Laboratory, Human Resources Directorate, Brooks AFB, TX.
- CHENG, C. (1996). A sequential optimization algorithm for personnel assignment based on cut-off profiles and a revision of the Brogden table. Final Report of 1996 AFOSR Summer Faculty Research Program, Armstrong Laboratory, Human Resources Directorate, Brooks AFB, TX.
- GROBMAN, J. H., ALLEY, W. E. and PETTIT, R. S. (1995). The optimality of sequential personnel assignments using a decision index. Armstrong Laboratory, AL/HR-TR-1995-0025, Brooks AFB, TX.
- HENDIRX, W. H., WARD, J. H., PINA, M. and HANEY, D. L. (1979). Pre-enlistment person-job match system. AFHRL-TR-79-29. Occupation and Manpower Research Division, Brooks AFB, TX.

OPTICAL DETECTION
OF INTRACELLULAR PHOTOOXIDATIVE REACTIONS

Randolph D Glickman
Associate Professor
Department of Ophthalmology

University of Texas Health Science Center
at
San Antonio
7703 Floyd Curl Drive
San Antonio, TX 78284-6230

Final Report for:
Contract SREP 96-0102
Summer Research Extension Program
US Air Force Research Laboratory

Sponsored by:
Air Force Office of Scientific Research
801 N. Randolph St., Rm 732
Arlington, VA 22203-1977

and

Air Force Research Laboratory
(formerly Armstrong Laboratory)

December 1998

OPTICAL DETECTION OF INTRACELLULAR PHOTOOXIDATIVE REACTIONS

Randolph D. Glickman, Ph.D.
Associate Professor
Department of Ophthalmology
University of Texas Health Science Center at San Antonio

ABSTRACT

The cellular pigments of the retinal pigment epithelium (RPE) have been shown to catalyze free radical activity, especially when illuminated with visible or ultraviolet light. This activity is sufficient to cause photooxidation of several major cellular components, including proteins, fatty acids, antioxidants, and enzyme cofactors. The photochemistry of the RPE melanosomes has been studied in considerable detail, although almost entirely in experiments utilizing pigment granules isolated from the RPE cells. The photoactivated reactions of these granules, characterized in the original AFOSR Summer Research Program, have an action spectrum peaking between 450 and 500 nm. In the research supported in the Extension Program, we have been able to demonstrate that similar, wavelength-dependent reactions occur within intact RPE cells. This was accomplished with the oxidation-sensitive chemical probe, 2',7'-dichlorofluorescein, which is non-fluorescent when chemically reduced and fluorescent when oxidized. Another oxidation-sensitive fluorescent probe, dihydrorhodamine 123, was not oxidized intracellularly in a wavelength-dependent fashion, and in fact, was found to have a higher oxidation potential which may have inhibited its reaction with light-excited reactive species within the cell. The experiments were conducted in cultured bovine and baboon RPE cells that were labeled with these probes, and then exposed to quantum-equivalent, 488, 514.5 or 647.1 nm emissions from Argon and Krypton ion CW lasers. The probes were isolated from the cells by solid phase extraction, and the amount of oxidized probe quantified by HPLC with fluorescence detection. Alternatively, cells were imaged with a fluorescence microscope. Images were acquired at various intervals after the cells were exposed to blue ($\lambda_{\text{max}} = 490$ nm) and yellow ($\lambda_{\text{max}} = 582$ nm) light derived from the microscope exciter lamp. The kinetics and amplitude of the fluorescence change in the cells were quantified with image processing software. Both types of experiments yielded the conclusion that blue-green wavelengths, on a quantal basis, most efficiently induced photooxidative stress in the pigmented cells. The microscopy also showed that fluorescence was restricted to the cells' cytoplasm. These findings indicate that the melanosomes of pigment cells are involved in intracellular photooxidative reactions.

OPTICAL DETECTION OF INTRACELLULAR PHOTOOXIDATIVE REACTIONS

Randolph D. Glickman, Ph.D.

INTRODUCTION

The retinal pigment epithelium (RPE) of the eye contains several pigments, including melanin, lipofuscin, and melanolipofuscin. The amount of pigmentation in the RPE cells changes with age, i.e. melanin tends to decrease and lipofuscin tends to increase [1]. Environmental and systemic factors also affect pigment content. The biological role and significance of these pigments is not entirely understood. For example, melanin is a broadband absorber and is generally thought to protect ocular tissues against excess light. The protection could derive from melanin's ability to absorb and screen light from reaching sensitive target tissues [2], to sequester heavy metals that might otherwise catalyze oxidative reactions [3], or to trap free radicals produced by photochemical reactions or ionizing radiation [4,5]. Lipofuscin is considered an aging pigment resulting from lysosomal accumulation of peroxidative end products of lipid decomposition [6] and, in the eye, polymerization of remnants of retinaldehyde, the chromophore of the visual pigment [7]. Lipofuscin is known to produce reactive oxygen species when illuminated with UV light [8]. Melanolipofuscin also is associated with aging and represents degenerated melanosomes combined with lipofuscin [9]. The accumulation of these substances has been associated with pathological changes [6]. We have previously demonstrated that melanin, as well as the other RPE pigments, all have some photoactivity with respect to the initiation of lipid peroxidation [10,11]. Lipofuscin also is able to promote peroxidative reactions in the dark, probably because the granules contain labile hydroperoxides that themselves are reactive, as well as metal ions (especially iron) that catalyze oxidative (Fenton-type) reactions.

Melanin-mediated photooxidative reactions

In spite of its presumed protective role, melanin (a) induces oxidative changes in physiological substrates such as ascorbic acid, fatty acids, and proteins during irradiation with visible light [12-16], (b) is a photoinducible free radical [17,18], (c) produces reactive oxygen species when irradiated by UV and visible light [19,20], and (d) promotes photochemical oxidations [15,21,22]. While the significance of these findings for photooxidative stress *in vivo* is not entirely clear, the possibility exists that pigments in the RPE cells may have a dual role in both protecting against and promoting photooxidative reactions, depending on the cellular environment and the nature of the oxidizing stressor.

Laser-induced melanosome disruption as a precursor to photochemical damage

Although the role of melanin and melanosomes in mediating thermal damage in the eye following continuous wave (CW) laser exposure is quite well understood, and has been successfully modeled based on the linear absorption of optical radiation by the pigment granules [23], the involvement of pigment granules in mediating damage produced by

short pulse (i.e. relative to the time constant of thermal diffusion or $<1\ \mu\text{s}$ approximately) laser exposures is less well known. For extremely short laser pulses ($\leq 100\ \text{ps}$), tissue damage (ionization and optical breakdown) results as a function of peak power during the pulse and is less dependent on the specific tissue absorption of the laser wavelength [24]. In the RPE, short pulse laser exposures above the damage threshold do cause disruption of the melanosomes [25]. The explosive disruption of the melanosome is undoubtedly fatal to the cell, and produces immediate damage to surrounding cells by transmission of mechanical forces. Yet, in some cases, the damage may take 24 hours or more to become apparent [25]. Based on the enhanced photochemical activity of isolated melanosomes disrupted by exposure to Q-switched Nd:YAG laser [26,27], Glickman proposed that the elevated photochemical activity of laser-damaged melanosomes may be responsible for the delayed onset of lesions after some short-pulse laser exposures, especially near threshold exposures [28]. Recently, a formal model incorporating the photochemical activity of damaged melanosomes to explain the delayed formation of threshold laser lesions has been proposed [29]. The need to detect or identify increased photooxidative stress in the cytoplasm of RPE cells following laser injury was a major motivation for the present research.

Detecting photooxidative reactions within the RPE cell

Most of the data on the photochemistry of the RPE pigments has been obtained in studies with isolated pigment granules. There is little published information on photooxidative reactions within the RPE cell itself. Although photochemical damage to the retina and RPE, defined as light-induced tissue damage resulting in the absence of significant tissue heating, is well documented [30,31], there is continuing controversy about the chromophore responsible for these changes [32,33]. In an effort to determine if one or all of the RPE pigments are responsible for photooxidative stress, we utilized oxidation-sensitive vital fluorescent probes to measure the redox state of the RPE cell following exposure to various wavelengths of visible light produced by continuous wave lasers and other light sources.

Scope of the project

The major goals of this project were to determine (1) if oxidation-sensitive fluorescent probes could be taken up by RPE cells in culture, (2) if the probes were tolerated over the 2-3 hr time course of the typical experiment; and (3) if light exposure from laser and other light sources could induce sufficient oxidative stress in the cells to oxidize the probes and thereby produce a fluorescent signal. In addition, the optimal methodology for studying the fate of the probes in the cells was evaluated, i.e. direct optical detection by fluorescence microscopy was compared to the extraction of the probes from the cells followed by biochemical analysis. The results of this project show that the use of oxidation-sensitive fluorescent probes is a powerful new way to characterize laser-tissue interaction.

METHODS

RPE Cell Cultures

Primary cultures of RPE cells were prepared from bovine eyes freshly obtained from a local slaughterhouse, and from baboon eyes generously provided by the Southwest Foundation for Biomedical Research (San Antonio). After opening the globes and removing the retinæ, RPE cells were gently brushed off the choroid into a pool of culture medium. Collected cells were centrifuged and plated at a constant density in 24-well plastic culture plates. Cells were grown in Dulbecco's Minimum Essential Medium (DMEM) containing 10% fetal calf serum and maintained at 37 °C in an atmosphere supplemented with 5% CO₂.

Viability testing of the cells by MTT test

The so-called MTT test is a cell viability test that utilizes dehydrogenase enzymes located in the mitochondria or elsewhere in the cell to catalyze the conversion of nitro tetrazolium salts to a colored formazan product. This assay has been validated in a number of cell models [34,35]. A commercial MTT test kit (active reagent: 3-[4,5-Dimethylthiazol-2-yl]-2-5-diphenyltetrazolium bromide, MTT) was obtained from Sigma Chemical Co. (St. Louis, MO). RPE cells of either bovine or baboon origin were used. Each assay used 150,000 - 600,000 cells. Assays were either run in bulk, by carrying out the reactions with the harvested cells in a 1.5-ml Eppendorf plastic microcentrifuge tube and, after spinning out the melanosomes, reading the results in a Beckman DU-640 spectrophotometer, or, by adding the reagents directly to the cells in their 24-well culture plates and monitoring the results in a Packard Instruments Spectracount plate reader. In either case, after adding the MTT reagent (5 mg/ml) and incubating the cells for 3 hr, the reactions were stopped and the formazan product solubilized by addition of 0.1 N HCl in absolute isopropanol. Samples were mixed and the reaction result was read as the difference in optical absorbance between the test wavelength at 570 nm and the reference wavelength at 630 nm. The extent of the MTT reaction in live cells was compared to that of "dead cell" controls, which were aliquots of cells killed by heating at 100 °C for 10 min.

Preparation of Probes

The oxidation-sensitive probes, 2'-7'-dichlorofluorescein (DCFH) and dihydrorhodamine 123 (DHR123) were obtained from Molecular Probes (Portland, OR). These probes have the property of being nonfluorescent when chemically reduced and highly fluorescent when chemically oxidized. DCFH was supplied from the manufacturer as the diacetate ester (DCFH-DA), and a 1 mM stock solution was prepared by dissolving 10 mg in 20 ml of methanol. For studies involving cellular uptake, the ester form was hydrolyzed by the cells themselves (see Results). For studies in cell-free experiments, 0.5 ml of DCFH-DA stock solution was hydrolyzed with 2.0 ml of .01N NaOH for 30 min at room temperature. Hydrolysis was stopped by adding 10 ml of 25 mM NaH₂PO₄ (pH=7.5). DHR123 was supplied as a dry powder of which 10 mg were added to 1 ml of N,N-dimethylformamide and then diluted to a 1 mM stock solution using methanol [36]. Working dilutions (usually 10 µM) of the probes were made by diluting stock solutions with culture

medium. Both probes were stored under nitrogen at -20°C, and working solutions were prepared fresh each day.

Fluorescence Microscopy

RPE cells were plated on Lab-Tek ChamberSlides (Nalge/Nunc) and allowed to attach to the ChamberSlides. Prior to microscopy, the cells were incubated in 10 µM DCFH or 10 µM DHR123 for 1 hr. After incubation, the cells were briefly washed in probe-free medium and cover-slipped. Photooxidative reactions were activated by exposing the probe-labeled RPE cells to the exciter source in an Olympus BX-60 fluorescence microscope. The fluorescein exciter ($\lambda_{\text{max}}=490$ nm) and the Texas red exciter ($\lambda_{\text{max}}=582$ nm) were used in different experiments. Fluorescence images were captured on a computer frame grabber at timed intervals during exposure to the excitation source. Image analysis was performed on these images with *Image-Pro* software (Media Cybernetics) by defining a constant Area of Interest (AOI) in the images, and measuring the mean and standard deviation of the AOI pixel intensity in each image. These values were plotted against the time of image acquisition to construct a fluorescence growth curve.

HPLC Analysis

Probes were analyzed by high performance liquid chromatography (HPLC) on a Waters µBondapak-C₁₈ or a Phenomenex Bondclone-C₁₈ column (which gave equivalent results), with one of the following mobile phases: DCFH and its derivatives were eluted with 8mM ammonium phosphate (pH 8.0) modified with 60% methanol, and DHR123 was eluted with 8mM ammonium phosphate (pH 8.0) modified with 60% acetonitrile. The flow rate was 1 ml/min. Fluorescence was measured by a Waters 474 detector with λ_{ex} at 488 nm and λ_{em} at 530 nm. For determination of the oxidation potential of the probes, chromatographic separation was carried out with these same conditions, except that electrochemical detection was performed with a Waters 460 electrochemical detector. Hydrodynamic voltammograms were constructed by systematically increasing the detection potential for successive sample injections, and measuring the resulting oxidation current. The half-wave potential, $E_{1/2}$, and the threshold response, E_0 , were determined from the data by fitting a sigmoidal function of the form

$$y = a_0 + \left(a_1 / (1 + e^{-(x-a_2) / a_3}) \right) \quad (\text{equation 1})$$

to the data set. The Y-axis intercept of this function was taken as the threshold for oxidation (E_0) and the coefficient, a_2 (which corresponds to the value of X at which the function amplitude is at half-maximum), as the value for $E_{1/2}$.

Extraction of Probes for HPLC Analysis

For cellular uptake experiments, aliquots of 10⁶ RPE cells were incubated in 10 µM probe for varying times. After the desired incubation time, the cells were centrifuged and the resulting pellet washed once in probe-free culture medium. The probe contained within the cells was isolated using solid phase extraction (SPE). This technique of sample preparation employs the retention of sample and impurities on a sorbent material similar to that used in reverse-phase HPLC analytical columns, followed by selective elution of the sample molecule(s) with a specific solvent. The

impurities are retained on the extraction cartridge. Cells were lysed with 500 μ l of 0.5% Triton X dissolved in Tris buffered saline and then incubated for 10 min. The samples were centrifuged, and the supernatant containing the probe and soluble components of the cytosol were processed with Waters Oasis HLB SPE cartridges using the following protocol: the cartridge was initially washed and the sorbent wetted by the passage of 1 ml each of methanol and distilled H₂O. The cartridge was not allowed to dry out before the sample was introduced into it. Then, 0.5 ml of the supernatant was passed through the cartridge. Finally, 1 ml of methanol was passed through the cartridge to elute the probes. Recovery efficiency for the probes was about 85%. Aliquots of this eluant were analyzed by HPLC using the conditions described above.

Chemical oxidation of probes for estimation of total uptake

In order to measure total probe content in the uptake experiments, probes extracted from RPE cells were subjected to chemical oxidation to convert all the probe molecules to the oxidized, highly fluorescent moiety. This was accomplished by combining the eluants obtained from SPE extraction with 5 μ l each of horseradish peroxidase (HRP, 5 mg/ml) and H₂O₂, (20 mM) for 30 min at 37°C [36]. These processed samples were then analyzed by HPLC with fluorescence detection.

Statistical Analysis

Routine statistical analysis, including the Bonferroni test for multiple comparison between groups, was performed with the *ProStat* statistical computer program (Poly Software International, Sandy, UT).

RESULTS

Viability of RPE cells following labeling with fluorescent probes

A classic test of cellular viability is the uptake of the dye, Trypan Blue. Live cells tend to exclude this dye, while dead or dying cells allow the penetration of the dye into the cytoplasm. The pigmentation, however, of the RPE cells interferes with the interpretation of this test, rendering it useless for evaluating cellular viability in these cells. We then adopted the so-called MTT test which measures metabolic activity in the cells. This test was also rendered more difficult to read by the presence of pigment granules, however, sufficient replications indicated that while cell viability was somewhat reduced by exposure to DCFH (Table I), over the two hour duration of the experiment, this reduction did not reach statistical significance (Table II: comparison of No Probe condition to 1-hour and 2-hour probe incubation conditions).

Table I. Effect of 1- and 2-hour incubations in DCFH on MTT test of RPE cell viability.

Treatment	# Expts.	MTT, mean \pm s.d.
Killed Cells	5	.167 \pm .017
No Probe	4	.240 \pm .024
+Probe, 1 h incubation	4	.232 \pm .023
+Probe, 2 h incubation	4	.216 \pm .018

Table II. Probability matrix. Statistical significance of effect of DCFH on RPE cell viability (Bonferroni multiple comparison test).

	Killed Cells	No Probe	1 Hour incubation
No Probe	0.000	****	****
1 Hour incubation	0.000	0.588	****
2 Hour incubation	0.003	0.119	0.286

Fluorescence microscopy studies of photooxidative stress in RPE cells

The use of a vital, fluorescent stain initially offered the possibility of obtaining direct visualization of photooxidative stress within the RPE cells, especially the spatial localization of oxidative reactions. Although the early data were encouraging, two factors prevented this imaging approach from yielding the quantitative data desired. One was the difficulty in calibrating the fluorescence signal so that meaningful comparisons could be made between experiments. The second problem resulted from the cells' pigmentation. Many of the primary RPE cell cultures used in these studies were heavily pigmented, retaining most if not all of their melanosome content. We found that the presence of the heavy pigment tended to quench or block the fluorescence signal from the cells. In many experiments, only a bright, fluorescent halo could be observed around the cell. However, one salient observation was made when intracellular fluorescence was clearly observed: that fluorescence was limited to the cytoplasm, and did not extend into the nucleus (Figure 1). This was of interest because it implied that photooxidative reactions occurred in the vicinity of the melanosomes. In these experiments, the photooxidative stress was not produced with laser exposure, but with the exciter of the fluorescence microscope which was simply allowed to illuminate the cells for various lengths of time. As described in the Methods, two exciter wavelengths were used, one with a spectrum centered at 490 nm and the other at 582 nm. Several cells, such as the group of cells pictured in Figure 2, were imaged clearly enough to measure the relative increase in fluorescence with increasing exposure time. The images of five RPE cells were selected for this type of image analysis. The changes in pixel intensity of a defined AOI in each image, during exposure to the microscope exciter lamp, are plotted in Figure 3. These observations indicated that the 490 nm light caused an increase in the intracellular fluorescence, while there was little or no increase when cells were exposed to the 582 nm light.

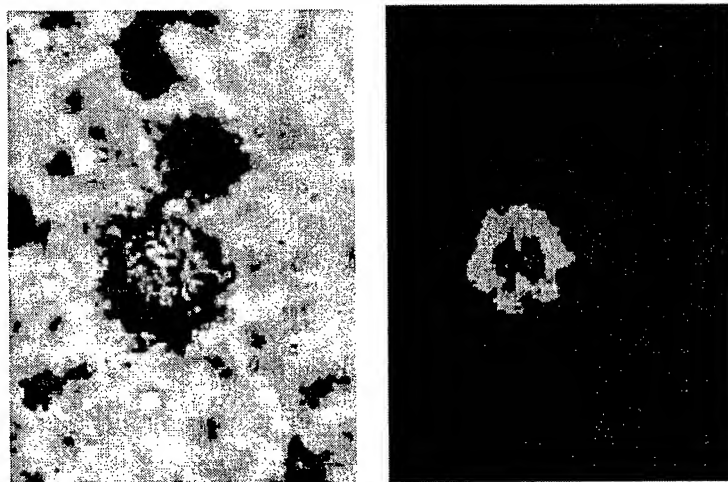


Figure 1. Micrographs of DCFH-labeled RPE cells. Left: bright field image. Right: fluorescence micrograph of same cell using fluorescein exciter, showing fluorescence in cell's cytoplasm.

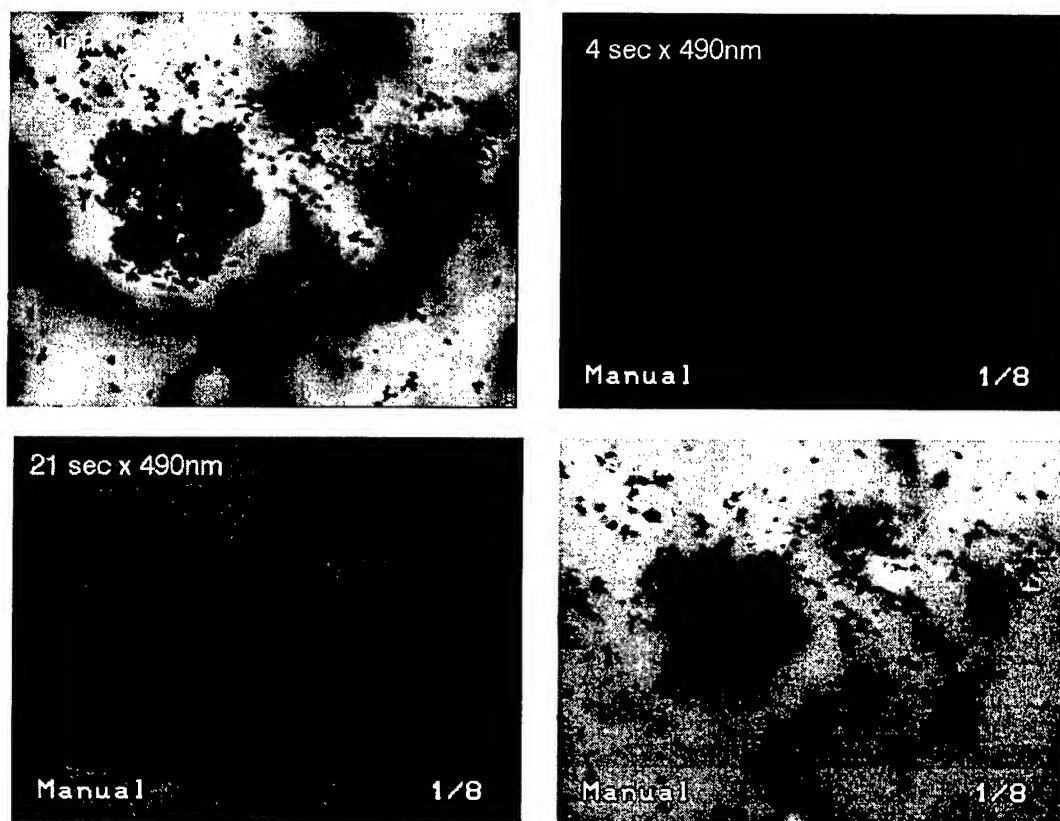


Figure 2. Fluorescence micrographs of a group of RPE cells loaded with DCFH and exposed to the fluorescein exciter lamp of the microscope ($\lambda_{\text{max}} = 490 \text{ nm}$). Top row: (left) bright field view of the cells; (right) 4 sec exposure to exciter lamp. Bottom row: (left) 21 sec exposure; (right) 90 sec exposure to the exciter lamp.

Fluorescence Microscopy of RPE Cells

Photooxidation of probe-labelled cells

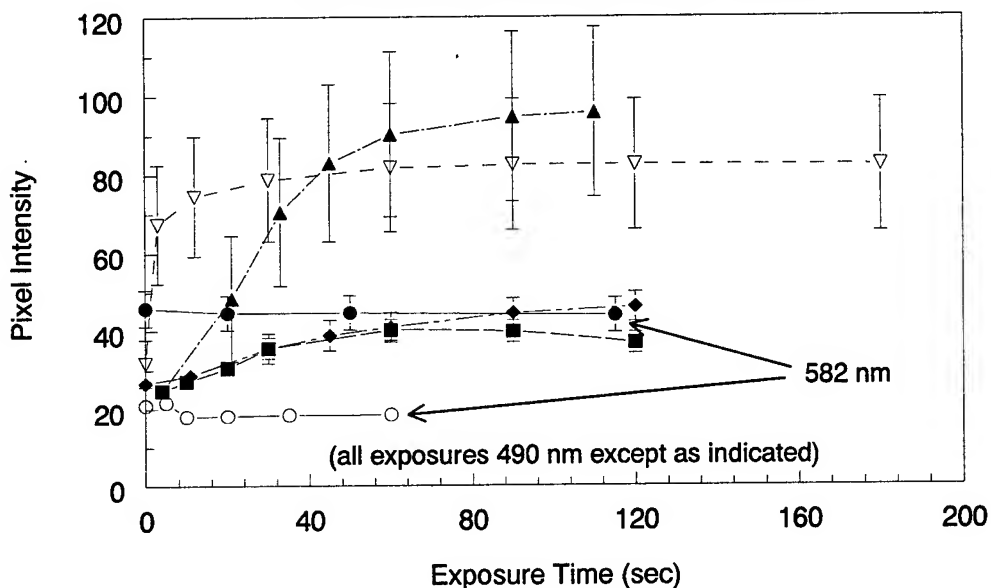


Figure 3. Increase in fluorescence of probe-labeled RPE cells continuously exposed to microscope exciter lamp (wavelengths indicated in figure). Data points are the mean \pm s.d. of the pixel intensity of a defined AOI positioned within the image of a cell and followed over time in successive images.

Nevertheless, the limited, qualitative nature of the imaging data led us to develop a biochemical methodology for the direct analysis by HPLC of the amount of the DCFH and DHR123 probes oxidized by various wavelengths of light. The results of these studies are described in the following sections.

HPLC method for analysis of DCFH and DHR123

Development of a suitable HPLC method for the separation of each probe allowed us to isolate the probe from cell lysates, and quantify the probe fluorescence with precision. Figures 4 and 5 show, respectively, chromatograms of DCF (oxidized DCFH) and DHR123 (also oxidized) standards. Under our analytical conditions, DCF had a retention time of about 4.1 min, while that of DHR123 was 5.5 min. Each figure also shows a sample of "aged" probe, indicating that each probe was susceptible to autoxidation leading to the formation of oxidative breakdown products. For this reason, working dilutions of the probes were made up fresh for each day's experiments.

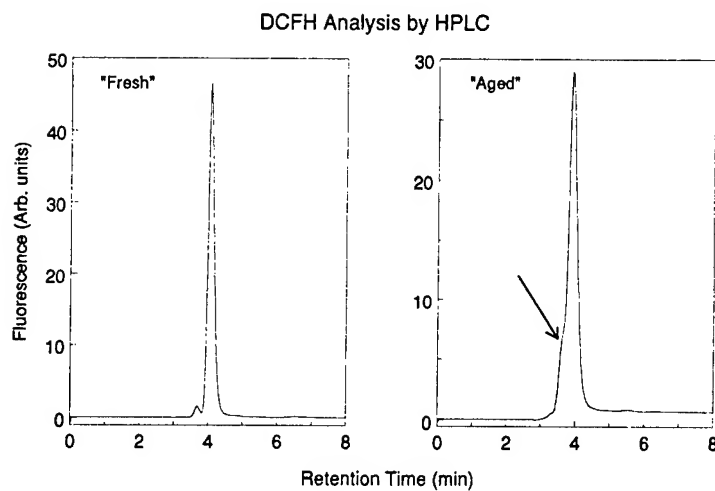


Figure 4. HPLC chromatograms of fresh DCF (left) and autoxidized (“aged”) DCF (right). Arrow points to appearance of oxidative breakdown products

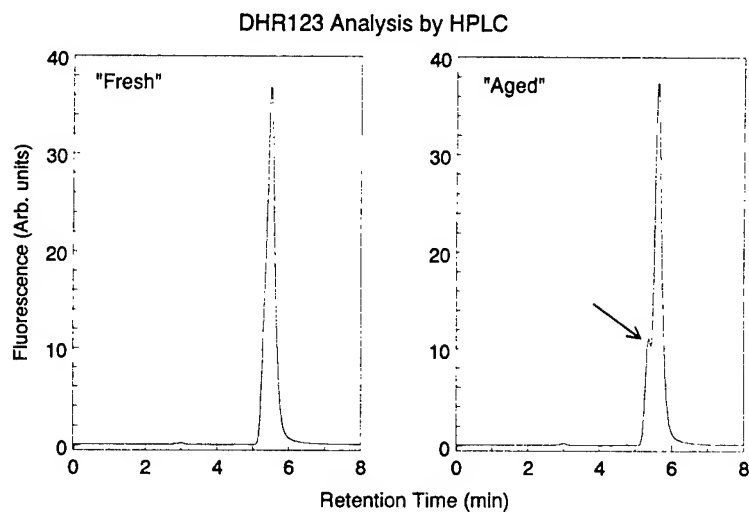


Figure 5. HPLC chromatograms of DHR123. Freshly oxidized probe is shown on the left, and autoxidized (“aged”) probe on the right. Arrow points to appearance of oxidative breakdown products.

Kinetics of DCFH and DHR123 uptake by RPE cells

To characterize the uptake of the probes, RPE cells were incubated for various time periods in 10 μ M DCFH-DA or DHR123, and then the probes were extracted from the cells using SPE. The probe content in the cell extracts was

oxidized (in order to make it fluorescent) by reaction with HRP and H_2O_2 , and then aliquots were analyzed on HPLC with fluorescence detection. The time course of probe uptake versus time is shown in Figure 6. DCFH-DA was generally taken up quickly and reached a maximum in about 20 min, after which the intracellular content of the probe gradually declined (Figure 6, left). DHR123 was accumulated more slowly, reaching a plateau at about 60 min which was maintained for up to another hour (Figure 6, right)

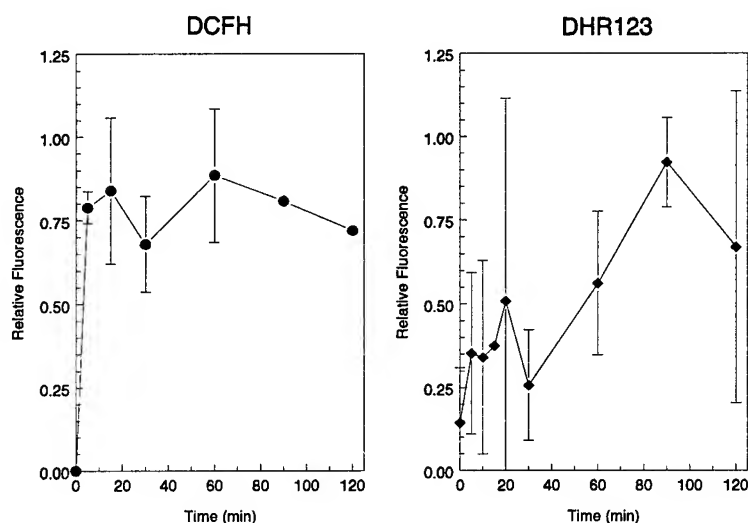


Figure 6. Kinetics of fluorescent probe uptake into cultured RPE cells, determined by HPLC analysis of cell lysates. Left panel: DCFH; right panel: DHR123. Each time point represents the mean \pm s.d. of at least 4 measurements.

DCFH-DA Uptake and Hydrolysis

DCFH-DA and its two principal metabolites, the hydrolyzed-reduced form DCFH, and the hydrolyzed-oxidized form DCF, exhibited distinct retention times in HPLC analysis (Figure 7). In this figure, the left-hand panel shows a chromatogram of the stock probe, DCFH-DA. This form elutes as a single peak at about 6.2 min under our HPLC conditions. After the probe is chemically hydrolyzed and oxidized, HPLC analysis reveals a single, highly fluorescent peak (note difference in vertical scale between the right hand panel and the other two) eluting at slightly over 4 min. HPLC analysis of a sample of probe that was chemically hydrolyzed, but **not** oxidized, is shown in the central panel. Note that all forms of DCFH have some degree of fluorescence, which enables the detection of each moiety. The hydrolyzed-reduced form, DCFH, elutes at about 5 min, between DCF and DCFH-DA.

Because the three principal forms of DCFH can be separated and identified on HPLC, the uptake and processing of DCFH-DA by RPE cells could be followed, which proved that, following cellular uptake, the probe is hydrolyzed to DCFH by intracellular esterases. RPE cells were incubated with a 10 μ M solution of DCFH-DA, and aliquots were

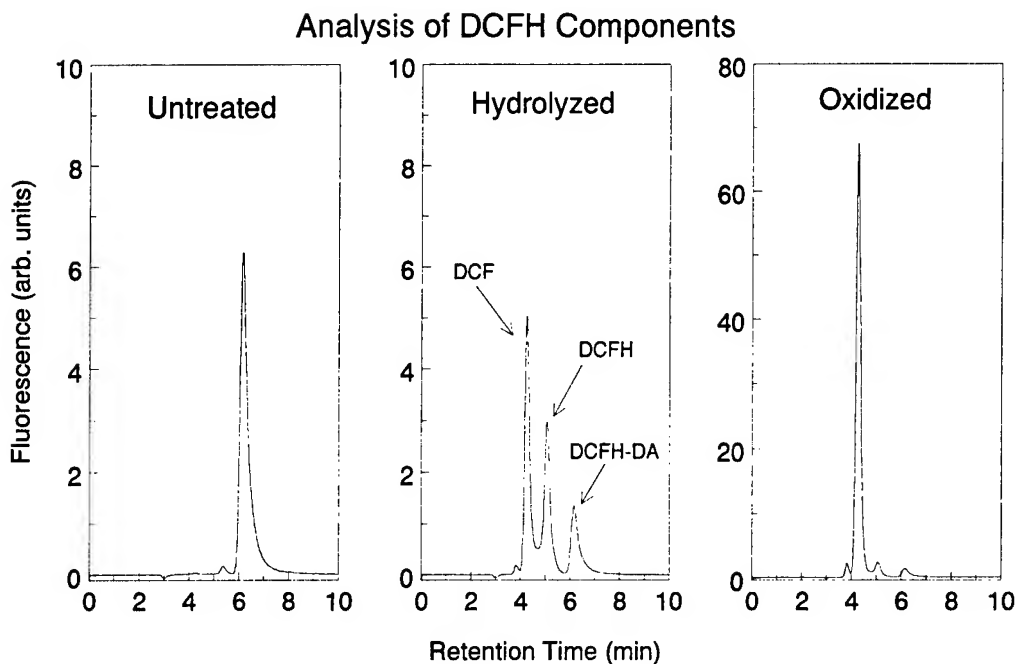


Figure 7. HPLC analysis of DCFH components. Left panel: DCFH-DA (i.e. working dilution of the probe as supplied by manufacturer). Center panel: DCFH-DA + DCFH + DCF (analysis of probe following hydrolysis with NaOH). Right panel: DCF (analysis of hydrolyzed probe following chemical oxidation with HRP and H_2O_2 ; note difference in vertical scale).

removed for assay at 20 minute intervals, beginning at 0 min of incubation (the probe was added to the cell cultures, and the sample was then immediately processed). The sample was extracted using SPE, chemically oxidized to enhance detection of the compounds, and analyzed by HPLC with fluorescence detection. The peaks in the chromatograms obtained were identified by comparison to the known retention times of the identified probe components shown in Figure 7. The chromatograms obtained at $t = 0'$, $15'$, $20'$, and $60'$ are shown in Figure 8. At time = $0'$, all of the probe is present as DCFH-DA. By $15'$, probe has accumulated in the cells and is starting to be hydrolyzed. (Note that because these samples have been manually oxidized prior to HPLC analysis, little or no DCFH is found, because all DCFH produced by the action of cellular esterases is oxidized to DCF by our procedure). By $20'$, most accumulated probe has been hydrolyzed, and by $60'$ virtually all detectable probe in the cells has been hydrolyzed. Apparently, the total probe content in the cells declines by $60'$ either because of efflux from the cell, or metabolic breakdown to a form that is either non-fluorescent or not captured by our isolation procedure.

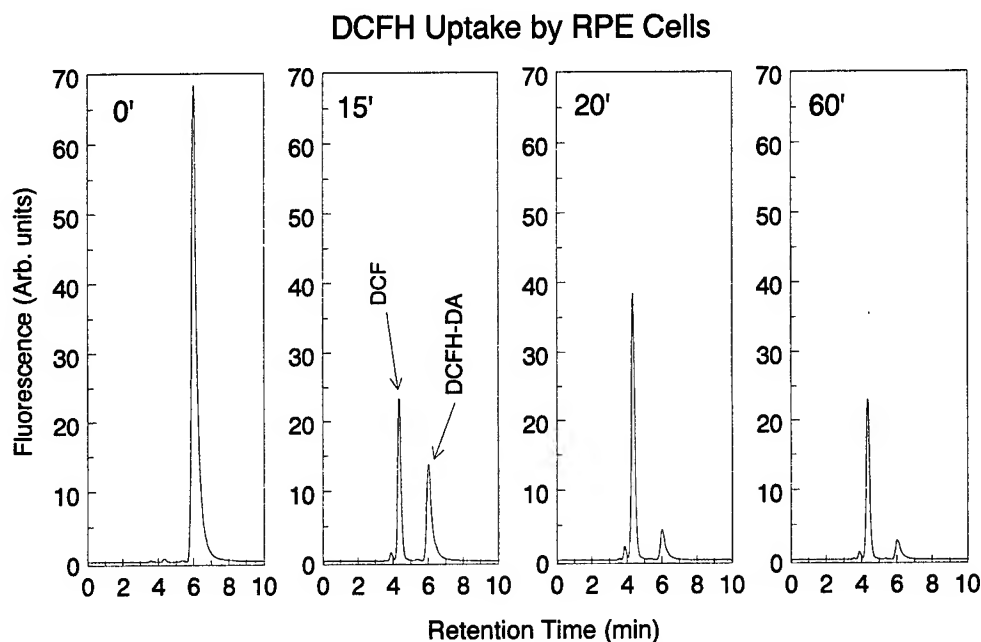


Figure 8. Uptake and processing of DCFH-DA by RPE cells. HPLC analysis of cell lysates following incubation for the indicated times in 10 μ M DCFH. Note that at 0', all the recovered probe is in the diacetate form, but by 20' of incubation, most of the probe has been hydrolyzed by the action of cellular esterases. See text for further details.

Photooxidation of Intracellular Probe

Aliquots of RPE cells were incubated with 10 μ M DCFH or DHR123 for 1 hr, and then were either exposed to light or maintained in the dark as a control. Ten-minute light exposures were made with the 488 or 514.5 nm emissions of the Argon ion laser, or the 647.1 nm emission of the Krypton ion laser. All exposures were quantum-equivalent, delivering $\sim 4.99 \times 10^{18}$ photons/cm²-sec in the 10 min period. Following the laser exposure, the cells were lysed and the probe isolated from the lysates by SPE. Twenty- μ l aliquots were injected into the HPLC column and the probe content quantified by fluorescence detection. DCFH exhibited a clear pattern of photooxidation by laser exposure, as shown in Figure 9. In the dark, or in cell free media, there was a low level of DCF fluorescence detected, indicating that most of the probe remained in the reduced form. All three laser wavelengths resulted in DCFH oxidation, but the degree to which the probe was oxidized was clearly wavelength dependent. On a quantal basis, the Argon 488 nm output was the most efficient in producing photooxidation. In contrast, DHR123 was not consistently photooxidized (Figure 10). The amount of fluorescence recovered from exposed RPE cells labeled with DHR123 did not bear any clear relationship to the wavelength or intensity of the laser irradiation.

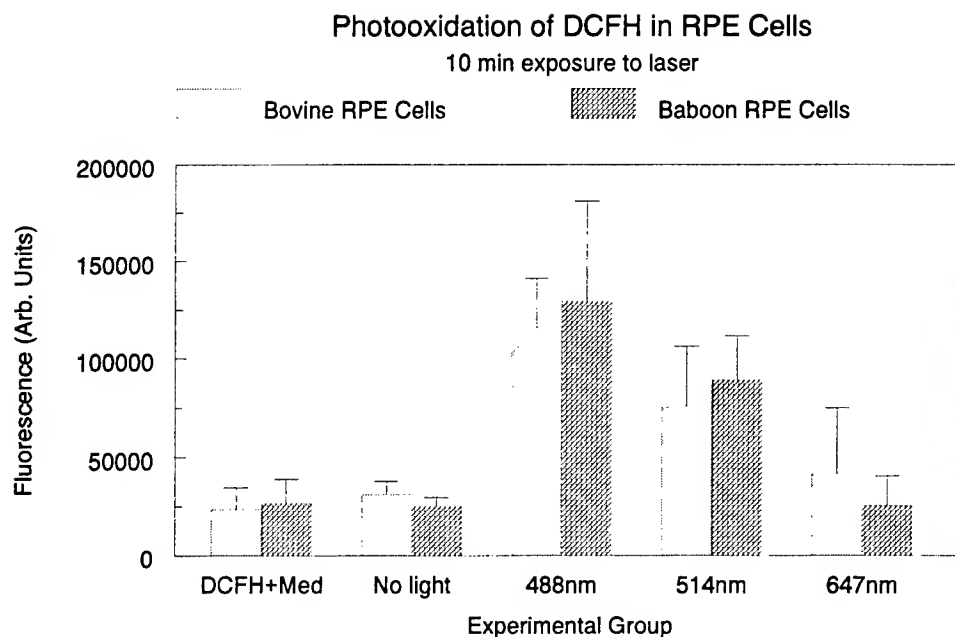


Figure 9. Photooxidation of DCFH incorporated into cultured bovine and baboon RPE cells and exposed to the indicated argon ion (488 and 514 nm) and krypton ion (647 nm) laser lines. All exposures were quantum equivalent, delivering $\sim 4.99 \times 10^{18}$ photons/cm²-sec. Further experimental details are given in the text.

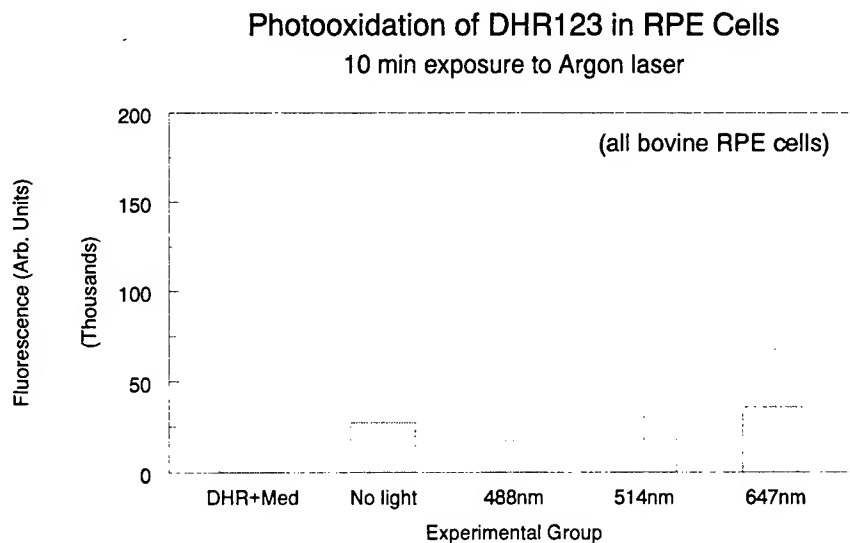


Figure 10. Photooxidation of DHR123 in RPE cells exposed to quantum-equivalent exposures at several laser lines. DHR123 is not oxidized in a wavelength-dependent manner. Experiment conducted as in Figure 9.

The failure *in situ* of DHR123 to be oxidized consistently by light exposure was puzzling, especially because it had been oxidized by laser-excited isolated melanosomes in the original pilot study. However, in the intact cell (= *in situ*), the mode of interaction between the photoactivated melanosome and the probe may be different from the *in vitro* case, perhaps requiring the intervention of a reactive intermediate that may or may not be present in adequate quantities to mediate the reaction. Another possibility is that the oxidation potential of the probes may differ enough to lead to different reaction pathways. Because there was no published information on the oxidation potential of the probes, nor was any data available from the manufacturer, we determined the half-wave oxidation potential of both probes by use of HPLC analysis with electrochemical detection. The hydrodynamic voltammograms produced by this technique are shown in Figure 11. A sigmoidal mathematical function was fit to these data, and the $E_{1/2}$ and E_0 parameters were calculated as described in the Methods. The values of these parameters are shown in Table III.

Table III
Oxidation potentials of DCFH and DHR123

(potentials in V)	DCFH	DHR123
E_0	.279	.513
$E_{1/2}$.633	.712

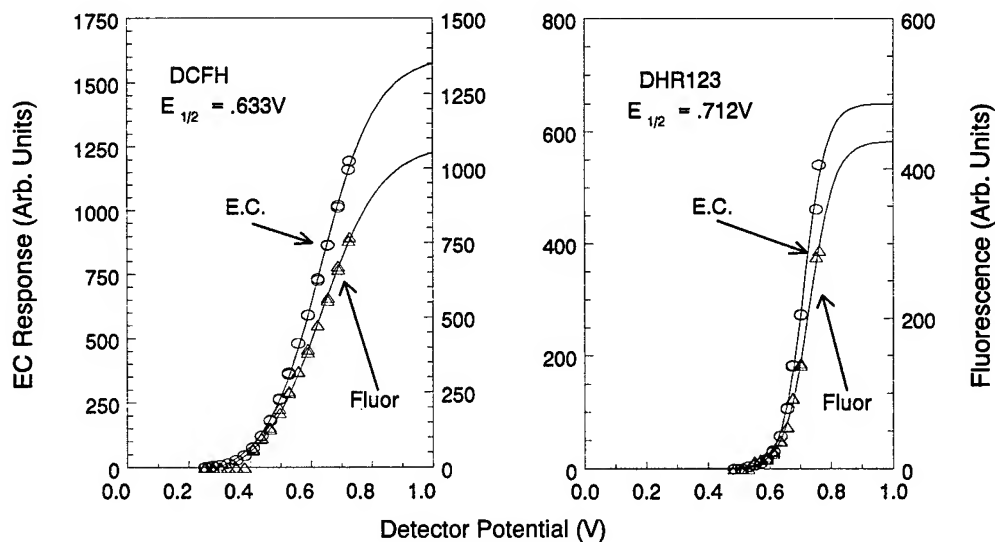


Figure 11. Hydrodynamic voltammograms of DCFH (left) and DHR123 (right). The oxidation potentials were determined by HPLC with electrochemical (E.C.) detection. A downstream fluorescence detector measured the fluorescence of the probes oxidized by the E.C. detector. As the probes were increasingly oxidized by higher working potentials in the E.C. flow cell, probe fluorescence increased. The values of the half-wave and threshold oxidation potentials were calculated from the sigmoidal functions fit to the data as described in the text.

DISCUSSION

Utility of oxidation-sensitive probes for the study of laser-induced cellular photooxidative stress

At least in the case of DCFH, the results of the present investigation show that an oxidation-sensitive probe can be introduced into a living cell, and that the fluorescence signal derived from the cell is related to the cell's recent light exposure history. Moreover, the intensity of the fluorescence is related to the wavelength of the incident light, which points to the involvement of a specific chromophore with a characteristic action spectrum. A biochemical approach, using HPLC analysis of extracted probe, proved to be the most productive method for studying photooxidative stress in RPE cells because of interference of the pigmentation itself with a strictly optical approach. Although fluorescence microscopy was not as useful as originally hoped in studying the photochemical reactions of these probes in the pigmented cells, it did reveal that the spatial extent of the fluorescence increase in the cell was restricted to the cytoplasm. While the actual cellular distribution of the probe was not determined in this study - it is possible that the probe simply did not penetrate the nucleus - there is no published data that suggests that the nucleus excludes these molecules. Additional work is necessary to resolve this issue. However, the increase in fluorescence in the cytoplasm indicates that the photoactive chromophore is located there. Further discussion below will argue that this chromophore is melanin.

Significance of the wavelength dependence of DCFH photooxidation

Although the intracellular photooxidative conversion of DCFH to DCF has been characterized for only three major laser wavelengths, the results obtained are very consistent with the action spectrum reported for the photochemical oxidation of NADPH by laser-excited RPE melanin [15]. The oxidation of NADPH in that study was used as an assay for the excitation of reactive free radical sites in the melanin heteropolymer, and the resulting action spectrum exhibited a peak in the visible spectrum between 450 and 500 nm (see Figure 12). For comparison, the data shown in Figure 9 has been normalized and superimposed on the melanin action spectrum in Figure 12. It is clear that photooxidation of DCFH in laser-exposed RPE cells follows a very similar wavelength dependence as that of NADPH. It is unclear why DHR123 was not similarly photooxidized in the RPE cell, but recently we have found that this probe has a higher oxidation potential than that of DCFH (.712 V as compared to .633 V) [37]. The higher redox potential may prevent it from reacting with the principal oxidizing species in the cell. Another possibility is that because DHR123 is more lipophilic than DCFH, the probe may be selectively taken up in membranous structures such as mitochondria where it is inaccessible to the pigment granules.

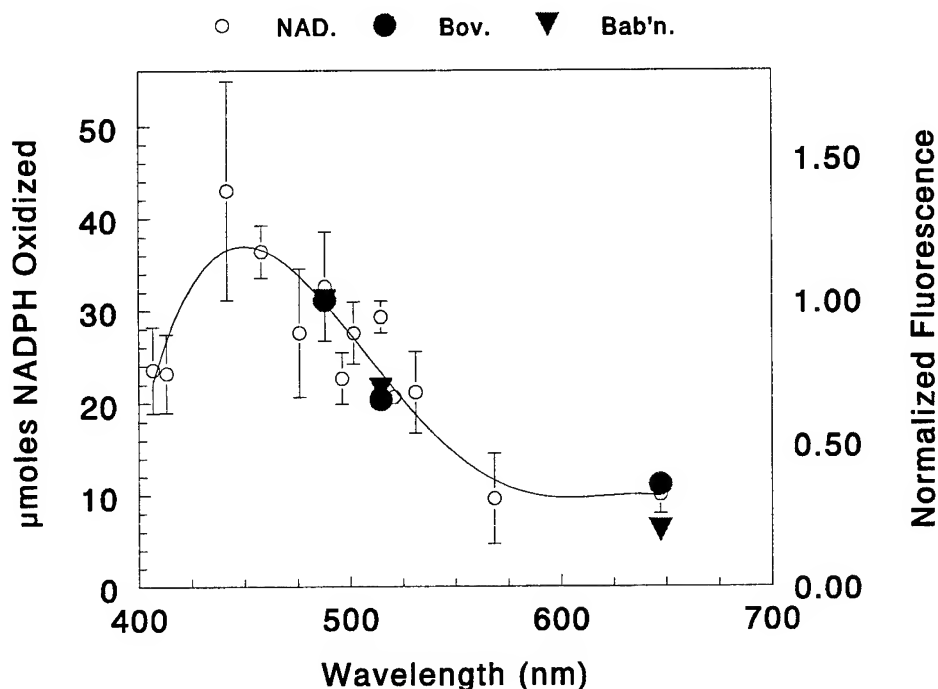


Figure 12. Action spectrum of NADPH oxidation by laser-excited melanin (all exposures $\approx 3.18 \times 10^{21}$ photons/cm²/300 sec). Open circles: photooxidation of NADPH. Superimposed data: normalized fluorescence of DCFH in bovine (filled circles) and baboon (filled triangles) RPE cells following CW laser exposure.

The localization of DCF fluorescence only in the cytoplasm of the cell argues strongly that the chromophore responsible for this photochemical reaction is one of the RPE pigment granules. Melanin is the most likely candidate; one, because of the overlap of the DCFH photooxidation data with the melanin action spectrum, and two, because lipofuscin and melanolipofuscin, the other two RPE pigment granules, are not found in appreciable quantities in the young bovine eyes used in some of the present experiments [11]. The baboon eyes were from older animals that may have contained larger amounts of lipofuscin, therefore the contribution of lipofuscin cannot be totally excluded. There was insufficient tissue available from the baboon eyes to analyze for lipofuscin. Nevertheless, because lipofuscin is capable of inducing oxidative reactions even in the dark [11], the low level of dark oxidation in our preparations suggests that the contribution of lipofuscin granules was not significant.

Consequences of photooxidation in the RPE cell

The oxidation of DCFH in laser-exposed RPE cells serves only as a beacon of oxidative stress. In the absence of any

other information, it would have limited significance. However, there are several reports in the literature concerning oxidative damage to physiological molecules due to light-activated RPE pigment granules [8,11,13,14,16,38]. Because most of these observations have been made with isolated pigments, the significance of these findings for oxidative stress *in vivo* are not yet known. The importance of the present finding is that an intracellular reporter of oxidative stress (i.e. the fluorescent probe DCFH) yields a positive signal in light-exposed pigmented cells. It is known that these probes can be oxidized by hydroxyl radical ($E^{\circ'} = +1.060\text{V}$ for $\text{HOO}\cdot \rightarrow \text{H}_2\text{O}_2$), and probably by singlet oxygen - at least for DCFH ($E^{\circ'} = +.650\text{V}$ for $\text{O}_2^1 \rightarrow \text{O}_2^{\bullet-}$). These reactive oxygen species can be produced by photochemical reactions, and indeed have been reported in studies on light-activated melanin [19,20]. Normally the RPE cells have antioxidants that quench reactive species produced directly or indirectly by light-activated pigment granules, preventing cellular damage. The cumulative effects of oxidative damage may be the basis of some of the age-related retinal degenerations. The melanosome breaks down in age, leading to the accumulation of melanolipofuscin granules along with the lipofuscin granules [1]. The melanosome is also damaged by short-pulse laser exposures [25]. The breakdown of the melanosome structure has been shown to increase its photochemical reactivity [26]. Taken together, all of these observations lead to the general conclusion that the RPE pigments may play dual roles in the eye: protecting against light damage as long as sufficient antioxidants such as ascorbic acid are present to quench the light-excited pigment radicals, but promoting light damage in the event of melanosome structural damage, antioxidant depletion, or the inability to recycle antioxidants, which is an energy-dependent process. Examination of these related aspects of RPE cell metabolism may yield new insights into the prevention of oxidative stress in the retina and its supportive tissues. The use of oxidation-sensitive fluorescent probes to provide an intracellular measure of oxidative stress ("redox status") will greatly aid research on oxidative stress in the eye resulting from laser injury, as well as from metabolic and environmental factors.

CONCLUSIONS

The oxidation-sensitive fluorescent probe, 2',7'-dichlorofluorescein diacetate, can be used to detect laser- and light-induced oxidative stress in retinal pigment epithelial (RPE) cells. This probe, which becomes fluorescent when chemically oxidized, interacts with melanosomes in the cytoplasm of the RPE cells in a wavelength-dependent fashion. Wavelengths in the region between 440 and 500 nm are the most effective in producing a fluorescence increase; longer wavelengths in particular do not induce these reactions. Another fluorescent probe, dihydrorhodamine 123, is not oxidized in a wavelength-dependent manner. DCFH, at least for short term experiments, is relatively nontoxic and appears to be a novel and sensitive reporter for intracellular photochemical damage produced as a consequence of laser and light exposures.

ACKNOWLEDGMENTS

This research was supported by Subcontract 97-0836, AFOSR/SREP. Technical assistance was provided by Ms. Neeru Kumar. Meena Vendal and Mary Ann Gonzales participated in this research project while they were Lions Summer Research Scholars.

REFERENCES

1. L. Feeney-Burns, E. S. Hilderbrand, and S. Eldridge, "Aging human RPE: morphometric analysis of macular, equatorial and peripheral cells", *Invest. Ophthalmol. Vis. Sci.* **25**, pp. 195-200, 1984.
2. M. L. Wolbarsht, A. W. Walsh, and G. George, "Melanin, a unique biological absorber", *Appl. Opt.* **20**, pp. 2184-2186, 1981.
3. T. Sarna, "Properties and function of the ocular melanin - A photobiophysical view", *J. Photochem. Photobiol. B* **12**, pp. 215-258, 1992.
4. M. Porebska-Budny, N. L. Sakina, K. B. Stepień, A. E. Dontsov, and T. Wilczok, "Antioxidative activity of synthetic melanins. Cardiolipin liposome model", *Biochim. Biophys. Acta* **1116**, pp. 11-16, 1992.
5. N. L. Sakina, A. E. Dontsov, G. G. Afanas'ev, M. A. Ostrovski, and I. I. Pelevina, "The accumulation of lipid peroxidation products in the eye structures of mice under whole-body x-ray irradiation" [Russian], *Radiobiologiya* **30**, pp. 28-31, 1990.
6. D. Yin, "Biochemical basis of lipofuscin, ceroid, and age pigment-like fluorophores", *Free Rad. Biol. Med.* **21**, pp. 871-888, 1996.
7. G. E. Eldred and M. R. Lasky, "Retinal age pigments generated by self-assembling lysosomotropic detergents", *Nature* **361**, pp. 724-726, 1993.
8. E. R. Gaillard, S. J. Atherton, G. Eldred, and J. Dillon, "Photophysical studies on human retinal lipofuscin", *Photochem. Photobiol.* **61**, pp. 448-453, 1995.
9. L. Feeney-Burns, R. P. Burns, and C. L. Gao, "Age-related macular changes in humans over 90 years old", *Am. J. Ophthalmol.* **109**, pp. 265-278, 1990.
10. R. D. Glickman, A. E. Dontsov, and M. A. Ostrovsky, "Relative photoreactivity of the pigment inclusions of the retinal pigment epithelium". In *Laser-Tissue Interaction IX*, (Edited by S. L. Jacques), **3254**, pp. 46-51, Proc. SPIE, Bellingham, WA, 1998.
11. A. E. Dontsov, R. D. Glickman, and M. A. Ostrovsky, "RPE pigments stimulate the photooxidation of

unsaturated fatty acids", *Free Rad. Biol. Med.* **in press**, 1999.

12. R. D. Glickman and K.-W. Lam, "Oxidation of ascorbic acid as an indicator of photooxidative stress in the eye", *Photochem. Photobiol.* **55**, pp. 191-196, 1992.
13. R. D. Glickman, R. Sowell, and K.-W. Lam, "Kinetic properties of light-dependent ascorbic acid oxidation by melanin", *Free Rad. Biol. Med.* **15**, pp. 453-457, 1993.
14. R. D. Glickman and K.-W. Lam, "Melanin may promote photooxidation of linoleic acid". In *Laser-Tissue Interaction VI*, (Edited by S. L. Jacques), **2391**, pp. 254-261, Proc. SPIE, Bellingham, WA, 1995.
15. R. D. Glickman, B. A. Rockwell, and S. L. Jacques, "Action spectrum of oxidative reactions mediated by light-activated melanin". In *Laser-Tissue Interaction VIII*, (Edited by S. L. Jacques), **2975**, pp. 138-145, Proc. SPIE, Bellingham, WA, 1997.
16. M. Rozanowska, A. Bober, J. M. Burke, and T. Sarna, "The role of retinal pigment epithelium melanin in photoinduced oxidation of ascorbate", *Photochem. Photobiol.* **65**, pp. 472-479, 1997.
17. H. S. Mason, D. J. E. Ingram, and B. Allen, "The free radical property of melanins", *Arch. Biochem. Biophys.* **86**, pp. 225-230, 1960.
18. F. W. Cope, R. J. Sever, and B. D. Polis, "Reversible free radical generation in the melanin granules of the eye by visible light", *Arch. Biochem.* **100**, pp. 171-177, 1963.
19. T. Sarna and R. C. Sealy, "Free radicals from eumelanin: quantum yields and wavelength dependence", *Arch. Biochem. Biophys.* **232**, pp. 574-578, 1984.
20. W. Korytowski, B. Pilas, T. Sarna, and B. Kalyanaraman, "Photoinduced generation of hydrogen peroxide and hydroxyl radicals in melanins", *Photochem. Photobiol.* **45**, pp. 185-190, 1987.
21. M. H. van Woert, "Reduced nicotinamide-adenine oxidation by melanin: Inhibition by phenothiazines", *Proc. Soc. Exp. Biol. Med.* **129**, pp. 165-171, 1968.
22. I. A. Menon and H. F. Haberman, "Mechanisms of action of melanin in photosensitized reactions". In *Pigment Cell*, (Edited by S. N. Klaus), pp. 345-351, Karger, Basel, 1979.

23. C. R. Thompson, B. S. Gerstman, S. L. Jacques, and M. E. Rogers, "Melanin granule model for laser-induced thermal damage in the retina", *Bull. Math. Biol.* **58**, pp. 513-553, 1996.
24. S. L. Jacques, "Laser-tissue interactions". In *Non-ionizing radiation: An overview of the physics and biology*, (Edited by K. Hardy, M. Meltz, and R. Glickman), pp. 81-98, Medical Physics Publishing, Madison, WI, 1997.
25. C. P. Cain, C. A. Toth, C. D. DiCarlo, C. D. Stein, G. D. Noojin, D. J. Stolarski, and W. P. Roach, "Visible retinal lesions from ultrashort laser pulses in the primate eye", *Invest. Ophthalmol. Vis. Sci.* **36**, pp. 879-888, 1995.
26. R. D. Glickman, S. L. Jacques, J. A. Schwartz, T. Rodriguez, K.-W. Lam, and G. Buhr, "Photodisruption increases the free radical reactivity of melanosomes isolated from retinal pigment epithelium". In *Laser-Tissue Interaction VII*, (Edited by S. L. Jacques), **2681**, pp. 460-467, Proc. SPIE, Bellingham, WA, 1996.
27. S. L. Jacques, R. D. Glickman, and J. A. Schwartz, "Internal absorption coefficient and threshold for pulsed laser disruption of melanosomes isolated from retinal pigment epithelium". In *Laser-Tissue Interaction VII*, (Edited by S. L. Jacques), **2681**, pp. 468-477, Proc. SPIE, Bellingham, WA, 1996.
28. R. D. Glickman, "Is there a photochemical component to retinal damage produced by ultrashort pulse laser exposures?", 4th AFOSR Ultrashort Laser Pulse Collaborative Workshop, San Antonio, TX, 24-26 March, 1996.
29. B. S. Gerstman and R. D. Glickman, "Activated rate processes and a specific biochemical mechanism for explaining delayed laser induced thermal damage to the retina", *J. Biomed. Opt.*, **Submitted**, 1999.
30. M. E. Moon, A. M. Clarke, J. J. Ruffolo Jr., H. A. Mueller, and W. T. Ham Jr., "Visual performance in the rhesus monkey after exposure to blue light", *Vis. Res.* **18**, pp. 1573-1577, 1978.
31. W. T. Ham Jr., H. A. Mueller, J. J. Ruffolo Jr., and A. M. Clarke, "Sensitivity of the retina to radiation damage as a function of wavelength", *Photochem. Photobiol.* **29**, pp. 735-743, 1979.
32. L. M. Rapp and S. C. Smith, "Evidence against melanin as the mediator of retinal phototoxicity by short-wavelength light", *Exp. Eye Res.* **54**, pp. 55-62, 1992.
33. T. G. Gorgels and D. Van Norren, "Two spectral types of retinal light damage occur in albino as well as in

pigmented rat: no essential role for melanin", *Exp. Eye Res.* **66**, pp. 155-162, 1998.

34. B. E. Loveland, T. G. Johns, I. R. Mackay, F. Vaillant, Z. X. Wang, and P. J. Hertzog, "Validation of the MTT dye assay for enumeration of cells in proliferative and antiproliferative assays", *Biochem. Int.* **27**, pp. 501-510, 1992.
35. D. T. Vistica, P. Skehan, D. Scudiero, A. Monks, A. Pittman, and M. R. Boyd, "Tetrazolium-based assays for cellular viability: a critical examination of selected parameters affecting formazan production", *Cancer Res.* **51**, pp. 2515-2520, 1991.
36. J. A. Royall and H. Ischiropoulos, "Evaluation of 2',7'-dichlorofluorescein and dihydrorhodamine 123 as fluorescent probes for intracellular H_2O_2 in cultured endothelial cells", *Arch. Biochem. Biophys.* **302**, pp. 348-355, 1993.
37. R. D. Glickman, M. A. Gonzales, N. Kumar, and M. Vendal, "Oxidative stress in retinal pigment epithelium", *Free Rad. Biol. Med.* **25(suppl 1)**, p. S102, 1998.
38. M. Rozanowska, J. Jarvis-Evans, W. Korytowski, M. E. Boulton, J. M. Burke, and T. Sarna, "Blue light-induced reactivity of retinal age pigment. In vitro generation of oxygen-reactive species", *J. Biol. Chem.* **270**, pp. 18825-18830, 1995.

PREDICTING ALTITUDE DECOMPRESSION SICKNESS
USING SURVIVAL MODELS

Nandini Kannan
Assistant Professor
Division of Mathematics and Statistics

University of Texas at San Antonio
6900 N. Loop 1604 West
San Antonio, TX 78249

Final Report for:
Summer Research Extension Program
Armstrong Laboratory

Sponsored by:
Air Force Office of Scientific Research
Bolling Air Force Base, DC

and

Armstrong Laboratory

December 1997

PREDICTING ALTITUDE DECOMPRESSION SICKNESS USING SURVIVAL MODELS

Nandini Kannan
Assistant Professor
Division of Mathematics and Statistics
University of Texas at San Antonio

Abstract

The application of survival models to predict the probability of altitude decompression sickness was studied. Bootstrap methods were used to develop confidence bands for the survival function to ascertain the accuracy of the predictions. Estimates of the change point of the risk function were obtained and bootstrap methods used to construct confidence intervals for the change point. Data on bubbles was incorporated into the survival model to assess the effect of bubble onset time on symptoms.

PREDICTING ALTITUDE DECOMPRESSION SICKNESS USING SURVIVAL MODELS

Nandini Kannan

1. INTRODUCTION

Individuals exposed to significant changes in environmental pressure encountered during diving, high altitude exposures or artificially induced pressure changes in hyperbaric or hypobaric chambers may experience symptoms of Decompression Sickness (DCS). These include joint pain, respiratory difficulties, nervous system problems, and in some extreme situations, even death. The onset of these symptoms have been attributed to the growth of nitrogen bubbles in body tissue. When there is a significant change in ambient pressure, the gas exchange processes in the tissues are unable to expel the excess nitrogen causing supersaturation. These gases which come out of solution when tissues are sufficiently supersaturated collect as bubbles in the tissue. The location of these bubbles and their size are thought to have a significant effect on the manifestation of symptoms.

Crews operating in unpressurized/ inadequately pressurized aircraft or performing extravehicular activity (EVA) in space must assume some level of DCS risk. The range of this risk depends on the length of exposure, final altitude, level of physical activity, preoxygenation time, type of breathing gas mixture, and several other factors that affect bubble formation and growth. The ability to predict/ assess the risk of DCS real-time, as well as for planning of future missions is an operational need in both military and civilian aerospace applications. The High Altitude Protection Function at Armstrong Laboratory, Brooks Air Force Base has been actively pursuing the development of an appropriate model to answer these very practical and important questions.

The Armstrong Laboratory has for many years conducted research using human subjects exposed to simulated altitude in hypobaric chambers. The subjects are

exposed to different altitudes, varying denitrogenation times, different breathing gas mixtures, and levels of exercise determined by the flight protocol. They are monitored constantly for symptoms of DCS. The experiment either lasts the entire exposure period or terminates when an individual exhibits symptoms. While at altitude, subjects are also monitored for venous gas emboli (VGE) using echocardiography. Data from these experiments has been deposited in the Armstrong Laboratory database and will provide the foundations for the modeling efforts.

Over the past two years, statistical models have been developed to predict the probability/ risk of DCS for different flight profiles. These models use techniques from survival analysis to express the probability/ risk of DCS as a function of several risk factors. As part of the AFOSR Summer Research Extension Program, I have been involved in examining the properties of the models and conducting further statistical analysis of the data. This report summarizes the findings and results of this investigation.

At present, a validation study is underway at the Armstrong Laboratory to investigate the performance of these survival models. The final product of this and other research efforts will be a validated statistical and mathematical model that will be used for risk assessment in USAF flight and altitude chamber operations. The model will provide the foundation for advanced development of a standardized altitude decompression computer.

2. BACKGROUND

A survey of the literature in the area of DCS modeling reveals a large body of work devoted to diving models. Those articles that do deal with altitude DCS are simply modifications of diving models. This approach has its limitations because there are certain characteristics unique to high altitude exposure. The first difference is the faster ascent rate in high altitude situations compared to the slower ascent rates for divers. In aircraft, there is a significant threat of instantaneous loss of pressure. In

addition, in most aerospace operations, symptoms of DCS occur during the mission. In contrast, in the diving field, symptom occurrence is post mission. In light of these differences, it seems unreasonable to use diving models to predict altitude DCS. There are a limited number of articles that do deal with models for altitude DCS, but a standardized approach does not seem to be available. We briefly describe some of the relevant literature in this area.

One of the earliest attempts at modeling DCS was by Weathersby [1], [2]. He described several probabilistic models for predicting the occurrence of DCS, using maximum likelihood methods to fit these models to DCS data. The first article only considered the presence/ absence of symptoms as the response variable. The second article, did however, incorporate some information on the onset time of symptoms. Both articles considered data from diving experiments. Van Liew et al [3] developed a probabilistic model of altitude DCS assuming that the risk of DCS is related to the number of bubbles and the volume of gas that can be liberated from a unit of tissue. A dose-response model relating the probability of occurrence of symptoms and several independent variables accounting for decompression stress was considered. The risk function incorporated several mathematical equations describing the mechanistic principles of bubble growth. Several models were tested and evaluated on the basis of how well they fit the data. The data used in the article was an accumulation of records on human exposures in altitude chambers from different sources. The factors affecting DCS used in this article were 100% O_2 at ground level (preoxygenation), atmospheric pressure after ascent, and exposure duration.

Models for bubble growth have also been studied by Gerth and Vann [4]. In their paper, they developed an extensive model for bubble dynamics to provide an assessment of DCS. The equations considered in the paper to describe bubble dynamics are similar to those in Van Liew et al. The models considered in the article are the standard dose-response models with the percentage of symptomatic individuals being the response variable. The unknown parameters in the model were estimated using

maximum likelihood methods. In the report, the authors make the observation that symptom onset times need to be included for the model to be more realistic.

There are some drawbacks to the approaches used in the articles described above. Most of these models involve complex equations describing bubble growth based on certain physiological assumptions. It is extremely difficult to verify these assumptions with real data, data on bubble characteristics is limited to VGE measurements on the Spencer scale. These models only use the percentage of symptomatic individuals and ignore the symptom onset time. Information on asymptomatic individuals (a very large percentage of individuals complete the experiment without exhibiting any symptoms) is not adequately incorporated into the model. In addition, these models offer limited information about the effects of different risk factors on the occurrence of DCS.

Methods based on survival analysis seem to be the most appropriate for modeling DCS because the time to occurrence of symptoms is not fixed but a random event. Individuals exposed to identical experimental conditions will not all display symptoms, and the onset times for those that do exhibit symptoms vary widely. Kumar et al [5], [6], [7] in a series of papers, discussed survival models for predicting DCS. Logistic and loglinear models were developed to predict DCS as a function of Tissue Ratio (a measure of tissue nitrogen decompression stress) and CMB (circulating microbubbles) status. Maximum likelihood techniques were used to estimate the parameters of the models, the response variable being the logarithm of symptom onset time. Conkin et al [8] in a recent article developed loglogistic survival models using data from 66 NASA and USAF hypobaric chamber tests. The models examined the effects of Tissue Ratio and exercise status (yes, no) on the risk of DCS and also incorporated some of the mechanistic principles of bubble growth.

All the articles referenced above are limited to examining the effects of one or two risk factors on the probability of DCS. However, the risk of DCS over time is influenced by several competing factors like altitude, preoxygenation duration, ex-

posure duration, and level of exercise performed during the exposure. In order to develop a comprehensive model that describes altitude DCS, it is essential to include all these factors and determine their relative importance. In addition, these models do not account for the varying number of subjects in different protocols and the large variation in exposure times.

To address these limitations, Kannan, Raychaudhuri, and Pilmanis [9] developed a model based on the loglogistic distribution incorporating several risk factors. Using data from the Armstrong Laboratory database, the model identified pressure, ratio of preoxygenation to exposure time, and exercise level as the most significant risk factors. The model also adjusted for the large variation in exposure times by assigning weights to the observations. Maximum Likelihood methods were used to obtain the parameter estimates. The estimated survival function was used to predict the probability of DCS for a variety of exposure profiles. The predictions from this model agreed closely with empirical data from the USAF database. However, further analysis is necessary in order to evaluate the performance of the model.

In this study, several aspects of the loglogistic model have been examined in detail. In particular, confidence bands for the survival function have been developed using bootstrap techniques. Estimates of the time at which the instantaneous risk is maximum have also been derived. Data on bubbles and their onset times have also been incorporated into the model.

In the next section, we discuss the role of survival analysis in DCS modeling and provide details about the loglogistic model.

3. METHODOLOGY

The onset time of DCS symptoms varies from individual to individual and also depends on the flight characteristics. It is also evident from the data that not all individuals exposed to the same flight conditions will exhibit symptoms. These observations suggest the need for survival analysis techniques to develop models for

predicting the probability/ risk of DCS. Survival Analysis refers to statistical methods for analyzing data on the lifetime or failure time of humans or components.

The primary variable of interest is the survival time, the time to occurrence of a disease/ symptom. For the dataset under investigation, the survival time is the onset time of DCS symptoms. In recent years, the focus of research in survival analysis has been the identification of risk or prognostic factors related to the development of the disease or symptom. We provide some basic definitions from survival analysis in the appendix. However, for a comprehensive treatment we refer the reader to the books by Lee [10], Lawless [11], and Kalbfleisch and Prentice [12].

The first step in survival analysis is to develop an appropriate model for the survival time T using various forms of the probability density function (pdf). Each pdf has its unique characteristics and determines its' corresponding survival and risk functions. The most widely used distributions in survival analysis are the exponential, gamma, Weibull, lognormal, and loglogistic.

The choice of the appropriate distribution is usually made by determining the shape of the risk function that best describes the data. The risk function can be a constant function of time (exponential), increasing/ decreasing (Gamma) or bathtub shaped, i.e. nonmonotonic (lognormal). From empirical evidence, and the physiology of DCS it is known that the risk of DCS increases over time as nitrogen bubbles form in the tissues, reaches a maximum, and then decreases because of denitrogenation. This limits the choice of models to distributions whose risk function have an inverted bathtub shape. The lognormal, loglogistic, and inverse gaussian distribution all fall into this category.

One of the problems unique to survival data is the notion of "censored" or incomplete data. In the chamber experiments, a subject is brought down to ground level as soon as he or she experiences any symptoms associated with DCS. For these individuals, the time to onset of symptoms is available. However, several individuals remain in the chamber for the entire exposure period without experiencing any

symptoms. In these cases, we have no information on their symptom onset time. It is possible that these individuals would become symptomatic if the exposure duration were increased. These are the censored observations and it is vital that information from these individuals be appropriately incorporated into the model.

Once an appropriate model has been selected, we may obtain the likelihood function which describes the probability of observing the actual data points and includes information from both censored and uncensored individuals. The likelihood function depends on several unknown parameters corresponding to the risk factors as well as parameters unique to the underlying distribution. The likelihood is maximized to obtain estimates of the underlying parameters.

In the paper by Kannan, Raychaudhuri, and Pilmanis [9], both the loglogistic and lognormal distributions were fit to the database. To examine the fit of the model, the loglikelihood values can be compared. Since both models produced almost identical loglikelihood values, the loglogistic model was selected because of its' simpler form. The survival function for the loglogistic distribution is given by

$$S(t) = \frac{1}{1 + (\lambda * t)^\gamma}$$

where the parameter λ is related to the risk factors through the following function

$$\lambda = \exp(-\beta' x)$$

Here x is the vector of risk factors, and β the vector of corresponding parameters. The parameter γ is the scale parameter for the loglogistic distribution. The hazard/risk function for the loglogistic distribution is given by

$$r(t) = \frac{\lambda \gamma (\lambda * t)^{\gamma-1}}{1 + (\lambda * t)^\gamma}.$$

The likelihood function is given by

$$L(\beta, \gamma) = \prod_{i=1}^M f(t_i) \prod_{j=1}^{N-M} S(t_j),$$

where $f(t)$ is the loglogistic probability density function, N is the total number of subjects, and M denotes the number of symptomatic individuals. The LIFEREG procedure of the statistical software package SAS can be used to maximize $L(\beta, \gamma)$ to obtain the maximum likelihood estimates of the parameters. Because of the large variability in the exposure times (180-480 minutes), and subsequently the large variations in the onset times, it was decided to include weights in the model. The weights were determined by forming groups based on environmental and physiological conditions and computing the standard deviation of DCS onset times in the different groups. The likelihood function can be modified to incorporate these weights as follows:

$$L(\beta, \gamma) = \prod_{i=1}^M [f(t_i)]^{w_i} \prod_{j=1}^{N-M} [S(t_j)]^{w_j}.$$

Once estimates of the parameters β and γ are computed, we obtain estimates of the survival and risk functions, viz. $\hat{S}(t)$ and $\hat{r}(t)$ by replacing the parameters by their maximum likelihood estimates. These estimates can then be used to predict the probability/ risk of DCS over time for a variety of exposure profiles.

When using models for prediction purposes, it is also very important to provide a measure of accuracy of these predictions. Most statistical packages that analyze survival data will provide confidence intervals for the survival probability at different time points. However, we would like an overall assessment of accuracy of the estimated survival/ risk functions. This can be achieved by constructing a confidence band that will contain, with a high confidence level, the entire unknown survival function. In the next section, we discuss the methods available in the literature for constructing confidence bands, and examine their properties.

3.1 Confidence Bands

Most confidence bands for the cdf or survival function are based on applications of the classical Kolmogorov-Smirnov test for an empirical distribution function. However this approach leads to bands that are of constant width. This is unreasonable

especially in the tails of the function. The bands also tend to exceed one or become negative which again is not a desirable property. To avoid this problem, Srinivasan and Wharton [13] have constructed confidence bands for the Weibull distribution exploiting certain properties of the distribution. If the form of the distribution is known except for certain unknown parameters, Chang and Iles [14] have developed a method based on maximum likelihood estimation of the parameters. The method automatically provides a band whose ordinate values lie between 0 and 1. Detailed results are provided for a location-scale parameter model.

These methods however deal with complete data. If censoring is present, the problem can be quite challenging. Nair [15] compares the performance of several methods for arbitrarily right censored data. Most of the literature is based on the Kaplan-Meier estimator of the survival function and its' limiting distribution. The Kaplan-Meier estimator reduces to the usual empirical distribution function in the absence of censoring. The most widely used confidence band is that of Hall and Wellner [16]. The band is constructed assuming large samples and reduces to the Kolmogorov band in the absence of censoring. In the article, Nair discusses an Equal Precision band constructed by adapting the standard confidence intervals based on Greenwood's variance formula. A numerical example is provided to compare the widths of the bands for three different methods.

Most of the methods discussed above are based on asymptotic theory, i.e. hold only for large samples. If the form of the distribution is known, these bands tend to be overly conservative, i.e. the bands are very wide. For small samples, exact confidence bands are extremely difficult to obtain. In these situations, resampling techniques like the bootstrap provide a powerful and efficient alternative. Bickel and Krieger [17] discuss the construction of bootstrap confidence bounds for any arbitrary cdf. These bands are known to have the correct coverage probability for large samples. In addition, a simulation study shows that the bootstrap works well for small samples, and outperforms traditional methods based on the Kolmogorov-Smirnov test statistic.

Based on the above observations, it seems reasonable to construct confidence bands based on the bootstrap. A brief outline of the basic principles of the bootstrap as applied to DCS data is given below.

3.2 Bootstrap Confidence Bands

Let $x = (x_1, \dots, x_n)$ be a random sample of size n from a probability distribution F . We will assume that F depends on an unknown parameter θ . Let \hat{F} be the empirical distribution, which puts a probability of $1/n$ on each of the observed values $x_i, i = 1, \dots, n$. A bootstrap sample is defined to be a random sample of size n drawn from \hat{F} , i.e. a bootstrap sample is nothing but a sample of size n drawn with replacement from the original data. Let us denote the bootstrap sample by $x^* = (x_1^*, \dots, x_n^*)$. Using the bootstrap sample, we maximize the loglikelihood function to obtain an estimate of the parameter θ . This provides an estimate of the survival function $\hat{S}(t)$ and the risk function $\hat{r}(t)$.

We generate $B = 500$ bootstrap samples and repeat the entire process. For each sample, the survival and risk functions are evaluated at several time points. At each time point, the 5th and 95th percentiles of these estimates provide the lower and upper confidence bound for a 90 % confidence band. These points together generate the confidence band for the survival/ risk function. For further details on the bootstrap, we refer the reader to the book by Efron and Tibshirani [18].

The DCS database consists of multiple observations for each flight profile. The sample size varies from profile to profile. In order to adapt the bootstrap method, we consider our initial sample to be all observations on a particular flight profile. Since the levels of the risk factors are the same for all the datapoints, the likelihood function depends on only two parameters: λ and γ . To obtain the parameter estimates, the likelihood function must be maximized. The likelihood equations are highly nonlinear and explicit solutions are not available. We need to use numerical techniques to obtain a solution to the likelihood equation. For each bootstrap sample, an iterative

algorithm will be used. Clearly the computational complexity of the problem is extensive. We have written a program in Fortran using optimization subroutines from the IMSL Math/ Stat library to solve the numerical problem. We have illustrated the performance of the bands in the Results section.

3.3 Estimation of the Change Point

The risk of DCS is known to increase over time, reach a maximum, and then decrease because of denitrogenation. It is clearly of interest to obtain an estimate of the time at which the instantaneous risk is maximum. Providing a time interval in which the pilot is at maximum risk for DCS could be used in mission planning. In this interval, perhaps additional precautions could be taken like reducing the level of exercise or descending to a lower altitude. There have been some studies which require staged decompression or multiple decompressions. Staged decompressions are profiles where the individual remains at certain altitudes for specified intervals of time before they reach the target altitude. Multiple decompressions are profiles where the individual reaches a certain altitude and remains there for a specified interval, then comes down to a lower altitude and goes back up again. Preliminary analysis of such data shows a reduced rate of DCS when compared to regular profiles. Estimates of the change point could be used in designing a mission with a reduced risk of DCS. The analysis of data based on staged/ multiple decompressions is a challenging problem and definitely needs further investigation.

We now derive the expression for the change point for the loglogistic distribution. The risk function is

$$r(t) = \frac{\lambda\gamma(\lambda * t)^{\gamma-1}}{1 + (\lambda * t)^\gamma}$$

and for $\gamma > 1$ has an inverted bathtub shape. To determine the time at which the risk function is maximum, we set the derivative of $r(t)$ with respect to t equal to zero and solve for t_{max} . The exact solution to this equation is given by

$$t_{max} = \frac{(\gamma - 1)^{1/\gamma}}{\lambda}.$$

The maximum likelihood estimate of t_{max} is obtained by substituting the maximum likelihood estimates of λ and γ in the above equation. To draw inferences about the change point, we need an estimate of the standard deviation. Since \hat{t}_{max} is a nonlinear function of $\hat{\lambda}$ and $\hat{\gamma}$, an explicit formula for the variance is not available. We will therefore resort to resampling techniques like the bootstrap and the jackknife to obtain an estimate of the variance and construct confidence intervals.

For the bootstrap method, we select B samples of size n with replacement from the original data. For each sample, we maximize the loglikelihood function to obtain estimates of the parameters, and consequently an estimate of t_{max} . The bootstrap estimate of the standard deviation is given by

$$\hat{\sigma} = \left[\frac{1}{B-1} \sum_{i=1}^B (\hat{t}_i^* - \bar{t}^*) \right]^{1/2}$$

where \hat{t}_i^* is the estimate of t_{max} from the i -th bootstrap sample, and \bar{t}^* is the average of the bootstrap replications. Confidence intervals for the change point can also be constructed using the percentiles of the bootstrap replicates.

As discussed earlier, the resampling can be done using the entire dataset or only the data on a particular profile. If the entire dataset is used, the likelihood function now involves many more parameters, i.e. we would need to estimate the vector β as well as γ . This multidimensional optimization problem is exceedingly complex and very challenging to implement. A Fortran program has been written to maximize the loglikelihood function using subroutines from the IMSL library.

In the results section, we have provided the estimates of the change point for different flight profiles along with the bootstrap average and the confidence limits.

3.4 Bubble data

The last part of the study involved assessing the effects of VGE data on the manifestation of symptoms and on the probability of DCS.

The symptoms of DCS are caused by the growth of nitrogen bubbles in the tissue. The size and locations of these bubbles are believed to have a significant effect on the manifestation of symptoms. However, it is still not clear where these bubbles originate, and how exactly they affect the onset of symptoms. To study these issues, subjects are monitored for venous gas emboli (VGE) during the entire exposure period using echocardiography (Hewlett Packard SONOS 500, 1000, and 1500). Readings are taken at regular intervals on the density of bubbles observed. The severity of microbubbles detected are graded on Spencer's scale as follows: Grade 0 indicates no bubbles, Grade 1 indicates very few bubbles, Grade 4 indicates large numbers of circulating microbubbles. The data recorded includes the bubble density and the time of occurrence.

The bubbles that are observed are circulating microbubbles and it is clear that these are not directly the cause of symptoms. It is also unclear whether the presence of these bubbles is somehow correlated to the size or growth of the bubbles that do cause symptoms. However, it is not possible to obtain measurements on the size or location of the bubbles that directly impact symptoms, and VGE data is the only observable measurement of bubble activity.

In a previous report, Kannan and Raychaudhuri [19] have shown that in individuals who have at least bubbles of grades 2 or more, the time at which the bubble grade is maximum (MAXT) is highly correlated with symptom onset time. A loglogistic model was fit to the data adding MAXT as a risk factor. The results indicate that MAXT is highly significant, dampening the effects of the other risk factors. Considering the effects that the risk factors like exposure time, altitude, and exercise level have on the size and onset of bubbles, this was not surprising.

The loglogistic model using MAXT was used to predict the probability of DCS for several profiles. For profiles with low preoxygenation times, the predictions were

significantly closer to the database values compared with the model that did not include bubble data. However, the problem with considering MAXT as a risk factor is that, unlike, the other risk factors, it is not fixed by the profile but varies from individual to individual. An estimate of MAXT must be provided before the model can be used for prediction. Petropoulos et al [20] have developed a mathematical model describing the growth of bubbles in tissue. The model provides an estimate of the time at which the bubble reaches its' maximum size. This time has been used as an estimate of MAXT in the loglogistic model and works reasonably well.

There is, however, a lot of information in the database on bubbles that could possibly be used to improve the model. The time at which the first bubbles are detected, though not as highly correlated with symptoms as MAXT may provide an early warning of symptoms. Another variable that seems relevant is the interval between the first occurrence of bubbles and the time at which the bubble grade is highest. We fit loglogistic models to the database adding these risk factors and evaluated the predictions from these models. The results are provided in the next section.

4. RESULTS

The database maintained at the Armstrong Laboratory includes detailed information on the flight protocol and subject information. Both male and female subjects participated in the study. The subjects were all Air Force personnel aged 18-45 with similar physical characteristics, representative of the USAF rated aircrew population. The data collected in the study included the time to onset of DCS symptoms (ONSET), time of preoxygenation (BR), pressure/ altitude (PRES), time at maximum altitude (TALT), and exercise code (EX). Other variables included in the database are gender, age of subject, blood pressure, measure of bodyfat, smoking status etc. While in the chamber, subjects were constantly monitored for VGE and symptoms. If the subject exhibited any symptoms indicative of DCS, the experiment was termi-

nated and the subject brought down to ground pressure. If the subject reported no symptoms, the subject remained in the chamber for the entire exposure duration.

For individuals reporting no symptoms, their onset time was replaced by their corresponding TALT times. A censoring variable (CENSOR) was created to indicate the status of each individual: 1-DCS and 0-No DCS (Censored). The dataset used in the analysis contained 975 subject exposures of which 469 were censored, i.e. 48 % of individuals were asymptomatic.

The pressure levels used in the analysis ranged from 141 mm Hg to 314 mm Hg. The preoxygenation times ranged from 0 to 240 minutes. Different types of exercise were performed during altitude. These were classified as rest, mild exercise, or heavy exercise according to the oxygen consumption. All exposures in this database used the same ascent rate and the same breathing gas mixture.

Once the data were available, an exploratory analysis was conducted. In decompression studies, the amount of time spent in preoxygenation is known to have a significant effect on reducing DCS risk. However, a cursory examination of the database indicated an increase in the rate of DCS for increased preoxygenation times. This anomaly was because higher preoxygenation times were commonly observed for flight profiles with long exposure times and higher altitudes. To adjust for these differences, a new variable BRTALT was created which is the percentage of total exposure time spent in preoxygenation. Clearly a high value of BRTALT indicates one of two possibilities: longer preoxygenation times or shorter flight durations. High values of this variable are associated with low risks of DCS which is in line with empirical evidence.

In the paper by Kannan et al [9], a loglogistic distribution was fit to the data. Three covariates or risk factors were included in the model: PRES, BRTALT, EX. The pressure values were included on a log scale. Weights were incorporated into the likelihood equation to adjust for the large dispersions in the data set. These weights were obtained by computing the standard deviation of onset times in different groups. The groups were created based on environmental and physiological conditions.

The output from the SAS programs (Table 1) provides the parameter estimates, the standard error of the estimates and a chi-square value used to determine the relative importance of the different factors. Pressure was clearly the most important determinant, followed by exercise and the proportion of total exposure time spent in prebreathing. The coefficients for all three covariates were highly significant (p-value < 0.001), indicating their importance in predicting the risk of DCS. The loglikelihood value (a measure of how well the model fits the data) was -560.84. The estimate of γ is the reciprocal of the SCALE parameter given in the table.

Table 1: Parameter estimates for the weighted model

Variable	DF	Estimate	Std. Err.	Chi-sq	p-value
INT	1	-8.00	2.45	10.63	0.0011
PRES	1	2.53	0.44	32.57	0.0001
BRTALT	1	1.29	0.39	11.26	0.0008
EX	1	-0.53	0.14	13.68	0.0002
SCALE	1	0.60	0.03		

Using these parameter estimates, we obtain estimates of the survival and risk functions. These estimates can be used to predict the probability/ risk of DCS over time for specific flight profiles. In the next subsection, we provide bootstrap confidence bands for the survival function based on this model.

4.1 Bootstrap Confidence Bands

Using the bootstrap algorithm discussed earlier, we computed the confidence bands for a variety of different profiles. These profiles were selected because of their relatively large sample sizes. The 90 % confidence bands for the cdf for three different profiles are given in Figures 1-3. The lower and upper confidence limits are denoted by the dotted lines. The solid line is the predicted cdf obtained using the parameter

estimates from Table 1.

The points represent the actual data values, i.e. the empirical distribution function. The graphs clearly indicate that the 90 % confidence bands based on the loglogistic distribution do indeed cover the empirical data. There are some points that are outside the bands, but overall the model does seem to perform well. One can clearly see that these confidence bands are not of equal width, and are also not symmetric with respect to the predicted cdf. This is not unusual when using bootstrap techniques.

The bootstrap confidence intervals have provided statistical evidence that the loglogistic model does indeed provide very good predictions. Further research is needed to develop confidence bands for profiles not available in the database.

4.3 Inference on the Change Point

The maximum likelihood estimate of the change point for a particular profile is given by

$$\hat{t}_{max} = \frac{(\hat{\gamma} - 1)^{1/\hat{\gamma}}}{\hat{\lambda}}.$$

where the estimates of the parameters are obtained from Table 1. In Table 2, we provide the maximum likelihood estimate of t_{max} , the average of the bootstrap replications (BAV), and the lower and upper confidence limits using the percentiles of the bootstrap replications. In the bootstrap algorithm implemented here, we resampled from the entire dataset. For each sample, a function of 5 variables was maximized to obtain the parameter estimates.

The results show that the mle and the bootstrap average are quite close. The 90 % confidence interval clearly contains the mle. This confidence interval provides the time interval that includes the point at which the instantaneous risk is maximum. Similar results held for a variety of different profiles.

4.1 Models for Bubble Data

Table 2: Estimates of t_{max}

Profile	MLE	BAV	LCL	UCL
PRES = 231, BR = 75 TALT = 240, EX = 2	131.29	133.12	119.99	145.74
PRES = 253, BR = 60 TALT = 480, EX = 2	129.19	131.03	117.73	144.09

We fit loglogistic models to the data using the risk factors considered earlier with the addition of MAXT-the time at which the bubble grade is maximum, FTIME-the time at which the first bubbles are detected, and TINT-the difference in times between MAXT and FTIME. Since not all individuals had bubbles, we only considered individuals whose maximum bubble grade was 2 or more. In the presence of bubble onset times, the exercise factor was found to be insignificant and was dropped from further analyses. However, it is still implicitly accounted for because exercise affects the onset time of bubbles. The first model considered used MAXT and FTIME along with the other risk factors. The ANOVA table from SAS is provided below.

Table 3: Parameter estimates using Bubble Data

Variable	DF	Estimate	Std. Err.	Chi-sq	p-value
INT	1	-3.31	1.78	3.47	0.0627
PRES	1	1.27	0.32	16.09	0.0001
BRTALT	1	0.91	0.29	9.34	0.0022
MAXT	1	0.01	0.01	88.93	0.0001
FTIME	1	-.003	0.01	5.06	0.0245
SCALE	1	0.36	0.02		

The group consisted of 623 individuals who recorded atleast maximum grades of 2 or higher. Clearly, MAXT has a tremendous effect on the probability/ risk of DCS accounting for a very, very high Chi-squared value. The first time of occurrence is not that significant. In order to assess the impact of introducing FTIME, we compared the predictions from the models with and without FTIME to see if there is any improvement. The graphs of the cdf for a specific profile are given in Figure 4. The points represent the empirical data. The graph that includes FTIME is marginally closer to the datapoints. We may infer that the addition of FTIME does indeed improve predictions.

The second model included TINT and FTIME as risk factors. In this case, only individuals with maximum grades of 3 and 4, and an initial bubble grade of 2 or higher were included in the analysis. The ANOVA table is given below.

Table 4: Parameter estimates using Bubble Data

Variable	DF	Estimate	Std. Err.	Chi-sq	p-value
INT	1	-3.02	1.75	2.97	0.0846
PRES	1	1.22	0.31	15.29	0.0001
BRTALT	1	0.83	0.29	7.99	0.0047
TINT	1	0.01	0.01	94.81	0.0001
FTIME	1	0.01	0.01	122.97	0.0001
SCALE	1	0.35	0.02		

The dataset consisted of 589 individuals. The ANOVA table shows that the time at which bubbles first occur is highly significant, however so is the interval between the first occurrence and the time at which the grade is maximum. This suggests that not only is the time of occurrence important, so is the speed with which bubbles grow. Again we compared the cdf's for this model with the model that includes just MAXT (Figure 5). Again there is an improvement (though slight) using additional

information about bubbles.

There is still a lot of work to be undertaken in this area. Mathematical models that describe bubble growth need to be incorporated into the statistical model. A better understanding of the relation between circulating microbubbles and bubbles that cause symptoms needs to be obtained. This is ongoing research in collaboration with researchers at Brooks AFB. The validation study currently underway will provide an opportunity to assess the performance of these models in greater detail.

5. CONCLUSION

Survival analysis techniques have been used to determine an appropriate model to predict the probability/ risk of DCS as a function of several risk factors. The loglogistic model was found to provide the best fit, and indicated that pressure, ratio of preoxygenation to exposure time, and exercise were the most significant risk factors. Predictions from this model for different profiles agreed closely with empirical evidence from the database. Confidence bands for the survival function were constructed using bootstrap techniques and provided statistical evidence that the predictions from the model are very accurate.

Estimates of the change point of the risk function were also obtained and confidence intervals constructed using the bootstrap. Data on bubbles was incorporated into the model, and, specially for low preoxygenation times improved predictions significantly.

Current research includes the assimilation of mathematical models of bubble growth into the loglogistic model to provide a comprehensive description of DCS. The validation study will provide the opportunity to assess the model further and provide the framework for development of a standardized altitude decompression computer.

Acknowledgments:

The author would like to thank Dr. Andrew A. Pilmanis, Chief, High Altitude Protection Function, Armstrong Laboratory, Brooks AFB, Dr. James T. Webb and Mr. Lambros Petropoulos of Krug Life Sciences for their assistance during this project.

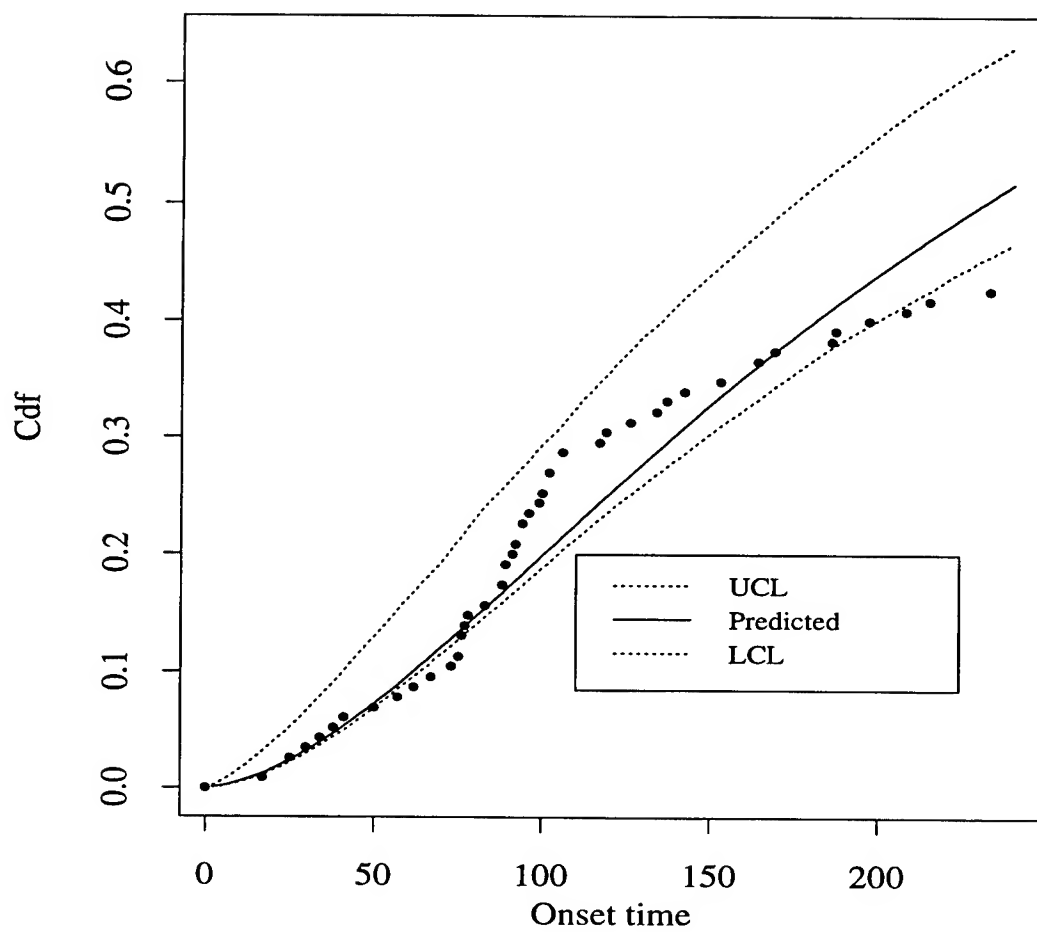


Figure 1: Confidence bands: PRES = 231, TALT = 240, EX = Mild, BR = 135

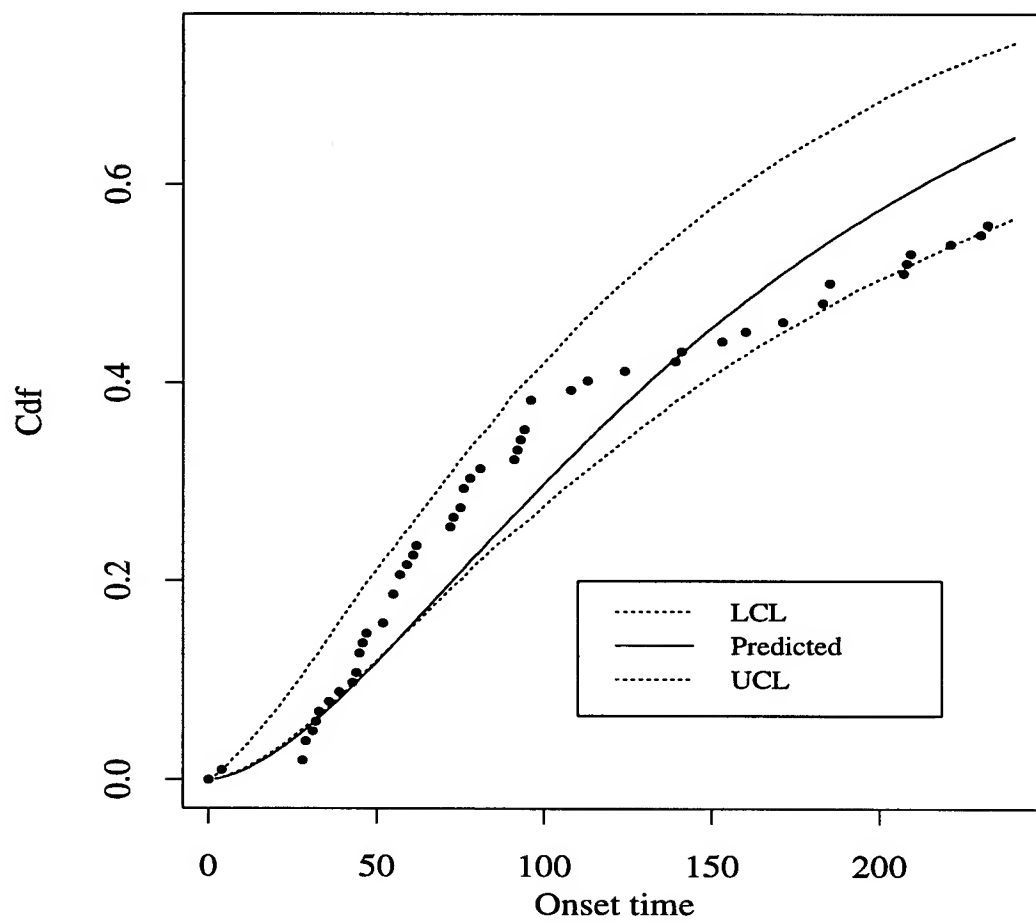


Figure 2: Confidence bands: PRES = 231, TALT = 240, EX = Mild, BR = 75

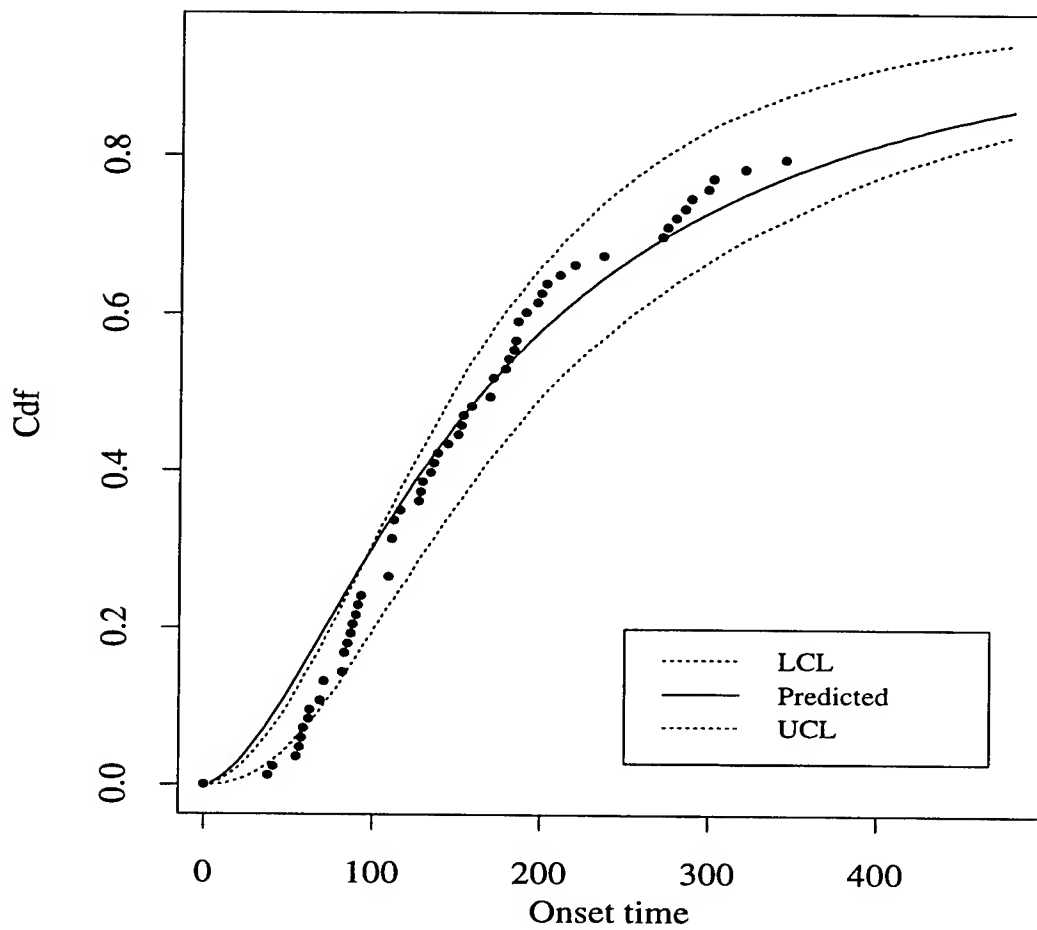


Figure 3: Confidence bands: PRES = 253, TALT = 480, EX = Mild, BR = 60

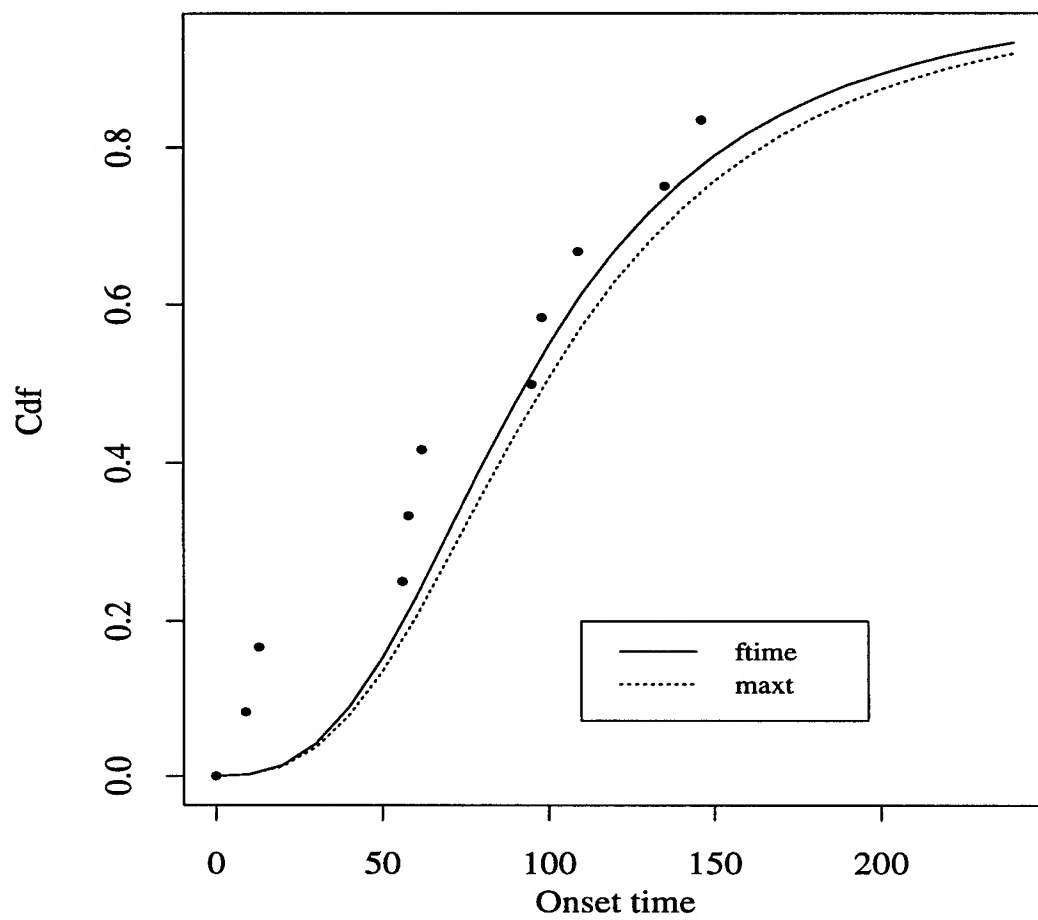


Figure 4: PRES = 282, TALT = 240, EX = Mild, BR = 0

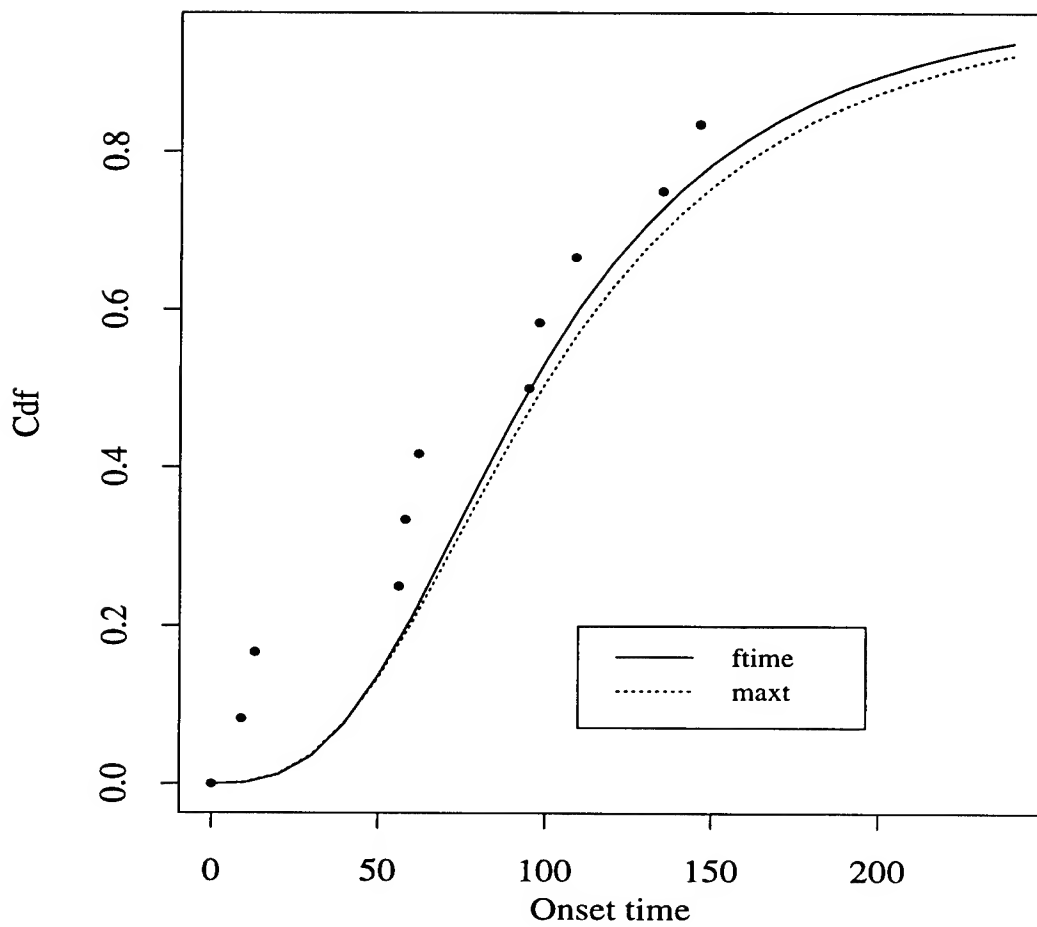


Figure 5: PRES = 282, TALT = 240, EX = Mild, BR = 0

Bibliography

- P. K. Weathersby, L. D. Homer, and E. T. Flynn, "On the likelihood of decompression sickness," *Journal of Applied Physiology*, vol. 57, pp. 815-825, 1984.
- P. K. Weathersby, S. S. Survanshi, L. D. Homer, E. Parker, and E. D. Thalmann, "Predicting the time of occurrence of decompression sickness," *Journal of Applied Physiology*, vol. 72, pp. 1541-1548, 1992.
- H. D. Van Liew, J. Conkin, and M. E. Burkard, "Probabilistic model of altitude decompression sickness based on mechanistic premises," *Journal of Applied Physiology*, vol. 76, pp. 2726-2734, 1994.
- W. A. Gerth and R. D. Vann, "Statistical bubble dynamics algorithms for assessment of altitude decompression sickness incidence," tech. rep., Armstrong Laboratory, 1995.
- K. Kumar, J. Waligora, and D. Calkins, "Threshold altitude resulting in decompression sickness," *Aviation, Space, and Environmental Medicine*, vol. 61, pp. 685-689, 1990.
- K. Kumar, D. S. Calkins, J. Waligora, J. Gilbert III, and M. Powell, "Time to detection of circulating microbubbles as a risk factor for symptoms of altitude decompression sickness," *Aviation, Space, and Environmental Medicine*, vol. 63, pp. 961-964, 1992.
- K. Kumar and M. Powell, "Survivorship models for estimating the risk of decompression sickness," *Aviation, Space, and Environmental Medicine*, vol. 65, pp. 661-665, 1994.
- J. Conkin, K. Kumar, M. Powell, P. Foster, and J. Waligora, "A probabilistic model of hypobaric decompression sickness based on 66 chamber tests," *Aviation, Space, and Environmental Medicine*, vol. 67, pp. 001-008, 1996.

- N. Kannan, Raychaudhuri, and A. A. Pilmanis, "A loglogistic model for altitude decompression sickness," *Aviation, Space, and Environmental Medicine*, 1997. submitted.
- E. T. Lee, *Statistical Methods for Survival Data Analysis*. Wiley, New York, 1992.
- J. F. Lawless, *Statistical Methods for Survival Data Analysis*. Wiley, New York, 1982.
- J. D. Kalbfleisch and R. L. Prentice, *The Statistical Analysis of Failure Time Data*. Wiley, 1980.
- R. Srinivasan and R. M. Wharton, "Confidence bands for the weibull distribution," *Technometrics*, pp. 375-380, 1975.
- R. C. H. Cheng and T. C. Iles, "Confidence bands for cumulative distribution functions of continuous random variables," *Technometrics*, pp. 77-86, 1983.
- V. N. Nair, "Confidence bands for survival functions with censored data: A comparative study," *Technometrics*, vol. 26, pp. 265-275, 1984.
- W. J. Hall and J. A. Wellner, "Confidence bands for a survival curve," *Biometrika*, pp. 133-143, 1980.
- P. J. Bickel and A. M. Krieger, "Confidence bands for a distribution function using the bootstrap," *Journal of the American Statistical Association*, pp. 95-100, 1989.
- B. Efron and R. J. Tibshirani, *An Introduction to the Bootstrap*. Chapman and Hall, 1993.
- N. Kannan and Raychaudhuri, "Survival models for predicting altitude decompression sickness," tech. rep., Armstrong Laboratory, Brooks Air Force Base, 1996.
- L. J. Petropoulos, P. G. Petropoulos, and A. A. Pilmanis, "Mathematical analysis of bubble growth models applied to altitude decompression sickness." submitted.

Appendix

We introduce some of the common definitions and terminology used in survival analysis literature.

Let T denote the time to onset of DCS. The survival function is defined as

$$S(t) = P(T \geq t),$$

i.e. the probability that the individual is symptom free upto time t . The survival function is a nonincreasing (decreasing) function of time t with the properties that

$$S(0) = 1, \quad S(\infty) = 0,$$

i.e. the probability of being symptom free for an infinite time is zero.

The Cumulative Distribution Function (cdf) is defined as

$$F(t) = P(T \leq t) = 1 - S(t),$$

the probability that DCS symptoms occur before time t . The Cdf starts at 0 and increases to 1. A steep cdf indicates the rate of survival is low or that onset time is relatively quick. A gradual, slow rising graph indicates the time to onset is higher. The survival function or cdf can be estimated from the data very easily using,

$$\hat{F}(t) = \frac{\# \text{ of individuals with onset times less than } t}{\text{total } \# \text{ of individuals}}.$$

The probability density function (pdf) $f(t)$ of the survival/onset time T is defined as the probability that an individual exhibits DCS symptoms in a small interval per unit time. The usual relation between the cdf and the pdf is:

$$F(t) = \int_0^t f(x)dx.$$

The hazard or risk function $r(t)$ specifies the instantaneous rate of developing the symptoms at time t , given that the individual is symptom free up till t . Therefore

$r(t)$ can be interpreted as the conditional failure rate. The risk function is appealing since it describes the way in which instantaneous risk of DCS changes with time in the chamber. The risk function is defined as

$$r(t) = \frac{f(t)}{S(t)}$$

where $f(t)$ is the probability density function of the onset time as defined before.

The likelihood equation is given by

$$L(\beta) = \prod_{i=1}^M f(t_i) \prod_{j=1}^{N-M} F(t_j)$$

where M is the number of uncensored observations.

When weights are included, the likelihood is proportional to

$$L(\beta) = \prod_{i=1}^M [f(t_i)]^{w_i} \prod_{j=1}^{N-M} [F(t_j)]^{w_j}.$$

SKILL IMPROVEMENTS VIA REFLECTED FORCE FEEDBACK

Antti J. Koivo
Professor
Department of Electrical Engineering

Purdue University
West Lafayette, IN 47907

Final Report for:
Summer Research Extension Program
Armstrong Laboratory

Sponsored by:
Air Force Office of Scientific Research
Bolling Air Force Base
Washington, D.C.

and

Armstrong Laboratory

December 1997

SKILL IMPROVEMENT
VIA
REFLECTED FORCE FEEDBACK

Antti J. Koivo
Professor
School of Electrical and Computer Engineering
Purdue University

ABSTRACT TO PART I

The skills of humans performing tasks can be evaluated using Fitts' law, which is described by a straight line in the coordinate system of execution time and task difficulty index. The inverse of the slope of the straight line is called the execution capacity of a human. The aforementioned variables can be calculated from experimental data collected for a task.

Experimental data were collected in the task in which a peg attached to the hand of an exoskeleton guided by a human arm was placed into a hole. Indeed, we have determined the mean and standard deviations for *individual* performances and also for the performances of a *group* of individuals. Thus, the numerical values calculated to describe the skills of an individual form a basis for comparison of the skills of the individuals.

Since Fitts' law is a geometric one-dimensional approach to skill evaluation, it is difficult to apply when the task performance is characterized by two or more variables. Our study introduces a novel probabilistic skill index to evaluate skills of operators performing tasks characterized by two or more variables. The probabilistic skill index provides a broader basis for the skill evaluations of the individuals. Moreover, the skills of the individuals performing tasks can be compared objectively by using the probabilistic skill index introduced.

ABSTRACT TO PART II

The system studied consists of a human operator, a stick driven by the force generated by the human hand, and a plant (e.g., a robotic arm) whose input comes from the stick. The system output is the position which is to be placed on a specific location by the human operator. The force from the stick output can be fed back (as a reflected force) and combined with the force applied by the human. The goal here is to study the effects of the reflected force feedback on the skills of the human operator. The recently induced probabilistic skill index is used to evaluate the performance of the operator performing specified tasks. The tasks are quantified by means of difficulty index. Four cases of different reflected feedback loops are studied. For each case, experimental data were collected when a human operator was performing a task of a known difficulty index. The probabilistic skill index is then used to quantify the effects of the reflected force feedback loop. Thus, this study provides evidence for evaluating the relative effects of the reflected forces on operator's skills in the teleoperation.

SKILL IMPROVEMENT
VIA
REFLECTED FORCE FEEDBACK

Antti J. Koivo

PART I: SKILL EVALUATION OF HUMAN OPERATORS

1. INTRODUCTION

The ability of a person to perform a task is often referred to as the skill that he/she has acquired. A human often gains skills by using his/her past knowledge and experience and by repeating the task. When a person performs a task, the success of the performance depends strongly on the difficulty of the task. A possible way to quantify the complexity of a task is by specifying an index of difficulty (ID), as proposed in [1]. The levels of skills are difficult to evaluate and quantify for many tasks. Yet, the skills of a human in certain applications can be quantified by evaluating his/her capacity to execute a specific task. It can be determined on the basis of one variable that can be measured in the experiments, for example the execution time, or it is calculated from experimental data. When such a variable is graphed as a function of the difficulty index of the task, a straight line can be fitted to the data points, for example, by the regression analysis. This straight line represents so-called Fitts' law. The inverse of the slope coefficient in the straight line equation is the execution capacity of the human performing the task. This concept, "the execution capacity", is analogous to the channel transmission capacity introduced by Shannon in communication theory [1]. The skill level of a person performing the task can be expressed by means of the execution capacity. It is clear that this measure of the skill level is the same for all values of the difficulty index. However, it is common that a person's skill level is quite high in easy tasks (ID is small), and low in difficult tasks; this suggests that some other criterion should be used to evaluate the skill level of a person. It should also be noticed that the execution capacity represents only one characteristic variable associated with the task that is used in the determination of the skill level.

In this paper, the evaluation of skill levels is studied by interpreting the execution capacity of a person in a broader sense. Specifically, the execution capacity is considered here as a random variable which is characterized by means of the statistical average and variance. Then, these parameters are introduced for skill evaluation to calculate the statistical execution capacity of a person and that of a group of persons. In this way, the person's task performance can be evaluated relative to that of the average performance of the entire group. Finally, a novel way of evaluating the skills of a person performing a task is proposed by introducing a probabilistic skill index. This approach can accommodate several variables which are used in the characterization of the person's skills.

2. DATA REPRESENTATION FOR A TASK

It is widely accepted that the magnitude (and variability) of the human responses and the information capacity of the human motor system play important roles in the human operators' motor skills. According to Fitts [1], the human capacity to execute a task can be related to the index of difficulty (ID) of a task defined as

$$ID = \log_2[A/(W/2)] \quad (1)$$

where A is the average amplitude of a human movement, and W is the admissible range of terminal movement error ("target bandwidth").

It was conjectured in [1] that the average movement time (MT) should remain constant for different values of A and W as long as the value of the ID remains constant. The ratio (ID)/(MT) expressed in bits per seconds may be interpreted as human's capacity to execute a particular class of tasks. By postulating that motor movements follow a law similar to perceptual motor processes, it is proposed in [1] that MT and ID are related as

$$(MT) = b + m (ID) \quad (2)$$

where m and b are constants. Equation (2) is often referred to as Fitts' law. In the framework of response duration, it may be considered as the traditional Weber function (the variability of a response as a function of its amplitude) written for the response duration. Subsequently performed experiments [1,2] have supported the relationship expressed in equation (2).

3. EXECUTION CAPACITY FOR SKILL EVALUATION

The constants m and b in equation (2) can be determined from experimental data. Indeed, if operator i, $i = 1, 2, \dots, N$ consumes the movement time t_i in performing a task of difficulty index ID, and the same person has a reaction time of t_{oi} (i.e., when $ID = 0$, t_{oi} is the pure reaction time), then one may write the straight line equation that corresponds to equation (2) as

$$t_i = t_{oi} + m_i (ID) \quad (3)$$

where m_i is a constant. The value of the reaction time t_{oi} is usually in the range 160 ms to 180 ms, which is small as compared with the movement time t_i in most cases.

It is a fairly common practice to use the inverse of the slope m_i , i.e., $1/m_i$ as a measure of the tracking skills of a person. If one considers t_{oi} negligible, then $1/m_i = (ID)/t_i$. If t_i is replaced by the average movement time, then this ratio may be interpreted as analogous to human's average capacity for executing a particular class of motor tasks. Its unit (bits/sec) is the same as that of the channel capacity in the information theory. The value $1/m_i = C_i$ is referred to as the execution capacity of person i .

3.1 DETERMINATION OF EXECUTION CAPACITY

It is a usual practice to determine constants t_{oi} and m_i in equation (3) by fitting equation (3) to the (measured) data points using the least squared error method (regression analysis). It gives numerical values t_{oi}^{ls} and m_i^{ls} for the constants. Then, equation (3) specifies Fitts' law as a straight line for person i as

$$t_i^{ls} = t_{oi}^{ls} + m_i^{ls}(ID) \quad (4)$$

The inverse m_i^{ls} of the slope characterizes human's capacity C_i^{ls} to execute a particular task, i.e., the execution capacity of person i . A small value of $C_i^{ls} = 1/m_i^{ls}$ signifies that the movement time can become very large when the task difficulty index increases, i.e., the human has poor skills to execute the task. A large value of $C_i^{ls} = 1/m_i^{ls}$ corresponding to a small value of m_i^{ls} indicates that the movement time for person i executing a task does not vary much even though the difficulty of the task varies, i.e., the person has good skills for performing tasks even when the task difficulty index varies over a wide range. It is emphasized that only one variable ($C_i^{ls} = 1/m_i^{ls}$) is utilized here to measure human's capacity to execute a particular task.

Example 1

An exoskeleton arm having seven rotary joints is attached to the arm of a human operator. It is moved by the human arm, and its joint motions are recorded by means of the encoders attached to the joint shafts. The exoskeleton arm is equipped with a force measuring pad attached to the elbow which can be used to compensate for the inertial torques. Moreover, a force/torque sensor (type JR3) has been installed on the wrist of the exoskeleton to measure the forces/torques generated by the human. The joint shafts are connected via steel wires and pulleys to the shafts of the motors. This system allows for the compensation of the gravity and the inertial torque effects caused by the exoskeleton. A peg of three different diameters may be attached to the gripper of the exoskeleton.

The task of a human operator here is to transfer the aforementioned peg from one hole to another specified hole as fast as possible. There are several holes in a vertical panel, and they all have the same diameter. Thus, the difference between the diameter of a hole and that of the peg can be chosen by the selection of a particular peg size.

One-half of this difference (tolerance) specifies $W/2$ in equation (1). The distance between the center points of the holes specifies A in equation (1). Hence, the task difficulty index can be calculated.

When a person is performing the described task, the time consumed for the completion of the task is measured electrically by means of the microswitches installed on the bottoms of the holes. A typical set of data points is shown in Table 1 for $i = 1$.

RUN#	0	1	2	3	4	5	6	7	8	9
ID	9.64	8.06	9.06	8.06	9.06	9.64	8.06	9.06	8.06	9.06
t_1	1711	671	1150	823	1602	1014	689	1465	7701	1560

RUN#	10	11	12	13	14	15	16	17	18	19
ID	7.58	6	7	6	7	7.58	6	7	6	7
t_1	1028	733	768	678	1232	1085	619	1004	673	841

RUN#	20	21	22	23	24	25	26	27	28	29
ID	11.64	40.06	11.06	10.06	11.06	11.64	10.06	11.06	10.06	11.06
t_1	1397	692	1331	1373	1483	1626	904	1885	982	1798

Table 1
Experimental data for person 1 ($i = 1$)

The data points of Table 1 for person $i = 1$ collected on the first day of the experiments can be displayed on the (t_1, ID) plane. A straight line is fitted to the data points using the regression analysis on equation (3). Thus, parameters t_{01}^{ls} and m_1^{ls} for equation (4) of person $i = 1$ and his execution capacity $C_1^{ls} = 1/m_1^{ls}$ for the task are calculated.

The least squared error method gives the numerical value of the parameter $m_1^{ls} = 151.7\text{ms/bits}$. Thus, equation (4) assumes the following form:

$$y = 151.7(\text{ms/bits})x - 208.7(\text{ms}) \quad (5)$$

where $x = ID$ is the index of difficulty (in bits), and $y = t_1$ (in milliseconds) is the movement time, which the person needs to complete the task.

Therefore, the execution capacity of person $i = 1$ is $C_1^{ls} = 1/m_1^{ls} = (1/151.7)\text{bits/ms} = 6.59(\text{bits/s})$ for the task in question. The calculated execution capacity is the same for all values of the task difficulty.

3.2 COMPARISON OF SKILLS USING EXECUTION CAPACITY

Person i repeated the experiments described in Example 1 usually on six successive days. The samples measured on a particular day can be graphed on the $(t_i, (ID))$ plane. The regression analysis is applied to the data collected on that day to determine the constants in equation (1). It results in a set of linear equations for each day the experiment was performed. The six equations (one for each day) are shown for person i in the second column of Table 2. Then, the execution capacity C_i^{ls} for person i on the particular day is calculated.

As an example for person $i = 1$, the set of equations calculated is displayed in the second column of Table 2. The execution capacity $C_i^{ls} = 1/m_{mi}^{ls}$ is shown in the fourth column of Table 2. The sample average of the execution capacity of this person is determined from the data: $\hat{C}_1^{ls} = 8.31$ (bits/s) with the sample standard deviation $\hat{\sigma}_{c_1} = 1.30$ (in the fifth column of Table 2). If it is assumed that the range of the execution capacity for person i is specified as $(C_i^{ls} - \sigma_{c_i}, C_i^{ls} + \sigma_{c_i})$, then for person $i = 1$ this range is (7.01, 9.61).

The comparison of the relative skills of the persons in the group can be performed by calculating $(\hat{C}_i^{ls}, \hat{\sigma}_{c_i})$ for each person, and the corresponding values $(\hat{C}^{ls}, \hat{\sigma}_c)$ for the entire group. An example is next presented to illustrate the comparisons of the skills of the persons.

Example 2

The execution capacity C_i^{ls} for person $i = 1, \dots, 7$ was calculated from the measured experimental data. The sample values C_i^{ls} for $i = 1, 2, \dots, 7$ are displayed in the fourth column of Table 2. The sample average \hat{C}_i^{ls} for each person i was calculated. The results are shown in the fifth column of Table 2.

The sample average of the execution capacity \hat{C}_i^{ls} of the entire population determined from the values of Table 2 is $\hat{C}^{ls} = 7.57$ and the sample standard deviation $\hat{\sigma}_c = 2.64$. Thus, the range of the execution capacity of the group is estimated as $(\hat{C}^{ls} - \hat{\sigma}_c, \hat{C}^{ls} + \hat{\sigma}_c) = (4.93, 10.21)$.

P e r s o n i=	Equation (4) $y = t_i, x = ID$	Sample mean/stand deviation $\hat{m}_i / \hat{\sigma}_{mi}$	Exec. cap. C_i^{ls}	Sample mean/Stand deviation $\hat{C}_i^{ls} / \hat{\sigma}_{C_i^{ls}}$
1	y=151.7x-208.71 y=121.69x-26.12 y=131.37x-45.75 y=98.49x+37.13 y=105.33x+46.05 y=127.9x-80.91	122.75/19.14	6.59 8.21 7.61 10.15 9.49 7.81	8.31/1.30
2	y=224.16x-275.17 y=173.75x+151.43 y=157.3x+11.88 y=315.62x-1086.2	217.71/71.20	4.46 5.75 6.35 3.16	4.93/142
3	y=157.06x-285.33 y=140.86x-221.88 y=66.84x+477.34 y=138.62x-146.73 y=134.23x-48.16 y=157.04x-289.41	132.54/33.58	6.36 7.10 14.96 7.21 7.45 6.37	8.24/3.32
4	y=133.77x-70.57 y=137.47x-25.47 y=160.81x-204.18 y=146.46x-104.28 y=164.53x-227.78	148.61/13.70	7.47 7.27 6.21 6.82 6.07	6.77/1.62
5	y=248.46x-519.21 y=227.27x-357.11 y=312.27x-651.73 y=246.48x-360.75 y=165.74x-70.28 y=229.73x-330.5	238.33/47.12	4.02 4.40 3.20 4.05 6.03 4.35	4.34/93
6	y=93.86x+163.5 y=126.54x-79.09 y=81.91x+278.45 y=93.95x+231.33 y=102.59x+186.43 y=124.87x+2.27	103.95/18.10	10.65 7.90 12.20 10.64 9.74 8.00	9.86/1.67
7	y=89.69x+193.51 y=96.211x+203.5 y=114.44x-9.152 y=128.46x-57.10 y=87.68x+215.58	103.30/17.58	11.15 10.39 8.73 7.78 11.40	9.87/1.57

Table 2

The skills of a particular person i can now be compared with the average skills of the group. For example, person $i = 1$ possesses skills for the task under consideration which are higher than those of an average person in the group. In particular, the range of the execution capacity for person $i = 1$ is (7.01, 9.61) which is entirely inside the range of the execution capacity of the entire group.

As another example, person $i = 4$ has skills for this task described by $\hat{C}_4^{ls} = 6.77$ with sample standard deviation $\hat{\sigma}_{c_4} = 0.62$. Thus, his skills in the average are below the average execution capacity $\hat{C}^{ls} = 7.57$ of the group. His range of the execution capacity on the days of the experiments was (6.15, 7.39). A part of this range intersects with the range of the execution capacity of the entire group, while another part of this range is outside the range of the entire group. It can thus be expected that he has potential to perform on the average level of the other individuals in the group.

It should be noted that the execution capacity is the same over the entire range of the index difficulties of the task.

4. PROBABILISTIC CRITERION FOR SKILL EVALUATION

Equation (3) is a straight line on a plane with (t_i, ID) as the coordinates. The constants t_{oi} and m_i of the straight line are used to characterize the human performance. The values of these constants in equation (3) depend on the distribution of the measured sample values. These measured samples can directly be used for the skill evaluation after realizing that they are samples of a random variable.

4.1 PROBABILISTIC SKILL INDEX FOR A SINGLE SKILL

It will be assumed that an approximate density function for the "general" population has been determined. Then, a probabilistic measure for the execution skills of a group of persons performing a task of a given difficulty index can be defined.

Definition: The probabilistic skill index for a group of humans executing a task is the probability that the humans in the group perform successfully the task of difficulty index $ID \in [d_1, d_2)$ in time less than α where d_1 , d_2 and α are positive numbers.

The probability skill index defined specifies the performance of the group. Indeed, the skill index SI^D at the specified task difficulty level is mathematically expressed as

$$SI^D = \Pr[t^D < \alpha | d_1 \leq ID < d_2] \quad (6)$$

where \Pr signifies the conditional probability and t^D is the movement time in the task of difficulty index.

Example 3

In order to determine the conditional probability in equation (6), a histogram of the data (such as in table 1) was drawn. It suggested the choice of the gamma density function for a given range of the difficulty index (ID). Thus, it is assumed that the (experimental) samples represent a random variable t that is characterized by the gamma density function $f(t; \eta, \lambda)$ where $\lambda > 0$ and $\eta > 0$ are constant parameters:

$$f(t; \lambda, \eta | 6 \leq ID < 7) = \lambda^\eta t^{\eta-1} e^{-\lambda t} / \Gamma(\eta), \quad t \geq 0 \quad (7)$$

$$0 \text{ elsewhere}$$

where $\Gamma(\eta)$ is the well-known gamma function. It is straightforward to calculate the mean of t to be η/λ and the variance η/λ^2 .

By calculating the sample mean \hat{t} and the sample variance $\hat{\sigma}_t^2$, the values of λ and η can be estimated: $\hat{\lambda} = \hat{t} / \hat{\sigma}_t^2$ and $\hat{\eta} = \hat{t}^2 / \hat{\sigma}_t^2$.

As an illustration, the skills of two persons "sm" and "rc" were compared for a task of index of difficulty in the range: $6 \leq ID < 8$. The parameters for the density function were estimated from the experimental data: $\hat{\lambda}_{sm} = 0.132$, $\hat{\eta}_{sm} = 26.90$ and $\hat{\lambda}_{rc} = 0.157$, $\hat{\eta}_{rc} = 13.76$. The probability density and distribution function for "rc" are graphed in Figure 1. It follows then that for "sm": $\Pr[t < 1000ms | 6 \leq ID < 8] = 0.852$ and for "rc": $\Pr[t < 1000 | 6 \leq ID < 8] = 0.803$. Hence, "sm" is more skilled in this particular task in the given range of the index difficulty.

It should be noticed that the probabilistic skill index introduced here will, in general, vary with the task difficulty index (ID). Moreover, this skill index allows one to consider several variables in the evaluation.

4.2 PROBABILISTIC SKILL INDEX FOR MULTIPLE SKILLS

Fitts' law describes the performance of an individual executing a task which is quantified by means of one variable. Due to its geometric nature, it is difficult to use it in a task characterized by means of several variables. On the other hand, the probabilistic skill index introduced here can be used equally well to describe the performance of a person executing a task that is characterized using several variables. Indeed, a multivariate probability density function can be used in the multivariable case, and the basic approach described in Section 4.1 can be applied to calculate the probabilistic skill indices for multivariate cases as well.

The use of a probabilistic skill index can be demonstrated in the evaluation of a person's skills in a task that is characterized by two variables. For example, the execution of the task "peg into a hole" may be quantified by means of the time (t^D) as well as the energy (en^D) used by a human. Thus, the probabilistic skill index of individuals is then

$$SI^D = \Pr[t_i^D < \alpha_1, en^D < \alpha_2 \mid d_1 \leq ID < d_2] \quad (8)$$

The probability in equation (8) can be calculated using a multivariate probability density function. Indeed, using experimental data the mean and variance of the chosen multivariate density function can be estimated. Then, the probability skill index in equation (8) can be obtained.

5. CONCLUSIONS

The skill evaluation of human operators is often based on Fitts' law. It provides us with the execution capacity for a human performing a task. It can be used to compare the skill performances of humans. Due to the random nature of the data which are used to determine the execution time, we propose to use the average execution capacity and the region about the foregoing mean to compare the skills of humans. Examples are presented to illustrate the approach.

Since many tasks are characterized by several variables and Fitts' law uses only one variable, we are proposing the use of a multivariate probability conditioned on the range of the task index of difficulty as the skill index. This probabilistic skill index, is calculated here by assuming that the experimental data obey the gamma distribution.

This paper thus, extends the concept execution capacity so that the ranges of these values can be used to evaluate the skills of humans performing a task. Moreover, a new multivariable probabilistic skill index is proposed for cases that a task is characterized by several variables.

REFERENCES:

- [1] P. M. Fitts and J. R. Peterson, "Information Capacity of Discrete Motor Responses", *Journal of Experimental Psychology*, Vol 67, No. 2, February 1964, pp. 103-112.
- [2] P. M. Fitts, "The Information Capacity of the Human Motor System in Controlling the Amplitude of Movement", *Journal of Experimental Psychology*, 1954, pp. 381-391.
- [3] S. Shapiro, Statistical Models in Engineering, book, John Wiley & Sons, Inc., 1967, pp 83-93.
- [4] D. W. Repperger, C. A. Phillips and T. L. Chelette, "A Study on Spatially Induced 'Virtual Force' with an Information Theoretic Investigation of Human Performance", *IEEE Trans. on Systems, Man, and Cybernetics*, Vol 25, No. 10, October 1995, pp. 1392 - 1404.

PART II: EFFECTS OF FORCE FEEDBACK ON OPERATOR'S SKILLS IN TELE-OPERATED SYSTEMS

1. INTRODUCTION

Skills are required to perform a task well.² The skills are acquired by past experiences, learned knowledge, and repetitions of the performance.² Difficult tasks require advanced skills. The complexity of a task can be quantified by defining the index of difficulty (ID).^{1,2}

The knowledge of the skill levels for humans in many situations would be helpful in evaluating the performances of the persons for a task. The levels of skills in certain applications can be quantified by determining the execution capacity for a human to perform a specific task.¹ It is based on graphing experimental data as a function of the ID of the task and then using the inverse of the slope of the regression line (Fitt's law) to obtain the execution capacity. An alternative approach² is to determine a probabilistic skill index conditioned on the specified ID of the task. This skill index can be applied to the evaluation of the skill level represented by several variables of a task, whereas the execution capacity considers only one variable of a task.

An active (computer realized) force feedback has been applied to stick control of carts used by paraplegics in order to make the motion smooth.³ It is known that an aggressive use of stick control can lead to unwanted oscillations of the pilot-aircraft coupling systems. An active reflected force feedback can be expected to effect these oscillations, which provides the major motivation to the study reported here. The effects of reflected force feedback on the skills of a human operator in tele-operated systems are studied here by using a probabilistic skill index. The paper is organized as follows: the experimental setup is described in Section 2. Section 3 presents the analysis of the experimental data. The results are discussed in Section 4, and the conclusions are presented in Section 5.

2. EXPERIMENTAL SETUP

An exoskeleton arm having seven rotary joints is attached to the arm of a human operator. It is moved by the human arm, and its joint motions are recorded by means of the encoders attached to the joint shafts. The exoskeleton arm is equipped with a force measuring pad attached to the elbow which can be used to compensate for the inertial torques. Moreover, a force/torque sensor (type JR3) has been installed on the wrist of the exoskeleton to measure the forces/torques generated by the human. The joint shafts are connected via steel wires and pulleys to the shafts of the motors. This system allows for the compensation of the gravity and the inertial torque effects caused by the exoskeleton.

The block diagram of the system used in the experiment is shown in Figure 1. The position of the (joy) stick provides the input to the plant (i.e. the exoskeleton), which produces the motion for a peg to be inserted into a hole of a specified diameter. The input to the stick consists of the force generated by the human and the reflected

force (if present) via the negative feedback. The outer feedback is from the output and it contains the human vision system.

The task for the human operator is to transfer a peg of a known diameter from a given hole to another specified hole of a known diameter as quickly as possible. This time is recorded. The diameters of the peg and the hole specified for the insertion determine the ID of the task.

3. EXPERIMENTAL DATA AND ANALYSIS

It is widely accepted that the magnitude (and variability) of the human responses and the information capacity of the human motor system play important roles in the human operators' motor skills. According to Fitts¹, the human capacity to execute a task can be related to the index of difficulty (ID) of a task defined as

$$ID = \log_2[A / (W / 2)] \quad (1)$$

where A is the average amplitude of a human movement, and W is the admissible range of terminal movement error.

In the experimental setup, the vertical panel has several holes of the same diameters. The difference between the diameter of a hole and that of the peg can be chosen by the selection of a particular peg size. One-half of this difference (tolerance) specifies W/2 in equation (1). The distance between the center points of the holes used in the insertion task specifies A in equation (1). Hence, the task difficulty index can be calculated.

The experiments were performed (i) without the reflected force (inner loop) feedback (to be denoted as nf); (ii) with the (inner loop) feedback (fcl); (iii) with the reflected force of the inner loop being generated by means of a spring with a constant K(fws); (iv) the same as in (iii) but the spring constant being K/2(fhs). Thus, the effects of the inner feedback loop can be studied.

When a person is performing the described task, the time consumed for the completion of the task is measured. A typical set of experimental data points is shown in Table 1 for case (nf).

The collected data were displayed on histograms for each of the foregoing cases. For a functional representation, a gamma density function $f(\cdot)$ conditioned on a specific ID of the task and the form of the inner feedback loop (il) was chosen:

$$f(t, \lambda, \eta / ID, il) = \begin{cases} e^{-\lambda t} t^{\eta-1} \lambda^\eta / \Gamma(\eta) & \text{for } \lambda > 0, \eta > 0, t \geq 0 \\ 0 & \text{elsewhere} \end{cases} \quad (2)$$

RUN#	0	1	2	3	4	5	6	7	8	9
ID	9.64	8.06	9.06	8.06	9.06	9.64	8.06	9.06	8.06	9.06
t	1711	671	1150	823	1602	1014	689	1465	770	1560

RUN#	10	11	12	13	14	15	16	17	18	19
ID	7.58	6.0	7.0	6.0	7.0	7.58	6.0	7.0	6.0	7.0
t	1028	733	768	678	1232	1085	619	1004	673	841

RUN#	20	21	22	23	24	25	26	27	28	29
ID	11.64	10.06	9.64	8.06	9.06	8.06	9.06	9.64	8.06	9.06
t	1397	692	1711	671	1150	823	1602	1014	689	1465

Table 1
Experimental data for a person

where t signifies the time needed to complete the task, λ and η are constants. These were calculated by using the expressions for the mean m and variance σ^2 , i.e.,

$$\begin{aligned} m &= \eta / \lambda \\ \sigma^2 &= \eta / \lambda^2 \end{aligned} \quad (3)$$

The values of m and σ^2 were approximated by their sample values calculated on the basis of the experimental data. The approximated values for the four cases of the inner loop (il) and the given values of the ID are displayed in Table 2, where the upper number is $\hat{\eta}$ and the lower number $1/\hat{\lambda}$. A typical graph for the gamma density functions and the corresponding distribution functions for the cases ID = 8.06 and 11.06 are shown in Figures 2a and b for the four cases of the minor loop (force) feedback.

i\ID	6.0	8.06	9.64	11.06
(i)	9.3798	14.5652	18.9314	13.7914
nf	0.0217	0.0951	0.0258	0.0158
(ii)	13.845	8.1314	7.7490	9.6224
fcl	0.0158	0.0065	0.0046	0.0054

(iii)	8.8679	9.3668	6.5190	5.3542
fws	0.0188	0.0076	0.0036	0.0022
(iv)	9.0660	7.9629	5.5413	7.1991
fhs	0.0109	0.0069	0.0032	0.0040

Estimates of $\hat{\eta}$ and $1/\hat{\lambda}$ for Equation (1).

Table 2

4. DISCUSSION

The probabilistic skill index SI of a population or human is defined² as

$$SI = \text{Pr ob}[t < \alpha \mid ID = \beta, il] \quad (4)$$

When the probability distribution function (in Figure 2) is given, the SI for a specific case can be read immediately. For the case that $ID = 8.06$, Figure 2 shows that the probabilistic skill index for case i (nf) is largest for all values of the ID. For easy tasks, the contribution of the half-spring force (iii) results in a better probabilistic skill index than the fcl-case (ii). However, when the value of α is made larger, the effects of these feedbacks reverse, although the differences are small.

5. CONCLUSIONS

The effects of a reflected (inner loop) feedback force on the motion of a stick operated by a human has been studied. Experimental data have been collected for various tasks quantified by means of the index of difficulty. A gamma density function has been used to describe the time to complete a task of known difficulty (ID). The affects of various forms of the reflected force feedback on the probabilistic skill index can be evaluated on the basis of the analyzed data. Thus, the relative benefits of the reflected force feedback to the human operator can be evaluated.

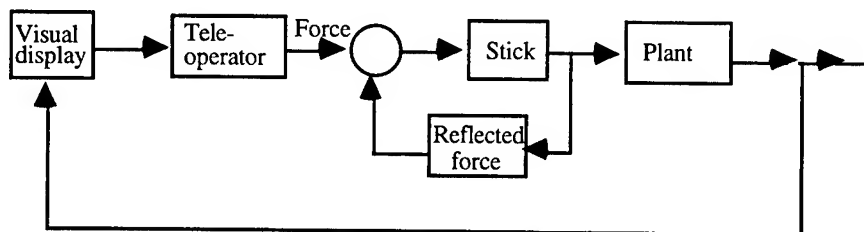


Figure 1

REFERENCES

1. P. M. Fitts and J. R. Peterson, "Information Capacity of Discrete Motor Responses", *Journal of Experimental Psychology*, Vol. 67, No. 2, February, 1964, pp. 103-112.
2. A. J. Koivo and D. W. Repperger, "Skill Evaluation of Human Operators," *Proc. of 1997 IEEE International Conference on Systems, Man and Cybernetics*, Orlando, Florida, October, 1997.
3. D. W. Repperger, "Active Force Reflection Devices in Tele-operation", *IEEE Control Systems*, January 1991, pp. 52-56.

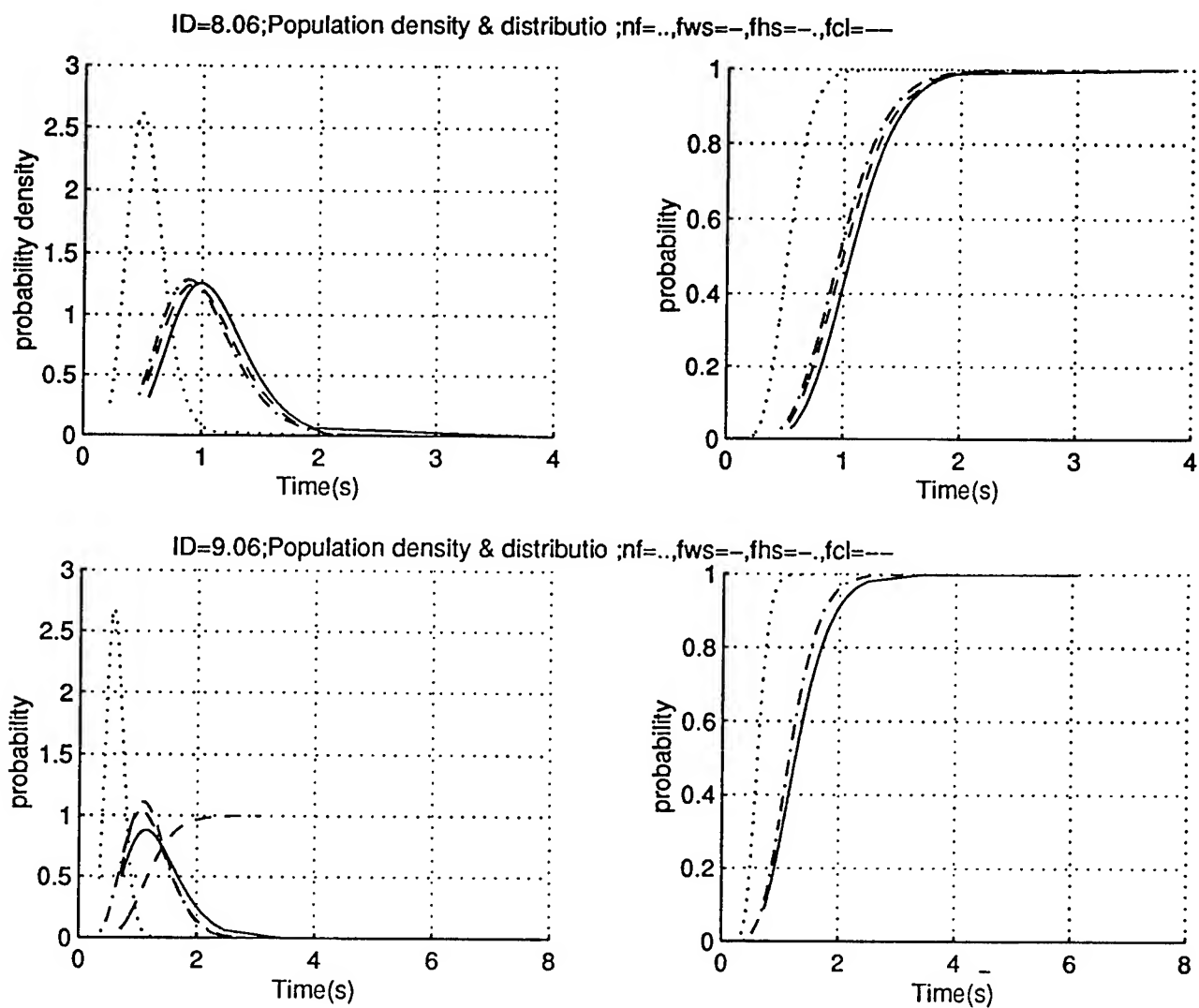


Figure 2a.

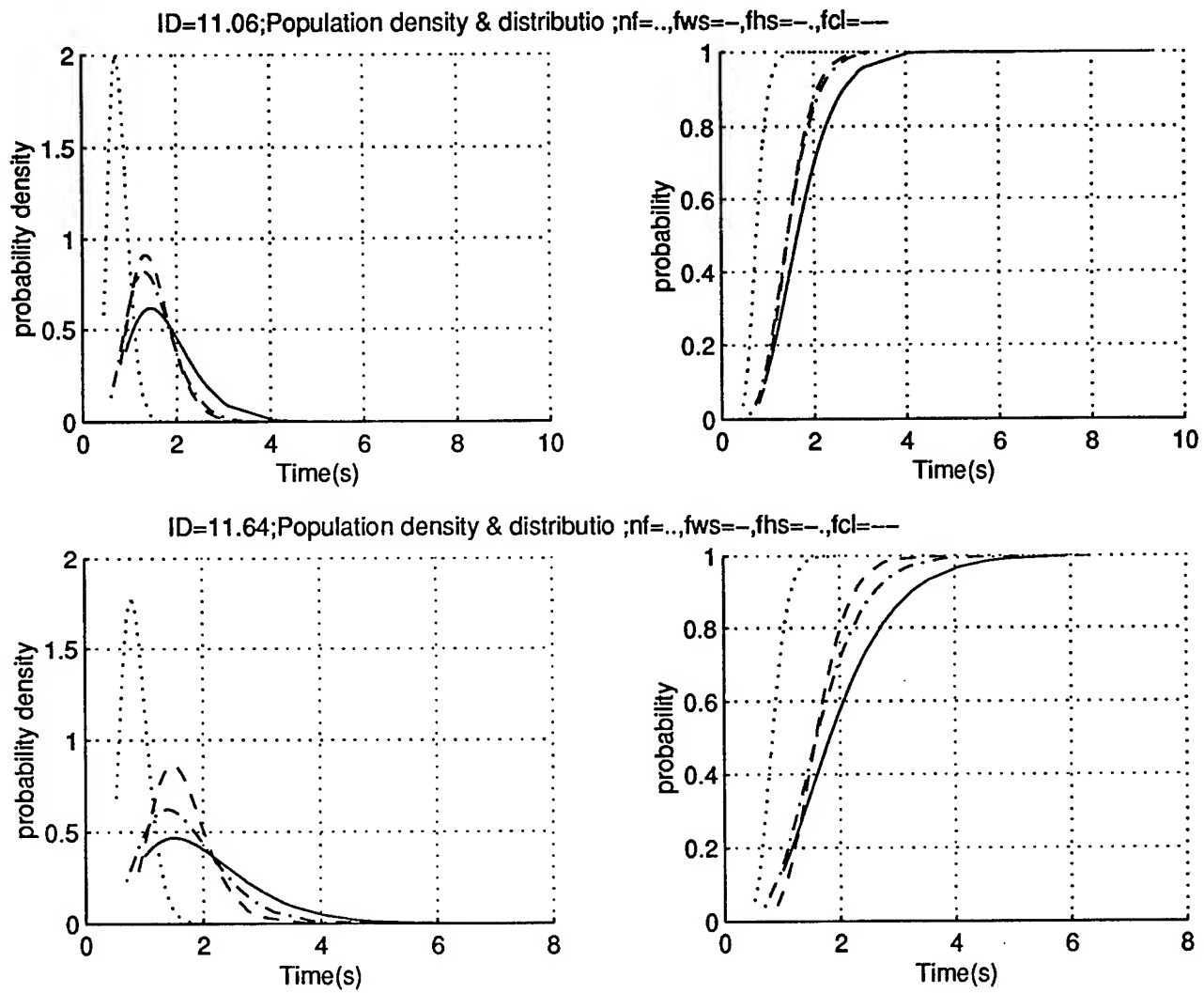


Figure 2b.

DEGRADATION AND MORTALITY STUDIES OF JP-8, DIESEL AND UNLEADED GASOLINE WITH
FRESH WATER SNAILS

S. Bin Kong, Ph.D.
Associate Professor
Department of Chemistry

University of the Incarnate Word
4301 Broadway
San Antonio, TX 78209

Final Report for:
Summer Faculty Research Extension Program
Armstrong Laboratory

Sponsored by:
Air Force Office of Scientific Research
Bolling Air Force Base, DC

And
Armstrong Laboratory

December 23, 1997

DEGRADATION AND MORTALITY STUDIES OF JP-8, DIESEL AND UNLEADED GASOLINE WITH FRESH WATER SNAILS

S. Bin Kong, Ph.D.
Associate Professor
Department of Chemistry
University of the Incarnate Word

Abstract

Petroleum, including gasoline, diesel, and jet fuels have been studied to determine the toxic effects on an aqueous environment. This research utilized fresh water mollusks as an indicator organism. The initial biological species tested was Biomphalaria glabrata, which was then replanced by Physa virgata, a species of snail local to the San Antonio area. After collection from the San Antonio river, Physa virgata were instpected for tremetode parasites, which could affect susceptibility to toxicants. Uninfected snails (10 specimens/container) were placed in water soluble extractions from each fuel, along with 1 and 0.5 percent solutions of the fuel itself. Mortality was observed over a 120-hour period. Preliminary results have shown that solutions of JP-8, in quantities of 1 and 0.5 percent, are more toxic than the water soluble fraction. Diesel fuel followed the same patter as JP-8, with solutions having a higher toxicity rate than its water soluble components. However, gasoline water extractions were found to be more toxic than its 1 and 0.5 percent solution and had the highest toxicity overall. Preliminary testing on component compounds of petroleum indicate molluscicidal activity, particularly in ethylbenzene.

DEGRADATION AND MORTALITY STUDIES OF JP-8, DIESEL AND UNLEADED GASOLINE WITH FRESH WATER SNAILS

S. Bin Kong, Ph.D.

Introduction

Jet fuels and diesel fuels are complex mixtures of hydrocarbons produced by distillation of crude oil. The composition of fuels varies depending on the source of crude oil, distilling process, and specifications. The hydrocarbons in diesel and jet fuels are less volatile than those in gasoline. JP-8 is similar to commercial Jet-A fuel and consists primarily of C8 - C17 hydrocarbons with approximately 18 % aromatics. For diesel (marine), these are roughly 13 % paraffins, 43 % benzene aromatics, and 44 % naphthalenes (Henderson, 1996). It might also contain less than 10 % polycyclic aromatic hydrocarbons. Many compounds in the fuels do not exist in the vapors (Bishop, 1982).

Fuels can be released to the environment by in-flight exhaust and from spills and leaks to soil and water. Some of the aromatic hydrocarbons making up fuels may dissolve in water and then partition to sediment or be biodegraded. Some components may migrate through the soil in to the groundwater. It is not possible to fully describe the toxicokinetics of the individual hydrocarbons that are present in the petroleum (Satcher, 1993). However, it is important to identify the individual chemicals as a base for the future environmental studies.

Biomphalaria glabrata, the aquatic species first used is found in Africa, India, and South America. The abundance required to run petroleum mortality tests and the unavailability of the species made it insufficient for more than preliminary testing. Physa virgata a species found locally, in the San Antonio River, replaced Biomphalaria glabrata. Its accessibility and lack of any dangerous parasites made it a suitable test subject. Present testing has focused on short term effects in aqueous samples, primarily mortality tests run over a 120 hour period using JP-8 (jet fuel), diesel fuel, and unleaded gasoline. Experiment consisted of 50/100 and 25/100 water soluble extractions and 1% and 0.5% solutions. Snails were placed in a 10/100 ml container of each and checked, at 24 hour intervals, for the duration of the experiment.

Methodology

1. Animal Care and housing

For this study two species were used, Biomphalaria glabrata and Physa virgata. P. virgata which is a native to the San Antonio and surrounding areas were collected from the San Antonio River, where it runs through Espada Park. B. glabrata were originally donated from Dr. Sullivan's lab. The snails were kept in 10 and 20 gallon tanks, set up with underground filters, air-pumps, natural colored gravel and glass covers. The water was treated with fresh water biological conditioner and chlorine remover 24 hours before P. virgata were introduced. Temperature of the water was kept between 78 and 80 Fahrenheit. The P. virgata were fed 3 times a week; two days they were fed basic flakes (for tropical fish) and shrimp pellets(sinking). The third day they were given both foods from the previous two days plus 2 leafs of Romain lettuce in each tank. The lettuce was washed and cooked for 6 minutes, in the microwave. After it had cooled off, the leafs were removed from the inner system. The leaves were placed in the tanks, while the stem was disposed of. The specimens were undisturbed, until day of collection, for tests, which was on the average of once a week. Snails, which were collected from the river, were first placed in small, individual containers with enough water to cover them. P. virgata were left to shed possible parasites overnight. Infected specimens were disposed of in a container consisting of 2 gallons of 6 percent solutions of Chlorox. Snails not found to be infected with parasites were placed in tanks, until needed for tests. Specimens, which were not perished during the testing, were disposed of in the same manner as parasite infected snails.

A. Method: Test #1

- 1) Place 50 ml of JP-8 in a 125 ml separatory funnel.
- 2) Add 50 ml of dechlorinized water to the funnel.
- 3) After shaking for about 5 minutes set in ring to let water and JP-8 separate.
- 4) Drain the water layer into 200 ml petri dish.
- 5) Place 10 snails in petri dish and cover with petri lid.
- 6) Repeat procedures #2 through #5
- 7) Repeat entire procedure for Diesel fuel and Gasoline.
- 8) Repeat entire procedure for all three substances reducing the amount from 50 ml to 25 ml of said substance.

B. Method: Test #2

- 1) Place 99 ml of dechlorinized water into a 200 ml petri dish. Add 1 ml of JP-8.
- 2) Add 10 snails and cover with petri lid.
- 3) Repeat entire procedure for Diesel and Gasoline.

2. Chemical analysis

Diesel and JP-8 were obtained from Kelly Air Force Base, San Antonio, Texas. Unleaded gasoline was obtained from a local gas station.

Analyses of the chemical components were done with GC crosslinked silicate capillary column interfaced with HP 5970 mass selective detector. Hydrocarbon standards were also used to identify n-paraffins and naphthalene-d8 was used as an internal standard. The injection mode was splitless and the column was temperature programmed (100 m x 0.25mm ID. Column temperature: 35 C' for 15 minutes then to 230 C' at 2 C' /minute. He carrier gas flow rate was 50 mm/min.) (Supelco, 1996, Restek, 1996 and Brook, 1978).

Results and Discussion

The results of the preliminary snail essays study are presented in Figure 3a-d. The biodegradation of the petroleum should be tested with the water soluble extracts along with the fuel toxicity. We also would like to use salt water snail in the next experiments. However, this essay test gave us some idea of the sensitivity of fresh water snails to the toxic petroleum components. It may also be feasible to scaling down the test volumes to small amount of fuels.

Electron Ionization (EI) was used for mass analysis. EI plays an important role in the routine analysis of small molecules. Its technique is straightforward and the databases contain the EI mass spectra of over 100,000 compounds and are used daily by thousands of chemists. However, it is difficult to analyze heavy molecules even if the backgrounds are subtracted due to the degree of fragmentation. It can limit the chemist to small molecules well below the mass range of common bioorganic compounds. Chemical Ionization(CI), electrospray ionization(ESI) or fast atom/ion bombardment(FAB) can be useful tools for future investigation. The usefulness of EI decreases significantly for compounds above a molecular weight of 400. The requirement that the sample be thermally desorbed into the ionization source often leads to decomposition prior to vaporization. The principal problems associated with thermal desorption in EI are the involatility of large molecules, thermal decomposition, and in many cases, excessive fragmentation. Too much fragmentation often results in no observable molecular ion. However, most of the aromatic hydrocarbons in fuels that we are dealing with are not huge molecules. Therefore, if we combine the data derived from EI and CI with GC/MS/IRD, that could be very useful for analyzing most of the aromatic hydrocarbons (Hafner et al., 1987 and Fodor, 1992).

Aromatic hydrocarbons usually occur naturally and most of them are not harmful to human health. But some of them are known to be health hazards and are found throughout the environment in the air, water, and chemical waste site soil (Purcell, et al. 1990, Satcher, 1993). Like many other chemicals, we still are not aware the environmental or occupational health effects of many aromatic hydrocarbons at this time. Petroleum contains many substituted benzenes, naphthalenes and other aromatic hydrocarbons and we are exposed to many of these

substances by breathing, eating, drinking, or skin contact. It was reported that repeated contact with fuel oils could cause skin and liver cancer in mice. However, there is some conflicting information (Andrews and Snyder, 1991 and Henderson, 1996).

Mass spectra

There were 182 peaks on mass spectra of JP-8 (Figure 1 and 2). JP-8 contains 11% benzenes and 6 % naphthalenes (Table 1). There were 28 benzenes and 13 naphthalene derivatives (Table 2). Most of the alkylbenzenes had molecular weight less than 150 such as ethylbenzene, dimethyl-, ethylmethyl-, methylpropyl-, ethyldimethyl-, trimethyl-, diethylbenzenes. Naphthalene derivatives were decalin, methyldecaline, methyl-dimethyl and trimethylnaphthalenes. It was difficult to identify the chemical components with mass spectra only: in many cases due to the overlapping of the retention times of molecules. Even if we try to change the column conditions, carrier gas or flow rate, the interpretation can be tricky, despite making background subtractions. We should consider other ionization methods such as CI or methods for high molecular weight determination.

Jet-A has 8 % benzenes and 4 % naphthalenes. There were 18 alkylbenzene and 12 naphthalene derivatives in Jet-A (Table 3). Most of the alkylbenzenes were similar to that of JP-8 such as ethylbenzene, dimethyl-, ethylmethyl-, trimethyl-, ethyldimethyl-, methylpropyl-, isopropylmethyl- and trimethylbenzenes. Naphthalene derivatives were methyldecalin, methyldecahydronaphthalene, methyl-, ethenyl-, dimethyl and trimethylnaphthalenes.

Aromatic hydrocarbons are the major components in water soluble extracts because of their greater solubility even though they are a minor components in petroleum (Figure 4, 5 and Table 5). Most of the aromatic hydrocarbons were benzene, xylene and naphthalene derivatives. We found toluene, ortho- meta- para-xylenes, isobutenyl-, dimethylpropenyl-, trimethylethenyl-, propenylbenzenes, but the characterization was difficult to be perfect. We may need several hundreds internal standards with high resolution MS data for the identification. Naphthalenes were dimethyl-, trimethyl-, dimethyltetrahydro-, trimethyltetrahydronaphthalenes. Identification of fuel components can be done more efficiently if we use GC/FT-IRD/MS.

Chemical Ionization(CI) should be applied along with EI. To characterize biodegraded molecules which can have high molecular weights, FAB , electron spray(ESI) or other methods can also be considered. Mass spectra are effective to identify the aromatic hydrocarbons but are not accurate for determining positional isomers. To solve the problem above, we also need individual aromatic hydrocarbon standards in different concentrations.

We have characterized fuels to identify the chemical components as a basis for future research. We will use these data for chemical and biodegradation studies in the following years. After we establish the routine procedure and identification of fuels, we can proceed to weathered JP-8 and other samples for degradation studies in chemical waste sites. Microorganism remediation study is also possible.

File : C:\HPCHEM\1\DATA\F200696\JP8KELLY.D
Operator :
Acquired :
Instrument : 5970 - IN
Sample Name : jp-8 Kelly AFB
Misc Info :
Vial Number : 1
AcqMethod FUELS

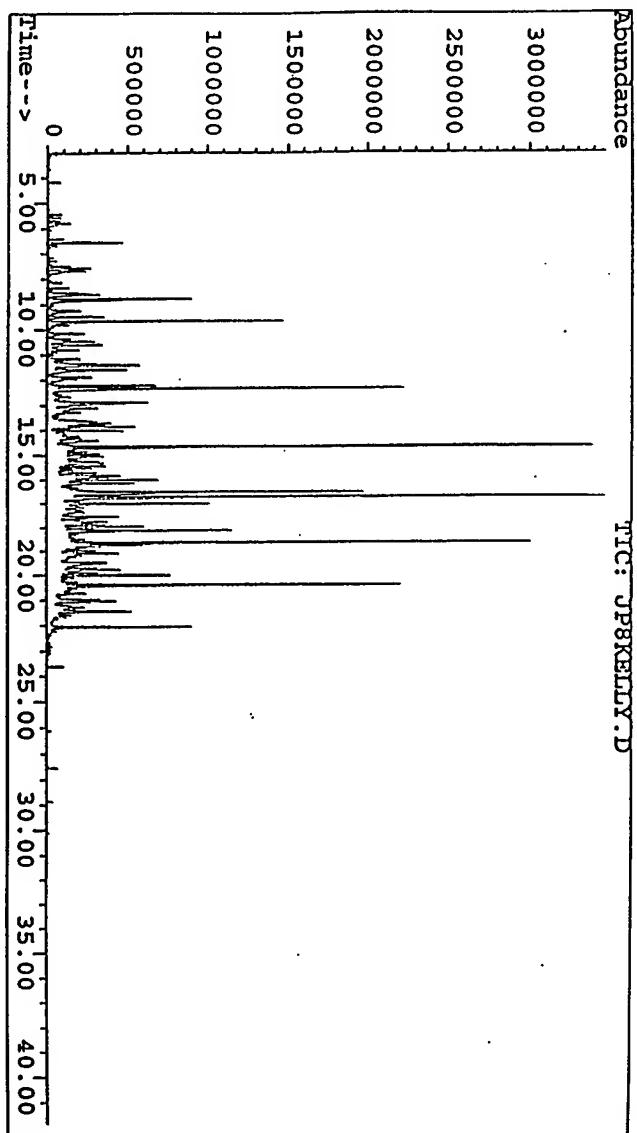


Figure 1. Gas Chromatogram of JP-8 fuel (Kelly A. F. B.)

Figure 2. Chemical Components of JP-8.

1	cyclohexane
2	?
3	methylcyclohexane
4	2-hexenol
5	pyrrolidine
6	toluene
7	?
8	cyclohexane, 1,4-dimethyl-
9	?
10	?
11	?
12	?
13	cyclohexane, 1,2-dimethyl-
14	octane
15	cyclohexane, 1,4-dimethyl-
16	hexane, 2,2,5-trimethyl-
17	heptane, trimethyl-
18	?
19	?
20	heptane, 2,6-dimethyl-
21	cyclohexane, ethyl-
22	cyclohexane, 1,1,3-trimethyl-
23	nonene, 2,4,6-trimethyl-
24	?
25	cyclohexane, 1,2,4-trimethyl-
26	?
27	heptane, 2,4-dimethyl-1-
28	?
29	benzene, ethyl-
30	octane, 4-methyl-
31	octane, 1-methyl-
32	benzene, 1,4-dimethyl
33	?
34	?
35	? pentenal
36	?
37	? 1-hexene, 6-bromo
38	heptene, 2-
39	cyclohexane, 4-ethyl-methyl-
40	benzene, 1,3-dimethyl-
41	nonene

- 42 pentenal, 2-ethyl-
- 43 cyclohexane, 1-ethyl-3-methyl-
- 44 heptyne
- 45 decane
- 46 1-hexene, 3,5,5-trimethyl-
- 47 cyclohexanepropanol
- 48 nonane, 4-methyl-
- 49 cyclohexane, propyl-
- 50 nonene, 3-methyl-
- 51 heptane, 3-ethyl-2-methyl-
- 52 3-nonene-1-ol
- 53 octyne
- 54 undecene
- 55 benzene, propyl-
- 56 pentane, tetramethyl-
- 57 nonene, 4-methyl-
- 58 benzene, 1-ethyl-2-methyl-
- 59 decanal
- 60 benzene, 1,2,4-trimethyl-
- 61 heptane, propyl-
- 62 benzene, 1-ethyl-2-methyl-
- 63 cyclohexane, 1-ethyl-2-methyl-
- 64 4-cyclohexyl-1-butanol
- 65 pentanal, ethyl-
- 66 benzene, 1,2,4-trimethyl-
- 67 decane
- 68 benzene, butyl-
- 69 ?
- 70 benzene, methylpropyl-
- 71 decane, 2,5,6-trimethyl-
- 72 decane, 4-methyl-
- 73 benzene, 1-ethyl-4-methyl-
- 74 decane, dimethyl-
- 75 cyclohexane, 1-methylpropyl-
- 76 ?
- 77 cyclohexane, butyl-
- 78 4-pentenal, 2-methyl-
- 79 6-octenal, 3,7-dimethyl-
- 80 2-decenal
- 81 benzene, 2-ethyl-1,3-dimethyl
- 82 benzene, 1-methyl-3-propyl

83	naphthalene, decahydro-, trans-	
84	decane, 5-methyl-	
85	benzene, 1-ethyl-2,3-dimethyl	
86	decane, 2-methyl	
87	decane, 3-methyl	
88	nonenal	
89	nonadiene, dimethyl	
90	? benzene, dimethylethyl	
91	benzene, 1-ethyl-2,3-dimethyl	not in
	order	
92	, 4-ethyl-2,3-dimethyl	
	, 2-ethyl-1,3-dimethyl	
	cyclohexane, 1-ethyl-1-methyl-	
93	cyclohexane, 1-methyl-1-propyl	
	benzene, 2-ethyl-1,3-dimethyl	
94	benzene, 1-ethyl-2,3-dimethyl	
	cyclohexane, 1-ethyl-2-propyl	
95	benzene, 4-ethyl-1,2-dimethyl	
96	undecene	
97	benzene, [1,1-dimethylpropyl]-	
98	?	
99	octane, 2-methyl	
100	benzene, 1,2-diethyl	
101	benzene, 1-methyl-2-(1-methylethyl)-	
102	dodecane, 2,6,10-trimethyl	
103	naphthalene, decahydro-2-methyl	
104	? dodecanol, trimethyl	
105	cyclohexane, pentyl	
106	benzene, 4-ethyl-1,2-dimethyl	
107	? azulene	
108	? benzene, 1,4-dimethyl-2-[2-methylpropyl]-	
109	? 2-hexyl-1-decanol	
110	? undecene, 5-methyl	
111	decane, 2,3-dimethyl	
112	? heptadecane, methyl	
113	? dodecane, 3-methyl	
114	benzene, [1,1-dimethylpropyl]-	
115	? tetradecyne	
116	naphthalene d8 standard	
117	azulene	

- 118 1H-indene, 1-methylene-naphthalene
dodecane
- 119 benzene, e-ethenyl-1,3,5-trimethyl
- 120 ?
- 121 undecane, 2,6-dimethyl
- 122 ? decane, 2,2,3-trimethyl
- 123 1H-indene, 2,3-dihydro-1,1,5-trimethyl-
- 124 decane, 2,3,7-trimethyl
- 125 ? phosphoric acid, dioctadecyl ester
- 126 naphthalene, decahydro-2.6-dimethyl-
- 127 ?
- 128 cyclohexyl, hexyl
- 129 1-tridecanol
- 130 ? octadecyne
- 131 ? decane, 2,6,7-trimethyl
- 132 dodecane, 5-methyl
- 133 ? heptane, 2,4-dimethyl
- 134 nonadecane
- 135 dodecane, 3-methyl
- 136 nonane, 3-methyl
- 137 ? octanol, hexyl
- 138 ? octadecane, 1-chloro
- 139 ?
- 140 ? tridecanediol, diacetate
- 141 1-hexadecanol
- 142 tridecane
- 143 naphthalene, 1-methyl
- 144 ? 6-octene-1-ol, 3,7-dimethyl-
- 145 ?
- 146 benzocycloheptatriene
- 147 benzene, [3-methylcyclopentyl]
- 148 ? pyridinol, acetate(ester)
- 149 ?
- 150 ? 7-hexadecyne
- 151 ? tridecane, methyl
- 152 ?
- 153 eicosane, 10 methyl
- 154 pentacosane
- 155 10-methylnonadecane
- 156 dodecane, 2,6,10-trimethyl

157 ?
158 naphthalene, 2-ethenyl
159 biphenyl
tetradecane
160 octadecane, 1-chloro
161 naphthalene, 1,2-dimethyl
162 ?
163 octadecanol
164 naphthalene, 2,7-dimethyl
165 naphthalene, 2,6-dimethyl
166 ?
167 ? 2-hexyl-1-decanol
168 octylcyclohexane
169 ? quinolinone, hydrazone
170 pentadecane
171 butane, 2-iodo-2-methyl
172 3-dodecyne
173 ? decane, 3-methyl
174 ?
175 ? 1,2'-biphenyl-2-methyl
176 ? methylphenylhexatriene
177 ?
178 tetradecane
179 ?
180 ?
181 ?
182 ?

Figure 3a.

Mortality rates of a 1% solution of petroleum products

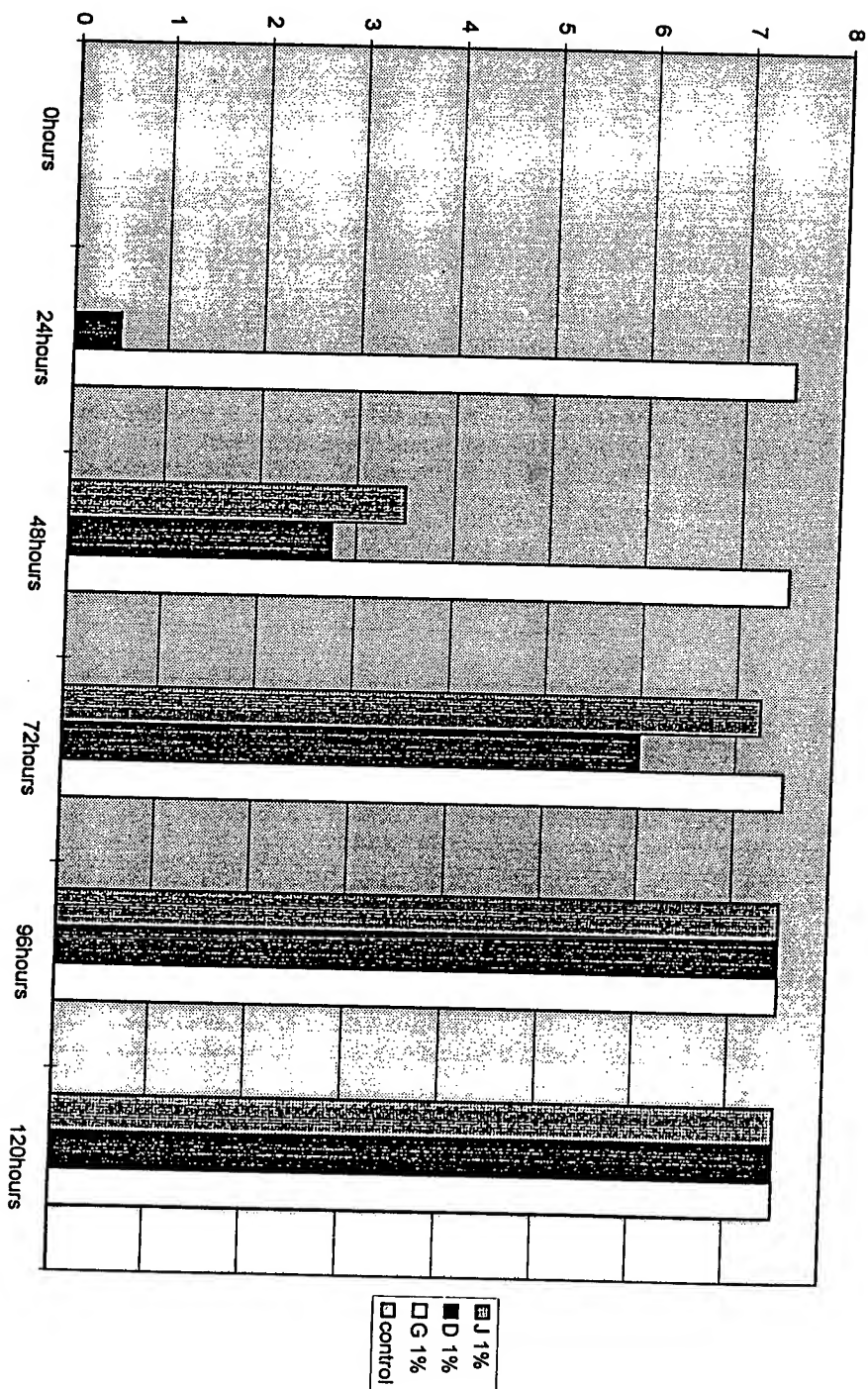


Figure 3b.

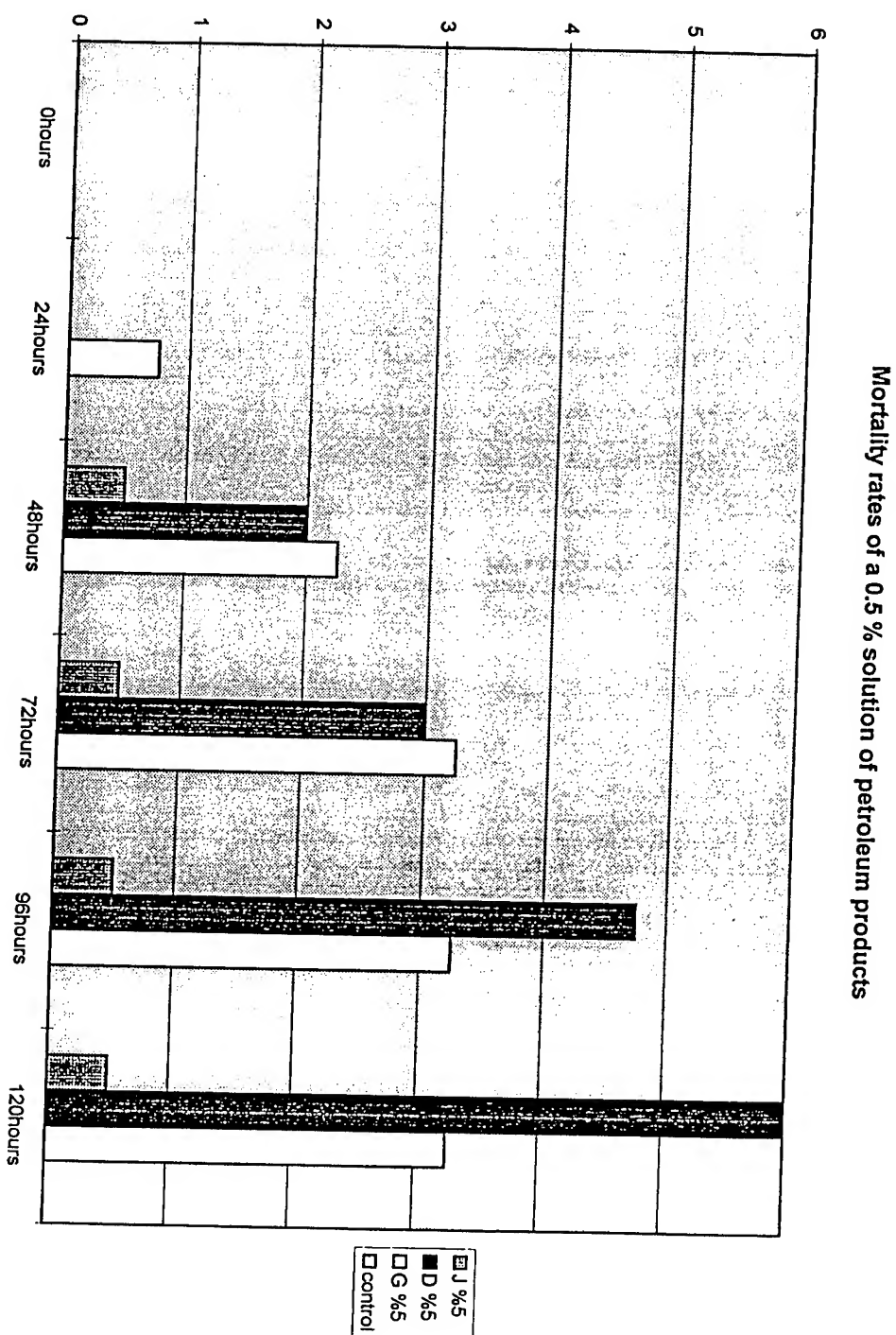


Figure 3c.

Mortality rates of a 50/100 water extraction of petroleum products

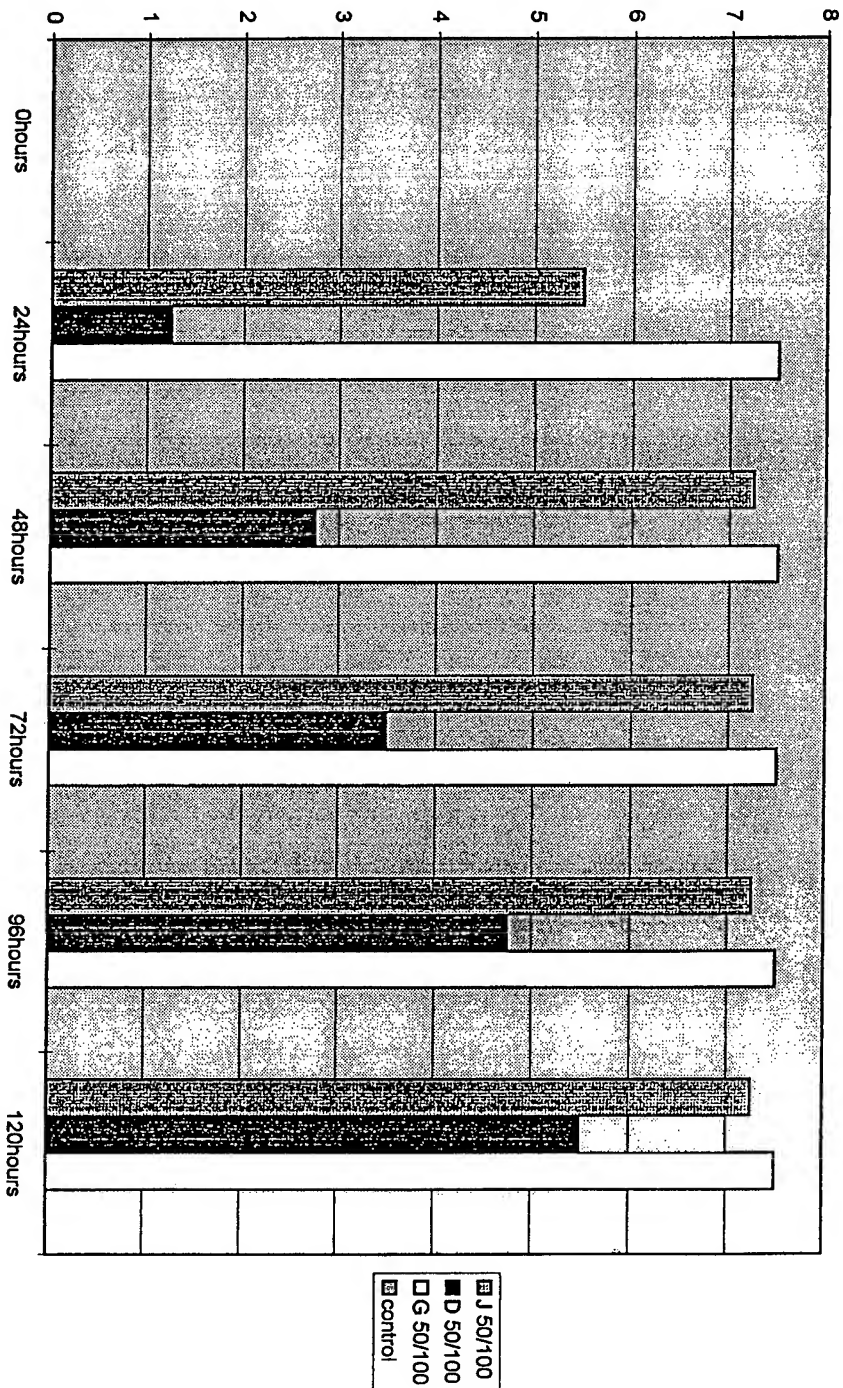


Figure 3d.

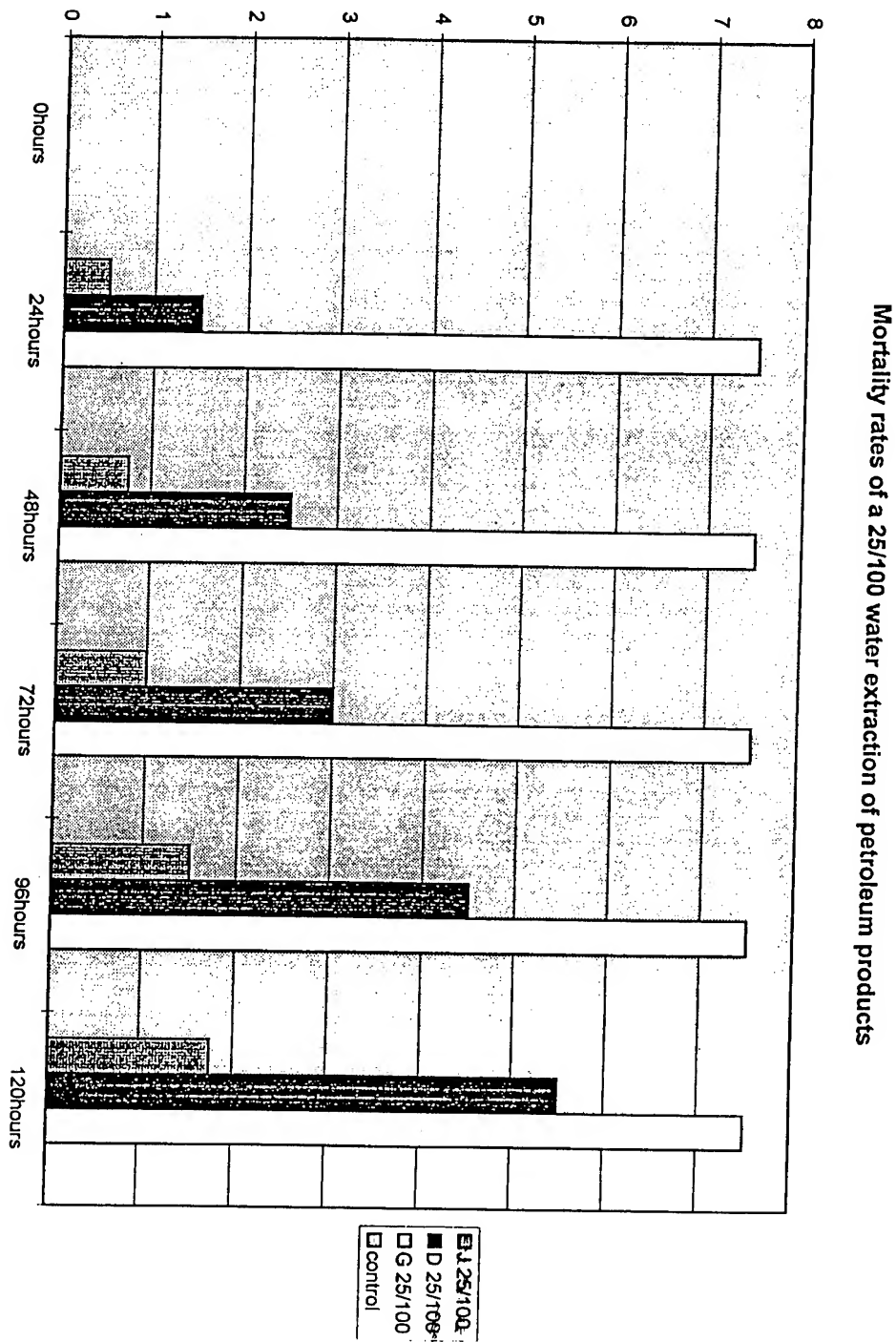


Figure 4. Water soluble extract of JP-8.

File : C:\HPCHEM\1\DATA\28AUG97\JP8.D
 Operator : CARLOS
 Acquired : 28 Aug 97 2:14 pm using AcqMethod FUELS
 Instrument : 625_1
 Sample Name: JP8 STANDARD FOR BEN
 Misc Info :
 Vial Number: 1

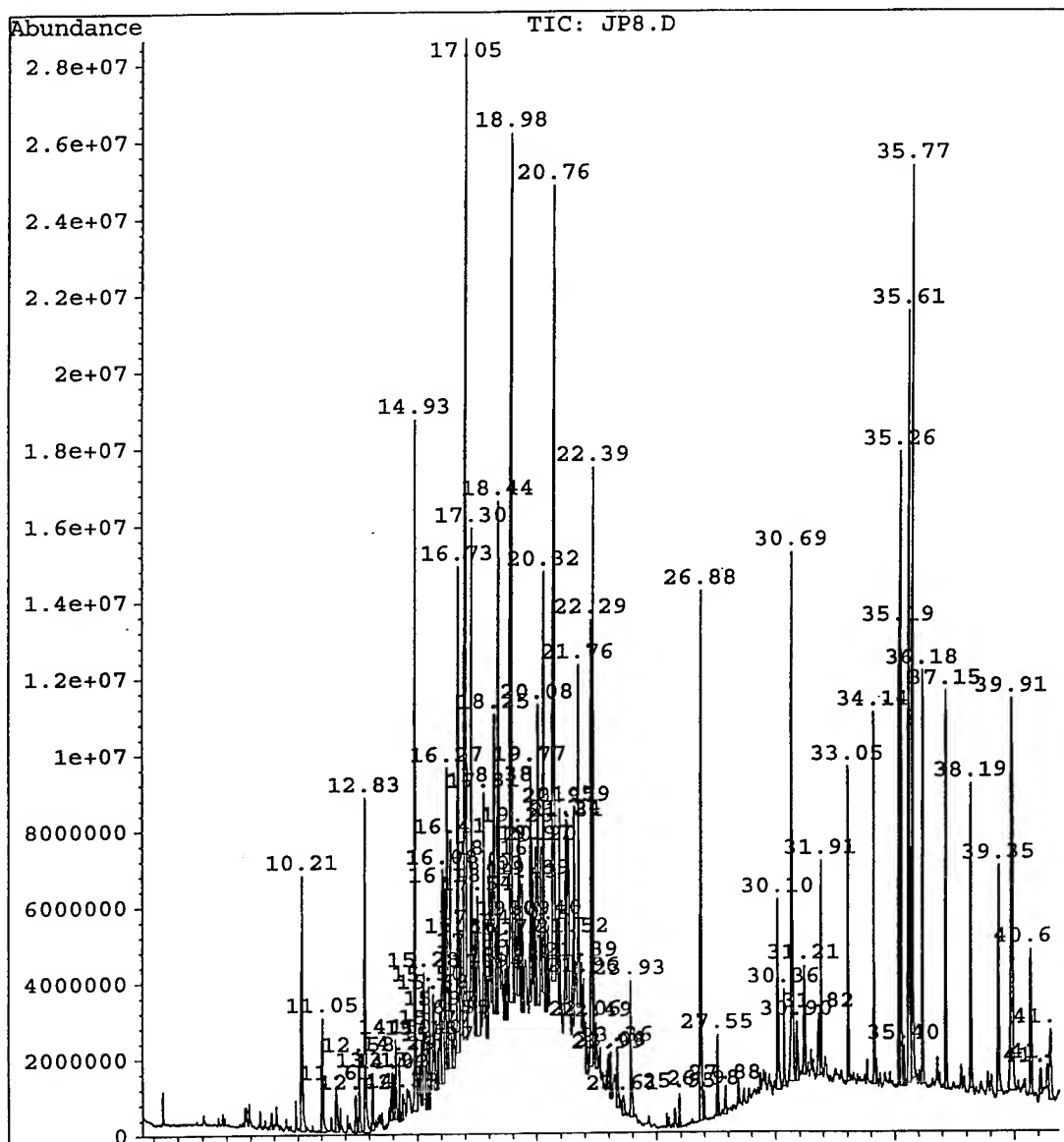


Figure 5. Water soluble extract of gasoline.

File : C:\HPCHEM\1\DATA\28AUG97\GAS.D
Operator : CARLOS
Acquired : 28 Aug 97 3:09 pm using AcqMethod FUELS
Instrument : 625_1
Sample Name: GAS STANDARD FOR BEN
Misc Info :
Vial Number: 2

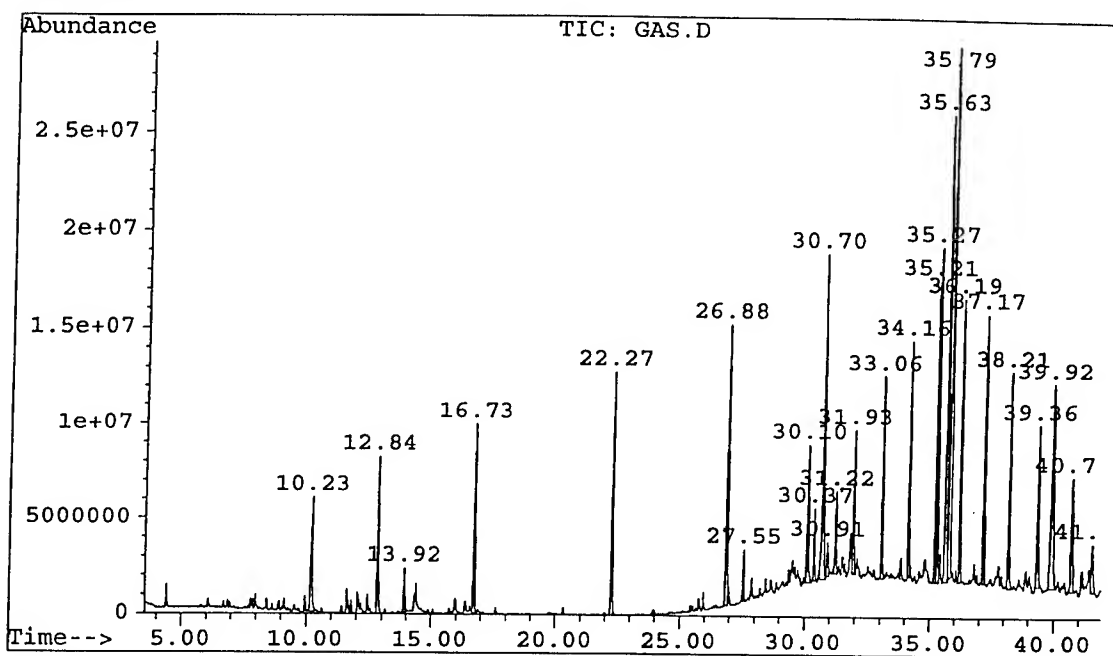


Table 1. Alkylbenzenes and naphthalenes of JP-8 (Kelly A. F. B.), Jet-A (Berry Airfield), and Diesel (Kelly A. F. B.).

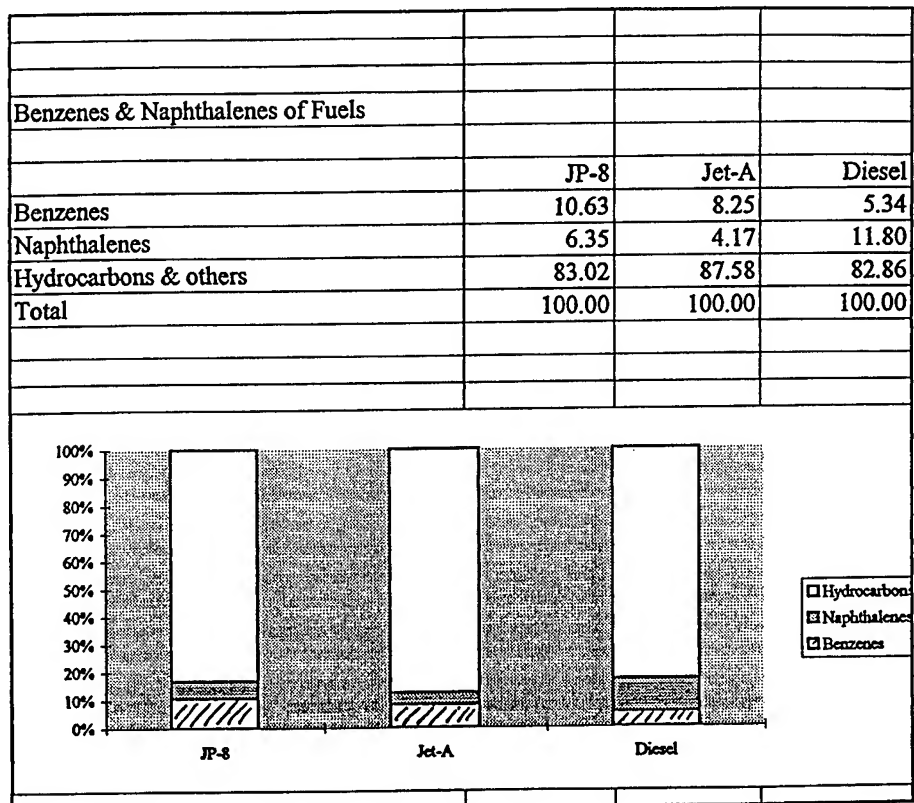


Table 2. Alkylbenzenes and naphthalenes of JP-8.

Benzenes and Naphthalenes in JP-8		
12 5.58 0.16 C:\DATABASE\NBS75K.L	CAS #	area%
Toluene	000108-88-3	0.16
Ethylbenzene	000100-41-4	0.31
Benzene, 1,3-dimethyl-	000108-38-3	2.73
p-Xylene	000106-42-3	
Benzene, 1,2-dimethyl-	000095-47-6	0.68
Benzene, 1-ethyl-2-methyl-	000611-14-3	1.44
Benzene, 1-ethyl-3-methyl-	000620-14-4	
1,2,4-Trimethylbenzene	000095-36-3	1.3
Benzene, 1,2,3-trimethyl-	000526-73-8	1.58
Benzene, butyl-	000104-51-8	0.14
Benzene, 1-ethyl-4-methyl-	000622-96-8	0.59
Benzene, 1-methyl-2-(1-methylethyl)-	000527-84-4	0.37
Benzene, 1-methyl-3-(1-methylethyl)	000535-77-3	
Benzene, methyl(1-methylethyl)-	025155-15-1	
Benzene, 2-ethyl-1,3-dimethyl-	002870-04-4	0.21
Benzene, 1-methyl-4-(1-methylethyl)	000099-87-6	
Benzene, 4-ethyl-1,2-dimethyl-	000934-80-5	0.78
Benzene, 1-ethyl-2,3-dimethyl-	000933-98-2	
Benzene, (1,1-dimethylpropyl)-	002049-95-8	0.2
Benzene, 1-ethyl-2,4-dimethyl-	000874-41-9	
Benzene, 1,2-diethyl-	000135-01-3	?
Benzene, 1,2,3,4-tetramethyl-	000488-23-3	?
Benzene, 1,2,4,5-tetramethyl-	000095-93-2	?
Naphthalene, decahydro-2-methyl-	002958-76-1	1.23
Benzene, 1,3-diethyl-5-methyl-	002050-24-0	0.63
Benzene, 1-ethyl-3,5-dimethyl-	000934-74-7	
Benzene, (1,1-dimethylpropyl)-	002049-95-8	0.31
Naphthalene-d8-	001146-65-2	
1H-Indene, 2,3-dihydro-1,1,5-trime	040650-41-7	? 0.28
1H-Indene, 2,3-dihydro-1,1,3-trime	002613-76-5	?
Benzene, 1-(1-methylethenyl)-3-(1-methyl	001129-29-9	?
Naphthalene, 1-methyl-	000090-12-0	1.15
Benzocycloheptatriene	000264-09-5	?
Naphthalene, 2-methyl-	000091-57-6	0.93
1H-Indene, 2,3-dihydro-1,1,3-trime	002613-76-5	
Naphthalene, 1,2,3,4-tetrahydro-1-methyl-	004175-54-6	0.09

1H-Indene, 2,3-dihydro-1,4,7-trime	054340-87-3	
Naphthalene, 2-ethenyl-	000827-54-3	0.32
Biphenyl	000092-52-4	
Naphthalene, 1,2-dimethyl-	000573-98-8	0.1
Naphthalene, 2,3-dimethyl-	000581-40-8	
4-Hexenoic acid, 3-methyl-2,6-diox	056771-77-8	?
Naphthalene, 2,6-dimethyl-	000581-42-0	0.73
Naphthalene, 1,4-dimethyl-	000571-58-4	0.55
Naphthalene, 2,7-dimethyl-	000582-16-1	0.87
Naphthalene, 1,3-dimethyl-	000575-41-7	
Naphthalene, 1,4,6-trimethyl-	002131-42-2	0.07
Naphthalene, 2,3,6-trimethyl-	000829-26-5	

Table 3. Alkylbenzenes and naphthalenes of Jet-A.

Benzenes and Naphthalenes		
Jet-A Fuel, Berry		
NAME	CAS#	%
Ethylbenzene	000100-41-4	0.15
Benzene, 1,2-dimethyl-	000095-47-6	0.64
p-Xylene	000106-42-3	
Benzene, 1-ethyl-3-methyl-	000620-14-4	1.16
Benzene, 1-ethyl-4-methyl-	000622-96-8	0.68
Benzene, 1-ethyl-2-methyl-	000611-14-3	0.40
1,2,4-Trimethylbenzene	000095-36-3	1.32
Benzene, 1,2,3-trimethyl-	000526-73-8	0.25
Benzene, 1-methyl-3-propyl-	001074-43-7	0.83
Benzene, (1-methylpropyl)-	000135-98-8	0.10

Benzene, 4-ethyl-1,2-dimethyl-	000934-80-5	0.28
Benzene, 1-ethyl-2,4-dimethyl-	000874-41-9	0.18
Benzene, 2-ethyl-1,3-dimethyl-	002870-04-4	0.20
Benzene, 1-ethyl-2,3-dimethyl-	000933-98-2	0.97
Benzene, 1-methyl-3-(1-methylethyl	000535-77-3	0.69
Benzene, 1-methyl-2-(1-methylethyl	000527-84-4	0.40
Naphthalene, decahydro-2-methyl	002958-76-1	0.47
Naphthalene, 1,2,3,4-tetrahydro-1-methyl-	004175-54-6	0.21
Octadecanal	000638-66-4	
Naphthalene, 2-methyl-	000091-57-6	0.36
Naphthalene, 1-methyl-	000090-12-0	0.20
Naphthalene, 2-ethenyl-	000827-54-3	0.44
Naphthalene, 2,7-dimethyl-	000582-16-1	0.48
Naphthalene, 2,6-dimethyl-	000581-42-0	0.72
Naphthalene, 1,3-dimethyl-	000575-41-7	0.48
Naphthalene, 1,6-dimethyl-	000575-43-9	0.1
Naphthalene, 1,5-dimethyl-	000571-61-9	0.36
Naphthalene, 1,6,7-trimethyl-	002245-38-7	0.35
Naphthalene, 2,3,6-trimethyl-	000829-26-5	
Naphthalene, 1,4,6-trimethyl-	002131-42-2	

Table 4. Alkylbenzenes and naphthalenes of Diesel.

Benzenes and Naphthalenes		
Diesel Fuel , Kelly A. F. B.		
NAME	CAS#	%
Ethylbenzene	000100-41-4	0.11
p-xylene	000106-42-3	0.30
Benzene, 1,2-dimethyl-	000095-47-6	0.03
Benzene, propyl-	000103-65-1	0.01
Benzene, 1-ethyl-4-methyl-	000622-96-8	0.42
Benzene, 1-ethyl-2-methyl-	000611-14-3	0.34
Benzene, 1-ethyl-3-methyl-	000620-14-4	0.39
1,2,4-Trimethylbenzene	000095-36-3	0.47
Benzene, 1,2,3-trimethyl-	000526-73-8	
Benzene, 1-methyl-3-propyl-	001074-43-7	0.52
Benzene, 1-ethyl-2,3-dimethyl-	000933-98-2	0.49
Benzene, 1-ethyl-2,4-dimethyl-	000874-41-9	0.2
Benzene, 4-ethyl-1,2-dimethyl-	000934-80-5	0.12
Benzene, 1-methyl-3-(1-methylethyl)	000535-77-3	0.11
Benzene, 1-ethyl-2,3-dimethyl-	000933-98-2	0.78
Benzene, 2-ethyl-1,3-dimethyl-	002870-04-4	
Benzene, 4-ethyl-1,2-dimethyl-	000934-80-5	
Benzene, 1-methyl-2-(1-methylethyl)	000527-84-4	0.19
Benzene, tert-butyl-	000098-06-6	0.08
Naphthalene, 1,2,3,4-tetrahydro-	000119-64-2	1.08
Naphthalene-d8- standard	001146-65-2	7.17
Naphthalene, 1,2,3,4-tetrahydro-2-methyl-	003877-19-8	2.44
Naphthalene, 1,2,3,4-tetrahydro-1-methyl-	001559-81-5	0.5
Naphthalene, 1,2,3,4-tetrahydro-6-methyl-	001680-51-9	1.21
Naphthalene, 1,2,3,4-tetrahydro-5-methyl	001680-51-9	
Naphthalene, 1-methyl-	000090-12-0	1.15
Naphthalene, 1,2,3,4-tetrahydro-2,7-dimethyl-	013065-07-1	1.71
Benzene, 1-(1-methylethenyl)-2-(1-methylethyl)-	005557-93-7	0.24
Biphenyl		0.54
Naphthalene, 2-ethenyl-		
Naphthalene, 1,2,3,4-tetrahydro-1,5-dimethyl-	021564-91-0	1.31
Naphthalene, 2,6-dimethyl-	000581-42-0	0.35
Naphthalene, 2,7-dimethyl-	000582-16-1	0.87
Naphthalene, 1,6-dimethyl-	000575-43-9	1.08

Naphthalene, 1,2,3,4-tetrahydro-1,1,6-trimethyl-	000475-03-6	0.05
Naphthalene, 1,2,3,4-tetrahydro-1,5,7-trimethyl-	021693-55-0	0.05
Indan, 1,1,6,7-tetramethyl-	016204-58-3	
Naphthalene, 2,3,6-trimethyl-	000829-26-5	0.45
Naphthalene, 1,4,6-trimethyl-	002131-42-2	
Naphthalene, 1,6,7-trimethyl-	002245-38-7	
Naphthalene, 1,4,5-trimethyl-	002131-41-1	
9-H-Fluorene, 2,3-dimethyl		0.01
Phenanthrene, 2,5-dimethyl-	003674-66-6	0.30

Table 5. Water soluble extracts of JP-8.

Information from Data File:

File: C:\HPCHEM\1\DATA\28AUG97\JP8.D
 Operator: CARLOS
 Date Acquired: 28 Aug 97 2:14 pm
 Method File: FUELS
 Sample Name: JP8 STANDARD FOR BEN
 Misc Info:
 Vial Number: 1

Search Libraries: C:\DATABASE\NBS75K.L Minimum Quality: 0

Unknown Spectrum: Apex
 Integration Events: AutoIntegrate

Pk#	RT	Area%	Library/ID	Ref#	CAS#
Qual					
1	10.21	1.66	C:\DATABASE\NBS75K.L		
			Ethanol, 2-butoxy-	64439	000111-
76-2	87				
			Ethanol, 2-butoxy-	64441	000111-
76-2	83				
			Ethanol, 2-butoxy-	3544	000111-
76-2	53				
2	11.05	0.70	C:\DATABASE\NBS75K.L		
			Ethanol, 2-(2-methoxyethoxy)-	64524	000111-
77-3	83				
			Ethanol, 2-(2-methoxyethoxy)-	3719	000111-
77-3	78				
			Ethane, 1,2-dimethoxy-	62991	000110-
71-4	37				
3	12.83	1.55	C:\DATABASE\NBS75K.L		
			1,4-Dichlorobenzene-d4	9593	003855-
82-1	95				
			Benzene-1,2,3,4-d4-, 5,6-dichloro-	9592	002199-
69-1	50				
			Benzenamine, 2-methyl-4-nitro-	10129	000099-
52-5	22				
4	14.93	3.36	C:\DATABASE\NBS75K.L		
			Undecane	11611	001120-
21-4	97				
			Undecane	67317	001120-
21-4	94				
			Undecane	67318	001120-
21-4	91				

TMPLIBRP.TXT

5	15.28	0.61	C:\DATABASE\NBS75K.L	
			Dodecane	68254 000112-
40-3	60			
			2,6-Dimethyldecane	15357 013150-
81-7	55			
			Dodecane	68252 000112-
40-3	55			
6	15.50	0.48	C:\DATABASE\NBS75K.L	
			Dodecane, 2,6,10-trimethyl-	70270 003891-
98-3	90			
			Undecane, 3,8-dimethyl-	19009 017301-
30-3	80			
			Nonane, 3-methyl-5-propyl-	19054 031081-
18-2	80			
7	16.08	1.25	C:\DATABASE\NBS75K.L	
			3-Undecanone	15322 002216-
87-7	25			
			1-Octanol, 2-butyl-	69110 003913-
02-8	25			
			Decane, 2,5,6-trimethyl-	19019 062108-
23-0	22			
8	16.18	0.62	C:\DATABASE\NBS75K.L	
			Undecane, 4-methyl-	68256 002980-
69-0	70			
			Undecane, 4-methyl-	15354 002980-
69-0	64			
			Decane, 3-methyl-	11604 013151-
34-3	64			
9	16.27	1.30	C:\DATABASE\NBS75K.L	
			Undecane, 2-methyl-	68257 007045-
71-8	81			
			Undecane, 2-methyl-	15356 007045-
71-8	74			
			Hexadecane	70787 000544-
76-3	72			
10	16.41	1.15	C:\DATABASE\NBS75K.L	
			Decane, 3,8-dimethyl-	68255 017312-
55-9	74			
			Decane, 3-bromo-	27510 030571-
71-2	50			
			Undecane, 5-ethyl-	19036 017453-
94-0	50			
11	16.73	2.63	C:\DATABASE\NBS75K.L	
			Naphthalene-d8-	6596 001146-

TMPLIBRP.TXT

65-2 97		Benzenemethanol, 3,5-dimethyl-	6537 027129-
87-9 53		6H-Purin-6-one, 1,7-dihydro-	65642 000068-
94-0 40			
12 16.86 0.49	C:\DATABASE\NBS75K.L		
	Cyclopentane, 1-methyl-3-(2-methyl	7554 029053-	
04-1 42		Cyclopentane, 1,1,3-trimethyl-	2676 004516-
69-2 38		Dodecane, 1-cyclopentyl-4-(3-cyclo	49134 007225-
68-5 27			
13 17.05 6.44	C:\DATABASE\NBS75K.L		
	Dodecane	68254 000112-	
40-3 96		Dodecane	68251 000112-
40-3 95		Dodecane	68249 000112-
40-3 95			
14 17.30 1.90	C:\DATABASE\NBS75K.L		
	Undecane, 2,6-dimethyl-	19058 017301-	
23-4 96		Undecane, 3,6-dimethyl-	19000 017301-
28-9 78		Heptadecane, 2,6-dimethyl-	37466 054105-
67-8 64			
15 17.44 0.38	C:\DATABASE\NBS75K.L		
	Nonane	65143 000111-	
84-2 64		Heptane, 2,4-dimethyl-	65120 002213-
23-2 58		Dotriacontane	74491 000544-
85-4 52			
16 17.54 1.18	C:\DATABASE\NBS75K.L		
	2,7-Octadiene, 4-methyl-	4209 000000-	
00-0 43		Aspidospermidin-17-ol, 1-acetyl-19	54883 002122-
26-1 43		Cyclohexane, 2-butyl-1,1,3-trimeth	68867 054676-
39-0 38			
17 17.81 1.12	C:\DATABASE\NBS75K.L		
	Cyclohexane, (4-methylpentyl)-	14775 061142-	
20-9 87		Cyclohexane, hexyl-	14757 004292-
75-5 83			

TMPLIBRP.TXT

42-3 81	Cyclohexane, 2-propenyl-	64813 002114-
18 18.03 0.45	C:\DATABASE\NBS75K.L	
23-4 62	Undecane, 2,6-dimethyl-	69032 017301-
23-4 53	Undecane, 2,6-dimethyl-	19058 017301-
22-3 52	Undecane, 2,5-dimethyl-	69031 017301-
19 18.16 0.48	C:\DATABASE\NBS75K.L	
97-1 91	Dodecane, 4-methyl-	19025 006117-
33-6 87	Undecane, 4,8-dimethyl-	69027 017301-
33-6 80	Undecane, 4,8-dimethyl-	19026 017301-
20 18.25 1.27	C:\DATABASE\NBS75K.L	
97-0 86	Dodecane, 2-methyl-	69030 001560-
27-8 81	Undecane, 2,10-dimethyl-	18997 017301-
08-4 64	Dodecane, 2-methyl-6-propyl-	29264 055045-
21 18.38 0.89	C:\DATABASE\NBS75K.L	
57-1 59	Dodecane, 3-methyl-	69025 017312-
00-0 58	10-Methylnonadecane	39858 000000-
26-7 58	Undecane, 2,9-dimethyl-	18994 017301-
22 18.44 1.63	C:\DATABASE\NBS75K.L	
34-6 78	Octane, 2,3,7-trimethyl-	11603 062016-
04-6 78	Nonane, 3-methyl-	66201 005911-
04-6 78	Nonane, 3-methyl-	8075 005911-
23 18.77 0.41	C:\DATABASE\NBS75K.L	
23-2 49	Cyclohexane, (2,2-dimethylcyclopentyl)-	17943 061142-
85-9 49	Cyclopentane, 2-isopropyl-1,3-dimethyl-	7525 032281-
00-0 49	Triallylmethylsilane	14075 000000-

TMPLIBRP.TXT

24	18.98	6.23	C:\DATABASE\NBS75K.L	
			Tridecane	69019 000629-
50-5	93		Tridecane	69021 000629-
50-5	92		Dodecane, 2-methyl-	69030 001560-
97-0	81			
25	19.09	0.34	C:\DATABASE\NBS75K.L	
			Decanedioic acid, didecyl ester	58384 002432-
89-5	46		1-Hexacosanol	52385 000506-
52-5	38		1-Tetracosanol	49775 000506-
51-4	38			
26	19.26	0.74	C:\DATABASE\NBS75K.L	
			Tetracontane, 3,5,24-trimethyl-	60914 055162-
61-3	72		Nonane, 3,7-dimethyl-	11601 017302-
32-8	53		Dodecane, 3-methyl-	69025 017312-
57-1	53			
27	19.43	0.65	C:\DATABASE\NBS75K.L	
			1H-Imidazole, 4,5-dihydro-4-methyl	12483 000939-
06-0	53		Benzene, 1-(1,1-dimethylethyl)-4-e	12543 001746-
23-2	41		Benzene, cyclohexyl-	12560 000827-
52-1	41			
28	19.77	1.17	C:\DATABASE\NBS75K.L	
			Cyclohexane, hexyl-	68123 004292-
75-5	58		Cyclohexane, pentyl-	11044 004292-
92-6	58		Cyclohexane, octyl-	69530 001795-
15-9	53			
29	19.97	0.60	C:\DATABASE\NBS75K.L	
			Tridecane, 4-methyl-	22537 026730-
12-1	93		Tridecane, 4-methyl-	69665 026730-
12-1	68		Heptadecane, 8-methyl-	34816 013287-
23-5	58			
30	20.08	1.47	C:\DATABASE\NBS75K.L	
			Tridecane, 2-methyl-	22536 001560-
96-9	81			

TMPLIBRP.TXT

96-9 76	Tridecane, 2-methyl-	69663 001560-
00-0 64	10-Methylnonadecane	39858 000000-
31 20.20 0.57	C:\DATABASE\NBS75K.L	
41-3 87	Tridecane, 3-methyl-	22540 006418-
02-4 72	Octacosane	74211 000630-
03-5 68	Nonacosane	54526 000630-
32 20.32 1.58	C:\DATABASE\NBS75K.L	
98-3 91	Dodecane, 2,6,10-trimethyl-	70270 003891-
98-0 86	Dodecane, 2,7,10-trimethyl-	26005 074645-
62-9 80	Pentadecane	26001 000629-
33 20.40 0.42	C:\DATABASE\NBS75K.L	
00-0 93	Decahydro-4,4,8,9,10-pentamethylna	24990 000000-
56-6 38	2(1H)-Naphthalenone, octahydro-4a,	21384 007056-
31-9 38	2(1H)-Naphthalenone, octahydro-4a,	21369 054699-
34 20.51 0.33	C:\DATABASE\NBS75K.L	
54-3 64	Naphthalene, 2-ethenyl-	11097 000827-
52-4 55	Biphenyl	67194 000092-
52-4 55	Biphenyl	67192 000092-
35 20.76 4.90	C:\DATABASE\NBS75K.L	
59-4 98	Tetradecane	69661 000629-
59-4 95	Tetradecane	22534 000629-
59-4 94	Tetradecane	69662 000629-
36 20.97 0.87	C:\DATABASE\NBS75K.L	
61-9 96	Naphthalene, 1,5-dimethyl-	11633 000571-
16-1 96	Naphthalene, 2,7-dimethyl-	11619 000582-
	Naphthalene, 1,5-dimethyl-	67354 000571-

TMPLIBRP.TXT

61-9 96			
37 21.24 0.98	C:\DATABASE\NBS75K.L		
	Naphthalene, 1,5-dimethyl-	11633	000571-
61-9 97			
	Naphthalene, 2,3-dimethyl-	67332	000581-
40-8 97			
	Naphthalene, 1,7-dimethyl-	67343	000575-
37-1 97			
38 21.52 0.42	C:\DATABASE\NBS75K.L		
	1-Pentadecene	70191	013360-
61-7 56			
	Decane, 5-propyl-	19035	017312-
62-8 42			
	Octadecane, 1-chloro-	72490	003386-
33-2 38			
39 21.59 0.66	C:\DATABASE\NBS75K.L		
	Naphthalene, 2,6-dimethyl-	67335	000581-
42-0 76			
	Naphthalene, 1,5-dimethyl-	11633	000571-
61-9 76			
	Naphthalene, 2,7-dimethyl-	67328	000582-
16-1 76			
40 21.76 1.43	C:\DATABASE\NBS75K.L		
	Tridecane	69017	000629-
50-5 90			
	Eicosane	72326	000112-
95-8 87			
	Pentadecane	26001	000629-
62-9 87			
41 22.29 2.45	C:\DATABASE\NBS75K.L		
	Acenaphthene-d10	13561	015067-
26-2 90			
	Papaveroline, 1,2,3,4-tetrahydro-5	42927	000000-
00-0 10			
	Methanimidamide, N'-(4-hydroxyphen	13383	002350-
51-8 9			
42 22.39 2.47	C:\DATABASE\NBS75K.L		
	Pentadecane	26001	000629-
62-9 98			
	Pentadecane	70275	000629-
62-9 97			
	Pentadecane	70277	000629-
62-9 96			
43 23.36 0.35	C:\DATABASE\NBS75K.L		

TMPLIBRP.TXT

26-5 95	Naphthalene, 2,3,6-trimethyl-	68266 000829-
26-5 91	Naphthalene, 2,3,6-trimethyl-	68265 000829-
42-2 91	Naphthalene, 1,4,6-trimethyl-	15380 002131-
44 23.93 0.65	C:\DATABASE\NBS75K.L Hexadecane	29267 000544-
76-3 98	Hexadecane	70788 000544-
76-3 97	Hexadecane	70790 000544-
76-3 96		
45 26.88 3.04	C:\DATABASE\NBS75K.L Phenanthrene-d10	19958 001517-
22-2 95	Anthracene-d10-	19957 001719-
06-8 94	Selenide, ethyl 1-methyl-1-penten-	19733 025128-
48-7 45		
46 27.55 0.35	C:\DATABASE\NBS75K.L 2,4-Diphenyl-4-methyl-2(E)-pentene	31185 000000-
00-0 95	Benzene, 1,1'-(3,3-dimethyl-1-bute	31190 023586-
64-3 78	(1H)2,3-Dihydroindene, 1,1,3-trime	31188 000000-
00-0 78		
47 30.10 1.03	C:\DATABASE\NBS75K.L 2-t-Butyl-4-(dimethylbenzyl)phenol	37458 000000-
00-0 91	1,5-Diphenyl-2H-1,2,4-triazoline-3	34508 005055-
74-3 50	Benzene, 1-methyl-3,5-bis[(trimeth	37301 089267-
67-4 12		
48 30.36 0.47	C:\DATABASE\NBS75K.L s-Indacene-1,7-dione, 2,3,5,6-tetr	32402 055591-
17-8 64	1,4-Naphthalenedione, 2-hydroxy-3-	32357 000084-
79-7 46	1,4-Naphthalenedione, 2-hydroxy-3-	32368 004042-
39-1 38		
49 30.69 2.95	C:\DATABASE\NBS75K.L 5-Methoxy-1-(3-methoxy-4-methylphe	46156 000000-
00-0 72	2,6-Bis(t-butyl)-4-(dimethylbenzyl	46161 000000-

TMPLIBRP.TXT

00-0 60				
		4,6-Bis(t-butyl)-2-(dimethylbenzyl	46160	000000-
00-0 42				
50 30.90 0.37	C:\DATABASE\NBS75K.L			
	2-Pyrimidinamine, 4-methyl-6-pheny	19183	015755-	
15-4 35				
	Benz[e]acephenanthrylene	34432	000205-	
99-2 25				
	Anisindione	34359	000117-	
37-3 25				
51 31.21 0.54	C:\DATABASE\NBS75K.L			
	4b,5,6,12-Tetrahydrochrysene	30407	031570-	
60-2 49				
	Benzene, (chloromethyl)ethenyl-	10204	030030-	
25-2 25				
	1,2,3,4-Tetrahydrobenz[A]anthracen	30405	004483-	
98-1 14				
52 31.82 0.45	C:\DATABASE\NBS75K.L			
	1'R-Methyl-2,2'-spirobiindan-1-one	33603	082309-	
97-5 25				
	Benzo[b]naphtho[2,3-d]thiophene, 8	33589	024964-	
07-6 25				
	1,4-Naphthoquinone, 6-acetyl-2,5,8	33412	013379-	
24-3 25				
53 31.91 0.81	C:\DATABASE\NBS75K.L			
	Docosane	44318	000629-	
97-0 99				
	Docosane	72998	000629-	
97-0 99				
	Octadecane	71560	000593-	
45-3 93				
54 33.05 1.24	C:\DATABASE\NBS75K.L			
	Docosane	72998	000629-	
97-0 96				
	Octadecane	71560	000593-	
45-3 95				
	Pentadecane, 3-methyl-	29258	002882-	
96-4 94				
55 34.14 1.51	C:\DATABASE\NBS75K.L			
	Tetracosane	73541	000646-	
31-1 97				
	Tricosane	73319	000638-	
67-5 95				
	Tetracosane	73542	000646-	
31-1 95				

TMPLIBRP.TXT

56	35.19	2.08	C:\DATABASE\NBS75K.L	
			Docosane	72997 000629-
97-0	97			
			Heptadecane	71191 000629-
78-7	95			
			Heptadecane	71193 000629-
78-7	94			
57	35.26	3.77	C:\DATABASE\NBS75K.L	
			Chrysene-d12	32068 001719-
03-5	93			
			9,10-Anthracenedione, 1,4-dihydrox	71175 000081-
64-1	58			
			Naphtho[2,1-b:7,8-b']difuran, 1,2,	32043 068873-
21-2	50			
58	35.61	4.33	C:\DATABASE\NBS75K.L	
			2,4-Bis(dimethylbenzyl)phenol	46982 000000-
00-0	94			
			1H-Dicyclooct[e,g]isoindole-1,3(2H	44974 051624-
47-6	9			
			2-Hydroxy-3-(2-hydroxy-1-naphthoyl	44972 000000-
00-0	9			
59	35.77	4.87	C:\DATABASE\NBS75K.L	
			2,4-Bis(dimethylbenzyl)-6-t-butylp	52799 000000-
00-0	78			
			N-Acetylcolchinol methyl ether	51472 065967-
01-3	9			
			1H-Pyrrole, 2,3,4,5-tetraphenyl-	51488 003263-
79-4	9			
60	36.18	1.73	C:\DATABASE\NBS75K.L	
			Hexacosane	51010 000630-
01-3	98			
			Tricosane	73319 000638-
67-5	98			
			Heptadecane, 9-octyl-	49558 007225-
64-1	95			
61	37.15	1.70	C:\DATABASE\NBS75K.L	
			Pentacosane	49559 000629-
99-2	98			
			Heptacosane	52248 000593-
49-7	97			
			Heptacosane	74082 000593-
49-7	96			
62	38.19	1.38	C:\DATABASE\NBS75K.L	
			Pentacosane	73719 000629-

TMPLIBRP.TXT

99-2 98	Tricosane	46165 000638-
67-5 97	Tricosane	73318 000638-
67-5 96		
63 39.35 1.24	C:\DATABASE\NBS75K.L Pentacosane	49559 000629-
99-2 97	Heptacosane	74082 000593-
49-7 94	Docosane	44318 000629-
97-0 91		
64 39.91 3.47	C:\DATABASE\NBS75K.L Perylene-d12	36687 001520-
96-3 97	Sericic acid	59077 055306-
03-1 46	1(3H)-Isobenzofuranone, 3-(3-oxo-1	36597 000482-
23-5 42		
65 40.69 0.89	C:\DATABASE\NBS75K.L Pentacosane	49559 000629-
99-2 97	Hexacosane	73944 000630-
01-3 93	Nonadecane, 9-methyl-	39865 013287-
24-6 91		
66 41.51 0.53	C:\DATABASE\NBS75K.L 2,4,6-Tri(dimethylbenzyl)phenol	56999 000000-
00-0 90	2-Propanone, 1-(2-nitro-1(5H)-phen	56141 021589-
31-1 23	Chamaecydin	56997 086746-
82-9 10		

Tue Sep 02 09:35:06 1997

Conclusion

Preliminary bioassay tests on the JP-8, Diesel and gasoline and their water soluble extracts have been conducted with two species of fresh water snails.

Both JP-8 and diesel fuels one percent and half percent solutions were found to be more toxic than their 50 to 1000 and 25 to 100 water extractions. However, gasoline was determined to be just the opposite, with its water extractions of 50 to 100 and 25 to 100 showing a higher mortality rate than its one percent and half percent solution. Overall, gasoline was established as the most mephitic of the three followed by diesel fuel and finally JP-8. Out of the nine compound, which were tested to establish toxic substances within the petroleum, only one, ethylbenzene has shown dramatic toxicity rates. Experimentation of chemical compounds will continue. Further tests using P. virgata eggs, to determine hatch ability, in petroleum products are underway.

Gas chromatograms of JP-8 and gasoline water soluble extracts contain aromatic hydrocarbons as the major components.

References

- Andrews, L. S., and Snyder, R., 1991. Toxic effects of solvents and vapors. p681-722 in Casarett and Doull's Toxicology: The basic Science of Poisons, 3rd Ed., Klassen, C. D., Amdur, M. O., and Doull, J., eds. New York: Pergamon.
- Bishop, E. C., 1982. Evaluating health hazards associated with aircraft fuel cell maintenanc. Proceedings of the twelfth conference on environmental toxicology, AMRL-TR-79-68. Wright-Patterson Air force Base, Dayton, Ohio.
- Brook, J. J., 1978. Jet Engine exhaust analysis by subtractive chromatography, USAF Report SAM-TR-37.
- Fodor, G. E., and Naegeli, 1992. Development of a method to determine the autoxidation of turbine fuels, AD A260578, Southwest Research Institute, San Antonio, Texas.
- Hafner, A. M., Norton, K. L., and Griffiths, P. R., 1987. Interfaced gas chromatography and fourier transform infrared transmission spectrometry by elute trapping at 77K, Analytical Chemistry, 60, 2441.
- Henderson, R. F., 1996. Permissible exposure levels for selected military fuel vapors, p18, National Academy Press, Washington, D. C.
- Purcell, K. J., Cason, G. H., Gargas, M. L., and Anderson, M. E., 1990. In vivo metabolic interactions of benzene and toluene, Toxicol. Lett. 52, 141.
- Restek Corporation, 1996. Product Guide, Bellefonte, PA.
- Satcher, D., 1993. Toxicological profile for fuel oils, U.S. Dept. of Health & Human Services. Contract No. 205-93-0606.
- Supelco, 1996. Chromatography Products, Supelco Park, Bellefonte, PA.
- USAF OEHL Report 84-148SZ111CFC, 1984. Characterization and evaluation of JP-4, Jet A and mixtures of these fuels in environmental water samples, Suffolk County Airport, N. Y..

Acknowledgement

LTC Kenny D. Locke, Dr. George H. Lee, Mr. Andy Richardson and Dr. William D. Gould are gratefully acknowledged for their interest and support of this project. Other individuals who provided information to me were Mr. Henry B. Forjohn, Carlos and Ms. Saad of Armstrong Laboratory. I acknowledge technical advice on the identification of fuel components by infrared spectra from Dr. George E. Fodor, Southwest Research Institute. This report also could not have been produced without the untiring support and advice from LTC, Dr. John T. Sullivan, University of the Incarnate Word. Finally, I would like to thank all the members of Analytical Services Division of Armstrong Laboratory, Brooks Air Force Base and the financial assistance from U.S. Air Force Summer Research Faculty project (Air force Office of Scientific Research 1996 Summer Research Extension Program Subcontract 97-0835, United States AFOSR contract number F49620-93-C-0063).

Biogeochemical Assessment of Natural Attenuation of JP-4-Contaminated Ground Water
in the Presence of Fluorinated Surfactants

Dr. Audrey D. Levine
Professor
Department of Environment Engineering

Utah State University
Logan, UT 84322-8200

Final Report for:
Summer Research Extension Program
Armstrong Laboratory

Sponsored by:
Air Force Office of Scientific Research
Bolling Air Force Base
Washington, D.C.

and

Armstrong Laboratory

December 1995

Biogeochemical assessment of natural attenuation of JP-4-contaminated ground water in the presence of fluorinated surfactants

A.D. Levine^{a,*}, E.L. Libelo^b, G. Bugna^c, T. Shelley^b, H. Mayfield^b,
T.B. Stauffer^b

^aDepartment of Civil and Environmental Engineering, Utah State University, Logan, UT 84322-8200, USA

^bAnnstrong Laboratory, Environics Directorate, 139 Barnes Drive, Suite 2, Tyndall Air Force Base, Florida, FL 32403-5323, USA

^cFlorida State University, Department of Oceanography, Tallahassee, Florida, USA

Received 30 January 1997; accepted 24 September 1997

Abstract

The biogeochemistry of the natural attenuation of petroleum-contaminated ground water was investigated in a field study. The focus of the study was a fire training site located on Tyndall Air Force Base in Florida. The site has been used by the Air Force for approximately 11 years in fire fighting exercises. An on-site above-ground tank of JP-4 provided fuel for setting controlled fires for the exercises. Various amounts of water and aqueous film forming foams (AFFF) were applied to extinguish the fires. The sources of contamination included leaks from pipelines transporting the fuel, leaks from an oil/water separator and runoff and percolation from the fire fighting activities. Previous investigations had identified jet fuel contamination at the site, however, no active remediation efforts have been conducted to date. The goal of this study was to use biogeochemical monitoring data to delineate redox zones within the site and to identify evidence of natural attenuation of JP-4 contamination. In addition to identifying several hydrocarbon metabolites, fluorinated surfactants (AFFF) were detected down-gradient of the hydrocarbon plume. © 1997 Elsevier Science B.V.

Keywords: Biogeochemistry; Petroleum-contaminated groundwater; Hydrocarbon metabolites; Intrinsic remediation

1. Introduction

Over the past decade significant research has been conducted to evaluate the fate, transport

and environmental and health risks associated with ground water contamination. Recently there has been increased interest in promoting the use of passive remediation processes based on natural biogeochemical attenuation of contaminants. The major objectives of this study were to identify biogeochemical indicators of natural attenuation

* Corresponding author.

of petroleum hydrocarbon contaminants under field conditions. The focus of the study was to evaluate relationships between redox conditions and the presence of metabolic byproducts of alkyl benzene degradation at a field site under quasi-steady-state conditions.

2. Background

Natural attenuation of petroleum hydrocarbons in stationary phase and dissolved plumes has been demonstrated in a number of field and laboratory studies (Hill, 1981; Wilson et al., 1986, 1990; Environmental Science and Engineering, 1988; Kuhn et al., 1988; Cozzarelli et al., 1989, 1990, 1994, 1995; Beeman and Suffita, 1990; Kehew and Passero, 1990; McMahon et al., 1990; Geraghty and Miller, 1991, 1994; McNichol et al., 1991; Barbaro et al., 1992; Bellar et al., 1992, 1995; Evans et al., 1992; Chapelle and Lovely, 1992; Baedeker et al., 1993; Bennett et al., 1993; Chapelle, 1993; Eganhouse et al., 1993; Edwards et al., 1994; Lovely et al., 1994; OHM Remediation Services Corp., 1994; Seyfried et al., 1994; Vroblesky and Chapelle, 1994; Bjerg et al., 1995; Jackson et al., 1996; Landmeyer et al., 1996; Stumm and Morgan, 1996; Vroblesky et al., 1996). Attenuation mechanisms encompass physical dilution, physicochemical sorption and ion exchange, chemical dissolution/precipitation or complexation and microbial metabolic processes. Key issues influencing the rate and extent of natural attenuation of contaminated ground water include contamination hydrogeochemistry in conjunction with the availability of subsurface

electron acceptor processes, pH, temperature, site geochemistry and hydrology. Modeling and prediction of the rate of natural attenuation and the fate of metabolic by-products is hampered by the lack of field data that integrates geochemical data with contaminant degradation and by-product formation. A brief review of the major factors relevant to the determination of dominant redox reactions and a summary of field evidence of metabolic by-product formation is given below.

2.1. Redox zones

Redox zones have been characterized in a variety of contaminated aquifers including down-gradient of fuel spills (Wilson et al., 1986, 1990; Cozzarelli et al., 1989, 1990, 1994; Barbaro et al., 1992; Baedeker et al., 1993; Bennett et al., 1993; Eganhouse et al., 1993; Vroblesky and Chapelle, 1994; Landmeyer et al., 1996; Vroblesky et al., 1996) and landfill leachate plumes (Kehew and Passero, 1990; Chapelle, 1993; Bjerg et al., 1995; Stumm and Morgan, 1996). It is widely reported that pH and redox buffering are major controls on biogeochemical reactions in contaminant plumes. A summary of the major types of redox that occur in ground water are given in Table 1 with the standard Gibbs free energy ΔG° values. The compound CH_2O is used to refer to a generic organic compound. The actual free energy values depend on the chemical composition of the organic substrate(s) and the concentrations of reactants and products present at a specific location.

In general, if oxygen is present, biogeochemical reactions tend to be mainly aerobic reactions.

Table 1
Summary of major oxidation–reduction reactions that occur in ground water^a

Type of reaction	Reaction	ΔG° (kJ), kcal/mol
Methanogenic	$2\text{CH}_2\text{O} \rightarrow \text{CH}_3\text{COOH} \rightarrow \text{CH}_4 + \text{CO}_2$	–22
Sulfate reduction	$2\text{CH}_2\text{O} + \text{SO}_4^{2-} + \text{H}^+ \rightarrow 2\text{CO}_2 + \text{HS}^- + 2\text{H}_2\text{O}$	–25
Ferric iron reduction	$\text{CH}_2\text{O} + 4\text{Fe}(\text{OH})_3 + 8\text{H}^+ \rightarrow \text{CO}_2 + 4\text{Fe}^{2+} + 11\text{H}_2\text{O}$	–28
Manganic reduction	$\text{CH}_2\text{O} + 2\text{MnO}_2 + 4\text{H}^+ \rightarrow \text{CO}_2 + 2\text{Mn}^{2+} + 3\text{H}_2\text{O}$	–81
Denitrification	$5\text{CH}_2\text{O} + 4\text{NO}_3^- + 4\text{H}^+ \rightarrow 5\text{CO}_2 + 2\text{N}_2 + 7\text{H}_2\text{O}$	–114
Oxygen reduction	$\text{CH}_2\text{O} + \text{O}_2 \rightarrow \text{CO}_2 + \text{H}_2\text{O}$	–120

^aAdapted from Kehew and Passero (1990), Bennett et al. (1993), Chapelle (1993), Lovely et al. (1994), Vroblesky and Chapelle (1994), Bjerg et al. (1995), Cozzarelli et al. (1995) and Stumm and Morgan (1996).

Due to the limited availability of natural mechanisms to replenish oxygen supplies in the subsurface, ground water that contains degradable organic material is likely to be depleted in dissolved oxygen (Kehew and Passero, 1990; Bennett et al., 1993; Chapelle, 1993; Lovely et al., 1994; Vroblecky and Chapelle, 1994; Bjerg et al., 1995; Cozzarelli et al., 1995; Stumm and Morgan, 1996). Under anoxic conditions, electron acceptors, such as nitrate, sulfate, Mn(IV), Fe(III) and CO_2 are reduced as organic compounds are oxidized resulting in changes in the redox conditions in the aquifer and increases in concentration of reduced aqueous species, such as sulfides, Fe (II), methane and ammonia. In contaminated aquifers, the sequence of the reactions down-gradient of a contaminant plume typically follows the sequence given in Table 1 and has been observed in many aquifers with variations depending on the local geochemistry (Wilson et al., 1986, 1990; Cozzarelli et al., 1989, 1990, 1994; Barbaro et al., 1992; Baedeker et al., 1993; Bennett et al., 1993; Eganhouse et al., 1993; Vroblecky and Chapelle, 1994; Landmeyer et al., 1996; Vroblecky et al., 1996). Some overlap occurs along the interface of successive redox zones.

In sandy aquifers, manganese reduction is a minor electron accepting process and Fe (III) is a major contributor to the oxidation capacity (Wilson et al., 1986, 1990; Cozzarelli et al., 1989, 1990, 1994; Barbaro et al., 1992; Baedeker et al., 1993; Bennett et al., 1993; Eganhouse et al., 1993; Vroblecky and Chapelle, 1994; Landmeyer et al., 1996; Vroblecky et al., 1996). When Fe (III) is available, iron reduction has been reported to out-compete sulfate reduction and methanogenesis in mediating the oxidation of organic matter (Chapelle and Lovely, 1992; Vroblecky et al., 1996). High concentrations of dissolved iron develop if there is minimal sulfate reduction because generation of sulfide results in the formation of iron sulfide precipitates (Chapelle and Lovely, 1992). Methanogenic and sulfate-reducing populations compete for the same substrates (acetate and hydrogen) and concurrent methanogenesis and sulfate reduction have been reported in some cases (Vroblecky and Chapelle,

1994). Methanogenesis is inhibited by acidic pH levels and low temperature (Beeman and Suffita, 1990). Fermentation products, such as organic acids accumulate in the absence of terminal electron accepting processes.

Due to the dynamic nature of redox processes, it is difficult to measure redox potential directly in the subsurface (Stumm and Morgan, 1996). At a fixed point in the subsurface, changes in the available electron acceptors caused by shifting groundwater flows, surface precipitation events and seasonal temperature fluctuations result in temporal variations in the dominant terminal electron acceptor processes. In addition, electron acceptors and reduced products of bioreactions can be transported by groundwater convection and may persist down-gradient in zones where there is minimal production of these compounds. Therefore, prediction of local redox reactions from substrate and product measurements and reaction stoichiometrics cannot be based on a single measurement.

A detailed look at the reactions listed in Table 1 provides insight into methods for characterizing the operative redox zones within an aquifer. The constituents that are consumed or generated during redox processes include CO_2 , CH_4 , H_2 , NO_3^- , N_2 , SO_4^{2-} , H_2S and organic substrate(s). The accumulation of biochemically active elements reflects an imbalance of one or more redox reactions. While no single measurement can provide a true assessment of the operative redox reactions, integrated analyses of the major constituents provides a means of estimating redox conditions. Dissolved hydrogen monitoring has been proposed as a reliable and responsive measure of dominant redox processes (Lovely et al., 1994).

Using the thermodynamic equations given in Table 1, the oxidation reduction potential can be calculated using the Nernst equation. Calculated values of redox potential must be interpreted in the context of site hydrogeochemistry to be of practical value. The relative abundance of oxygen, nitrate, ferrous iron, methane, sulfide and hydrogen in conjunction with ground water hydrodynamics can be used to substantiate and verify redox calculations.

2.2. Carbon isotope ratios

An alternative approach to delineate redox zones is to use measurements of dissolved carbon dioxide and carbon isotope ratios (Jackson et al., 1996). Carbon in the environment exists in one of two stable isotopes: ^{12}C and ^{13}C . The ratio of ^{13}C to ^{12}C in dissolved CO_2 is a function of the source of the gas. Isotope ratios are used to evaluate the degree of depletion or enrichment of ^{13}C in a given environment. The standard method for reporting isotope ratios in parts per thousand (‰) is:

$$\delta^{13}\text{C} - \Sigma\text{CO}_2 = \left[\frac{(^{13}\text{C}/^{12}\text{C})_{\text{sample}}}{(^{13}\text{C}/^{12}\text{C})_{\text{standard}}} - 1 \right] \times 1000$$

In natural waters the $\delta^{13}\text{C} - \Sigma\text{CO}_2$ is controlled by the source and partial pressure of CO_2 and the speciation of dissolved carbon dioxide (McNichol et al., 1991; Chapelle and Lovely, 1992; Baedeker et al., 1993; Bennett et al., 1993; Jackson et al., 1996; Landmeyer et al., 1996). In waters with low levels of organic carbon and pH levels below approximately 6, $\delta^{13}\text{C} - \Sigma\text{CO}_2$ is dominated by equilibria between dissolved CO_2 and H_2CO_3 and tends to be more depleted in ^{13}C (Stumm and Morgan, 1996). Photosynthetic reactions selectively utilize $^{12}\text{CO}_2$ over $^{13}\text{CO}_2$ therefore the residual CO_2 in water supporting photosynthesis typically reflects isotope ratios that are enriched in ^{13}C . Oils and synthetic chemicals tend to be

depleted in ^{13}C , the production of carbon dioxide from contaminant mineralization tends to result in lower $\delta^{13}\text{C} - \Sigma\text{CO}_2$ ratios.

Isotope ratios are composite measures of all dissolved carbon in water and therefore, the concentration and composition of dissolved organic compounds in water can be significant. Natural organic matter (NOM) in ground water is derived from biogeochemical reactions and consists of residual heterogeneous, hydrophilic, macromolecular compounds that are operationally defined as humic and fulvic compounds (Stumm and Morgan, 1996). Depending on aquifer geohydrology, NOM can be a significant component of the dissolved organic matter (measured as TOC) in ground water (McNichol et al., 1991; Stumm and Morgan, 1996). Isotope ratios for NOM vary with its genesis thus posing difficulties in using isotope ratios to differentiate CO_2 produced from contaminant mineralization. Some researchers have evaluated isotope ratios for methane (Baedeker et al., 1993). Under anaerobic conditions, ^{12}C is metabolized preferentially to methane and $\delta^{13}\text{C} - \Sigma\text{CO}_2$ is enriched while $\delta^{13}\text{C} - \Sigma\text{CH}_4$ is depleted in ^{13}C . A summary of reported values of $\delta^{13}\text{C} - \Sigma\text{CO}_2$ isotope ratios for various redox conditions is presented in Table 2. The highest isotope ratios are associated with reducing conditions and the lowest ratios are associated with aerobic and nitrate-reducing environments. Reported values for methane isotope ratios are approximately -55‰ (Baedeker et al., 1993).

Table 2

Comparison of reported values of $\delta^{13}\text{C} - \Sigma\text{CO}_2$ in ground water under various redox conditions

Source of CO_2	$\delta^{13}\text{C} - \Sigma\text{CO}_2$	Reference
Methanogenic	-11 to +11	Baedeker et al. (1993), Landmeyer et al. (1996)
Iron reducing	-6 to +8	Bennett et al. (1993), Landmeyer et al. (1996)
Near oil lens	-4 to -5	Baedeker et al. (1993)
Atmospheric CO_2	-8 to -9	Landmeyer et al. (1996)
Anoxic zone	-8 to -9	Baedeker et al. (1993)
Uncontaminated ground water	-11 to -15	Baedeker et al. (1993), Landmeyer et al. (1996)
Sulfate reducing	-12 to -18	Landmeyer et al. (1996)
Salt marsh	-14 to -17	Jackson et al. (1996)
Natural organic matter	-15 to -20	McNichol et al. (1991)
Soil CO_2	-20 to -26	Chapelle and Lovely (1992), Landmeyer et al. (1996)
Aerobic processes	-19 to -29	Bennett et al. (1993), Landmeyer et al. (1996)
Nitrate reducing	-19 to -29	McMahon et al. (1990)
Oil	-27 to -32	Baedeker et al. (1993), Jackson et al. (1996)

2.3. Metabolic products of petroleum hydrocarbon degradation

Microbial attenuation of petroleum hydrocarbon plumes has been widely studied. In general, the most soluble and mobile fuel components found in contaminated ground water are benzene, toluene, ethyl benzene and xylene (BTEX). Degradation of these constituents has been demonstrated in multiple redox environments and relative rates of degradation have been characterized in laboratory and field studies (Wilson et al., 1986, 1990; Cozzarelli et al., 1989; Barbaro et al., 1992; Eganhouse et al., 1993; OHM Remediation Services Corp, 1994; Vroblesky and Chapelle, 1994). It has also been reported that *n*-propyl benzene and 1-methylethyl benzene are conservative within anaerobic plumes and the most stable soluble fuel component in petroleum-contaminated ground water is 1,2,3,4 tetramethylbenzene (Cozzarelli et al., 1990). The recalcitrance of methyl naphthalene has also been observed (Kuhn et al., 1988).

Intermediate products of microbial degradation of petroleum hydrocarbons provide biochemical evidence of microbial transformations. Under anaerobic conditions, metabolic by-products include, benzoic acid, one to three methyl benzoic acids and other aromatic acids that are structurally related to alkylbenzene precursors, alicyclic acids and low molecular weight aliphatic acids (Cozzarelli et al., 1989, 1994; Wilson et al., 1990; Barbaro et al., 1992; Bellar et al., 1992, 1995; Evans et al., 1992; Edwards et al., 1994; Seyfried et al., 1994). There is a need to determine if metabolites are biologically stable under field conditions and to determine the efficacy of their use as molecular markers of biological contaminant degradation. It is also important to characterize the fate and transport properties of stable metabolites and identify potential health or environmental risks.

A summary of aromatic anaerobic metabolites identified from petroleum hydrocarbon degradation at field sites and in laboratory studies is given in Table 3. Two metabolites of particular interest are: benzyl fumaric and benzyl succinic acids. It

has been postulated that benzyl fumaric and benzyl succinic acids are 'dead-end' metabolites that might be of significance as biogeochemical indicators of natural attenuation (Bellar et al., 1992). These acids have been identified in sulfate and nitrate-reducing environments, although they have not been widely reported as anaerobic metabolites at field sites. The yield of these metabolites is reported to be between 7 and 10% of the mineralized alkyl benzenes (Bellar et al., 1992, 1995; Evans et al., 1992). It has been postulated that benzyl succinic acid is microbially dehydrogenated to benzyl fumaric acid (Bellar et al., 1992) therefore the ratio of the two acids is likely to be related to site-specific factors, such as electron acceptor, pH, temperature and other microbial growth requirements.

Presently, limited field data exists on the concentration, stability, fate and transport of metabolites in petroleum hydrocarbon plumes. Extrapolation of laboratory data to field conditions is complex due to site specific biogeochemical conditions. In the laboratory studies summarized in Table 3, relatively high concentrations of xylene or toluene (0.5–1 mM) (Evans et al., 1992; Seyfried et al., 1994) were used. The field study (Bellar et al., 1995) was a controlled site in which the fate of injected quantities of BTEX of 2–3 μ M was tracked over a 60-day period. Contaminant concentrations and other biogeochemical factors vary over several orders of magnitude at field sites and therefore the relative abundance and long-term stability of these compounds remains to be established. If these compounds are stable in the environment it is reasonable to assume they should be present in bioactive hydrocarbon plumes under sulfate or nitrate-reducing conditions. One reason for the limited field data on benzyl fumaric and benzyl succinic acids is related to analytical limitations. Detection and identification is only possible by using a derivatization procedure to form methyl esters of the acids that can be quantified by GC/MS. Since the derivatization procedure is not part of routine ground water characterization tests, the presence of these metabolites in petroleum hydrocarbon plumes has not been routinely assessed.

Table 3
Aromatic anaerobic metabolites identified from petroleum hydrocarbon degradation

Site	Major metabolites	Reference
Methanogenic Bemidji, MN	Toluic acid Dimethyl benzoic acid Trimethyl benzoic acid Phenyl acetic acid Methyl phenyl acetic acid	Cozzarelli et al. (1994)
Bordon aquifer, Ontario	2-Methyl benzoic acid	Barbaro et al. (1992)
Laboratory study of toluene and xylene degradation	Benzaldehyde Benzoate <i>p</i> -Cresol	Edwards et al. (1994)
Iron reducing Traverse City, MI	Dimethyl benzoic acid Methyl benzoic acid Cresol	Wilson et al. (1990)
Sulfate reducing Bemidji, MN	Toluic acid Trimethyl benzoic acid Dimethyl benzoic acid	Cozzarelli et al. (1994)
Traverse City, MI	Methyl benzoic acid Cresol	Wilson et al. (1990)
Seal Beach, CA; in situ degradation of BTEX (2-3 μ M BTEX; 0.16 mM sulfate) 60-day duration	Benzyl fumaric acid Benzyl succinic acid	Bellar et al. (1995)
Laboratory study of toluene and xylene degradation	Benzyl fumaric acid Benzyl succinic acid <i>p</i> -Toluic acid	Bellar et al. (1992)
Nitrate reducing Bemidji, MN	Toluic acid Trimethyl benzoic acid Dimethyl benzoic acid	Cozzarelli et al. (1994)
Laboratory column study of alkylated benzene degradation	Methyl-benzyl alcohol <i>o</i> -Cresol	Kuhn et al. (1988)
Laboratory study of toluene degradation using pure cultures (0.5-1 mM toluene; 5 mM nitrate)	Benzyl fumaric acid Benzyl succinic acid Benzaldehyde Benzoate	Seyfried et al. (1994)
Laboratory: 0.5-1 mM <i>m</i> -xylene degradation (5 mM nitrate)	3-Methyl benzaldehyde 3-Methyl benzoate	Seyfried et al. (1994)
Laboratory: 1 mM toluene and xylene degradation (5 mM nitrate)	Benzyl fumaric acid Benzyl succinic acid	Evans et al. (1992)
Laboratory study of toluene and xylene degradation	Benzyl fumaric acid Benzyl succinic acid <i>p</i> -Toluic acid	Bellar et al. (1992)

3. Research methodology

A biogeochemical assessment of a petroleum

hydrocarbon-contaminated ground water was conducted to delineate quasi-steady-state redox zones and try to identify evidence of natural

attenuation and biological degradation of contaminants. For this study, pH, conductivity and profiles of SO_4 , CO_2 , CH_4 , Fe (II), organic acids, hydrocarbons and metabolites were monitored to investigate natural attenuation. Other parameters were estimated using geochemical analyses and existing data.

3.1. Site characteristics

The site used for this case study is located at Tyndall Air Force Base (TAFB). TAFB is located at 30° north latitude in the central part of the Florida Panhandle. The depth to the surficial ground water ranges from 2 to 10 feet and yearly fluctuations in ground water level of approximately 5 feet are typical. The aquifer consists of clean, fine-grained quartz and clayey sandy soils that are nearly level, poorly to moderately drained and extend to depths of 80 inches or more (CHZM Hill, 1981; Environmental Science and Engineering, 1988; Geraghty and Miller, 1991, 1994; OHM Remediation Services Corp, 1994).

The site is a decommissioned fire training area that had been used by the Air Force for approximately 11 years in fire fighting exercises (1981–1992). The site is a flat open grassy area. Fires were set in a pit consisting of a cleared, bermed 0.33 acre area containing an old aircraft or simulated aircraft. The fires were set using 'contaminated' JP-4 stored in a 12000 gallon steel above ground storage tank that was mounted on a concrete pad surrounded by a 3-feet high containment system. The fuel (JP-4) was pumped from the tank through an adjacent pump house and directed to the fire training pit through an underground distribution system. The pit was approximately 13 feet west of the pump house and was surrounded by a non-vegetated fire prevention zone consisting of shell and sand. Fires were extinguished using water in conjunction with various formulations of aqueous film forming foams (AFFF) consisting of fluorinated surfactants. The sources of contamination include leaks from pipelines transporting the fuel, leaks from an oil/water separator, overspill of fuel in the pit during exercises and runoff and percolation from the fire fighting activities.

Three ground water and soil investigations have been conducted as part of the Air-Force Installation Restoration Program and consequently 13 monitoring wells are currently distributed across the site. Twelve of the wells are shallow wells with screened intervals between 2 and 15 feet below the ground surface and one deeper well was screened to 37 feet to provide a single estimate of the vertical extent of hydrocarbon contamination at the site. The wells were installed using the hollow-stem auger method of drilling and consists of 10-foot sections of a 2-inch diameter PVC screen attached to PVC casing. Wells are sealed with bentonite and cement grout and protected by steel casings that are embedded in concrete pads at each well head (CHZM Hill, 1981; Environmental Science and Engineering, 1988; Geraghty and Miller, 1991, 1994; OHM Remediation Services Corp, 1994).

A plan view of the site is shown in Fig. 1. The land slopes gently towards Little Cedar Bayou. Structures at the site included a fuel storage tank, a lined training pit where fires were set and extinguished, an oil/water separator that discharges wastewater to Little Cedar Bayou. A storm water drain and outfall are located to the east of the oil/water separator and drainfield. Soil vapor analyses in conjunction with ground water sampling were used to characterize the site. No estimate of the mass of contamination at the site is available at present. A small plume was delineated at the south side of the pump house that encompasses the above ground storage tank and pump house (MW-5). This plume contained the free phase product up to 3 feet in thickness in 1994. A second larger plume which contained approximately 0.5 inches of free product was observed along the distribution piping and under the fire training pit (AFMW-1). The vertical extent of the contamination was assessed by a single deep well (DMW-1). No petroleum hydrocarbons were detected in the deeper well (Beeman and Sufita, 1990; McMahon et al., 1990; Geraghty and Miller, 1991; McNichol et al., 1991; Vroblesky and Chapelle, 1994).

The hydraulic gradient at the site was evaluated in previous studies using water table elevation measurements in existing wells. Slug tests in

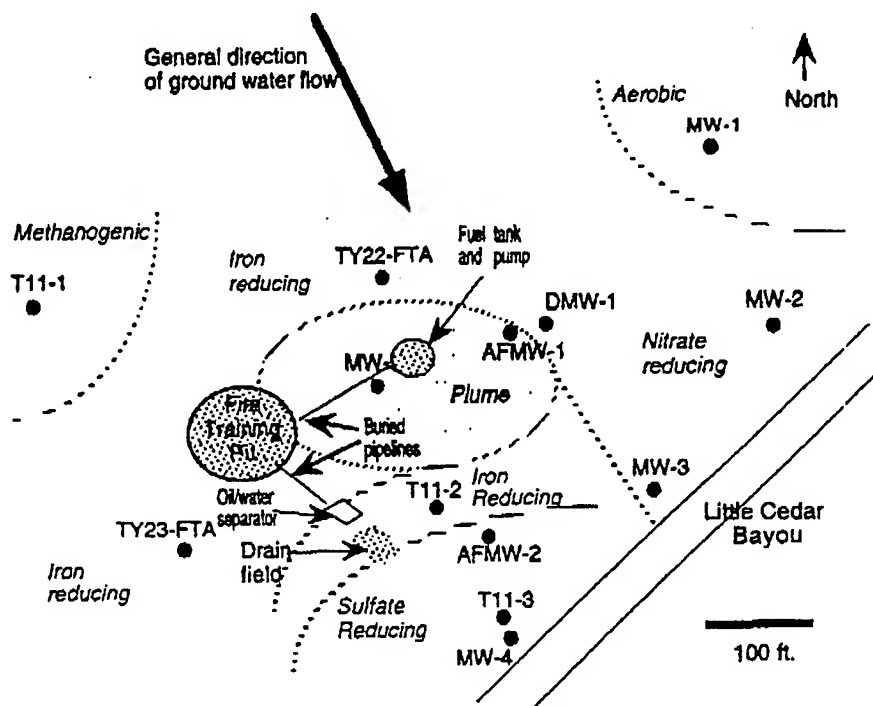


Fig. 1. Schematic of the fire training site at Tyndall Air Force Base. Approximate location of fire training pit, fuel storage tank, underground pipelines, monitoring wells, oil/water separator and drainfield are shown. The general location of redox zones is also indicated (adapted from the reference to OHM Remediation Services Corp, 1994).

wells were used to estimate hydraulic conductivity. In general, hydraulic gradient and conductivity vary over the site. Up-gradient of the plume the hydraulic conductivity ranges from 0.881 (T11-3) to 1.781 (TY22FTA) feet/day. Down-gradient of the plume the hydraulic conductivity is approximately 0.348 (T11-3) feet/day. Near the Little Cedar Bayou hydraulic conductivity has been reported as 1.274 feet/day (MW-1) and 0.091 ft/day (MW-2). The slope of the water table is relatively shallow with a hydraulic gradient of approximately 0.01–0.03 feet/feet. The ground water velocity has been estimated to range from 0.03 to 0.112 feet/day (CHZM Hill, 1981; Environmental Science and Engineering, 1988; Geraghty and Miller, 1991, 1994; OHM Remediation Services Corp, 1994).

3.2. Sampling

The sampling program was based on sampling

from 13 existing wells on the site. For the purposes of this study it was assumed that each well represented quasi-steady-state well-mixed conditions reflective of the region of the well. Existing data from the site were reviewed to determine appropriate sampling strategies. Four sampling events were conducted during the summer of 1996. For each sampling event, each well was pre-bailed using a bottom discharge bailer. Samples were collected with the bailer and either transferred to sampling containers; filtered and transferred to sampling containers; or used for on-site analyses. On site measurements of pH, conductivity, temperature and dissolved oxygen were made using field calibrated probes.

3.3. Analyses

The analytical methods used were based on Standard Methods. pH, conductivity, dissolved oxygen and temperature were measured in the

field using calibrated probes. Samples for analyses of anions, total organic carbon and ultraviolet absorbance were preserved at 4°C and usually completed within 24 h of sample collection. For analysis of ferrous iron, samples were poured immediately after collection into pre-washed 5-ml syringes (to prevent oxidation of iron) and a measured volume was filtered (0.45 μm pore size) into glass vials containing 2 ml of Ferrozine-Herpes buffer solution. The iron concentration was determined spectrophotometrically by reading the absorbance at 652 nm and comparing readings to a standard curve. Anions (nitrate, chloride, bromide and sulfate) were measured using a Dionex ion chromatography system with isocratic sodium hydroxide eluent and quantified by conductivity. Total organic carbon was measured using a Shimadzu Total Organic Carbon analyzer. Ultraviolet absorbance was measured using a Cary UV-VIS spectrophotometer. Surfactant levels were estimated using a Hach chloroform extraction to determine methylene blue active substances (MBAS). Samples for measurement of DIC, methane, $\delta^{13}\text{C}$ were transferred to 10 ml syringes and filtered into evacuated vials. Sample vials were pressurized to ambient pressure with nitrogen gas before they were analyzed for DIC and $\delta^{13}\text{C}$ with an IR/GC mass spectrometer. All analyses were conducted using standardized QA/QC protocols.

3.3.1. Metabolite derivitization and analysis

Metabolite sample collection, processing and analysis followed the procedure outlined by Bellar et al. 1992; Bellar et al., (1995). Samples were collected in 1-l glass bottles and immediately acidified to pH 1 using HCl. Each sample was spiked with 0.1 μM of 4-fluorobenzoic acid to track the efficiency of the extraction. Standards of benzyl succinic acid in water were run in parallel with the field samples to verify the derivitization procedure. Samples were extracted three times with high purity diethyl ether using liquid-liquid extraction in 2-l separatory funnels. Extracted samples were rotary evaporated to a volume of 2–5 ml and dried with pre-cleaned Na_2SO_4 . Dried samples were derivitized with ethereal diazomethane and exchanged into high purity

dichloromethane using high purity N_2 at room temperature. Samples were spiked with crysene as an internal standard and analyzed with a GC/MS DB-5 fused silica capillary column. Internal standard quantification was used to evaluate GC/MS response factors. Fluorinated surfactants were also determined by this derivitization and analysis procedure.

3.3.2. Analysis of hydrocarbons

Samples for hydrocarbon analysis were collected in 40-ml VOA vials with hole caps and Teflon-faced septa. During sample collection, the vials were allowed to overflow to eliminate headspace, preserved with HCl and capped with septa. Hydrocarbon analyses were conducted using a Solid Phase Micro Extraction (SPME) and analyzed using gas chromatography with flame ionization detection.

4. Results

The major contaminants of concern at the fire training site are petroleum hydrocarbons and monitoring data has been collected sporadically since 1988 in conjunction with various studies (Hill, 1981; Environmental Science and Engineering, 1988; Geraghty and Miller, 1991, 1994; OHM Remediation Services Corp, 1994). Variations in BTEX and methyl-naphthalene concentrations at the two wells within the plume (MW-5 and AFMW-1) are presented in Figs 2 and 3. Data from a down-gradient well (T11-3) are shown in Fig. 4. As shown, significant fluctuations have occurred in the reported levels for BTEX in each well over the 8-year monitoring period with a

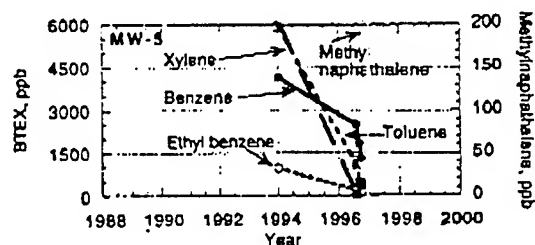


Fig. 2. Summary of BTEX and methyl-naphthalene monitoring data for well MW-5.

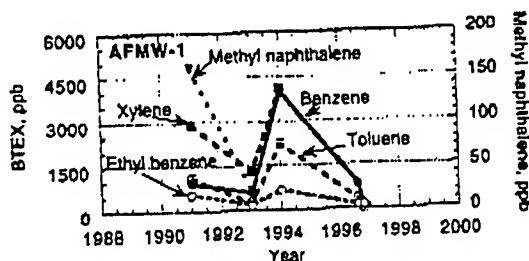


Fig. 3. Summary of BTEX and methyl-naphthalene monitoring data for well AFMW-2.

general decrease in contaminant levels since the 1994 sampling. The site has not been used for fire training since 1992 and the storage tank has been removed eliminating additional sources of contamination outside of the existing plumes.

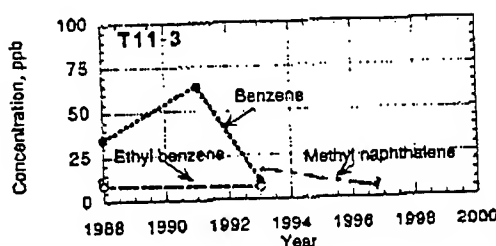


Fig. 4. Summary of BTEX and methyl-naphthalene monitoring data for well T11-3.

4.1. Water quality analysis

For preliminary assessment of site geochemistry, the site was divided into four general regions with respect to the hydrocarbon plume: up-gradient; within the hydrocarbon plume, up-gradient; within the hydrocarbon plume, down-gradient; and down-gradient and outside of the zone of influence of the plume. A summary of general water quality characteristics from each zone is given in Table 4. As shown, there is a significant variability in the data. Several of the wells down-gradient of the plume had strong sulfide odors, however, sulfate was not detected in any of the samples. It is likely that sulfate was reduced at the same rate as it became bioavailable and therefore was below detection limits even in the sulfate-reducing zone (Chapelle and Lovely, 1992; Vroblesky et al., 1996). The wells that are up-gradient and within the plume generally reflect anaerobic conditions and the down-gradient wells tend to be more iron or sulfate-reducing. The wells that are near the bayou and outside of the zone of influence display nitrate-reducing or aerobic conditions. The pH of the site is generally below 6 with slightly higher values in the down-gradient wells. The water temperature ranged between 25 and 30°C (reflecting ambient conditions). The TOC levels across the site are

Table 4
Summary of water quality data from fire training area wells sampled during summer 1996

Parameter	Up-gradient wells (T112-1; TY22 FTA; TY23 FTA)		Plume wells (MW-5; AFMW1)		Down-gradient (T11-2; T11-3; AFMW-2; MW-4)		Outside of zone influence (MW-1; MW-2; MW-3)	
	Range	(Mean \pm S.D.)	Range	(Mean \pm S.D.)	Range	(Mean \pm S.D.)	Range	(Mean \pm S.D.)
pH	5.2-6.6	(5.8 \pm 0.51)	5.3-5.6	(5.5 \pm 0.12)	5.6-6.8	(6.2 \pm 0.5)	4.1-5.8	(5 \pm 0.8)
Temp (°C)	26-29	(27.7 \pm 1.4)	26-28	(26.8 \pm 0.7)	24-29	(26.8 \pm 1.7)	27-29	(27.7 \pm 1.0)
Bromide (ppm)	0.1-1.2	(0.6 \pm 0.4)	0.9-1.7	(1.4 \pm 0.3)	0.4-2.1	(1.1 \pm 0.66)	0.2-1.1	(0.7 \pm 0.3)
Chloride ^a (ppm)	6-17	(12.6 \pm 5.9)	20-28	(24 \pm 6)	4-32	(19 \pm 9)	34-55	(44 \pm 15)
Iron (II) (ppm)	0.2-16	(3.9 \pm 6.3)	3-19	(10 \pm 8)	0.4-15	(5.6 \pm 5.9)	0.9-14	(5.7 \pm 4.4)
Nitrate ^a (ppm)	1-17	(6.3 \pm 6.3)	0.4-2	(1.3 \pm 0.7)	0.4-3	(1.2 \pm 1.5)	0.2-28	(17.7 \pm 12.5)
TOC (ppm)	25-68	(41 \pm 16)	72-119	(86 \pm 22)	29-122	(58 \pm 25)	2-61	(30 \pm 21)
DIC (mM)	5-13	(9.4 \pm 2.6)	7-13	(9.9 \pm 2.4)	4-12	(6.9 \pm 2.5)	2-4	(2.7 \pm 0.9)
Methane (μ M)	429-764	(637 \pm 127)	288-651	(501 \pm 154)	79-525	(201 \pm 163)	0.2-146	(45 \pm 57)
$\delta^{13}\text{C}-\Sigma\text{CO}_2$ (‰)	-8.5-2.0	(-1.2 \pm 4.3)	-2.4-1.1	(-0.4 \pm 1.6)	-12.1-1.4	(-7.1 \pm 4.1)	-9.4-20	(2-14 \pm 4.8)

^a Due to co-elution of sulfide with nitrate and chloride peaks, values for samples containing sulfides were estimated.

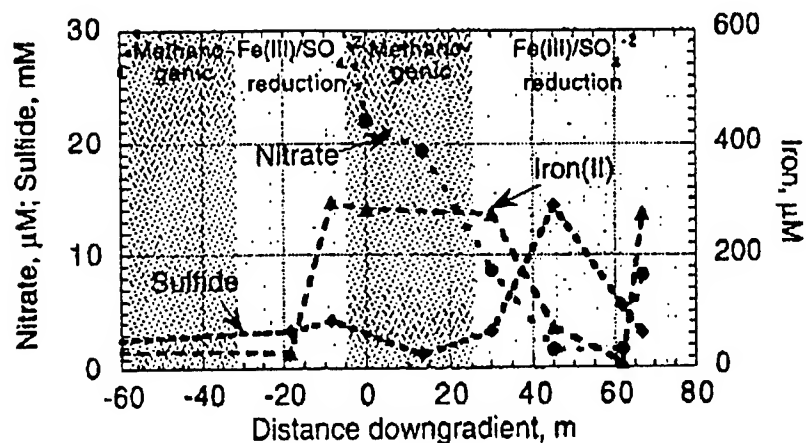


Fig. 5. Comparison of redox intermediates (nitrate, ferrous iron and sulfide) as a function of distance down-gradient at the Fire Training Site (data from summer, 1996).

high reflecting significant dissolved natural organic matter. The DIC, methane and carbon isotope values are consistent with levels reported in the literature (see Table 2) for the various redox zones.

4.2. Dominant redox zones

Based on assessment of key redox indicators, dominant redox zones for this site were delineated. The key redox intermediates measured in this study were nitrate, iron and methane. Sulfide levels were estimated from conductivity levels and

water quality data. The levels of inorganic redox intermediates (nitrate, ferrous iron and sulfide) as a function of distance down-gradient are shown in Fig. 5 and the levels of methane, inorganic carbon, carbon isotopes, hydrocarbon levels and TOC are shown in Fig. 6. As shown the level of nitrate is depleted within the plume and immediately down-gradient. Iron decreases down-gradient of the plume due to precipitation as iron sulfide, changes in the operative redox processes, or other factors. As shown in Fig. 6, methane, DIC and carbon isotope data are consistent with water quality data. Methane, dissolved inorganic carbon

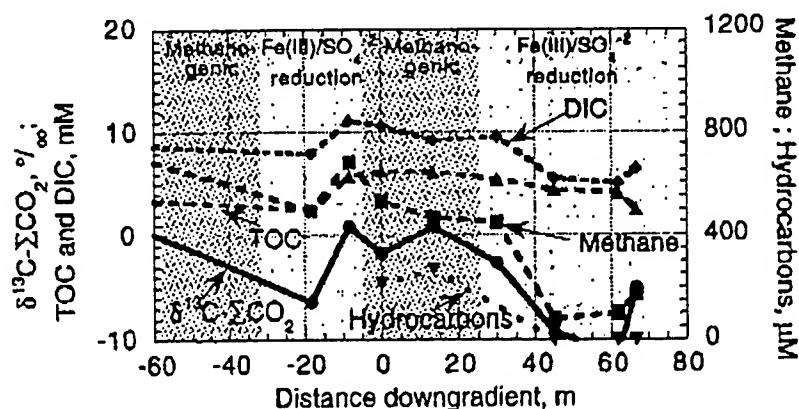


Fig. 6. Comparison of dissolved and organic carbon, carbon isotopes and hydrocarbon levels as a function of distance down-gradient at the fire training site.

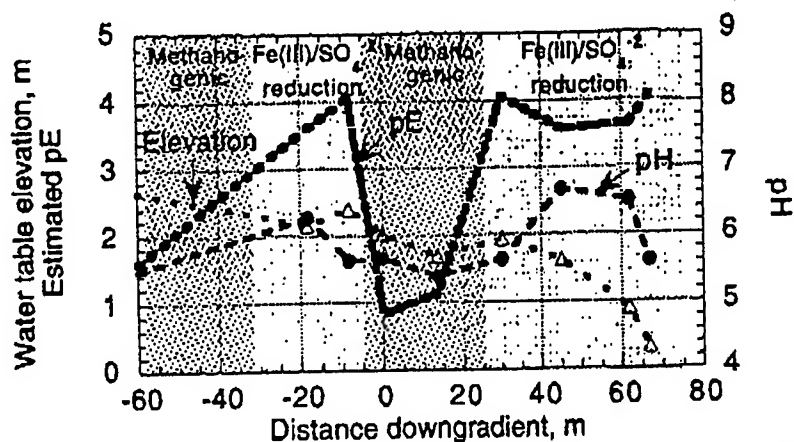


Fig. 7. Comparison of calculated pE and measured pH values as a function of distance from the hydrocarbon plume. Hydraulic gradient data are from OHM Remediation Services Corp, 1994).

and carbon isotope ratios tend to decrease down-gradient of the plume in parallel with reductions in hydrocarbon concentrations. TOC levels throughout the site are quite high due to natural sources of organic matter.

The water quality data were used to determine the dominant redox conditions for each well and relative redox potentials were calculated. A summary of the calculated redox potential as a function of distance down-gradient from the highest zone of contamination (MW-5) is shown in Fig. 7 in comparison with the hydraulic gradient and measured pH at each location.

4.3. Contaminant transport

The concentrations of BTEX, methyl naphthalene, isopropyl benzene and *n*-propyl benzene as a function of distance down-gradient are presented in Figs. 8 and 9. As shown, the BTEX levels are non-detectable within approximately 65 m down-gradient. Consistent with previous findings isopropyl benzene and *n*-propyl benzene are not degraded within the methanogenic zone of the plume, but are rapidly degraded in the Fe (III) and sulfate reduction zone.

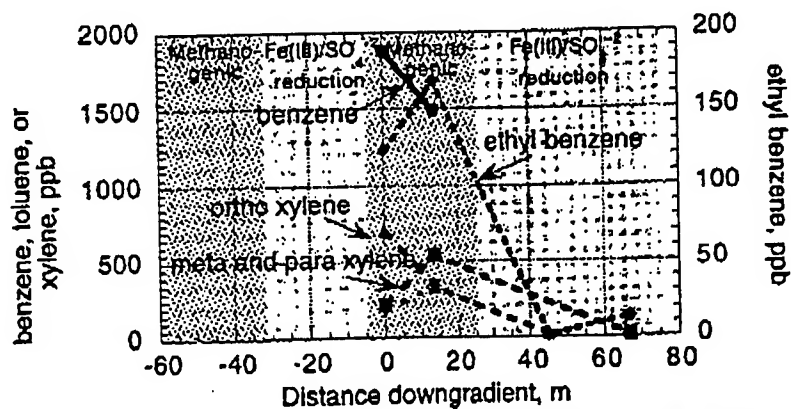


Fig. 8. Comparison of benzene, toluene, ethyl benzene and xylenes as a function of distance down-gradient from MW-5. Data are average values from summer 1996 sampling.

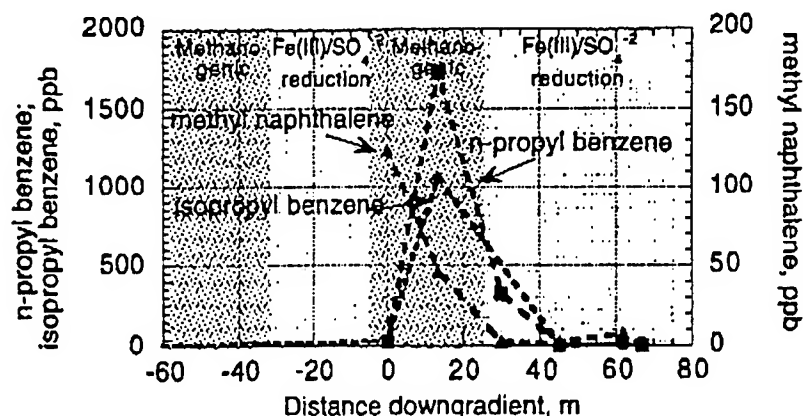


Fig. 9. Comparison of *n*-propyl benzene, isopropyl benzene and methyl naphthalene as a function of distance down-gradient from MW-5. Data are average values from summer 1996 sampling.

4.4. Carbon isotope ratios

A comparison of carbon isotope ratios for carbon dioxide and methane as a function of distance down-gradient is shown in Fig. 10. The isotope results generally follow the trends reported in Table 2 with higher values associated with methanogenic conditions and lower values for sulfate reduction. However, interference from the background NOM in delineating the zone of contamination using this approach is evident. Down-gradient of the plume, the methane isotope ratio increases while the carbon dioxide ratio decreases reflecting utilization of the hydrocarbon substrate.

Relationships between measured methane concentrations and dissolved organic carbon and carbon isotope ratios are shown in Fig. 11. In general there is a linear relationship between methane and the inorganic carbon, however, there is a good deal of scatter in the data most likely due to interferences from NOM.

4.5. Dissolved organic carbon and metabolite measurements

The shallow ground water at this site contains relatively high levels of NOM that may be of significance in biogeochemical attenuation of the hydrocarbon plume. Some preliminary effort at

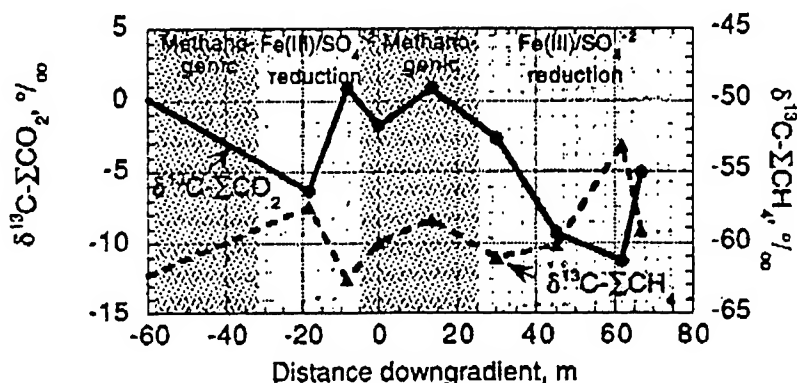


Fig. 10. Comparison of carbon dioxide and methane isotope ratios as a function of distance down-gradient from MW-5 (data from Florida State University, 1996).

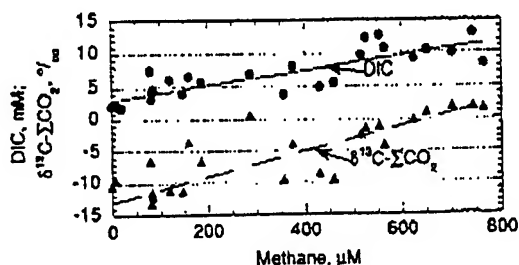


Fig. 11. Correlation of methane levels in ground water at the fire training site with levels of dissolved organic carbon (DIC) and carbon isotope ratios (data from Florida State University, 1996).

characterizing the dissolved TOC were conducted during this study. An analysis of the degree of aromaticity of TOC can provide an insight into biogeochemical transformations that occur across the site. The specific ultra violet absorbance (SUVA) is a measure of the degree of aromaticity of the dissolved organic materials. Since aromatic and double-bonded compounds have strong UV absorbance spectra, the ratio of UV absorbance to TOC (SUVA) provides a means to track aromaticity across the site. A comparison of dissolved organic carbon, SUVA and surfactant measurements as a function of distance down-gradient is given in Fig. 12. As shown, while the TOC values are fairly high across the site, the SUVA decreases indicating a decrease in aromaticity in the iron and sulfate-reducing zones

down-gradient. The up-gradient wells contain higher levels of natural organic matter that appears to have a higher aromatic content. The down-gradient wells are in close proximity to the Little Cedar Bayou and may be subject to some tidal influence that could modify the concentration and composition of the TOC.

It is also interesting to note the surfactant concentration around the site. There should be no natural sources of surfactant in the ground water. However, the AFFF used in fire training appears to be transported in the ground water. The apparent solubility of contaminants and TOC can be increased in the presence of surfactants. In some cases surfactants can reduce the degree of sorption and increase contaminant mobility and reactivity.

4.6. Metabolite derivitization and analysis

Multiple samples from each well up-gradient and down-gradient of the contaminant plume were derivitized and analyzed using GC/MS to identify potential metabolites of anaerobic degradation with specific focus on benzyl succinic and benzyl fumaric acids. Based on previous findings (Bellar et al., 1992, 1995; Evans et al., 1992; Seyfried et al., 1994) the most likely zone for formation of these acids would be down-gradient from the source (MW-5) under sulfate-reducing conditions (AFMW-2, T11-3 and MW-4) or ni-

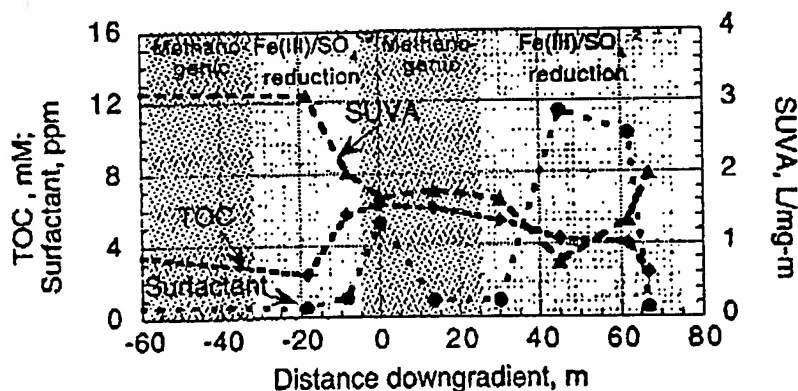


Fig. 12. Comparison of dissolved organic carbon (TOC) levels with surfactant estimates and specific UV absorbance (SUVA) as a function of distance down-gradient from MW-5.

Table 5

Summary of anaerobic metabolites detected in ground water at fire training site

Zone	Wells	Metabolites detected
Upgradient methanogenic	T11-1	None
Upgradient iron and/or sulfate-reducing	TY-22FTA; TY23FTA	None
Deep monitoring well (25 feet)	DMW-1	None
Plume	MW-5; AFMW-1	Methyl benzoic acid Benzene acetic acid
Down-gradient iron-reducing	T11-2	Benzene acetic acid Dimethyl benzoic acid
Down-gradient sulfate-reducing	AFMW-2; T11-3; MW-4	Trimethyl benzoic acid
Nitrate-reducing and/or aerobic (outside plume)	MW-1; MW 2; MW 3	None

trate-reducing conditions. However, neither benzyl succinic nor benzyl fumaric acid were detected in multiple samples from all zones of the site. A summary of the metabolites identified in each zone is given in Table 5. These findings are consistent with data reported from other field sites (Wilson et al., 1986; Barbaro et al., 1992; Cozzarelli et al., 1994).

In addition to metabolite evaluation, fluorinated surfactants (AFFF) were detected up-gradient of the plume (TY22 FTA), within the plume (MW-5 and AFMW-1) and down-gradient of the plume (T11-2, AFMW-2, T11-3 and MW-4). The transport of AFFF down-gradient of the plume is not surprising due to the large quantities of foam that were applied to the site during its operation in fire training. An unexpected finding, however, was the detection of AFFF in MW-3 which appeared to be outside of the zone of influence of the plume based on all other analyses. The presence of AFFF within the ground water introduces several important questions relating to attenuation processes in progress at this site. Limited information is currently available about transport properties of AFFF in the subsurface. If AFFF are transported more rapidly than the other dissolved constituents, the detection of AFFF outside of the active plume zone (MW-3) may serve as an 'early warning' of continued migration of the plume. In addition, the role of AFFF in mediating or inhibiting biogeochemical reactions needs to be elucidated. The absence of benzyl succinic and benzyl fumaric acids in sulfate-reducing zone may be related to the fate and transport of AFFF within the ground water. Al-

ternatively, if AFFF is not-reactive in a biogeochemical context, then the use of benzyl succinic and benzyl fumaric acids as indicators of anaerobic hydrocarbon degradation does not appear appropriate for this site. The higher temperatures, high background levels of TOC, low pH levels, surfactant matrix characteristic of this site may have promoted alternative pathways for microbial degradation of hydrocarbons that do not yield stable forms of benzyl succinic and benzyl fumaric acids.

5. Conclusions

Current theories of biogeochemical attenuation were tested in this field study.

The major conclusions are listed below

- The characteristics of this field site containing JP-4-contaminated ground water from a decommissioned Air Force fire training area are consistent with patterns observed at other petroleum-hydrocarbon-contaminated sites (CH2M Hill, 1981; Wilson et al., 1986, 1990; Environmental Science and Engineering, 1988; Kuhn et al., 1988; Cozzarelli et al., 1989, 1990, 1994, 1995; Beeman and Suffita, 1990; Kehew and Passero, 1990; McMahon et al., 1990; Geraghty and Miller, 1991, 1994; McNichol et al., 1991; Barbaro et al., 1992; Bellar et al., 1992, 1995; Evans et al., 1992; Chapelle and Lovely, 1992; Baedeker et al., 1993; Bennett et al., 1993; Chapelle, 1993; Eganhouse et al., 1993; Edwards et al., 1994; Lovely et al., 1994; OHM Remediation Services Corp., 1994;

Seyfried et al., 1994; Vroblesky and Chapelle, 1994; Bjerg et al., 1995; Jackson et al., 1996; Landmeyer et al., 1996; Stumm and Morgan, 1996; Vroblesky et al., 1996). This site tended to display higher temperatures and higher background levels of TOC than are typically reported. These factors play a key role in microbial reaction rates.

- Monitoring of redox intermediates, dissolved inorganic and organic carbon, methane and carbon isotope ratios provided a basis for estimating dominant redox processes at this site. Carbon isotope data tracked biological changes but did not provide effective 'stand-alone' assessments of contaminant degradation due to the high background levels of TOC.
- The composition of TOC varies across the site in terms of aromaticity. Further characterization of the role of dissolved organic matter in biogeochemical attenuation would be of value.
- Metabolites of anaerobic degradation were identified in methanogenic, iron-reducing and sulfate reduction regions of the site. Benzyl succinic and benzyl fumaric acid were not identified in any of the samples collected from this site. The absence of these metabolites at this site casts doubt upon the efficacy of their use as molecular markers of biological attenuation and should be verified by additional analyses in the zone down-gradient from the hydrocarbon plume.
- Significant levels of AFFF in the ground water were detected at this site. The presence of these compounds may be of significance in biogeochemical attenuation of hydrocarbon contaminants.

Acknowledgements

This study was funded by the United States Air Force Office of Scientific Research (AFOSR) as part of the Summer Faculty Research Associate Program. Mr. Michael Henley provided assistance and support with liquid chromatography and mass spectrometry. Ion chromatography, TOC analyses and general laboratory assistance by Ms. Eila

Burr and Ms. Marlene Cantrell are appreciated. Assistance with field sampling and analysis of carbon isotopes by Ms. Glynnis Bugna and her assistants from Florida State University is appreciated.

References

- Baedecker MJ, Cozzarelli IM, Eganhouse RP. Crude oil in a shallow sand and gravel aquifer III. Biogeochemical reactions and mass balance modeling in anoxic groundwater. *Appl Geochem* 1993;8:569–586.
- Barbato JM, Barker JF, Lemon LA, Mayfield CL. Biotransformation of BTEX under anaerobic, denitrifying conditions: field and laboratory observations. *J Contam Hydrol* 1992;11:245–272.
- Beeman RE, Suffita JM. Environmental factors influencing methanogenesis in a shallow anoxic aquifer: a field and laboratory study. *J Ind Microbiol* 1990;5:45–58.
- Bellar HR, Reinhard M, Grbic-Galic D. Metabolic by-products of anaerobic toluene degradation by sulfate reducing enrichment cultures. *Appl Environ Microbiol* 1992;58:3192–3195.
- Bellar HR, Ding W-H, Reinhard M. By products of anaerobic alkylbenzene metabolism useful as indicators of in situ bioremediation. *Environ Sci Technol* 1995;29:2864–2870.
- Bennett PC, Sigel DE, Baedecker MJ, Hult MF. Crude oil in a shallow sand and gravel aquifer I. Hydrogeology and inorganic geochemistry. *Appl Geochem* 1993;8:529–549.
- Bjerg PL, Ruge K, Pedersen JK, Christensen TH. Distribution of redox sensitive groundwater quality parameters down-gradient of a landfill. *Environ Sci Technol* 1994;29:1387–1394.
- Chapelle FH. Ground water and microbiology and geochemistry. New York: John Wiley, 1993.
- Chapelle FH, Lovely DR. Competitive exclusion of sulfate reduction by Fe (III) reducing bacteria: a mechanism for producing discrete zones of high-iron ground water. *Ground Water* 1992;30:29–36.
- Cozzarelli IM, Baedecker MJ, Eganhouse RP, Goerlitz D. The geochemical evolution of low-molecular weight organic acids derived from the degradation of petroleum contaminants in groundwater. *Geochim Cosmochim Acta* 1994;58:863–877.
- Cozzarelli IM, Eganhouse RP, Baedecker MJ. Transformation of monoaromatic hydrocarbons to organic acids in anoxic groundwater environment. *Environ Geol Water Sci* 1990;16:1335–1411.
- Cozzarelli IM, Eganhouse RP, Baedecker MJ. The fate and effects of crude oil in a shallow aquifer II. Evidence of anaerobic degradation of monoaromatic hydrocarbons.

- USGS Water-Resources Investigation Report, 1989:88–4220.
- Cozzarelli IM, Herman JS, Baedeker MJ. Fate of microbial metabolites in a coastal plain aquifer: the role of electron acceptors. *Environ Sci Technol* 1995;29:458–469.
- Edwards E, Grbic-Galic A, Grbic-Galic D. Anaerobic degradation of toluene and o-xylene by a methanogenic consortium. *Appl Environ Microbiol* 1994;60:313–332.
- Eganhouse RP, Baedeker MJ, Cozzarelli IM, Aiken GR, Thorn KA, Dorsey TF. Crude oil in a shallow sand and gravel aquifer II. Organic geochemistry. *Appl Geochem* 1993;8:551–567.
- Environmental Science and Engineering. Installation restoration program, Phase II. Contamination/quantification, Stage 2, vol 1. Florida: Tyndall AFB, 1988.
- Evans PJ, Ling W, Goldschmidt B, Ritter ER, Young LY. Metabolites formed during anaerobic transformation of toluene and O-Xylene and their proposed relationship to the initial steps of toluene mineralization. *Appl Environ Microbiol* 1992;58:496–501.
- Geraghty and Miller, Inc. Analytical results report for fire training areas. Florida: Tyndall Air Force Base, 1991.
- Geraghty and Miller, Inc. Draft contamination assessment report for active fire training area site FT-23. Florida: Tyndall Air Force Base, 1994.
- Hill CHZM. Installation restoration program records search for Tyndall Air Force Base. Florida, Phase I, Stage I of the installation restoration program. Florida: Tyndall AFB, 1981.
- Jackson AW, Pardue JH, Araujo R. Mineralization in salt marshes: use of stable carbon isotope ratios. *Environ Sci Technol* 1996;30:1139–1144.
- Kehew AE, Passero RN. pH and redox buffering mechanisms in a glacial drift aquifer contaminated by landfill leachate. *Ground Water* 1990;28:728–737.
- Kuhn EP, Zeyer J, Eicher P, Schwarzenbach R. Anaerobic degradation of alkylated benzenes in denitrifying laboratory aquifer columns. *Appl Environ Microbiol* 1988; 54:490–496.
- Landmeyer JE, Vroblesky DA, Chapelle FH. Stable carbon isotope evidence of biodegradation zonation in a shallow jet-fuel contaminated aquifer. *Environ Sci Technol* 1996;30:1120–1128.
- Lovely DR, Chapelle FH, Woodward JC. Use of dissolved H₂ concentrations to determine distribution of microbially catalyzed reactions in anoxic groundwater. *Environ Sci Technol* 1994;28:1205–1210.
- McNichol AP, Druffel ERM, Lee C. Carbon cycling in coastal sediments: 2. An investigation of the sources of SCO₂ to pore water using carbon isotopes. In: Baker RA, editor. Organic substance in ground water, vol. 2, Processes and Analytical. Michigan: Lewis Publishers, 1991:249–272.
- McMahon PB, Williams DF, Morris JT. Production and carbon isotopic composition of bacterial CO₂ in deep coastal plain sediments of South Carolina. *Ground Water* 1990;28:693–702.
- OHM Remediation Services Corp. Free-phase hydrocarbon delineation and soil quality investigation fire training area 23, Tyndall Air Force Base. Pilot test work plan of in-situ bioremediation using microbubbles active fire training area FT-23. Florida: Tyndall Air Force Base, 1994.
- Seyfried B, Gold G, Schocher R, Tschetch A, Zeyer J. Initial reactions in the anaerobic oxidation of toluene and m-xylene by denitrifying bacteria. *Appl Environ Microbiol* 1994;60:4047–4052.
- Stumm W, Morgan JJ. Aquatic chemistry: chemical equilibria and rates in natural waters. New York: Wiley Interscience, 1996.
- Vroblesky DA, Chapelle FH. Temporal and spatial changes of terminal electron processes in a petroleum hydrocarbon-contaminated aquifer and the significance for contaminant biodegradation. *Water Resour Res* 1994;30:1561–1570.
- Vroblesky DA, Bradley PM, Chapelle FH. Influence of electron donor on the minimum sulfate concentration required for sulfate reductions in a petroleum hydrocarbon-contaminated aquifer. *Environ Sci Technol* 1996;30:1377–1381.
- Wilson BH, Bledsoe BE, Armstrong JM, Sammons JH. Biological fate of hydrocarbons at an aviation gasoline spill site. Proceedings of the NWWA/API Conference on Petroleum Hydrocarbons and Organic Chemicals in Ground Water-Prevention, Detection, and Restoration, National Water Well Association, 1986:78–90.
- Wilson BH, Wilson JT, Kampbell DH, Bledsoe BE, Armstrong JM. Biotransformation of monoaromatic and chlorinated hydrocarbons at an aviation gasoline spill site. *Geomicrobiol J* 1990;8:225–240.

THE EFFECT OF VIDEO IMAGE SIZE AND SCREEN REFRESHER RATE ON
CONTENT MASTERY AND SOURCE CREDIBILITY IN DISTANCE LEARNING
SYSTEMS

Robert G. Main, Ph.D.
Professor
Department of Communication Design
California State University, Chico

John F. Long, Ph.D.
Associate Professor
Department of Communication Design
California State University, Chico

Wendi A. Beane
Research Assistant
Department of Communication Design
California State University, Chico

California State University, Chico
400 W. First Street
Chico, California 95929-0504

Final Report For:
Summer Faculty Research Extension Program
Armstrong Laboratory
Subcontract 97-0873

Sponsored by:
Air Force Office of Scientific Research
Bolling Air Force Base, DC
and
Armstrong Laboratory

August 1997

THE EFFECT OF VIDEO IMAGE SIZE AND SCREEN REFRESHER RATE ON CONTENT MASTERY AND SOURCE CREDIBILITY IN DISTANCE LEARNING SYSTEMS

Robert G. Main, Ph.D.
John F. Long, Ph.D.
Wendi A. Beane
Department of Communication Design
California State University, Chico

Abstract

In a laboratory setting, this study examined the effect of image size and refresh rate of those images on the subjects' abilities to recall content, and subjects' perceptions of source credibility. The results suggest that larger images and faster refresh rates do not increase content retention. Further analysis revealed that larger, more realistic televised lectures do not significantly enhance source credibility along the dimensions of attention, confidence, relevance, or satisfaction. This study lends evidence to the notion that Internet based course delivery, using small, slow images may be as effective in terms of learning outcomes and satisfaction, as high bandwidth networks.

THE EFFECT OF VIDEO IMAGE SIZE AND SCREEN REFRESHER RATE ON CONTENT MASTERY AND SOURCE CREDIBILITY IN DISTANCE LEARNING SYSTEMS

Robert G. Main, Ph.D.
John F. Long, Ph.D.
Wendi A. Beane

Introduction

The rapid rise of digital telecommunication and the transformation of media from analog to digital formats have opened the door to instructional delivery possibilities that have not been seen before. Distance learning resources and technologies are no longer restricted to a select academic community and they are changing the nature of education and training across a broad spectrum (Capell, 1995). Organizations are beginning to change their question from "Should we be doing distance learning?" to "When are we going to begin distance learning?" The demand will be on improved access, sophisticated interfaces and more interesting and stimulating presentations for an expanded learner base (Main, 1996). Most of the research on distance learning presentations has focused on system capabilities. Transmission rates and methods, media capabilities and interactions (two-way or one-way audio and video, synchronous or asynchronous).

Distance learning has evolved from analog distribution systems whether by conventional broadcast, microwave, fixed site, satellite or cable to digital formats using computer mediated communication. Desktop video conferencing systems are a reality in some workplaces because of developments in compression method, high bandwidth networks and faster computers (Gale, 1992).

Computer mediated communication using real time video and audio places great demand on network capacities (Kies, 1997). Video frame rate and image size are the two major factors in determining computing power and network speed. Most U.S. systems employ the NTSC standard of 30 frames per second (fps) screen refresh rate. A 2:1 interlace in the presentation produces 60 seams (or fields) per second (Ramachandran and

Anstis, 1982). Lower frame rates result in “choppy” video motion which may lead to decreased user satisfaction (Kies, Williges and Rosson, 1996).

Image size for computer mediated communication is commonly a small window where motion video appears. Using contemporary technology to fill the entire screen with information requires much greater computing speed or greatly reduced video quality.

A high proportion of the published research about distance learning are descriptive analyses based on field studies and case studies. Those studies which do attempt quasi-scientific comparisons with traditional delivery modes offer little control over confounding or contaminating variables. This study used a laboratory experiment to investigate some of the basic questions facing distance learning instructional designers and developers.

Research question 1:

Motion video has become an increasingly common component of distance learning digital workstations. It is axiomatic with satellite or cable based analog systems that the video picture will cover the entire screen. There are exceptions, for example, when special effects switching superimpose a small circular or rectangular video of the instructor as a talking head in a portion of a graphic display. But, these are generally rare. With the advances in digital audio and video and compression technology, desktop computer based distance learning stations linked by local and wide area networks have appeared with regularity. While motion video is available on these digital systems for the instructional designer/developer to use, it is often only a small window in the screen. The first research question for this project is, “What effect does the screen size of the instructor’s image have on the learner’s perception of source credibility and retention of the message. The results of the study have implications for decision makers in assessing system capabilities for purchase as well as for instructional designers and developers in designing multimedia presentations.

Hypotheses:

Two hypotheses were generated by the research question. The first hypothesis was that learner retention of lecture material, as measured on a ten question multiple choice exam, varies directly with the image size of the instructor's videotaped lecture. The experiment allowed for three variations of image size.

The second hypothesis was that the learner's perception of the credibility of the instructor has a direct relationship with the image size of the instructor's videotaped lecture. For purposes of this study, credibility is defined as a composite of four sub-variables, in particular, attention confidence, relevance and satisfaction. This measure was developed from the work of Keller (1983). The independent variable in the experiment was the size of the video image in the computer screen. The video window was manipulated in three sizes-four inch square, six inch square and a full 17 inch diagonal screen surface (approximately 12 X 15 inches). The dependent variables (instructor credibility, information retention, and satisfaction with message content and presentation) were measured by questionnaires.

Research question two:

Another characteristic of PC-based digital video is that the compression technology permits transmission via telephone networks but the traditional full motion screen refreshment rate of 30 frames per second (fps) is reduced about one-half to 15 fps screen refresh rate. The question to be answered is; "What effect does reduced screen motion capability have on learner retention of content and perception of source credibility?"

Hypotheses:

The Two hypotheses generated by the second research question about video motion speed parallel those concerning screen size. The first hypothesis is that presentation of an instructor lesson in full motion video increases learner retention compared with 15 fps motion video. The second hypothesis is that instructor credibility is greater when 30 fps video is used than 15 fps video is used for the lesson presentation. The independent variable in this parallel experiment is the screen refresh rate. Identical lessons were

presented with one using a full motion (30 fps) screen refreshment and information retention, instructor credibility and subject and presentation satisfaction, are the same as those for the research question of screen size and were measured with the same questionnaires.

Experimental design:

An experiment was designed in which one 40 minute lesson presentation was manipulated in a two by three experimental model design (see Figure 1.) Three treatments of screen size (4x4 inch, 6x6 inch and full screen) were presented on a PC based learning station with a 17 inch diagonal monitor. The same 40 minute lesson was presented over all three screen sizes in two speeds (15 and 30 fps refresh rates) and manipulated with the size dependent variable.

	4X4 inch Image	6X6 inch Image	Full Screen Image
15 fps	credibility retention subject satisfaction presentation	credibility retention subject satisfaction presentation	credibility retention subject satisfaction presentation
30 fps	credibility retention subject satisfaction presentation	credibility retention subject satisfaction presentation	credibility retention subject satisfaction presentation

Figure 1. Research Model

Four dependent measurements were taken for each of the six treatment conditions (4x4 inch image with 15 fps, 4x4 inch image with 30 fps, 6x6 inch image with 15 fps, 6x6 inch image with 30 fps, full screen with 15 fps and full screen with full motion). The dependent variable concerning lecture retention was measured by paper/pencil test covering the learning objectives of the 40 minute lesson. Content mastery was measured

immediately after each session, and was also imbedded in the final examination administered three weeks after exposure. The dependent variable of credibility was self reported from a questionnaire administered with the content examination.

Conduct of the Experiment:

A laboratory with eight PC- based multimedia learning stations was set up within the Department of Communication Design at California State University, Chico. Each learning station was configured with hardware and software to allow the manipulation for the treatment groups. The learning stations were linked by a local area network to a server. Technical assistance for the project was provided by students in the Department of Communication Design.

A 50 minute class, a course that is regularly taught as a lower division Introduction to Broadcasting/Cable in the Department of Communication Design, was used for the stimulus content. The instructor of the class was assisted by students in the Instructional Technology degree program at the University to design and develop the lesson for delivery via the interactive digital multimedia network. The instructor's presentation was video taped and edited into a 40 minute lesson. The completed lesson was digitized and a master tape was prepared for each of the six treatment modes. The same source video was used for each treatment.

The delivery vehicle for the distance learning lesson was hardware and software developed by SUN Microsystems Incorporated for conducting research in distributed tutored video instruction (DTV). The system consisted of seven student stations and one instructor controlled station with proprietary software developed by SUN Microsystems, which permitted a segmented screen with nine images displayed simultaneously in a 3x3 matrix. The student work station and the instructor workstations were isolated from one another and connected through a local area network (LAN). Each workstation was equipped with a camera and microphone so that student could interact with the facilitator at the instructor's workstation as well as each other.

The system was modified for this experiment by creating only one display window for each screen. The windows were 4x4 inch, 6x6 inch and the full 17 inch diagonal monitor screen. To control for student interaction as a confounding variable this experiment was conducted as a one way linear audio visual presentation. In each trial, the appropriate lesson format was distributed to each of the students present on all eight workstations from facilitator workstation that had the primary controls for the video showing. Student video cameras as well as microphones were disabled at each station. The students could not hear or see other students participating in the class.

Students in an introductory communication survey course were randomly assigned to one of the six treatment groups. The stimulus lesson dealt with the history of radio and was an integral component of the course curriculum. The class had 180 students enrolled and each treatment group had 30 subjects. Since the laboratory system could accommodate only eight subject for each trial, the groups were randomly assigned to times from six until nine in the evening for six nights over a two week period. The laboratory was available only on Monday, Tuesday and Wednesday evenings. One Thursday evening session was scheduled to accommodate the last few randomly assigned groups. From the 24 trials, 148 data scores were obtained. The 32 students who failed to show up for their scheduled time gave a number of reasons, the most common being a conflict with a previous commitment. Some admitted they just forgot and at least one of the students strongly objected to being a part of a military experimental study and was excluded from the analysis of data.

Because of the high rate of no shows (almost 25 percent), a Chi Square goodness of fit test was conducted between the groups using gender and class level (Freshman, Sophomore, Junior and Senior) as the variables. No systematic bias to the random assignment of subjects appeared.

The students watched the presentation in the image size and screen refresher rate for their particular trial as passive viewers of a linear audio video format. At the completion of the lesson, the students were given a paper and pencil test with ten questions measuring the

cognitive content of the presentation. On the back of the paper and pencil test were eight questions measuring the credibility variables.

The credibility measurement instrument was constructed from items developed and validated by John Keller to determine how well presentations hold a learner's attention, is considered relevant, instills confidence and provides satisfaction . Two items for each of these elements were included in the questionnaire.

The ten item learning measurement instrument was developed by the course instructor and designed to determine achievement of the learning objectives for the class. Information retention over time was measured by performance of the subjects on a delayed measure of the same items administered four weeks after the last trial. A copy of both measurement instruments are included in Appendix A.

Design

The critical independent variables for this study were (1) image size, and (2) refresh rate of those images. Performance on two primary dependent variables, "content mastery" and "credibility measures" were indexed. The "content mastery" variables consisted of an immediate posttest (0-10) and performance on a delayed measure of the same items (0-10). The "credibility measures" consisted of four attitudinal measures (1-5), attention, confidence, relevance, and satisfaction respectively.

These data were analyzed with repeated measures ANOVA's for each of the six dependent variables. Since the collective impact was not a pertinent question to these hypotheses, MANOVA was not applied.

Results

Descriptive statistics delineated by image size for content mastery variables appear in Table 1.

TABLE 1. Descriptive Statistics for content Mastery Delineated by Image Size

Image Size	Content Mastery				
	Posttest	M	SD	Delayed Test	
	n			M	SD
SMALL	43	5.44	1.88	4.74	1.96
MEDIUM	46	5.02	2.03	3.74	1.77
LARGE	47	5.56	2.20	4.14	1.85

Separate analyses were conducted for each of the dependent measures. The contribution of image size to immediate test performance was found to be non-significant. However, these data did reveal that image size had a significant effect on delayed test retention of lecture material ($F=3.53$, $p<.05$). Interestingly, those in the treatment with the smallest screen size outperformed the other conditions. It is possible that larger screen size may result in passive viewing behavior typical in television use, whereas a smaller screen size may mandate greater cognitive demand in information interpretation. Plausibly, since the lecture was rich in factual information, subjects in that condition were more attentive than the other groups.

The descriptive statistics for image size effect on credibility are displayed in Table 2. The mean scores for the attention, relevance, and satisfaction variables were each higher for the smallest image condition, however, analysis of variance on each of these variables failed to yield significance.

TABLE 2. Descriptive Statistics for Credibility Delineated by Image Size

Image Size	n	Credibility Variables							
		<u>Attention</u>		<u>Confidence</u>		<u>Relevance</u>		<u>Satisfaction</u>	
		<u>M</u>	<u>SD</u>	<u>M</u>	<u>SD</u>	<u>M</u>	<u>SD</u>	<u>M</u>	<u>SD</u>
SMALL	43	4.84	2.11	5.09	2.03	7.35	1.84	5.26	2.18
MEDIUM	46	4.73	1.99	4.93	2.23	6.59	2.21	4.96	2.18
LARGE	47	4.70	2.18	5.34	2.06	6.79	2.01	5.13	2.13

These data suggested that image size had no significant effect on learning as measured by the immediate posttest, or on the variable concerning the learner's confidence on test performance.

The descriptive statistics in Table 3 and 4 address the main effect of "refresh rate".

TABLE 3 Descriptive Statistics for Content Mastery Delineated by Screen Refresh Rate

Refresh Rate	Content Mastery				
	<u>Posttest</u>		<u>Delayed Test</u>		
	<u>n</u>	<u>M</u>	<u>SD</u>	<u>M</u>	<u>SD</u>
15 FPS	70	5.14	2.10	4.07	1.78
30 FPS	66	5.55	1.96	4.36	1.20

TABLE 4. Descriptive Statistics for Credibility Delineated by Screen Refreshment Rate

Refresh Rate	n	Credibility Variables							
		<u>Attention</u>		<u>Confidence</u>		<u>Relevance</u>		<u>Satisfaction</u>	
		<u>M</u>	<u>SD</u>	<u>M</u>	<u>SD</u>	<u>M</u>	<u>SD</u>	<u>M</u>	<u>SD</u>
15 FPS	70	4.84	2.22	4.94	2.33	6.67	2.14	4.97	2.25
30 FPS	66	4.67	1.93	5.32	1.82	7.14	1.93	5.26	2.05

Mean scores indicated that students receiving the lecture at thirty frames per second performed better on both the posttest, as well as the delayed test. Moreover, this condition indicated greater confidence in test performance, relevance of the subject matter, and satisfaction with the presentation. However, subsequent analysis of variance revealed that none of these differences are significant. Lack of significance is not surprising considering the wide variability of individual scores on both dependent variables as reflected by the large standard deviations. Replication of the study with subjects on a 2x2 design to afford a larger n for each cell might provide significance. Correlation analysis was conducted to examine the inter-relationships of the dependent variables measured in this study.

As Table 5 illustrates, the “content mastery” variables do correlate significantly ($p < .01$), with the “credibility variables”, however, the association level is not strong (none above .50).

TABLE 5 Correlation Matrix of Dependent Variables

Variable	2	3	4	5	6
1. Posttest #1	.43 ^(a)	.25 ^(a)	.45 ^(a)	.30 ^(b)	.17
2. Delayed Test	—	.16	.32 ^(a)	.21 ^(b)	.10
3. Attention		—	.47 ^(a)	.46 ^(a)	.60 ^(a)
4. Confidence			—	.53 ^(a)	.51 ^(a)
5. Relevance				—	.56 ^(a)
6. Satisfaction					—
(a) $p < .001$ (b) $p < .01$					

The credibility variables correlate strongly with each other and illustrate universally high levels of significance ($p < .001$). These results suggest that there is considerable

cohesiveness in the dependent data structure and depicts a conceptually solid relationship between the two content mastery variables and the four credibility measures.

Discussion

The findings in this study suggest that larger image sizes and increased refresher rate do not positively affect content retention or instructor credibility in the sense of attention, satisfaction with the material, relevance of the material or confidence in test performance. In essence, better quality images do not improve cognitive performance or perception of the affective domain of visual images.

These results should be of great interest to those engaged in the development of Internet based courses and those involved with desktop video conferencing (DVC). The issue of image quality should not be regarded as the driving force behind effective distance learning. Hence, designers of such systems and products can devote greater resources to content development. Moreover, without the need for greater bandwidth and processor speeds for image delivery, more dedicated network bandwidth might be allocated to development of interactive distance learning systems. In fact, most critics of web based learning resources and DVC claim that it lacks "social presence". Thus, given limited bandwidth, due either to system consideration or cost effectiveness, a portion could be deployed for interactive networking assuming, as this study suggests, that content mastery can be achieved with smaller, slower images as effectively as larger television format images.

Overall, these findings are encouraging to those involved with training and education using limited bandwidth networks. Without question, educational design, not image quality, is the most compelling factor in distance learning applications.

Limitations

The results of this study did not support the contentions of the original research hypotheses, and were, arguably, somewhat counterintuitive. It should be noted that this study, by design, was artificially induced, and students were therefore aware of their

collective experimental experience. Since this was only a forty minute presentation, it would be difficult to note any rendering of long term effects. If students were exposed to one of the specific conditions used in this study for an entire semester, it would be reasonable to expect some differences in information retention and credibility. Currently, this is a nearly untouched , yet important, area of inquiry. Future experimental designs need to examine image sizes and frame rate outcomes in more realistic settings. Learning style and other confounding variables should be taken into account in developing a comprehensive model. Finally, more sensitive instruments should be developed to understand the characteristics of attention, confidence, relevance, and satisfaction in the networked learning environment.

REFERENCES

- Biner, P.M. (1993) The development of an Instrument to Measure Student Attitudes Toward Televised Courses, *The American Journal of Distance Education*, Vol. 7, Issue (1), Pg. 62-73
- Biner, P.M., Dean, R.S., and Mellinger, A.E. (1994), Factors Underlying Distance Learner Satisfaction with Televised College-Level Courses, *The American Journal of Distance Education*, Vol. 8, Issue (1), Pg. 60-71.
- Bramble, W. J. And Martin B.L. (1995) The Florida Teletraining Project: Military Training in Two-Way Compressed Video, *The American Journal of Distance Education*, 9(1), 6-26.
- Capell, Peter (1995), *Report on distance Learning Technologies*, Software Engineering Institute, Carnegie Mellon University, Pittsburgh, PA.
- Gale, S. (1992) Desktop Video Conferencing: Technical Advances and Evaluation Issues. *Computer Communications*, 15(8), 517-526.
- Keller, J.M. (1983) Motivation and Instructional Design: A theoretical Perspective. *Journal of Instructional Development*. 2(4), 26-34.
- Krathwohl, D.R., Bloom B.S. and Masia, B.B. (1964) Taxonomy of Educational Objectives, The classification of educational goals, handbook II: Affective Domain. New York: David McKay Co., NY.
- Kies, K. J., Williges, R. C., and Rosson, M. B., (1996) *Controlled Laboratory Experimentation and field Study Evaluation of Video Conferencing for Distance Learning Applications*, Technical Report for SUCCEED, Blacksburg, Virginia.

Kies, K. J., (1997) Empirical Methods for Evaluating Video-Mediated Collaborative Work. Doctoral Dissertation. Blacksburg, Virginia: Virginia Tech.

Main, Robert G. (1996), *Designing Instruction for Distance Learning*, U.S. Air Force Technical Report, Armstrong Laboratory, Brooks Air force Base, TX.

Main, Robert G, and Riise, Eric O., (1995) *Creating a Virtual Classroom: Using Public Switched Networks for Distance Learning Applications*, U.S. Air Force Technical Report, Armstrong Laboratory, AFB, San Diego, CA.

Main, Robert G., Terry Curtis and Mick Presnell (1996), *Report of Findings Interactive Multimedia Distance Learning Experiment*, Darlene Hinds, ed., California State University. Chico, Chico, CA.

Ramachandran, V. S. And Anstis, S. M. (1986) *The Perception of Apparent Motion*. Scientific American, 254, 102-109.

Tang, J.C. and Isaacs, Ellen, (1993). *Why do Users Like Video?* Computer Supported Cooperative Work, (1)4, 163-195.

APPENDIX A

Measurement Instruments

Content Mastery

Page 16

Credibility

Page 17

1. The legislation that created the Federal Radio Commission was
 - a. the Post Roads Act of 1866.
 - b. the Wireless Ship Act of 1910.
 - c. the Radio Act of 1912.
 - d. the Radio Act of 1927.
2. The network that was formed from the NBC Blue Network was
 - a. CBS.
 - b. ABC.
 - c. RKO.
 - d. Mutual.
3. The person most closely associated with the development of CBS is
 - a. Marconi.
 - b. Weaver.
 - c. Sarnoff.
 - d. Paley.
4. The Federal Radio Commission was under the direction of
 - a. the Navy.
 - b. Department of Commerce.
 - c. Congress.
 - d. Defense Department.
5. The Radio Act of 1912
 - a. established the FCC.
 - b. established the FRC.
 - c. formed RCA.
 - d. required licenses to use radio frequencies.
6. NBC was originally owned by
 - a. the Red Network.
 - b. AT&T.
 - c. RCA, GE and Westinghouse.
 - d. RCA.
7. The cross-licensing agreements of 1926 prevented which of the following companies from entering the broadcasting business?
 - a. AT&T
 - b. RCA
 - c. Westinghouse
 - d. Mutual
8. The FCC replaced the FRC in 1934 because
 - a. the FRC was incompetent.
 - b. the FCC would be an agency independent from government.
 - c. the FRC could not oversee television.
 - d. the FRC was under the direction of the Navy.
9. The philosophy of private ownership of electronic communication began with
 - a. the Post Roads Act of 1866.
 - b. the Wireless Ship Act of 1910.
 - c. the Communications Act of 1934.
 - d. the Radio Act of 1927.
10. AT&T's chain broadcasting efforts in the 1920's would be characterized today as
 - a. advertising.
 - b. monopolistic.
 - c. networking.
 - d. violations of anti-trust rules.

Please read the following statements and select the response that most accurately reflects your feelings.

- | | | |
|---|---|-----------------|
| A | = | Not true |
| B | = | Slightly true |
| C | = | Moderately true |
| D | = | Mostly true |
| E | = | Very true |

1. The instructor made me feel enthusiastic about the subject matter of this course.
2. I feel confident that I did well on the quiz.
3. This presentation had very little in it that captured my attention.
4. The instructor made the subject matter of this course seem important.
5. I do NOT see how the content of this course relates to anything I already know.
6. I enjoyed this presentation.
7. I feel rather disappointed with this presentation.
8. I feel I have received a good foundation in broadcast history.

**ON THE RESILIENCE OF TIME-TO-CONTACT JUDGMENTS: THE DETERMINATION OF
INHIBITORY AND FACILITORY INFLUENCES, AND FACTOR STRUCTURE**

**Philip H. Marshall
Professor
Department of Psychology**

**Texas Tech University
Lubbock, TX 79409**

**Final Report for:
Summer Research Extension Program
Armstrong Laboratory**

**Sponsored by:
Air Force Office of Scientific Research
Bolling Air Force Base, DC**

and

**Texas Tech University
Lubbock, TX**

February 1998

ON THE RESILIENCE OF TIME-TO-CONTACT JUDGMENTS: THE DETERMINATION OF INHIBITORY AND FACILITORY INFLUENCES, AND FACTOR STRUCTURE

Philip H. Marshall
Professor
Department of Psychology
Texas Tech University

Abstract

The initial SFRP project which served as the basis for these SREP studies is reported here as Experiment 1. The results of that study lead to the conclusion that neither the mere presence of a number of irrelevant stimuli, their relative velocity, nor their movement direction adversely affected time-to-contact (TTC) judgments. There was, however, a significant improvement in TTC accuracy when the non-targets moved in the same direction and at the same velocity as the target. It was proposed that visible, non-target stimuli that continue to move in the same direction and at the same speed as the invisible target, may be used to guide the participant's TTC judgments. This was termed the surrogate target effect. Experiment 2 was a follow up study that confirmed the surrogate target explanation. Experiment 3 was conducted to determine the extent of the apparent resiliency of TTC judgments in the presence of non-target stimuli that were potentially more distracting than those used in the previous studies. Conditions of greater apparent distractibility tended to result in shorter TTC judgments. Experiment 4 investigated the effects of having the non-target stimuli appear in different phases of the TTC trial. Some resiliency to the presence of non-target stimuli was observed in that no differences were found, as was generally obtained in Experiment 1, between conditions where the non-targets were on the screen all of the time, or none of the time. When they were present only before the target became invisible, however, TTC judgments were longer, and when they appeared only after the target became invisible, TTC estimates were shorter. It was hypothesized that contrasting temporal dynamics may have affected arousal levels to produce these results. Experiment 5 investigated TTC judgments for curvilinear paths of varying fidelity. It appears that different cognitive processes may be involved for TTC decisions along straight lines and curves. In Experiment 6 a factor analytic model was proposed for TTC and related cognitive and perceptual processes.

ON THE RESILIENCE OF TIME-TO-CONTACT JUDGMENTS: THE DETERMINATION OF INHIBITORY AND FACILITORY INFLUENCES, AND FACTOR STRUCTURE

Philip H. Marshall

Introduction

For some time there has been a research interest in the ability of human observers to make time-to-contact (TTC) judgments. In one common version of this task, an observer watches a target traveling horizontally (at constant velocity) along a path for several seconds before that target disappears. The participant is to predict (usually by pressing a button) when the target would reach a predetermined end point, or finish line. Typically, performance is characterized by increasing underestimation of TTC (responding earlier than the target would have made contact) as actual TTC increases (Schiff & Detwiler, 1979; Caird & Hancock, 1991). Some researchers have suggested this ability to be solely a function of information from the optic array (Lee, 1976; Tresilian, 1991), while others have suggested the involvement of various cognitive processes and mechanisms such as memory, imagery, and internal clocks (see Tresilian, 1995).

The stimuli in most TTC tasks consist of simple, moving objects (e.g., a square) in uncluttered displays, with no other stimuli. There are attempts currently underway to assess some potential distractor effects in more complex arrays and tasks (Liddell, 1997; Novak, 1997), and one published study (Lyon & Wagg, 1995) reports limited non-target stimulus effects with a target moving in a circular path. In that study participants had to determine whether an invisible target, traveling a circular path, would have hit a target location presented after some variable time. Under some conditions a single moving distractor stimulus appeared going in either the same or opposite direction as the target, and at different speeds. Lyon and Wagg (1995) found that the distractor conditions did not have uniform effects, only sometimes degrading performance based on "some kind" of tracking mechanism.

Research incorporating potentially distracting or other stimuli in the visual field can make contributions in several ways. First, real world situations in which TTC judgments are made are very likely to contain distracting or other events, and this is so even if the "real world" task is only monitoring a computer display. Therefore, research incorporating non-target stimuli is somewhat more ecologically valid than that where only a single target is present and moves. Such research

could also contribute to the debate on the extent of involvement of cognitive processes in TTC decision tasks. Cognitive acts that require effort (as distinguished from those that have become automatic) require a share of our limited attentional resources. To the extent that, and under conditions where, TTC processing might be effortful, sufficiently distracting events could reduce attentional resources and affect TTC performance. Alternatively, there are other perceptual phenomena that might affect TTC accuracy when other stimuli, especially moving stimuli, are present in the visual array, and an example would be the so-called motion repulsion effect described by Marshak and Sekuler (1979). They found that the perceived direction of motion for a given dot can be affected by the motion of another dot in the visual array such that the perceived difference between their respective headings is exaggerated. If a similar process were to operate when a target was moving in the presence of moving non-target stimuli, the path of the target might be misperceived with resulting effects on TTC performance.

In one recent study, DeLucia and Novak (in press) investigated participants' ability to make relative TTC judgments in the presence of multiple moving targets, and whether such abilities are determined by limited-capacity cognitive processing. In their studies participants saw either various numbers of computer-simulated objects approaching them and had to decide which object would hit them first, or whether a target with a different TTC was present in an array. Their results showed, in part, that individuals performed generally at above chance levels even when up to eight objects moved in the display, but that reaction time was generally greater for eight than two object displays. DeLucia and Novak concluded that "the number of elements in the optic array may affect the speed and effectiveness of relative TTC judgments, that processing load as well as optic expansion information must be included in models of perceived collision, [and that] visual information other than optical TTC may contribute to relative TTC judgments." They go on to state that "it is important to determine the limits, relative strengths, and combinatorial rules for different sources of visual information."

It is important to note that the nature of the effects of non-target stimuli could be to move TTC judgments closer to actual times, that is, compensate for the underestimation normally observed. It would be naive to assume that the effects of the presence of non-target stimuli should always be in the direction of decreased performance as a simple diminished resources model would suggest. We recognize that stimuli may have various functional roles depending on the situations in

which they are present, and that "cognitive effects" may occur at a variety of levels and be manifested in a variety of ways. For example, they may include fundamental attentional processes or more complicated task-related strategic processes. We are, therefore, unwilling to presume that the presence of non-target stimuli can only decrease the accuracy of judgments, and opt, instead, for the more pragmatic perspective that one never knows if a stimulus is a distractor until the effects are known.

Experiment 1

This study serves as the basis for several of the studies conducted as SREP research, and it will be presented in some depth. In this initial study the presence, number, direction, and relative velocities of moving non-target stimuli were manipulated to determine possible effects on the accuracy of TTC judgments.

Method

Design. The variety of trials (stimulus scenes) in this study included those in which only target stimuli were present, those in which non-target stimuli were present but did not move (static), and those in which non-target stimuli were present and did move (dynamic). When non-target stimuli were present they varied according to how many there were (4, 8 or 16), and, when they moved, they varied according to their velocity relative to the target (same, or +/- 50%), and their direction of movement (0-315 degrees in 45-deg, counter-clockwise increments)

Participants. A total of 42 Air Force basic recruits participated at the start of this study as part of their basic military training requirements. All (but one) were right-handed, had normal or corrected-to-normal vision, participated according to standard Air Force privacy and confidentiality procedures, and none declined to participate. Two different computer systems were used (see below) and five participants using each had their data deleted because the participants either did not understand or follow the instructions. These individuals were identified by having a very large number of repeated trials relative to the majority of participants. The final distribution included 8 males and 9 females having used a Dell® computer system, and 7 males and 8 females having used a Micron® computer system.

Materials and computers. The two-dimensional scenes were designed to have a light gray background, black vertical start and finish lines, dark gray square targets, and somewhat lighter,

square non-target stimuli (approximately 83-, 0-, 16-, and 39-% of "pure" white, respectively, as defined by the graphics program that was used). The targets were made darker to distinguish them from the non-target stimuli. Brightness settings on all monitors were equated visually by turning all monitors to the brightest level. This had an overall effect of slightly reducing contrast, but still clearly retaining the distinction between target and non-target stimuli. In all conditions, when the target and a non-target stimulus overlapped or intersected, the target always appeared to be in front of the non-target stimulus. All paths "traveled" by the target had the same finish line, but the start lines, and hence total distance traveled, varied (see Table 1). All movements were from left to right.

Each scene came on and remained static (nothing moving) until the subject pressed the spacebar to initiate that trial. Initially, the target was entirely visible, its trailing edge at rest against the starting line. When the participant depressed spacebar the visible target traveled for 2-sec before it disappeared. Any non-target stimuli present remained static, or continued to move, until the participant responded.

The targets traveled at six different velocities (see Table 1 for specifications of travel distance, velocity and TTC). There were two different velocities and distances after disappearing for each of the three times to contact. The non-target stimuli, if assigned to move, traveled at one of three different velocities relative to the target depending on which condition the participant was in. One third of the participants saw the non-target stimuli moving at the same velocity as the target, one third saw them moving 50% faster than the target, and one third saw them moving 50% slower than the targets. On any given trial, if non-target stimuli moved, they all moved in the same direction, and followed a path defined by one of eight degrees of deviation from horizontal (in increments of 45-deg, counter-clockwise from the horizontal, left-to-right direction of 0-deg).

When they were present, there were either 4, 8 or 16 non-target stimuli, randomly positioned on the screen at the start of each trial. Initial non-target stimulus positions were determined by randomly choosing an x,y intersection from an imaginary 16x16 grid that filled nearly all of the viewable area on the computer monitor (inset about 2.54-cm on all sides), with the restriction that no x or y value was repeated. If and when a moving non-target stimulus "left" the screen, a new one immediately appeared and began to move at a location at the other end of an imaginary circular path around the screen. Figure 1 shows examples of scene presentations for 4,

8, and 16 stimuli, and also indicates examples of three of the eight different non-target stimulus movement directions.

The six-item TTC matrix (two different scene conditions for each of the three TTC durations, 2-, 4-, and 8-sec, as in Table 1) was crossed with the three levels of Number of non-target stimuli and the eight levels of Direction of Movement, for a total of 144 trials. There were also two replications of the TTC matrix on which no non-target stimuli were present (12 trials), and six replications of the TTC matrix on which 2, 4, and 8 non-target stimuli were present but did not move (36 trials). Thus, there were a total of 192 unique trials for each participant.

In each session some participants used either a Dell® computer configured with a 90-MHz Pentium® processor with 16 megabyte of RAM, and a 17-in color monitor set to a black and white monochrome screen, or a Micron® computer using a 166-MHz Pentium® processor with 16 megabyte of RAM, and a 17-in color monitor set to a black and white monochrome screen. The programs operated in EGA video, with a presentation rate of 14-msec per frame. We had no basis for predicting differences in performance based upon the systems, especially since frame rate was the same in both. In fact, a *t*-test on overall mean TTC estimates between the two systems resulted in an insignificant difference, 3.72-sec for the Dell® versus 3.81-sec for the Micron® [*t* (30) = -.31, *p* > .75], so the data from the two systems were pooled in the analyses presented below.

Procedure. The participants were run, on consecutive days, in two group sessions. They were pseudo-randomly assigned to one of the computer stations, with the only restriction being that we attempted to evenly distribute men and women across computer systems and relative non-target stimulus speed conditions (normal, slower, and faster). They were seated so as to be centered on the screen, with their eyes 24-in from the screen. The first part of the program gave instructions for the task, and demonstrated the stimulus conditions to be encountered during the study. There were also several familiarization trials with no non-target stimuli present, and which used a starting location longer than those used in the study, and a different (yet similar) velocity than any experienced in the study.

The presentation of criterion trials followed. To initiate each trial, the participant pressed the keyboard spacebar with left hand fingers to start the target moving, and pressed a mouse key using right hand fingers to make the TTC response. Upon the conclusion of the TTC response no

feedback was given, and the scene for the next trial immediately appeared. The sequencing of the 192 trials was randomly determined for each participant. To compensate for inadvertent responses and possible inattention, a trial on which a TTC response occurred before the target had disappeared was aborted and was presented again at the end of the original series, as was any trial for which the TTC response was shorter than .5-sec. or longer than 12-sec. No trial was repeated more than once, and the average number of repeated trials was 13.35 (sd = 11.2), or just about 7%. Finally, participants proceeded at their own pace with two one-minute rest breaks (remaining in their chairs and posturally oriented) after the 64th and 128th trials.

An important point needs to be introduced at this juncture. On day one of data collection there was an unplanned environmental occurrence, with the air conditioning in the testing center shutting down. Since the experimental sessions were conducted in mid-summer, the temperature and humidity in the testing center on that day became high enough to produce obvious general discomfort. Climatological data recorded in the testing center showed that the temperature had risen to 90°-F, with a humidity reading of 76%, sufficient to qualify for a "Category II" apparent heat index of approximately 110° F which can be associated with heat exhaustion in instances of prolonged physical activity (Steadman, 1979). Decrements in performance on visual processing tasks also have been found at this temperature (Hohnsbein, Peikarski, Kampmann & Noack, 1984). On day two of data collection the malfunction had been repaired, and readings were a much more comfortable 76°-F, with 72% humidity. In effect, we had an unplanned source of variance, a new factor - moderate heat-induced stress. This heat stress factor is introduced in the following analyses as the Day factor - high heat for day one, and normal conditions on day two.

Results

In each of the analyses that follow, mean TTC scores were computed over trials with actual TTC times of 2-, 4-, or 8-sec (respectively) in each condition, and those means were the data entered into the analyses of variance. Thus, for the target only condition and static non-target stimuli conditions, each TTC entry for each participant was based on four trials (observations), while in the dynamic non-target stimuli condition each TTC entry was based on two trials.

Does the presence or mere movement of non-target stimuli affect TTC accuracy? To answer this question TTC performance was assessed across the three task conditions with Gender and Day as between-subjects variables, and Task and TTC as within-subjects variables. That analysis

yielded only an overall effect for TTC, $F(2, 56) = 187.06, p < .0001$, with mean estimated TTC increasing as actual TTC increased, 2.17-, 3.68-, and 5.58-sec for actual TTC times of 2-, 4-, and 8-sec, respectively. No other main effects or interactions were significant at the .05 level. Thus, the mere presence (static condition) or movement (dynamic condition) of non-target stimuli did not have a significant affect on overall TTC estimates relative to the simple condition where only the target was present.

Does the number of non-target stimuli present have an effect on TTC accuracy? To answer this question an analysis of variance was performed on data from the static and dynamic conditions. In the latter, performance was pooled over the direction of movement manipulations. This analysis had Gender and Day as between-subjects variables and Task, Number of non-target stimuli (4, 8, or 16), and TTC as within-subjects variables. There was a significant effect for TTC, $F(2, 56) = 173.13, p < .0001$, with increasing mean TTC estimates of 2.18-, 3.69-, and 5.55-sec. For the record, there was also a significant interaction between Day and Number of non-target stimuli, $F(2, 56) = 3.85, p < .05$. Day 1 (Heat) participants gave slightly longer estimates of TTC than Day 2 (Normal) participants, especially for the eight non-target stimuli condition. Although we had no a priori hypothesis about the effects of heat, it might be that the high heat and moderate numbers of non-target stimuli combined to create an optimum arousal-optimal performance situation, but such an explanation is purely speculative, and, in any event, Day (testing temperature) did not interact with TTC duration. The number of non-target stimuli yielded no main effect, nor did that factor interact with TTC.

Do the number, relative speed and direction of movement of non-target stimuli have an effect on TTC performance? To answer this question an analysis of variance was conducted on data only from the dynamic condition. That analysis had Gender, Day, and Relative Speed of non-target stimuli as between-subjects factors, and Number of non-target stimuli, Direction of Movement, and TTC as within-subjects variables. That analysis yielded a significant main effect for TTC, $F(2, 40) = 137.25, p < .0001$, with increasing mean TTC scores of 2.12-, 3.66-, and 5.58-sec. There also was a significant interaction between Direction of movement and TTC, $F(14, 280) = 4.83, p < .0001$, and between Relative Speed of movement of non-target stimuli, Direction of movement, and TTC, $F(28, 280) = 1.91, p < .01$. This latter interaction, encompassing the effects of the former, is shown in Figure 2. Time to contact estimates increased as a function of

actual TTC, and there was the usual greater degree of underestimation of TTC as actual TTC increased. Further, with non-target stimuli moving at the same speed as the target, participants were much more accurate in their TTC estimates at the 8-sec TTC duration when the non-target stimuli traveled in the same direction as the target. No other effects were significant at the .05 level.

Discussion

We began this study with the expectation that the non-target stimulus manipulations would have an effect on TTC performance, but we were not sure how those effects would be manifested in performance. It appears from our results, however, that TTC performance is rather difficult to disrupt. Non-target stimuli, even when they are numerous and moving across the target's path, do not impair TTC judgments. We also had the opportunity to observe that not even a very hot and uncomfortable task environment produced a disruptive effect. In fact, the only substantial effect on TTC performance, other than the obvious effects of actual TTC, was the improvement in accuracy when the non-target stimuli moved at the same speed, and in the same direction as the target at the 8-sec TTC, but there is a plausible explanation for that facilitation effect.

A non-target stimulus traveling in the same direction and at the same speed as the target stimulus is essentially a running mate, and can become a surrogate target when the actual target disappears. This would require one to make a mental note of the degree of separation between the target and a correlated non-target stimulus, and use the movement and location of the surrogate non-target stimulus as a guide to judge when the target would reach the finish line. The longer the remaining travel time before the target would have contacted the finish line, the more time for the participant to make these mental compensations, and hence performance at the 8-sec TTC received the greatest benefit from the surrogate process. Non-targets moving at different speeds or directions would serve the surrogate function less well, if at all, and that also is consistent with our findings. This surrogate facilitation effect was examined in Experiment 2, the first of the SREP studies.

Experiment 2

The results of Experiment 1 suggested that non-target stimuli moving in the same direction and at the same speed as the target can become surrogate stimuli used to guide the participant's TTC judgment. This was based on the observation that the accuracy of TTC judgments were superior in the condition where non-target stimuli moved in the same direction and at the same

speed as the target in the 8-sec TTC condition. The purpose of this study was to directly test that hypothesis. Specifically, if non-target stimuli can become surrogates, the longer they are visible, the better surrogates they will be. Since it takes time to initiate and use the surrogate process, the benefit of such a process should be increasingly apparent as TTC increases. Non-target stimuli that disappear before or at the same time the target disappears will be totally useless as a surrogate, and non-target stimuli that disappear shortly after the target does will be much less useful as surrogates. Thus, in Experiment 2 we varied the offset of the non-targets relative to the offset of the target with the expectation that potential surrogate effects would be most obvious the longer the non-targets were visible.

Method

Participants. The participants in this study were 37, male Air Force basic recruits who participated in this study as part of their basic military training requirements. All were right-handed, had normal or corrected-to-normal vision, participated according to standard Air Force privacy and confidentiality procedures, and none declined to participate.

Materials and apparatus. The same computer systems and general procedures as described for Experiment 1 were used.

The scenes contained either just the moving target, or the target and 16, moving, non-target stimuli. Scenes containing the non-target stimuli were drawn from the 0-deg, same velocity scenes constructed for Experiment 1. That is, they moved in the same direction (horizontally, left to right) and at the same velocity as the target. For target-only scenes there were two replications of the TTC matrix for a total of 12 trials. For the scenes having non-target stimuli, the non-target stimuli appeared and moved with the target (as in Experiment 1), but disappeared at different times relative to the offset of the target. There were five offset intervals used for each TTC duration. For each of the three TTC durations, one non-target offset interval was -.5-sec (non-targets disappear .5-sec before the target), and one was 0-sec (non-targets disappear simultaneously with the target). The remaining three offset durations for each TTC were 25-, 50-, and 100-% of that TTC value. Therefore, the remaining offset intervals were .5-, 1-, 2-sec, 1-, 2-, 4-sec, and 2-, 4-, 8-sec for the three TTC durations of 2-, 4-, and 8-sec, respectively. For an example, for scenes with a 4-sec TTC duration, the non-targets disappeared either .5-sec before the target, at the same time as the target, or 1-, 2-, or 4-sec after the target disappeared.

The TTC matrix was repeated three times for each of the 15 conditions having non-target stimuli, for a total of 90 trials. Thus, there were a total of 102 trials in this study, with a 1-min rest break after the fiftieth trial.

Procedure. The procedures were the same as in Experiment 1.

Results

The data for all analyses were the mean judged TTCs for each participant under each condition. Data from the target only condition were entered into a one-way analysis of variance that had TTC as the within-subjects variable. That analysis yielded a significant effect for TTC, $F(2, 74) = 211.36$, $p < .001$, and showed the traditional underestimation as TTC increased (mean TTC estimates of 2.03-, 3.56-, and 5.67-sec as TTC increased over 2-, 4-, and 8-sec., respectively).

To test for the effects of the different non-target offset intervals an analysis of variance was conducted with TTC and Offset intervals (defined as -.5-, 0-sec, and, 25%-, 50%-, and 100%-sec after target) as within-subjects variables. That analysis yielded a significant effect for TTC, $F(2, 74) = 586.04$, $p < .001$; for the Offset interval, $F(4, 148) = 7.81$, $p < .001$; and for the interaction between the two, $F(8, 296) = 30.26$, $p < .001$. These effects are shown in Figure 3.

Discussion

The results of Experiment 2 confirm all expectations. When the non-target stimuli disappeared either .5-sec before, or simultaneously with, the target there was no advantage over the non-target condition. Thereafter, the longer the non-target stimuli were visible, the greater was the accuracy in TTC judgments. This pattern of results is consistent with the notion that the non-target stimuli can, in some situations, become surrogates for the target and benefit TTC estimation.

Experiment 3

With the exception of the unique combination of conditions that gave rise to surrogate processing in Experiment 1, no other condition had an effect on TTC judgments. This could have been because of several factors that may have produced little distraction from the non-target stimuli. For example, the non-targets were lighter than the targets, making the latter more easily visually acquired and maintained during the invisible period. Moving non-targets all moved in the same direction, and each was on the screen for its entire travel time making for a uniform background situation that may not have yielded higher levels of distraction. In this study several modifications were made in the characteristics of the non-target stimuli to make their presence

potentially more distracting.

Method

Participants. The participants in this study were 36, male Air Force basic recruits who participated in this study as part of their basic military training requirements. All were right-handed, had normal or corrected-to-normal vision, participated according to standard Air Force privacy and confidentiality procedures, and none declined to participate.

Materials and apparatus. The same computer systems and general procedures as described for Experiment 1 were used. Several alterations were made in the stimulus scenes in an attempt to increase possible distraction. There were 16 non-target stimuli for all conditions. On one half of the trials, all of the non-targets were lighter (as in Experiments 1 and 2), and on the other half they were the same shade as the target, and hence, potentially more distracting. Each non-target stimulus either remained on the screen for its entire possible travel time across the screen, or it disappeared at some point during travel across the screen, only to reappear at some other random location. Of the 16 possible such stimuli, the number that did this "popping" was varied, with the number that would pop on any given trial being 0, 8, or 16. Popping rates among non-targets were randomly determined within a 100-300-msec. interval. Additionally, the possible number of different directions the non-target stimuli could take was randomly determined to be one, four, or eight of the directions used in Experiment 1. So, in this study the new variables were Color of non-targets, number of Poppers, and number of possible Directions. These new variables (2x3x3) were crossed with the basic six-item TTC matrix used previously for a total of 108 trials. Finally, the relative movement of the non-target stimuli was manipulated as a between-subjects variable, with thirds of the participants seeing non-targets traveling at the same rate as the targets, or 50% faster or 50% slower than the target.

Procedure. The same testing procedures were used as in Experiments 1 and 2.

Results

An analysis of variance performed on these data yielded a significant effect for the TTC manipulation, $F(2,66) = 324.42$, $p < .001$, with the mean TTC estimates for 2-, 4-, and 8-sec being 2.22-, 3.83, and 5.90-sec, respectively. The only other significant effect was for the interaction between the number of poppers and the number of different directions of travel, $F(4, 132) = 3.80$, $p < .01$. This interaction is shown in Figure 4. Increasing the number of poppers

resulted in increasingly shorter overall TTC judgments when these non-targets traveled in only one, or in up to four, directions. Entirely different results were obtained when there were eight different directions of travel, most notably, an increase in overall TTC when only eight of the non-targets popped. There were no other significant effects, including no significant effects involving the TTC variable.

Discussion

There was some indication that increasing the level of distraction can, in some situations, have, what appears to be, a systematic effect on the overall estimate of TTC. A possible explanation for this effect is considered in the discussion of Experiment 4.

Experiment 4

The manipulations of possible distracting stimuli in the previous studies had such stimuli present during the entire trial. The stimuli came on, and moved if required, when the target was both visible and invisible. In this study we investigated the effect of non-target stimuli appearing (or not appearing) during various Phases of the trial: never present (no non-targets), present all of the time, present only during the target visible phase, or present only during the target invisible phase.

Method

Participants. The participants in this study were 49, male Air Force basic recruits who participated in this study as part of their basic military training requirements. All were right-handed, had normal or corrected-to-normal vision, participated according to standard Air Force privacy and confidentiality procedures, and none declined to participate.

Materials and apparatus. When conditions warranted, there were 16 non-target poppers in this study, and they were of the same color as the target, traveled in one of eight randomly chosen directions, and at the same speed as the target. The manipulation in this study was if, and when, the non-targets appeared, and for this there were four conditions, equally divided among the trials. On any given trial, there were either no non-targets; non-targets appearing just during the visible phase (i.e., the first 2-sec.) of target travel, and disappearing with the target; non-targets appearing appearing only when the target became invisible; or non-targets on during the entire trial (as in Experiments 1-3). These four conditions were crossed with the basic TTC matrix used previously, for a total of 72 trials.

Procedure. The same testing procedures were used as in Experiments 1 and 2.

Results

An analysis of variance was conducted with Phases and TTC as within-subjects variables. That analysis yielded a significant effect for TTC, $F(2,96) = 398.00$, $p < .001$, with judged TTC being 2.13-, 3.76-, and 5.84-sec, as actual TTC increased from 2-, to 4-, to 8-sec. There was also a significant effect for Phase, $F(3,144) = 17.03$, $p < .001$, and for the interaction between Phase and TTC, $F(6,288) = 2.82$, $p < .02$. That interaction is shown in Figure 5.

Similar effects of Phase can be seen in Figure 5 for all levels of TTC, but the nature of the effect becomes more pronounced as actual TTC increases. At any actual TTC level there is no difference in judged TTC between the conditions that have no non-targets present, and the condition that has non-targets present throughout the trial (e.g., during both target visible and invisible phases). When the non-targets appear only during the initial target's visible phase, however, there is an increase in judged TTC, and when the non-targets are visible only during the target's invisible phase there is a decrease in judged TTC.

Discussion

The absence of a difference between the no non-targets and the non-targets being present during the entire trial (both the target's visible and invisible phases) conditions is consistent with the general conclusions from Experiment 1 (excepting the special case of the surrogate target effect).

The non-target stimuli in all of these studies have been irrelevant initially (again, surrogate targets may be an exception, but they are neutral at least at the start of the trials) to the TTC task, and to any decision or response that the participant had to make. For that reason, the clearly uniform effects of the Phase manipulation have to be attributed to a nonspecific performance mechanism affecting TTC judgments. One such performance mechanism may have to do with the arousal inducing capability of these irrelevant stimuli and the dynamic temporal contrasts they may induce.

There is some literature on the effects of arousal on temporal judgments. Researchers (Delay & Richardson, 1981; Delay & Mathey, 1985) have suggested that ambient stimulation may alter performance on time estimation tasks through activation of the reticular formation (e.g., an arousal function). In one study, Delay and Mathey (1985) showed that in some conditions, as the

intensity of ambient noise increased, estimates of the time duration of a 10-sec. interval decreased. That is, subjectively, time (the 10-sec. interval) seemed to pass by faster. In the present study, the non-target stimuli could be considered ambient stimulation in the sense that they were not relevant to the participants' task, and unlike the surrogate effect conditions of Experiment 1, they offered no information to facilitate performance. Also, in Experiment 4 possible heightened levels of general arousal achieved in some conditions of greater distractibility may have been operating to shorten TTC judgments.

In the no non-target and always present non-target conditions the level of ambient stimulation (albeit different in each condition) is constant within a trial. There is just the target in the former, and always the target and the non-targets in the latter. Each of the other two conditions represent periods of change in the presence of the non-target stimuli. When the non-target poppers appear for only the first 2-sec. of visible target motion (and then disappear when the target becomes invisible), one may consider that there is a reduction in the level of ambient stimulation -- the popping stimuli are no longer on screen. Under these circumstances contrasting arousal situations might be set up. The result might have been the overestimation of travel time (TTC) for the now invisible target moving under a condition in which, in contrast with the previous 2-sec. of popping stimuli, arousal is reduced, and TTC estimates are larger than would have been the case if the two phases had the same level of ambient arousal. Similarly, under the condition where the non-target poppers appear only after the target has become invisible, the opposite arousal contrast might have occurred. Greater arousal by virtue of this contrast might have lead to the perception of faster passage of time, and hence, an underestimation of TTC.

Unfortunately, there was neither time nor resources to examine the possible effects of arousal on TTC performance. Future research, however, should address issues of this kind.

Experiment 5

The previous four experiments examined TTC performance effects in conditions that varied the presence, number, movement characteristics, structural properties, and location in the trial of non-target stimulus events. In this study, the influence on performance of characteristics of the path the target takes were investigated. With few exceptions (i.e., Lyon & Wagg, 1995) researchers have had targets travel straight lines in TTC studies. In this study TTC judgments also were made for target stimuli traveling along various kinds of curved paths.

Method

Participants. The participants in this study were 56, male Air Force basic recruits who participated in this study as part of their basic military training requirements. All were right-handed, had normal or corrected-to-normal vision, participated according to standard Air Force privacy and confidentiality procedures, and none declined to participate.

Materials and apparatus. The same computer systems were used as in the previous research, but the stimulus scenes were prepared in color. They had a black background, blue start and end lines, a yellow ball for a target, and gray lines for target paths. The end lines were of the same dimensions as those used previously, and the target paths, depicted here for the first time, were the same widths as the end lines. The diameter of the ball target was slightly larger than the width of the path.

In addition to the presence of paths, a new variable manipulated in this study was the Fidelity of the path, and it had four levels. A given trial scene contained either no path, a continuous line path, a somewhat broken, dashed path, or a severely broken, dashed path. In each case the manipulation of fidelity came after the target disappeared (i.e., after 2-sec of travel from the start point). That is, for the first 2-sec. of every trial the path was defined by a solid line. It is important to note that when the target became invisible, that initial solid segment remained on the screen, and the remaining path was defined by one of the four levels of fidelity. So, for example, on some trials the path had a solid beginning (2-sec. worth), followed by a dashed line indicating the remainder of the path.

Another new variable manipulated for the first time was the curvilinearity of the path. A given trial had a path that was either a straight line, or a curved line of varying degrees of complexity. The paths were drawn using a common drawing program that varied the number of attraction points for a given curve. Three levels of attraction points (5, 7, or 9 attraction points) defined paths of increasing Complexity. Figure 6 shows the six possible paths at each level of complexity that were used in this study. The top two lines contain the simplest curved paths, the middle two lines an intermediate level of complexity, and the bottom two lines the most complex curved paths that were used. For any given participant, one path at each level was chosen randomly to represent a given level of complexity.

A final new variable was the Length of the path that the target traveled. On any given trial it

was either 300-, 400-, or 500-pixels long. Of necessity, the start line-to-finish line straight line distance (or horizontal visual angle subtended) of any given length of curved line was always less than of the straight line of the same length, and more complex curved lines had shorter start-to-finish horizontal lengths. That is, even though the traveling length of the paths may have been the same, there was increasing horizontal compression of increasingly complex curves.

Design. The study had the following variables manipulated in a completely within-subjects design: Fidelity (four levels) X Complexity (four levels) X Length (three levels) X TTC (2-, 4-, or 8-sec.) for a total of 144 trials.

Procedure. The same essential procedures were used as in the previous studies, with participants receiving instructions showing the various conditions, and a practice trial for familiarization.

Results and discussion

Analysis of variance yielded several main effects and interactions among these new variables, some involving TTC.

Judged TTC increased in the expected manner (2.34-, 4.02-, and 6.19-sec), $F(2,110) = 481.64$, $p < .001$. Mean, overall judged TTC increased as a function of Complexity, $F(3,165) = 25.38$, $p < .001$, with average TTC judgments being 3.98-, 4.13-, 4.23-, and 4.38-sec., for straight paths, and increasingly complex curves, respectively. Mean, overall judged TTC varied as a function of Fidelity, $F(3,165) = 20.58$, $p < .001$, with the average TTC judgments being 4.24-, 4.30-, 4.19-, and 3.99-sec., for solid, dashed, severely dashed, and invisible paths, respectively. Overall, mean TTC judgments increased, $F(2,110) = 20.08$, $p < .001$, as overall path length increased, respectively, from 300- to 500-pixels.

The interaction between Complexity and Fidelity was also significant, $F(9,495) = 3.66$, $p < .001$, and is shown in Figure 7. For straight paths, solid and invisible remaining paths yielded very similar overall TTC judgments, but the dashed paths resulted in an increase in TTC judgments. For curved paths, TTC judgments generally decreased as fidelity decreased, reaching their lowest values with invisible paths. It would seem that as long as the path is a straight line, marking the path with a solid line does not affect TTC performance, but that inserting a dashed path during the invisible period of time increases TTC judgments. One may speculate that the dashed lines disrupt either a timing or a visual scanning process. It is unclear how this may

happen, but it may have to do with the loss and reacquisition of attentional processes as one visually scans over the dashes. That is, if one were visually scanning a broken path, maintaining smooth travel time across broken segments may be a difficult process, adding to the anticipated arrival time at the end point.

In each case, TTC judgments for curves were greater for solid paths than for invisible paths. Increasingly complex curved paths are more difficult to follow, even though they may be of the same length, as is the case in Figure 7. This difficulty may be due, in part, to the horizontal compression associated with increased complexity for any given path length. Possibly, participants try to follow the paths when the curves are shown in solid lines, but adopt a strategy of "skipping ahead" when they are dashed or invisible. One should also consider that a memory factor might be operating such that, with increasingly complex curves any memory of the path would be harder to maintain for low fidelity paths. This could result in a functional shortening of the path in memory, and a quicker TTC judgment. Of course, straight paths wouldn't need the memory function since the length of the remaining path is clearly defined by the distance to the vertical finish line, so there would be no functional difference between solid or invisible paths. For straight paths, following a dashed path may be, however, another matter, as discussed above.

The interaction between Fidelity and TTC was also significant, $F(6,330) = 6.25, p < .001$, and is shown in Figure 8. It appears that, overall, longer TTCs were most affected by differences in Fidelity, with shorter times associated with invisible paths, especially for the 8-sec. TTC.

These results raise interesting issues about the cognitive and strategic components people may use when making timing judgments along straight versus curved paths, and they should serve as the basis for future research.

Experiment 6

This study was conducted as a collaborative effort with Dr. William Tirre and Dr. Virginia Goff of Armstrong Laboratory, Brooks AFB, and I am indebted to them for helping to prepare much of the following presentation. The study was motivated by an interest in how visual timing performance might relate to other abilities in the visual perception and timing domains. Tests of visual timing performance were administered along with tests of six other ability factors in the visual perception and timing domains: spatial reasoning, inspection time, visual search, dynamic visual perceptual identification, auditory temporal discrimination, and auditory rate extrapolation.

Two previous studies conducted by Tirre and associates (Tirre, 1997; Tirre & Guggerty, 1997) point to the importance of perceptual ability factors in the prediction of performance in tasks with significant real-time processing demands such as flying and driving. The timing and dynamic visual processing factors were distinguishable, but perhaps only because the timing tasks involved auditory stimuli. In the present study, a set of structural hypotheses about human abilities was tested, focusing on timing, visual search, dynamic visual processing, perceptual speed/inspection time, and spatial reasoning. Multiple indicators were available for each of these hypothesized abilities. In addition to primary factors which could be assessed using confirmatory factor analysis, we suspected that a set of second-order factors would be present. Because we were uncertain about the second order factors, we conducted this part of the factor analysis in the exploratory mode, using primary factor intercorrelations as input to EQS (Bentler, 1993), and then completing the analysis in both orders in LISREL. As an aid in interpreting the factors underlying the experimental tests, we related the factors to a set of fairly well understood factors underlying the Armed Services Vocational Aptitude Battery (ASVAB). The results of this study were intended to indicate how visual timing processes fit into the structure of perceptual abilities, and how perceptual abilities relate to abilities already measured by traditional tests.

Method

Participants. The sample consisted of 363 male airmen basics at Lackland Air Force Base, Texas. The mean age was 19.1 years (range 17 to 35). The modal educational level was high school diploma (78%). Nearly 18% had some college but no degree; 2% had an associate's degree, 2% had bachelor's degrees, and .6% (2 persons) had some graduate credits. The sample was diverse in ethnicity: 76% were Caucasian/white; 12.9% were African American/black; 7.2% were Hispanic; 1.4% were Asian; .3% were Native American; and 1.9% came from other racial groups.

Tests. A simplified version of the TTC task used in Experiments 1-4 was constructed for this study. It consisted of the same stimulus scenes as used in those studies, but contained no non-target stimuli. There six replications of the basic TTC matrix used in those studies, resulting in 12 trials at each of the three TTC levels, 2-, 4-, and 8-sec. The performance score of interest was the slope of the TTC function obtained by the regression of actual vs. obtained TTC judgments based on the 12 observations at each level. A value of 1.0 would have represented perfect TTC

performance.

Other tests included: three auditory temporal discrimination (AUDTDIS) tasks, three versions of the auditory rate extrapolation (AUDREX) task, Disappearing Line Time to Contact test (DLTTC), Shrinking Circle Visual-search task (VISSRCH), a computerized version of the AFOQT Table Reading test, a computerized version of the AFOQT Scale Reading test, the AFOQT Block Counting test was also computerized and used as a measure of spatial reasoning, quantitative versions of two inspection time (quantitative and spatial) tasks, the Direction Detection Test, the Rapid Serial Classification Test, the Dynamic Visual Identification test, the Moving Target Test, and the Dynamic Contrast Sensitivity test. (See Tirre, 1997; and Tirre & Guggerty, 1997 for test details.)

Results

The fit for the initial model that was tested was quite good (see Figure 9). The factors proved to be intercorrelated in such a way to imply higher order factors (see Table 2). The final model that was tested (see Figure 10) posited three higher order factors: visual search and identification, general timing processes, and a third factor which was tentatively labeled "Gf/attention." The overall fit of this hierarchical model to the data was marginally better than the primary factors model. The Gf/attention factor was specified to be uncorrelated with visual search and identification, but correlated with timing processes. Gf/attention and timing, in fact, were correlated .86.

Additional analyses related the experimental factors to well-established factors underlying the Armed Services Vocational Aptitude Battery (ASVAB): Quantitative, Speed, and Technical Knowledge. Gf/attention had its highest correlation (.55) with Gc, which is consistent in magnitude (mean $r=.61$) with prior research conducted on enlisted personnel. Visual search and identification had its highest correlation with ASVAB Speed ($r=.47$), and low correlations with the other ASVAB factors. The general timing performance factor and visual timing factor had identical correlations with ASVAB factors, the only significant correlation being with Gc ($r=.37$) as would be expected from its correlation with Gf/attention.

This factor analytic study suggests that visual and auditory timing performance spring from the same underlying ability, and that this ability is strongly related to a higher order ability that appears to be fluid intelligence. We tentatively equated fluid intelligence with a general attention

ability construct, similar to what Crawford (1991) has previously argued. Further research is needed to test the relationship between the factors identified here with Gf identified through conventional tests, and with attentional abilities factors identified through experimental tasks usually selected for that purpose, such as those developed by Washburn and Putney (1997).

Conclusions

The results of these several studies have extended our knowledge of the possible operations, processes, and mechanisms involved in TTC judgments over fairly short time intervals. Experiments 1 and 2 confirmed that cognitive processes can be recruited at strategic levels of task performance. Participants can be very good at noticing that otherwise irrelevant stimuli can help in the task. Two of the experiments have opened areas of unique interest. The possibility of an arousal mechanism derived from contrasting visual dynamics produced by irrelevant (Experiment 4) stimulation points to a new line of research in the TTC arena. Similarly, the manipulations used in Experiment 5 may provide a new methodology for investigating the role of memory in TTC judgments, since curvilinear paths require a visual memory component unlike that for linear paths. Finally, the factor analysis of Experiment 6 concerns the ongoing issue of determining and classifying human abilities. The alternative models that were proposed need to be researched further before their validity and usefulness can be decided.

References

- Bentler, P. M. (1993). EQS: Structural equations program modeling. Los Angeles: BMDP Statistical Software, Inc.
- Caird, J.K., & Hancock, P.A. (1994). The perception of arrival time for different oncoming vehicles at an intersection. Ecological Psychology, 6, 83-109.
- Crawford, J.D. (1991). The relationship between tests of sustained attention and fluid intelligence. Personality and Individual Differences, 12, 599-612.
- Delay, E. R., & Mathey, M. E. (1985). Effects of ambient noise on time estimation. Perceptual and Motor Skills, 61, 415-419.
- Delay, E. R., & Richardson, M. A. (1981). Time estimation in humans: Effects of ambient illumination and sex. Perceptual and Motor Skills, 53, 747-750.
- DeLucia, P. R., & Novak, Jennifer B. (in press). Judgments of relative time-to-contact of more than two approaching objects: Toward a method. Perception & Psychophysics.
- Hasher, L. & Zacks, R. (1979). Automatic and effortful processes in memory. Journal of Experimental Psychology: General, 108, 356-388
- Lee, D.N. (1976). A theory of visual control of braking based on information about time-to-collision. Perception, 5, 437-459.
- Liddell, G. (1997). Interfering and updating cognitive representations used in judgments of absolute time-to-contact in a prediction motion task. Unpublished doctoral dissertation, Texas Tech University.
- Lyon, D.R., & Wagg, W.L. (1995). Time course for visual extrapolation accuracy. Acta Psychologica, 89, 239-260.
- Marshak, W. & Sekuler, R. (1979). Mutual repulsion between moving visual targets. Science, 205, 1399-1401.
- Novak, J. L. (1997). Judgments of absolute time-to-contact in multiple object displays: Evaluating the role of cognitive processes in arrival-time judgments. Unpublished doctoral dissertation, Texas Tech University.
- Schiff, W. & Detwiler, M.L. (1979). Information used in judging impending collision. Perception, 8, 647-656.
- Steadman, R.C. (1979). The assessment of sultriness. Journal of Applied Meteorology.

18, 861-884.

Tirre, W. C. (1997). Steps toward an improved pilot selection battery. In R. Dillon (Ed.), *Handbook on Testing* (pp. 220-255) Westport, CT: Greenwood Press.

Tirre, W.C. & Gugerty, L.J. (October, 1997). Ability factors in situation awareness. Paper presented at the University of Minnesota Conference on the Future of Individual Differences Research, Minneapolis, MN.

Tresilian, J.R. (1991). Empirical and theoretical issues in the perception of time to contact. Journal of Experimental Psychology: Human Perception and Performance, 17, 865-876.

Tresilian, J.R. (1995). Perceptual and cognitive processes in time-to-contact estimation. Analysis of prediction motion and relative judgment tasks. Perception and Psychophysics, 57, 231-245.

Washburn, D.A. & Putney, R.T. (October, 1997). Individual differences in attention profiles. Paper presented at the University of Minnesota Conference on the Future of Individual Differences Research, Minneapolis, MN.

Table 1

Target and Stimulus Specifications

Overall distance (degrees of visual angle)	Velocity (degrees/second)	Time to Contact (seconds)
<hr/>		
23.5	5.9	2.0
17.8	4.5	2.0
17.6	2.9	4.0
15.2	2.5	4.0
13.4	1.3	8.0
11.2	1.1	8.0

Length of "start" and "finish" vertical lines was 5.6 degrees of visual angle.

The target and distractor squares had sides of .7 degrees of visual angle.

Table 2

Intercorrelations of Primary Factors

Visual Search	1.00					
Spatial Reasoning	.15	1.00				
Inspection Time	.58	.79	1.00			
Auditory Rate Extrap.	.13	.37	.44	1.00		
Auditory Temporal Disc.	.17	.54	.54	.34	1.00	
Visual Timing	.22	.65	.79	.45	.63	1.00
Dynamic Visual Ident.	-.63	.07	-.15	-.03	.11	1.00

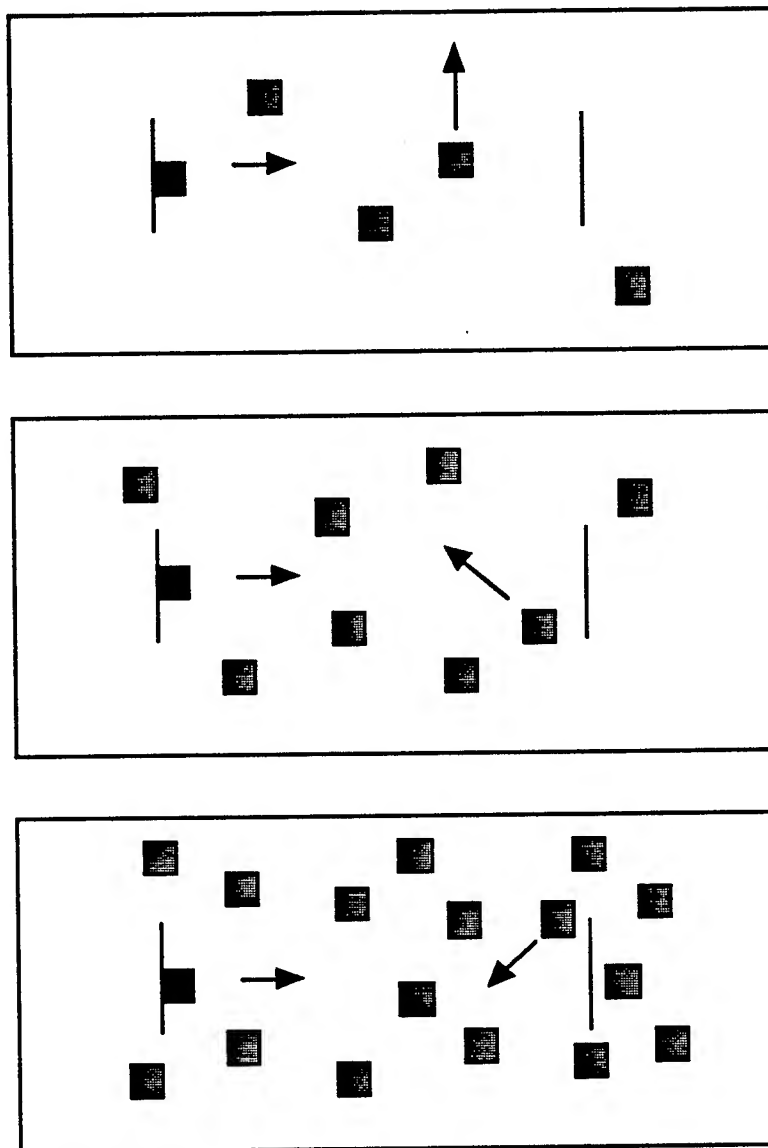


Figure 1

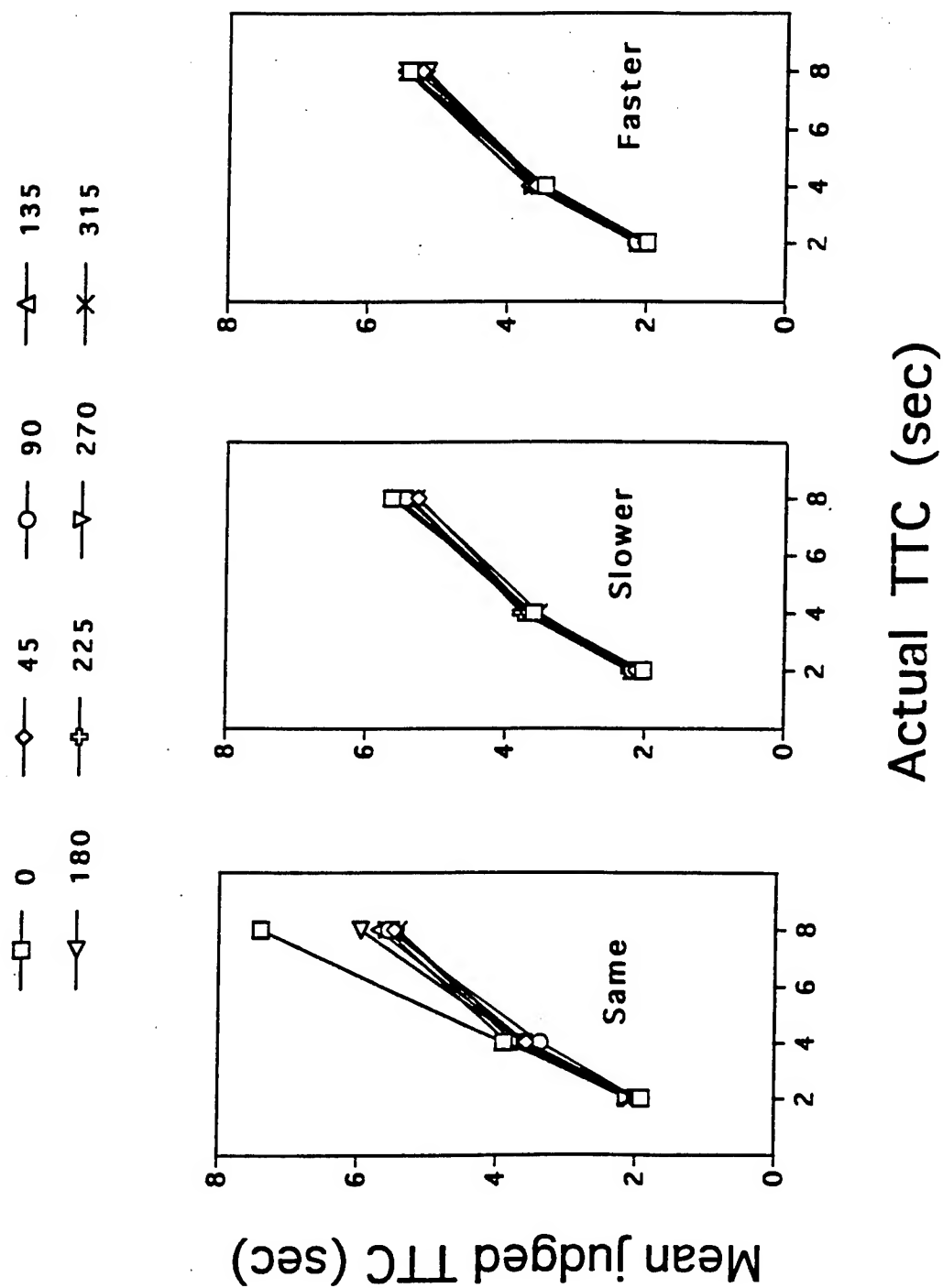


Figure 2

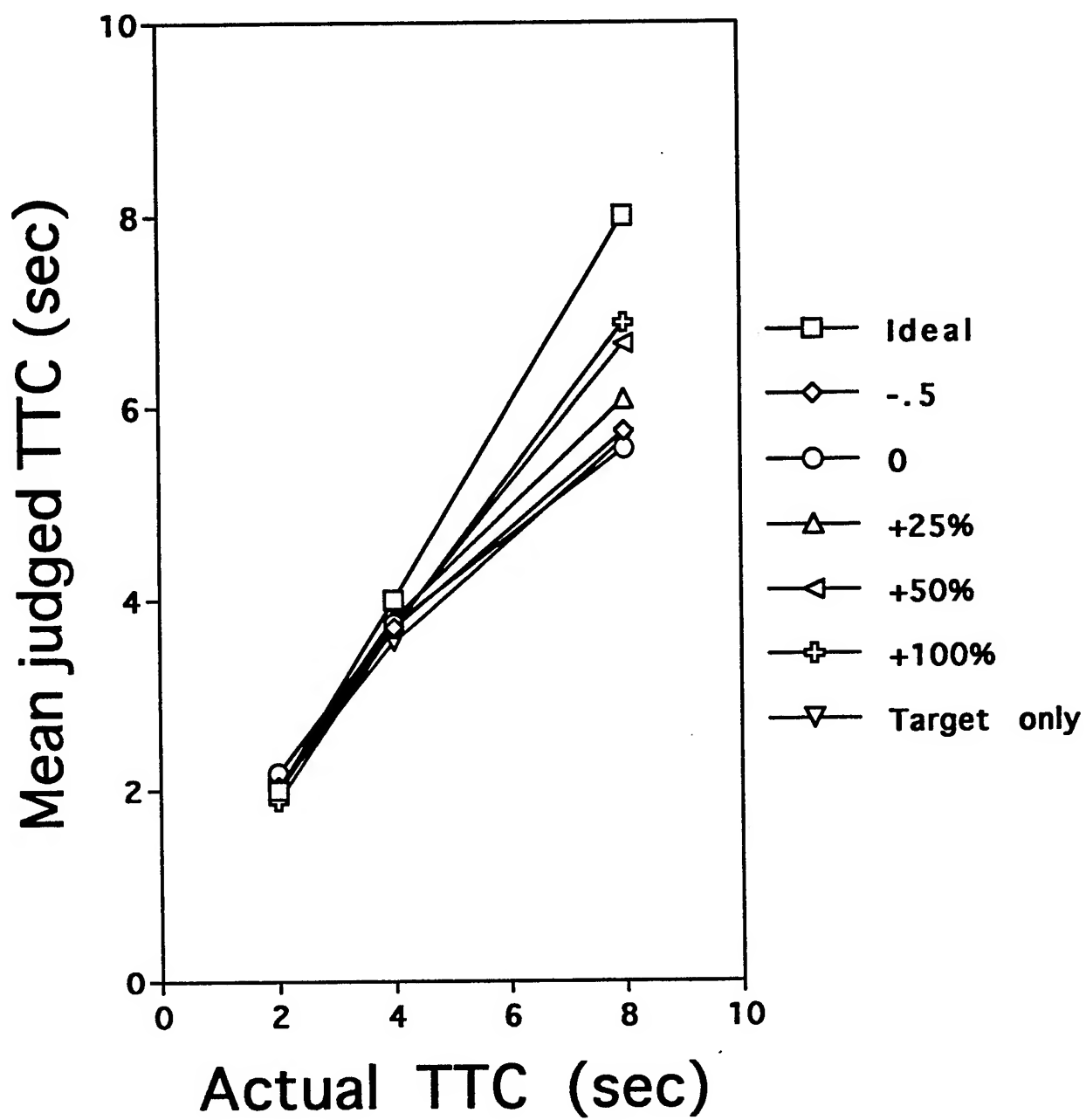


Figure 3

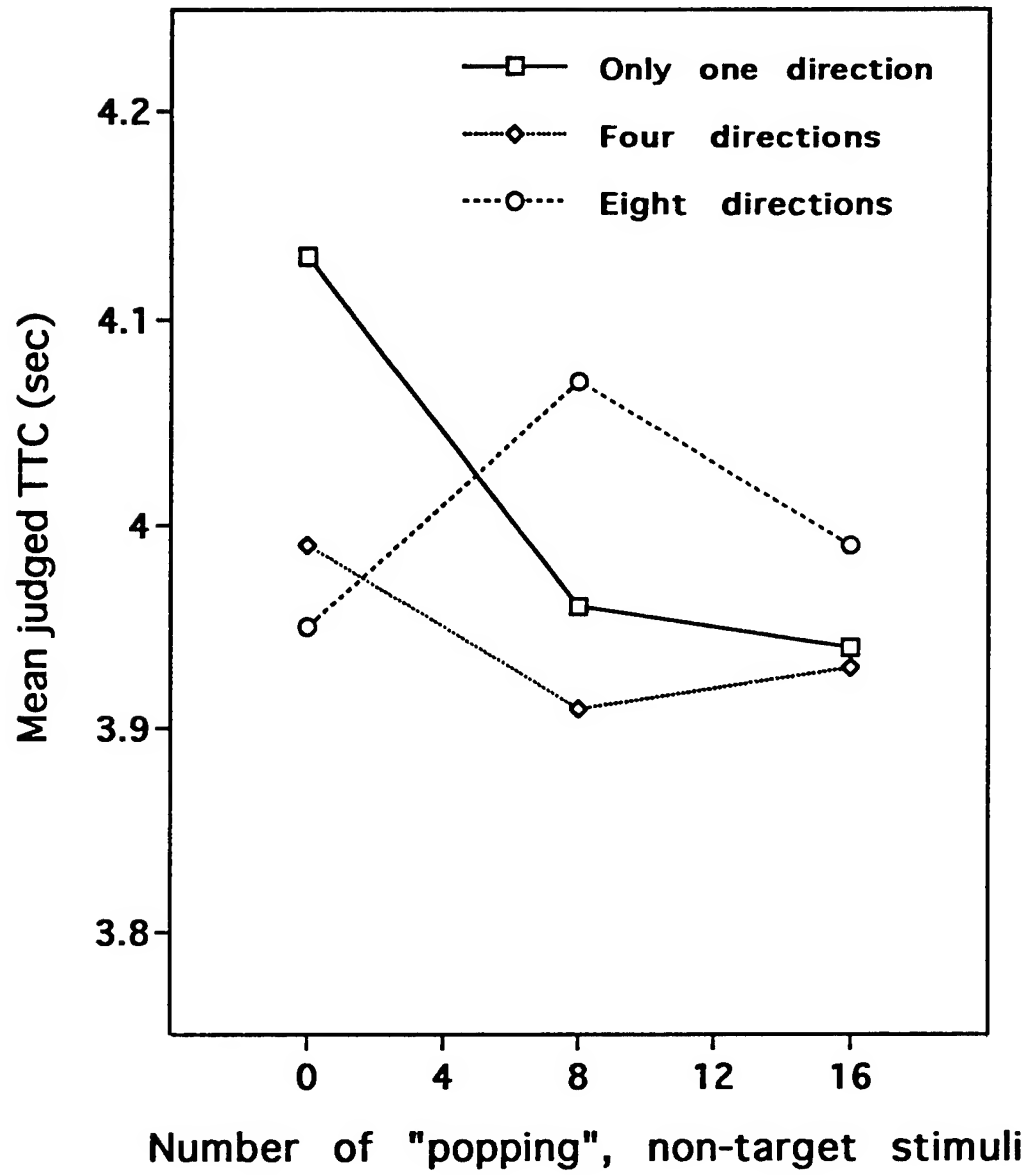
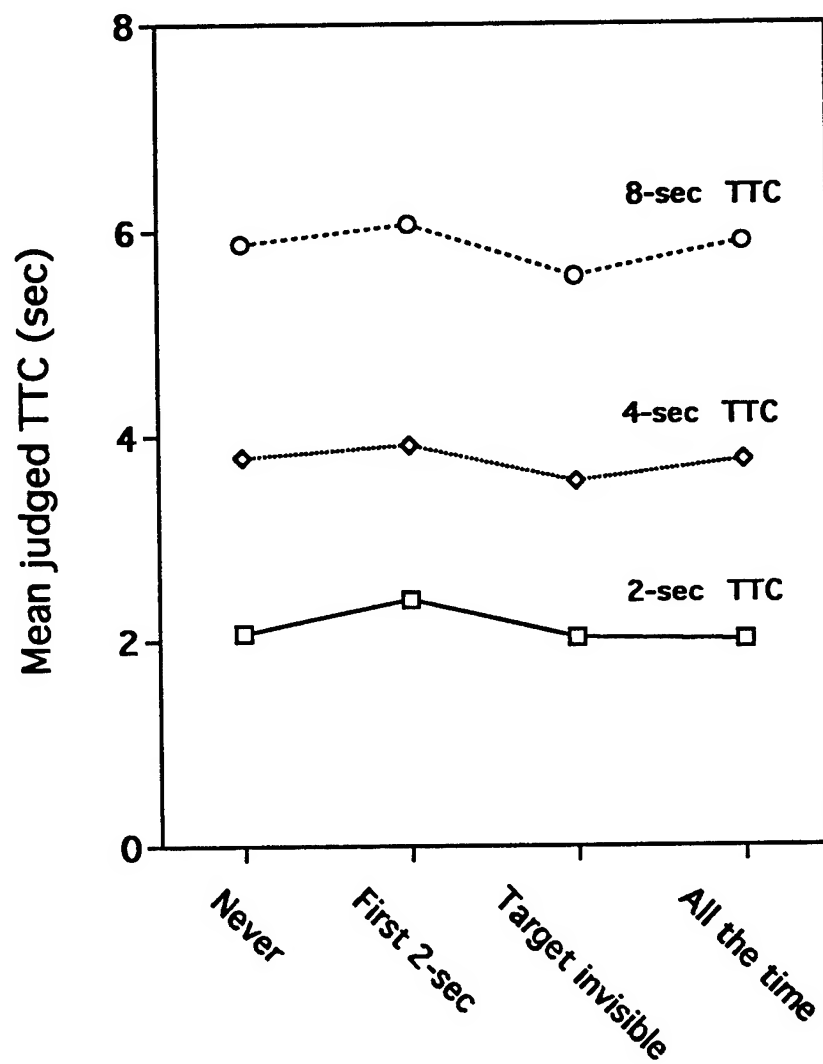


Figure 4



Phase in which non-targets appeared

Figure 5

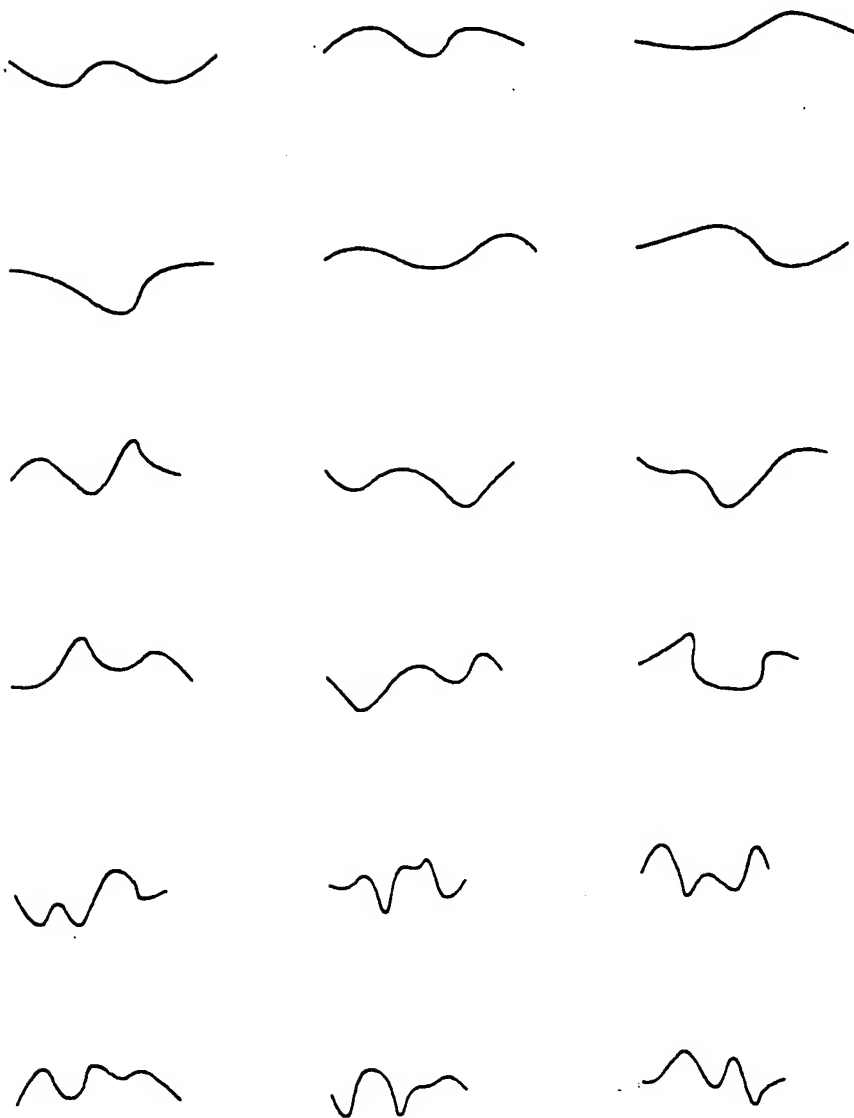


Figure 6

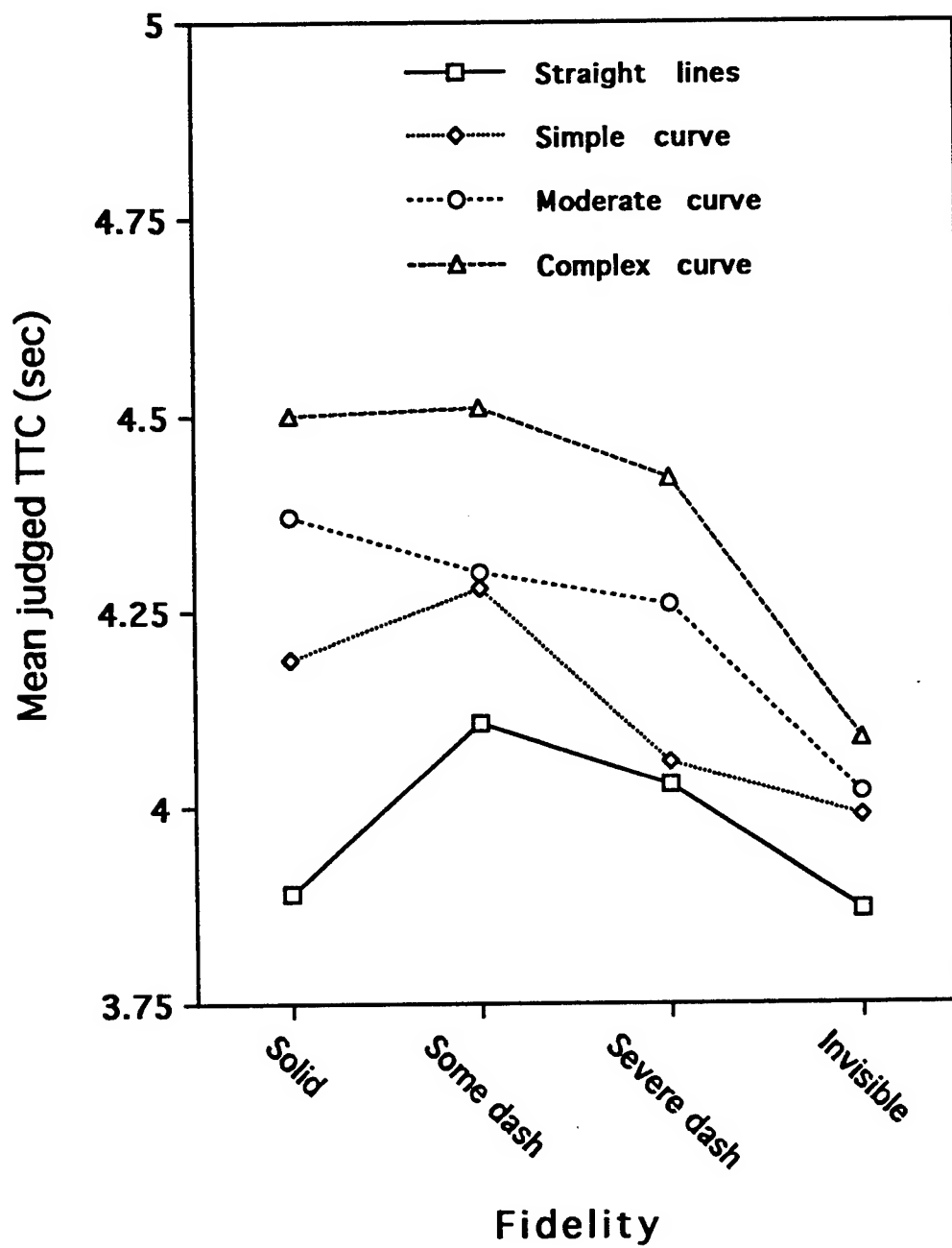


Figure 7

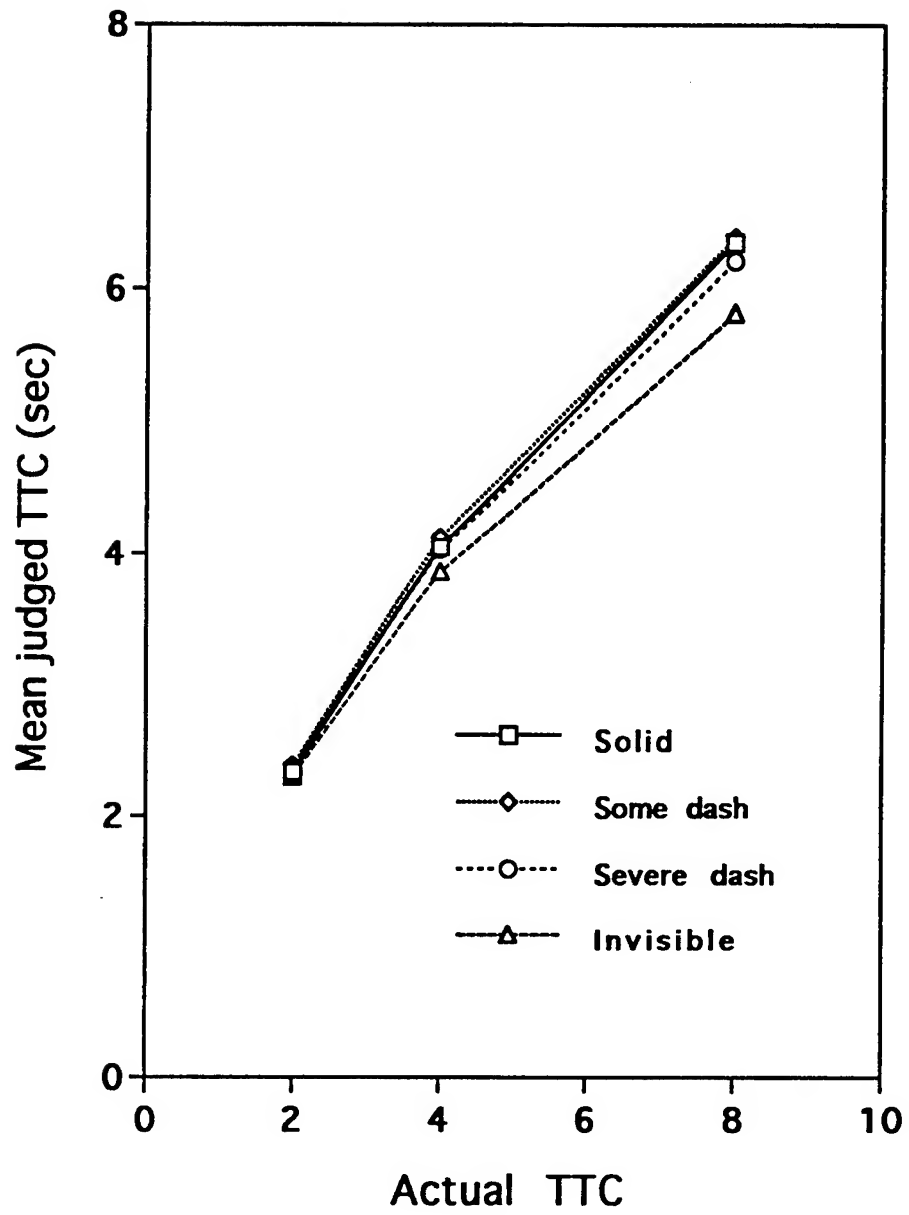


Figure 8

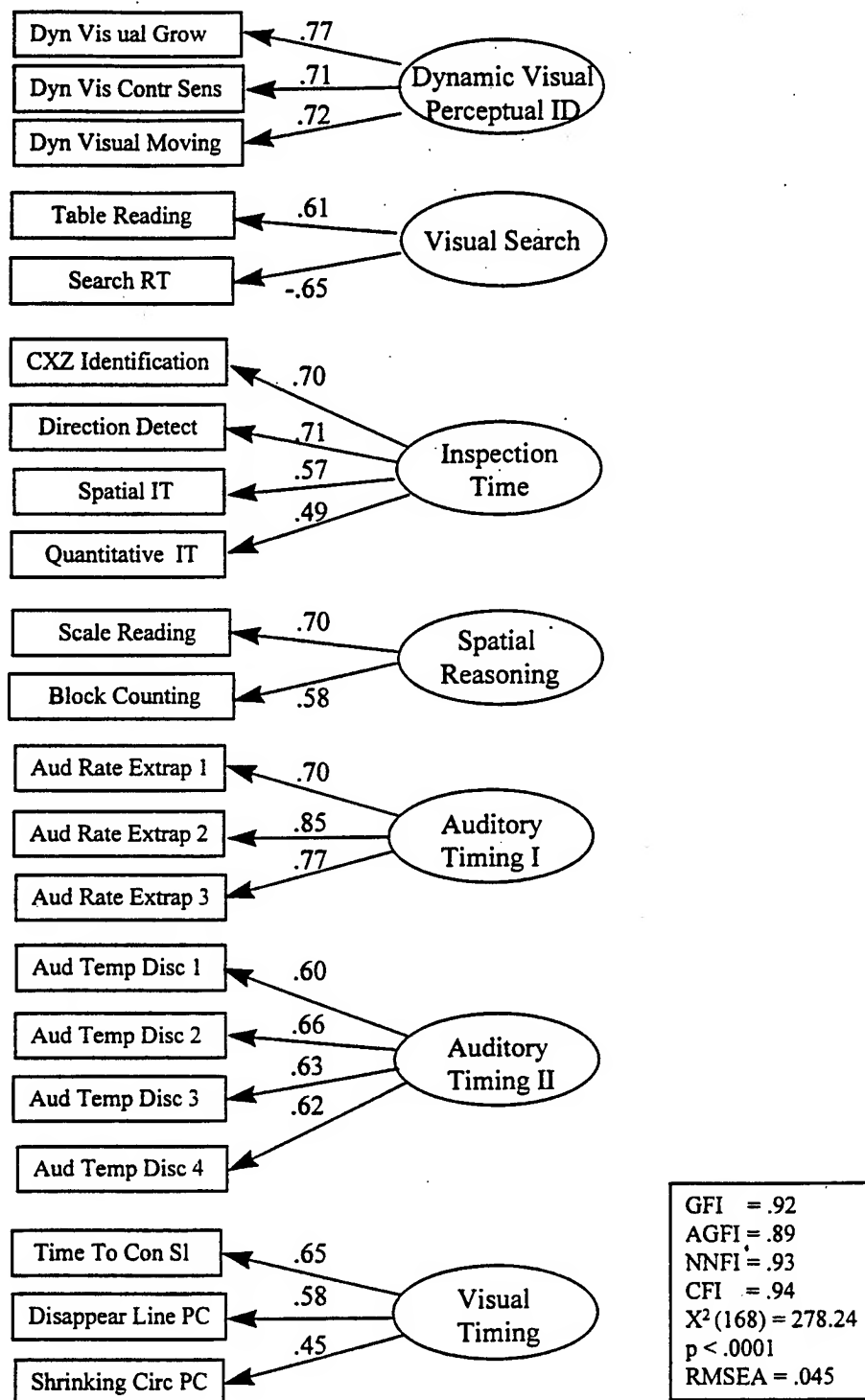


Figure 9

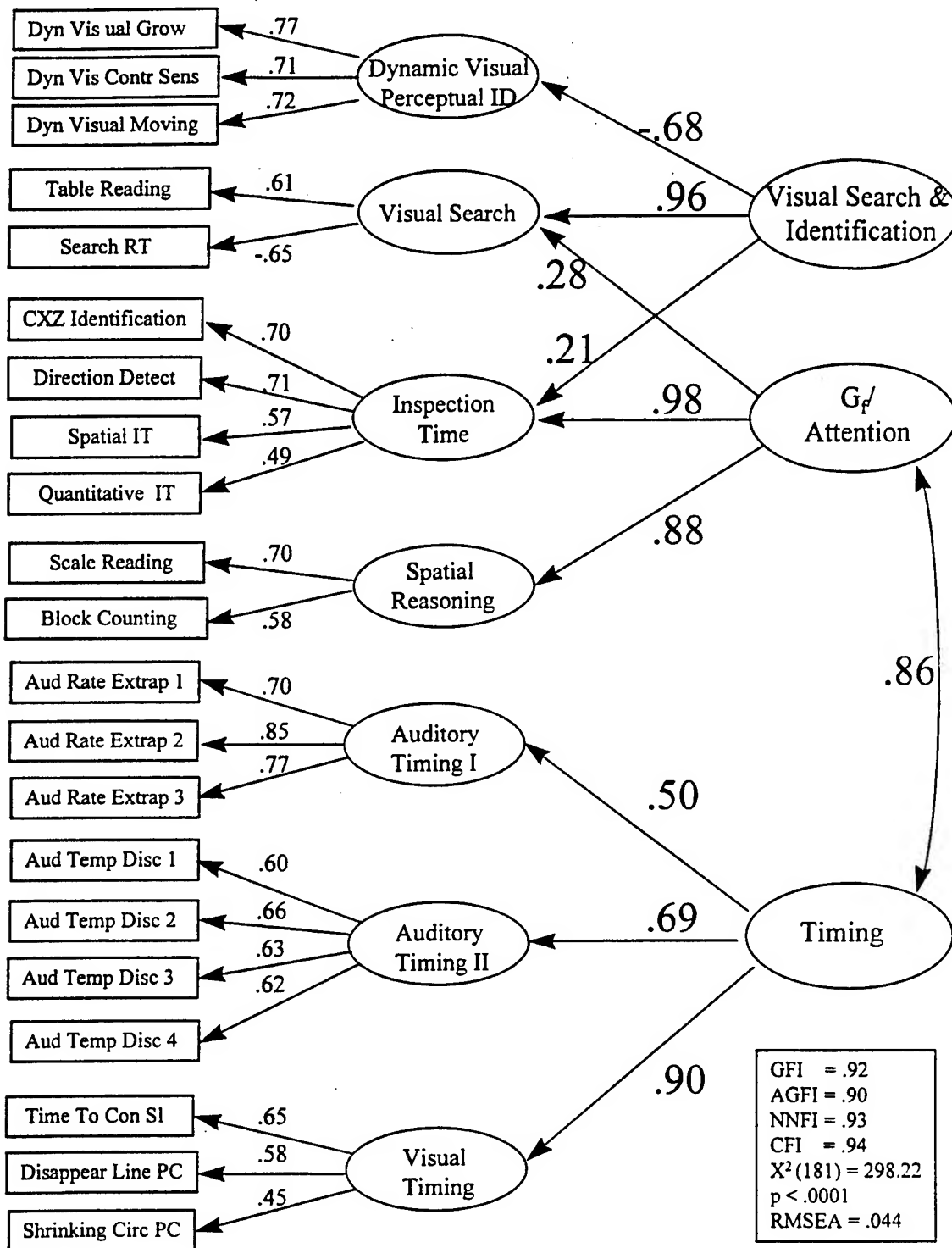


Figure 10

**ENVIRONMENTAL COST ANALYSIS:
CALCULATING RETURN ON INVESTMENT
FOR EMERGING TECHNOLOGIES**

Bruce V. Mutter
Associate Professor
Division of Engineering Technology

Bluefield State College
219 Rock Street
Bluefield, West Virginia

Progress Report for
Summer Faculty Research Program
Armstrong Laboratory

Sponsored by:
Air Force Office of Scientific Research
Bolling Air Force Base, DC

and

Armstrong Laboratory
Tyndall Air Force Base, FL

August 1996

**ENVIRONMENTAL COST ANALYSIS:
CALCULATING RETURN ON INVESTMENT
FOR EMERGING TECHNOLOGIES**

Bruce V. Mutter
Associate Professor
Division of Engineering Technology
Bluefield State College

Abstract

This research examines the process of calculating the Return on Investment (ROI) for emerging technologies. The report illustrates the relationship between means and costs associated with implementing appropriate technologies to solve a compliance, remediation or source reduction problem. Major cost factors were identified by comparing emerging technologies to a baseline capable of achieving equivalent end results. The range of the costs captured for each alternative was developed by a decision criteria model and included: direct, indirect, liability, and intangible costs. The tabulation of total costs was input to conventional Net Present Worth (NPW), Internal Rate of Return (IRR), and Benefit Cost Ratio (BCR) equations, which were presented to solve for the time value of the total cost estimates. Finally, the Return on Investment (ROI) was calculated for an emerging technology based on results of the life-cycle cost estimate.

ENVIRONMENTAL COST ANALYSIS: CALCULATING RETURN ON INVESTMENT FOR EMERGING TECHNOLOGIES

Bruce V. Mutter

Introduction

The inherent limitations of conventional cost analysis become apparent when assessing the financial performance of an investment in emerging environmental technologies. These limitations appear to be widely recognized. We now know that some short-sighted *nondecisions* were made, in business past, because we were ignorant of the true costs. If we had known of our future obligations to comply, the cost of our liabilities, then we would have probably taken those costs into account and made more informed decisions. We now have the opportunity to learn from this past to make better investment decisions in the future. Organizations will to return, again and again, to reinforce the fact that all business decisions will be forever linked to the cost of one option compared to the cost of another. The difference, from now on, should be that the costs are more accurately allocated to a process or activity, and are reflective of the true cost of doing business. How?

The practice of merging and comparing the success of environmental processes with asset, resource, income, cost and managerial data is a complex process that defies convention. Accounting for the full cost of project alternatives is not an "easy sell" in any organization. When environmental costs are identified and quantified, the direct (capital, operating, and regulatory), indirect (training, audits, fines, etc.), and intangible (contingent, liability, good will, etc.) costs provide insight into the real cost of the effort (Kirschner, 1994: p.25). Certain limitations of conventional cost analysis surface immediately. Uncertainty in quantifying environmental costs is the primary cause for these limitations. We should focus on minimizing the uncertainty associated with calculating the return on investment.

Environmental research will continue to yield innovative solutions, but the questions remain: What is the nature of the true environmental costs? How large could the liability costs be? When will the costs occur? If investments in innovative control, compliance, and remediation methods are in the interest of the organization, then what accounts for the reluctant approach to invest the capital in new solutions? How can management afford to invest in new programs in an atmosphere of limited resources, where these projects compete with more pressing mission tasks (White et al.,1991)?

There are a few readily apparent explanations for the contradiction drawn between environmental policies and the final financial analysis used to make the decision to carry the policies forward. First, available alternatives might be precluded from the decision making process, from the outset, due to organizational structure or the general attitude toward progressive environmental projects. In this case, there will be no cost analysis. Second, if the decision to undertake a new environmental project has been made, then the not-so-obvious economic or financial barriers tied to methods of costing or the budgeting process block the inclusion of the total cost and/or the proper life-cycle for the project in question (White et al.,1992-93: p. 35). Third, there is a general lack of credibility or stigma attached to liability costs and less tangible qualifiers, which can lead to their exclusion. These costs are often referred to as "externalities" for this reason. Evidence has shown that externalities can rather quickly become internal costs under certain circumstances. Can we afford to completely exclude these future costs from the evaluation of our options?

All organizations, whether large entities or small businesses, face the dilemma of calculating how to appropriate scarce resources to competing projects. However funded, most environmental control, compliance, or remediation projects are subject to some sort of profitability analysis. This process is used to assess the desirability of one project over another, or the break-even point established by the organization for undertaking a project. Organizations need to examine innovative environmental cost analysis techniques that measure up to the task of calculating Return on Investment (ROI) for current and emerging environmental technologies.

New ROI strategy will be founded on capturing the total costs throughout the life-cycles of the emerging technologies versus continued use of current methods. For some environmental projects, there will be no return on investment. In these cases, we can devise a system to consistently select the alternative that minimizes the cost of what we must do anyway. Within the context of the corporate budgeting structure, we should determine if, and to what degree, conventional methods of investment analysis act to distort the cost of innovative methods in favor of more conventional measures (White et al., 1991: p.9).

Since we are, in essence, determining how to best allocate funds, the organization's budget becomes one of the constraints. Budgeting is a strategic process of analyzing alternative investments and deciding which one is best for the organization. The nature of budgeting for capital expenditures often requires a five, ten, or more years' outlook. This is important because it will indicate how far into the future the organization is willing to analyze costs or accept life-cycles of competing alternatives. Large corporate entities should primarily focus on long-term operations for calculating return on investment. Therefore, they require a formal budgeting process involving input from many departments within the organization (Todd, 1993: p. 3-9). This can cause the collection and dissemination of detailed cost data to be conflicting and laborious. However, the sophistication of the financial analysis should match the size and long range expectations of the organization and assembling this cost data is key to the success of the analysis. Small private firms are better able to focus on short term profit and more often than not make decisions based on simple payback calculations, but institutions with centuries old financial histories and long range plans that the future itself depends upon, can ill afford to use of such capricious decision-making techniques to manage their finances (White et al., 1991: p.10).

The challenge is to develop a framework that can be relied upon to consistently help make the best selection among alternatives, and help answer the question: where is the best investment of scarce capital resources for environmental projects? The technology alternative that offers the largest return or minimizes the financial burden relative to cost should be chosen.

This involves quantifying; placing some dollar value, whenever possible, to risks and uncertainties that traditional cost analyses have not yet articulated. Rapidly changing regulations, and the court decisions that define them, continually alter costs. Determining risk associated with treatment, storage, and disposal facilities (TSDF) for hazardous materials further complicates the cost analysis. However, we should continually adapt environmental cost analysis in response to these complexities, so that we make the most informed decision possible and hopefully select the lowest cost alternative that will best serve our future needs.

Problem Statement

The development of new environmental technology requires investment decisions to be made in an atmosphere of limited resources. The competing project alternative with the greatest return on investment or lowest opportunity costs should be selected. The objective is to develop guidance for evaluating emerging environmental technologies in comparison to a baseline that leads to the selection of the better investment. The comparison must take into account the total costs, while making sure the competing technologies can accomplish the same end result. A five step approach will be necessary to calculate the return on investment for emerging technologies, which consists of the following required elements: specify the environmental cost problem, develop a decision criteria model that allows comparison of the alternatives within the constraints of the model, capture the total costs of alternatives, apply the life-cycle to the cost estimates, and finally, calculate the return on investment. Case studies will be presented to illustrate the capabilities of this procedure in actual practice. These examples will demonstrate the return on investment for several emerging environmental technologies. The sample analysis will be capable of spelling out the costs and benefits of varying types of emerging technologies, at different stages of development, so decisions are more universally well informed.

Methodology

Specifying the Cost Problem

All environmental costing problems are of a common nature. These problems have two essential characteristics. First, there is a deviation between what managers think it will cost and the *actual* cost to solve an environmental problem. The second characteristic is that the deviation is important enough that the responsible decision maker thinks it should be corrected. The second part of the cost deviation is what makes it a problem. Why are excessive costs created? Deviation from the cost as planned could be brought about by an unanticipated regulatory change. Some of the other excessive cost generators may include: lack of cost information on new processes, myopic financial analysis, immature stage of technology development, lack of standards for performance measurement, and shortage of time available to analyze the costs and implement a solution. The implementation of new technology has a long term economic impact that is sufficiently important to be part of any analysis leading to a decision. There may well be a great many other aspects of the problem to consider before making a decision, but cost will dominate any decision process, and therefore, should be the focus of the problem specification (Newman and Johnson, 1995 p:4).

There will usually be several technologies, methods, or processes that could solve a compliance, remediation, or source reduction problem. The combination of attributes for each alternative can complicate side by side comparisons, turning the valuation process into an intricate matrix instead of a step by step approach. The objective is to identify the costing problem, and continue with problem formulation, including all relevant goals and objectives. This will eventually lead to the establishment of operating profile criteria. When specifying the cost problem, the analyst searches for those constraints that draw a boundary line around the relevant and important cost drivers. The cost problem can be properly specified by systematically answering the following questions:

What is the process in which the cost deviation was observed? Where is the process ? When did/will the excessive cost first appear? What is the amount of the cost deviation? What regulatory factors may have contributed to this cost difference (Macedo et al., 1978: p.42)? In a continuing process we need to recognize the environmental cost problem, state the specifics of the problem, develop possible causes of cost deviations, then test the problem specifications, until satisfied that the true cost drivers have been identified. This will ensure that we have considered all relevant information, achievable goals, and feasible alternatives and filtered this through the organization, so that a reliable decision criteria model can be developed.

Developing a Decision Criteria Model

The technology will be selected from feasible alternatives. These alternatives need to be identified and then defined for subsequent analysis. When an emerging technology is compared to a baseline, then a set of decision parameters must be established for the scope of work involved. The context of comparison affects the end result, therefore, the analyst needs to determine how and where the new technology would be applied. Assessing the situation in such a way, as to realize the constraints (strengths and limitations) of the competing technologies. This is an important part of making sure the alternatives will meet common achievable objectives. We need to base the selection of competing alternatives on performance under the most probable set of conditions, then proceed with the cost analysis. The technology profile can be brought to light by such questions as: What is the nature of the contamination? Where are the projects located? What is the capacity of the assembly, device, or technology units that are to be installed? How many units or assemblies are needed based on their performance? How long would the technology need to be in place? What level of cost reporting detail is required to assess relative performance? If care is taken in understanding the big picture first, then properly detailed descriptions can be used to identify the components that make up the assembly of technologies (U. S. Army, EIWR, 1995: p.38).

The purpose of establishing the decision criteria model is to synthesize the goals and objectives of the technologies, with the relevant cost and performance data available for both the baseline and the emerging. This will increase the awareness of cost drivers within the applications of the technologies. We should focus on the differences; only the differences in expected future outcomes among the alternatives are relevant to their comparison and ought to be considered in the analysis. For example, research and development cost data may not be relevant to the cause, if this cost data is not available for both the old and the new process. We want to measure the corresponding performance attributes of the alternatives. This objective can be realized by monitoring proper gauges of performance. We should measure enough parameters to indicate the range of capabilities for the technologies. If comprehensive standards are established, then the resulting indicators can be a useful tool to compare alternatives, recognize constraints of available options, and in the context of one particular setting, determine whether the emerging technology is a functional alternative (Booth et al., 1991: p.13). An example of this approach could be applied to permeable barriers. This method is known to be an emerging technology. Profiling assemblies here would require comparing this passive (in situ) groundwater remediation technology to *other* treatment trains providing groundwater remediation solutions. It would be necessary to conceptualize the geometry and geography of the site, the nature and extent of the contamination, and the depth of the installation required to do this specific job. This would allow us to determine when an alternative is most effective.

The construction of the decision criteria model should ensure that the comparison will be technically consistent, and eliminate, or at least diminish the uncertainties of the cost problem. The intent is to compare practical applications of the competing alternatives and identify an approach that can be used to capture costs for further analysis. An alternative may drop out of consideration early because it offers little promise of meeting the performance requirements, or later on, because its relative cost is so great that it is not a reasonable cost alternative. We want to screen the approaches, and eliminate those options that do not fit the performance profile. An important tenet, at this stage of the process, is that we are working to develop scaled risk factors.

The decision criteria model illustrates, whether or not, research and development of the emerging technology is mature enough to predict performance with a reliable degree of confidence (Showalter et al.,1995: p.22).

Using a common unit of measure will allow appropriate comparison of the innovative technology to the baseline, leading to the decision to fund additional research, development, testing, evaluation, and the eventual implementation. The emerging technology must be better than the accepted technique, both technically and economically, to compete for limited resources (Showalter et al.,1995: p.18). This comparison should be as objective as possible to avoid any conflicts of interest in the decision making process.

The crucial part of developing the decision criteria model is to make sure the techniques are truly comparable. A common reference point might be established by some type of performance standard; that is, competing projects should be capable of achieving the same level of pollution control or source reduction. There will be few cases where the emerging technology serves as a direct replacement for an existing one. The nature of innovative processes is that these new technologies usually do not fit with current practices on a point by point basis; rather, they are a different means to the same end. Differences in capabilities will have to be articulated with the decision criteria model, which should incorporate real world analysis. For example, if the latest goal is to reduce the volume of exhaust requiring treatment of air contaminated with volatile organic compounds (VOC) passing through painting facilities by 90 percent, then a baseline technology that can reduce the volume by that amount would make an acceptable comparison. In addition, this particular case might call for comparison of two emerging technologies in tandem, in contrast to technologies that make up the conventional treatment train. The reason for pairing emerging technologies in the decision criteria model here is that recirculation in conjunction with a source leveling device, might be more cost effective than the independent application of each. It depends on how it fits into the rest of the treatment system.

Therefore, we compare the accompanying emerging technologies to those baseline technologies that make up the current train of treatment, being cautious, all the while, that the competing assemblies will yield the same end result or that the cost of any compromise is included in the final analysis.

Capturing the Total Costs

While the relative performance capabilities of the alternatives are being evaluated, we must also examine the elements associated with total cost analysis within the context of implementing these technologies. For environmental technology projects, there are four general cost categories: (1) direct costs (2) indirect costs (3) liability costs and (4) intangible costs. Emerging environmental technologies warrant the capture of a wider range of cost components for consideration than conventional cost analysis projects have traditionally required.

As we will see, the decision to invest in new technology may not be possible based purely on *direct* costs. We should consider all relevant cost data, if we want to capture the *true* costs that go into the decision (EPA, 1989). If costs can't be expressed in dollars, then these costs should at least be made explicit with descriptive qualifiers to accompany the cost figures. In certain cases, the probable costs avoided should be considered, along with conventional capital costs associated with the investment. A further breakdown of these costs is discussed in turn.

(1) Direct Costs

Capital Expenses - Initial Acquisition

- o Site Work - land acquisition, surveys, file fees, clearing, relocation, drilling, & fencing
- o Construction - general conditions, substructure, superstructure, enclosure, & finishes
- o Equipment - conveying systems, HVAC, fire protection, security, process, & non-process, operations supplies, mobilize and equipment set
- o Design & Review - A/E fees, consultants, testing, models, & data processing
- o Direct Labor - associated with mobilization, installation, and administration
- o Other - utility connection, legal fees, appraisal, and waste management equipment

Operations & Maintenance Costs - Recurring Expense

- o Materials - parts, supplies, process chemicals, and incidental tools
- o Direct labor - for operating equipment, supervision, maintenance & contract labor
- o Operating Overhead - payroll charges, shipping, transportation, insurance, & rentals
- o Utilities - fuels, water, energy, and sewerage
- o General Administration - indirect labor, interest, travel, communications, & marketing

(2) Indirect Costs*

Compliance Costs

- o Notification - based on directives to comply in time or frequency
- o Reporting - preparedness, medical surveillance, loaded wage rates
- o Monitoring/Testing - planning, studies, modeling, inspections
- o Recordkeeping - maintain files associated with regulatory activities
- o Manifesting - listing/labeling hazardous process materials
- o Others - recovery cost, maintenance contracts, waste disposal, safety, & closure

Insurance

- o Worker - incremental cost of higher premiums paid due to risk
- o Third Party - incremental cost of higher premiums paid due to risk

On-Site Waste Management

- o Waste Management - collection, storage, transportation, sampling, and disposal
- o Non-recovered Materials - incremental cost of lost marketable by-product

* These cost have been traditionally hidden in the sense that they have been considered a burden to overhead in the past, or treated as externalities in conventional from the project cost analysis. These costs are in reality part of the production process or the product (EPA, 1989: p.3-6).

(3) Liability Costs

Fines & Penalties

Remediation

- o Air - costs associated with liability under federal, state, and local regulations
- o Soil - costs associated with liability under federal, state, and local regulations
- o Water - (groundwater & surface water) costs associated with liability under regulations

Containment

- o Waste Disposal - eminent liability associated with surface sealing

Legal Fees

- o Personal Injury - third party lawsuits seeking compensation for bodily injury
- o Economic Loss - claims and internal incremental costs of production loss
- o Real Property Damage - third party claims for loss of property value
- o Natural Resource Damage - claims seeking compensation for natural resource damage

(4) Intangible Costs

Qualifiers & Irreducibles

- o decreased readiness from distressed product quality
- o decreased standards due to poor image- organization & product marketing
- o increased health maintenance costs due to current exposure
- o decreased efficiency from poor employee productivity/relations
- o increased production costs due to waste management decisions
- o increased operations & maintenance of facilities costs due to inefficient processes

When capturing the total costs of the alternative technologies we should attempt to quantify as many direct cost items as necessary; there will be little debate arising from the inclusion of the initial acquisitions cost or recurring O&M expense. The more controversial aspects of the analysis will stem from the attempt to quantify compliance or liability costs. Although these issues require the expenditure of *real* dollars, the line items would also have to be extracted from the accounting system, which would normally require "breaking out" costs that are normally considered operational overhead. This paradox will make the capture of these costs difficult.

For instance, liability costs are generated by fines and penalties usually levied for non-compliance (White et al., 1991: p.11). Most organizations are not well equipped to cost account for non-compliance, but business as usual can lead to the excessive costs due to this shortcoming. Moreover, legal awards or settlement costs can stem from remedial action and accidents causing personal injury or property damage. Superfund holds corporations financially responsible for environmental damage caused by previous waste disposal and management practices. Liability costs are difficult to estimate and predict their entry point into the life-cycle, so an emerging technology that effectively reduces the liability should be accounted for in a way that illustrates the potential cost savings. When future liability costs are included in the evaluation, the cost analyst introduces non-traditional uncertainties to decision makers (Peer & Beetle, 1990). For this reason, these potential costs are frequently omitted from the process, and if considered in the project analysis at all, management normally exercises caution in assigning a dollar value estimate to liability costs. The approach is too conservative and not realistic because these are real costs.

The initial research and development costs are generally not included, unless such costs are included for the base technology. It is crucial to perform cost analysis in an equitable atmosphere, in regard to both initial expenditures and future benefits. Benefits are more often considered to be costs avoided (Tarditi et al., 1995: p.18). In the case of some source reduction activities, there is no research and development, but decision costs are always present. Changing the way a filter is washed or the way a truck is unloaded might have no capital costs whatsoever, but have future benefits to the organization that can only be calculated by capturing the total costs of previous methods.

The less tangible costs and benefits are difficult to predict and estimate, but benefits or cost reductions of one system over another should be part of the evaluation of the assemblies because these benefits are real, even if there not easy to quantify (U.S. Army COE, 1995: p.8) The goal is to assign monetary value to environmental line items that have so far escaped analysis.

We are attempting to include a range of value for liability costs, so we should proceed cautiously, as not to over or under value the less tangible costs. Although qualitative analysis may be more appropriate and salable to in some cases, overstating qualifiers could be an impediment to promoting sound business decisions that take environmental factors into account, when selecting the alternative with the strongest economic benefit. In the final analysis, the bottom line will be the focus of the decision and any qualitative scoring or ranking system, no matter how well constructed will be looked upon as supporting information. Managers will typically skip ahead to the final number.

In addition, costs should be captured in a way that reflects the manner in which they were incurred. It is important not to cross operating centers when allocating costs; the type and quantity of contaminant reduced per center is more useful data than collecting the total for administration, research and development, etc. If possible, we should attempt to keep costs, such as those attributable to compliance, out of the general overhead category and move as many line items as possible to the direct cost category. This will focus attention on the proper source of the cost and make comparison of technologies more valid (West, 1993).

Life Cycle Cost Estimating

The time value of money becomes an important issue for costs that span more than one year. Techniques for making the analysis equitable over time will be applied to environmental technology projects. If we expand the list of cost components, then, at times, it is also necessary to look at an elongated time line for realizing the benefits of the investment. For instance, some pollution prevention projects might take many years to document costs and savings. A conventional time horizon for industrial project financial analysis might be less than five years. Accepting this typical five-year timeline could undermine the expanded cost-benefit component approach listed above.

The *reason* for considering an extended analysis period can be demonstrated by examining the life-cycle cost for conventional pump-and -treat remediation of a contaminated site, which is a process that will rather commonly exceed a 30-yr span (Pendergrass, 1991). The decision maker's willingness to work with an extended time period for analysis will depend on funding, size and structure of the organization, process lifetime, and finally, return on investment from competing projects (White et al, 1992-93: pp. 38).

Calculating the return on investment for new technology requires incorporation of long-term financial indicators in the decision-making process. Assessment tools must consider the time value of money, and positive and negative cash flows over the life of the project. The tools for developing the Life-Cycle Cost Estimate (LCCE) are accepted economic analysis standards: Internal Rate of Return (IRR), Net Present Worth (NPW), and Benefit /Cost Ratio (BCR). All three procedures can appropriately discount future cash flows. The ROI is closely related to these assessment tools, which solve the same equation for different variables, and precede the calculation of the return on investment. The selection of the assessment tool depends on the type of analysis required; the nature of total costs captured, and the desired expression of the final result, should lead to the proper analysis technique (General Electric, 1987). Key differences may include a increase in the number of line item costs, or an increase in the time period of the life-cycle, when appropriate. The use of these assessment tools is valid and straight forward, as long as the costs were captured in a comprehensive manner. Other methods, such as simple payback method, do not take into account cash flow beyond the "break-even" point or the cost of capital, but are none-the-less overused by large organizations as an inappropriate substitute for a more in-depth return on investment (ROI) calculation.

The calculation of Net Present Worth (NPW) is based on a known, or more likely assumed, discount rate. The sum of the discounted cash flows is the NPW of the project. If the project is worth pursuing, then the NPW is positive; a project with a negative NPW should be rejected. In general, a project with the higher NPW should be chosen over a lower NPW, if other parameters are equal.

The calculations will illustrate this present worth method as sensitive to the rate of discount. This is particularly evident when NPW is applied to longer-term initiatives with substantial cash flows in later years. For a "frontloaded" project with most cash flows occurring in early years, the NPW will not be lowered much by increasing the discount rate. The opposite is true for projects whose major cash flow comes later. This means that, when using this method, projects with a big payoff towards the end of their life-cycle could be presented by the calculations as a less than attractive investment. For this methodology, the NPW of life-cycle costs is the present worth of capital costs, plus the present worth of the annual operations and maintenance costs, plus the present worth of the indirect costs and liabilities, if known, for each year the project is operable (Macedo et al., 1978: p.295). If the technology warrants the inclusion, the present worth of the salvage value of the equipment is also considered. The following formula would be

used for a ten year life cycle:
$$NPW = \sum_{a=1}^F PW_a = PW_1 + PW_2 + PW_3 + \dots + PW_9 + PW_F + PW_{salvage}$$

The present worth of each year through ten plus the salvage value is calculated by

$PW = F(1+i)^{-n}$ where P represents a present sum of money, F is a future sum of money, i equals the interest rate per interest period (normally one year), and n is the number of interest periods. It is often necessary to calculate present worth for use in techniques other than *Net* present worth, as we will see below. There are many sources for compound interest factors at different rates. For instance, if we wanted to calculate the present worth of a series of equal annual cost that will occur for the next ten years and the discount rate is assumed to be 10%, then we would multiply one year's cost by (6.145), which is the value for (P/A, 10%, 10 years. This factor can be found on page 630, of Newman & Johnson's "*Engineering Economic Analysis*," Fifth Edition, 1995. This factor eliminates the need to individually calculate each annual cost in the series using the formula above. Once we have established a fundamental understanding of the methods, a spreadsheet could be constructed to automate any of these calculations and perform sensitivity analysis for various circumstances. Since one of our goals is to increase the understanding of the process, it is hardly a waste of time to look at what might be *behind* the use or construction of such a spreadsheet.

Using the internal rate of return (IRR) method, the discount rate that equates the present worth of cash inflow to present worth of expected project costs is calculated. A new technology would be worth using when the calculated IRR is greater than the cost of capital to finance its implementation. For the IRR, the net present worth is set to zero; the discount rate i , is calculated. In a situation where a minimum interest rate of return, sometimes called a “hurdle rate” has been established, and where several competing projects require analysis, the project having the greatest IRR would theoretically be selected. To calculate the internal rate of return, we must convert the various consequences of the investment into a cash flow. Then we will solve for the unknown value of i , which is the interest rate of return. There are five forms of the cash applicable to return on investment. **PW of benefits - PW of costs = 0, EUAB - EUAC = 0, PW of benefits / PW of costs = 1, NPW = 0, and PW of costs = PW of benefits.** These five equations represent the same concept in different forms (Newman & Johnson, 1995: p.165). The IRR method can relate costs and benefits with rate of return i as the only unknown. The calculation of IRR would be used in situations where decision makers wanted the final result expressed in percentage (%) form. The difficulty in solving for an interest rate is that there is no convenient direct method of solution. We solve the equations by trial and error, until one of the five conditions above is satisfied. A spreadsheet or software designed for this iterative process would be particularly useful for calculating the IRR.

The IRR is defined as the equivalent rate of return at which competing alternatives are equally attractive, For some firms , this is considered to be the ROI. Decision makers typically know the “hurdle rate” for investments; if the rate of return is above the hurdle rate, then the investment is acceptable. There are two main considerations that have a bearing on what interest rate to use in governmental investment studies. One obvious factor is the interest rate on borrowed capital, and the other is the sometimes overlooked opportunity cost of capital to the governmental agency and to the taxpayers. At present, the federal government uses a 10% standard hurdle rate, according to the Office of Management and Budget (OMB, 1992). OMB sets the guidelines for projects sponsored by the government.

This factor is based on a minimum rate calculated by subtracting the projected average annual rate of inflation from the nominal annual interest rate for Treasury notes and bonds. Currently, the factor for constant dollar analysis of ten year projects is would be about 4 percent (Ewer, 1992: p.71). Rates established by private businesses are dependent are relevant to this study only so far as they effect subcontract prices.

The Benefit/Cost Ratio (BCR) is sometimes called the Profitability Index. The BCR amounts to the present value of cash flow in (benefits) over the present value of cash flow out (costs). This illustrates the present worth of dollar value benefits per dollar spent or the relative profitability of the project. Projects with the highest ratio greater than one should be pursued. In governmental projects there may be difficulties deciding whether to classify various consequences as items for the numerator or for the denominator. An alternate computation for public funded projects is to consider user costs a *disbenefit* and to subtract them in the numerator rather than adding them in the denominator (Newman & Johnson, 1995: p.426).The reason for this suggested alteration to the common benefits/costs equation can be illustrated by using the example of a government project with the following consequences:

- o Initial cost of project to be paid by government is \$1,000,000*
- o Present Worth of future maintenance to be paid by government is \$423,000*
- o Present Worth of Benefits to the public is \$3,336,000*
- o Present Worth of additional public user costs is \$617,000*

If we put the benefits in the numerator and all the costs in the denominator it yields:

$$BCR = \$3,336,000 / \$1,000,000 + \$423,000 + 617,000 = \$3,336,000 / \$2,040,000 = 1.64$$

Using the alternate calculation below to consider user cost as a disbenefit, since the people receiving the benefits may pay none of the costs directly, would compute:

$$BCR = \frac{\text{Public benefits} - \text{Public costs} - \text{Maintenance costs}}{\text{Governmental costs}}$$

$$\text{BCR} = \$3,336,000 - \$617,000 - \$423,000 / \$1,000,000 = \$2,296,000 / \$1,000,000 = \mathbf{2.30} \text{ <-----}$$

We should note that, while this will yield a higher benefit - cost ratio than may be conventionally calculated, the NPW does not change.

$$\begin{aligned} \text{NPW} &= \text{PW of benefits} - \text{PW of costs} = \$3,336,000 - \$617,000 - \$423,000 - \$1,000,000 \\ &= \$1,296,000 \end{aligned}$$

Again, these are rather commonly used economic analysis techniques, but there were some new line item costs identified earlier that, in conjunction with the often extended analysis period, separate the analysis of emerging environmental technologies from typical industrial projects requiring similar analysis (DeGarmo et al., 1993; Newman & Johnson, 1995; Macedo et al., 1978). The key to assessing the economic viability of investment in new technology is to open an organization's accounting system, so that it can be used to track and allocate environmental costs to the process responsible for creating them. If this is done properly, the cost accounting system can provide relevant cost data and the time/rate constraints for analysis of the true life-cycle costs and operating budget. We should pursue the assessment of life-cycle cost in enough detail to allow for calculation of a reliable return on investment.

Return on Investment

The potential profitability of investing in an emerging environmental technology could be expressed in a variety of calculations described as return on investment. The IRR is defined as the equivalent rate of return at which competing alternatives are equally attractive--expressed a percentage rate. The ROI is defined in this report as the actual dollar benefit of an investment. This is a more straightforward expression than profitability percentages, especially when developing budgets within government agencies. For these organizations, reaching a certain profit-making percentage is not their primary mission. Furthermore, a relatively high *incremental* rate of return, of say--40%, placed in a final report, could mislead or encourage managers to believe that the entire project has a 40% *internal* rate of return.

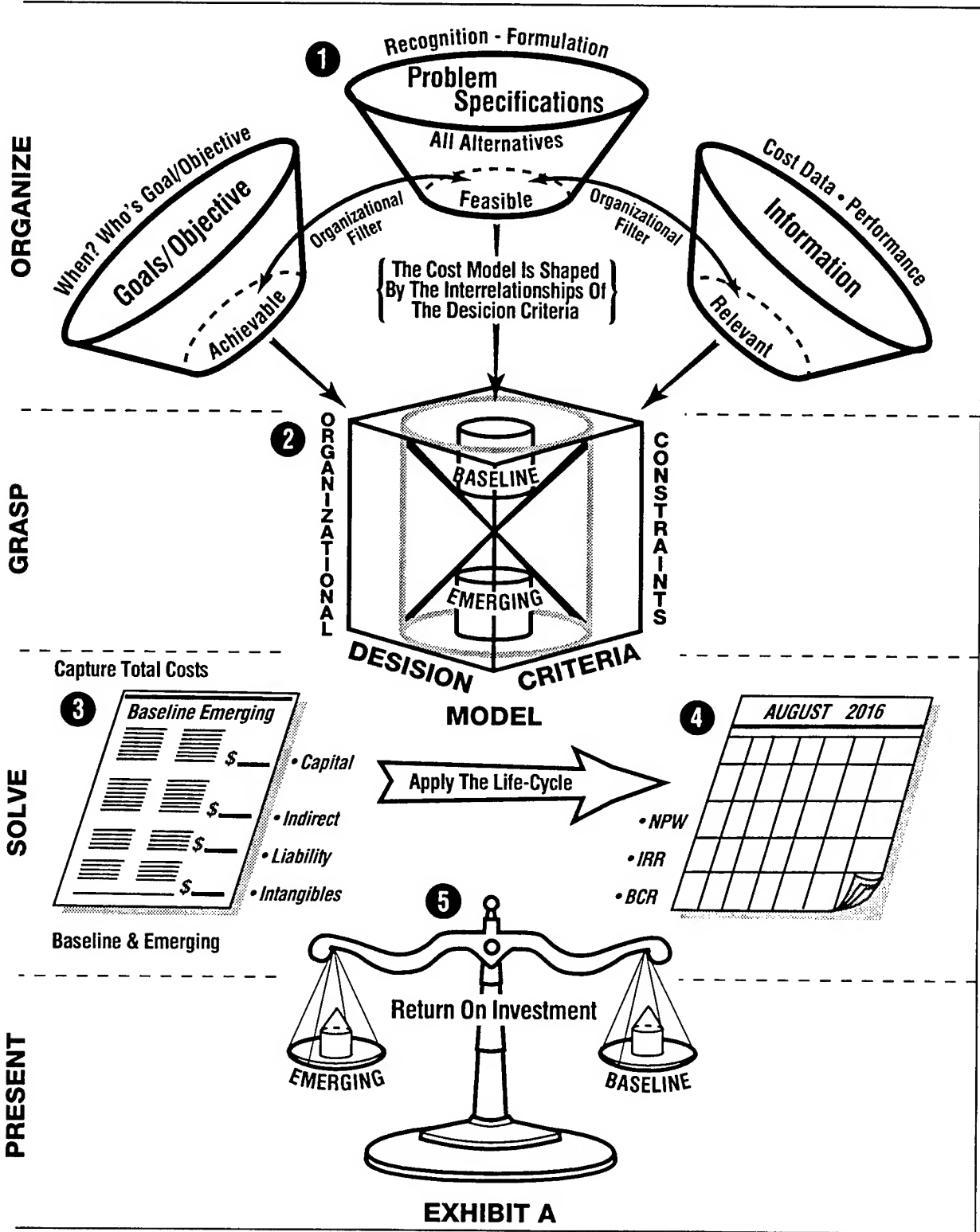
Return on Investment (ROI) is a criterion for judging the most efficient way of solving a given problem. The selected method should be the most efficient, that is, the least expensive way of meeting the performance objectives of the project. No matter what other decision making rule has been applied, we calculate the expected savings, from employing the new technology, relative to the existing alternatives. Calculating return on investment requires understanding the scope of the environmental problem and an estimate of the number of times the new technology would actually be used to solve the problem. The return on investment would ultimately equal the discounted cost savings minus the discounted cost of initial investment over a period of time. This final step is the culmination of our efforts to calculate the total life-cycle costs associated with alternative approaches to environmental solutions and should serve as a useful decision making tool, when presented to management with proper qualifications.

Summary of Methodology

The steps involved in evaluating return on investment for new technologies are to (1) **specify the cost problem**, using established goals and objectives and relevant data to define the alternatives, (2) **develop the decision criteria model**, so the performance of the competing technologies can be characterized within the context of application, and the predominate cost factors will be exposed, (3) **capture the total costs** to implement the alternatives, including direct, indirect, liability, and qualify the less tangible costs, (3) **estimate the life-cycle costs** associated with costs and benefits occurring at different times, while applying present worth methods with discount rates and life-cycles appropriate to the specific project, (4) calculate **return on investment** expressed as an actual dollar amount benefit of implementing the emerging technology. Collectively, this process should provide structure and promote consistency in evaluating investments in new technology.

Calculating Return On Investment For Emerging Technologies

SUMMARY OF METHODOLOGY



Results

Following the specification of the value problem, we begin by developing the decision criteria model, comparing like technologies with like, so as to avoid any distinctive benefits claimed by dissimilar projects being taken out of context. The scope and quality of the service to be provided must be closely defined, or quality differences in the proposed solutions can make the comparison invalid. If this is done carefully; then the technology yielding the greatest ROI among the various alternatives can be selected with fewer reservations (Burley & Phillips, 1993). This forces definition of the emerging technology and proposals for some general situations in which it could be implemented. This criterion assumes that the technologies are expected to carry out the same technical project goals equally well or that the cost of compromise will be captured.

Being able to conceptualize the implementation of a technology provides us with a tool for characterizing its effectiveness in a given set of circumstances. Note that it is not possible to foresee every situation, combination of technologies, or scope of work that could be applied to a given problem. However, this should not become a deterrent to developing good hypothetical settings and criteria, in which appropriate applications for a new technology can be demonstrated (Hombach, 1995). The challenge is to confine acceptable results to meaningful performance standards, without losing too much generality and making it impossible to come up with a cost.

The technologies must be compared in an atmosphere of requirements that would be encountered in actual practice, while emphasizing the individual performance attributes of each. This will bring to light the best use of new technologies, highlight differences, and demonstrate the relevancy of the comparison. An example of this principle is illustrated in the application of rapid optical screening tool (ROST). The real-time assessment of monitoring data on-site without laboratory analysis is a critical factor. It facilitates decision making during site investigation projects, and ensures accurate and efficient completion of site investigations and optimization of remedial activities.

Therefore, one of the parameters for determining when the technology is appropriate should call for rapid sample analysis rates because this is a real world requirement (Booth, et al., 1993: p.11).

Another one of the more difficult aspects of parameterizing the application of technology is that costs attributable to a particular environmental problem do not follow a linear scale in regard to their magnitude. A form of sensitivity analysis could be used to parameterize critical points within the range of values. This will highlight any economies of scale that could be realized which could reduce the cost of an assembly. Conversely, if a technology exceeds performance to a degree or level of detail that is not required, then there is no point in analyzing beyond artificial milestones that would never be encountered in the real world (Booth, et al., 1991: p.19)

In addition to these concerns, determining the level of a technology's performance within the context of its application calls to attention the strengths and limitations of competing projects. There is a need to measure parameters such as rate of reduction, refinement, accuracy, sensitivity, volume of reduction, and time saved or added per use. Volume of contaminant could be reduced, for example, to levels below one part per billion, but if requirements call for a much lower standard, then defining the alternatives based on the standard would not be relevant. Any added capabilities beyond that necessary to do the job adequately become part of the qualitative analysis that should accompany any set of cost calculations. However, if it is anticipated that systems requirements will change, thus calling for greater refinement in the technologies within the predicted life-cycle, then comparison on the basis of new standards can be justified (Surma and Vondra, 1992: pp. 52-53).

Defining the alternative assemblies of technology will certainly highlight non-quantifiable characteristics that are, none-the-less, critical to the decision making process. It is important to point out the qualifiers that are irrevocably connected with the calculated costs.

One system might be more portable or convenient to use; another might have more potential market or a planned future use not covered in the scope of the analysis. Usually, it will be adequate to note qualitative performance characteristics within the investment evaluation. The technologists should assist in the input of all parameters of the conceptual analysis, so that conclusions are not drawn without the inclusion of substantial field data, or at least an independent study of the predicted results (Schroeder et al., 1991:pp 11-17). The synthesis of the decision criteria profile and the comparison of the alternatives is illustrated in Exhibits B1 & B2 on the next two pages.

EMERGING TECHNOLOGY
BASELINE TECHNOLOGY
DECISION CRITERIA

Bioventing of Petroleum Hydrocarbons	Landfarming, Full Scale Windrow Composting, Solidification/Stabilization	<The volume and depth of possible excavation.> Is off-gas treatment necessary ? NO -- costs range \$10-\$40/cy. Yes -- costs range up to \$85/cy. Bioventing-10,000 cy costs \$15/cy.
Site Characterization and Analysis Penetrometer (SCAPS)& Rapid Optical Screening Technology (ROST)	Monitoring Wells Soil Borings	<Depth to groundwater and the soil conditions.> Does not replace monitoring wells; rather, used in combination with wells to avoid the over use and poor placement of wells (See Los Alamos cost effectiveness study) --% replaced
Bioremediation of Chlorinated Aromatic Solvents - Contaminated Groundwater	Granular Activated Carbon Fluid Bed Reactor Treatment, Air Stripping/ Vapor Phase Carbon Adsorption or Thermal Oxidation	Major cost factors include the microorganisms, influent & effluent piping, type of absorber bed, the pumps, substructure, saturation indicator, heaters, blowers electrical usage, operation and maintenance. (R.S. Means)
In Situ Dechlorination (Funnel & Gate)	Pump & Treat Technologies (Above)	Major concern is depth possible with permeable barrier = 50' so far, 80'-120' planned, reactive media thickness & weight also an issue.
In Situ Bioremediation of Chlorinated Solvents	Air Sparging with soil vapor extraction Carbon Adsorption or Air Stripping/ Thermal Oxidation/ Natural Attenuate	The stage of development of the proper electron donor for PCE is an important factor. Major baseline cost drivers include O & M, injection wells, piping, air compressor, blowers, monitoring, containment
Complex Resistivity	Drill Multiple Characterization Wells	Major cost considerations are well drilling and installation of equipment versus non invasive technique. <Geophysical reducing number will be required.>
Six Phase Resistive Heating	Excavation & Treatment/Pump & Treat	The emerging might be limited to less than a 100 foot thick aquifer, at this time, and has not yet been applied to saturated zones. O&M is major energy user.
Surfactant Curtain	Pump & Treat - Organic Contaminants	Surfactant material costs could be high. Does not remediate; rather a containment technique, with follow on to remove contaminant.
Environmental Systems Management Analysis & Reporting neTwork (E-SMART)	Manual Sampling with Standard Monitoring Wells	Works in tandem w/SCAPS/ROST to reduce manual sampling requirements by 75% versus costs of well drilling and installation of equipment.
Bioventing of Non-Petroleum Hydrocarbons	Windrow Composting, Solidification/Stabilization, Soil Vapor Extraction & Off Gas Treatment	Volume and depth of possible excavation, If off gas treatment is necessary, then it can cost up to \$120 per cy, if not required, then \$10-\$40/cy versus \$15 per cy for bioventing.
Paint Spray Booth Recirculation reduces the volume of air requiring treatment by 90 percent	Manage the entire volume of air contaminated with VOCs and treat with.....	Recirculation reduces volume requiring VOC treatment by 90%. Total costs of current facility & treatment train * 70 minus cost of new booths + treatment costs saved over lifetime =savings
Ferrous Sulfate/Sodium Sulfide (FS/SS) Wastewater Treatment	Chemical Treatment & Sludge Disposal	Current chemical usage to reduce chromium plus hazardous sludge versus metals removal method reducing chemicals and amount of sludge

EMERGING TECHNOLOGY**BASELINE TECHNOLOGY****DECISION CRITERIA**

Ion Vapor Deposition (IVD) of Aluminum	Cadmium Plating Bath Waste Stream Treatment	Emerging technology possibly a must due to new regulations requiring elimination of cadmium, therefore, common industrial cost analysis could be used prior to environmental.
Space Launch Risk Assessment Program	Conservative Atmospheric Transport & Diffusion Models	Emerging technology would safely reduce the number of launch holds, in both eastern and western test ranges, which have caused expensive operational delays. Percentage of delays avoided 50% or \$19M minus cost of S&T
Jet Engine Test Cell (JETC) NOx Emission Control	Possible Emission Reduction Treatment of JETC Effluents	Cost savings based on whether or not the EPA will require emission reduction treatment of JETC before technology can developed to reduce emissions. <Counter to mission.>
Internal Combustion Engine (ICE) & Aerospace Ground Equipment (AGE) NOx Emission Control	NOx reduction technique currently proposed by Federal, State, and local regulations, the Consolidated Aircraft Support System	Major cost concerns are the installation of current compliant device that would cost \$20M and is not realistic to deploy in exercises. New device to be compliant and deployable @ \$5M each
Mercury Recovery from Flue Gases with Innovative Sorption Materials	Waste incinerators will be out of compliance with new standards	At issue are incinerators that are or will be non-compliant. New incinerators cost less and would be compliant. Does the emerging meet DoD requirements? Any value to the mercury recovered ?
Source Characteristic Conversion Device	Intermittent & high volume exhaust air requiring treatment of VOCs	Emerging technology intended to be used in conjunction with recirculating paint spray booth to reduce idle time of VOC treatment allowing possible use of biofilter or smaller more active system.
Paint Stripping Waste Treatment	Combined waste stream disposed of as hazardous waste	Baseline technologies do not separate; Emerging technology would separate & reduce source requiring treatment.
Liquid-Phase Catalytic Reactor Development	Open burning and incineration of propellants	Baseline non-compliant and not a technology; Emerging compliant with latest regulations. \$ 3 million dollars minus the number of days fined * \$25,000/day for current EPA maximum.
Transportable AFFF Treatment System	Disposal by discharge to wastewater treatment plants at controlled rates	Cost of hydrothermal oxidation equipment @ 40 bases versus current treatment costs.
Aircraft Hydraulic Fluid Purification and Reuse	Hydraulic Fluid is disposed of as hazardous waste or mixed with fuels to be incinerated.	Major cost factors include total volume of hydraulic fluid used by AF times savings per gallon minus cost of purification & reuse over life cycle
Ion Vapor Deposition (IVD) of Heavy Metals	Disposal of heavy metal wastes by collection, containment, and landfill	Emerging technology costs versus hazardous waste disposal costs plus fines for non-compliance plus the costs of new heavy metal plating facilities
Natural Attenuation	Pump & Treat - low risk contaminants	If the risks are relatively low, then is there something more cost effective and safer than natural attenuation ?

**Capturing the Total Costs Associated with the Purification & Reuse of Aircraft Hydraulic Fluid Vs
Purchase of New Hydraulic Fluid to Meet Total Demand for 72 Bases**

Cost Category	Baseline (New Fluid)		Emerging (Reuse Fluid)	
(1) Direct Costs				
Capital Expenses - Initial Acquisition				
o Purification equipment - 160 units * \$14,000 ea (Pall, Inc.)	nil		\$	2,240,000.00
o Design & Review - new purification process development (?)	nil		\$	10,000,000.00
o Direct Labor -to deliver/start-up purification equipment (bvm)	nil		\$	160,000.00
o Other - Wear test to follow up on performance (WL/MLBT)	nil		\$	150,000.00
Total Capital Investment	\$	0.00	\$	13,550,000.00
Operations & Maintenance Costs				
o Hydraulic Fluid - total demand 3.5 Mgal @ \$10/gal (WPAFB)	\$ 35,000,000.00	reduce to 1/4th	\$	8,750,000.00
o Replacement parts - filters for purification equipment (Pall,Inc)	nil		\$	400,000.00
o Subcontract - disposal (incinerate) 63,636 @ \$400.00 (Means)	\$ 25,454,000.00	reduce to 1/4th	\$	6,364,000.00
o Operating Overhead - insurance & fees 40 barrel shipment ("	\$ 4,162,000.00	reduce to 1/4th	\$	1,041,000.00
o Utilities - 2.5 kW * \$0.10 * 250 days * 8 hrs/day (bvm)	nil		\$	80,000.00
o General Administration - marketing, travel communication	\$ 0.00		\$	0.00
Total Annual O&M Costs	\$	64,616,000.00	\$	16,635,000.00
(2) Indirect Costs				
Compliance Costs = Professional labor - Frequency * [Material + (Time * Loaded Wage)] (EPA, 1989: pp. 3-9 through 3-35)				
o Notification = 432 occurrences/yr * [3 hrs * \$25/hr] =	\$ 32,400.00	reduce to 1/4th	\$	8,100.00
o Reporting = 288 occurrences/yr * [8hrs * \$25/hr] =	\$ 57,600.00	reduce to 1/4th	\$	14,400.00
o Monitoring = 3744 occurrences/yr. * [1 hr * \$25/hr] =	\$ 93,600.00	reduce to 1/4th	\$	23,400.00
o Recordkeeping = 3744 occurrences/yr * [1 hr * \$15/hr] =	\$ 56,160.00	reduce to 1/4th	\$	14,040.00
o Manifesting = 1600 * [3 hrs * \$25/hr] =	\$ 120,000.00	reduce to 1/4th	\$	30,000.00
o Training = 360 employees/yr * [\$1000 +(8 hrs * \$20/hr)] =	\$ 360,160.00	reduce to 1/4th	\$	90,040.00
o Inspection = 18,000 occurrences/yr * [0.25 hrs * \$20/hr] =	\$ 90,000.00	no reduction	\$	90,000.00
o Labeling = 63,636 * [\$15 + (0.25 hrs * \$15/hr)] =	\$ 1,193,175.00	reduce to 1/4th	\$	298,294.00
o Preparedness =864 * [0.5 hrs * \$15/hr] =	\$ 6,480.00	no reduction	\$	6,480.00
o Medical Surveillance = 720 * [\$100 + (1hr * \$25/hr)] =	\$ 90,000.00	reduce to 1/2	\$	45,000.00
Subtotal Compliance Costs	\$	2,129,575.00	\$	619,754.00
Insurance & Special Taxes				
o Requirements - Contractor's pollution liability insurance (5%)	\$ 106,500.00	reduce to 29 %	\$	30,900.00
o Requirements - Public liability insurance (3%)	\$ 63,900.00	reduce to 29 %	\$	18,500.00
o Permits - Location / Project specific				
Total Indirect Costs	\$	2,299,975.00	\$	666,993.00
(3) Liability Costs (These values were calculated using the EPA Pollution Prevention Benefits Manual, Phase II: Exhibit C)				
Year liabilities will occur(1 to 20) + [(Distance to GW 150 to 3200m) * (RF = 1 to 1000)]/ [Velocity (30 to 3000m/yr)] Within 20 years				
Fines & Penalties				
o Federal - (Cost present, but no model to calculate at this time)	unknown		unknown	
o State - (Cost present, but no model to calculate at this time)	unknown		unknown	
o Local - (Cost present, but no model to calculate at this time)	unknown		unknown	
Remediation				
o Air	nil		nil	
o Soil - 8.9k * 1 * (0.002) * Q temporary storage in drums	\$ 62,300,000.00	reduce to 1/4th	\$	15,575,000.00
o Soil - 8.9k * 1 * (0.0000024 * 50 * + 0.00029) * Q transport	\$ 12,772,000.00	reduce to 1/4th	\$	3,193,000.00
o Groundwater - \$5,425,000 + (1,258,000 * 6) = \$ 12,973,000	\$ 12,973,000.00	reduce to 1/4th	\$	3,243,000.00

Containment (Surface Seal) = (7 to 46 k\$/ acre) * (65 to 150 acres)	\$ 2,849,000.00	reduce to 1/4th	\$ 712,000.00
Legal Fees - (Cost present, but no model to calculate at this time)	unknown		unknown
Personal Injury = \$56,000/ person * population affected (100)	\$ 5,600,000.00	reduce to 1/4th	\$ 1,400,000.00
Economic Loss = Cost to replace water supply (\$350,000 to \$334,000,000)	\$ 38,784,000.00	reduce to 1/4th	\$ 9,696,000.00
Real Property Damage = (0.15 to 0.30) * (\$1000 to \$3500/ acre) (default)	\$ 250,000.00	reduce to 1/4th	\$ 63,000.00
Natural Resource Damage			
o Water - (Surface) = \$692k/Ac * 1 to 3 acres	\$ 2,076,000.00	reduce to 1/4th	\$ 692,000.00
(4) Intangible Costs	\$ 137,604,000.00		\$ 35,574,000.00

Qualifiers & Irreducibles

- o Decreased costs due to increased aircraft in-commission rate through purification and reuse of hydraulic fluid
- o Decreased costs due to increased sortie generation - more reliable aircraft hydraulic systems through purification and reuse
- o Decreased health maintenance costs due to reduction in exposure to hazardous material with purification and reuse
- o Decreased costs due to improved relations with employees & surrounding community through hazardous material reduction
- o Decreased costs due to lessened dependence on imported oil through purification and reuse of hydraulic fluid

$$\begin{aligned}
 NPW_{Baseline} &= PW_{Capital} + PW_{Annual\ O\&M} \\
 &= \$ 0 + \$ 64,616,000 (P/A, 10\%, 10yrs) \\
 &= \$ 64,616,000 (6.145) = \$ 397,065,320
 \end{aligned}$$

$$\begin{aligned}
 NPW_{Emerging} &= PW_{Capital} + PW_{Annual\ O\&M} \\
 &= \$ 13,550,000 + \$ 16,635,000 (P/A, 10\%, 10yrs) \\
 &= \$ 13,550,000 + \$ 16,635,000 (6.145) = \$ 115,772,075
 \end{aligned}$$

$$\begin{aligned}
 NPW_{Savings} &= NPW_{Baseline} - NPW_{Emerging} = \$ 397,065,320 - \$ 115,772,075 \\
 &= \$ 281,293,245 <-----
 \end{aligned}$$

If we consider the NPW of the indirect and the liability costs, in addition to the industrial analysis above, then the potential NPW of both the baseline & the emerging technology costs become:

$$\begin{aligned}
 NPW_{Baseline} &= PW_{Indirect} + PW_{Liability} \\
 &= \{[\$ 2,299,975 + \$ 137,604,000 (P/F, 10\%, 10yrs)](P/A, 10\%, 10yrs)\} \\
 &= \$ 2,299,975 (6.145) + \$ 137,604,000 (0.3855)(6.145) \\
 &= \$ 340,103,118
 \end{aligned}$$

$$\begin{aligned}
 NPW_{Emerging} &= PW_{Indirect} + PW_{Liability} \\
 &= \{[\$ 666,993 + \$ 35,574,000 (P/F, 10\%, 10yrs)](P/A, 10\%, 10yrs)\} \\
 &= \$ 666,993 (6.145) + \$ 35,574,000 (0.3855)(6.145) \\
 &= \$ 88,369,832
 \end{aligned}$$

$$\begin{aligned}
 NPW_{Savings} &= NPW_{Baseline} - NPW_{Emerging} = \$ 340,103,118 - \$ 88,369,832 \\
 &= \$ 251,733,286 <-----
 \end{aligned}$$

If we collect the NPW of cost savings including direct, indirect, and liability, then the total potential NPW of the savings is:

$$NPW_{Total} = \$ 281,293,245 + \$ 251,733,286 = \$ 533,026,531 <-----$$

Capturing the Total Costs

The total costs associated with implementing a technology are based on the performance capabilities highlighted in the conceptual stages, and the total costs captured above that are applicable to the project. This means that we must assess all of the costs associated with achieving the desired goals established for using the technology in the first place (Hoult et al., 1994: p.10). These include costs connected with acquiring equipment and materials, manifesting and mobilizing personnel and equipment, installation, operation and maintenance, site secondary disposal, and closure.

Technology acquisition costs should have captured the purchase cost of all assemblies necessary to obtain the desired result, and any modifications necessary to allow the technology to perform in the specific situation as envisioned (Carter, 1992: p.59). Under current acquisition reform initiatives, the general approach would be to purchase off-the shelf technology whenever possible; this may often require alterations that make the equipment more durable or portable in actual practice. The objective is to capture total costs for a complete system, without overlooking the costs of any necessary labor or equipment to deliver it whole.

The decision concerning whether or not we should buy or rent the equipment needed to mobilize and install the technology is itself based on the "return on investment"; It would depend on how long it takes to complete the installation and/or how often the equipment would be used. This is a further complication since there are no hard and fast rules , especially when working new technology, but again, we should rely on the context of the decision criteria profile to make this decision too (Showalter et al., 1995: p.22). Transportation costs dedicated to making the technology readily operable should be included; this is one of the modifications mentioned earlier that can make an existing assembly more portable, but add to the cost.

Internal Rate of Return for Aircraft Hydraulic Fluid Purification and Reuse

Incremental Analysis

Year	PW* <i>@ 0%</i>	PW* <i>@ 10%</i>	PW* <i>@ 60%</i>	PW* <i>@ ◎%</i>
0	-13,550,000	-13,550,000	-13,550,000	-13,550,000
1	47,981,000	43,619,527	29,988,125	0
2	47,981,000	39,651,498	18,741,379	0
3	47,981,000	36,048,125	11,712,162	0
4	47,981,000	32,771,023	7,321,901	0
5	47,981,000	29,791,403	4,577,387	0
6	47,981,000	27,085,275	2,859,668	0
7	47,981,000	24,623,849	1,789,691	0
8	47,981,000	22,383,137	1,117,957	0
9	47,981,000	20,348,742	700,523	0
10	47,981,000	18,496,676	436,147	0
	<u>466,260,000</u>	<u>281,269,255</u>	<u>65,694,940</u>	<u>-13,550,000</u>

* **Note:** Each year the cash flow difference is multiplied by (P/F, i%, n yrs)

$$\begin{aligned}
 @ \ 0\%; \ (P/F, \ 0\%, \ n \ \text{yrs}) &= 1 \ \text{for all values of } n \\
 @ \ ◎\% \ (P/F, \ ◎\%, \ 0) &= 1 \\
 (P/F, \ ◎\%, \ n \ \text{yrs}) &= 0 \ \text{for all other values of } n
 \end{aligned}$$

Therefore, the incremental rate of return on the additional initial acquisition costs is greater than 60%. We know this because it would require an IRR greater than 60% to satisfy NPW set equal to zero. We should also note that the cash flow total for present worth set to 10% equals \$281,269,255, which is nearly the same value calculated in the previous step. The difference is due to rounding. The negative 13,550,000 value comes from calculating the difference in acquisition costs. The positive 47,981,000 is the amount of annual savings in operations and maintenance cost realized, by using the emerging technology, as opposed to the baseline.

Benefit-Cost Ratio for Aircraft Hydraulic Fluid Purification and Reuse

$$\frac{\text{Benefit}}{\text{Cost}} = \frac{B}{C} = \frac{\text{Equivalent Uniform Annual Benefit}}{\text{Equivalent Uniform Annual Cost}} = \frac{EUAB}{EUAC}$$

$$\frac{EUAB_{\text{baseline}}}{EUAC_{\text{baseline}}} = \frac{3,500,000 \text{ gal/yr @ \$10 per gallon}}{\$ 64,616,000 / \text{year (O\&M)}} = 0.54$$

$$\frac{EUAB_{\text{emerging}}}{EUAC_{\text{emerging}}} = \frac{(3,500,000 \text{ gal/yr @ \$10 per gallon}) + \$ 47,981,000/\text{yr savings}}{[\$ 13,550,000 (\text{A/P, } 10\%, 10 \text{ yrs})] + \$ 16,635,000/\text{year (O\&M)}} =$$

$$\frac{EUAB_{\text{emerging}}}{EUAC_{\text{emerging}}} = \frac{\$ 35,000,000/\text{yr} + \$ 47,981,000/\text{yr}}{[\$ 2,204,585] + \$ 16,635,000/\text{yr}} = \frac{82,981,000}{18,839,585}$$

$$= 4.41 <-----$$

The emerging technology yields the higher benefit to cost ratio. The benefits are the value of new hydraulic fluid plus any savings in operations and maintenance costs. The costs are attributed to the annualized cost of the initial acquisition plus the annual operations and maintenance cost.

The completion of the benefit-cost ratio analysis is the final step involved in our life-cycle cost estimate. Using the results of this section, along with a synopsis of the other process steps, we should summarize the results for the decision maker. This will form the cover for individual technology economic analysis reports. The bottom line will be the return on investment for the emerging technology.

Return on Investment for Aircraft Hydraulic Fluid Purification and Reuse

Technology Summary : Large quantities of waste aircraft fluid are generated each year from routine operations within the Air Force. Most of the hydraulic fluid is reusable, but is limited by particulate and water build-up, causing it to be disposed of as hazardous waste or mixed with fuels to be incinerated. Equipment was identified to purify hydraulic fluid for reuse to minimize this waste generation and reduce hydraulic fluid replacement costs. This equipment demonstrated that waste hydraulic fluid can be purified to acceptable military specifications without degrading the working properties or additives of the fluid. Follow-on aircraft pump wear testing in aircraft hydraulic pumps will thoroughly evaluate the purified hydraulic fluid.

Capturing the Total Costs : *Associated with the Purification & Reuse of Aircraft Hydraulic Fluid Vs Purchase of New Hydraulic Fluid to Meet Total Demand for 72 Bases*

Cost Category		Baseline (New Fluid)	Emerging (Reuse Fluid)
(1) Direct Costs			
Capital Expenses - Initial Acquisition	Total Capital Investment	\$ 0.00	\$ 13,550,000.00
Operations & Maintenance Costs	Total Annual O&M Costs	\$ 64,616,000.00	\$ 16,635,000.00
(2) Indirect Costs			
Compliance Costs = Professional labor Insurance & Special Taxes	Total Indirect Costs	\$ 2,299,975.00	\$ 666,993.00
(3) Liability Costs (EPA Manual, 1989)			
	Total Liability Costs	\$ 137,604,000.00	\$ 35,574,000.00
(4) Intangible Costs			
<i>Qualifiers & Irreducibles</i>			
o Decreased costs due to increased aircraft in-commission rate through purification and reuse of hydraulic fluid			
o Decreased costs due to increased sortie generation - more reliable aircraft hydraulic systems through purification and reuse			
o Decreased health maintenance costs due to reduction in exposure to hazardous material with purification and reuse			
o Decreased costs due to improved relations with employees & surrounding community through hazardous material reduction			
o Decreased costs due to lessened dependence on imported oil through purification and reuse of hydraulic fluid			

Life-Cycle Cost Estimates :

- o The USAF will save \$ 251,733,286 over ten years by using the new process instead of the baseline *without* considering the added environmental benefits.
- o The USAF will realize an internal rate of return of more than 60% on the investment in the new process over the baseline considering direct costs only.
- o The benefit to cost ratio of the new process is approximately 4.40. The baseline process has a BCR of approximately 0.54.

Return on Investment: The USAF should save \$ 251,733,286 through purification and reuse of hydraulic fluid, and could save up to \$ 533,026,531 considering indirect and liability costs.

**Capturing the Total Costs Associated with New Electroless Nickel Plating Bath Rejuvenation Process Vs
Conventional Electrolytic Nickel Plating for 5ALC's**

Cost Category	Baseline (Electrolytic)	Emerging (Electroless)
(1) Direct Costs		
<i>Capital Expenses - Initial Acquisition</i>		
o Purchased equipment - 5 units * \$10,500/ \$61,740 ea (Battelle)	\$ 53,000.00	\$ 309,000.00
o P.E. Installation - 5 units * \$4,095/ \$6,000 ea	\$ 20,475.00	\$ 30,000.00
o Instrumentation & Control - 5 units * \$1365/ \$1000 ea	\$ 6,825.00	\$ 5,000.00
o Piping - 5 units * \$2,625 / \$3,087 each	\$ 13,125.00	\$ 15,435.00
o Electrical - 5 units * \$1050/ \$3087 each	\$ 5,250.00	\$ 15,435.00
o Engineering & Supervision - 5 units * \$10,915/\$21,887 ea	\$ 54,575.00	\$ 109,435.00
o Working Capital & Startup - 5 units * \$15,978/ \$23,075 ea	\$ 79,890.00	\$ 115,375.00
Total Capital Investment	\$ 233,140.00	\$ 599,680.00
<i>Operations & Maintenance Costs</i>		
o Raw Materials - chemicals for plating process	\$ 319,570.00	\$ 309,805.00
o Labor - operating, maintenance, & supervision	\$ 358,205.00	\$ 284,430.00
o Operating Overhead - insurance & fees 40 barrel shipment	\$ 214,925.00	\$ 170,660.00
o Utilities - electricity & process water	\$ 15,740.00	\$ 17,330.00
o Depreciation -	\$ 12,220.00	\$ 38,720.00
Total Annual Costs	\$ 1,045,635.00	\$ 898,280.00
(2) Indirect Costs		
<i>Compliance Costs = Professional labor - Frequency * [Material + (Time * Loaded Wage)] (EPA, 1989: pp. 3-9 through 3-35)</i>		
o Notification = 60 occurrences/yr * [3 hrs * \$25/hr] =	\$ 4,500.00	reduce to 1/12th \$ 375.00
o Reporting = 20 occurrences/yr * [8hrs * \$25/hr] =	\$ 4,000.00	reduce to 1/4th \$ 1,000.00
o Monitoring = 1825 occurrences/yr * [1 hr * \$25/hr] =	\$ 45,625.00	reduce to 1/12th \$ 3,800.00
o Recordkeeping = 913 occurrences/yr * [1 hr * \$15/hr] =	\$ 13,695.00	reduce to 1/12th \$ 1,140.00
o Manifesting = 60 * [3 hrs * \$25/hr] =	\$ 4,500.00	reduce to 1/12th \$ 375.00
o Training = 25 employees/yr * [\$1000 + (8 hrs * \$20/hr)] =	\$ 29,000.00	reduce to 1/4th \$ 7,250.00
o Inspection = 1250 occurrences/yr * [0.5 hrs * \$20/hr] =	\$ 12,500.00	no reduction \$ 12,500.00
o Labeling = 600 * [\$15 + (0.25 hrs * \$15/hr)] =	\$ 11,250.00	reduce to 1/12th \$ 940.00
o Preparedness = 60 * [0.5 hrs * \$15/hr] =	\$ 450.00	no reduction \$ 450.00
o Medical Surveillance = 50 * [\$100 + (1hr * \$25/hr)] =	\$ 6,250.00	reduce to 1/2 \$ 3,125.00
Subtotal Compliance Costs	\$ 132,770.00	\$ 30,955.00
<i>Insurance & Special Taxes</i>		
o Requirements - Contractor's pollution liability insurance (5%)	\$ 6,640.00	reduce to 31 / 133 \$ 1,550.00
o Requirements - Public liability insurance (3%)	\$ 3,985.00	reduce to 31 / 133 \$ 930.00
o Permits - Location / Project specific		
Total Indirect Costs	\$ 143,395.00	\$ 33,435.00
(3) Liability Costs (These values were calculated using the EPA Pollution Prevention Benefits Manual, Phase II: Exhibit C)		
<i>Year liabilities will occur(1 to 20) + [(Distance to GW 150 to 3200m) * (RF = 1 to 1000)]/ [Velocity (30 to 3000m/yr)] Within 20 years</i>		
<i>Fines & Penalties</i>		
o Federal - (Cost present, but no model to calculate at this time)	unknown	unknown
o State - (Cost present, but no model to calculate at this time)	unknown	unknown
o Local - (Cost present, but no model to calculate at this time)	unknown	unknown
<i>Remediation</i>		
o Air	nil	nil
o Soil - 8.9k * 1 * (0.002) * Q temporary storage	\$ 623,000.00	reduce to 1/12th \$ 52,000.00
o Soil - 8.9k * 1 * (0.0000024 * 50 * + 0.00029) * Q transport	\$ 132,000.00	reduce to 1/12th \$ 11,000.00
o Groundwater - \$5,425,000 + (1,258,000 * 6) = \$ 12,973,000	\$ 130,000.00	reduce to 1/12th \$ 11,000.00

Containment (Surface Seal) = (7 to 46 k\$/ acre) * (65 to 150 acres)	\$ 455,000.00	reduce to 1/12th	\$ 38,000.00
Legal Fees - (Cost present, but no model to calculate at this time)	unknown		unknown
Personal Injury = \$56,000/ person * population affected (25)	\$ 1,400,000.00	reduce to 1/4th	\$ 350,000.00
Economic Loss = Cost to replace water supply (\$350,000 to \$334,000,000)	\$ 1,750,000.00	reduce to 1/4th	\$ 438,000.00
Real Property Damage = (0.15 to 0.30) * (\$1000 to \$3500/ acre) (default)	\$ 250,000.00		\$ 63,000.00
Natural Resource Damage			
o Water - (Surface) = \$692k/Ac * 1 to 3 acres	\$ 692,000.00		\$ 173,000.00
Total Liability Costs	\$ 5,432,000.00		\$ 1,136,000.00

(4) Intangible Costs

Qualifiers & Irreducibles

- o Decreased costs due to increased aircraft in-commission rate because of more consistent plating quality
- o Decreased costs due to increased sortie generation - more reliable nickel plated aircraft components
- o Decreased health maintenance costs due to reduction in exposure to hazardous material with bath rejuvenation process
- o Decreased costs due to improved relations with employees & surrounding community through hazardous material elimination

$$\begin{aligned}
 NPW_{Baseline} &= PW_{Capital} + PW_{Annual\ O\&M} \\
 &= \$ 233,140 + \$ 1,045,635 (P/A, 10\%, 10yrs) \\
 &= \$ 233,140 + \$ 1,045,635 (6.145) = \$ 6,658,567
 \end{aligned}$$

$$\begin{aligned}
 NPW_{Emerging} &= PW_{Capital} + PW_{Annual\ O\&M} \\
 &= \$ 599,680 + \$ 898,280 (P/A, 10\%, 10yrs) \\
 &= \$ 599,680 + \$ 898,280 (6.145) = \$ 6,119,611
 \end{aligned}$$

$$\begin{aligned}
 NPW_{Savings} &= NPW_{Baseline} - NPW_{Emerging} = \$ 6,658,567 - \$ 6,119,611 \\
 &= \$ 538,956 <-----
 \end{aligned}$$

If we consider the NPW of the indirect and the liability costs, in addition to the industrial analysis above, then the potential NPW of both the baseline & the emerging technology costs become:

$$\begin{aligned}
 NPW_{Baseline} &= PW_{Indirect} + PW_{Liability} \\
 &= \{[\$ 143,395 + \$ 5,432,000 (P/F, 10\%, 10yrs)](P/A, 10\%, 10yrs)\} \\
 &= \$ 143,395 (6.145) + \$ 5,432,000 (0.3855)(6.145) \\
 &= \$ 13,749,014
 \end{aligned}$$

$$\begin{aligned}
 NPW_{Emerging} &= PW_{Indirect} + PW_{Liability} \\
 &= \{[\$ 33,435 + \$ 1,136,000 (P/F, 10\%, 10yrs)](P/A, 10\%, 10yrs)\} \\
 &= \$ 33,435 (6.145) + \$ 1,136,000 (0.3855)(6.145) \\
 &= \$ 2,896,526
 \end{aligned}$$

$$\begin{aligned}
 NPW_{Savings} &= NPW_{Baseline} - NPW_{Emerging} = \$ 340,103,118 - \$ 88,369,832 \\
 &= \$ 10,852,488 <-----
 \end{aligned}$$

If we collect the NPW of cost savings including direct, indirect, and liability, then the total potential NPW of the savings is:

$$NPW_{Total} = \$ 538,956 + \$ 10,852,488 = \$ 11,391,444 <-----$$

Internal Rate of Return for New Electroless Nickel Plating Bath Rejuvenation Process
Incremental Analysis

Year	PW*<i>@</i> 0%	PW*<i>@</i> 10%	PW*<i>@</i> 40%	PW*<i>@</i> 39%
0	-366,540	-366,540	-366,540	-366,540
1	147,355	133,960	105,256	0
2	147,355	121,774	75,181	0
3	147,355	110,708	53,696	0
4	147,355	100,644	38,357	0
5	147,355	91,493	27,393	0
6	147,355	83,182	19,569	0
7	147,355	75,623	13,984	0
8	147,355	68,741	9,991	0
9	147,355	62,493	7,132	0
10	147,355	56,805	5,099	0
	1,107,010	538,956	-10,882	-366,540

* **Note:** Each year the cash flow difference is multiplied by (P/F, i%, n yrs)

@ 0%; (P/F, 0%, n yrs) = 1 for all values of n

@ 39% (P/F, 39%, 0) = 1

(P/F, 39%, n yrs) = 0 for all other values of n

Therefore, the incremental rate of return on the additional initial acquisition costs is approximately 39%. We know this because it would require a value for incremental IRR of about 39% to satisfy NPW set equal to zero. We should also note that the cash flow total for present worth set to 10% equals \$538,956, which is the same value calculated in the previous step. The negative 366,540 value comes from calculating the difference in acquisition costs. The positive 147,355 is the amount of annual savings in operations and maintenance cost realized, by using the emerging technology, as opposed to the baseline.

Benefit-Cost Ratio for New Electroless Nickel Plating Bath Rejuvenation Process

$$\frac{\text{Benefit}}{\text{Cost}} = \frac{B}{C} = \frac{\text{Equivalent Uniform Annual Benefit}}{\text{Equivalent Uniform Annual Cost}} = \frac{EUAB}{EUAC}$$

$$\frac{EUAB_{\text{baseline}}}{EUAC_{\text{baseline}}} = \frac{(\$ 635 / \text{kg} * 329.3 \text{ kg/yr} * 5 \text{ locations})}{[\$ 233,140 (\text{A/P}, 10\%, 10\text{yrs}) + \$ 1,045,635]} = 0.97$$

$$\frac{EUAB_{\text{emerging}}}{EUAC_{\text{emerging}}} = \frac{\$ 147,355 + (\$ 635 / \text{kg} * 329.3 \text{ kg/yr} * 5 \text{ locations})}{[\$ 599,680 (\text{A/P}, 10\%, 10 \text{ yrs}) + \$ 898,280]} = 1.20 <$$

The emerging technology yields the higher benefit to cost ratio. The benefits are the value of nickel plating on aircraft parts plus any savings in operations and maintenance costs. The costs are attributed to the annualized cost of the initial acquisition plus the annual operations and maintenance cost.

The completion of the benefit-cost ratio analysis is the final step involved in our life-cycle cost estimate. Using the results of this section, along with a synopsis of the other process steps, we should summarize the results for the decision maker. This will form the cover for individual technology economic analysis reports. The bottom line will be the return on investment for the emerging technology.

Return on Investment for New Electroless Nickel Plating Bath Rejuvenation Process

Technology Summary : Electroless Nickel (EN) is routinely performed at USAF-ALCs as a means of providing corrosion resistance to aircraft parts. EN plating is an autocatalytic chemical reaction with reaction byproducts accumulating in the bath. With usage, the byproducts accumulation slows the plating rate and renders the bath inoperable. Traditionally, EN baths were dumped once a month, constituting a significant hazardous waste source from plating shops. Bath rejuvenation equipment has been developed that will remove byproducts and thereby extend bath life to a conservative assumption of dumping the bath once a year. This new process has the added benefit of consistent plating quality because of uniform bath composition over a prolonged period. The decision to deploy the process will remove hazardous waste from the EN process, which will eliminate the hazardous waste costs and risks associated with managing the waste disposal.

Capturing the Total Costs : *Associated with New Electroless Nickel Plating Bath Rejuvenation Process Vs Conventional Electrolytic Nickel Plating for 5ALC's*

Cost Category		Baseline (Electrolytic)	Emerging (Electroless)
(1) Direct Costs			
<i>Capital Expenses - Initial Acquisition</i>	Total Capital Investment	\$ 233,140.00	\$ 599,680.00
<i>Operations & Maintenance Costs</i>	Total Annual Costs	\$ 1,045,635.00	\$ 898,280.00
(2) Indirect Costs			
<i>Compliance Costs = Professional labor Insurance & Special Taxes</i>	Total Indirect Costs	\$ 143,395.00	\$ 33,435.00
(3) Liability Costs (EPA Manual, 1989)	Total Liability Costs	\$ 5,432,000.00	\$ 1,136,000.00
(4) Intangible Costs			
<i>Qualifiers & Irreducibles</i>			
o Decreased costs due to increased aircraft in-commission rate because of more consistent plating quality			
o Decreased costs due to increased sortie generation - more reliable nickel plated aircraft components			
o Decreased health maintenance costs due to reduction in exposure to hazardous material with bath rejuvenation process			
o Decreased costs due to improved relations with employees & surrounding community through hazardous material elimination			

Life-Cycle Cost Estimates:

- o The USAF will save \$539,000 to \$ 1,474,000 over ten years by using the new process instead of the baseline *without* considering the added environmental benefits.
- o The USAF will realize an internal rate of return of approximately 39% on the investment in the new process over the baseline considering direct costs only.
- o The benefit to cost ratio of the new process is approximately 1.20. The baseline process has a BCR of approximately 0.97.

Return on Investment: The USAF should save \$539,000 by implementing this new bath rejuvenation process and could save up to \$2,600,000 considering indirect and liability costs.

Conclusion

We can appreciate that we face a formidable challenge when using somewhat irreducible monetary values for less tangible considerations in return on investment (ROI) analysis, but what would happen if these- more difficult to quantify- values were completely omitted? When only easily quantifiable cost factors are used in the analysis, the importance of the seemingly irreducible factors may be totally neglected at great expense to the organization in the future. There will always be leniency toward technologies that have mostly tangible monetary benefits and require less capital upfront. Decision makers require a bottom line to either give the "go ahead" or "kill" the project. The focus of this challenge is to heavily emphasize the less tangible cost items in the discussion of a project, by assigning a reliable dollar value to these items, so that they may then become part of the bottom line and thus used to make the decision. A 1980 congressional committee concluded that "whenever some quantification is done - no matter how speculative or limited - the number tends to get into the public domain and the qualifications tend to get forgottenThe number is the thing (DeGarmo, 1993: p.508)."

In order to face these challenges squarely, we have attempted to specify the environmental cost problem from a viewpoint at least as broad as the perspective of those who pay the costs and those who receive the benefits. When an environmental problem is totally confined to the internal workings of an organization, for example, it might be appropriate to concentrate on elements that only generate capital expenditures, but when the problem goes beyond that point it begins to take on elements that require a broader vantage point (U.S. EPA, 1994: p.8) This required assembling environmental cost information to be filtered for relevancy to the achievable goals of the organization. External consequences that could become future liability costs to the organization were made part of the decision making criteria.

The decision criteria models will need to be expanded beyond the few limited statements presented in exhibit B of this report. The current matrix was presented to provide insight, into the type of questions we should ask, when trying to identify major cost factors associated with

the comparison of an emerging technology to a baseline. The next step will be to develop these models to a greater detail, so that we might increase our understanding of the context and performance of the comparative technologies. The models would still be most useful in a tabular or flowchart format, depending on the process and preference of the user. We want to filter out sufficient cost problem constraints to establish an abstract comparison of the technologies. As we have emphasized throughout the report, the decision criteria model must be solvable and representative of the situation at hand.

The practical application of the decision criteria was to guide the capture of total costs for both current practices and the emerging technologies. At this point, the principle caution would be to consider the source of the cost data. We have expanded the inventory of line item costs to include non-traditional considerations, which could lead to erroneous conclusions about the cost-effectiveness of a technology in a real world situation, unless proper care is taken to ensure that the cost data obtained is relevant, timely, and as objective as possible. This call for more work to update equations for predicting indirect, hidden, liability, and less tangible costs, and validating traditional capital cost with additional sources.

Calculating the return on investment for emerging environmental technologies can be accomplished with conventional economic analysis tools with few exceptions. We should use principled caution when defining the alternatives for subsequent analysis, focusing on the differences in emerging technologies and baseline processes, viewing the situation from a consistent perspective with common units of measure, considering all relevant cost data, making uncertainty explicit, and revisiting our analysis in an adaptive process. This calls for sensitivity analysis to consider all relevant time periods and discount rates. Finally, a careful presentation of the final result is required to make sure decision makers understand the qualifications that go along with the bottom line.

JAVA-BASED INTERACTIVE SIMULATION ARCHITECTURE FOR AIRBASE LOGISTICS
MODELING

S. Narayanan
Assistant Professor
Department of Biomedical and Human Factors Engineering

Wright State University
207 Russ Engineering Center
Dayton, OH 45435

Final Report for:
Summer Research Extension Program

Sponsored by:
Air Force Office of Scientific Research
Bolling Air Force Base, DC

and

Wright State University

December 1997

JAVA-BASED INTERACTIVE SIMULATION ARCHITECTURE FOR AIRBASE LOGISTICS MODELING

S. Narayanan
Assistant Professor
Department of Biomedical and Human Factors Engineering
Wright State University

Abstract

User interfaces in interactive simulations not only display the state of the simulated system, but also allow an analyst to interact with the executing simulation. As the simulation executes in real time or scaled time, users can modify the parameters and alter the dynamics of the simulated system. The major challenges in developing interactive simulations are in overcoming problems associated with computer hardware and software. In this research project, we have developed a portable, object-based interactive simulation architecture called Java-based architecture for developing interactive simulations on the web (JADIS-Web). The architecture is designed to overcome the hardware and software problems in developing interactive simulations. Through the architecture, multiple users can interact concurrently with an executing simulation from distributed locations through an Internet browser. The architecture integrates concepts from object-oriented programming, model-view-controller paradigm, graphical user interface design, and distributed computing in providing a portable and flexible interactive simulation infrastructure that can be executed on the Internet. This report discusses the components of the architecture and demonstrates its application to an aircraft repair time analysis problem in the domain of airbase logistics.

JAVA-BASED INTERACTIVE SIMULATION ARCHITECTURE FOR AIRBASE LOGISTICS MODELING

S. Narayanan

Introduction

With the advances in computing power and graphical user interfaces, there is an increasing interest in the area of visual interactive simulations (VIS). In VIS, interfaces serve not only to display the state of the simulated system, but also to allow an analyst to interact with the executing simulation (Bell, 1991; Bell & O'Keefe, 1987). As the simulation executes in real time or scaled time, the analyst can modify the parameters and alter the dynamics of the simulated system.

The VIS approach offers several potential advantages. O'Keefe (1987) outlines different perspectives of visual interactive simulations: statistical, decision support, and simulator. Under the statistical view, there is little or no user interaction with the simulation model during program execution. The interfaces under this mode are primarily for post-simulation animation or performance analysis (Bishop & Balci, 1990). Under the decision support perspective, emphasis is placed on what-if analysis by the user. A user can evaluate alternate scenarios through interaction with the simulation model. The interaction can be user initiated or model prompted. Prompting the user to make a scheduling decision is an example of model-prompted interaction. A situation where a user observes a critical situation in the simulated system and dispatches a constrained resource during the execution of the simulation program is an example of user-initiated interaction (Hurion, 1980). Under the simulator view, interactive simulation architectures can be used to develop human-in-the-loop simulations (Ammons, et al., 1988; Dunkler, et al., 1988). Such simulators can provide a powerful synthetic environment for training of human operators in complex systems. Interaction with a high-fidelity synthetic representation of the system can be effective in enhancing user understanding of the complexities of the large, dynamic system (Kirkpatrick & Bell, 1989).

The major challenges in developing interactive simulations are problems associated with computer hardware and software (Bell & O'Keefe, 1987). Bell (1991) highlights the historic struggle of the early VIS development efforts with advances in computer hardware. Early VIS systems including See-Why were developed for large main frames. Currently, personal computers and workstations have become the standard for systems development. Most VIS packages currently available are still hardware dependent and suffer from problems of portability.

Interactive simulations suffer from software problems as well. Several early interactive simulation packages were developed in FORTRAN (e.g., FORSSIGHT). Developmental interest has moved towards C and recently towards object-oriented languages (e.g., ProfiSEE in Smalltalk-80). While object-oriented

programming offers many advantages for simulation modeling in terms of modularity, software reuse, and natural mapping with real world entities (Narayanan, et al., 1996), their application to developing interactive simulations has not been widespread (Bell, 1991). The software to display the simulation model and to facilitate user interaction are often embedded in the simulation model. Such tight integration makes it difficult to maintain large simulation programs and pose limitations in the development of multiple interfaces to a simulation model. The coupling of the simulation model with the interface also makes it difficult for the concurrent development of simulation models and their user interface.

The central thesis of this research is that developments in distributed computing offer a significant potential in overcoming the hardware and software problems with the interactive simulation methodology. We describe an architecture that integrates concepts from object-oriented programming, concurrent processing, and graphical user interfaces (GUI) to provide a powerful design approach to interactive simulations. The architecture called JADIS-Web (Java-Based Architecture for Developing Interactive Simulations on the Web) is portable, object-oriented, and supports development of interactive simulations. The simulation model and the user interface are separate processes. Through our architecture, users can interact concurrently with the simulation from distributed locations through a Java-enabled Internet browser. We present the design goals, discuss the architectural components, and outline the application of JADIS-Web to an aircraft repair time analysis problem in the domain of airbase logistics.

Methodology

We describe the methodology in terms of design goals, implementation of the architectural components, and application of JADIS-Web.

Design Goals

There were four major goals of this research effort. First, the components of JADIS-Web are designed such that they can be assembled rapidly for implementing simulations and developing interfaces. Second, JADIS-Web is designed on the Model-View-Controller (MVC) paradigm (Goldberg, 1990), where the simulation model is separated completely from the graphical interface and user interactions. This mechanism of partitioning the model from the view and the controller is intended to support software reuse, facilitate code maintenance, and promote interface reconfigurability. Third, JADIS-Web is designed to support multiple views to the same underlying simulation model. Interfaces to simulations can be tailored according to the context of user interaction and should be designed to facilitate concurrent user interaction through an Internet browser. Finally, we want to design JADIS-Web such that it supports execution of simulations from multiple platforms with concurrent user interaction from distributed locations.

Components Implementation

Broadly, the JADIS-Web architecture consists of two major elements: (1) classes forming the application-independent portion and (2) modeling classes for the application domain. The application-independent portion comprises the simulation infrastructure, the interface infrastructure, and the communications infrastructure.

The elements of the simulation infrastructure include a random number generator, various standard statistical distributions, an event calendar which keeps track of future events, simulation clock, main simulation loop, and general queueing support. The interactive simulation infrastructure in JADIS-Web differs from most traditional discrete-event simulations in two major ways. First, the main simulation loop can operate in real-time or next event time transition mode. In traditional discrete-event simulations, the time transition takes place between one event and another ordered as a sequence on the event calendar. In interactive simulations, the simulation can operate in this mode or it can operate in real-time mode where the simulation clock corresponds to a real clock or a scaled version of a real clock. Second, user input can be obtained through interaction even while the simulation continues to execute. Most simulation languages have the capability of interruption where the simulation is halted and the user modifies some parametric aspect of the simulation process or the simulation model. In interactive simulations, the processes continue and system state can change even while the user makes decisions and alters the simulation model or process. JADIS-Web supports concurrent processing of the simulation process and the processing of user input. Therefore, JADIS-Web is useful in developing high-fidelity simulations that explicitly incorporate human supervisory control by presenting a real-time view of the system to the user (Ammons, et al., 1988). The JADIS-Web architecture can also be used to develop traditional discrete-event simulations for detailed output analysis of the system. The simulation is then set to operate in the traditional mode. Since JADIS-Web uses the MVC framework, a simulation model can be rapidly implemented with a limited graphical interface view of the state of the entities in the simulation.

The elements of interface infrastructure must provide the software building blocks to create different views and to accommodate user interactions with the simulation model. Many simulation views can be composed by assembling one or more graphical windows, menus, scrolling lists, pop-up boxes, push buttons, and graphical objects to visualize activities and state of the system. The JADIS-Web architecture contains several of these building blocks inherited from the Java language's abstract windowing toolkit and is specialized for simulation applications.

Users can develop interactive simulations in JADIS-Web by instantiating the simulation process from the simulation infrastructure and interfaces from the interface infrastructure through an Internet browser such as HotJava. The elements of the communication infrastructure in JADIS-Web enable the simulation model to send status updates to the different views and to receive input from the user through the interface views. The simulation must continue to execute even while sending and receiving messages. The communication

between the simulation and the interfaces in JADIS-Web occurs through Java's Remote Method Invocation (RMI) calls. Once the simulation process receives a message from an interface process, it must parse the input, interpret the message, and alter the state of the simulated system. For example, consider the situation where the user presses the exit button on the interface. The interface process will send the message "exit" to the simulation process. When the simulation process receives the input from the interface, it must parse the input to obtain the command "exit", interpret its meaning to realize that the message "exit" must result in an action to halt the simulation, and perform the desired action. Similarly, when the interface process receives a message from the simulation process, it must interpret the input and update the appropriate displayed object. Inter-process communication in the JADIS-Web architecture is designed to take place through RMI calls.

Figure 1 illustrates the RMI communication between simulation and interfaces in JADIS-Web. The communication between the simulator and the interface take place through the RMI layers that come as part of the Java programming language. On the server side are skeletons and on the client side are stubs. The figure shows two different types of interface objects instantiated as applets, which can be accessed through a HotJava browser.

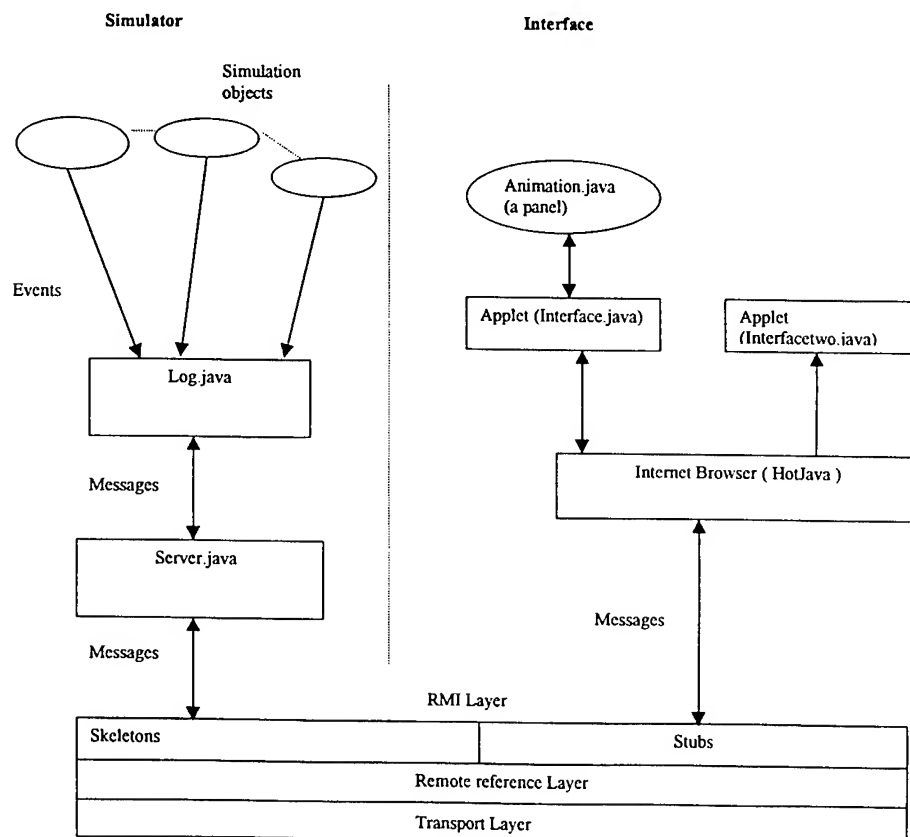


Figure 1. Remote Method Invocation communication between simulation and interfaces in JADIS-Web.

The simulation objects run on the server and communicate with the server process through a Log object. The server object registers the interface objects, sends initialization data to the interfaces, and also sends information on simulated events to the interfaces. All the interfaces are registered with the server object. The interface objects are initialized before any event begins and join the simulation event loop. An object of class Datastruct captures the current state of the simulation. The current state is passed to the interfaces when a new interface is begun after the simulation has started. Thus, a user can connect in to an executing simulation at any time. The interface that is used is initialized using the current simulated state as stored in the Datastruct object on the server. The server keeps track of a list of applets currently used in interacting with the simulation. Whenever a user opens the applet view to the simulation, the applet identifier is added to the list. When the state of the simulation object is altered, the state change information is conveyed to all the viewers. The simulation process has to be started by a user on the server. Once the simulation process is active on the server, a user can start the simulation through an Internet browser. The inheritance hierarchy of the various classes implemented in JADIS-Web is described in the context of the application in airbase logistics.

Application

Airbase logistics is a large and complex domain involving logistics processes that support aircraft sortie generation at operational airbases. For fighter aircraft, a sortie is the takeoff, mission execution, and landing of a single aircraft. Several aircraft may be required to fly together in a mission. Airbase logistics involves aircraft maintenance, parts supply, and munitions loading (Popken, 1992). Models of logistics processes are useful in analysis for aircraft acquisition planning, maintenance personnel allocation, and theater-level supply redistribution.

In an airbase, there are aircraft of different kinds with varying configurations and capabilities. An aircraft is comprised of several subsystems. A typical fighter aircraft, for example, has over 300 subsystems. Sortie take-off times can be scheduled in a variety of ways from uniform random generation, flying when refueled and ready, to a specific launch schedule. Each sortie specifies the number of aircraft required, the type of each aircraft, and the details of the mission. While the aircraft is in operation one or more of its subsystems may fail. When a subsystem of an aircraft fails, it is sent to the maintenance for repairs.

In a typical Air Force squadron or wing, there will be a pool of manpower assigned to maintenance. Within this pool will be a variety of specialties which correspond to areas in which the technicians are certified to perform repairs. Each repair evaluation may require aerospace ground equipment (AGE), test equipment, or special tools. Most repairs also require replacement parts.

For each configuration of aircraft, manpower, equipment, and spares, there will be a wide range of sortie generation criteria that can be satisfied. The challenge is to determine if any given set of sortie requirements can be sustained for a period of time without generating excessive resource queue wait times. Each time an aircraft cannot fly due to repair problems, it is considered a maintenance abort. Simulation studies are useful to determine an efficient mix of logistics resources including spare parts, personnel, support equipment, and facilities to achieve a desired sortie rate (Boyle, 1990). Various related performance measures include maintenance cost, sorties completed, sorties aborted, facility utilization, and personnel utilization (Carrico & Clark, 1995; Carrico et al., 1995). The design and implementation of Java classes to represent the entities in this system and to specify their interaction are discussed in the following paragraphs.

The development of the JADIS architecture is driven by the desire to simplify the process of creating portable, interactive simulations. In order to accomplish this goal, we applied a set of design principles to translate our conceptual model of airbase logistics to the implementation of software abstractions and interfaces to the simulations. The design principles are as follows:

1. Simulation objects in JADIS should have an obvious correspondence to the resources, material, and logistic processes in the airbase logistics domain. Through object-oriented programming it is possible to develop software abstractions in simulations that have a direct correspondence with real world objects (Narayanan et al., 1996). In the application of JADIS to airbase logistics modeling, we exploited the natural mapping and modularity features of object-oriented programming and developed a large number of Java classes such as *Aircraft*, *Hangar*, *Spares*, and *Equipment* that have a direct mapping to real world entities and logistic processes.
2. In the JADIS architecture, objects that represent decision making are designed to be distinct from physical objects and information storage objects. In applying JADIS to airbase logistics, physical objects such as *Aircraft* are distinguished from decision making objects (e.g., *ResourceManager*) and information storage objects (e.g., *ResourceStatistics*). Since simulations are built to study the effects of complex decisions, by decomposing the decisions, the data used by the decision logic, and the results of the decisions on the physical system in a structured manner, analysis of these systems are likely to be facilitated. The approach of making the physical-control-information decomposition has been successfully applied by several researchers in object-oriented simulations of large manufacturing systems (Adiga & Glassey, 1991; Mize et al., 1992; and Narayanan et al., 1992 & 1996). Hence,

applying a similar principle in modeling large, complex, and dynamic airbase logistics systems is appealing.

3. The components of the JADIS architecture are designed such that they can be assembled rapidly for implementing simulations and for prototyping user interfaces to interactive simulations. The hierarchy of classes permits modeling at different levels of abstraction. Both on the simulation side and the interface side, the hierarchy is structured to facilitate successive refinement. In airbase logistics, for example, a modeler can construct an initial model at the air base level and then refine the representations to model systems at the hangar level. Similarly, on the interface side, information can be presented hierarchically. The analyst can get to view the overall dynamics of the system and if desired could then look at the details of the individual components. The feature of hierarchic presentation of information is illustrated in the context of an air craft maintenance problem in the next subsection.
4. The interface components of the JADIS architecture are developed to feature a standard look and feel of conventional windowing system. On UNIX systems, the interface follows the framework of Motif window manager. On PCs, the interface follows the framework of Microsoft Windows, and on Macintoshes, it appears as a typical Macintosh application. This capability is derived primarily from using the Java programming language.

Figure 2 shows the inheritance hierarchy of the simulation classes in JADIS-Web. The notation used is a variation of UML in the static structure diagram (Unified Modeling Language) (UML document set, 1997). In the notation, a rectangle represents a class. A dash dotted rectangle is an abstract class, a dotted rectangle shows a Java interface, and the triangle shows the superclass at the apex and subclass at the lower end of the line. All classes in JADIS are subclasses of the base Java class `Object`. In addition, there is an abstract class `SimBase` from which several of the simulation infrastructure classes are inherited. Class `Distribution` encapsulates a portable random number generator using the linear congruential method (Law & Kelton, 1991). Classes `Exponential` and `Uniform` use the inverse transformation method in generating exponential and uniform distributions respectively. Class `Rnormal` generates a standard normal distribution using the composition method described in Brantley, Fox, and Schrage (1987, p.318). Class `Normal` generates a normal distribution with a given mean and variance by transforming the standard normal.

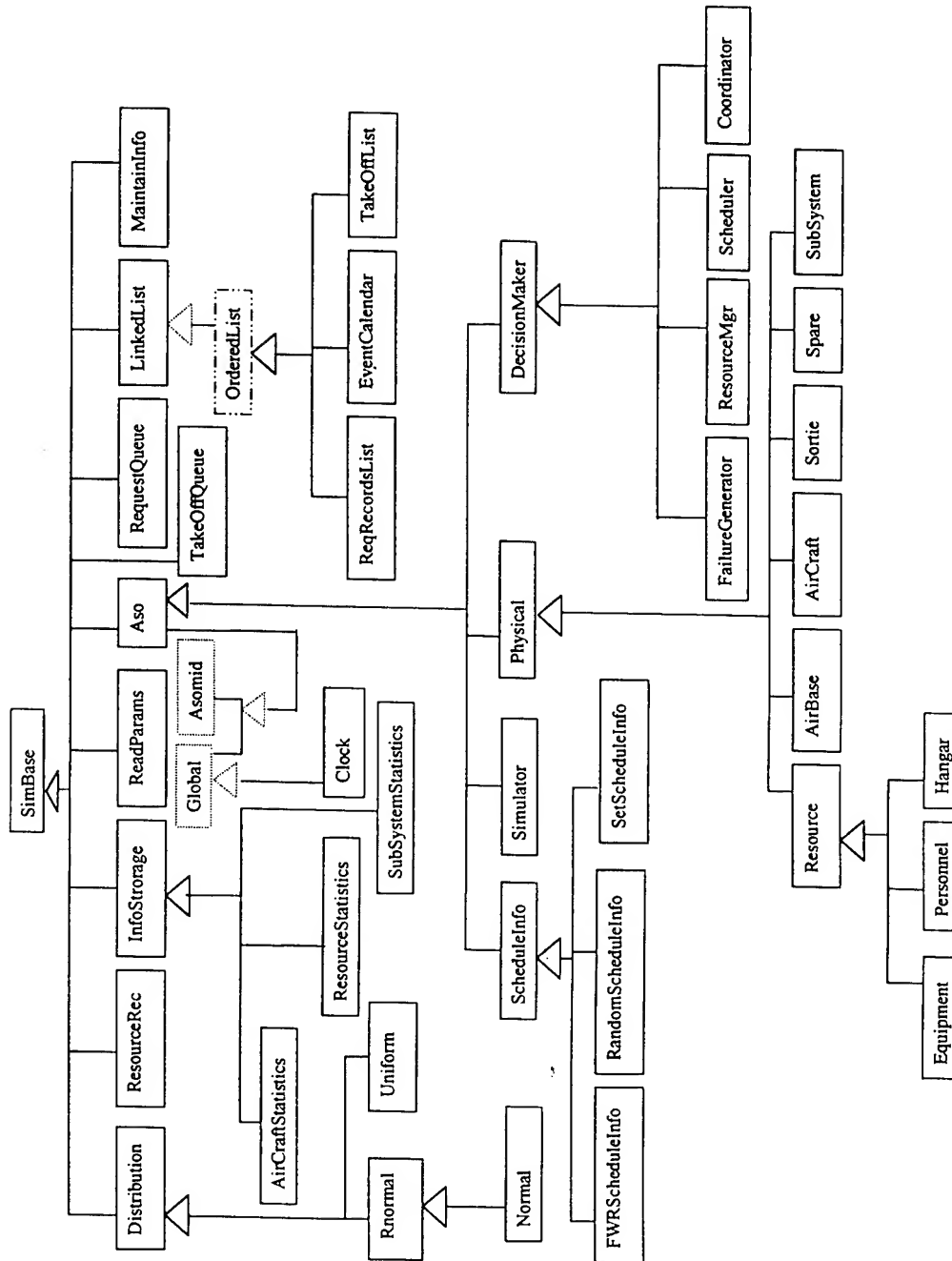


Figure 2. Inheritance hierarchy of the simulation classes in JADIS-Web.

Class `Clock` encapsulates the simulation clock. `Clock` has an `updateClock` method which updates the simulation clock to the next event time if the simulation is not operating in real time or updates the clock in microseconds corresponding to the computer system clock. Classes `LinkedList` and `OrderedList` are queueing utilities available in JADIS. Class `EventCalendar` keeps track of the details of the events including information about the event ordered by the time when it needs to be executed. Events which are placed on the `EventCalendar` must be encoded as methods of class `ActiveSimulationObject` or its subclasses. Class `Main` encapsulates the main simulation loop in JADIS. The main loop generates a thread to obtain input from the interface process and creates another for the simulation process to continue to execute. The main simulation loop invokes an event from the `EventCalendar` at the scheduled time and updates the simulation clock appropriately. Class `Simulator` is a subclass of `ActiveSimulationObject` and has methods to initialize the simulation parameters and exit at the end of the simulation.

Objects that encapsulate events in the simulation are subclasses of `ActiveSimulationObject`. These include physical objects such as `Aircraft`, `Subsystem`, `Spare`, `Sortie`, `Airbase`, and `Resources` such as `Equipment`, `Hangar`, and `Personnel`. The physical objects have a one-to-one mapping to objects in the real world. Class `Aircraft` is a representation of aircraft in an airbase and is comprised of several `Subsystems`. Class `Spare` represents consumable spare parts used during maintenance. Class `Sortie` models sorties generated during a time horizon. Class `Airbase` is a collection of several entities including `Aircraft`, `Spares`, and `Resources` such as `Equipment`, `Hangar`, and `Personnel`. Class `Equipment` represents aircraft ground equipment needed for maintenance operations. Class `Hangar` represents a hangar in an airbase and class `Personnel` represents maintenance operators.

Class `DecisionMaker` and its subclasses encapsulate logistical decision making. Subclasses of `DecisionMaker` include `ResourceManager`, `Scheduler`, `FailureGenerator`, and `Coordinator`. The `Scheduler` generates sorties for an airbase. The `FailureGenerator` enables subsystems in aircraft to fail according to their failure behavior. The `ResourceManager` controls the handling and distribution of all resources including equipment, hangar, and personnel needed for maintenance. The `Coordinator` is an overall airbase controller responsible for controlling the movements of various physical objects in an airbase. There is at least one instance of all the decision making classes in any simulation of airbase maintenance operations.

Class `InformationStorage` and its subclasses encapsulate data associated with the simulation. Subclasses of `InformationStorage` include `ResourceStatistics`, `MaintenanceInfo`, `AircraftStatistics`, `SubsystemStatistics`, and `ScheduleInfo`. Class `MaintenanceInfo` encapsulates data associated with the maintenance operations including type of failure, repair time, and the necessary type and number of personnel, spares, and equipment. Class `ScheduleInfo` encapsulates information associated with the sortie generation. There are three subclasses of `ScheduleInfo`: `SetScheduleInfo`, `RandomScheduleInfo`, and `FlyWhenReadyScheduleInfo`, each encapsulating sortie information according to the appropriate mode of sortie generation. Classes `ResourceStatistics`, `AircraftStatistics`, and `SubsystemStatistics` all encapsulate statistical information of relevant performance measures gathered during the execution of the simulation program.

Figure 3 shows the inheritance hierarchy of interface and communication classes in JADIS-Web. The abstractions comprising the interface infrastructure include the main interface process and building blocks such as windows, menus, scrolling lists, pop-up boxes, and push buttons which are useful in developing an interface to an interactive simulation. JADIS classes in the interface infrastructure include `CommandEntry` useful for gathering user commands to the simulation through a text-based command line, `EventLog` is a scrolling list to output a log of the events occurring in the simulation, `Exit` is a push button to halt the simulation and close the interface, `PicWin` is useful to display icons of the simulated system, `PopUp` is useful to implement windows that pop up as a result of user action on the interface. Classes `GraphWin` is window used to display graphs of the simulated system's performance measures with class `Graphs` providing the drawing area canvas. Class `Animation` assembles all the necessary interface building blocks for a simulation. `Animation` has a method called `processEvent` which in turn invokes a `processEvent` method of displayed objects. Class `Interface` initiates the interface process and spawns another process to concurrently receive input from the simulation model. Users of JADIS typically create additional subclasses of the classes in the interface infrastructure to tailor it to the application domain. Class `Interface` is created as a subclass of `Applet`. The remote objects enable communication between the simulation and the interface.

Figure 4 illustrates the aggregation relationships between the JADIS-Web classes. The aggregation diagram shows the whole part relationship. In the diagram, a solid line is used from the part to the whole with filled diamond at the end of the path where it meets the whole element. For example, an `EventCalendar` contains several `EventRecord` objects. Similarly, a `PicWin` object contains an `Animation` object and an `Animation` object contains a `PicWin` object.

Over seventy classes comprise the software abstractions in JADIS-Web for the airbase logistics application. Java contains a utility called `javadoc` used to automatically generate source code documentation with hypertext link for Java code. The utility turns comments of code into hypertext markup language (HTML) code with links to the parent class and the overridden methods. The URL for the source code documentation of JADIS-Web and its application to airbase maintenance is in <http://isis.cs.wright.edu:1947/jadisWeb/airbase/tree.html>.

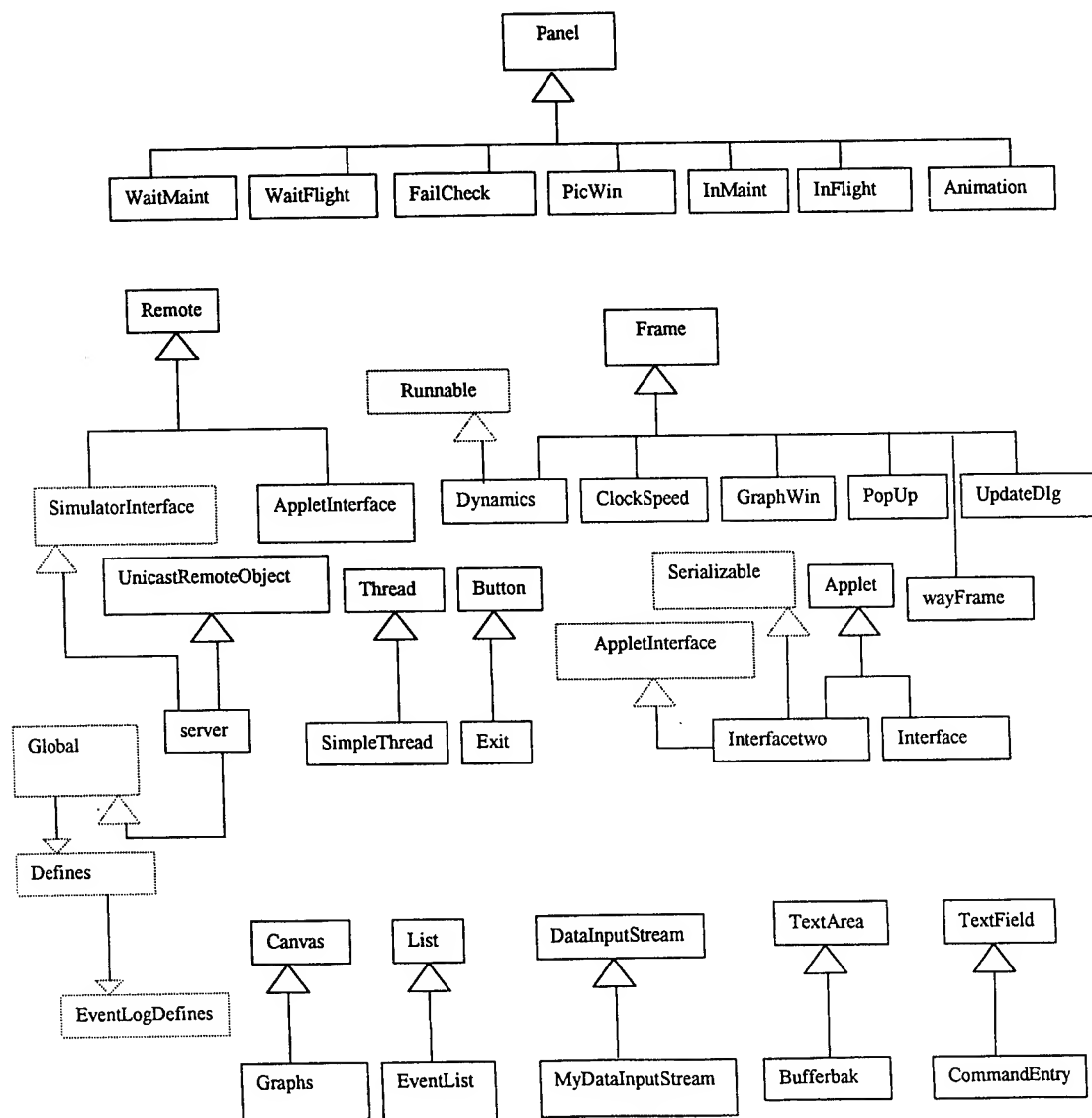


Figure 3. Inheritance hierarchy of the interface classes in JADIS-Web.

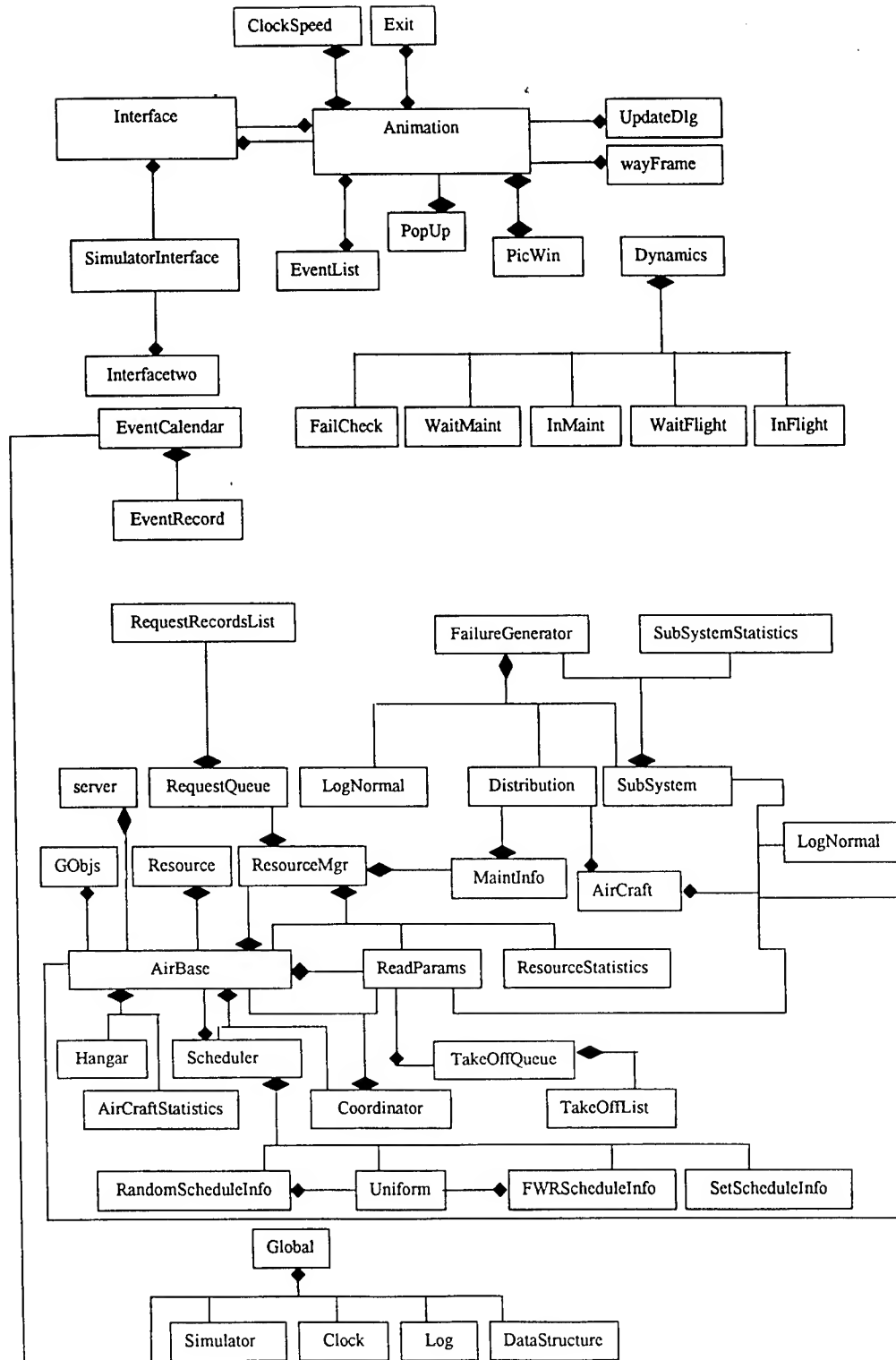


Figure 4. Aggregation relationships between the classes in JADIS-Web.

Once the simulation process is active, interfaces to JADIS-Web for airbase logistics modeling can be triggered using one of two URLs <http://isis.cs.wright.edu:1947/jadisWeb/airbase/interface1.html> or <http://isis.cs.wright.edu:1947/jadisWeb/airbase/interface2.html>. Several interface instances of these two interfaces can also be opened concurrently.

Figure 5 shows one interface to JADIS-Web for the airbase logistics application accessed through a HotJava browser. An analyst can view the system state and as shown in the snapshot, can also modify a system parameter such as personnel value at run time. User can also pause the simulation clock, alter sortie scheduling discipline and view various performance measures.

Figure 6 depicts another completely different interface to the same application. In this interface, users can primarily view the system performance measures displayed as dynamic bar graphs animation to the simulation.

Figure 7 depicts two similar interfaces opened at different times to the same underlying airbase simulation. Both views are synchronized through the inter-applet communication using RMI. Thus, the graphs on completed sorties show similar output at the same simulation clock time.

Figure 8 shows two different interfaces overlaid on top of each other, one interface shows the bar graph while the other shows the detailed first interface panel. Both interface views are tailored to different users and depict the same simulation model.

Similarly, Figure 9 illustrates two similar interfaces with a visualization of the simulation model placed together to emphasis view synchronization. Again, these interfaces were started at different times. Through RMI calls and the data structure to capture the state of the simulated system, both interfaces capture the simulation snap shot.

The specific airbase logistics application overcomes several limitations pointed out in our prior research (Narayanan, et al., 1997). First, the subsystems could have multiple failures. Second, the architecture can readily model airbases at the theater level. Third, dynamic resource constraints in terms of personnel, spares, and equipment were modeled. Users, at run time, can modify the number and type of personnel and equipment. The result is a more powerful testbed to develop models of airbase logistics processes useful for analysis on maintenance resource allocation and theater-level supply redistribution. As a result of the capability to run JADIS-Web on the Internet, analysts from different locations can connect in to the same underlying simulation and make dynamic changes to the simulation.

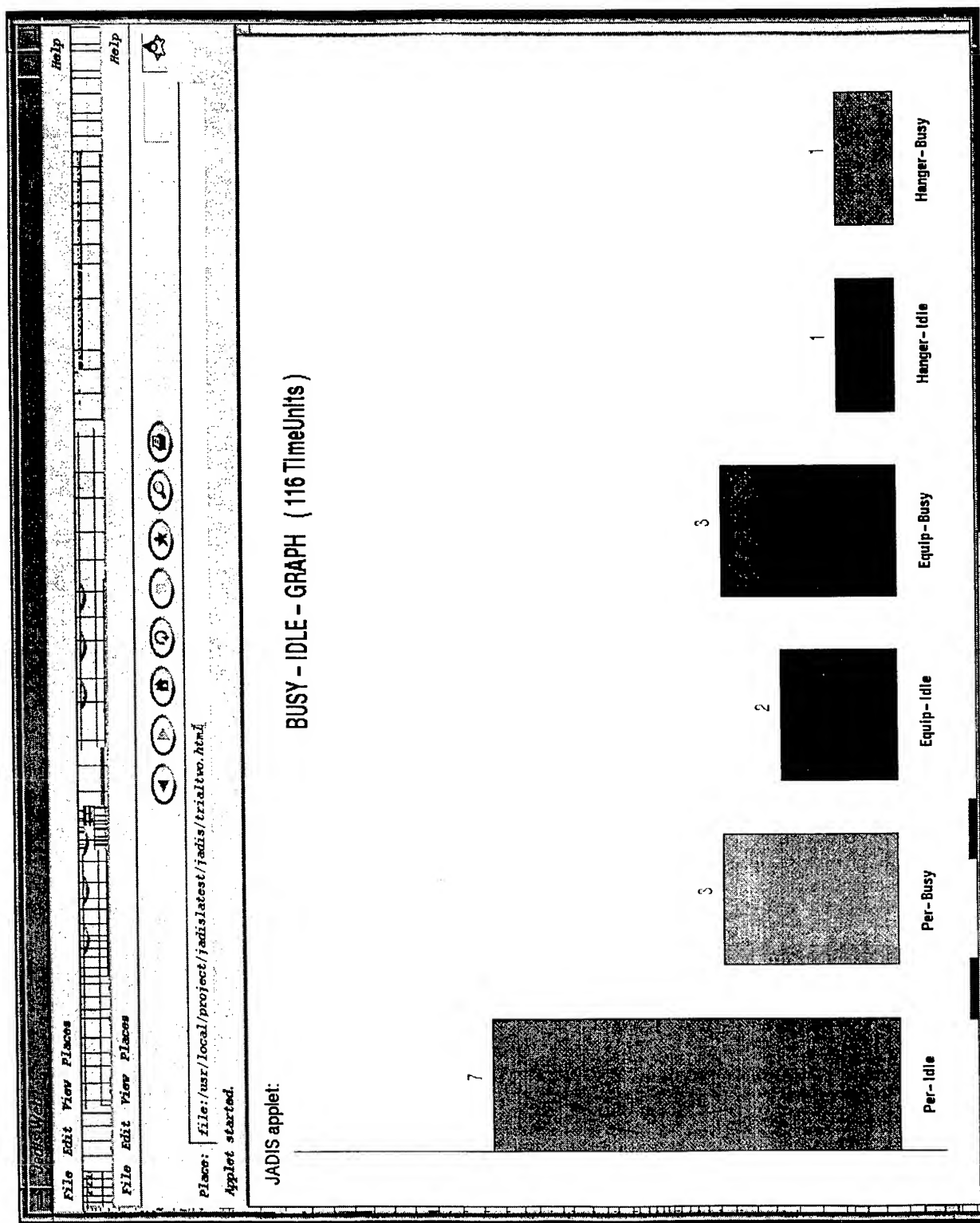


Figure 6. Another interface to JADIS-Web for the airbase logistics application.

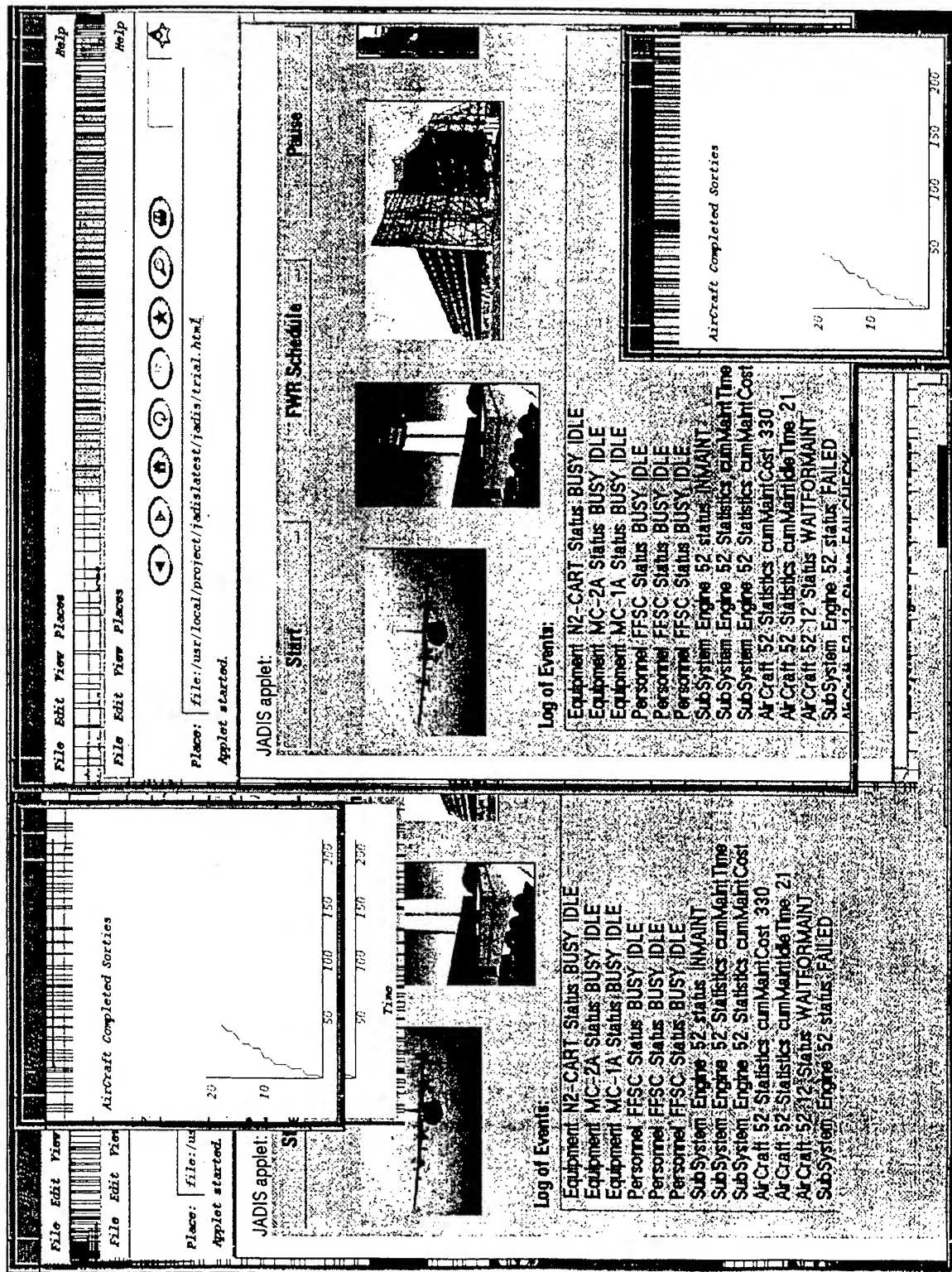


Figure 7. Two similar synchronized interfaces to the same simulation.

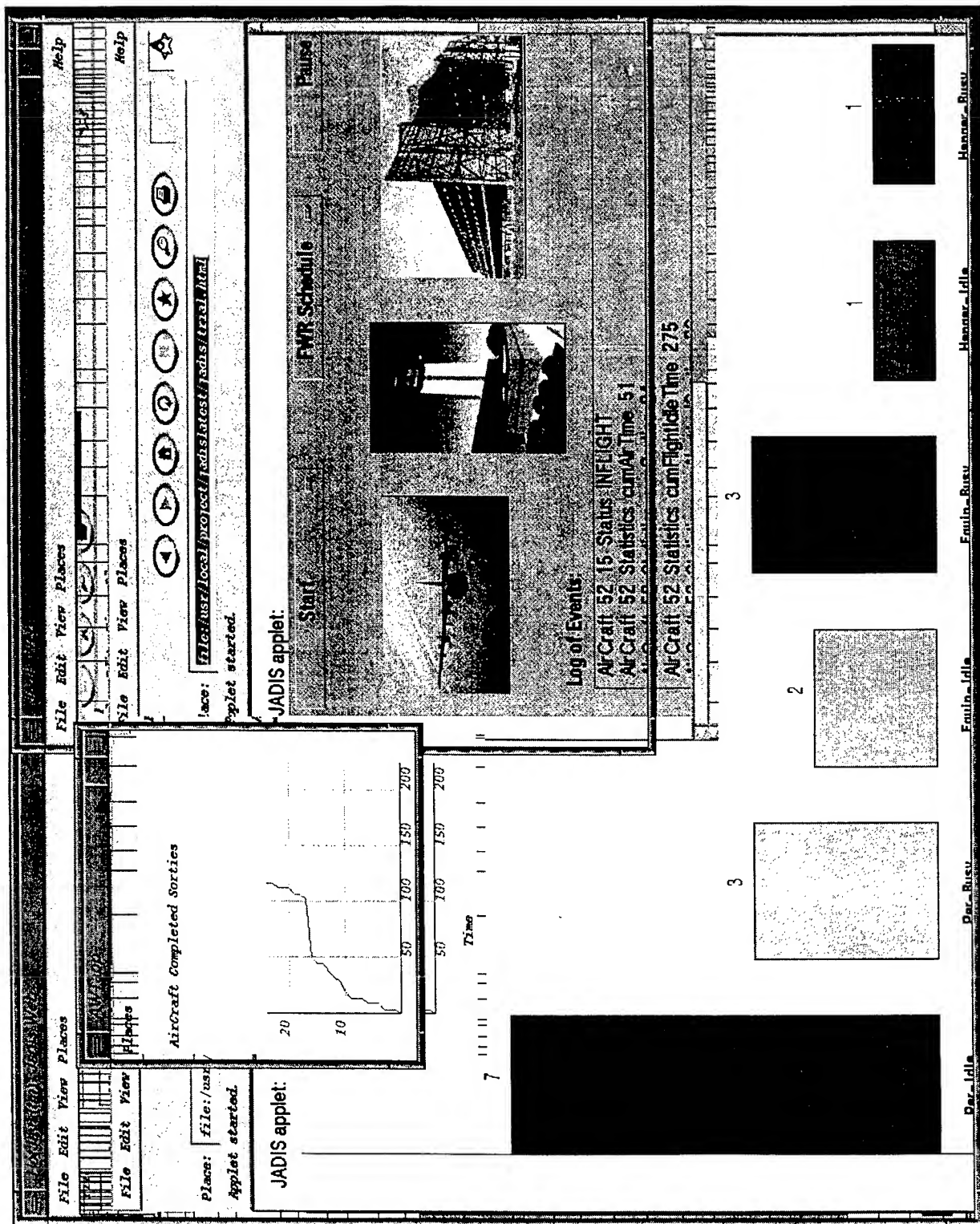


Figure 8. Two different interfaces to the same simulation model.

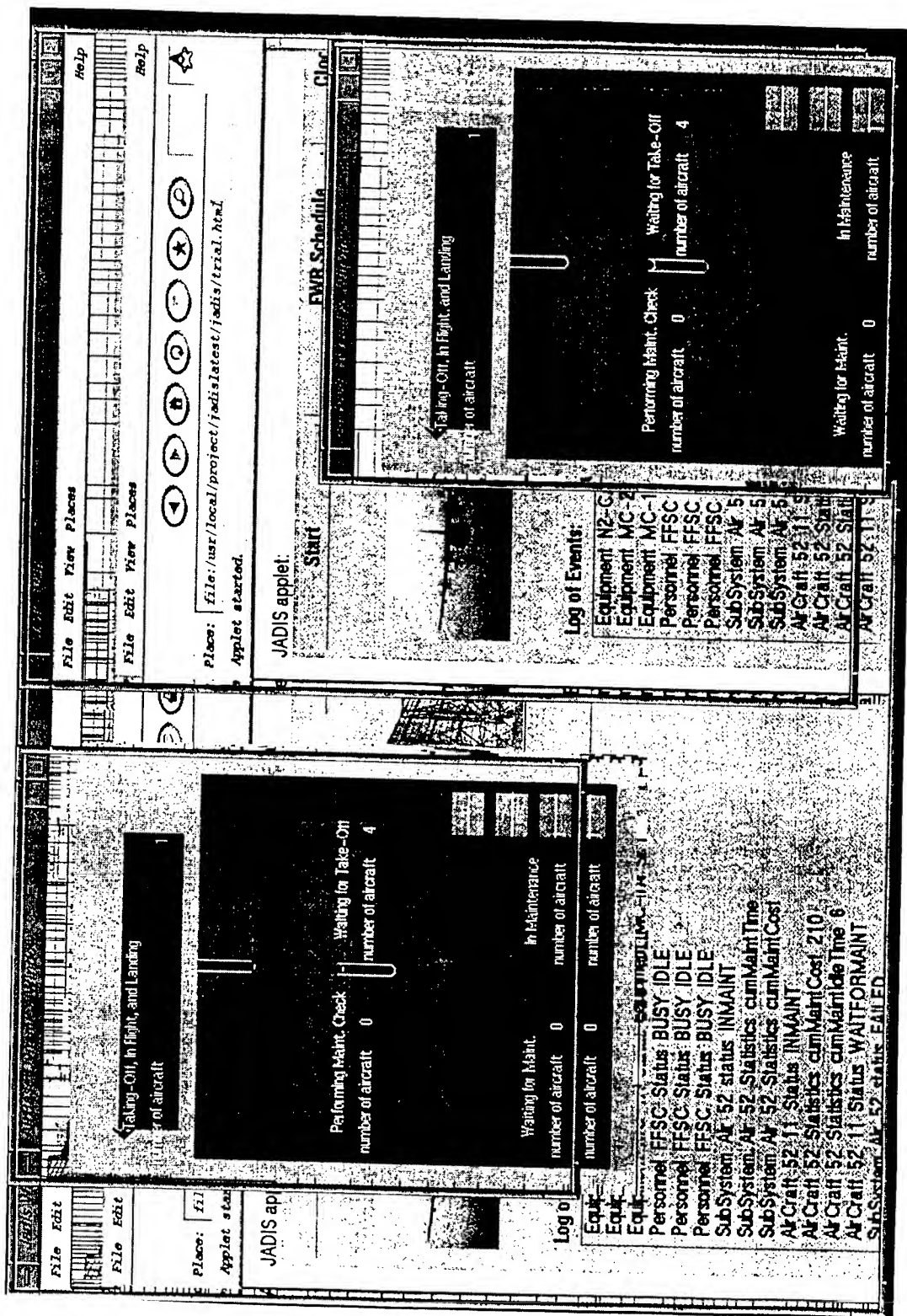


Figure 9. Two similar interfaces depicting synchronized visualization to the system.

Related Research

Recently, there has been an increasing interest in applying the World Wide Web infrastructure to simulation modeling and analysis (Fishwick, 1996). Examples of recent java-based simulations include Simkit (Buss & Stork, 1996) and Simjava (McNab & Howell, 1996). There are a few simulation applications written in Java as well. Example applications include modeling CPU disk performance (Fishwick, et al., 1997) and graphical turbine simulator (Reed, 1997). Most of these applications have used Java for portability, reuse, object-orientation, Internet programming, and graphical capabilities. The simulations mentioned above can all be run on the web using a Java-enabled browser. The simulations, however, seem to be completely embedded in the interface code and do not support concurrent multi-user interaction. Thus, inter-applet communication is not a salient issue dealt with by these research efforts. User interaction is also quite limited.

JADIS-Web research was in part motivated by the need to overcome the software and hardware problems associated with the interactive simulation methodology. Hardware-independent architectures that facilitate high-fidelity representation of the problem domain and enable rapid development of graphical interfaces to interactive simulations are critically important. JADIS-Web uses the Internet as a medium to overcome the portability problems. Multiple users from heterogeneous platforms can interact concurrently with the simulation. The interactive capability goes well beyond animating discrete-event simulations such as seen in most commercial packages. In JADIS-Web, users can not only alter the parameters of the simulation, but also modify system dynamics at run time.

Research Contributions and Limitations of the Study

The JADIS-Web architecture facilitates development of interactive simulations. This capability goes well beyond animating discrete-event simulations such as seen in most commercial packages. In JADIS-Web simulations, users can not only alter the parameters of the simulation, but also modify the system dynamics. For example, users in the airbase logistics simulation can alter the parameters of the maintenance resources and the mode of sortie generation at run time. Real-time human decision making can therefore be readily studied using JADIS simulations. While several researchers have acknowledged the value of interactive simulations in modeling and analysis of complex, dynamic systems, the development of interactive simulations have been hampered due to hardware and software problems (Bell, 1991). There is need for hardware-independent architectures that facilitate high-fidelity representation of the problem domain and enable the development of graphical interfaces to interactive simulations. We integrated concepts from object-oriented programming, distributed computing, and graphical user interfaces to interactive simulations.

JADIS-Web is hardware independent. Users can connect into a JADIS-Web simulation from a client side computer, which can be a PC, Macintosh, or a UNIX workstation. The only requirements are that they be

connected to the Internet and that they have a HotJava browser. The JADIS-Web simulation process itself must be run on a server with Java Development Kit.

The JADIS-Web architecture applies the Model-View-Controller framework in interactive simulations to facilitate reconfigurability of interfaces. Thus, in JADIS-Web, the interfaces to interactive simulations can be readily tailored to the types of users and the tasks for which users interact with the simulation. JADIS-Web, however, goes beyond the traditional implementation of the MVC framework. While the MVC framework provides a powerful metaphor for developing interactive simulations, practical implementations often lead to complicated, unwieldy class inheritance structures (Krasner & Pope, 1988; Shan, 1990). In JADIS-Web, the model and views are completely separated. The inheritance structure also maps well to the real world objects. The semantics of how displayed objects are updated is encapsulated well within the class representation. In traditional MVC, a model broadcasts that its status has changed, all views and controllers tied to that model are required to query it to discover exactly what the change is before they can update themselves. Finally, in contrast to the polling protocol applied in the traditional MVC, JADIS-Web applies a process-based, event-driven protocol which maps well with simulations where behavior is represented as events occurring at different time units. Interactive simulation architectures such as *ProfiSEE* which are implemented in Smalltalk use the traditional MVC framework and support reconfigurability of interfaces. Other interactive simulation architectures do not use the MVC framework.

The JADIS-Web architecture also enables an analyst to run the simulation and interfaces to it concurrently on multiple machines. This feature of concurrent processing is valuable in harnessing the power of distributed, parallel, computing systems. Existing interactive simulation architectures do not appear to have the capability of distributed, concurrent processing.

In the application of JADIS-Web to airbase logistics simulation, we developed a hierarchy of Java classes based on an extensive domain analysis and a set of software design principles. The architecture enabled rapid development of an interactive simulation for an airbase repair time analysis problem. A major strength of the JADIS-Web architecture is the decomposition between physical, decision making, and information storage objects to enhance its applicability to what-if analysis. Starting from the basic application-independent JADIS-Web infrastructure, it took about one person month to design and implement a large interactive logistics simulation for a prototypical application. This includes the time to develop the simulation model and implement appropriate user interfaces. It is straight forward to tailor the architecture to a class of similar problems. Based on our development experience using the JADIS-Web architecture, we estimate that it would take less than three person weeks for a developer with basic programming experience in C++ or Java to apply JADIS-Web to other similar problems in airbase logistics simulation.

The current implementation of JADIS-Web has a few limitations as well. First, the RMI system used for communication between the simulation and the interfaces limits the interface to be viewed using a HotJava

browser. Current versions of Netscape and Internet Explorer need to be extended through patches to facilitate their use to view the JADIS-Web interface. HotJava browsers, however, are available freely for a number of computing platforms. Second, in this research, we have not focused our efforts on making the JADIS-Web architecture compliant to the emerging standards on High Level Architecture (HLA), which is gaining a lot of attention in the Distributed Interactive Simulation (DIS) community (IEEE, 1993). Third, the reuse of the classes at the theater level has not been investigated in this study. Finally, the speed of the RMI system in conjunction with a HotJava browser for this application needs to be systematically evaluated.

Conclusions

Interactive simulation is an effective methodology for systems analysis of large, complex systems. We have applied Java programming language and integrated concepts from object-oriented programming, model-view-controller, and distributed computing to develop JADIS-Web, an architecture to facilitate development of interactive simulations on the Internet. Using JADIS-Web, simulations can be implemented as a Java application and their interfaces are implemented as Java applets that can be viewed using an Internet browser. The simulations and the interfaces are hardware independent. Multiple users can connect in to the same underlying simulation executing on a continuous basis. Users can concurrently modify the parameters of the simulation at run time.

The JADIS-Web architecture was evaluated for an aircraft repair time analysis problem in the domain of airbase logistics. The classes for this application were based on principles designed to enhance reuse, exploit natural mappings, and rapidly test different decision-making strategies. The resulting application is an interactive visual simulation accommodating active human interaction for aircraft maintenance manpower and spares analysis.

Our research contributes to the area of interactive simulations in several ways. The JADIS-Web architecture offers a solution to the hardware and software problems encountered in interactive simulation development. Through application of the Model-View-Controller framework, simulation model development and interface design can take place concurrently thereby potentially reducing the simulation development life-cycle cost. The architecture facilitates the study of human interaction with complex systems by providing a test bed to investigate the effectiveness of tailored views to interactive simulations. JADIS-Web can be used to generate a high-fidelity synthetic environment for training human operators in complex systems. The airbase logistics problem studied in evaluating the JADIS-Web architecture appears to be a ripe application domain for implementing interactive simulations.

Future research extensions include making JADIS-Web HLA compliant, evaluating scalability of the RMI system used for communication between the simulation and interfaces, and further developing software modeling abstractions that can be highly reused at the theater level.

References

- Adiga, S. & Glassey, C. R. (1991). Object-oriented simulation to support research in manufacturing systems. *International Journal of Production Research*, 29 (12): 2529-2542.
- Ammons, J. C., Govindaraj, T., & Mitchell, C. M. (1988). A supervisory control paradigm for real-time control of flexible manufacturing systems. *Annals of Operations Research*, 15: 313-335.
- Bell, P. C. (1991). Visual interactive modelling: The past, the present, and the prospects. *European Journal of Operational Research*, 54, 274-286.
- Bell, P. C. & O'Keefe, R. M. (1987). Visual interactive simulation - History, recent developments, and major issues. *Simulation*, 49(3):109-116.
- Bishop, J. L. & Balci, O. (1990). General purpose visual simulation system. *Proceedings of the 1990 Winter Simulation Conference*. 504-512.
- Boyle, E. (1990). LCOM explained. Technical report, *AFHRL-TP-90-58*, Air Force Human Resources Laboratory, Wright-Patterson Air Force Base, OH.
- Brantley, P., Fox, B. L., & Schrage, L. E. (1987). *A Guide to Simulation*, 2nd Edition, Springer-Verlag, New York.
- Buss, A. H., & Stork, K. A. (1996). Discrete-event simulation on the world wide web using Java. *Proceedings of the 1996 Winter Simulation Conference*, San Diego, CA, 780-785.
- Carrico, T., Clark, P. K., Shute, N. J., and Zahn, E. A. (1995). Integrated Model Development Environment (IMDE) multi-function aerospace support system. Technical report, *AL/HR-TR-1995-0186*, Armstrong Laboratory, WPAFB, Dayton, OH.
- Carrico, T. & Clark, P. K. (1995). IMDE support for Air Force logistics. Technical report, *AL/HR-TR-1995-0187*, Armstrong Laboratory, WPAFB Dayton, OH.
- Dunkler, O., Mitchell, C. M., Govindaraj, T., & Ammons, J. C. (1988). The effectiveness of supervisory control strategies in scheduling flexible manufacturing systems. *IEEE Transactions on Systems, Man, and Cybernetics*, SMC-18, 223-237.

- Fishwick, P. A. (1996). Web-based simulation: some personal observations. *Proceedings of the 1996 Winter Simulation Conference*, San Diego, CA, 772-779.
- Fishwick, P. A., Belk, M., & Spatz, B. (1997). An interactive web simulation of CPU/Disk performance. Available on <http://www0.cise.ufl.edu/~fishwick/CPUDISK>.
- Goldberg, A. (1990). Information models, views, and controllers. *Dr. Dobbs's Journal*, July, 54-61.
- Hurion, R.D. (1980). An interactive visual simulation system for industrial management. *European Journal of Operational Research*, 5(2): 86-94.
- IEEE Standard for Information Technology. (1993). Protocols for distributed simulation applications: Entity information and interaction. *IEEE Standard 1278-1993*. New York: IEEE Computer Society.
- Kirkpatrick, P.F. & Bell, P.C. (1989). Visual interactive modeling in industry: Results from a survey of visual interactive model builders. *Interfaces*, 19, 71-79.
- Krasner, G. E. & Pope, S. T. (1988). A cookbook for using the model-view controller user interface paradigm in Smalltalk 80. *Journal of Object Oriented Programming*, August/September, 26-49.
- Law, A. M. & Kelton, W.D. (1991). *Simulation Modeling and Analysis*, 2nd Edition, McGraw-Hill, New York.
- McNab, R., & Howell, F. A. (1996). Using Java for discrete-event simulation. *Proceedings of the Twelfth UK Computer and Telecommunication Performance Engineering Workshop (UKPEW)*, University of Edinburgh, 219-228.
- Mize, J. H., Bhaskute, H. C., Pratt, D. B., & Kamath, M. (1992). Modeling of integrated manufacturing systems using an object-oriented approach. *IIE Transactions*, 24 (3), 14-26.
- Narayanan, S., Bodner, D. A., Mitchell, C. M., McGinnis, L. F., Govindaraj, T., & Platzman, L. K. (1992). Object-oriented simulation to support modeling and control of automated manufacturing systems. In *Proceedings of the 1992 Western Multiconference*, San Diego: Society for Computer Simulation, 55-63.
- Narayanan, S., Bodner, D. A., Sreekanth, U., Govindaraj, T., McGinnis, L. F., & Mitchell, C. M. (1996). Research in object-oriented manufacturing simulations: An assessment of the state of the art. To appear in *IIE Transactions*.
- Narayanan, S., Schneider, N. L., Patel, C., Carrico, T. M., & DiPasquale, J. (1997). An object-based architecture for developing interactive simulations using Java. *Simulation*, 69(3), 153-171.

O'Keefe, R. M. (1987). What is visual interactive simulation? (and is there a methodology for doing it right?). In *Proceedings of the 1987 Winter Simulation Conference*. A. Thesen, H. Grant, & W. D. Kelton (Eds.), IEEE, Piscataway, NJ, 461-464.

Popken, D. A. (1992). An object-oriented simulation environment for airbase logistics. *Simulation*. 59(5): 328-338.

Reed, J. A. (1997). The Java gas turbine simulator. Available on: http://www-mime.eng.utoledo.edu/research/thermalsciences/jet_engine_simulation/jgts/JavaGasTurbineSimulator.html.

Shan, Y-P. (1990). MoDE: A UIMS for Smalltalk. University of North Carolina, Chapel Hill, *TR90-017*, DTIC.

UML Document Set. (1997). *UML Document Set Version 1.0*, Available on <http://rational.com/uml/start/index.html>.

DINITROTOLUENE BIODEGRADATION UNDER NITRATE REDUCING CONDITIONS

Barth F. Smets
Assistant Professor
Environmental Engineering Program

University of Connecticut
261 Glenbrook Rd, U-37
Storrs, CT 06268

Final Report for:
Summer Faculty Research Extension Program
Armstrong Laboratory

Sponsored by:
Air Force Office of Scientific Research
Bolling Air Force Base, DC

and

Armstrong Laboratory

January 1998

DINITROTOLUENE BIODEGRADATION UNDER NITRATE REDUCING CONDITIONS

Barth F. Smets
Assistant Professor
Environmental Engineering Program
University of Connecticut

Abstract

The mineralization kinetics of 2,4-dinitrotoluene by JS867 *Alcaligenes sp.* under varying degrees of oxygen limitation were examined. Batch growth experiments were initiated with ≈ 2.25 mg of 2,4-DNT and 15.63 (O_2 excess), 2.25, 1.5, 0.6, and 0.3 mg of oxygen. Complete 2,4-DNT mineralization was observed under oxygen excess with near stoichiometric release (83%) of nitrite. Average kinetic parameters were estimated based on a dual Monod model with 2,4-DNT and dissolved oxygen as growth limiting substrates, modified by incorporating the noncompetitive inhibition by NO_2^- . Under aerobic conditions, μ_{max} , K_{sDNT} , and K_{iNO} were $0.058(\pm 0.004) \text{ hr}^{-1}$, $3.3(\pm 1.3) \text{ mg 2,4-DNT/L}$, and $1.2(\pm 0.2) \text{ hr}^{-1}$, respectively. Nitrite accumulation negatively impacted the specific growth rate. At increasing oxygen limitation, the rates of 2,4-DNT disappearance and nitrite production decreased. Complete mineralization of 2,4-DNT was no longer observed. The test strain JS867 was able to use NO_2^- as a terminal electron acceptor when grown on glucose or succinate under anaerobic conditions. However, during growth on 2,4-DNT and under limiting O_2 conditions, JS867 did not use nitrite as an electron acceptor. The nearly constant ratios of DNT removed over NO_2^- released under various degrees of oxygen limitation suggested oxygenolytic denitration pathways. These observations suggest that the affinity of the terminal electron acceptor train for O_2 exceeds the affinity exhibited by the oxygenases. Oxygen limited DNT mineralization was (adequately) modeled using dual substrate limited kinetics incorporating non-competitive NO_2^- inhibition. Strain JS867 exhibited an average affinity for oxygen (K_{SO_2}) of $0.285(\pm 0.198) \text{ mg } O_2/\text{L}$.

DINITROTOLUENE BIODEGRADATION UNDER NITRATE REDUCING CONDITIONS

Barth F. Smets

Introduction

Dinitrotoluenes (DNTs) are anthropogenic compounds synthesized as precursors or byproducts in the manufacturing of commodity chemicals, toluene diamine, or the explosive TNT. U.S. production of toluene diamines, themselves precursors to toluene diisocyanate used in the manufacture of adhesives, sealants, and coatings, and polyurethane foams, require millions of pounds of DNT each year as a primary starting material (Agency for Toxic Substances & Disease Registry, 1989). Waste streams from mass production of TNT contain high concentrations of DNT which may enter soil and groundwater when improperly disposed. Due to military decommissioning, the close of military bases across the world may lead to the discovery of many new sites contaminated with TNT and DNT; and a treatment technology for the impacted soils and waters is needed.

Significant contamination of soil and groundwater with DNTs from industrial and military practices has prompted an interest in their cleanup. Because dinitrotoluenes are toxic, mutagenic and/or potentially carcinogenic they pose a human health risk (Marinkas, 1996).

Currently, soil and groundwater contaminated with DNT are treated by physical and chemical separations such as adsorption to activated charcoal, filtration, solvent extraction, or surfactant precipitation and incineration (Freedman, 1995). High costs and undesirable wastes products associated with traditional technologies hinder the disposal process of DNT laden soils.

Biodegradation of dinitrotoluenes, on the other hand, can result in complete mineralization of the compounds. Therefore, biochemical technologies offer an attractive alternative.

Biochemical Pathways for Anaerobic and Aerobic Transformations

Under both anaerobic and aerobic conditions, DNT can be biotransformed (Spain, 1995). Anaerobic biotransformation typically involves unspecific reduction of the nitro groups to nitroso, hydroxylamino, and eventually amine groups (Freedman, 1995; Spain, 1995; Noguera, 1996). The

potential accumulation of the highly reactive nitroso and hydroxylamino intermediates, which are more toxic than the parent compounds, plagues anaerobic processes for DNT biotransformation (Haigler, 1996).

Although several bacterial strains transform DNTs via nitro-reduction even under aerobic conditions (Freedman, 1995; Noguera, 1996) some strains have been isolated that can completely mineralize both 2,4-DNT and 2,6-DNT as a sole carbon and energy source through oxygenolytic denitration pathways (Spain, 1995). Aerobic biodegradation of DNT involves the incorporation of molecular oxygen into the aromatic ring with simultaneous or subsequent release of nitro groups as nitrite molecules.

The degradation of 2,4-DNT (①; Figure 1) by *Burkholderia cepacia* involves an initial dioxygenase attack producing 4-methyl-5-nitrocatechol (②, Figure 1) (Spanggord, 1991). The 4-methyl-5-nitrocatechol serves as the substrate for a monooxygenase that catalyzes the replacement and release of the second nitro group producing 2-hydroxy-5-methylquinone and finally 2,4,5-trihydroxytoluene (③, Figure 1). Ring cleavage of 2,4,5-trihydroxytoluene is mediated by an additional dioxygenase (Spanggord, 1991; Spain, 1995). Three moles of oxygen are needed as oxygenase substrates for NO_2^- elimination and ring cleavage; additional oxygen may be required as a terminal electron acceptor (TEA) for the complete mineralization of 2,4-DNT. Therefore, large amounts of oxygen are needed to completely mineralize 2,4-DNT.

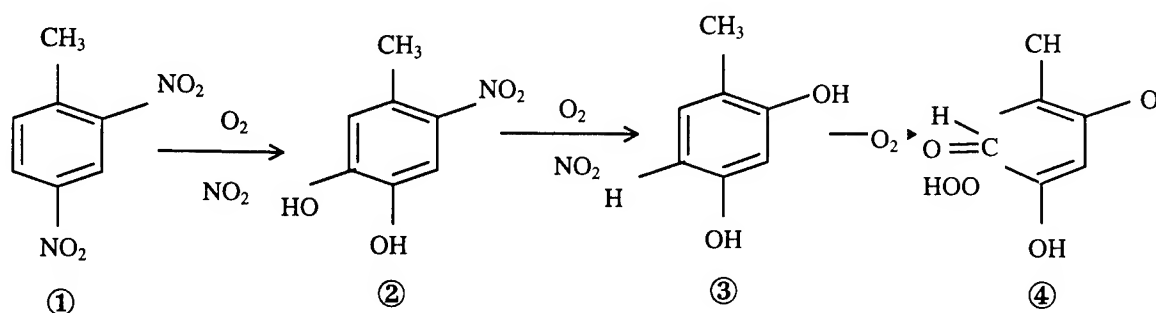


Figure 1 Sequential biodegradation of 2,4-DNT by an aerobic *Burkholderia cepacia* (after Spain, 1995). The enzyme cofactor requirement (NADH.H^+ and NADPH.H^+) is not indicated. ① 2,4-DNT ② 4-methyl-5-nitrocatechol ③ 2-hydroxy-5-methylquinone ④ 2,4-Dihydroxy-5-methyl-6-oxo-2,4-hexadienoic acid

End-Products of DNT Transformation

Anaerobic biotransformation of DNT produces highly reactive nitroso and hydroxylamino intermediates and therefore is not productive. The ultimate products of aerobic mineralization of DNT are

carbon dioxide, water, and nitrite (Haigler, 1996). If NO_2^- is oxidized to NO_3^- by abundant nitrifying populations, the end products of aerobic biodegradation of DNT are therefore completely innocuous to human and ecological receptors. However, nitrite concentrations can be inhibitory to bacterial growth (Almeida, 1994). Nitrite can interfere with energy conservation in aerobic bacteria by inhibition of oxygen uptake, oxidative phosphorylation, or proton-dependent active transport (Yarborough, 1980). Nitrite can act as an uncoupler, causing a collapse of the proton gradient (Yarborough, 1980). Therefore, the impact of nitrite accumulation, an end product of aerobic DNT mineralization, on the growth kinetics are to be examined.

Fate of Nitrogenous Oxides

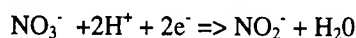
Removal of nitrite can occur through several mechanisms. In the absence of other nitrogen species, some of the nitrite released can be incorporated into biomass. If nitrifiers are present, nitrite can be oxidized to nitrate. Under low dissolved oxygen concentrations, denitrifiers may use NO_2^- as a TEA and reduce it sequentially to nitrogen gas. Although molecular oxygen is required for oxygenolytic DNT cleavage, under limiting DO conditions, it is conceivable that NO_2^- could be used as a TEA by facultative heterotrophs (including DNT mineralizers themselves). The use of nitrite as the TEA offers many advantages: First, DNT mineralization would supply the nitrite needed. Second, nitrite is more mobile than oxygen in the soil making it more available. Third, elimination of nitrite through respiration could prevent nitrite toxicity. Finally, reduction in total oxygen needed to completely mineralize DNT would decrease overall costs.

Denitrification

Denitrification is an anaerobic bacterial respiratory process that converts nitrate into nitrogen gas (Brock, 1994). Under oxygen limitations and when present, nitrate or nitrite can be used as a terminal electron acceptor offering a bioenergetic option for the cell (Zumft, 1992; Carter, 1995). The denitrification pathway is a sequential reduction of the nitrogenous oxides: $\text{NO}_3^- > \text{NO}_2^- > \text{NO} > \text{N}_2\text{O} > \text{N}_2$.

Four specific oxido-reductase enzymes facilitate the conversion of each step in complete denitrification (Sears, 1993). Nitrate reductase (NAR), nitrite reductase (NIR), nitric oxide reductase

(NOR), and nitrous oxide reductase (NOS) sequentially reduce nitrate to nitrogen gas. The first step in denitrification is the conversion of nitrate to nitrite (Zumft, 1992; Brock, 1994):



Bacteria can contain three types of nitrate reductases; a membrane bound dissimilatory respiratory nitrate reductase (NAR), a soluble assimilatory-type nitrate reductase (NAS), and a dissimilatory periplasmic nitrate reductase (NAP) (Zumft, 1997).

Under anaerobic conditions, dissimilatory nitrate reductase synthesis is induced when nitrate is present (Krul, 1976). The active site of the enzyme is located on the inner side of the cytoplasmic membrane (Averill, 1996). Oxygen has been found to inhibit the transport of nitrate across the cytoplasmic membrane (Hernandez, 1988). The periplasmic nitrate reductase is present and active under aerobic conditions and therefore is linked to nitrate reduction in the presence of oxygen (Hernandez, 1988; Sears, 1993).

Effects of Oxygen on Denitrification

Although some bacteria lose the ability to denitrify in the presence of molecular oxygen (Robertson, 1984), aerobic denitrification has been widely documented (Krul, 1976; Meiberg, 1980; Hochstein, 1984; Bell, 1991; Arts, 1995). The degree to which oxygen affects a microorganism's ability to denitrify varies greatly from strain to strain (Bonin, 1991; Patureau, 1994; Thomas, 1994). For example, *Thiosphaera pantotropha* can denitrify under completely aerobic conditions (Robertson, 1988) and certain *Alcaligenes* strains can denitrify under conditions of 50% air saturation (Robertson, 1988; Korner, 1989).

Synthesis and Activity of Each Enzyme in Denitrification Pathway

In general, when denitrifying strains are shifted to aerobic conditions, the rate of denitrification decreases, production of N_2 decreases, and N_2O , NO , NO_2^- accumulation occurs (Patureau, 1994). Several mechanisms of oxygen inhibition have been documented (Wu, 1994): oxygen can suppress the activity and/or synthesis of the denitrification enzymes (John, 1976; Stewart, 1988; Remde, 1991; Thomas, 1994); oxygen can compete for a limited supply of electrons (Hochstein, 1984); oxygen can inhibit nitrate transport

into the cell (Hernandez, 1988) or oxygen can prevent insertion of nitrate reductase into membrane (Hackett, 1981).

Production, sensitivity, and expression of reductases vary with oxygen concentration and denitrifying strain. In *Pseudomonas aeruginosa*, *Pseudomonas stutzeri*, and *Azospirillum brasilense*, NO production is more sensitive to oxygen than NO consumption. After synthesis, different nitrogenous reductases exhibit different oxygen sensitivities. In *Pseudomonas nautica*, NOS is more sensitive to oxygen than NAR and NIR (Bonin, 1989). NIR is more sensitive to oxygen than NAR and NOS in *Achromobacter cycloclastes*, while in *Pseudomonas stutzeri* NOS is synthesized continuously, even at air saturation (Korner, 1989). Maximum expression of the denitrification enzymes does not always coincide with completely anaerobic conditions. *Pseudomonas stutzeri* showed maximum expression of NIR and NOR at or around 0.6 mg of O₂ per liter (Korner, 1989). In *Thiosphaera pantotropha*, the enzymes of denitrification are also synthesized and active under aerobic conditions (Robertson, 1984). Some microorganisms can even use oxygen and nitrogenous oxides simultaneously as a TEA e.g. *Thiosphaera pantotropha*, *Comamonas sp.*, *Alcaligenes faecalis*, and *Pseudomonas nautica* (Bonin, 1991; Patureau, 1994; Robertson, 1995; John, 1976; Robertson, 1988).

Conclusion

Several bacterial strains can aerobically mineralize DNT. The biotransformation process requires large amounts of molecular oxygen and releases significant amounts of nitrite. The accumulation of nitrite may inhibit cell growth. In addition NO₂⁻ is a regulated pollutant. Many bacterial strains can reduce nitrite in the presence of oxygen. The potential for DNT degrading strains to remove nitrite through respiration at low oxygen concentrations could enhance biodegradation of DNT contaminated soils by eliminating high aeration costs and removing toxic nitrite.

There were four main objectives to this research. The first objective was to evaluate the denitrification potential of several DNT mineralizing bacterial strains. Second, the effects of limiting dissolved oxygen conditions on 2,4-DNT mineralization were examined. Third, the inhibitory effects of nitrite on the biodegradation of 2,4-DNT mineralization were examined. Finally, the kinetics of DNT

mineralization in aqueous batch experiments were described and the appropriate kinetic and stoichiometric parameters were estimated.

Material and Methods

Bacterial Inoculum

Alcaligenes sp. JS867, a bacterial strain known to degrade 2,4-DNT, was used for most experiments. It was pregrown at 30°C in shake flasks containing a mineral medium supplemented with 2,4-DNT. The medium contained XAD-7 Tenax beads (Sigma, St. Louis, MO) at 10 g/L to maintain a sub-toxic, aqueous concentration of DNTs. The mineral salts medium, termed BLKN, was free of inorganic nitrogen, and provided macronutrients and buffering capacity. In addition, strains JS871, JS872 (also DNT 2,4-DNT degrading strains), *Pseudomonas fluorescens* and *Pseudomonas aeruginosa* were used during screening.

Cell Maintenance

Freeze-dried DNT cultures of known 2,4-DNT mineralizing strains, JS867 (*Alcaligenes* sp.), JS871 (*Alcaligenes xylosoxidans*), and JS872 (*Burkholderia cepacia*), were obtained from Shirley Nishino (Air Force Research Lab, Tyndall AFB). Stocks were rehydrated and streaked on solid media containing 3mM 2,4-DNT and 10 g/L XAD-7 Tenax beads (Sigma, St. Louis, MO) in BLKN mineral media (Bruhn, 1987). Plates were incubated at 30°C and restreaked approximately every 6 weeks to maintain fresh working cultures.

HPLC Analysis

2,4-DNT concentrations were measured via high performance liquid chromatography (HPLC) separation followed by a UV-detection at 254 nm. The method used a C6-hexyl column (Spherisorb, Alltech, Deerfield, IL) and a solvent system consisting of 50% deionized water and 50% methanol.

Nitrite Analysis

Nitrite analysis was performed by a modified standard method (Eaton, 1995). A 0.7 ml sample was centrifuged at 14,000 rpm for 5 minutes. The supernatant was analyzed colorimetrically by mixing 4

ml of deionized water and 0.4 ml of sulfanilamide with 0.4 ml of sample. The solution was allowed to react for 5 minutes before 0.4 ml of N-(naphthyl)diethylenediamine was added. Samples were vortexed and allowed to react for 15 minutes prior to reading their absorbance at 543 nm using a UV-spectrophotometer.

Determining Denitrification Potential

Strains were grown aerobically in 10 ml TSB (Difco, Detroit, MI). Duplicate experiments were performed to examine both nitrate and nitrite reduction by each species. Test tubes containing ten ml of $\frac{1}{4}$ x TSB medium, supplemented with 0.01% NaNO_3 or 0.01% NaNO_2 and 0.17% agar were inoculated with 0.1 ml of individual overnight cell cultures. Aerobic control growth tubes to check inoculum viability containing ($\frac{1}{4}$ x TSB without nitrogenous oxides or agar) and negative control tubes containing ($\frac{1}{4}$ x TSB and 0.17% agar without nitrogenous oxides) were inoculated with overnight cultures as well. All test tubes were shaken vertically in a 25°C constant temperature room. The cultures were examined periodically (2, 4, 8, 12, and 24 hrs) during incubation for gas bubble (N_2) formation.

The reduction of nitrate to nitrite was determined colorimetrically by performing nitrite analyses. Formation of a purple color confirmed nitrate reduction. Nitrite accumulation with age of the culture results in an increase in color intensity. Decreasing color intensity indicates a further ability to reduce nitrite. If no purple color develops, zinc powder was added to reduce any nitrate present to nitrite. Color formation after zinc addition verifies inability to reduce nitrate.

Aerobic Batch Mineralization Experiments

Seventy-five ml of BLKN solution containing ≈ 30 mg/L 2,4-DNT was added to sterile 125 ml serum bottles. Bottles were inoculated with cell culture JS867, pregrown aerobically in BLKN containing 3mM 2,4-DNT and Tenax beads (10g/L), resuspended in BLKN. Vials were capped with rubber septums and aluminum crimp seals and incubated on a shaker table (150 rpm) at 30°C. Nitrite and DNT disappearance were monitored on 1 ml aliquots drawn by a syringe (B-D Disposable, polypropylene, 3 cc, Franklin Lakes, NJ) at various time intervals.

Use of Nitrite Released From Mineralization 2,4-DNT as TEA

To test whether nitrite released from the mineralization of 2,4-DNT could be used rapidly as a terminal electron acceptor, aerobic batch experiments were performed. Initial 2,4-DNT concentration was ≈ 13 mg/L. Serum bottles were incubated aerobically and monitored until removal of 2,4-DNT was complete. Upon DNT depletion aliquots of glucose or succinate stock solutions were added using a sterile syringe equipped with a $0.2\mu\text{m}$ filter at final concentrations of 10 mM and 6 mM, respectively. Anaerobic conditions were created by purging bottles with N_2 gas. Subsequently, samples were monitored every 12 hrs for nitrite disappearance.

Oxygen Limited Batch Mineralization Experiments

Seventy-five ml of a BLKN solution with ≈ 23 mg/L 2,4-DNT was added to sterile, 125 ml serum bottles. Bottles were inoculated with cell culture JS867, pre-grown aerobically in BLKN containing 3mM 2,4-DNT and Tenax beads (10g/L), resuspended in BLKN. Vials were capped with rubber septums and aluminum crimp seals. Oxygen limited bottles were purged with N_2 gas before injecting a fixed amount of air. Using a syringe equipped with a $0.2\mu\text{m}$ filter, separate injections of 5, 2, and 1 ml of lab air were made into bottles through the rubber septum (injections were made directly into liquid media). A second set of oxygen limited bottles were made to analyze oxygen partial pressure. A 50 μl sample of the head space was removed using a gas tight syringe (Hamilton) and injected into a gas chromatograph analyzer to determine percent oxygen in the headspace. Vials were incubated on a shaker table (150 rpm) at 30°C . Nitrite and DNT disappearance were monitored on samples periodically removed with a syringe.

Sampling of Batch Experiments

One ml of aqueous phase was removed from serum bottles using a syringe (B-D Disposable, polypropylene, 3 cc, Franklin Lakes, NJ) and placed into a polypropylene microcentrifuge tube. A 0.7 ml aliquot was removed from the microcentrifuge tube and placed into an additional microcentrifuge tube that contains 0.3 ml of HPLC grade MeOH. Samples were centrifuged at 14,000 rpm for 5 minutes (Eppendorf, 5415C). A 0.1 ml of aqueous sample was used to perform the colorimetric nitrite test. Samples supplemented with MeOH were analyzed for 2,4-DNT by HPLC.

Results

Determining Denitrification Potential

Denitrification potential was investigated by inoculating $\frac{1}{4}$ x TSB media containing 0.01% NaNO_3 or 0.01% NaNO_2 supplemented with 0.17% agar. Reduction of nitrate results in its disappearance along with a transient increase in nitrite. Subsequent disappearance of nitrite verifies further nitrite reduction. *P. aeruginosa* and *P. fluorescens*, known denitrifiers, reduced nitrate and nitrite (Figure 2 & 3). JS867, JS871, and JS872 also reduced nitrate to nitrite (Figure 2), but only JS867 and JS871 were capable of reducing nitrite (Figure 3).

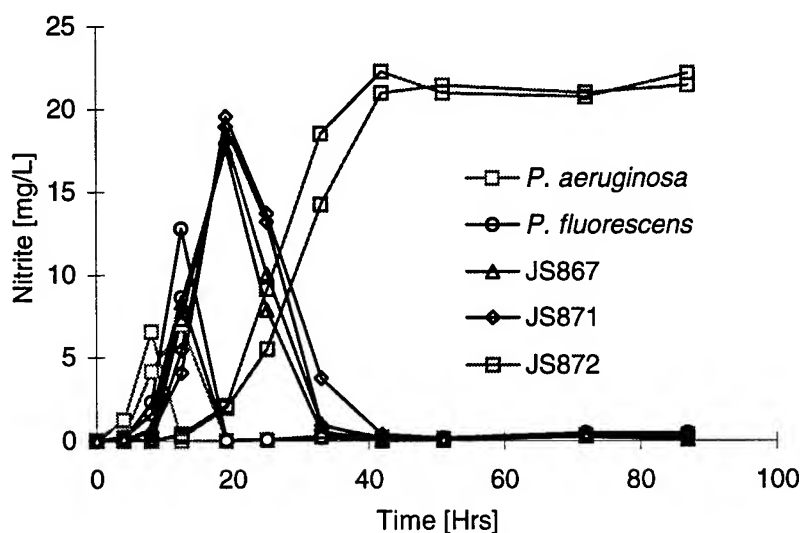


Figure 2 - Nitrite profiles from batch experiments containing $\frac{1}{4}$ x TSB as growth medium with initial concentration of 1.6 mM NO_3^- . Tubes contained 0.17% agar and were incubated at 25°C with gentle agitation.

The ability of strains JS867 and JS871 to degrade 2,4-DNT and reduce nitrate and nitrite suggest that they may have the potential to denitrify under oxygen limited conditions. Because JS872 could only reduce nitrate, it would not be effective in reducing high concentrations of nitrite released from DNT mineralization.

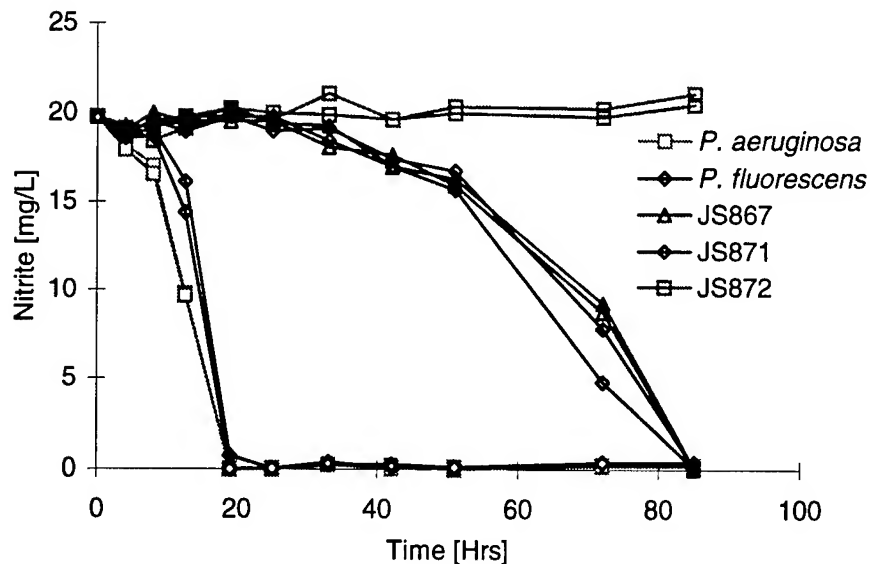


Figure 3 - Nitrite profiles from batch experiments containing $\frac{1}{4}$ x TSB as growth medium with initial concentration of 2.2 mM NO_2^- . Tubes contained 0.17% agar and were incubated at 25°C with gentle agitation.

Aerobic Batch Mineralization Experiments

Kinetics of aerobic biodegradation of 2,4-DNT by strain JS867 were examined. Batch aerobic mineralization experiments were performed in bottles containing a BLKN solution supplemented with 2,4-DNT. Complete disappearance of 0.165 mM of 2,4-DNT was observed after 140 hours (Figure 4) releasing 0.276 mM of nitrite. Theoretically, 0.33 mM of nitrite can be produced from degradation of 0.165 mM of 2,4-DNT. Thus, approximately 18% $[(1-0.276/0.332) \times 100\%]$ of the nitrite was incorporated into biomass.

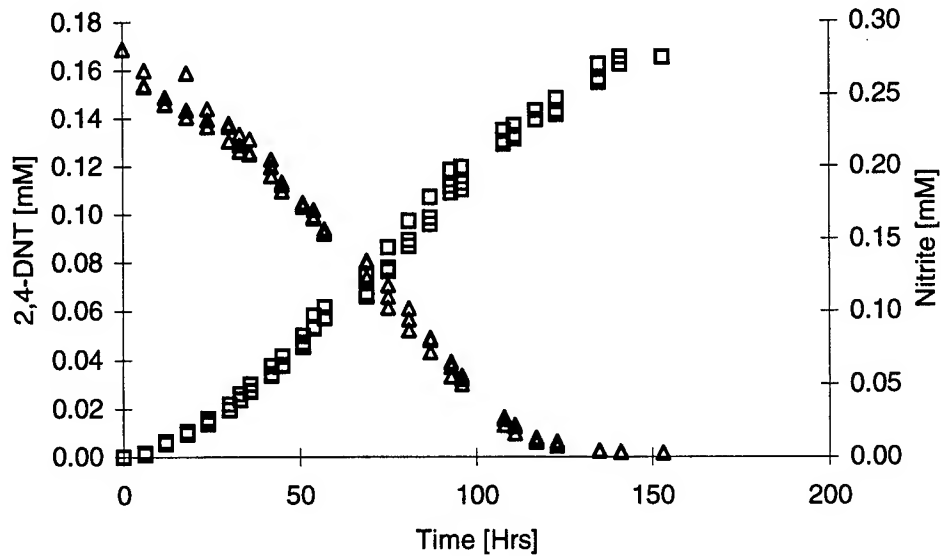


Figure 4 - Nitrite and 2,4-DNT profiles during aerobic batch mineralization experiments with strain JS867 / Triplicate samples / 30°C / Initial biomass = 0.2 mg/L / Δ = 2,4-DNT / \square = Nitrite

Experimental data were fit using a mathematical model (Figure 5) based on Monod kinetics and incorporating a non-competitive nitrite inhibition term:

$$\frac{dS_{DNT}}{dt} = \frac{-\mu_{\max}}{\left(1 + \frac{S_{NO}}{K_{iNO}}\right)} \left(\frac{S_{DNT}}{K_{S_{DNT}} + S_{DNT}} \right) X \quad (\text{Equation 3.1})$$

$$\frac{dNO_2^-}{dt} = \left(-2 \frac{dS_{DNT}}{dt} \right) - \left(0.123 \frac{dX}{dt} \right) \quad (\text{Equation 3.2})$$

$$\frac{dX}{dt} = -Y \frac{dDNT}{dt} \quad (\text{Equation 3.3})$$

Where S_{DNT} is the 2,4-DNT concentration (mg/L), S_{NO} is the nitrite concentration (mg/L), $\hat{\mu}$ is the maximum specific growth rate coefficient (hr^{-1}), K_S is the half-saturation coefficient (mg 2,4-DNT/L), K_{iNO} is the inhibition coefficient (mg NO_2^- -N/L), X is the biomass concentration (dry weight mg/L), Y is the growth yield coefficient (mg dry weight/L), and t is time (hrs). Numerical profiles of 2,4-DNT and NO_2^- -N, derived from simultaneous solutions to equations 1-3, were fit to experimental profiles and the goodness of

fit evaluated from the residual sum of squared errors (RSSE). The parameter values were adjusted until the RSSE was minimized (using SOLVER routine in EXCEL) and predicted curves adequately described the experimental data. Average best fit kinetic parameters were $\mu_{\max} = 0.058(\pm 0.004) \text{ hr}^{-1}$, $K_{s\text{DNT}} = 3.3(\pm 1.3) \text{ mg DNT/L}$ and $K_{\text{INO}} = 1.2(\pm 0.2) \text{ mg NO}_2^-/\text{L}$. The estimated K_s value is similar to other bacteria growing on xenobiotic compounds.

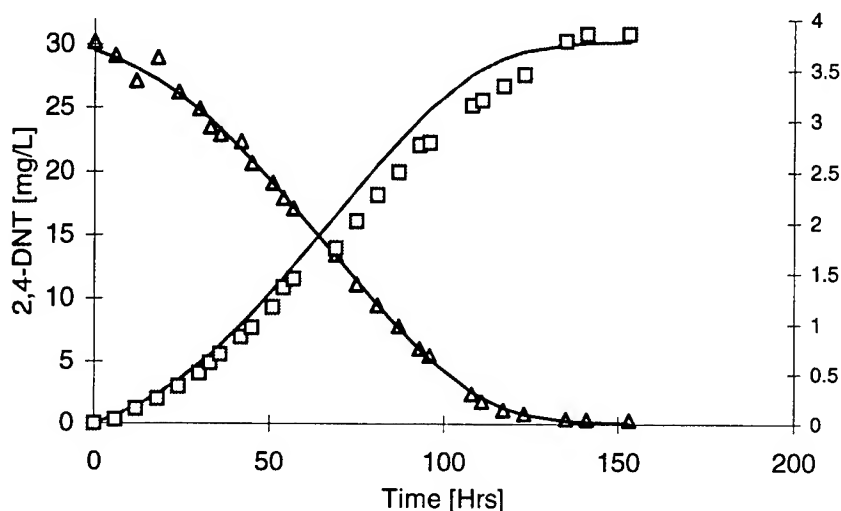


Figure 5 - Experimental and best fit profiles of Nitrite and 2,4-DNT from aerobic batch mineralization experiments. Smooth lines are predicted values and $\Delta = 2,4\text{-DNT}$ / $\square = \text{Nitrite}$

Use of Nitrite Released From Mineralization 2,4-DNT as TEA

To examine whether JS867 was capable of rapidly using nitrite released from 2,4-DNT denitration as a TEA a two phase batch experiment was performed. Phase one consisted of complete mineralization of 2,4-DNT under aerobic conditions. In phase two, anaerobic conditions were created by purging the vessels with N_2 gas and another carbon source was added. Complete disappearance of 2,4-DNT occurred in phase I with an increase in NO_2^- (Figure 6). Rapid removal of nitrite (from solution) was observed in phase II. Test vessels containing succinate showed complete nitrite removal in approximately 80 hrs, while complete nitrite removal in vessels containing glucose was observed after 190 hrs. Control vessels containing no additional carbon source showed no decrease in nitrite concentration over time (Figure 6) demonstrating denitrification's need for a carbon source. The rapid disappearance in NO_2^- confirms the ability of strain

JS867 to reduce NO_2^- in the absence of oxygen. Furthermore, the NO_2^- available for reduction resulted from the mineralization of 2,4-DNT.

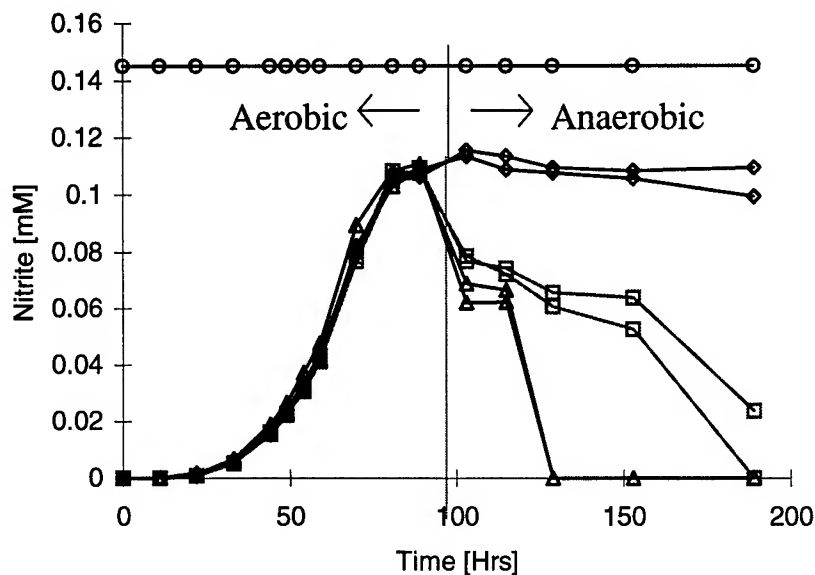


Figure 6 - Nitrite profiles from batch experiments evaluating use of NO_2^- as TEA. Flasks were purged with N_2 gas and supplemented with an additional carbon source after complete mineralization of 2,4-DNT (≈ 80 hrs). \diamond = no additional carbon source / \bullet = Glucose [10 mM] / Δ = Succinate [6mM] / \circ = Nitrite [0.145 mM]

Oxygen Limited Batch Mineralization Experiments

Batch mineralization experiments were performed under limiting oxygen conditions to test whether strain JS867 was capable of using nitrite as a TEA while mineralizing 2,4-DNT. Fixed volumes of air were injected into sealed bottles. Headspace gas make-up was measured (Table 1) and used to calculate the oxygen concentrations in aqueous and headspace volumes (Table 2). The experimental measurements matched the theoretical values well for 50 ml (aerobic), 7.5ml, 2ml, and 5 ml injections. Error appears to be more prevalent at low air injections.

One mole of 2,4-DNT reacts with 3 moles of oxygen in oxygenase catalyzed reactions (Figure 1). Therefore, degradation of ≈ 30 mg/L of 2,4-DNT (under oxygen limited conditions) requires a minimum of ≈ 1.2 mg of O_2 as reactant for oxygenases. The theoretical oxygen demand of 2,4-DNT (assuming complete

oxidation) is 8 moles of O₂ per mole of 2,4-DNT. If O₂ is the TEA during degradation of ≈ 30 mg/L, a total of 3.2 mg O₂ would therefore be required. Subtracting 1.2 mg of O₂ as reactant for the oxygenase catalyzed reaction indicates that 2 mg of O₂ is required for complete 2,4-DNT mineralization subsequent to aromatic ring cleavage.

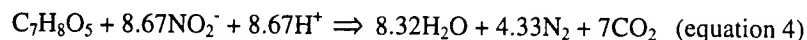
Table 1 - Oxygen Measurements: Theoretical and Experimental

Volume of Air Injected	Calculated Headspace P _{O2} (%)	Calculated O ₂ Mass in Bottle (mg)	Experimental Headspace P _{O2} (%)	Experimental O ₂ Mass in Bottle (mg)
50 ml Aerobic	21.00	15.63	20.1(±0.2)	14.96(±0.15)
7.5 ml	3.23	2.25	2.5(±0.3)	1.86(±0.22)
5 ml	2.15	1.5	2.1(±0.2)	1.56(±0.15)
2 ml	0.86	0.6	0.94(±0.07)	0.70(±0.05)
1 ml	0.43	0.3	0.78(±0.05)	0.58(±0.04)

Table 2 - Calculated Aqueous and Gaseous Oxygen Concentrations

Volume of Air Injected	From Theoretical Lab Air Injections		From Experimental Headspace Measurements	
	Aqueous O ₂ Conc. (M)	Gaseous O ₂ Conc. (M)	Aqueous O ₂ Conc. (M)	Gaseous O ₂ Conc. (M)
50 ml Aerobic	2.81×10^{-4}	9.36×10^{-3}	2.52×10^{-4}	8.38×10^{-3}
7.5 ml	4.04×10^{-5}	1.35×10^{-3}	3.16×10^{-5}	1.05×10^{-3}
5 ml	2.69×10^{-5}	8.98×10^{-4}	2.33×10^{-5}	7.76×10^{-4}
2 ml	1.08×10^{-5}	3.60×10^{-4}	1.17×10^{-5}	3.89×10^{-4}
1 ml	5.38×10^{-6}	1.80×10^{-4}	9.69×10^{-6}	3.23×10^{-4}

Aromatic ring cleavage results in the formation of 2,4-dihydroxy-5-methyl-6-oxo-2,4-hexadienoic acid (Figure 1④). The following equation describes the theoretical complete oxidation of 2,4-dihydroxy-5-methyl-6-oxo-2,4-hexadienoic acid to CO₂ using nitrite as an alternative terminal electron acceptor (i.e. oxidant).



During aerobic biodegradation of DNT, two moles of nitrite are released per mole of DNT. Degradation of 2,4-dihydroxy-5-methyl-6-oxo-2,4-hexadienoic acid would require 8.67 moles of nitrite as a terminal electron acceptor. Subtracting 2 moles of nitrite produced from the oxygenolytic denitration

reactions indicates that an extra 6.67 moles of nitrite are required for complete 2,4-DNT mineralization aromatic ring cleavage. Any biomass formation would reduce the total amount of nitrite required as an electron acceptor. In sum, if nitrite can serve as a TEA, the above calculation suggests that an excess of reducing power is available in the carbon substrate to achieve its complete reduction.

Nitrite production and 2,4-DNT disappearance occurred in all bottles. Complete mineralization of 0.161 mM of 2,4-DNT occurred in 62 hours under aerobic conditions (Figure 7). Approximately 87.5, 50, and 12.5 percent of the initial 2,4-DNT was mineralized in bottles that were injected with 5, 2, and 1 ml of air (Figure 7). In addition, rates of 2,4-DNT removal decreased under increasing oxygen limitations.

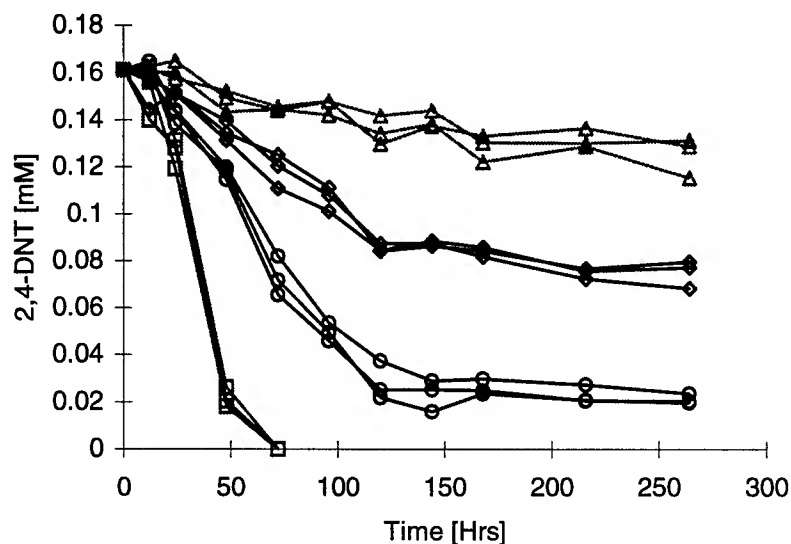


Figure 7 - 2,4-DNT removal profiles during batch assays with JS867 under oxygen limitations. Oxygen limited bottles were purged with N_2 gas before injection of a known volume of lab air.
 = aerobic / ○ = 5 ml / ◇ = 2 ml / △ = 1 ml

Rates of NO_2^- production also decreased as a result of decreased 2,4-DNT mineralization rates. Approximately 72, 42, and 17.5 percent of the total amount of NO_2^- available in the 2,4-DNT was released in bottles that were injected with 5, 2, and 1 ml of air, respectively (Figure 8). Ratios of 2,4-DNT removed over NO_2^- released ($\Delta 2,4\text{-DNT}/\Delta NO_2^-$) under various degrees of oxygen limitation were calculated (Table 3). If denitrification was occurring, $\Delta 2,4\text{-DNT}/\Delta NO_2^-$ would be larger under oxygen limited conditions than under aerobic conditions due to the use of nitrite released as a TEA. The calculated ratios suggested that

denitrification under oxygen limited conditions did not occur. The constant ratios of $\Delta 2,4\text{-DNT}/\Delta \text{NO}_2^-$ of 0.73 - 0.80 under various degrees of oxygen limitation suggested denitrification was not occurring.

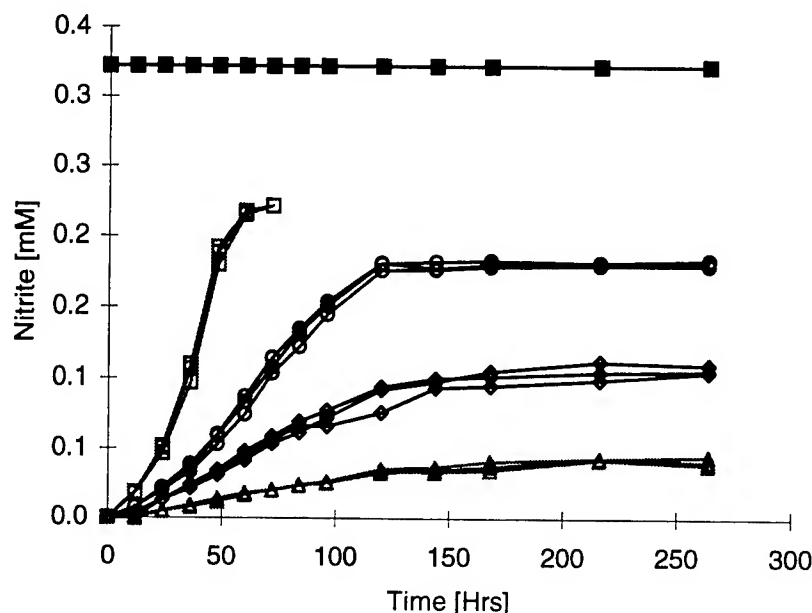


Figure 8 - Nitrite production profiles during batch assays with JS867 under oxygen limitations. Oxygen limited bottles were purged with N_2 gas before injection of a known volume of lab air. = aerobic / $\diamond = 2 \text{ ml}$ / $\Delta = 1 \text{ ml}$

Table 3 - Ratios obtained during oxygen limited mineralization experiments

Air Injected	$\Delta \text{DNT}/\Delta \text{NO}_2^-$	$\Delta \text{DNT}/M_{\text{O}_2, \text{initial}}$
50 ml (Aerobic)	0.73(± 0.00)	n/a
5 ml	0.76(± 0.01)	1.22 (± 0.01)
2 ml	0.79(± 0.02)	1.68 (± 0.10)
1 ml	0.80(± 0.08)	0.73 (± 0.02)

Experimental 2,4-DNT and nitrite profiles were fit using a mathematical model based on Monod kinetics incorporating dual substrate utilization (by 2,4-DNT and O_2) and a non-competitive nitrite inhibition term (as was found necessary in aerobic experiments). Oxygen is present in both the aqueous phase and head space in these experiments. The growth limiting substrate considered in the Monod expression is the true aqueous phase concentration. However, mass balances on O_2 need to consider both aqueous and headspace concentrations. This is done by introduction of a new term Ω ; this term measures the total mass of oxygen present in the system, expressed per unit volume of aqueous phase (the

mathematical relationship between Ω , $S_{O_2, LIQ} + S_{O_2, GAS}$ are fully developed in Naziruddin and Grady (1995):

$$\frac{dS_{DNT}}{dt} = \frac{-\mu_{max}}{\left(1 + \frac{S_{NO}}{K_{INO}}\right)} \left(\frac{S_{DNT}}{K_{SDNT} + S_{DNT}} \right) \left(\frac{\Omega}{K_{SO} \cdot \left(1 + K_H \frac{V_G}{V_L}\right) + \Omega} \right) X \quad (\text{Equation 5})$$

$$\frac{dNO_2^-}{dt} = \left(-2 \frac{dS_{DNT}}{dt} \right) - \left(0.123 \frac{dX}{dT} \right) \quad (\text{Equation 6})$$

$$\frac{d\Omega}{dt} = Y^{O_2/\Delta DNT} \left(\frac{dS_{DNT}}{dt} \right) \quad (\text{Equation 7})$$

Where S_O is the aqueous phase oxygen concentration (mg/L), K_{SO} is the half-saturation coefficient (mg oxygen/L), K_H is the Henry's Law constant (40 mg/L-atm), V_G is the volume of the headspace (0.05L), V_L is the volume of the liquid (0.075L), Ω is the amount of oxygen in the bottle at any time (mg/L), and $Y^{O_2/\Delta DNT}$ is the oxygen stiochiometric coefficient (mg O_2 /L). Predicted profiles of 2,4-DNT and NO_2^- -N, derived from simultaneous solutions of equations 4 - 5, were solved using initial conditions indicative of our experimental set-up. This exercise was performed to examine whether profiles simulated using our mathematical models (with varying Ω_0) qualitatively matched the experimental profiles obtained under oxygen limited conditions.

Synthetic data were generated with different Ω values to estimate how O_2 concentration affected the rate of 2,4-DNT mineralization (Figure 10). As oxygen concentrations decrease (decline in Ω) the rates of 2,4-DNT mineralization and nitrite release decrease, indicating qualitative agreement with our observation.

The experimental profiles from the aerobic, 5, 2, and 1 ml air injection were adequately fit using kinetic parameters indicative of those in the completely aerobic experiments (Figures 11-14). Oxygen

affinity (K_{SO_2}) was estimated under all three conditions by holding all other parameters constant (Table 4).

As oxygen limitation increased, so did K_{SO_2} . An overall average K_{SO_2} value of $0.30(\pm 0.23)$ mg O_2/L .

Table 4 - Estimated oxygen affinities (K_{SO_2}) and experimental Ω values

Air Injected	Average K_{SO_2}	Ω , mg O_2/L
5 ml	$0.083(\pm 0.03)$	$20.6(\pm 0.15)$
2 ml	$0.150(\pm 0.002)$	$9.3(\pm 0.05)$
1 ml	$0.591(\pm 0.116)$	$7.7(\pm 0.04)$

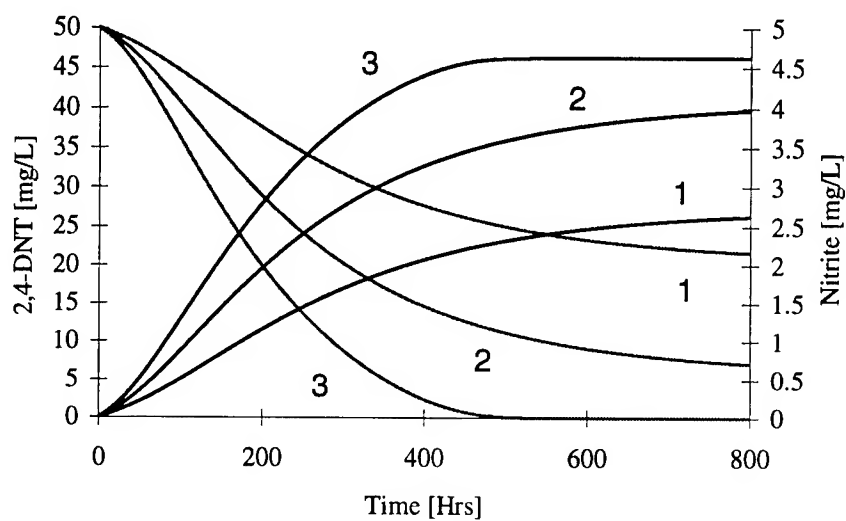


Figure 9 - 2,4-DNT and NO_2^- -N synthetic profiles under oxygen limitations.
 1 - $\Omega = 10$ mg/L / 2 - $\Omega = 15$ mg/L / 3 - $\Omega = 20$ mg/L

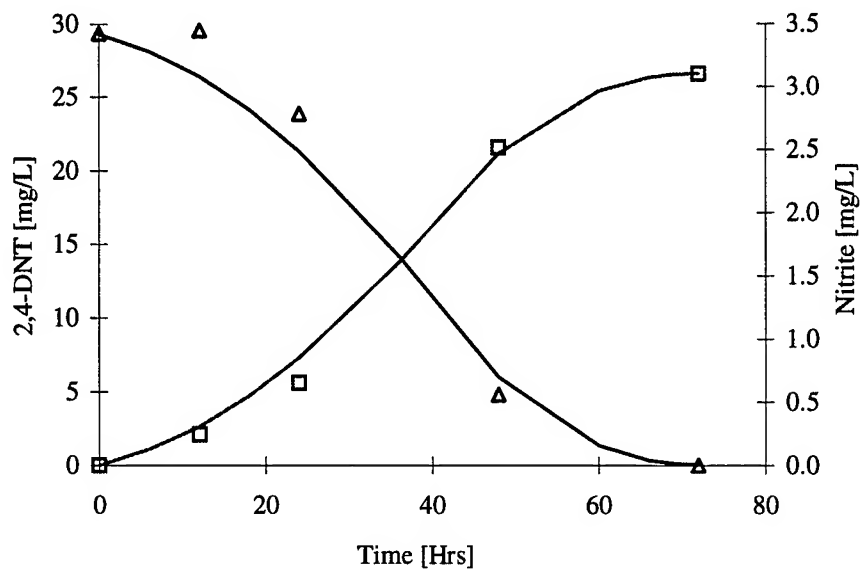


Figure 10 - Experimental and best fit 2,4-DNT and NO_2^- -N profiles under aerobic conditions.

Smooth lines are predicted values and $\Delta = 2,4\text{-DNT} / \text{Nitrite}$

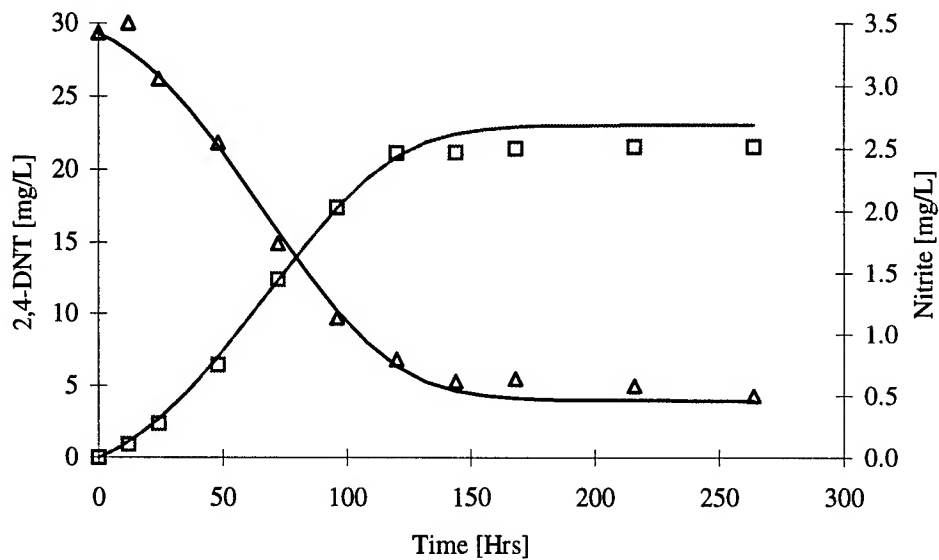


Figure 11 - Experimental and best fit 2,4-DNT and NO_2^- -N profiles under oxygen limitations (5 ml air injection). Smooth lines are predicted values and $\Delta = 2,4\text{-DNT} / \text{Nitrite}$

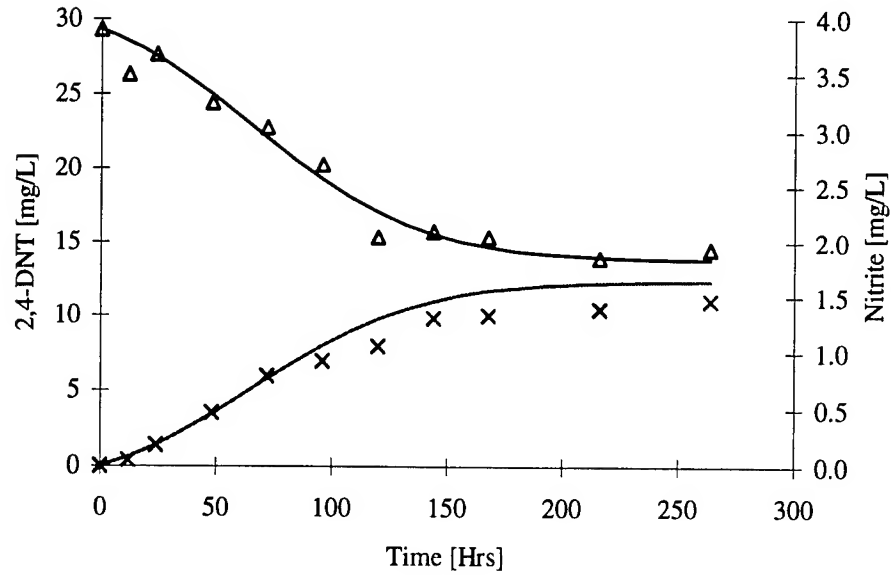


Figure 12 - Experimental and best fit 2,4-DNT and NO_2^- -N profiles under oxygen limitations (2 ml air injection). Smooth lines are predicted values and $\Delta = 2,4\text{-DNT} / \text{Nitrite}$

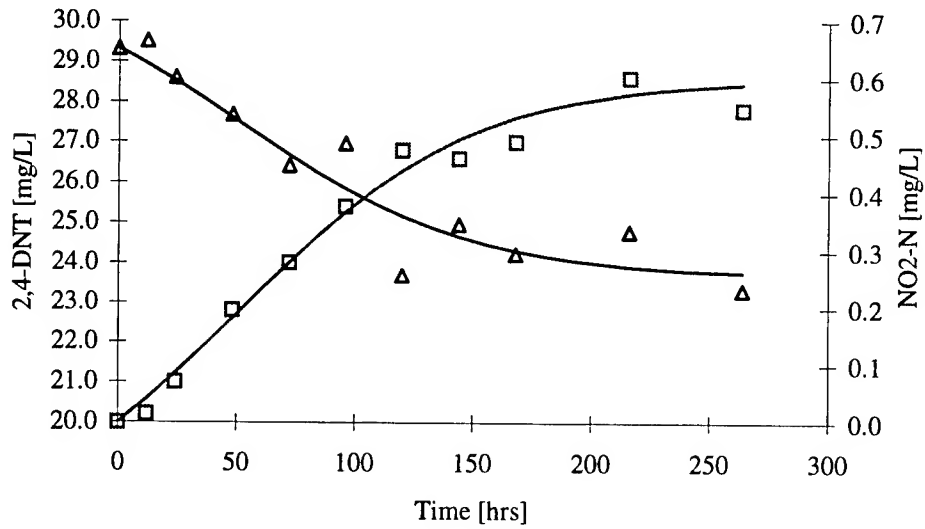


Figure 13 - Experimental and best fit 2,4-DNT and NO_2^- -N profiles under oxygen limitations (1 ml air injection). Smooth lines are predicted values and $\Delta = 2,4\text{-DNT} / \text{Nitrite}$

References

- Alefunder, P. R., Greenfield, Anthony J., McCarthy, John E. G., Ferguson, Stuart J. (1983). "Selection and organization of denitrifying electron-transfer pathways in *Paracoccus denitrificans*." Biochimica et Biophysica Acta **724**: 20-39.
- Almeida, J. S., Julio, S. M., Reis, M. A. M., Carrondo, M. J. T. (1994). "Nitrite inhibition of denitrification by *Pseudomonas fluorescens*." Biotechnology and Bioengineering **46**: 194-201.
- Arts, P. A. M., Robertson, Lesley A., Kuenen, J. Gijs (1995). "Nitrification and denitrification by *Thiosphaera pantotropha* in aerobic chemostat cultures." FEMS Microbiology Ecology **18**: 305-316.
- Averill, B. A. (1996). "Dissimilatory nitrite and nitric oxide reductases." Chemical Reviews **96**: 2951-2964.
- Bell, L. C., Ferguson, Stuart J. (1991). "Nitric and nitrous oxide reductases are active under aerobic conditions in cells of *Thiosphaera pantotropha*." Biochemical Journal **273**: 423-427.
- Bonin, P., Gilewicz, M. (1991). "A direct demonstration of "co-respiration" of oxygen and nitrogen oxides by *Pseudomonas nautica*: some spectral and kinetic properties of the respiratory components." FEMS Microbiology Letters **80**: 183-188.
- Brock, T. D., Madigan, Michael T., Martinko, John M., Parker, Jack (1994). Nitrate reduction and the denitrification process. Biology of Microorganisms. Englewood Cliffs, Prentice-Hall, Inc: 598-601.
- Bruhn, C., Lenke, H., Knackmuss, H. J. (1987). "Nitrosubstituted aromatic compounds as nitrogen source for bacteria." Applied and Environmental Microbiology **53**: 208-210.
- Carter, J. P., Hsiao, Wa Hsin, Spiro, Stephen, Richardson, David J. (1995). "Soil and sediment bacteria capable of aerobic nitrate respiration." Applied and Environmental Microbiology **61**: 2852-2858.
- Davies, D. J. P., Lloyd, David, Boddy, Lynne (1989). "The effect of oxygen of denitrification in *Paracoccus denitrificans* and *Pseudomonas aeruginosa*." Journal of General Microbiology **135**: 2445-2451.
- Eaton, A. D., Clesceri, L.S., Greenberg, A.E. (1995). Standard Methods for the Examination of Water and Wastewater. Washington, D.C.
- Freedman, D. L., Shanley, R. S., R. J. Scholze (1995). "Aerobic biodegradation of 2,4-dinitrotoluene, aminonitrotoluene isomers, and 2,4-diaminotoluene." Journal of Hazardous Materials **49**: 1-14.
- Hackett, C. S., MacGregor, C. H. (1981). "Synthesis and degradation of nitrate reductase in *Escherichia coli*." Journal of Bacteriology **146**: 352-359.
- Haigler, B. E., Spain, Jim C. (1996). Degradation of nitroaromatic compounds by microbes. SIM News. **46**: 59-68.
- Hernandez, D., Rowe, John J. (1988). "Oxygen inhibition of nitrate uptake is a general regulatory mechanism in nitrate respiration." The Journal of Biological Chemistry **263**: 7937-7939.
- Hochstein, L. I., Betlach, Michael, Kritikos, Gary (1984). "The effect of oxygen on denitrification during steady-state growth of *Paracoccus halodenitrificans*." Archives Microbiology **137**: 74-78.
- John, P. (1976). "Aerobic and anaerobic bacterial respiration monitored by electrodes." Journal of General Microbiology **98**: 231-238.
- Korner, H., Zumft, Walter (1989). "Expresion of denitrification enzymes in response to the dissolved oxygen level and respiratory substrate in continuous culture of *Pseudomonas stutzeri*." Applied and Environmental Microbiology **55**: 1670-1676.

- Krul, J. M. (1976). "Dissimilatory nitrate and nitrite reduction under aerobic conditions by an aerobically and anaerobically grown *alcaligenes* sp. and by activated sludge." Journal of Applied Bacteriology **40**: 245-260.
- Lloyd, D., Boddy, Lynne, Davies, Kathryn J. P. (1987). "Persistence of bacterial denitrification capacity under aerobic conditions: the rule rather the exception." FEMS Microbiology Ecology **45**: 185-190.
- Meiberg, J. B. M., Bruinenberg, P. M., Harder, W. (1980). "Effect of dissolved oxygen tension on the metabolism of methylated amines in *Hyphomicrobium* X in the absence and presence of nitrate: evidence for 'aerobic' denitrification." Journal of General Microbiology **120**: 453-463.
- Meijer, E. M., Ban Der Awaan, J. W., Wever, R., Stouthamer, A. H. (1979). "Anaerobic respiration and energy conservation in *Paracoccus denitrificans*. Functioning of iron-sulfur centers and the uncoupling effect of nitrite." European Journal of Biochemistry **96**: 69-76.
- Nakajima, M., Hayamizu, Teruyoshi, Nishimura, Hajime (1984). "Effect of oxygen concentration on the rates of denitrification and denitrification in the sediments of an eutrophic lake." Water Resources **18**: 335-338.
- Naziruddin, M., Grady, C. P. L. Jr, Tabak, H.H. (1995). "Determination of biodegradation kinetics of volatile organic compounds through the use of respirometry." Water Environment Research **67**: 151-158.
- Noguera, D. R., Freedman, David L. (1996). "Reduction and acetylation of 2,4-dinitrotoluene by a *pseudomonas aeruginosa* strain." Applied and Environmental Microbiology **62**: 2257-2263.
- Patureau, D., Davison, J., Bernet, N., Moletta, R. (1994). "Denitrification under various aeration conditions in *Comamonas* sp., strain SGLY2." FEMS Microbiology Ecology **14**: 71-78.
- Rake, J. B., Eagon, R. G. (1980). "Inhibition, but not uncoupling, of respiratory energy coupling of three bacterial species by nitrite." Journal of Bacteriology **144**: 975-982.
- Remde, A., Conrad, Ralf (1991). "Production and consumption of nitric oxide by denitrifying bacteria under anaerobic and aerobic conditions." FEMS Microbiology Letters **80**: 329-332.
- Robertson, L. A., Kuenen, J. Gijs (1984). "Aerobic denitrification: a controversy revived." Archives of Microbiology **139**: 351-354.
- Robertson, L. A., Van Niel, Ed W. J., torremans, Rob A. M., Kuenen, J. Gijs (1988). "Simultaneous nitrification and denitrification in aerobic chemostat cultures of *Thiosphaera pantotropha*." Applied and Environmental Microbiology **54**: 2812-2818.
- Robertson, L. A., Dalsgaard, Tage, Revsbech, Niels-Peter, Kuenen, J. Gijs (1995). "Confirmation of 'aerobic denitrification' in batch cultures, using gas chromatography and N mass spectrometry." FEMS Microbiology Ecology **18**: 113-120.
- Sears, H. J., Ferguson, Stuart J., Richardson, David J., Spiro, Stephen (1993). "The identification of a periplasmic nitrate reductase in *Paracoccus denitrificans*." FEMS Microbiology Letters **113**: 107-112.
- Spain, J. C. (1995). "Biodegradation of nitroaromatic compounds." Annu. Rev. Microbiol. **49**: 523-55.
- Spangord, R. J., Spain, Jim C., Nishino, Shirley F., Mortelmans, Kristien E. (1991). "Biodegradation of 2,4-Dinitrotoluene by a *Pseudomonas* sp." Applied and Environmental Microbiology **57**: 3200-3205.
- Stewart, V. (1988). "Nitrate respiration in relation to facultative metabolism in enterobacteria." Microbiology Reviews **52**: 190-232.
- Thomas, K. L., Lloyd, David, Boddy, Lynne (1994). "Effects of oxygen, pH and nitrate concentration on denitrification by *Pseudomonas* species." FEMS Microbiology Letters **118**: 181-186.

- Wu, Q., Knowles, R., Niven, D. F. (1994). "O₂ regulation of denitrification in *Flexibacter canadensis*." Canadian Journal of Microbiology **40**: 916-921.
- Yarborough, J. M., Rake, J. B., Eagon, R. G. (1980). "Bacterial inhibitory effects of nitrite: inhibition of active transport, but not of group translocation, and of intracellular enzymes." Applied and Environmental Microbiology **39**: 831-834.
- Ye, R. W., Averill, Bruce A., Tiedje, James M. (1994). "Denitrification: production and consumption of nitric oxide." Applied and environmental Microbiology **60**: 1053-1058.
- Ye, R. W., Haas, D., K. A., J. O., Krishnapillai, V., Zimmermann, A., Baird, C., Tiedje, J. M. (1995). "Anaerobic activation of the entire denitrification pathway in *Pseudomonas aeruginosa* requires ANR, an analog of Fnr." Journal of Bacteriology **177**: 3606-3609.
- Zumft, W. G. The Denitrifying Prokaryotes. The Prokaryotes: 554-573.
- Zumft, W. G. (1997). "Cell biology and molecular basis of denitrification." Microbiology and Molecular Biology Reviews **61**: 533-616.

***In vitro* detection of apoptosis in differentiating mesenchymal cells using
immunohistochemistry and image analysis**

Mary Alice Smith
Assistant Professor
Environmental Health Science Department

University of Georgia
206 Environmental Health Science Building
Athens, GA 30602-2102

Final Report for:
Summer Faculty Research Program Extension Grant
Armstrong Laboratory

Sponsored by:
Air Force Office of Scientific Research

and

Armstrong Laboratory

March 11, 1999

Introduction As women have entered the work force in increasing numbers and have continued to work during their pregnancies, identifying toxicants to developing systems has become increasingly important. Many women of reproductive age are potentially exposed to hazardous chemicals in the workplace. Developing systems are often susceptible to toxicants before the mother experiences toxicity. This embryonic susceptibility is the result of certain processes that are occurring rapidly in a developing embryo such as cell proliferation, movement, orientation, aggregation and differentiation. Consequently, tests are needed to predict which chemicals are likely to cause birth defects in humans and to develop interventions to prevent these defects (Smith, 1996).

The chick limb bud micromass culture is a well-established means for investigating normal differentiation of chondrocytes (Puzas et al, 1992). For this reason and because it demonstrates similar responses as mice to specific teratogens (Renault et al, 1989; Brown and Wiger, 1992), the chick limb bud micromass culture was used in this study.

Ethylene glycol monomethyl ether (EG) and diethylene glycol monomethyl ether (DEG) are the primary toxicants chosen for study in this experiment. It is known that glycol ethers are widely used in industry as solvents to make lacquers, varnishes, resins, inks (stamp pads, ballpoint pens and print shops), dyes and gasoline additives such as antifreeze. Glycol ethers available to consumers are found in latex paints, cleaners and other household products (Cassarett and Doulls, 1996). Because EG and DEG are in so many products that are used both commercially and domestically, there are ample opportunities for human exposure. EG is a clear, odorless, sweet tasting chemical at room temperature and persists in the water, soil and air for less than 3 weeks (ATSDR,

1997). Ethylene glycol ethers are well absorbed through the skin (Sabourin et al., 1992) and can cause reproductive toxicity (Wiley et al., 1938).

Lead Acetate (lead) and Chromium (III) Chloride (Chromium) are the comparison chemicals chosen for study in this experiment. Lead was specifically chosen as a positive control because there is published information of its effects on *in vitro* chick limb bud micromass cultures (Smith and Kanti, 1997; Sokol et al., 1994; Bress and Bidanset, 1990). Lead can affect the entire body, young or old. Exposure is particularly harmful to fetuses causing premature births, smaller size, decreased learning ability and even abortion (ATSDR, 1993).

Chromium(III) compounds are stable and an essential nutrient in our diet, although all forms of chromium are toxic at high levels (ATSDR, 1993). In industry it is used in steel, furnace bricks, dyes, chrome plating, leather tanning and wood preserving. Chromium can exist in three main valence forms: chromium(0), chromium(III) and chromium(VI).

This research supports the use of an *in vitro* system to screen hazardous chemicals of interest and their effects on proteoglycans and cell proliferation. The area of interest for these chemicals' teratogenic effects is chondrogenesis. If a chemical inhibits or promotes proteoglycan synthesis significantly, the fetus could be malformed. When grown under specified culture conditions, mesenchymal cells originating from embryonic limb buds will proliferate and differentiate into chondrocytes (George et al, 1983). Histochemical stains can be used to rapidly measure the amount of cell growth and cartilage specific products (such as proteoglycans) (Smith and Kanti, 1997; Bjornsson, 1993; Renault et al, 1989). These two developmental markers: chondrogenesis and cell

proliferation, were used to screen for specific chemicals of interest in occupational and environmental settings (Smith, 1996). Chondrogenesis and cell proliferation were chosen as markers because it is known that specific toxicants adversely effect these two markers in developing systems.

Method Fertilized chick eggs for tissue culture were obtained from CWT Farms (Gainesville, GA.) on day zero and incubated for five days in a humidified, constant temperature incubator. After five days of incubation, stage 25 embryos (Hamburger and Hamilton, 1951) were removed and the distal portion of the forelimbs was excised. The limbs were incubated in 1:2 trypsin (Sigma 4Na/l)/Tyrode's solution for one minute and were then rinsed with Tyrode's solution. A flamed bore pipet was used to disperse the cells into a single cell suspension. The suspension was filtered using a 20nm Nytex mesh filter to remove the ectoderm, diluted with complete media containing 16g/lm Hams F-12 nutrient mixture (Sigma, St. Louis, MO), 0.005mg gentamicin sulfate (Sigma), 0.05mg asorbic acid (Sigma) and 3.4ml per 50ml of complete media fetal bovine serum (Atlanta Biologicals, Norcross, GA) and plated in 48-well tissue culture plates (Corning) in 30ul drops. Once cultures were placed in the plates, they were incubated for 120 hours in a humidified constant temperature carbon dioxide incubator.

Cells were allowed to adhere to the bottom of the well plate (approximately 4 hours after plating), before treatment with the chemical of interest. After attachment, 1.0ml of complete media including the chemical treatment was added to each culture well. At twenty four hour intervals, 0.5ml of media was replaced by freshly prepared complete media and appropriate chemical solution. At 120 hours, the media was

removed and the cells were fixed in formalin for at least 18 hours and subsequently stained. Each experiment was conducted at least three times with a minimum of three replicates per trial.

The chemicals used in treatment were EG (Sigma), DEG (Aldrich Chemical Company, Milwaukee, WI), chromium III chloride (Sigma, hexahydrate) and lead acetate (Fisher Scientific, Pittsburgh, PA, trihydrate). The final concentrations in the culture well for EG were 1.31×10^{-8} , 1.31×10^{-7} , 1.31×10^{-6} , 1.31×10^{-5} , 1.31×10^{-4} and 1.31×10^{-3} M. For DEG the concentrations were 8.32×10^{-9} , 8.32×10^{-8} , 8.32×10^{-7} , 8.32×10^{-6} , 8.32×10^{-5} and 8.32×10^{-4} M. The final molar concentrations in the culture well for chromium were 1.877×10^{-7} , 1.877×10^{-6} , 1.877×10^{-5} , 1.877×10^{-4} , 1.877×10^{-3} and 1.877×10^{-2} . The final molar concentrations in each culture well for lead were 1.32×10^{-6} , 1.32×10^{-5} , 1.32×10^{-4} , 1.32×10^{-3} and 1.32×10^{-2} . For each chemical, 100 μ l/ml was added to each well on day zero.

Alcian green stain was used to identify chondrogenesis by binding to negatively charged molecules on the proteoglycans in the cell culture as described by Renault et al, 1989; Smith and Kanti, 1997 and Kanti and Smith, 1997. 0.1% of alcian green solution was added to the cell cultures for 15 minutes followed by three washes with tap water. Once this stain was dry, the culture was placed in a spectrophotometer (Cambridge Scientific,) and read at a single wavelength of 600nm. Subsequently, the crystal violet stain was applied. 1.0% crystal violet stain was detected spectrophotometrically at a single wavelength of 570nm. Detection of chondrogenesis and cell proliferation was completed using the same culture. Statistical analysis was conducted using a Dunnett's T-test.

Results At the highest concentration tested (100 μ l/ml) of DEG and EG, proteoglycan content was significantly reduced when compared to controls (0.033% and 0.017% of control, respectively) (Figures 1 & 3). Although proteoglycan content for some concentrations were significantly different from controls for both DEG and EG, neither chemical showed a consistent concentration dependent pattern. For DEG, all concentrations tested significantly reduced cell proliferation when compared to control cultures (Figure 2). For cell proliferation, all of the treatments except the lowest (0.001 μ l/ml) for EG, were significantly different ($p < 0.05$) from control (Figure 4). At the highest dose tested, cell proliferation was approximately 3.0% of control cultures for DEG and only 0.03% of control for EG (Figures 2 & 4). Absorbance for CV ranged from 1.46nm for control to 0.05nm for 100 μ l/ml and from 1.53nm to 0.04nm for DEG and EG, respectively.

For the time course studies, both chemicals had significant effects on proteoglycans and cell proliferation by the end of the first 24 hour period at the highest concentration (100 μ l/ml) (Figures 5, 6, 7 & 8). That effect lasted throughout the 120 hour culture period. At 24 hours post-treatment for DEG, proteoglycans at concentrations of 0.001 and 100 μ l/ml were significantly different from control (Figure 5). Similarly for EG at 24 hours post-treatment, proteoglycan abundance was also significantly different from control, but for all concentrations tested (0.001, 1.0 and 100 μ l/ml) (Figure 7). By 48 hours and throughout the 120 hour culture period, proteoglycan content was not significantly different from controls at the 0.001 and 1.0 μ l/ml concentrations for DEG or EG (Figures 5 & 7). Cell proliferation for both DEG and EG was only significantly different from control at the highest concentration (100 μ l/ml), 0.001 and 1.0 μ l/ml closely followed the cell proliferation pattern for control cultures (Figures 6 & 8).

Discussion Renault et al. (1989) demonstrated the effectiveness of the CV and the alcian blue stains to predict teratogenicity of specific chemicals to the skeletal system using rat embryo limb bud cells. Since previous studies have shown the chick embryo limb bud culture system is comparable to the rodent tissue culture system (Smith and Kanti, 1997), we adapted Renault et al.'s (1989) technique for use with the chick embryo limb bud system. Toxins can affect proteoglycans in two ways: directly on the biochemical pathway of proteoglycan synthesis and/or degradation (quantified by AG absorbance) or by exerting a general effect on cell growth (quantified by CV absorbance) (Smith and Kanti, 1997). Inhibition of proteoglycan synthesis may indicate developmental toxicity to the skeletal system; whereas, inhibition of cell proliferation indicates general cell toxicity (Brown and Wiger, 1992).

Evidence has been found that suggests EG is a teratogen (Nelson et al, 1984; Clothier et al, 1997 and Bowden et al, 1995) while not much research has been conducted on DEG (Bowden et al, 1995). Teratogenic defects of the skeleton were seen in rabbits exposed to EG vapor (Nelson et al, 1984). Clothier et al. (1997), conducted an in vitro study using mouse fibroblasts exposed to EG concentrations ranging from 138mg/ml to 4.6mg/ml. This study found that the highest dose of EG resulted in a 100% decrease of total protein in the fibroblast (Clothier et al, 1997). Bowden et al. (1995) exposed rats and hydra to DEG and EG in separate experiments and found that EG retarded the growth of the rat forelimb at 1mg/ml; while, DEG had no apparent adverse effects.

Conclusions

1. Treatment with DEG and EG resulted in a significant decrease in cell proliferation when compared to control cultures.
2. The proteoglycan decrease from control cultures for DEG and EG do not exhibit a concentration dependent pattern and appears to be a result of general cell toxicity.
3. For the time course experiment, the highest concentration tested (100 μ l/ml) for DEG and EG exerted its full effects on proteoglycans and cell proliferation by the end of the first 24 hour exposure period.
4. After 24 hours in the time course experiment 0.001 and 1.0 μ l/ml DEG and EG were not significantly different from control cultures for either proteoglycans or cell proliferation.

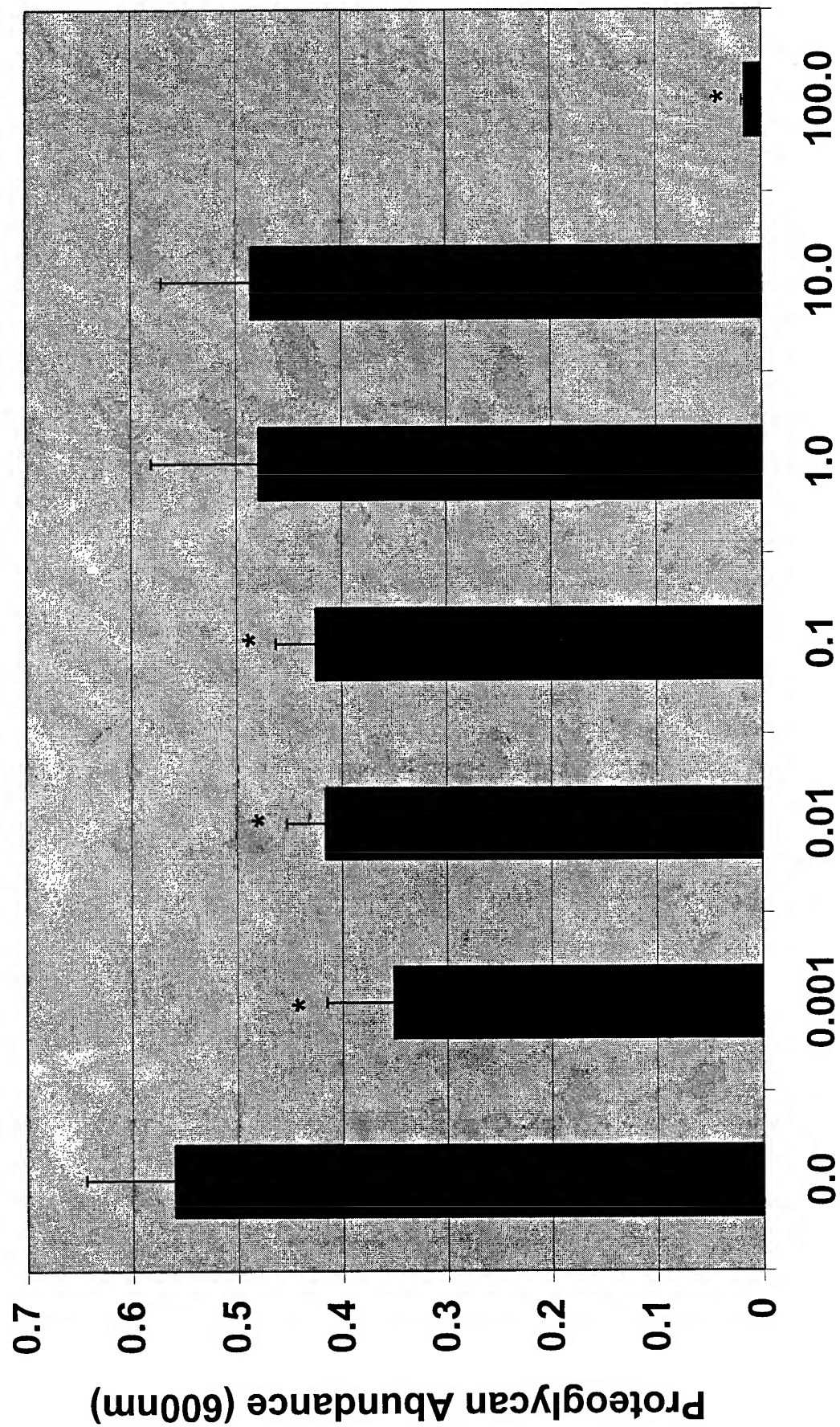


Figure 1: DEG Concentration (ul/ml)

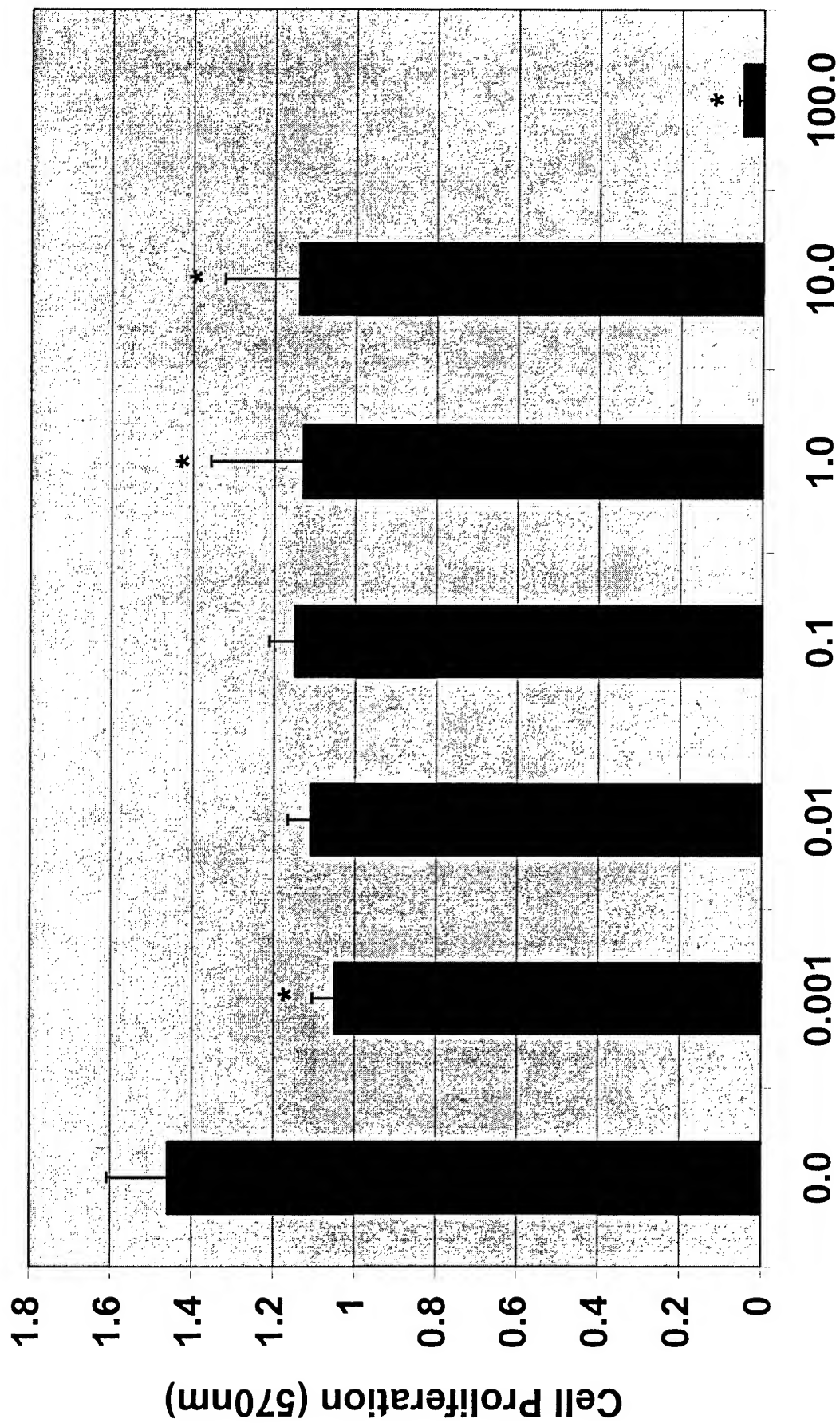


Figure 2: DEEG Concentration (ul/ml)

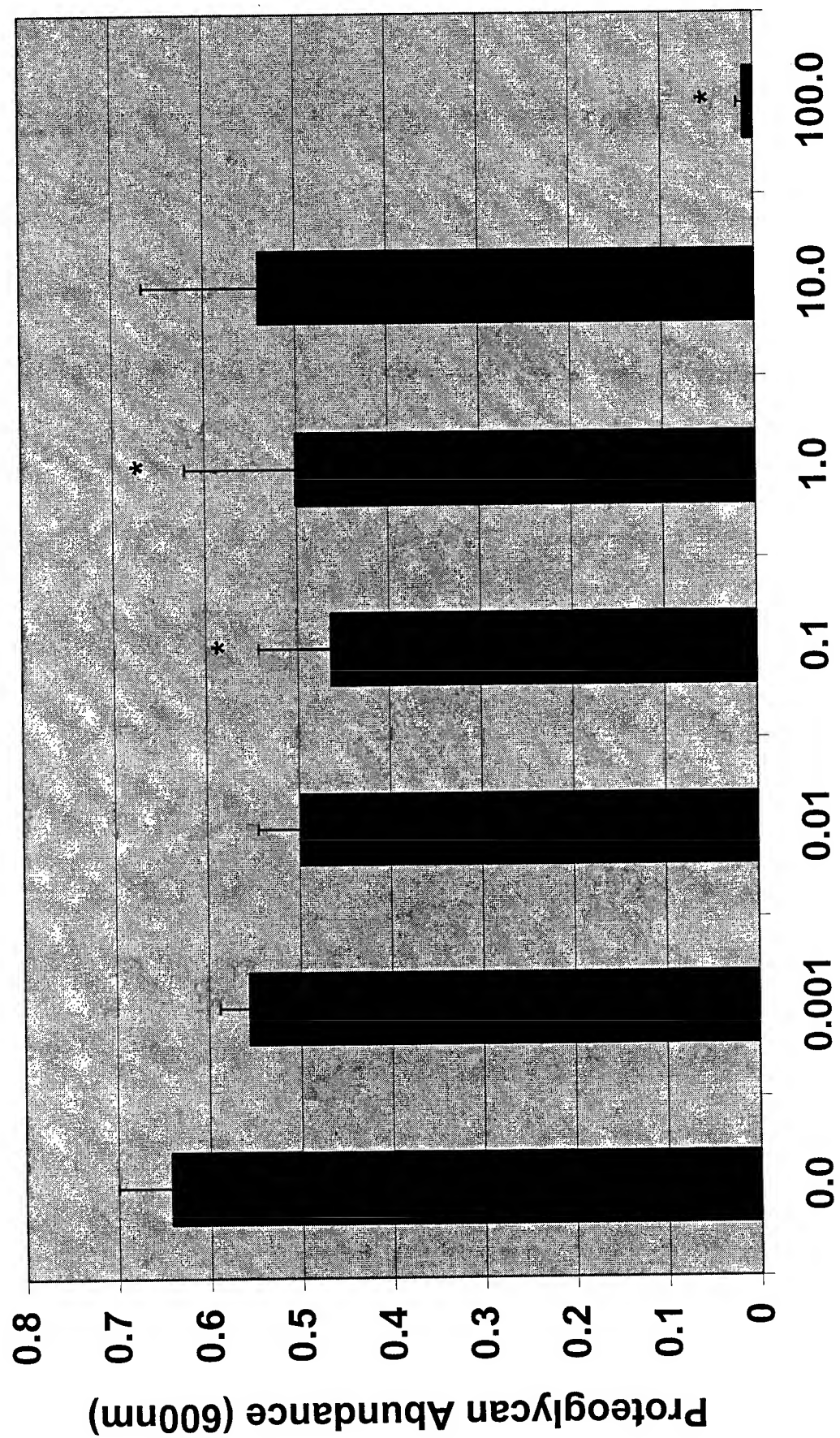


Figure 3: EG Concentration (ul/ml)

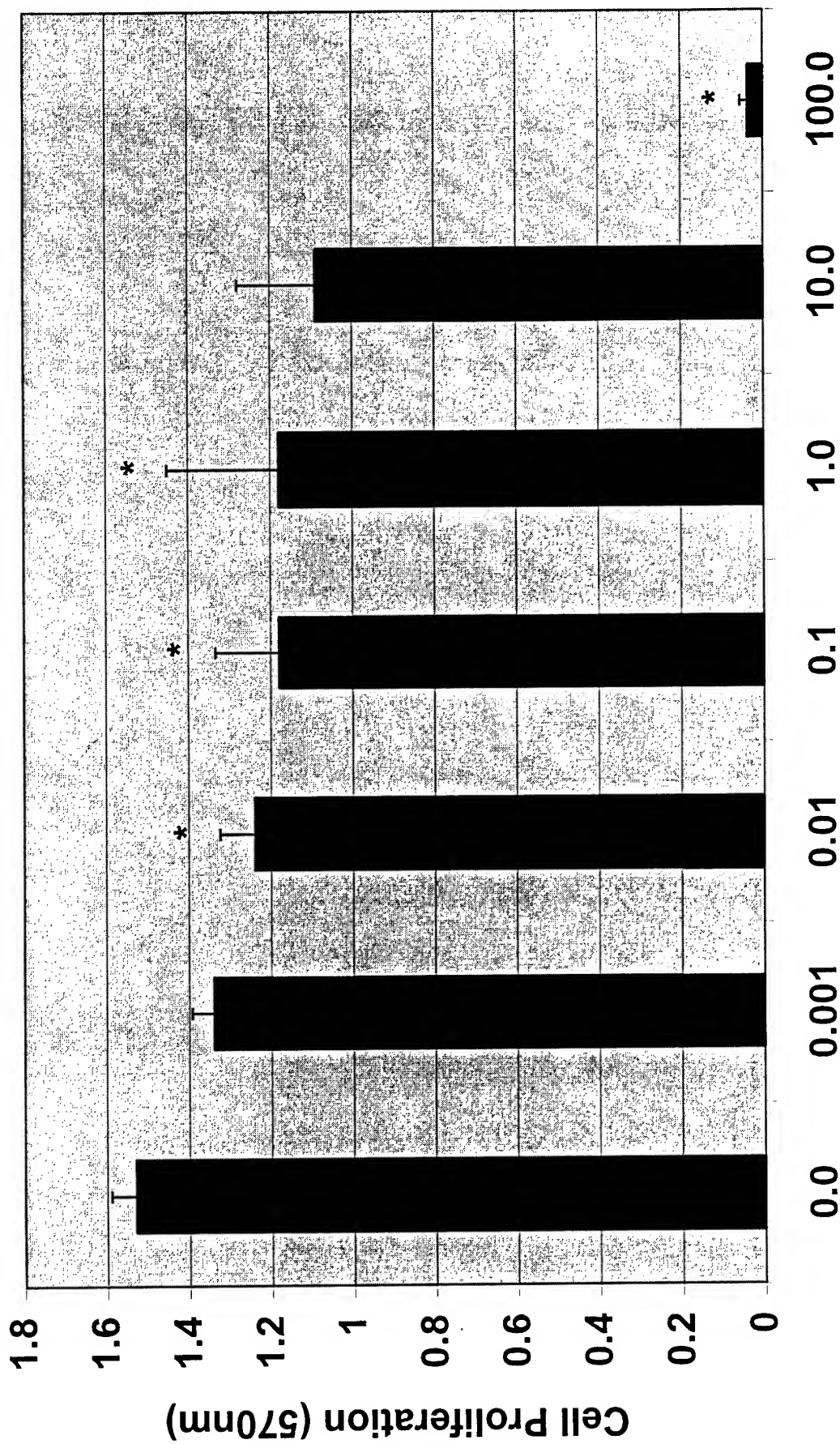


Figure 4: EG Concentration (ul/ml)

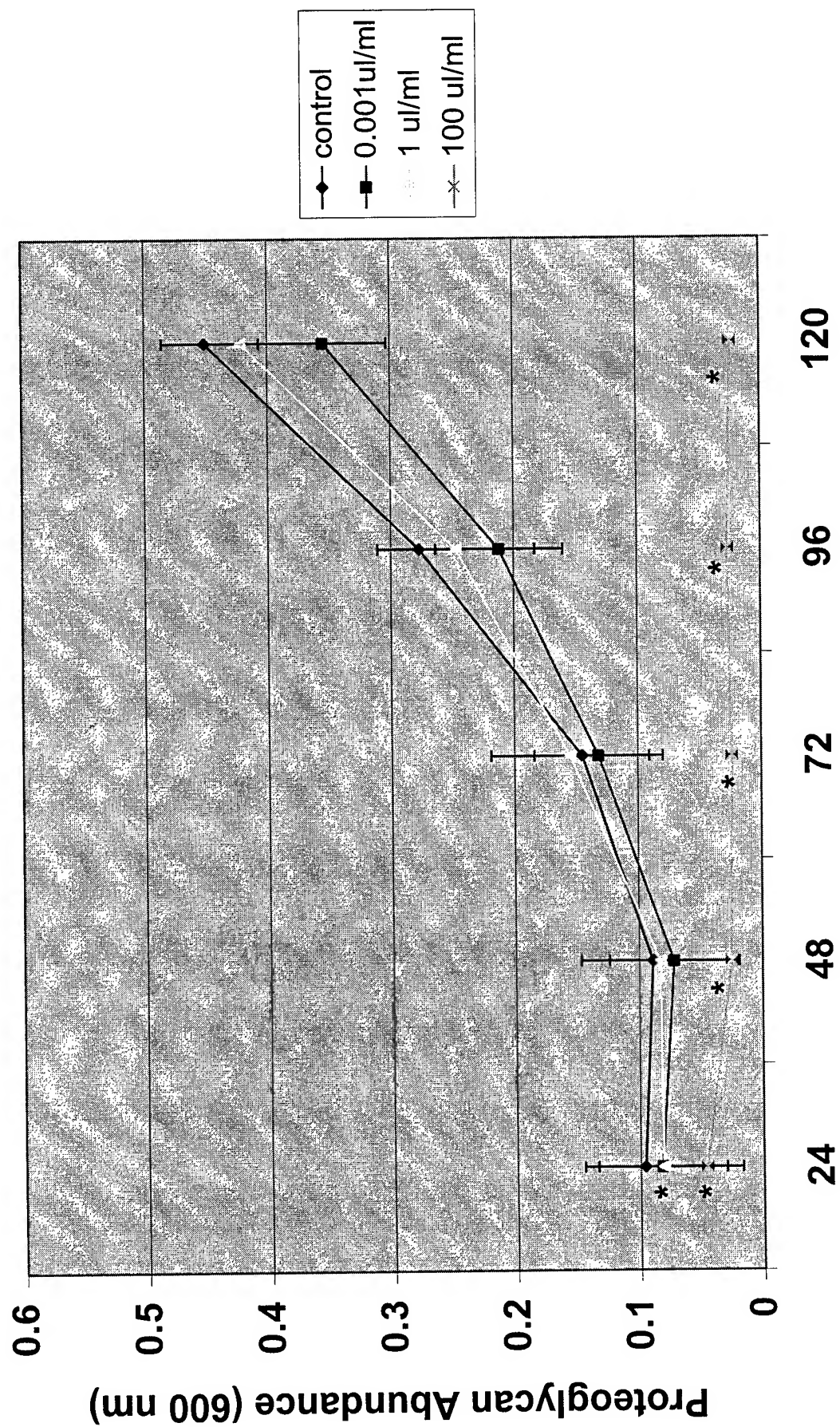


Figure 5: DEG Time Course (hours)

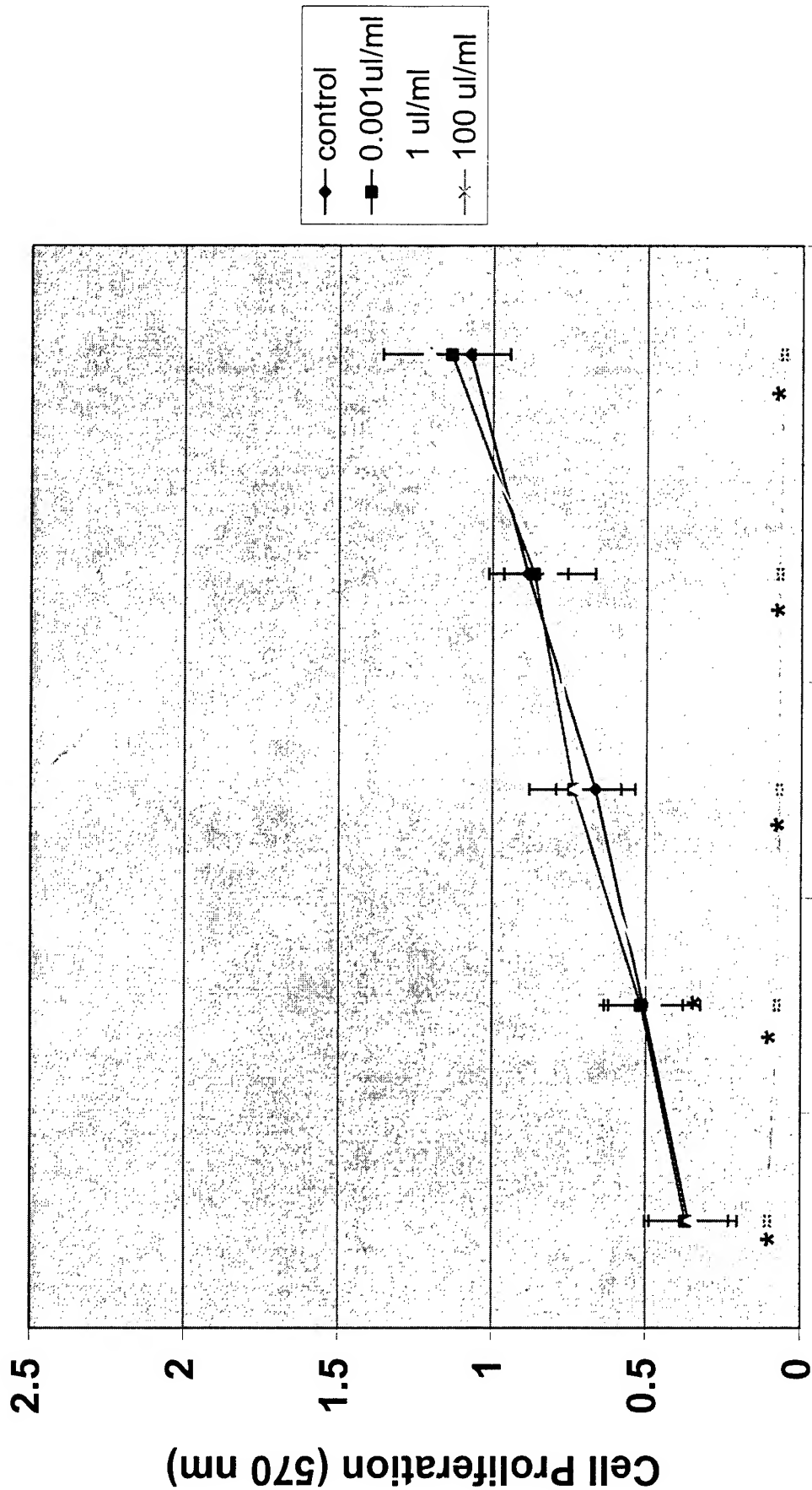


Figure 6: DEG Time Course (hours)

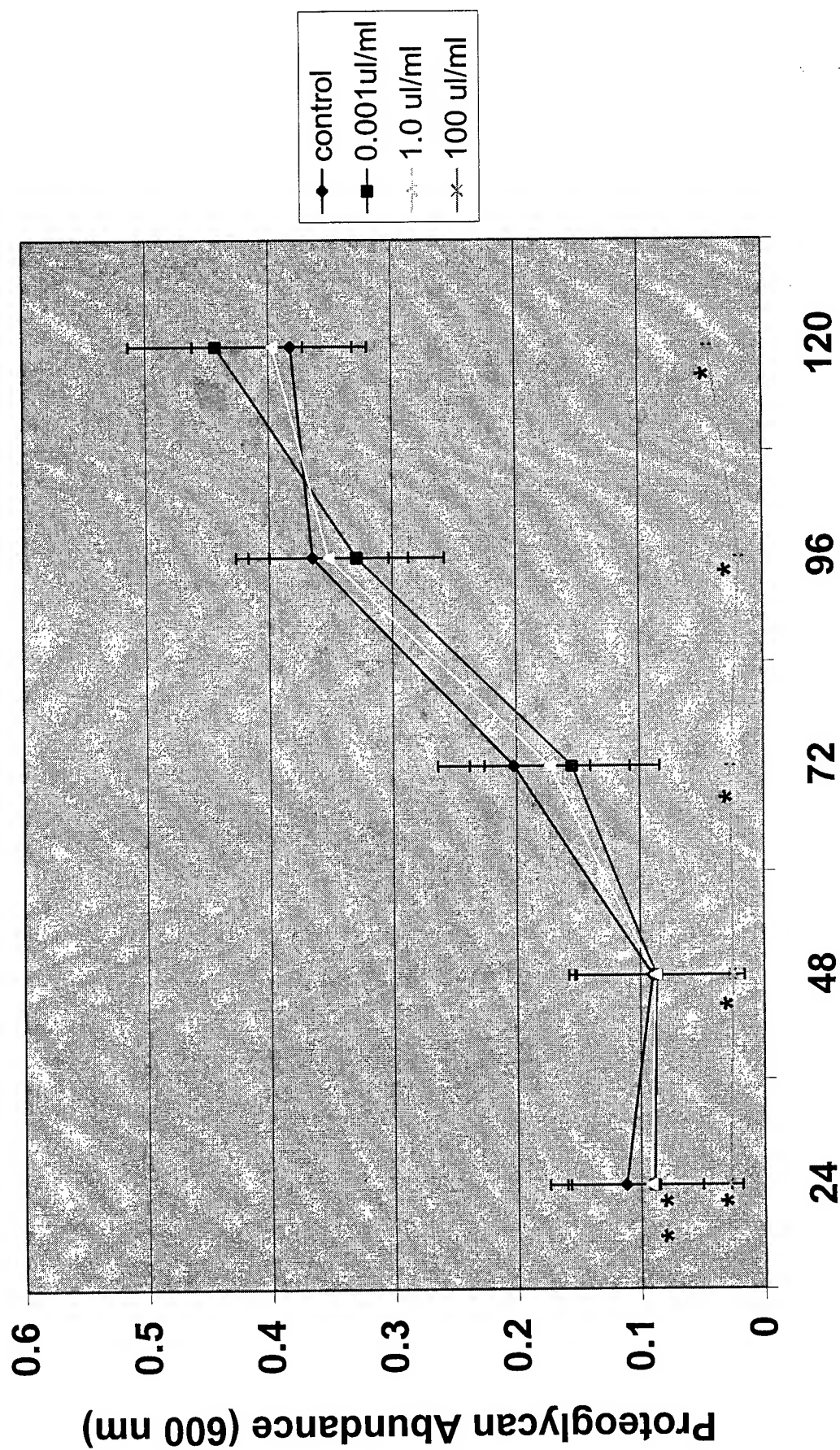


Figure 7: EG Time Course (hours)

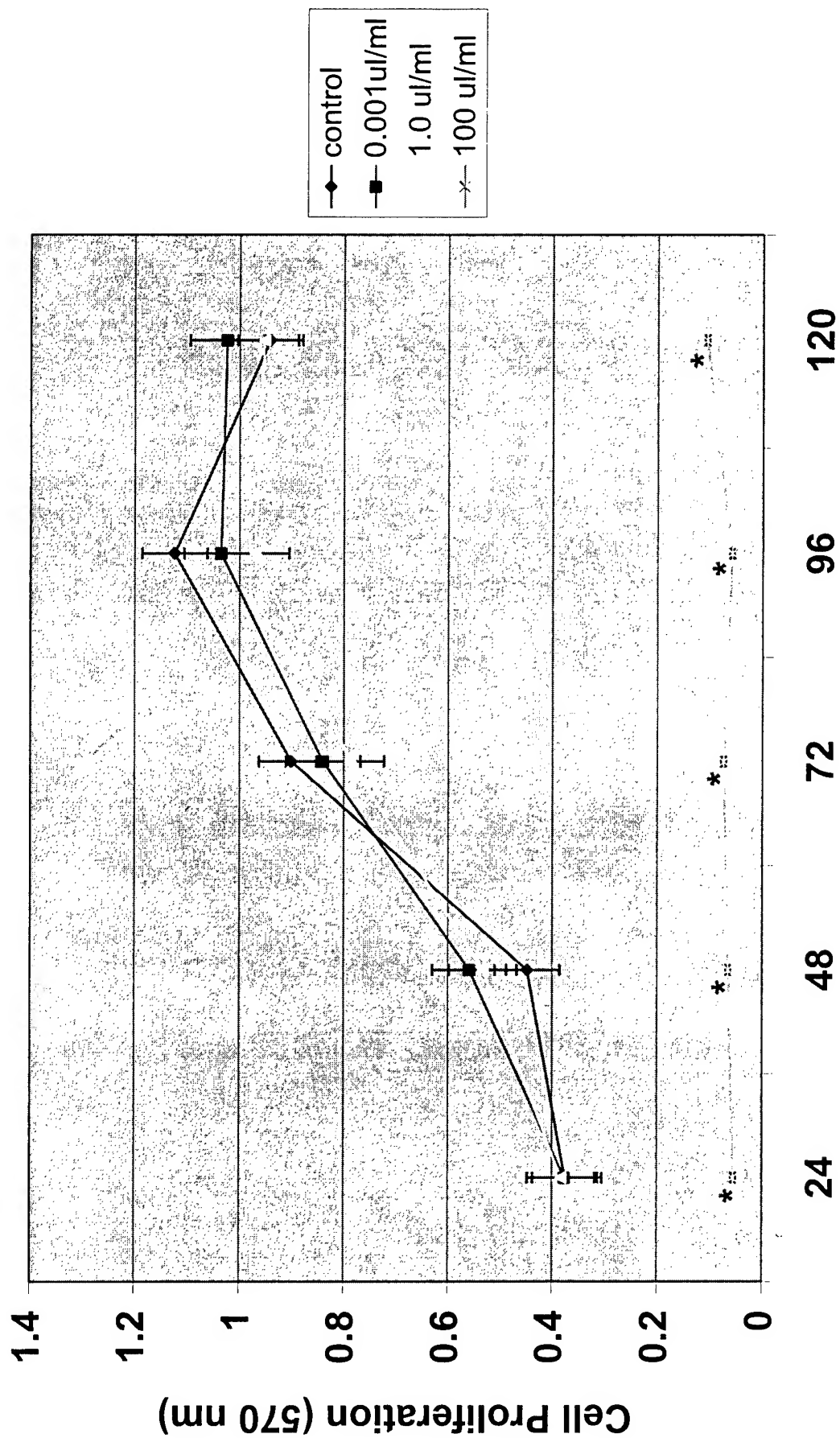


Figure 8: EG Time Course (hours)

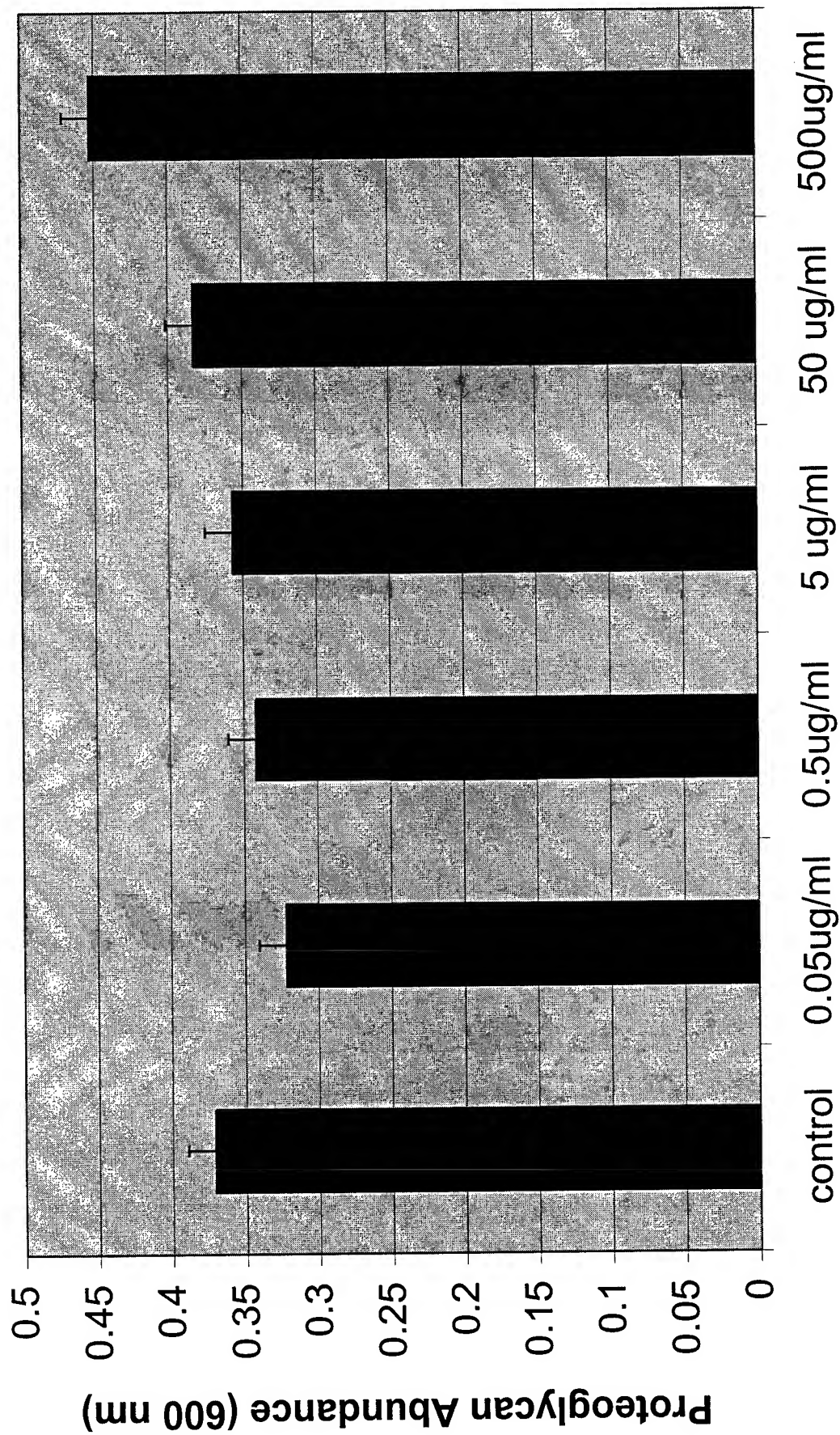


Figure 9: Cr+3 Concentration (ul/ml)

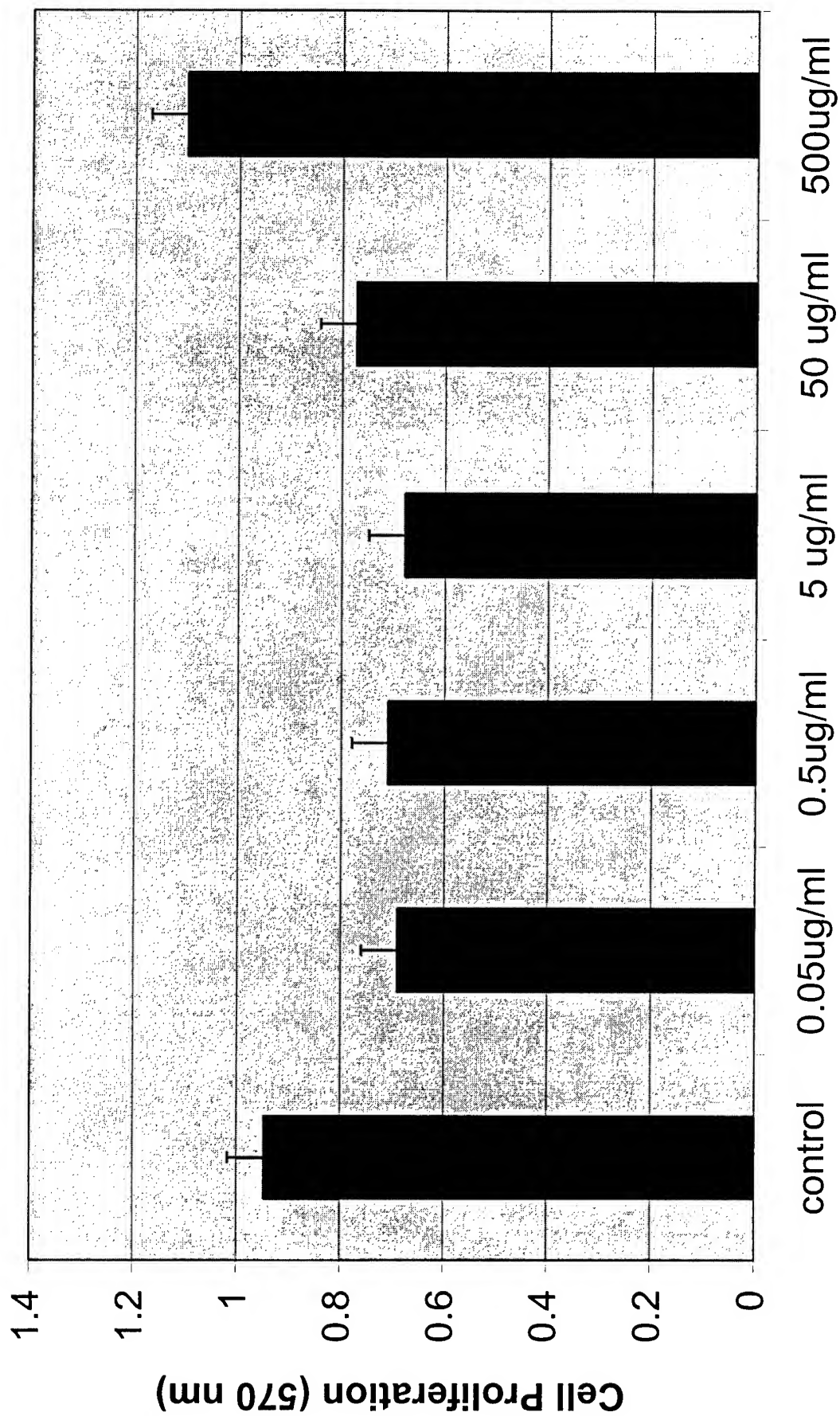


Figure 10: Cr+3 Concentration (ul/ml)

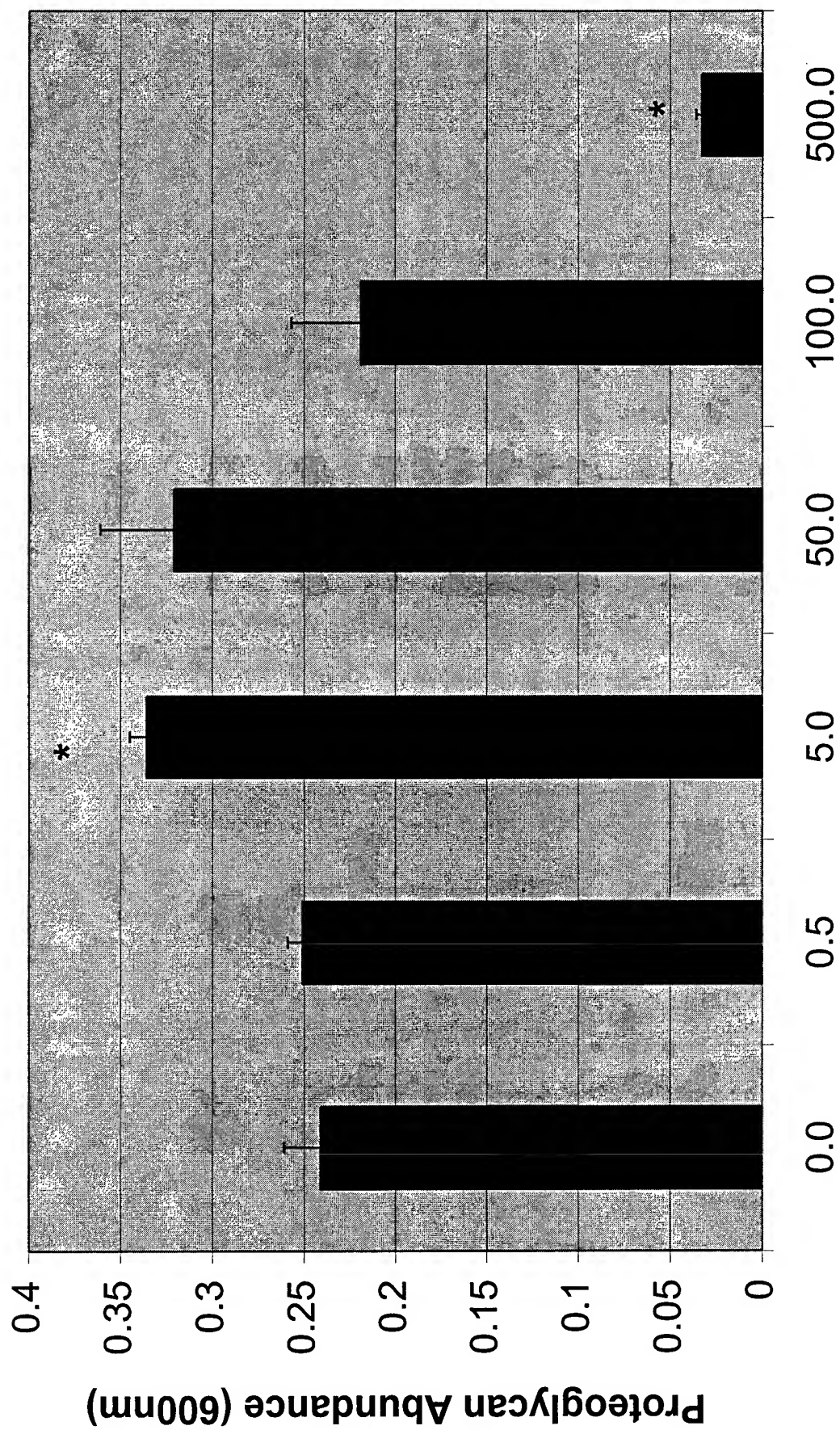


Figure 11: Pb Concentration (ug/ml)

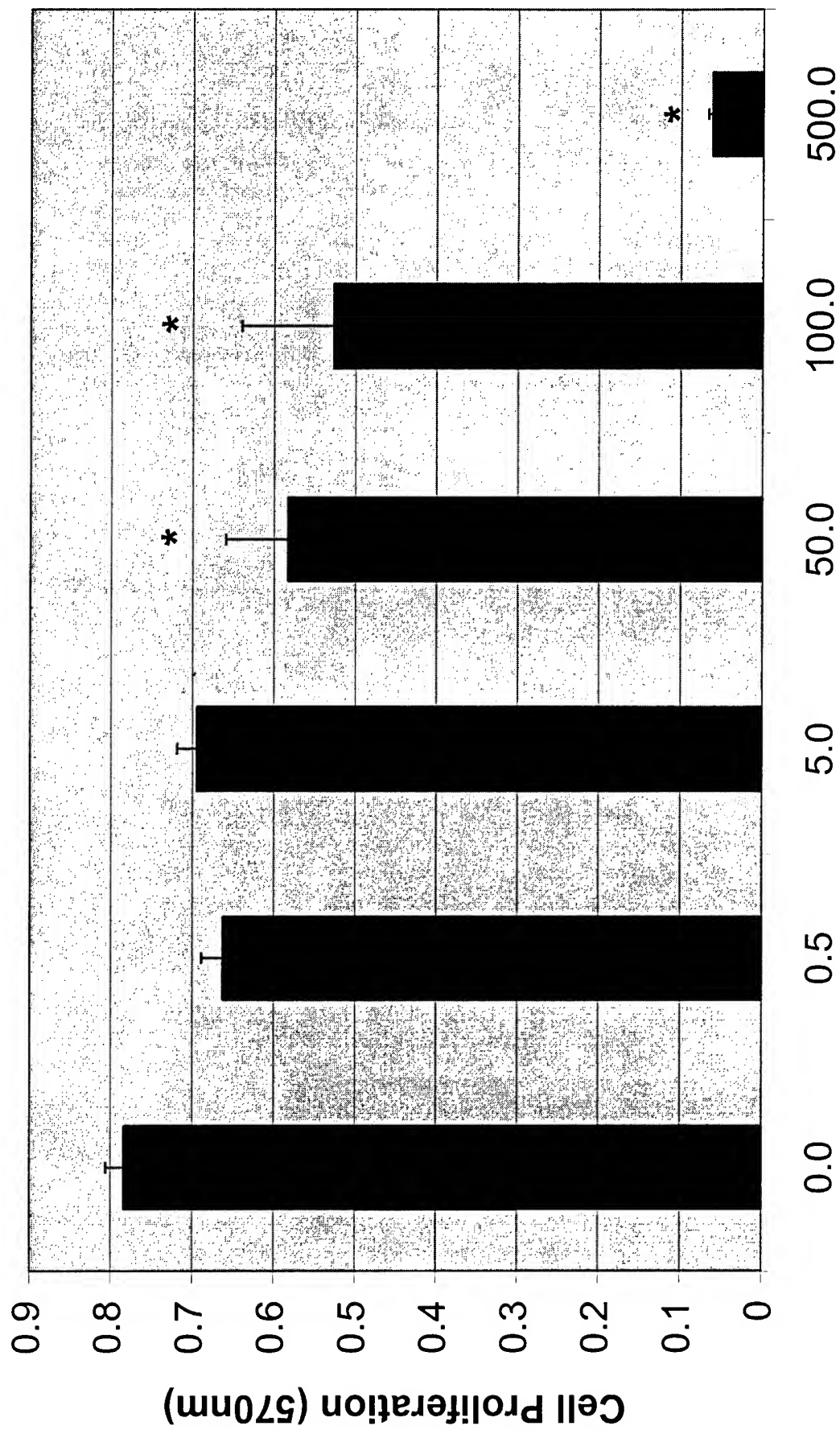


Figure 12: Pb Concentrations (ug/ml)

Figure 1 Concentration-response experiments showing the effects of DEG on proteoglycan abundance after 120 hours of culture (mean \pm S.E.). Asterisks indicate significant difference ($p < 0.05$) from control cultures. N=7.

Figure 2 Concentration-response experiments showing the effects of DEG on cell proliferation after 120 hours of culture (mean \pm S.E.). Asterisks indicate significant difference ($p < 0.05$) from control cultures. N=7.

Figure 3 Time course experiments showing the effects of DEG on proteoglycan abundance at 24 hour intervals (mean \pm S.E.). Asterisks indicate significant difference ($p < 0.05$) from control cultures. N=7.

Figure 4 Time course experiments showing the effects of DEG on cell proliferation at 24 hour intervals (mean \pm S.E.). Asterisks indicate significant difference ($p < 0.05$) from control cultures. N=7.

Figure 5 Concentration-response experiments showing the effects of EG on proteoglycan abundance after 120 hours of culture (mean \pm S.E.). Asterisks indicate significant difference ($p < 0.05$) from control cultures. N=6.

Figure 6 Concentration-response experiments showing the effects of EG on cell proliferation after 120 hours of culture (mean \pm S.E.). Asterisks indicate significant difference ($p < 0.05$) from control cultures. N=6.

Figure 7 Time course experiments showing the effects of EG on proteoglycan abundance at 24 hour intervals (mean \pm S.E.). Asterisks indicate significant difference ($p < 0.05$) from control cultures. N=3.

Figure 8 Time course experiments showing the effects of EG on cell proliferation at 24 hour intervals (mean \pm S.E.). Asterisks indicate significant difference ($p < 0.05$) from control cultures. N=3.

Figure 9 Concentration-response experiments showing the effects of Cr+3 on proteoglycan abundance after 120 hours of culture (mean \pm S.E.). Asterisks indicate significant difference ($p < 0.05$) from control cultures. N=5.

Figure 10 Concentration-response experiments showing the effects of Cr+3 on cell proliferation after 120 hours of culture (mean \pm S.E.). Asterisks indicate significant difference ($p < 0.05$) from control cultures. N=5.

Figure 11 Concentration-response experiments showing the effects of Pb on proteoglycan abundance after 120 hours of culture (mean \pm S.E.). Asterisks indicate significant difference ($p < 0.05$) from control cultures. N=6.

Figure 12 Concentration-response experiments showing the effects of Pb on cell proliferation after 120 hours of culture (mean \pm S.E.). Asterisks indicate significant difference ($p < 0.05$) from control cultures. N=6.

Works Cited

- Agency for Toxic Substances and Disease Registry (ATSDR), 1996. Toxicological Profile for Ethylene Glycol and Propylene Glycol (update), Atlanta: U.S. Department of Health and Human Services, Public Health Service.
- Agency for Toxic Substances and Disease Registry (ATSDR), 1993. Toxicological Profile for Lead, Atlanta: U.S. Department of Health and Human Services, Public Health Service.
- Bress, William C., and Jesse H. Bidanset, 1991. Percutaneous *In Vivo* and *In Vitro* Absorption of Lead, *Veterinary and Human Toxicology* 33:212-214.
- Bjornsson, S., 1993. Simultaneous Preparation and Quantitation of Proteoglycans by Precipitation with Alcian Blue, *Analytical Biochemistry* 210:282-291.
- Brown, NA and R Wiger, 1992. Comparison of Rat and Chick Limb Bud Micromass Cultures for Developmental Toxicity Screening, *Toxicology In Vitro* 6:101-107.
- George, M., K. Chepenik and M.H. Schneiderman, 1983. Proliferation of Cells Undergoing Chondrogenesis *In Vitro*, *Differentiation* 24:245-249.
- Hamburger, V and HL Hamilton, 1951. A Series of Normal Stages in the Development of the Chick Embryo, *Journal of Morphology* 88:49-92.
- Ivankovic, S. and R. Preussmann, 1975. Absence of Toxic and Carcinogenic Effects After Administration Of High Doses of Chromic Oxide Pigment in Subacute and Long-term Feeding Experiments in Rats, *Food Cosmetic Toxicology* 13:347-51.
- Klaassen, Curtis D., editor, 1996. *Casarett and Doull's Toxicology The Basic Science of Poisons 5th Edition* McGraw Hill, NY. pp.759-762.
- Price, C.J., C.A. Kimmel, R.W. Tyl and M.ZC. Marr, 1985. The Developmental Toxicity of Ethylene Glycol in Rats and Mice, *Toxicology and Applied Pharmacology* 81:113-127.
- Puzas, JE, MJ Sickel and ME Felter, 1992. Osteoblasts and Chondrocytes are Important Target Cells for the Toxic Effects of Lead, *Neurological Toxicology* 13:783-788.
- Renault, JY, C Melcion and A Cordier, 1989. Limb Bud Cell Culture for *In Vitro* Teratogen Screening: Validation of an Improved Assessment Method Using 51 Compounds, *Teratogenesis, Carcinogenesis and Mutagenesis* 9:83-96.

- Sabourin, P.J., M.A. Medinsky and F Thurmond, 1992. Effect of Dose on the Disposition of Methoxyethanol, Ethoxyethanol and Butoxyethanol Administered Dermally to Male F344/N Rats, *Fundamentals of Applied Toxicology* 19:124-132.
- Smith, MA, 1996. AFOSR Summer Research Extension Program Proposal, *unpublished*.
- Smith, MA and A Kanti, 1997. Chick Embryo Limb Bud Cell Culture for Screening Environmental Contaminants, Environmental Toxicology and Risk Assessment: Modeling and Risk Assessment (6th Volume). ASTM STP 1317, F. James Dwyer, Thomas R. Doane and Mark L. Hinman, Eds., American Society for Testing and Materials.
- Sokol, Rebecca Z., Helen Okuda, Harris M. Nagler and Nancy Berman, 1994. Lead Exposure *In Vivo* Alters the Fertility Potential of Sperm *In Vitro*, *Toxicology and Applied Pharmacology* 124:310-316.
- Wiley, F.H., W.C. Hueper, D.S. Bergen and F.R. Blood, 1938. The Formation of Oxalic Acid From Ethylene Glycol and Related Solvents, *Journal of Industrial Hygiene Toxicology* 20:269-277.

**APPLICATION OF META-ANALYSIS TO RESEARCH ON PILOT TRAINING:
EXTENSIONS TO FLIGHT SIMULATOR VISUAL SYSTEM RESEARCH**

**William A. Stock
Professor
Department of Exercise Science and Physical Education**

**Arizona State University
Tempe, AZ 85287-0701**

**Final Report for:
Summer Research Extension Program
Armstrong Laboratory**

**Sponsored by:
Air Force Office of Scientific Research
Bolling AFB
and
Armstrong Laboratory**

March, 1998

APPLICATION OF META-ANALYSIS TO RESEARCH ON PILOT TRAINING:

EXTENSIONS TO FLIGHT SIMULATOR VISUAL SYSTEM RESEARCH

William A. Stock

Professor

Department of Exercise Science and Physical Education

Abstract

In the present project, meta-analysis was used to synthesize nonclassified behavioral research conducted under the auspices of Armstrong Laboratory. A total of 599 effect sizes (mean effect size = .33) were extracted from 25 primary research reports dealing with flight simulator visual systems and the flying behaviors of pilots. Six of thirteen classes of experimental manipulations (density of features, presence of objects, presence of visual texture, vertical cues, visual details, and visibility) and three of eleven outcome classes (visual performance, altitude, bombing accuracy, and refueling) were associated with moderate to high mean effect sizes. Despite an inability to compute effect sizes from some studies, the overall results suggest a moderate to strong effect for a variety of manipulations in flight simulation systems across numerous outcome measures related to pilot performance.

APPLICATION OF META-ANALYSIS TO RESEARCH ON PILOT TRAINING: EXTENSIONS TO FLIGHT SIMULATOR VISUAL SYSTEM RESEARCH

William A. Stock

Introduction

Meta-analysis is the quantitative synthesis of primary research reports in a given domain. The methods used in meta-analyses have improved steadily since the seminal works of Glass and his associates (Glass, 1976; Glass, McGaw, and Smith, 1981), with most of the important changes documented in works by Hedges and Olkin (1985), Hunter and Schmidt (1990), and the *Handbook of Research Synthesis* (Cooper and Hedges, 1994). To conduct an effective meta-analysis one: (1) chooses, locates, and acquires the primary research reports in a given domain, (2) extracts effect sizes and other information from these reports, (3) codes the extracted information accurately and reliably (Stock, 1994; Stock, Gomez, and Balluerka, 1996), and (4) analyzes the effect sizes by means of appropriate models (Cooper and Hedges, 1994; Hedges and Olkin, 1985). When meta-analysis is applied to training research, the findings help: (1) distinguish effective from ineffective training methods and techniques, (2) estimate average effect sizes for successful interventions, and (3) provides objective bases for making decisions about the course of future work. In this manner, a meta-analysis provides a sound basis for making training, research, and policy decisions.

In a recently completed meta-analysis of Armstrong Laboratory research on the effects of scene content variables on low-altitude flight in flight simulators, one of more than 30 identified domains of flight simulator visual system research (Casey and McConnon, 1995; Warner and Casey, 1995), Stock (1996) found that changes in scene content were reliably related to positive changes in the low-altitude flying behaviors of pilots. He concluded that changes in scene content dramatically improve low-altitude flying in flight simulators. Specifically, increasing density of objects and textures, and introducing vertical cues (e.g., cones, trees and/or hills) were found to be the most effective manipulations. In addition, Stock found that some primary research reports failed to report sufficient statistics for the estimation of effect sizes -- a technical matter that can be addressed by providing investigators guidelines about what to present in primary research reports. These guidelines appear here in Part 2 of Appendix A. Finally, after determining that a large number of the primary reports involved applications of multi-dimensional scaling methods, Stock identified three problems associated with the use of this methodology. These problems included: (1) an absence of outcome

variables related to low-altitude flying, (2) a lack of experimental controls, and (3) limitations imposed by the choice of stimuli for the scaling tasks.

Although Stock (1996) identified effective interventions and suggested some changes in both the conduct and reporting of research, the scope of his project was limited to scene content and low-level flight. The goal of the present project was to expand Stock's previous meta-analysis to include other domains of Armstrong Laboratory research, specifically, studies that investigated the effects of manipulations of the visual systems of flight simulators on a variety of pilot behaviors – not just low-level flight.

Statement of the Problem

Whether pilot training occurs in planes or simulators, the cost is high. Quality research may decrease costs by determining more effective and/or efficient training procedures applicable in both environments, and/or by identifying behaviors that can be trained equally or more effectively in simulators -- where costs are lower. To these ends, the research staff of Armstrong Laboratory has conducted research on training since the early 1970's, and, as a result, there is a large body of competently designed and conducted, technically sophisticated, behavioral research that appears primarily in the technical research reports of Armstrong Laboratory.

Stock (1996) found that there was not a single quantitative syntheses of any portion of this body of research. He did locate a training report, the *Academic text: Low-altitude training* (Tactical Fighter Group, 1986), wherein the author reported the results of a thorough investigation of crash reports related to low-altitude flight. The changes in training that would reduce the dangers of low-altitude flight were identified, and a training program was subsequently created. That work demonstrated the usefulness of synthesizing findings presently available in Air Force documents, and led to important changes in training for low-altitude flight. However, in *Academic text: Low-altitude training*, the synthesis was not specifically a meta-analysis. Stock demonstrated that quantitative research synthesis provides a way to document and summarize a body of work, to communicate the findings of this work to a wider training community, and to base future training policy decisions on previously conducted research.

The premise of the present proposal was that a more comprehensive meta-analysis of the technical report series of Armstrong Laboratory would: (1) contribute to the training mission of the Air Force, (2) provide a basis for describing and communicating the findings of this body of research to the general training community, and (3) help guide decisions about training and future research. The specific overall goal of the present project was to initiate a comprehensive review of the entire corpus of flight simulator visual system research, comprised of research studies in 33 separate domains

(Casey and McConnon, 1995; Warner and Casey, 1995), so as to identify and synthesize those studies that investigated the effects of manipulations of the visual flight simulator systems on the flying behaviors of pilots.

Achievement of the overall goal depended on successfully completing a series of specific, enabling, objectives, each of which also contributes to the mission of Armstrong Laboratory. These specific objectives included the following.

Identification of the research literature. Due to efforts of the staff of the Library of Armstrong Laboratory, this objective was achieved in an efficient manner. The Library maintains and catalogs all research conducted under the auspices of Armstrong Laboratory. Extensive annotated bibliographies are periodically published by the staff. These bibliographies were the primary means of identifying the research that has been conducted and reported under the auspices of Armstrong Laboratory.

Identification of a general coding scheme for extracting information from the primary research reports. The ground work for completing this objective rested on previous work in meta-analysis methodology (Stock, 1994; Stock, Gómez, and Balluerka, 1996; Stock and Kulhavy, 1989) and the previously cited meta-analysis of scene content research at Armstrong Laboratory (Stock, 1996). The steps necessary to insure that a meta-analysis will have a high likelihood of success are specified in Appendix A. Included there are the steps of identifying the information to code, designing forms for coding, data entry, and analyses, and constructing a code book that provides specific guidance to present and future coders.

Extraction of the information to be coded. Extraction of information from the primary research reports was the most time-consuming aspect of the project. However, the research report series was not excessively large, and this aspect of the project was completed in a relatively timely fashion.

Creation of an electronic data base. Once the series of primary reports had been read, and the information extracted and coded, it was necessary to transfer the coded information to a data base, so that inquiries about the findings of the primary research reports could be quickly and effectively answered. Over time, with additional efforts, it should be possible to add new research studies and/or newly coded items to this data base. This data base provide a means by which researchers and policy makers can rapidly, systematically, and quantitatively assess the effects of specific experimental and/or training interventions. This data base currently exists in the form of an SPSS 7.5 save file.

Definition of the Variables of Interest. For those who train pilots and for those who design, conduct, or evaluate training that occurs in simulators, the tasks of conducting and evaluating training research are made more complex because the graphics imaging systems of simulators do not reproduce a real out-of-the-cockpit scene with complete fidelity (Andrews, Carroll, and Bell, 1996).

Nevertheless, a presupposition of the present project was that the outcome variables of interest are those behaviors that are related to flying an aircraft -- whether said behaviors occur in planes or simulators. These behaviors included but were not necessarily limited to: (1) aircraft control (e.g., altitude estimation, stick control, take off and landings), (2) mission completion (e.g., bombing, refueling, and carrier landing), and (3) minimization of performance errors.

The remaining information that was coded focused on attributes of interventions (training procedures and duration, experimental manipulations) and background variables of the studies (location, subjects, type of study, etc.). By examining the coding forms for this meta-analysis (Appendix B), the reader may better understand the scope and detail of the items coded.

Method

Literature Search for Data Base

The literature was restricted to behavioral research studies conducted under the auspices of Armstrong Laboratory. These studies are identified in annotated and categorized bibliographies maintained by the Library at Armstrong Laboratory, Williams Gateway Air Field, Mesa, Arizona. The Armstrong Laboratory Librarian provided copies of all of the required research reports. All behavioral research dealing with flight simulator visual systems and pilot flying behaviors was initially included in the project -- with the following restrictions. First, classified research was excluded because the author had no clearance to access this research. Second, research designed and conducted to assess or improve the performance of the flight simulator systems themselves was excluded because the primary intent of such research was not the training or performance of pilots. Finally, for obvious reasons, duplicate papers (e.g., a technical report and a paper presentation for the same study) were coded as a single source.

Choice of Effect Size

There are two major types of effect sizes. The first is a standardized mean difference on an outcome variable measured at two different levels of a manipulated variable. For example, if an investigator measured the proportion of time that pilots maintained their aircraft at a specified low altitude both when the scene did and did not contain vertical cues, then an effect size could be computed that reflected the effect of the presence of vertical cues on the behavior of maintaining altitude. The second type of effect size is a correlation between two measured variables. Prior to initiating this meta-analysis, it was planned to include both types of effect size in the study. However, at a later stage, preliminary screening of the primary research sources revealed that a very small proportion of studies provided the second type of effect size. Consequently, the latter type was

excluded. Effect size computations have been documented in the general academic literature (e.g., Cooper and Hedges, 1994; Glass, McGaw, and Smith, 1981; Hedges and Olkin, 1985; Hunter and Schmidt, 1990). The methods described in that literature were employed in the present project.

Selection and Coding of Data Base

A meta-analyst tries to identify attributes of studies that vary with effect sizes. Attributes that are causally linked to effect size magnitude are important because they provide a basis for designing and conducting new research, as well as making policy decisions about the nature of training. The information that defines these attributes has to be extracted and coded for analysis. Of a variety of possible categories of items to code (Stock, 1994), a standard set of items would include information about identification of studies, research setting, subjects, methodology, and effect size outcomes. Year and source of publication are examples of identification. Items in the setting category often describe the use of special populations, as well as the physical location in which the study took place. Characteristics of participants of a study are considered subject variables. Items that describe study design and sampling procedures pertain to methodology. Information about effect size forms the final category of items. Included in this category are the summary statistics used to compute effect sizes and information about the outcome measures. The final set of items selected for coding in this meta-analysis appear in Appendix B. A more extended presentation of the details associated with identification and selection of items to code appears in the Part 3 of Appendix A.

Categorization of Effect Size Conditions

The entire set of effect sizes was sorted by the type of: (1) experimental manipulation, and (2) outcome measure. These groupings formed the basis for the principal analyses reported in this paper.

Categories of Experimental Manipulation. Thirteen categories of experimental manipulation were coded across studies. These categories focused on changes in the: (1) density of objects (more minus less), (2) presence and/or types of objects (more minus less, or more minus less realistic), (3) visual texture (more minus less), (4) vertical cues (more minus less), (5) visual details (more minus less), (6) motion (more minus less), (7) type of display (more versus less complete types of simulation systems), (8) field of view (larger minus smaller) (9) g seat (on minus off), (10) turbulence (less minus more), (11) visibility (more minus less), (12) angle of attack (shallower minus steeper), and (13) wind (less minus more). Strictly speaking, changes in motion and g-seat configurations are not manipulations of the visual systems of flight simulators, nevertheless, it was judged to be reasonable to code and include them in subsequent analyses.

Categories of Outcome Measures. Eleven categories of outcome measures were employed. These categories included: (1) visual performance measures (e.g., target location and identification), (2)

flying within a specified tolerance on an performance measure, (3) airspeed measures, (4) altitude measures, (5) carrier landing measures, (6) transfer measures (including real flight after simulator training), (7) bombing accuracy indices, (8) root mean square measures of error for a variety of performance domains (hereafter, RMS), (9) roll, pitch and yaw indices, (10) outcomes associated with refueling performance, and (11) an eclectic group of summary and global indices of flying performance.

Selection of a Data Base and Analysis System

During the course of the project, a decision was made to use SPSS 7.5 to provide the combination of data base manipulation and data analysis tools. This off-the-shelf data statistical package is generally available.

Results

Overall Distribution of Effect Sizes

A total of 599 effect sizes were extracted from 25 primary research reports, representing more than four times as many effect sizes as found by Stock (1996). As with Stock (1996), some research reports were appropriate for the meta-analysis, but did not contain sufficient statistics to compute an accurate effect size estimate. Figure 1 depicts the distribution of effect sizes with a normal curve superimposed on the actual distribution. For this set of effect sizes, the mean and standard deviation were .33 and .69, respectively. An examination of Figure 1 reveals that the modal effect size was in the interval around zero. However, this modal phenomenon was due in large part to the effect sizes generated by two primary sources (Irish, Grunzke, Gray, & Waters, 1977; LeMaster & Longridge, 1978), which accounted for a total of 252 effect sizes – many of them quite small in value. Consequently, Figure 2 depicts the distribution of effect sizes for all but these two sources. For Figure 2, the mean and standard deviation were .54 and .79, respectively – a notable increase in the mean effect size. Further, a comparison of Figures 1 and 2 reveals that the latter distribution has a much larger proportion of effect sizes above zero. Interestingly, both the Irish et al. and Lemaster & Longridge studies generated a very large number of dependent measures using the Advanced System for Pilot Training, a system characterized by extensive automatic measurement capabilities.

Categorization of Effect Sizes by Conditions of Study and Outcome

Table 1 summarizes the descriptive statistics for effect sizes after cross-classification by type of experimental manipulation and by outcome measure. Note that the final row category of Table 1 Parts 1 and 2, and the final column category of Table 1 Part 2, are marginal summaries of the cells of Table 1. An examination of Table 1 reveals a number of interesting facts.

For the experimental manipulations, just three categories of manipulation (Visual Details, Type of Display, and Field of View) had effect sizes associated with a majority of the 11 outcome categories. The column marginal means for these three categories of experimental manipulation were .57, .17, and .31 respectively. Disregarding the outcome measures involved, six of the thirteen classes of experimental manipulations (density of features, presence of objects, presence of visual texture, vertical cues, visual details, and visibility) were associated with moderate to large mean effect sizes (above .5). Five of the classes (motion, type of display, field of view, angle of dive, and wind) were associated with small to moderate mean effect sizes (between .2 and .5). In this group, note that the marginal mean for motion is negative. This reflects the fact that the direction of the comparison was more minus less motion (e.g., 6 degree-of-freedom minus 3 degree-of-freedom motion, or 3 degree-of-freedom minus no motion). In short, the introduction of motion in the simulation system generally led to poorer flying behaviors in the flight simulation systems. Finally, manipulations involving the use of g-seats or simulating turbulence did not produce noticeable effects.

For outcome measures, only three outcome classes (Altitude, RMS, and General Flight) appeared in a majority of the classes of experimental manipulation. The row marginal mean effect sizes for these three classes of outcome were .72, .31, and .12, respectively. Disregarding the number of different types of experimental manipulations involved, moderate to high mean effect sizes were found with visual performance, altitude, bombing accuracy, and refueling outcome measures. Small to moderate mean effect sizes were found for the flying within tolerance, transfer, RMS, and roll, pitch and yaw outcome measures. Negligible marginal mean effect sizes were observed for airspeed and carrier landing outcome measures.

Finally, of the 143 cells representing a combination of an experimental manipulation and an outcome measure, 91 cells are empty – each one representing an experimental manipulation and outcome measure combination for which no effect size was found. These are areas in which new research might be conducted.

Functional Use of the Flight Simulator System

Effect sizes were divided into two groups, one for studies in which the subjects actually flew or had functional control of the simulator during measurement of the outcome measure, and the other for studies in which subjects lacked such functional control (e.g., subjects merely pressed a button to indicate a change in simulator conditions, say for detection of increases or decreases in the displayed altitude, or the appearance of a target, etc.). An analysis of variance indicated a large and reliable difference ($F_{1, 598} = 18.76$, $MS_{\text{error}} = .45$, $p < .001$) between the mean effect sizes (.29 and 1.1 for

the functional control and no functional control groups, respectively). Thus, where the study conditions were more complex and comparable to actual flying, effect size magnitude was typically more moderate.

Changes in Effect Size Magnitude Across the Study Period

Effect sizes were sorted by year of publication and examined for possible differences. Figure 3 depicts the mean effect size by year of publication. An analysis of variance confirmed what visual inspection of Figure 3 suggests. First, from earlier to later years there is increase in the average effect size difference (for the linear component, $F_{1, 586} = 17.52$, $MS_{\text{error}} = .38$, $p < .001$). Second, there are nonlinear elements in the trend in effect size magnitude (e.g., $F_{1, 586} = 21.47$, $MS_{\text{error}} = .38$, $p < .001$, and $F_{1, 586} = 55.72$, $MS_{\text{error}} = .38$, $p < .001$, for the quadratic and cubic effects, respectively). Two possible explanations for the simple linear increase were explored.

First, Figure 4 depicts the number of effect sizes associated with each year of publication. Examination of this figure reveals that many more effect sizes are associated with the earlier studies. With fewer effect sizes in the latter years, it is possible that observed phenomenon is due to sampling variability. Next, Figure 5 depicts, for each year of publication, the proportion of studies in which subjects had functional control of the flight simulation system. Visual inspection of Figure 5 confirms that the concentration of studies with functional control is much greater in earlier than later years. Unfortunately, these alternate explanations are essentially confounded.

Figure 1. Distribution of All Effect Sizes

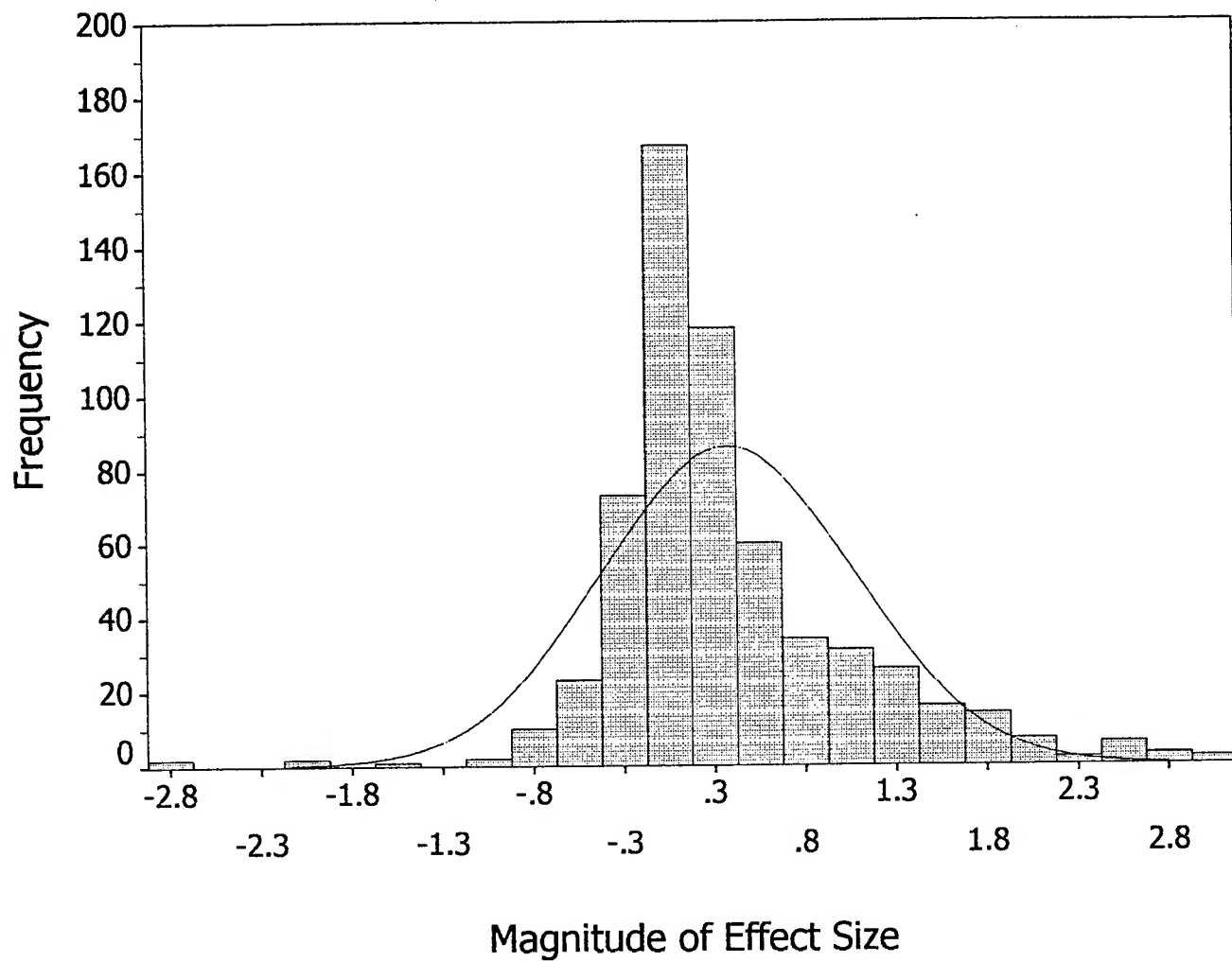


Figure 2. Distribution of All Effect Sizes
With Studies 16 and 17 Omitted

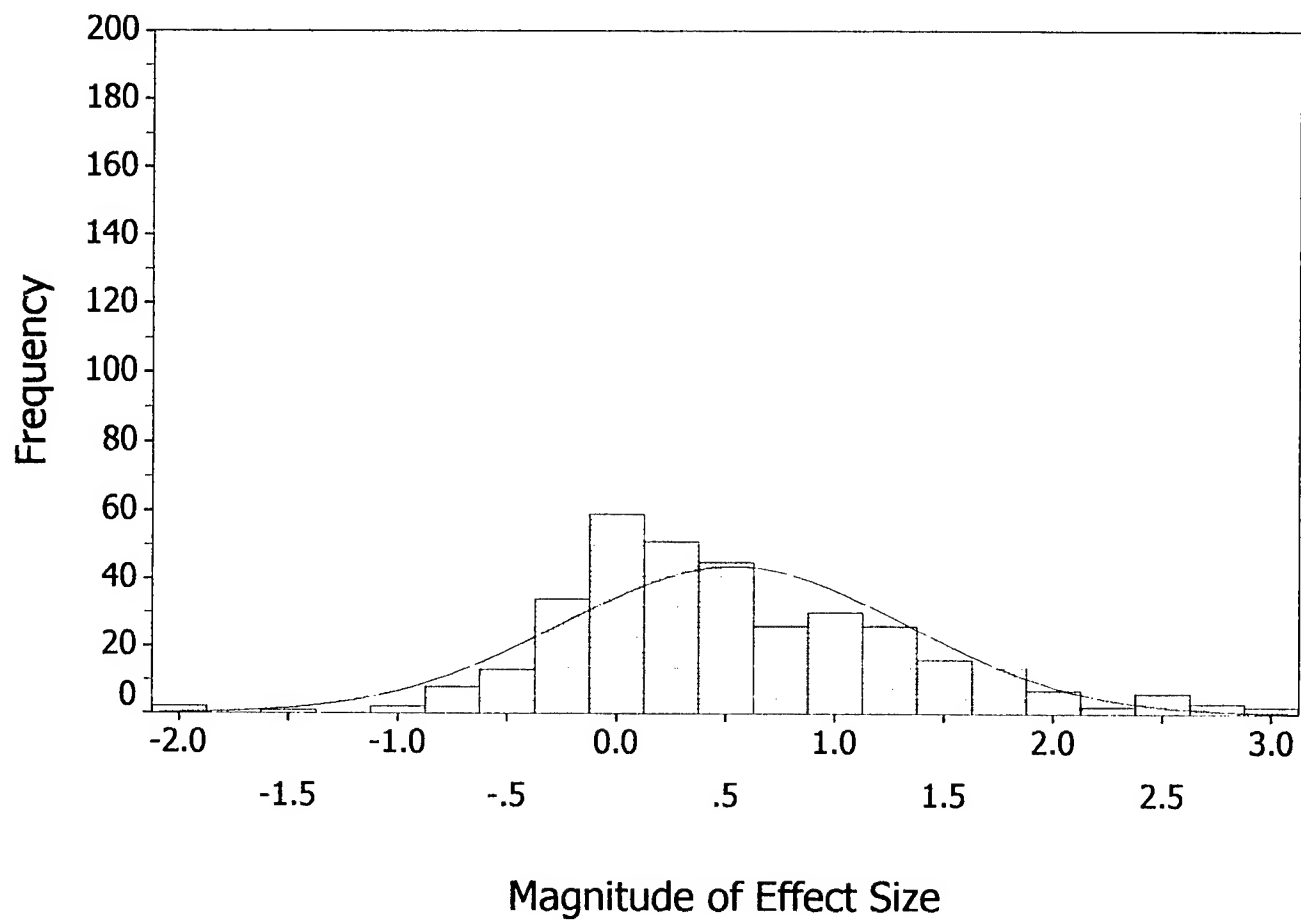


Table 1, Part 1. Statistical Summary of Effect Sizes as a Function of Experimental Manipulation and Type of Outcome Measure

Experimental Manipulations		Dependent Variables					
		Visual	Fly within Tolerance	Airspeed	Altitude	Carrier Landing	Transfer
Density	M		.92		.92		
	SD		.43		.74		
	N		3		57		
Objects	M				.92		
	SD				.85		
	N				79		
Visual Texture	M		.92	-.05	.85		
	SD		.26	.26	.85		
	N		3	3	55		
Vertical Cues	M				.95		
	SD				.54		
	N				8		
Visual Details	M			-.46	.57		
	SD				.67		
	N			1	19		
Motion	M						
	SD						
	N						
Type of Display	M	1.82		.06			
	SD	.87		.25			
	N	2		4			
Field of View/AOI	M	.32	-.07	.18	.21	-.08	.02
	SD	.79	.33	.31	.62	.31	.14
	N	11	6	4	13	24	12
G Seat	M						
	SD						
	N						
Turbulence	M						
	SD						
	N						
Visibility	M						.49
	SD						.84
	N						33
Angle of Dive	M				.16		
	SD				.67		
	N				12		
Wind	M						
	SD						
	N						
Across All Experimental Manipulation	M	.55	.26	.04	.72	-.08	.37
	SD	.95	.60	.32	.82	.31	.75
	N	13	9	11	135	24	45

Table 1, Part 2. Statistical Summary of Effect Sizes as a Function of Experimental Manipulation and Type of Outcome Measure

Experimental Manipulations	Dependent Variables						Across All Variables
		Bombing Accuracy	RMS Type	Roll, Pitch & Yaw	Refueling	General Flight	
Density	M					.03	.84
	SD					.21	.74
	N					6	66
Objects	M		1.10			.00	.82
	SD		.81			.18	.86
	N		18			9	88
Visual Texture	M		1.10			1.07	.82
	SD		.81			.22	.82
	N		18			3	.64
Vertical Cues	M						.95
	SD						.54
	N						8
Visual Details	M	.28	.31	-.10	.90	.08	.57
	SD	1.35	.52	.62	.44	.27	.70
	N	5	4	5	23	4	60
Motion	M		-.12			-.26	-.23
	SD		.16			.54	.51
	N		24			60	69
Type of Display	M	.04	.17	.09	.08	-.08	.17
	SD	.45	.28	.22	.23	.57	.50
	N	2	9	6	18	2	34
Field of View or AOI	M	.94	.21	.29	.54	.13	.31
	SD	1.17	.34	.52	.54	.36	.65
	N	22	35	9	41	46	183
G Seat	M		.10			.06	.06
	SD		.14			.15	.15
	N		10			31	31
Turbulence	M		.07			.11	.11
	SD		.18			.22	.22
	N		15			51	.51
Visibility	M		.34		.90	.42	.56
	SD		.23		.44	.66	.64
	N		5		23	56	81
Angle of Dive	M		1.00	1.00			.44
	SD		.73	.73			.79
	N		6	6			18
Wind	M		.40			.31	.31
	SD		.31			.31	.31
	N		9			33	33
Across All Experimental Manipulation	M	.76	.31	.33	.54	.12	
	SD	1.18	.57	.65	.54	.50	
	N	29	126	26	41	290	

Figure 3. Average Effect Size by Year of Publication

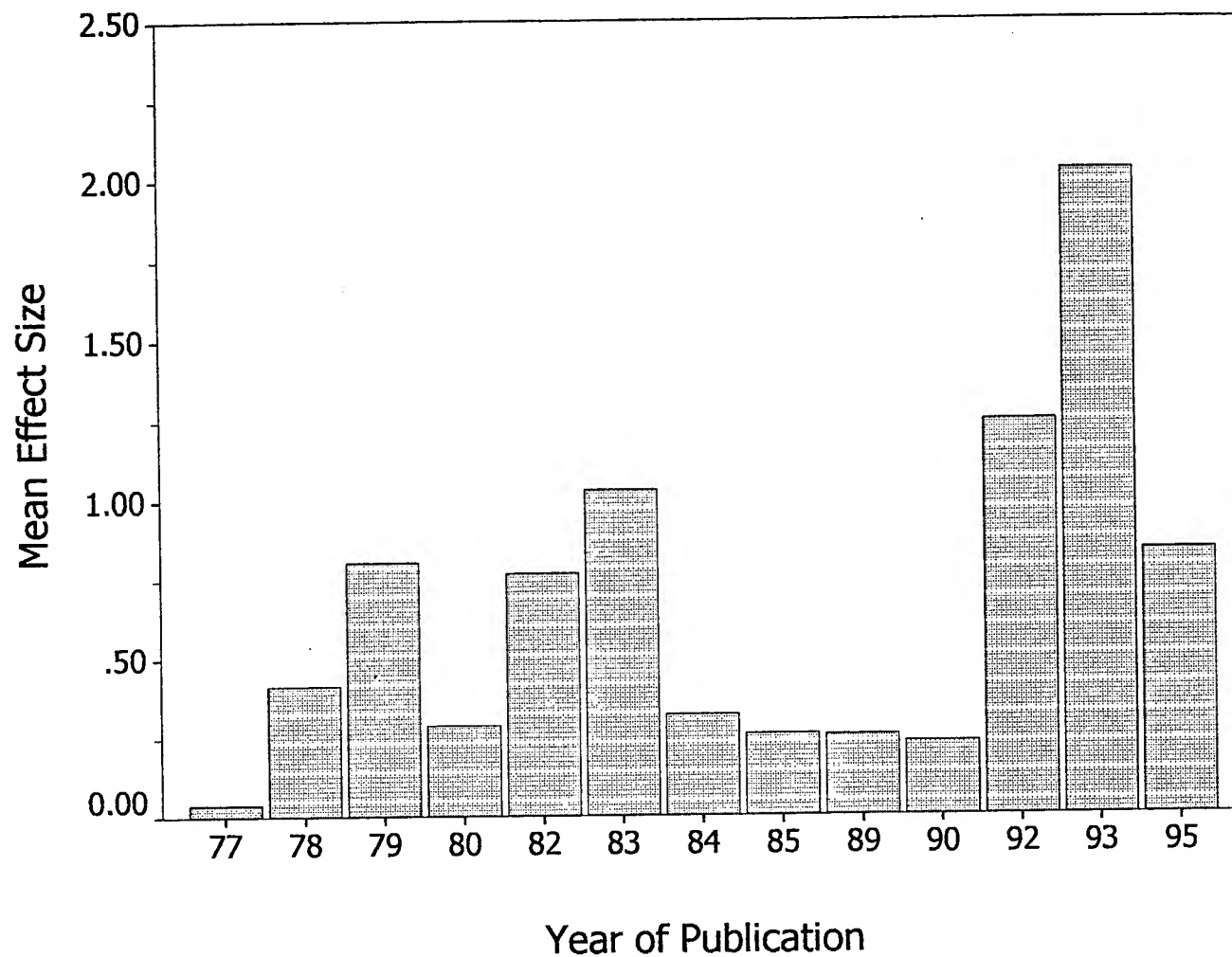


Figure 4. Effect Size Count by Year of Publication

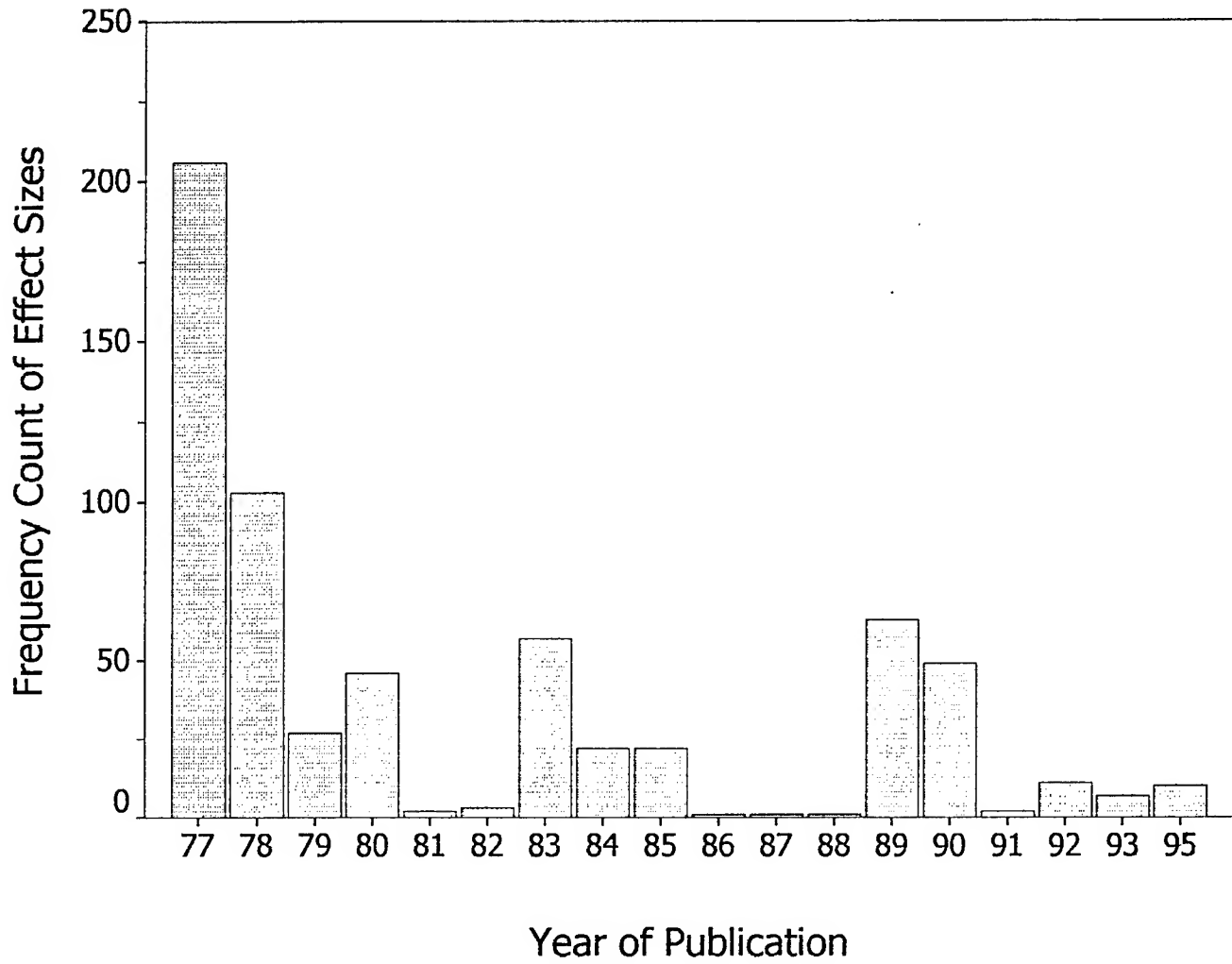
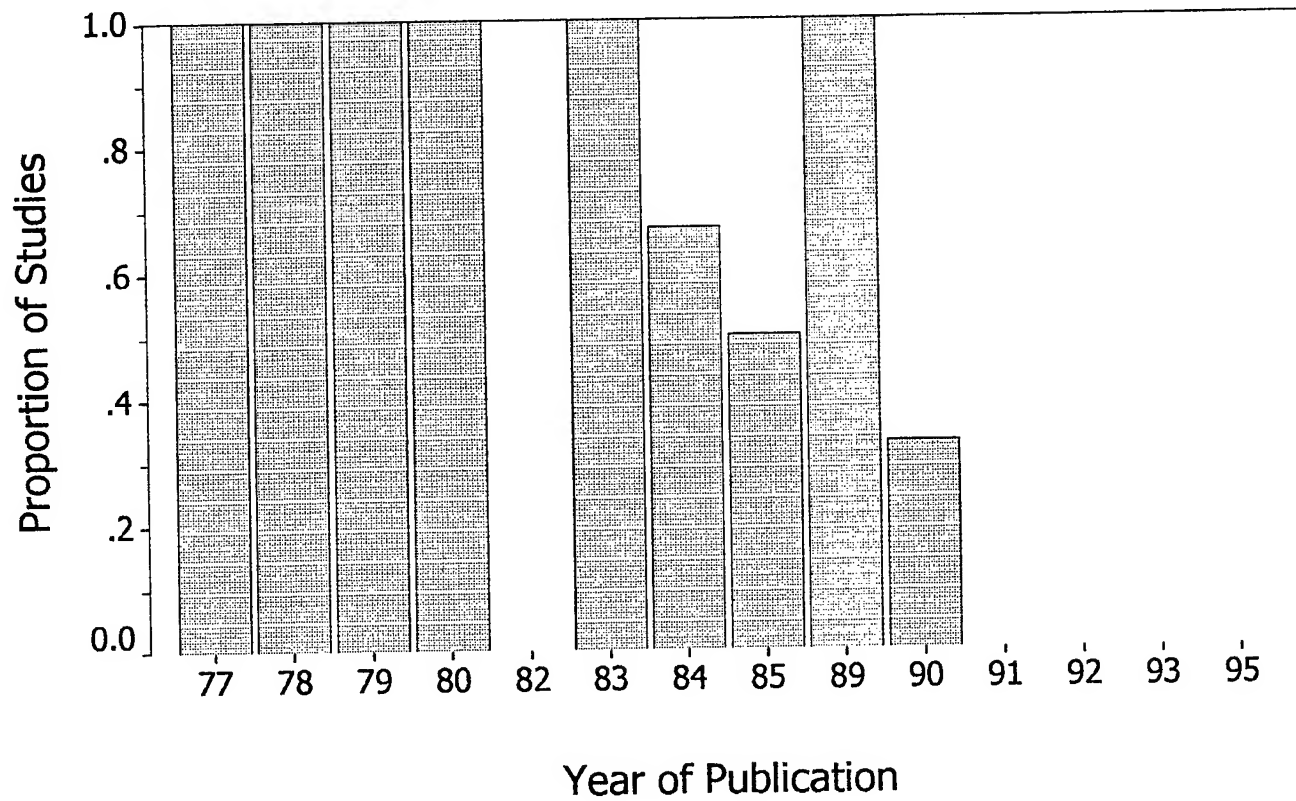


Figure 5. Proportion of Studies Where Subjects
Had Functional Control of the Simulator

Note. Zero in Years 82, 91, 92, 93, 95



Discussion

Across all effect sizes, a mean of .33 indicates a moderate level of effectiveness. To help interpret this level of effect, consider the following illustration. In the simplest case of a comparison between a treatment and a control condition, an effect size of .33 means that the typical person in the treated group performs the same as a person at the 63rd percentile in the control group. To place effect sizes in another perspective, consider the following. Say that the mean performance of pilots in the control group is considered a threshold of successful performance. Say also that a treatment leads to an effect size of .33. In this case, for every 100 successful pilots in the control group, there will be 126 successful pilots in the experimental group. If the effect size is small, say .1, there will still be 108 successful pilots in the experimental group for every 100 successful control pilots. When the effect sizes reaches 1.0, there are 168 successful experimental pilots for every 100 successful control pilots. The point is that even small effect sizes lead to important changes in training outcomes.

Most of the experimental manipulations were associated with effect sizes of moderate value, indicating that pilot performance was being substantively changed for the better. G-seat manipulations were least likely to have an appreciable effect – a finding in consonance with the fact that Air Force flight simulation systems now generally operate without this subsystem. Similarly, effect sizes associated with the introduction of motion systems were generally negative (mean = -.23). In itself, this effect is not surprising. Motion will increase the difficulty of task performance and produce lower scores. Although motion subsystems have generally been abandoned in Air Force flight simulators, an interesting issue remains. Because real flight occurs in a full 6 degree-of-freedom motion environment, the question of interest is not whether motion systems lead to better simulator performance, relative to non motion systems, but rather whether the use of motion systems, relative to nonmotion systems, lead to better flight performance in the real world. Unfortunately, in the present data base, this author was unable to find effect sizes in the transfer outcome category (i.e., comparisons of real flight performances between those trained in motion versus nonmotion systems).

With respect to the different classes of outcome measures, it may be said that the types of interventions investigated generally had substantive effects. In reviewing Table 1, it is interesting to note that general or global flight measures were less sensitive to manipulations than measures of more specific behaviors. This is understandable for the following reason. Most of the subjects were Air Force pilots with significant amounts of flying experience, all of whom had passed various training thresholds. Relative to the population of all pilots, they are likely to be fairly homogeneous with respect to global assessments of their flying skills. Further, when such subjects encounter a specific intervention, the outcome measure most likely to be affected is the one most directly affected by the

intervention (e.g., manipulations of visibility will affect the pilots ability to position his plane for refueling but not necessarily the airspeed at which he attempt to reach that position).

As in Stock (1996), here there were research reports that failed to report sufficient statistics for effect sizes to be computed. This deficiency may be corrected by creating standard formats for studies that report behavioral research. In particular, Part 2 of Appendix A provides an outline of these sufficient statistics and offers some guidance on the development of standard formats. However, the issue of reporting standards can become quite complex with complicated designs, and a full specification is beyond the scope of this project.

For the studies that did report sufficient statistics, an interesting historical phenomenon was observed. This was the fact that more recent studies of the visual flight simulator systems have actually involved less functional control of the simulators than earlier studies. The basic finding may be due to a number of possibilities. It may reflect a switch of interest from training to more basic research issues. It may reflect a difference between classified and unclassified research – the former not within the scope of this investigation. Finally, it may simply be an artifactual difference.

References

- 162nd Tactical Fighter Group. (1986). *Academic text: Low-altitude training*. Tucson, AZ: Author.
- Andrews, D. H., Carroll, L. A., & Bell, H. H. (1995). *The future of selective fidelity in training devices*. (AI/HR-TR-1995-0195). Aircrew Training Research Division, 6001 South Power Road, Mesa, AZ.
- Casey, E. P., & McConnon, M. E. (1995). *Annotated bibliography of Aircrew Training Research Division technical publications*. (AI/HR-TR-1995-0079). Aircrew Training Research Division, 6001 South Power Road, Mesa, AZ.
- Cooper, H., & Hedges, L. V. (Eds.). (1994). *Handbook of research synthesis*. New York: Russell Sage.
- Durlak, J. A., & Lipsey, M. W. (1991). A practitioner's guide to meta-analysis. American Journal of Community Psychology, 19, 291-332.
- Glass, G. V. (1976). Primary, secondary, and meta-analysis of research. *Educational Researcher*, 5, 3-8.
- Glass, G. V., McGaw, B., & Smith, M. L. (1981). *Meta-analysis in social research*. Beverly Hills, CA: Sage.
- Hedges, L. V., & Olkin, I. (1985). *Statistical methods for meta-analysis*. Orlando, FL: Academic Press.
- Hunter, J. E. & Schmidt, F. L. (1990). *Methods of meta-analysis: Correcting error and bias in research findings*. Newbury Park, CA: Sage.
- Kulik, J. A., & Kulik, C. L. C. (1989). Meta-analysis in education. International Journal of Educational Research, 13, 221-340.
- Orwin, R. G. (1994). Evaluating coding decisions. In H. Cooper, & L. V. Hedges (Eds.), The handbook of research synthesis. (pp. 139-162). New York: Russell Sage Foundation.
- Orwin, R. G., & Cordray, D. S. (1985). Effects of deficient reporting on meta-analysis: A conceptual framework and reanalysis. Psychological Bulletin, 97, 134-147.
- Rosenthal, R. (1994). Parametric measures of effect size. In H. Cooper, & L. V. Hedges (Eds.), *Handbook of research synthesis*. (pp. 231-260). New York: Russell Sage Foundation.
- Stock, W. A. (1994). Systematic coding for research synthesis. In H. Cooper, & L. V. Hedges (Eds.), *Handbook of research synthesis*. (pp. 139-162). New York: Russell Sage Foundation.
- Stock, W. A. (1996). Application of Meta-analysis to pilot-training research: A case study of research on scene content and low-level flight in simulators. Final Report for the AFOSR Summer Faculty Research Program.
- Stock, W. A., Gómez Benito, J., & Balluerka Lasa, N. (1996). Research synthesis: Coding and conjectures. *Evaluation and the Health Professions*, 19, 104-117.

- Stock, W. A., & Kulhavy, R. W. (1989). Reporting primary data in scientific articles: Technical solutions to a perennial problem. *American Psychologist*, 44, 741-742.
- Warner, H. D., & Casey, E. P. (1995). *Flight simulator visual system research and development: Bibliography of support provided by the Aircrew Training Research Division*. (AI/HR-TR-1995-0107). Aircrew Training Research Division, 6001 South Power Road, Mesa, AZ.

Appendix A: General Guidelines for Research Synthesis

Part 1. Different Families of Effect Sizes

There are two primary families of effect size. The first of these includes any effect size that is essentially a standardized mean difference between two conditions. In ideal circumstances, this type of effect size is computed from means and standard deviations reported in the primary research report for the two conditions compared – these ordinarily being either an experimental and a control condition, or two different levels on an experimental factor. Also, as there are a number of ways that a mean difference might be standardized, it is not surprising that there is family of effect size indices.

The second family of effect sizes includes any index that is a linear measure of association, i.e. a correlation. In optimal conditions, this effect size is a pearson correlation coefficient between two measured variables. It is also possible to conceive of circumstances in which a partial correlation is the effect size of interest. There also exists a number of other, more minor, classes of effect size, including omega and eta squared, and log-odds ratios for frequency tables. These types are not discussed further.

Rosenthal (1994) categorized and compared the two primary families of effect sizes. His summary not only explores the relations among measures within a family, but also specifies many connections that exist between the two families. The ability of a research synthesist to extract and or estimate effect sizes is determined by the information presented in the primary research report. As indicated immediately above, the most desirable information includes means and standard deviations for the first family, and pearson correlation coefficients for the second. However, effect sizes can also be extracted from a variety of less straightforward statistical summary information. For example, a t statistic can be directly transformed to an effect size if the degrees of freedom are available. Further, a one-degree-of-freedom F statistic can be transformed to a t statistic, and subsequently to an effect size (given the error degrees of freedom are provided). On the other hand, an F test with multiple degrees-of-freedom in the numerator may not be transformed to effect sizes unless the condition means and mean square error are provided. As the extraction of effect sizes from various arcane summary information has been treated in detail elsewhere, the reader is referred to these sources for further details (Rosenthal, 1994; Glass, McGaw, and Smith, 1981).

Part 2. What to Report in Primary Research Reports

The Sufficient Statistics for Effect Sizes that Compare Conditions. To compute effect sizes in this family, the sufficient statistics are means, standard deviations, and sample sizes within each condition being compared – for each original dependent variable. With these statistics, one may calculate

effect sizes using either a Glass, Hedges, or other estimator. For example, the Hedges' estimator uses the mean difference divided by the pooled standard deviation (In analysis of variance terms this is the square root of mean square error.) The principal concern in standardizing effect sizes is that the selected standard deviation is not contaminated by treatment effects or pre-existing differences among the groups. For this purpose, Glass (1976) recommended using the standard deviation of a control group, while Hedges and Olkin (1985) favored the pooled within-groups standard deviation. To this author, the latter selection seems preferable on the grounds that many studies lack a true control group.

Technically, most of the theory of effect sizes deal with comparisons between independently drawn comparison groups. However, in a wide variety of settings, interesting effect-size comparisons are observed within subjects. Rather than discard such effect sizes, one can employ the standard deviation of the difference as the denominator of the effect size. In such cases, it is necessary to have an estimate of the correlation between the dependent variable measured in the first and second conditions. Obviously, as the number of within subjects conditions and/or the number of dependent variables increases, the reporting requirements increase dramatically. There is no simple solution to this dilemma. Further thoughts on this problem are provided in a following section.

The Sufficient Statistics for Effect Sizes that Assess Degree of Relation. The Pearson correlation coefficients are both the effect sizes of interest and the sufficient statistics. A principal consideration when preparing to report correlations in a study centers on classifications of subjects into different groups (either naturally occurring groups like pilots and nonpilots, or experimental and control conditions). When a study has different groups of subjects for which there are expectations of mean differences on one or more of the dependent variables, then correlations within individual groups or pooled within-group (also called error) correlations are required. This is because a correlation estimated from data in which groups are mixed together (and mean differences exist) results in a spurious estimate of the correlation. Needless to say, when the strength of association between two variables is different from one group to the next, then the correlations in each group are required.

There are direct links between estimates of correlations and estimates of mean differences. Many formulas for making a transformation from one type of effect size to the other exist. Space does not permit listing them here (see Rosenthal, 1994 or Glass, McGaw, and Smith, 1981).

A Reporting Strategy Insuring that Studies Conform Well to Requirements for Meta-Analysis. For studies having all between-subjects conditions, one should report the mean(s) of the dependent variable(s) within each group of subjects. The sample sizes and standard deviations are also needed. However, if one adapts the Hedges and Olkin effect size, thereby using a pooled estimate of the

standard deviation, then one may simply report estimate(s) of the standard deviation(s) pooled across all between-subjects conditions. Note that this quantity is also the square root of mean square error from the analysis of variance corresponding to the study's design.

When studies have between and within-subjects factors, then the summary information for between subjects conditions should be reported as listed above (i.e., collapsed across levels of the within-subjects factors). This will facilitate the synthesis of information across studies for those factors that appear primarily as between-subjects conditions. For the within-subjects factors, technically, one should consider the observations under the various combinations of within-subjects conditions as different dependent variables; thereby creating vectors of variables for which vectors of means and standard deviations, and matrices of correlations are required. Unfortunately, as the number of true dependent variables increases and/or as the number of within-subjects factors (and levels) increase, the reporting requirements quickly become quite burdensome. At this point, very serious judgments about what to report are needed. With respect to an organization like the Air Force, this appears to be a perfect situation for which reporting standards should be created and implemented.

Part 3. Guidelines for Coding Research Reports

An effective meta-analysis is an insightful summary of primary research reports and provides a meaningful basis for making sound policy decisions. However, before one can address substantive issues by means of meta-analysis, it is first necessary to: (1) identify information to extract from primary research reports; (2) code this information in an accurate and reliable way, and (3) store the information so that it is easily accessed for analysis. Only an expenditure of significant amounts of time, effort, and thought insure that these needs are met in each individual meta-analysis. To insure that a prospective meta-analyst makes, more often than not, correct decisions about what and how to code information this appendix reviews six guidelines for coding [A complementary paper by Stock (1994) appears in the *Handbook of Research Synthesis* (Cooper and Hedges, 1994)]. With these guidelines, readers, particularly those encountering meta-analysis for the first time, will be aware of the many decisions that must be made in order to produce an effective meta-analysis. These guidelines also identify specific steps that all meta-analysts can take before, during, and after coding activities.

A meta-analysis leads to a long series of decisions. Early on, a meta-analyst must try to identify attributes of studies that covary with the magnitude of effect size. Attributes that covary with effect size are important if they are **causally** linked to changes in the magnitude of effect sizes. Thus, when a study attribute is statistically linked to changes in the magnitude of effect sizes, this may signal a

need for specific additional empirical research (to assess the likelihood of a causal relation). The information that defines such attributes has to be extracted and coded for analysis.

Guidelines one and two describe a framework for choosing both the attributes to code and the conventions for coding them. Given that attributes and their coding conventions have been selected, the resulting items must be organized on forms before actual coding can begin. Guidelines three and four outline methods for creating forms and a code book. Coders must reliably and accurately find, transform, and transcribe information from primary research reports onto a set of forms. Guidelines five and six deal with human factors — how to be reliable and vigilant, and how to remain so for extended periods. Each guideline is expressed in a proactive form that encourages prospective meta-analysts to undertake the efforts specified therein. In the domain of science, the notion that we stand on the shoulders of those who have preceded us is the appropriate framework for introducing guideline one, wherein encourage meta-analysts are encouraged to use the work of others.

Guideline 1: To identify possible items, review items that have been coded in the past. A standard classification of items provides an organized checklist of possible items. Durlak and Lipsey (1991), Kulik and Kulik (1989), and Glass, McGaw, & Smith (1981) are among those who have offered an extensive classification of items. Based on the work of these authors, and on his own experiences conducting meta-analyses, Stock (1994) suggested a set of seven general categories of items. He labeled these categories identification, setting, subjects, methodology, treatment, process, and effect size. A review of these papers provides a sound basis for initiating the selection of items. Reviewed below are a few specific items in the different categories suggested by Stock.

Year and source of publication, as well as identification of the person who coded a source, are examples of items dealing with the *identification*. A temporal shift in effect size (magnitude of effect sizes varies with year of publication) suggests that factors that change across time may be related to effect size in a causal manner. Items in the *setting* category describe general conditions of a study. General conditions include the scope of sampling, the use of special populations, and the "climate" of the setting in which the study took place. In distinction to general conditions of a study, specific characteristics of individuals in the sample(s) of a study are considered *subject* variables. Demographic information is included in the subject category. Items that describe study design, sampling procedures, rates of attrition, and the presence or absence of threats to validity all basically pertain to *methodology*. A bit of thought will show that the rating of study quality is derived from information present in other items in this category, and so study quality may be placed in this category. Items in the *treatment* category focus on the theoretical orientation that motivated a treatment and on specific attributes of treatment conditions. *Process* items describe behaviors and

dispositions of coders. Orwin and Cordray (1985) coded items and then rated their confidence in the study report -- with respect to inclusion of information required for the coding decision. Analyses by Orwin and Cordray that were based on these ratings revealed "... that deficient reporting injects considerable noise into meta-analytic data and can lead to spurious conclusions" (p. 134). As a consequence, Stock suggested confidence ratings be considered in conjunction with those items that are considered important on an a priori basis. Information about *effect size* forms the final category of items. Included here are the summary statistics (for computing effect size) and items that describe the nature of outcome measures (including estimates of the reliability of these measures).

In sum, general classifications of items already exist. These should be reviewed prior to a meta-analysis. Still, even after reviewing one or more of these citations, a prospective meta-analyst may wonder on what basis to select the final set of items. The answer is straightforward -- one can only proceed from a basis that is provided by what one already knows. The implications of this belief are explored in the next section.

Guideline 2: To select the items, base your choices on your knowledge of the domain of research.

The more a meta-analyst knows about a domain of research, the more likely s/he is to make correct choices in critical matters that shape the meta-analysis. The choice of what attributes to code is critical for two different reasons. First, both coding time and the chance of coding unimportant or irrelevant attributes increase as the number of items is increased. Second, one can fail to choose an important variable, i.e., a variable that is causally related to effect size magnitude. To maximize the likelihood of choosing items that are causally linked to effect size and to minimize the likelihood of selecting irrelevant items, the following strategy has previously been suggested by Stock (1994).

Based on domain-specific knowledge, do the following. First, formulate conjectures about how attributes of studies vary with effect size magnitude. Although this process may initially focus on items found in the various standard classifications of items identified in the preceding section, the process of forming conjectures should extend beyond these standard lists. This is so because the role of conjecture is to admit both the testing of interesting hypotheses and the appearance of serendipity in a meta-analysis. Second, judge how well each conjecture matches the: (1) goals of the synthesis, (2) adequacy of information in study reports, (3) ability of coders to reliably extract the necessary information, and (4) costs of coding. (Note: One also uses domain-specific knowledge to reject items that lack potential or are not frequently reported). Finally, for each conjecture that is evaluated favorably on these criteria, create a coded item and evaluate it analytically. Although Stock noted this procedure creates more coded items than a procedure that requires a formal justification for each item (as recommended by Hunter & Schmidt, 1990), the process described here encourages

speculations about the inadequacies of formal theories, an approach that fosters the advancement of study in particular fields.

It cannot be emphasized too strongly that the selection of items is the single most important set of choices a meta-analyst makes simply because an item that is not coded cannot be analyzed. However, assuming a set of items has been selected, the focus of activity turns to more mundane issues. Guidelines three and four describe the behaviors that are needed to transform the selected items into a set of coding forms and a code book. Considered first is the construction of forms.

Guideline 3: The benefits of well-designed forms appear during coding, data entry, and analyses.

After choosing a set of items, a meta-analyst has to construct forms and a code book, then revise both as needed, and subsequently train coders in their use. As with identification and selection of items, a meta-analyst should first review and adopt (as judgment indicates) coding conventions that appear in published work, thereby reducing the amount of preparatory work that is required. In addition to effective coding conventions, items have to be arranged and described in ways that foster error-free extraction.

A coding convention is a way to assign numbers to an attribute so as to capture sufficient information about an attribute that subsequent analyses realistically address whether or not the attribute is linked to effect size. As Stock (1994) noted, "One standard that guides the selection of coding conventions is to conserve as much of the original information as possible. The more directly information is transcribed from study to form, the fewer judgments a coder makes and, consequently, the fewer errors." (p. 129) He urged that numerical information be coded directly, whereas he recommended that nonnumerical descriptive information be coded using closed coding systems. For example, say we are coding treatment attributes. In a closed coding system, the common attributes of the variations of treatment conditions are listed and given code numbers. Coders used as many of these numbers as necessary to describe each treatment and control condition encountered. Whenever a new attribute is encountered during coding, it is given a unique number and added to the list.

Assembling information on forms is a behavior guided by the maxim that *information should never be coded more than once*. Items at the level of the study, sample, or effect size should be gathered together and placed on distinct forms. Since the location and appearance of items on a coding page affect accuracy, and because substantial benefits accrue from ordering and annotating items, one should not pack items densely onto the fewest possible forms. It is reasonable to group on a single form items that identify a study (authors, source and year of publication, coder, date coded, and coding time) and use this form as a cover sheet. Other items to be coded can be arranged in the order that they are ordinarily encountered in the original report. The items that describe setting,

subjects, and methodology may occupy several pages, but generally are coded at the same point in time. Grouped on separate forms are items about study quality and about subsamples. Finally, information related to effect size (summary statistics, context, size, type of scale, estimates of reliability, and treatment attributes) should be appear together. Items about process (e.g., estimates of coding time for items or ratings of confidence in the quality of report information) should appear with the corresponding substantive item. Such process items should be coded immediately after the item itself.

Think about the arrangement of items on the forms. There are tactics that aid both coders and data entry personnel. For example, the order of items on a form should reflect the typical order of information in primary research reports. Further, using a readable font, separating items from each another, and numbering each item are all actions that assist coding and subsequent data entry and verification. After items and conventions are chosen, and decisions are made about how many significant digits to record for numerical items, specific columns can be assigned to every item. If this column information is preprinted on coding forms, it serves as a way to verify the accuracy of data entry. To further assist coders, it is often useful to also construct a code book that describes the coding of each item in detail. In addition, a code book can provide a historical record of the procedures employed during a meta-analysis. These topics are the focus of the following section.

Guideline 4: Construct a code book to provide guidance to coders and document the meta-analysis.

A code book provides detailed guidance to coders. Consequently, every code book should have a section that is organized in the order that the forms are used. At that point, the detailed descriptions of coding conventions for each item should appear. The sequence of descriptions of conventions in the code book should follow the sequence of items -- as they are numbered on the forms. Under guideline 3, it was suggested that information that assists coding should be put on the forms themselves. However because of space limitations on forms, the information that can be included there is limited -- a limitation that does not exist in a code book. Descriptions of conventions in a code book should dispel as many ambiguities as possible about application of a convention. The copious use of examples provides helpful guidance to both novice and experienced coders.

Besides its primary role, a code book also provides a historical record of the meta-analysis -- accomplished by preparing sections that describe the: (1) domain and global objectives of the meta-analysis, (2) definitions of primary constructs, (3) processes of coding and using forms, and (4) data entry and management. These descriptions are a historical record that helps in two activities. First, these descriptions introduce new coders to the meta-analysis when new coders are required. Second, these descriptions facilitate writing (for publication) reports of the results of the meta-analysis.

Creation of a set of coding forms and a code book set the stage for actual coding. Because the reliability of coders is important, full-scale coding should begin only after coders competently and reliably code items on final versions of coding forms. The next two guidelines discuss the training of coders and maintenance of vigilance.

Guideline 5: Conduct training sessions to insure that the coders are as reliable as possible. Well-conceived and well-conducted training sessions will result in persons who use coding forms and conventions in a competent and replicable manner. Stock described eight steps in an effective training process (iterations of these eight are added as necessary). The steps are to : (1) provide an overview of the research domain, (2) read and discuss a sample of studies, (3) review each item on its coding form and in the code book, (4) outline the process for using forms, (5) complete a sample coding, (6) have everyone code the same study or studies, (7) compare and resolve discrepancies and errors, and (8) revise the forms and code book as necessary. Thereafter, a meta-analyst is ready to gather empirical evidence that coders are reliable. A complementary article on the assessment of the reliability of coders appears in chapter 11 of the *Handbook of Research Synthesis* (Orwin, 1994). Still, a few comments are in order.

The principles of sound research design apply to assessment of reliability in a research synthesis. Randomization should be employed wherever it is possible to do so (as in the selection of studies to code and in the assignment of these studies to coders). The instructions given to all persons should be identical. As coders, these persons should work independently and refrain from discussing studies or coding decisions with one another. As a general perspective, a low level of reliability on an item should be viewed as an opportunity to discuss coding discrepancies and identify possible revisions of the item (and forms and code book). When acceptable levels of reliability are achieved, coding can start. The fact that reliability goes down over time implies that it may be necessary to re-estimate the reliability of coders after an extended period of coding. In addition, this fact raises the issue of maintaining vigilance during extended periods of coding. The last guideline deals with the issue of maintaining vigilant behaviors.

Guideline 6: Efforts to maintain vigilance for extended periods lead to meta-analyses of higher quality. During a meta-analysis, the coding stage can take a significant amount of time, and so maintaining the vigilance of coders during this stage is critical to the project. To reach and sustain a high level of attentiveness, a meta-analyst should schedule meetings and reviews of the work of participants. If these meetings are attended by all persons who are coding, then the meeting itself provides an opportunity to report progress, discuss difficulties, and code in a group setting -- all of which encourage further progress and foster a critical appraisal of completed work. The ultimate

effect of these appraisals is a data base characterized by higher reliability. This completes our brief description of the six guidelines for coding information from primary research reports. This author is convinced that, properly implemented, these guidelines help produce high quality and informative meta-analyses.

Appendix B: Coding Forms

SREP Research Synthesis: Coding Form 1

Study Characteristics

Synthesis ID	
Year Published	
Type of Report (Check one)	
Technical Report	
Article	
Paper/Proceeding	
Other (specify here)	

Did the study relate simulation conditions or manipulations to pilot performance/training? If Yes, complete Simulator section on next form.	Yes	
	No	
Did the study report sufficient statistics to compute effect sizes?	Yes	
	No	
Did the study include pilots as subjects? If Yes, complete description Of pilots in global sample in the following table.	Yes	
	No	
Comments:		

Global Sample Characteristics

Total Number of Subjects in the Study (Sum across multiple experiments)		
Total Number of Pilots in the Study (Sum across multiple experiments)		
Mean Number of Flying Hours for Pilots in Study (Across multiple experiments)		
For pilots, check the principal type of aircraft experience		
F-15		
F-16		
A-10		
Big Body		
Trainer's only		
Other (Specify)		
For subjects who were not pilots, specify type		
Students		
Civilians associated with AL		
Other civilians		
Comments:		

SREP Research Synthesis: Coding Form 2

Synthesis ID	
--------------	--

Methodological Characteristics of the Study

Location of Study		
		Location Code
Was a true experiment conducted in study.	Yes	
	No	
Describe the basic experimental manipulation below		
Experimental Manipulation Description Code 1		
Experimental Manipulation Description Code 1		
If not a true experiment, describe the basic type of study		
Non-Experimental Manipulation Description Code 1		
Non-Experimental Manipulation Description Code 1		
Was a plausible alternate study methodology available?	Yes	
	No	
Describe the plausible alternate methodology.		

Simulator Use in the Study

Was a simulator used in any way in the study	Yes	
	No	
If Yes, describe the nature of simulator use		
Simulator Use Code 1		
Simulator Use Code 2		
If Yes, also describe the type of simulator		
Type-of-Simulator Code		
Total number of simulator hours		
Total number of simulator sessions		
Comments:		

SREP Research Synthesis: Coding Form 3

Synthesis ID	
---------------------	--

Sample Characteristics of Specific Experiment (for Multi-experiment Studies)

Total Number of Subjects in experiment (individual investigation)		
Number of Pilots		
Mean Number of Flying Hours for Pilots		
For pilots, check the principal type of aircraft experience		
F-15		
F-16		
A-10		
Big Body		
Trainer's only		
Other (Specify)		
For subjects who were not pilots, specify type		
Students		
Civilians associated with AL		
Other civilians		
Comments:		

SREP Research Synthesis: Coding Form 4

Synthesis ID	
--------------	--

Effect Size Estimates

[illegible]

Appendix C: Source Documents Providing Effect Sizes

- Bell, H. H., & Ciuffreda, K. J. (1985). Effects of collimation on accommodation and vergence in the Advanced Simulator for Pilot Training (AFHRL-TP-85-27 AD-A159 545). Williams AFB, AZ: Operations Training Division, Air Force Human Resources Laboratory.
- Buckland, G. H. (1980). Visual cue requirements for terrain flight simulation. In Proceedings of the 2nd Interservice/Industry Training Systems Conference and Exhibition (pp. 92-93). Arlington, VA: National Security Industrial Association.
- Collyer, S. C., Ricard, G. L., Anderson, M., Westra, D. P., & Perry, R. A. (1980). Field of view requirements for carrier landing training (NAVTRAEQUIPCEN-IH-319/AFHRL-TR80-10, AD-A088 701). Williams AFB, AZ: Operations Training Division, Air Force Human Resources Laboratory; Orlando, FL: Naval Training Equipment Center.
- DeMaio, J., & Brooks, R. (1982). Assessment of simulator visual cueing effectiveness by psychophysical techniques. In Proceedings of the 4th Interservice/Industry Training Equipment Conference (Vol. 1, pp. 379-381). Arlington, VA: National Security Industrial Association.
- DeMaio, J., Rinalducci, E. J., Brooks, R., & Brunderman, J. (1983). Visual cueing effectiveness-Comparison of perception and flying performance. In Proceedings of the 5th Interservice/Industry Training Equipment Conference (Vol. 1, pp. 92-96). Arlington, VA: Defense Preparedness Association.
- Dixon, K. W., & Curry, D.G. (1987). Effect of scene content and field of view on weapons delivery training. In Proceedings of the 9th Interservice/Industry Training Systems Conference (pp.247-256). Arlington, VA: American Defense Preparedness Association.
- Dixon, K.W., & Curry, D. G. (1990). Weapons delivery training: Effects of scene content and field of view (AFHRL-TP-88-29, AD-A227 968). Williams AFB, AZ: Operations Training Division, Air Force Human Resources Laboratory.
- Dixon, K.W., Martin, E. L., Rojas, V. A., & Hubbard, D. C. (1988). The effects of field-of-view on pilot performance in the C-130 WST. In Proceedings of the 10th Interservice/Industry Training Systems Conference (pp. 362-371). Arlington, VA: National Security Industrial Association.
- Dixon, K. W., Martin, E. L., Rojas, V. A., & Hubbard, D. C. (1990). Field-of-view assessment of low-level flight and an airdrop in the C-130 Weapon System Trainer (WST) (AFHRL-TR-89-9, AD-A218 504). Williams AFB, AZ: Operations Training Division, Air Force Human Resources Laboratory.
- Irish, P.A., III, & Buckland, G. H. (1978). Effects of platform motion, visual and G-seat factors upon experienced pilot performance in the flight simulator (AFHRL-TR-78-9, AD-A055 691). Williams AFB, AZ: Flying Training Division, Air Force Human Resources Laboratory.
- Irish, P.A., III, Grunzke, P.M., Gray, T.H., & Waters, B.K. (1977). The effects of system and environmental factors upon experienced pilot performance in the Advanced Simulator for Pilot Training (AFHRL-TR-77-13, AD-A043 195). Williams AFB, AZ: Flying Training Division, Air Force Human Resources Laboratory.
- Kleiss, J. A. (1992). Tradeoffs types of scene detail for simulating low-altitude flight. In Proceedings of 1992 IEEE International conference on Systems, Man, and Cybernetics (Vol. 2, pp. 1141-1146). New York, NY: Institute of Electrical and Electronics Engineers.
- Kleiss, J. A., Hubbard, D. C., & Curry, D. G. (1989). Effect of three-dimensional object type and density in simulated low-level flight (AL-TR-1988-66). Williams AFB, AZ: Aircrew Training Research Division, Armstrong Laboratory.

- Kellogg, R.S., Hubbard, D. C., & Sieverding, M. J. (1989). Field-of-view variations and strip-texturing effects on assault landing performance in the C-130 Weapon System Trainer (AFHRL-TR-89-3, AD-A212 763). Williams AFB, AZ: Operations Training Division, Air Force Human Resources Laboratory.
- Kruk, R., & Longridge, T. M. (1984). Binocular overlap in a fiber optic helmet mounted display. In E. G. Monroe (Ed.), Proceedings of the 1984 IMAGE III Conference (AFHRL-TR-84-36, AD-A148 636, pp. 363-378). Williams AFB, AZ: Operations Training Division, Air Force Human Resources Laboratory.
- LeMaster, W. D., & Longridge, T. M., Jr. (1978). Area of interest/field-of-view research using ASPT (AFHRL-TR-78-11, AD-A055 692). Williams AFB, AZ: Flying Training Division, Air Force Human Resources Laboratory.
- Martin, E. L., & Cataneo, D. F. (1980). Computer generated image: relative training effectiveness of day versus night visual scenes (AFHRL-TR-79-56, AD-A088 313). Williams AFB, AZ: Operations Training Division, Air Force Human Resources Laboratory.
- Martin, E. L., & Lindholm, J. M. (1992). Effects of image update rate on target identification range. In Proceedings of the Thirteenth Symposium Psychology in the Department of Defense (USAFA TR 92-2, pp. 178-182). Colorado Springs, CO: Department of Behavioral Sciences and Leadership, U.S. Air Force Academy.
- Martin, E. L., & Rinalducci, E. J. (1983) Low-level flight simulation: Vertical cues (AFHRL-TR-83-17, AD-A133 612). Williams AFB, AZ: Operations Training Division, Air Force Human Resources Laboratory.
- Rinalducci, E. J., Patterson, M. J., & De Maio, J. (1984). Static vs. dynamic presentation of visual cues in simulated low level flight. In Proceedings of the Ninth Symposium Psychology in the Department of Defense (USAFA-TR-84-2, AD-A141 043, pp. 667-671). Colorado Springs, CO: Department of Behavioral Sciences and Leadership, U.S. Air Force Academy.
- Thorpe, J. A., Varney, N. C., McFadden, R. W., LeMaster, W. D., & Short, L. H. (1978). Training effectiveness of three types of visual systems for KC-135 flight simulators (AFHRL-TR-78-16). Williams AFB, AZ: Flying Training Division, Air Force Human Resources Laboratory.
- Warner, H. D., Serfoss, G. L., & Hubbard, D. C. (1993). Effects of area-of-interest display characteristics on visual search performance and head movements in simulated low-level flight (AL-TR-1993-0023, AD-A264 661). Williams AFB, AZ: Aircrew Training Research Division, Armstrong Laboratory.
- Woodruff, R. R. (1979). Effects of varying visual display characteristics of the T-4G, a T-37 flight simulator (AFHRL-TR-79-17, AD-A071 410). Williams AFB, AZ: Flying Training Division, Air Force Human Resources Laboratory.
- Woodruff, R. R., Hubbard, D. C., & Shaw, A. (1985). Advanced simulator for Pilot Training and helmet-mounted visual display configuration comparisons (AFHRL-TR-84-65, AD-A155 326). Williams AFB, AZ: Operations Training Division, Air Force Human Resources Laboratory.
- Woodruff, R. R., Longridge, T. M., Jr., Irish, P. A., III, & Jeffreys, R. T. (1979). Pilot performance in simulated aerial refueling as a function of tanker model complexity and visual display field-of-view (AFHRL-TR-78-98, AD-A079 231). Williams AFB, AZ: Flying Training Division, Air Force Human Resources Laboratory.

EVALUATION OF A SCALE DESIGNED TO MEASURE THE UNDERLYING CONSTRUCTS OF
ENGAGEMENT, INVOLVEMENT, AND SELF-REGULATED LEARNING

Nancy J. Stone
Assistant Professor
Department of Psychology

Creighton University
2500 California Plaza
Omaha, NE 68178

Final Report for:
Summer Research Extension Program
Armstrong Laboratory

Sponsored by:
Air Force Office of Scientific Research
Bolling Air Force Base, Washington DC,

Armstrong Laboratory,

and

Creighton University

March 1998

EVALUATION OF A SCALE DESIGNED TO MEASURE THE UNDERLYING CONSTRUCTS OF
ENGAGEMENT, INVOLVEMENT, AND SELF-REGULATED LEARNING

Nancy J. Stone
Assistant Professor
Department of Psychology
Creighton University

Abstract

A measurement scale was designed after the literature on engagement, involvement, and self-regulated learning was reviewed, including the correlates and current measures of these constructs. It was proposed that there are unique underlying characteristics of engagement, involvement, and self-regulated learning. To determine that these characteristics are distinct, a sorting task was conducted first followed by an exploratory factor analysis. These preliminary data support the notion that the unique underlying characteristics exist and they correlate differently with various measures of academic performance. The implications of these findings suggest that different learner characteristics correspond to different types of academic performance. Applications of the results and suggestions for future research are discussed.

EVALUATION OF A SCALE DESIGNED TO MEASURE THE UNDERLYING CONSTRUCTS OF ENGAGEMENT, INVOLVEMENT, AND SELF-REGULATED LEARNING

Nancy J. Stone

Introduction

In educational and training environments, it is critical that students and trainees have the opportunity to assimilate and master as much of the course information in order to increase achievement. Engagement (e.g., Finn, Folger, & Cox, 1991; Skinner & Belmont, 1993), involvement (e.g., Reed & Schallert, 1993), and self-regulated learning (e.g., Zimmerman, 1986, 1990) appear to be three related, yet somewhat distinct areas of research which address the process by which students do or do not acquire knowledge. Because college and many training environments are much less controlled than elementary and/or secondary schools (specifically concerning study time), it is important to identify what determines whether individuals will become totally engrossed in, own, or monitor their learning process. Thus, it is necessary to develop a measure that taps the underlying constructs of engagement, involvement, and self-regulated learning.

In order to develop such a measurement tool, the relationships among the three areas of engagement, involvement, and self-regulated learning are clarified first, including inconsistencies in the terminology, to identify the unique characteristics which underlie engagement, involvement, and self-regulated learning. Then, the correlates (i.e., possible determinants) of engagement, involvement, and self-regulated learning are reviewed. Next, an evaluation of current measurement tools for these constructs precedes the development of a comprehensive set of items for use in measuring the unique characteristics underlying these constructs. Many of the current measures

tend to be study specific as opposed to validated assessment tools. Validated measures should be useful in identifying who will succeed in educational and training situations as well as who needs assistance in order to increase their engagement, involvement, and/or self-regulated learning.

To develop an understanding of the differences between the three constructs, the following information is intended to be descriptive in nature. A complete discussion of how these constructs were operationalized occurs when the current measurement scales are evaluated.

Engagement has been defined as an orientation, purpose (Ainley, 1993), and motivation (Lee & Anderson, 1993) to learn. From the literature, and based mostly on teacher observations, engagement spans a continuum from disengaged to engaged. Disengaged elementary students tend to display restless behavior, to annoy others, and to need reprimands (Finn et al., 1991). Additionally, to be disengaged is to be passive in learning, to expend little effort, to give up easily, and to be bored, depressed, anxious, angry, withdrawn from learning, and rebellious (Skinner & Belmont, 1993). Students who use direct observation and verbal rehearsal are not disengaged, but they are still considered to be relatively passive learners (Helstrup, 1989). When sixth grade students invoked strategies to understand the material, as determined by informal interviews and observation, they were considered to be more engaged (Lee & Anderson, 1993). At a moderate level of engagement, teenage students focused on achieving minimal tasks (Ainley, 1993), and elementary students were observed, usually by teachers, to display behaviors such as being attentive (Finn et al, 1991; Lee & Anderson, 1993), being involved in class activities (Lee & Anderson, 1993), completing homework on time, and being persistent (Finn et al., 1991; Skinner & Belmont, 1993).

Fully engaged students tend to focus on achieving a deep understanding of the material (Ainley, 1993), to display initiative (Finn et al., 1991; Lee & Anderson, 1993; Skinner & Belmont, 1993), to study or work beyond course requirements (Finn et al., 1991; Lee & Anderson, 1993), to be thorough (Finn et al., 1991), to verbally discuss ideas with others (Finn et al., 1991; Goff & Ackerman, 1992), to be completely absorbed in one's work whereby time becomes distorted (Goff & Ackerman, 1992), to exhibit intense concentration (Helstrup, 1989; Skinner & Belmont, 1993), to desire engagement (Goff & Ackerman, 1992), to display persistence and effort (Finn et al., 1991; Skinner & Belmont, 1993), to challenge their abilities (Skinner & Belmont, 1993), and to display positive affect (Skinner & Belmont, 1993). Engaged students also use active strategies such as associations and visual imagery (Helstrup, 1989), which are related to levels of processing (Craik & Lockhart, 1972).

Engaged students also have been described as involved in class activities (Lee & Anderson, 1993). In turn, students identified as "involved" have been described as absorbed in their work, displaying intense concentration, challenging their abilities, and exhibiting positive affect (Reed & Schallert, 1993). Wehlage (1989) considered using the term involvement, but switched to engagement in order to be more descriptive of students' investment of attention and effort in school work and activities. Wehlage (1989) defined "engagement" as an investment of student attention and effort in school work and activities and "involvement" as an attachment and commitment to the beliefs of the school. This represents a social bond, or even an ideological or value bond.

Much of the literature on involvement has referred to teacher and parent activity, but also has included student participation in various activities.

The need for clarification of the involvement construct is not unique to these learning areas; even in the business world the concept of involvement needs clarification (Goldsmith & Emmert, 1991).

Even though the concepts of engagement and involvement appear to be similar, no studies were found to evaluate these constructs as distinct and to determine the relationship between these constructs. Given the overlap in some of the terminology (e.g., involved students are engaged in their learning), it is necessary to clarify the distinctions between these two constructs. Therefore, it is proposed that engagement refers to intense concentration on, attention to, and absorption in a task as well as a desire to learn the material thoroughly and to learn more beyond the specified requirements. Because involvement has been measured using adapted job and work involvement scales (Farrell & Mudrack, 1992), involvement is hypothesized to tap the learner's commitment to, perceived importance of, and ownership of learning.

There is also the need to distinguish self-regulated learning from engagement and involvement. In particular, there is a need to clarify what self-regulated learning (Howard-Rose & Winne, 1993) and engagement are. The literatures on self-regulated learning and engagement often share common elements. Due to this partial overlap of the two constructs in the literature, the term engagement is often used interchangeably with the phrase self-regulated learning. For example, Corno and Mandinach (1983) identified self-regulated learning as the highest form of cognitive engagement, and Butler and Winne (1995) considered self-regulation to be a style of engagement. Also, McCombs and Whisler (1989) and Pintrich and de Groot (1990) concluded from their reviews of the literature that self-regulated learning

included various cognitive strategies, some of which could be construed as engagement strategies (e.g., elaboration, attaching personal meaning to activities).

Butler and Winne's (1995) model clearly defines a self-regulated learner as one who, given a task, evaluates the task, sets goals based on that evaluation, uses strategies to meet those goals, and monitors activities to assess progress and to make a reinterpretation of the task, given internal (self) or external (teacher) feedback about the task. This model closely resembles Dickinson's (1992) description of autonomous learners. Self-regulated learners, as opposed to engaged learners, were described as autonomous (Dickinson, 1992; McCombs & Whisler, 1989), self-regulated or self-monitored (Corno & Mandinach, 1983; McCombs & Marzano, 1990; McCombs & Whisler, 1989; Pintrich & de Groot, 1990), resourceful (Zimmerman, 1990), and strategic (i.e., make plans, organize; McCombs & Whisler, 1989).

The self-regulation process may be considered a result of two processes: acquisition and transformation. Acquisition concerns the uptake of information and transformation involves the manipulation of the information once the student possesses it (Corno & Mandinach, 1983). If a student actively seeks information (i.e., is resourceful) and is involved in the acquisition process and also manipulates the data by making connections among the information, then the individual is a self-regulated learner (Corno & Mandinach, 1983). At the other extreme, where students are given the information (low acquisition) and then told how it should or could be categorized, grouped, or manipulated (low transformation), the student is merely a recipient of information (Corno & Mandinach, 1983). Therefore, self-regulated learning is posited to reflect an autonomous and systematic process

by which students attain a learning goal through the gathering (acquisition) and manipulation (categorizing, organizing, processing) of information, strategic planning (setting goals, monitoring progress), and feedback to continue the self-evaluative cycle.

Self-regulation may induce moderate levels of engagement (e.g., attention), but just because a student plans, sets goals, organizes, self-monitors, self-evaluates, or creates a better learning environment in order to enhance academic achievement, the student may not be engaged (i.e., absorbed in one's work). Although Zimmerman (1986, 1990) considered self-regulated learners to be metacognitively, motivationally, and behaviorally active in their learning, this might not include engagement (or only moderate levels). A self-regulated learner who gathers information, establishes goals as to what needs to be done, and monitors progress toward those goals will not necessarily become thoroughly and deeply engrossed in the topic. It is also possible for someone to be engaged without being a self-regulated learner. One could be completely absorbed in what one is doing, but not monitoring one's work according to a set of goals, whereby all aspects of one task or other tasks might not be completed. From this review of the literature, the only apparent overlap between engagement and self-regulated learning occurred when terminology suggested that students displayed initiative (Schunk, 1990), a desire to engage (McCombs & Marzano, 1990), persistence (Pintrich & de Groot, 1990; Schunk, 1990; Zimmerman, 1986) and effort (Pintrich & de Groot, 1990).

Involvement, on the other hand is proposed to include one's ownership and/or responsibility of learning (e.g., work ethic, commitment). It may be possible to have high commitment or a strong work ethic, but not to be engaged

or self-regulated. An individual highly committed to a project may not become absorbed in the project and may not monitor one's progress on the project. Because of the overlapping definitions in the literature, it is proposed that there are unique characteristics underlying these three constructs that could and should be defined as distinct from each other.

Another way to identify these unique characteristics is by reviewing the correlates of engagement, involvement, and self-regulated learning. Although engagement can be described and defined, and its effects have been identified, only self-interest (Wehlage, 1989) and affect (Skinner & Belmont, 1993) were found in the literature as correlates of engagement. Given that engagement is an engrossing process, it is reasonable that topics must tap students' interest (Wehlage, 1989), perhaps by being relevant to the students' career goals (Morrison & Brantner, 1992) as opposed to achievement goals in order to capture the students' attention. Thus, self-interest could be construed as relevance, although relevance was not found to be tested as a correlate of engagement. Similarly, positive affect may be related to student interest, which may increase the potential for engagement. Furthermore, as correlates, it is possible that interest and affect are determinants as well as effects of engagement, which affect the likelihood of future engagement. There may be a cyclical process between these correlates and engagement (Kinzie, 1990).

Similar to engagement, few correlates of involvement have been identified. Academic involvement correlated with need for achievement (Farrell & Mudrack, 1992), task difficulty (Reed & Schallert, 1993), Protestant work ethic (Farrell & Mudrack, 1992), importance of school activities (i.e., relevance; Farrell & Mudrack, 1992; Reed & Schallert, 1993), and positive affect (Reed & Schallert, 1993).

Most of the literature focuses on the correlates of self-regulated learning. From numerous models and some correlational studies, the proposed correlates of self-regulated learning include confidence (Zimmerman, 1990), self-efficacy (Henderson, 1986; Kinzie, 1990; McMillan, Simonetta, & Singh, 1994; Pintrich & de Groot, 1990; Schunk, 1990, 1994; Zimmerman, 1990), self-esteem (McCombs & Marzano, 1990), self-concept (Howard-Rose & Winne, 1993; Thomas et al., 1993), learned helplessness (Henderson, 1986), locus of control (Henderson, 1986; Wilhite, 1990) including strategy and capacity beliefs (Skinner, Wellborn, & Connell, 1990), learner or personal control (Kinzie, 1990), relevance (Kinzie, 1990), task importance (Pintrich & de Groot, 1990), curiosity (Kinzie, 1990) or interest (Pintrich & de Groot, 1990), motivation (Kinzie, 1990; McCombs & Marzano, 1990), personal development goals (McCombs & Marzano, 1990), achievement goals (McCombs & Marzano, 1990; Schunk, 1990) or level of challenge (Pintrich & de Groot, 1990), affect or mood (McCombs & Marzano, 1990), and prior achievement (Pintrich & de Groot, 1990). Categorizing similar correlates together reveals four groups of correlates relating to self-concept, relevance, goals, and affect.

A couple of the correlates are suspected to be influenced by other variables. Motivation is conceived to be influenced by a number of correlates such as self-efficacy (Kinzie, 1990; McMillan, et al., 1994) personal control, relevance, curiosity (Kinzie, 1990), self-esteem, personal development goals, affect, mood (McCombs & Marzano, 1990), and attitudes (McMillan et al., 1994). Similarly, will (described as an innate state of motivation) is proposed to be influenced by self-esteem, personal development, goals, affect, and mood (McCombs & Marzano, 1990). McCombs and Marzano (1990) proposed that an individual's will is necessary for self-regulated learning.

Although engagement, involvement, and self-regulated learning correlate with relevance and affect, the majority of correlates of self-regulated learning tend to reflect the likelihood that one will set challenging goals and monitor one's performance relative to those goals. That is, learners who have high positive perceptions of themselves (i.e., high levels of self-efficacy, confidence, self-esteem), identify relevance in the material (i.e., exhibit interest, curiosity), and experience positive affect are more likely to set challenging goals relative to task difficulty, role clarity, and prior achievement, and to monitor their performance relative to those goals than learners with low self perceptions.

Besides reviewing the correlates of engagement, involvement, and self-regulated learning, current measures also were evaluated. The most common form of measurement is the questionnaire (Ainley, 1993; Farrell & Mudrack, 1992; Finn et al., 1991; Goff & Ackerman, 1992; Goldsmith & Emmert, 1991; Howard-Rose & Winne, 1993; Pintrich & de Groot, 1990; Reed & Schallert, 1993; Skinner & Belmont, 1993; Wilhite, 1990), which is used to collect self-reports (Pintrich & de Groot, 1990; Reed & Schallert, 1993; Skinner & Belmont, 1993; Skinner et al., 1990; Wilhite, 1990), or teacher ratings or observations (Finn et al., 1991; Lee & Anderson, 1993; Skinner & Belmont, 1993; Skinner et al., 1990). Usually students are asked to consider what they do when studying or working on a task, but have also been asked to consider a hypothetical situation or to recall their actions during various phases of a task. On occasions, structured interview questions were used to elicit preliminary information (Reed & Schallert, 1993). Others have used student and teacher reports (Skinner & Belmont, 1993) or personality measures (Goff & Ackerman, 1992) to assess students' engagement levels.

What must be avoided are measures which are based on teacher defined behaviors. In a review of how engagement was operationalized for learning disabled individuals, Sturmey & Crisp (1994) found engagement to be operationalized often as tasks specified by teachers (i.e., what the child should be doing). So, if the child was manipulating an item, but not exhibiting teacher specified behavior, the child was not considered engaged (Sturmey & Crisp, 1994). Therefore, it is important to determine what researchers have measured as engagement, involvement, and self-regulated learning and to combine that information with the correlates and descriptors of these constructs in order to develop quality measures. How these constructs were operationalized in various studies is evaluated next.

Current measures of engagement include the Learning Process Questionnaire (LPQ) and the Study Process Questionnaire (SPQ; Biggs, 1987), designed to capture whether students have a surface, deep, or achieving approach to learning. A surface approach tends to reflect the desire to minimally pass a subject without putting out too much effort. In contrast, a student who attempts to gain a thorough understanding of the material by integrating new information with other subject material and current knowledge is said to have a deep approach to learning. Finally, students who have an achieving approach set goals to achieve the highest grades possible, regardless of whether they find the material interesting or not (Biggs, 1987). These approaches, in turn, influence student motives and strategies, which are measured in the questionnaires.

The LPQ (36 items) and the SPQ (42 items) assess surface, deep, and achieving motives and strategies in six subscale scores, using a 5-point Likert scale. A student's approach scale score is the sum of the respective

motive and strategy subscale scores (Biggs, 1987). In review of these items, it appears as though the deep approach items most closely resemble engagement, as presently defined. The achieving approach, and somewhat the surface approach, items tend to reflect self-regulated learning. Biggs (1987) tended to combine the deep and achieving approaches into a single score. Although some of these scales have sufficient alpha reliabilities (ranging from .45 to .81), only one or two factors are identified in the research (Biggs, 1987), suggesting the need for combining the deep and achieving scale scores.

Another measure, the 29-item Student Participation Questionnaire (SPQ; Finn et al., 1991) was used by the classroom teacher to assess fourth grade students' level of participation. The items tend to tap concepts of engagement such as persistence, effort, attention, and interest. These classifications of the items, though, are not necessarily the same as identified by Finn et al. (1991). In fact, Finn et al. (1991) identified three factors: nonparticipatory behavior (e.g., annoys others, restless behavior, needing reprimand), effort (e.g., passive but adequate participation, pays attention, persistent, completes homework on time), and initiative (does more than assigned work, attempts to work thoroughly, verbal participation). A fourth factor, value, was also identified and the items were on the questionnaire, but these items were not included in the factor analysis. The three factors mentioned above had high reliabilities (.89, .89, and .94, respectively), yet the factors may not be as distinct as they could be. That is, although the items had the highest loading on their respective factors, these items also loaded on other factors. For example, one item had a loading .89 with Factor I and loadings of -.52 and .58 on Factors 2 and 3, respectively.

Similarly, Skinner & Belmont (1993) used student and teacher reports to measure students' engagement levels. Third, fourth, and fifth grade students and teachers used a 4-point Likert format from not at all true to very true to assess behavioral and emotional engagement. Behavioral engagement tapped effort, attention, and persistence (38 items for teachers, e.g., "student does not try when faced with difficult problems"; 29 student items, e.g., "I think about other things when in class"). Emotional engagement tapped interest, happiness, anxiety, and anger (24 teacher items, e.g., "student appears worried"; 36 student items, e.g., "in class I feel happy").

Engagement has also been conceived of as a personality trait (Goff & Ackerman, 1992). This measure of engagement was labeled intellectual engagement. Testing the measure of intellectual engagement on undergraduate students revealed 5 subcategories: typical intellectual engagement (e.g., engagement in thoughtful or intellectual pursuits, a desire to engage and understand the material, a preference for puzzles in life that must be solved), extroverted and introverted intellectual engagement (e.g., enjoying involved discussions; pleasure in evaluating one's own thoughts and feelings), absorption (e.g., other people seem not to exist when concentrating), interest in arts and humanities (e.g., interest in understanding poetry), and social science (e.g., interest in the cause of societal problems). Although intellectual engagement is related to the personality trait of openness (open to new experiences and interests; Ackerman & Goff, 1994; Goff & Ackerman, 1992; Rocklin, 1994), these constructs appear to be distinct (Ackerman & Goff, 1994; Goff & Ackerman, 1992). Intellectual engagement is also distinct from factors identified as directed activity (lack of distractibility and energy; not easily distracted from the task; much energy, rarely tired), science/

technology interests (likes science; likes technical problems), and conscientiousness (e.g., prefers hard work; likes work requiring conscientiousness, perfectionism) (Goff & Ackerman, 1992). The description of this conscientiousness factor appears to reflect the proposed construct of involvement which supports the notion that engagement and involvement may be distinct constructs. Typical intellectual engagement (TIE), a component of the engagement measure, may reflect measurable individual differences which influence choice of activities, engagement with those activities, and possibly achievement.

Another method of measuring engagement is using the effective time within an allotted time period during which students were actively participating in learning (Kumar, 1991). The length of time of participation may not be as good a measure of engagement as the quality of the learning participation. Yet, if engaged students become so engrossed in their work that time becomes distorted (Goff & Ackerman, 1992), then perceived and actual time may be crude measures of engagement. That is, students who spend more time on task may be more engaged in the material, especially students who lose track of time. Thus, time spent studying may be another means to measure engagement if engaged students become so engrossed in their work that time becomes distorted (Goff & Ackerman, 1992).

Finally, Thomas et al.'s (1993) Study Activity Questionnaire measures cognitive and effort management study activities by assessing six areas: level of cognitive processing, representational level, initiative, autonomous management, memory augmentation, and effort management. Time spent studying was also assessed. No alpha reliability values were reported for the measures of effort or time, but the alpha reliabilities for the other scales were .84,

.75, .84, .71, .49, respectively. It is important to note that there were some inconsistencies between the data reported in the text and tables. Nevertheless, level of processing, representational level, and initiative were the only positively correlated dimensions with the achievement test for this study (.18, .34, .30, respectively) (Thomas et al., 1993). Given the descriptions of these items, as the actual items were not provided, these three aspects tend to reflect engagement, while the other dimensions unrelated to achievement seem to overlap with self-regulated learning.

It is apparent that these measures assess more than engagement. In fact, all measures identified in the literature tended to tap aspects of engagement, involvement, and/or self-regulated learning.

Unlike engagement, few, if any, involvement measures exist. Most are adaptations of Kanungo's (1982) job and work involvement scales. Reed and Schallert (1993) developed a questionnaire which identified two dimensions of involvement, concentration and understanding. Concentration included items related to attention (high), task difficulty (moderate, but achievable), and importance (high) (Reed & Schallert, 1993). Several of the items on this questionnaire actually appear to be measures of engagement. Nevertheless, involvement was found to be different than interest (Reed & Schallert, 1993).

Although measures of student involvement are limited, a review of involvement measures in other areas provide insight into the involvement measure. In testing three measures of consumer product involvement, Goldsmith and Emmert (1991) found the three measures to be convergent, but divergent from measures of general marketplace involvement. The three measures tapped personal qualities (inherent interests, values, needs that motivate); physical characteristics (characteristics of an object that increase interest);

situational conditions (something that temporarily increases relevance or interest toward an object); perceived risk (importance); the rewarding nature of a product; the ability of a brand to convey status, personality, and identity; and purchase decision involvement (Goldsmith & Emmert, 1991). These aspects may be classified into interest, relevance, and importance categories.

Similarly, Farrell and Mudrack (1992) adapted two of the job and work involvement scales of Kanungo (1982) to measure academic involvement of older students in an organizational behavior course. Kanungo's (1982) work and job involvement questionnaires included six and ten items, respectively, which were rated on a 7-point Likert scale ranging from strongly disagree to strongly agree. The two graphic items were positively correlated with the questionnaire items, so only the questionnaire items were evaluated for this review.

Although several models of self-regulated learning have been proposed (e.g., Butler & Winne, 1995; Kinzie, 1990; McCombs & Marzano, 1990), few well developed measures of self-regulated learning have emerged. The Learning and Study Strategies Inventory (LASSI, Weinstein, Palmer, & Schulte, 1987) was developed and validated (Weinstein, Zimmerman, & Palmer, 1988), but the emphasis is on strategies, not whether the individuals are engaged, involved, or self-regulated. Likewise, Zimmerman, Bandura, and Martinez-Pons (1992) developed two reliable scales for assessing learners' self-efficacy for self-regulated learning and for academic achievement. Self-efficacy appears to be an important aspect of self-regulated learning. Even McMillan et al. (1994) validated a measure of student motivation, which assessed general self-efficacy and attitudes as well as self-efficacy and attitudes toward math, reading/English, and science for fourth, eighth, and eleventh graders.

The Everyday Memory Questionnaire (EMQ; Martin & Jones, 1984) and Christopoulos, Rohwer, and Thomas's (1987) Study Activity Survey (SAS) also appear to assess self-regulated learning characteristics. The EMQ was significantly related to two dimensions on the SAS, uniform processing and generation of interpreted information. Uniform processing included indiscriminant processing that was voluntary, intense, or earnest. Attempting to interpret the material for a deeper understanding described the generation of interpreted information (Wilhite, 1990).

Students' ability to monitor time is assessed by the LASSI (Weinstein et al., 1987), while the Student Progress Management (SPM) program helps students monitor time (Judd, McCombs, & Dobrovolsky, 1979). Study time should be evaluated because lower performing students tend to spend less time studying difficult topics than higher performing students (Zimmerman, Greenberg, & Weinstein, 1994). It is important to note that measures of time appear to be related to engagement and self-regulated learning; however, time for engaged students tend to become distorted whereas self-regulated learners tend to be cognizant of time in order to complete all tasks.

Finally, researchers usually develop scales for their specific studies, often tapping the 14 self-regulated strategies identified by Zimmerman and Martinez-Pons (1986). Previously, though, Corno, Collins, and Capper's (1982) Self-Regulated Learning Scale tapped five general areas of self-regulated learning strategies including deliberate alertness, selectivity, accessing schemata, planning, and monitoring. Only a few descriptions were given to describe some of these learning activities. Nevertheless, these categories seem to encompass the 14 self-regulated learning strategies identified by Zimmerman and Martinez-Pons (1986). The alpha reliabilities for these five

categories were reported as .70 and .80 on pre- and post-tests (Corno et al., 1982).

Working from the definitions of the constructs, the review of the correlates of these constructs, and the current measures available, the following are descriptions of the unique characteristics proposed to underlie engagement, involvement, and self-regulated learning.

Engagement should tap six areas: interest, attention, absorption, persistence, effort, and level of cognitive processing. Students who become engaged with material should characteristically find topics to be inherently interesting, which draws their attention to the subject matter, whereby they are not easily distracted from the material. Such directed attention should be related to a distortion of time and a lack of awareness of their task-irrelevant environment. That is, the student should be absorbed in the material. Being absorbed, the student would be persistent in the quest for information about the topic and would display effort in mastering the material, but not necessarily relative to a specific goal. Finally, such intense focus on this material should be related to a deeper level of cognitive processing.

The concept of involvement appears to involve school and learning importance, commitment, and conscientiousness. School and learning importance reflects the students' perception of how relevant the topic or topics are to them and whether schooling in general is important. Commitment is one's connection with the institution (e.g., involvement in activities outside the classroom). Conscientiousness is one's belief in the virtue or value of hard work (e.g., strong work ethic).

A self-regulated learner develops goals for the task, establishes an

environment conducive to learning; uses various processing techniques or strategies; and monitors the environment, strategies, and progress toward the goals. The factors of this construct should include: goal development, planning, strategies, and monitoring.

It was hypothesized that these subscales within and between the scales are distinct.

Experiment 1

Method

Participants

Undergraduate students (14 females, 5 males) from a mid-sized, private, mid-western university volunteered for this experiment and received extra credit to be applied toward one of their psychology courses.

Materials

To determine whether the subscales of the 3 constructs are distinct, scale items were developed from current measures, and from descriptions and correlates of these constructs. Obviously redundant items were eliminated by the experimenter, leaving a total of 134 items for the three constructs. Each of the 134 items was printed on a separate index card.

Procedure

In order to eliminate other redundancies before collecting the factor analytic data, students performed one or two card sorting tasks within 30 min, after signing a consent form. Before the sorting began, card sorting was explained using sample cards, indicating that cards representing similar concepts should be grouped together. Most students sorted cards for 2 constructs. Half the students were given the items for one construct and asked to sort the cards before given a second set of items to sort. The other

students were given items for 2 constructs in one set of cards. The combination and order of the card sets were counterbalanced.

Results and Discussion

Comparisons of the sorting patterns revealed a great deal of consistency within the engagement and involvement subscales as proposed. Given the large number of self-regulated learning items, there was less consistency, but some patterns emerged. Only 6 redundant items (1 engagement, 1 involvement, 4 self-regulated learning) were identified and eliminated. These preliminary data suggest that the proposed unique subscales of engagement, involvement, and self-regulated learning are distinct. Based on these findings, a questionnaire using a 7-point Likert-type format with the remaining 128 items was developed. Experiment 2 was conducted in order to clarify further the underlying factors, to identify other redundant items within and across the scales, and to validate the scales.

Experiment 2

Method

Participants

Undergraduate students (45 males, 55 females) from a small, private commuter university and (157 males, 303 females) from a mid-sized private university, both in the midwest, volunteered for this experiment, for a total sample of 560 participants. Students from the commuter university and 294 students from the mid-sized university received extra credit which could be applied toward one of their psychology courses. The remaining 176 students at the mid-sized university completed the surveys as part of their Freshman Seminar course. Students at the commuter institution were between the ages of

18 and 65, with a median age of 21. The ages of the students at the mid-sized university ranged between 16 and 27, with a median age of 19.

Materials

Based on the data from the card sort conducted in Experiment 1, a 128 item survey was created. The items were alphabetized within each subscale (engagement, involvement, and self-regulated learning). The involvement scale was appended to the engagement scale and the self-regulated learning scale was appended last. Students responded using a 7-point Likert-type response scale (1=never, 7=always).

Procedure

Students were first given a consent form to read and sign, except the students in the Freshman Seminar courses. For the Freshman Seminar students, the survey was administered following another survey distributed during the same Freshman Seminar session. The freshmen were informed that the survey was voluntary. Otherwise, the procedures were the same as follows. After the consent forms were collected, the experimenter informed the students that people have different attitudes toward and approaches to learning; therefore, the reason for the study was to identify and clarify the underlying student characteristics which had been identified in three different areas of research. Students at the mid-sized university were also asked to give the experimenter authorization to tap their academic records for academic measures such as ACT or SAT scores, GPA, and high school rank. These students were informed that they did not have to give such authorization, that it was voluntary. Issues of confidentiality were also discussed. The experimenter also explained to all students that they should use the scale listed at the top of each page to respond to the items and that they should consider

themselves when responding. Finally, before the questionnaire was administered, students were asked if they had any questions about the questionnaire or confidentiality (if applicable).

After all questions were answered the questionnaire was administered. Students normally completed the questionnaire within 15 to 20 minutes. Once the questionnaires had been collected, the students were fully debriefed and thanked for their participation.

Results

The data were analyzed using exploratory factor analysis with varimax rotation. Because of missing data, a correlation matrix was used as the input data, resulting in 556 observations. The first analysis resulted in 30 factors. The scree plot was difficult to read, but indicated that 12 factors might be more appropriate. To reduce the number of factors, the number of factors desired in the factor analysis was specified based on the number of factors that had 3 or more variables with loadings of .30 or higher. After the first analysis, 5 factors had less than 3 variables with loadings of .30 or higher. Thus, the second analysis requested that the number of factors be 25. This process was continued until all factors had 3 or more variables with loadings of .30 or higher. This iterative process ended when there were 13 factors. Then, each variable was evaluated. If a variable loaded .40 or higher on 2 or more variables, it was deleted (Hatcher, 1994). This process was continued until 109 variables remained as well as 13 factors. Some of the variables loaded .30 or higher on more than one factor, but not .40 or higher on more than one factor. These variables were not eliminated, but they were not included in the next phase of the analysis, which included the development of scaled scores and identification of the factors. Because of space

limitations, the actual factor loading data are not presented here, but may be requested from the author.

The variables included in the scale development phase had loadings of .30 or higher on only one factor. The number of variables retained for each factor based on the alpha reliabilities and the alpha reliabilities of those variables are presented in Table 1. Factors 12 and 13 each had one variable dropped from their scales because the respective variables drastically lowered the alpha reliabilities. Upon evaluation of the items, it was appropriate that these variables were not included in the scaled score.

As expected, there was little overlap between the engagement, involvement, and self-regulated learning scales, although there was some. Often it was the self-regulated learning strategies which appropriately overlapped with the engagement or involvement items. Based on an evaluation of the items on each factor, it was possible to label each factor and to identify the constructs each factor tapped (see Table 1).

Once the factors were identified and alpha reliabilities were calculated, the factors were correlated with the performance measures, which included individuals' best ACT score, SAT scores, high school rank, and semester and cumulative GPAs. High school rank was calculated as a proportion of the student's rank relative to the number of students in the graduating class. It was easier to compare relative proportions than actual rankings. These data are reported in Table 2.

Discussion

Students responded to a questionnaire designed to tap the unique underlying characteristics of engagement, involvement, and self-regulated learning. It is important to note that although certain unique underlying

characteristics or factors were proposed to exist, no research was found that statistically evaluated the measures from the engagement, involvement, and self-regulated learning literatures. Thus, it was more appropriate to use exploratory as opposed to confirmatory factor analysis. Although tentative, these results suggest that the items proposed to be unique to engagement, involvement, and self-regulated learning do tap relatively distinct characteristics. In fact, all three constructs were tapped in the first three identified factors (see Table 1). In addition, several of the proposed factors were identified, even though some of the items shifted. Therefore, it appears as though the hypothesis that the underlying characteristics are distinct was partially supported. Further research is needed to confirm these factors and refine the measurement scales.

Even though these data are preliminary, scaled scores were calculated based on the items loaded .30 or higher on only one factor. For Factors 1, 2, 3, 4, 6, and 13, the alpha reliabilities ranged from .71 to .88. These factors were significantly related to different measures of academic performance and are now discussed. Factor 1: Interest was related to high school rank, and university grade point averages, but not ACT or SAT scores. This suggests that individuals who are interested in learning, seek related information, and apply their knowledge perform better in learning environments, especially when there is a predetermined time period for learning the material (e.g., a semester). These individuals will not necessarily perform better on general achievement or aptitude tests such as the ACT or SAT because students who successfully complete only what is required should also do well on these exams.

On the other hand, planning and monitoring (Factor 2) may be detrimental

to performance on general achievement tests and to have no effect on course performance. It should be noted that the relationship between Factor 2 and ACT score is significant, but the practical significance is tenuous. As indicated before, though, it is possible to monitor and plan in order to complete tasks, but to learn the material well. This notion needs to be investigated further.

Factor 3: Commitment tapped how much education was a part of one's life; however it was positively related to only one set of semester grades. It is possible that many of the freshmen who completed this survey indicated high commitment, but grades varied among them. The fall 1996 grades, though, may have tapped more senior students who may have indicated greater variance in the prominence of education in their lives. Finally, how much one values education may not translate into actual success, as reflected in the negligible relationships between Factor 3 and ACT and SAT scores. It is possible that education is a primary part of one's life, even if one is not successful in education.

Even if success is not enhanced when one's life is dominated by education, Effort/Initiative (Factor 4) was related to high school rank and cumulative grade point averages. As effort and initiative increased, students were ranked higher in the class (closer to 1) and also performed better, at least according to cumulative grades. Similar to Interest (Factor 1), people who display effort and initiative are likely to be more successful in timed constrained learning situations.

Another factor that is not related to ACT or SAT scores, or high school rank, but is related to most academic performances is Self-Concept (Factor 6). Self-concept, which taps self-efficacy, is a major correlate of self-regulated

learning (e.g., Howard-Rose & Winne, 1993; Pintrich & de Groot, 1990; Schunk, 1994). It is possible that individuals can learn general knowledge necessary for the ACT and SAT exams regardless of their levels of self-concept. Perhaps this learning occurs outside of classrooms. When learning takes place at college, though, the environment is likely to be more competitive in college whereby one must be more independent and possibly more assertive. Therefore, self-concept is likely to have a greater impact on semester grades than general knowledge exams.

Finally, Commitment to School Activities (Factor 13) was negatively related to SAT scores and high school rank, which seems to be a contradiction, and was not correlated with ACT scores or university success. Although SAT scores tended to decrease with increased commitment, the students' rankings went down (i.e., the student was nearer the top of the class). If students participate in school activities at the expense of learning new material, this would decrease SAT scores. High school rank might increase, though, if these same activities are part of the course grade. These relationships need further clarification.

For the remaining factors (5, 7, 8, 9, 10, 11, 12), the alpha reliabilities were lower than .70; however, it is interesting to note the relationships between these factors and the measures of academic performance. For instance, the greater the students' level of conscientiousness (Factor 5), the higher the high school class standing and university performance. Interestingly, though, conscientiousness was not related to ACT or SAT scores. Again, a student may not be conscientious, but will still learn the basic materials. Conscientious students, though, appear to excel in the classroom.

It is also interesting that Factors 8 (Seeks Assistance) and 12

(Ownership in Assessment) were not related to any academic performance measures. Also, Factor 9 (School/Learning Importance - Purpose) was significantly related to ACT scores. If doing well in order to get a good job or career is important to the students, they tended to perform better on the ACT. Their success in university, though, does not appear to be that greatly enhanced.

On the other hand, Factor 11 (Absorption) was only related to university performance in the fall of 1996. Because of the earlier grade point averages, perhaps this factor tapped more senior students. It is possible that absorption has a greater impact on higher level course work, but not general knowledge tapped in the ACT or SAT exams, or in lower level courses. This notion could easily be evaluated by assessing students' levels of absorption in higher and lower level courses.

Relatedly, Factor 7 (School/Learning Importance - General), only impacted recent grades. The notion that education is a good thing may have impacted the lower level students in the lower level courses (spring grades) more than senior students in senior courses (e.g., fall grades). This, however, does not explain why Factor 7 is not correlated with ACT and SAT scores.

Finally, Factor 10 (Feedback) was related to high school rank and recent grades. This suggests that feedback is important for success in school, but it may not impact what is actually learned. That is, without feedback, one can still perform well on the ACT or SAT. To perform well in courses, though, one often needs feedback in order to make adjustments in studying. Although the students may be learning a great deal, if what is being learned is not related to how learning is assessed, these students will not perform well in

the course. Thus, the students need to self-monitor themselves, which can be enhanced with performance feedback.

These data support the notion that the unique underlying characteristics of engagement, involvement and self-regulated are distinct and that they tap different aspects of learning and academic success. There are, though, some limitations to this study and, thus, to the application of these results. First, more data is needed to support these results. Although some indicate that a sample size greater than 500 is sufficient, either more data combined with this set of data or a new set of data is needed to retest the assumptions tested here. Also, test-retest reliabilities would be useful to determine the consistency of the scale. Finally, although it was possible to assess students from two universities, more diversity in the population studied is needed.

General Discussion and Conclusions

Based on the card sort and factor analysis data, these distinct factors appear to exist and to affect different measures of academic performance. Because engaged (Greenwood, Terry, Marquis, & Walker, 1994) and self-regulated learners (Butler & Winne, 1995) tend to be, and involved learners are proposed to be (Farrell & Mudrack, 1992), better learners, identification of these unique underlying characteristics is beneficial. If these factors can be assessed accurately, then it will be possible to predict to what extent a learner will be engaged, involved, or self-regulated and how a student will perform.

Based on this study, there are several avenues of research still needed. If the unique characteristics a learner possesses suggest the learner may not be successful, future research could investigate whether these individual

characteristics can be altered or if the learning environment can be altered to tapped into the learner's characteristics. It is also possible that these factors have indirect effects on various academic measures, which should be investigated.

Furthermore, a potential benefit of engagement, involvement, and self-regulated learning is that students may become better calibrated. Well calibrated learners accurately assess whether they do or do not know something. Zimmerman (1990) proposed that self-regulated learners are aware of whether they do or do not know something, although the direct relationship between engagement, involvement, or self-regulated learning and calibration does not appear to have been tested. Intuitively it seems that we should know what we do or do not know, but calibration tends to be low (Wagenaar, 1988). In fact, individuals are generally found to be overconfident (Bjorkman, 1992). Because overconfidence is high, people are assessing their confidence in their knowledge to be greater than what their knowledge actually is. One measure of calibration is the correlation between confidence ratings and actual performance; therefore, calibration is low.

Nevertheless, calibration appears to improve with more knowledge (Bjorkman, 1992), but not general knowledge (Trafimow & Sniezek, 1994). That is, the student must have knowledge of the content tested. The improvement in calibration due to more knowledge may be influenced by how information is processed. Strategies for engagement, involvement, and self-regulated learning, such as increased processing (Maki, Foley, Kajer, Thompson, & Willert, 1990; Walczyk & Hall, 1989) and monitoring (Schraw, Potenza, & Nebelsick-Gullet, 1993) effected better calibration scores, which suggests that strategies to improve calibration may exist as well as possible

relationships between calibration and these three constructs. Certain types of processing, though, may increase confidence ratings, but not necessarily calibration (Trafimow & Snizek, 1994).

To ensure proper processing, it may be possible to use incentives to improve calibration, thereby decreasing bias and increasing accuracy in calibration (Schraw et al., 1993). Students who received incentives to improve calibration apparently shifted their attention from performance to monitoring, facilitating self-generated cognitive feedback (Schraw et al., 1993). It is important to note that self-generated feedback was also suspected to develop when questions and examples were imbedded in the text students' studied (Walczyk & Hall, 1989). This suggests that feedback, which is a critical component of self-regulated learning, may also be a critical component for improved calibration if it includes achievement as well as calibration information. It is likely that calibration may be low for engaged learners because these learners theoretically lack the feedback loop required to monitor their performance relative to some goal.

Therefore, research is planned to evaluate the relationship between the measurement scale currently being developed and calibration. If the current measure is correlated with academic performance and calibration, it would be possible to detect or predict individuals' calibration levels. Because it is suspected that students' levels of engagement (Greenwood et al., 1994), involvement (Jacobi, 1991), and self-regulation (Henderson, 1986) can be taught or influenced, it should be possible to increase learners' performance and calibration levels.

References

Ackerman, P. L. & Goff, M. (1994). Typical intellectual engagement and personality: Reply to Rocklin (1994). Journal of Educational Psychology, 86, 150-153.

Ainley, M. D. (1993). Styles of engagement with learning: Multidimensional assessment of their relationship with strategy use and school achievement. Journal of Educational Psychology, 85, 395-405.

Biggs, J. B. (1987). Student approaches to learning and studying. Melbourne, Australia: Australian Council for Educational Research.

Bjorkman, M. (1992). Knowledge, calibration, and resolution: A linear model. Organizational Behavior and Human Decision Processes, 51, 1-21.

Butler, D. L. & Winne, P. H. (1995). Feedback and self-regulated learning: A theoretical synthesis. Review of Educational Research, 65, 245-281.

Christopoulos, J. P., Rohwer, W. D. Jr., & Thomas, J. W. (1987). Grade level differences in students' study activities as a function of course characteristics. Contemporary Educational Psychology, 12, 303-323.

Corno, L., Collins, K., & Capper, J. (1982). Where there's a way there's a will: Self-regulating the low-achieving student. ERIC Document ED 222 499.

Corno, L. & Mandinach, E. B. (1983). The role of cognitive engagement in classroom learning and motivation. Educational Psychologist, 18, 88-108.

Craik, F. I. M. & Lockhart, R. S. (1972). Levels of processing: A framework for memory research. Journal of Verbal Learning and Verbal Behavior, 11, 671-684.

Dickinson, L. (1992). Collaboration in assessment: Empowering the individual course member. In E. Sadtono (Ed.) Language teacher education in a fast-changing world. Anthology series 29. Eric Document ED 369 275.

Farrell, G. M. & Mudrack, P. E. (1992). Academic involvement and the nontraditional student. Psychological Reports, 71, 707-713.

Finn, J. D., Folger, J., & Cox, D. (1991). Measuring participation among elementary grade students. Educational and Psychological Measurement, 51, 393-402.

Goff, M. & Ackerman, P. L. (1992). Personality-intelligence relations: Assessment of typical intellectual engagement. Journal of Educational Psychology, 84, 537-552.

Goldsmith, R. E. & Emmert, J. (1991). Measuring product category involvement: A multitrait-multimethod study. Journal of Business Research, 23, 363-371.

Greenwood, C. R., Terry, B., Marquis, J., & Walker, D. (1994). Confirming a performance-based instructional model. School Psychology Review, 23, 652-668.

Hatcher, L. (1994). A step-by-step approach to using the SAS system for factor analysis and structural equation modeling. Cary, NC: SAS Institute.

Helstrup, T. (1989). Active and passive memory: States, attitudes, and strategies. Scandinavian Journal of Psychology, 30, 113-133

Henderson, R. W. (1986). Self-regulated learning: Implications for the design of instructional media. Contemporary Educational Psychology, 11, 405-427.

Howard-Rose, D. & Winne, P. H. (1993). Measuring component and sets of cognitive processes in self-regulated learning. Journal of Educational Psychology, 85, 591-604.

Jacobi, M. (1991). Mentoring and undergraduate academic success: A literature review. Review of Educational Research, 61, 505-532.

Judd, W. A., McCombs, B. J., & Dobrovolsky, J. L. (1979). Time management as a learning strategy for individualized instruction. In H. F. O'Neil, Jr. & C. D. Spielberger (Eds.), Cognitive and affective learning strategies (pp. 133-175). New York: Academic Press.

Kanungo, R. N. (1982). Measurement of job and work involvement. Journal of Applied Psychology, 67, 341-349.

Kinzie, M. B. (1990). Requirements and benefits of effective interactive instruction: Learner control, self-regulation, and continuing motivation. Educational Technology Research and Development, 38, 5-21.

Kumar, D. D. (1991). A meta-analysis of the relationship between science instruction and student engagement. Educational Review, 43, 49-61.

Lee, O. and Anderson, C. W. (1993). Task engagement and conceptual change in middle school science classrooms. American Educational Research Journal, 30, 585-610.

Maki, R. H., Foley, J. M., Kajer, W. K., Thompson, R. C., & Willert, M. G. (1990). Increased processing enhances calibration of comprehension. Journal of Experimental Psychology: Learning, Memory, and Cognition, 16, 609-616.

Martin, M. & Jones, G. V. (1984). Cognitive failures in everyday life. In J. E. Harris & P. E. Morris, (Eds.), Everyday memory, actions and absent-mindedness (pp.173-190). London: Academic Press.

McCombs, B. L. & Marzano, R. J. (1990). Putting the self in self-regulated learning: The self as agent in integrating will and skill. Educational Psychologist, 25, 51-69.

McCombs, B. L. & Whisler, J. S. (1989). The role of affective variables in autonomous learning. Educational Psychologist, 24, 277-306.

McMillan, J. H., Simonetta, L. G., & Singh, J. (1994). Student opinion survey: Development of measures of student motivation. Educational and Psychological Measurement, 54, 496-505.

Morrison, R. G. & Brantner, T. M. (1992). What enhances or inhibits learning a new job? A basic career issue. Journal of Applied Psychology, 77, 926-940.

Pintrich, P. R. & de Groot, E. V. (1990). Motivational and self-regulated learning components of classroom academic performance. Journal of Educational Psychology, 82, 33-40.

Reed, J. H. & Schallert, D. L. (1993). The nature of involvement in academic discourse tasks. Journal of Educational Psychology, 85, 253-266.

Rocklin, T. (1994). Relation between typical intellectual engagement and openness: Comment on Goff and Ackerman (1992). Journal of Educational Psychology, 86, 145-149.

Schraw, G., Potenza, M. T., & Nebelsick-Gullet, L. (1993). Constraints on the calibration of performance. Contemporary Educational Psychology, 18, 455-463.

Schunk, D. H. (1990). Goal setting and self-efficacy during self-regulated learning. Educational Psychologist, 25, 71-86.

Schunk, D. H. (1994). Self-regulation of self-efficacy and attributions in academic settings. In D. H. Schunk & B. J. Zimmerman (Eds.). Self-regulation of learning and performance: Issues and educational applications, (pp.77-99). Hillsdale, NJ: Lawrence Erlbaum Associates.

Skinner, E. A. & Belmont, M. J. (1993). Motivation in the classroom: Reciprocal effects of teacher behavior and student engagement across the school year. Journal of Educational Psychology, 85, 571-581.

Skinner, E. A., Wellborn, J. G., & Connell, J. P. (1990). What it takes to do well in school and whether I've got it: A process model of perceived control and children's engagement and achievement in school. Journal of Educational Psychology, 82, 22-32.

Sturmey, P. & Crisp, A. G. (1994). Group engagement: A conceptual analysis. Journal of Intellectual Disability Research, 38, 455-468.

Thomas, J. W., Bol, L., Warkentin, R. W., Wilson, M., Strage, A., & Rohwer, W. D. Jr. (1993). Interrelationships among students' study activities, self-concept of academic ability, and achievement as a function of characteristics of high-school biology courses. Applied Cognitive Psychology, 7, 499-532.

Trafimow, D. & Snizek, J. A. (1994). Perceived expertise and its effect on confidence. Organizational Behavior and Human Decision Processes, 57, 290-302.

Wagenaar, W. A. (1988). Calibration and the effects of knowledge and reconstruction in retrieval from memory. Cognition, 28, 277-296.

Walczyk, J. J. & Hall, V. C. (1989). Effects of examples and embedded questions on the accuracy of comprehension self-assessments. Journal of Educational Psychology, 81, 435-437.

Wehlage, G. G. (1989). Engagement, not remediation or higher standards. In J. M. Lakebrink (Ed.) Children at Risk. Springfield, IL: Charles C. Thomas, Publisher.

Weinstein, C. E., Palmer, D. R., & Schulte, A. C. (1987). Learning and study strategies inventory. Clearwater, FL: H & H Publishing Company.

Weinstein, C. E., Zimmerman, S. A., & Palmer, D. R. (1988). Assessing learning strategies: The design and development of the LASSI. In C. W. Weinstein, E. T. Goetz, & P. A. Alexander (Eds.), Learning and study strategies: Issues in assessment, instruction, and evaluation (pp.25-40). San Diego: Academic Press.

Wilhite, S. C. (1990). Self-efficacy, locus of control, self-assessment of memory ability, and study activities as predictors of college course achievement. Journal of Educational Psychology, 82, 696-700.

Zimmerman, B. J. (1986). Becoming a self-regulated learner: Which are the key subprocesses? Contemporary Educational Psychology, 11, 307-313.

Zimmerman, B. J. (1990). Self-regulated learning and academic achievement: An overview. Educational psychology, 25, 3-17.

Zimmerman, B. J., Bandura, A., & Martinez-Pons, M. (1992). Self-motivation for academic attainment: The role of self-efficacy beliefs and personal goal setting. American Educational Research Journal, 29, 663-676.

Zimmerman, B. J., Greenberg, D., & Weinstein, C. E. (1994). Self-regulating academic study time: A strategy approach. In D. H. Schunk & B. J. Zimmerman (Eds.). Self-regulation of learning and performance: Issues and educational applications. Hillsdale, NJ: Lawrence Erlbaum Associates. (pp. 181-199).

Zimmerman, B. J. & Martinez-Pons, M. (1986). Development of a structured interview for assessing student use of self-regulated learning strategies. American Educational Research Journal, 23, 614-628.

Table 1

Identified Factors and Their Related Labels, Construct, Number of Items used for the Scaled Scores, and Alpha Reliabilities.

	Factor Label	Construct	Total Items	Alpha
Factor 1	Interest	ENG	15	.88
Factor 2	Planning/Monitoring	SRL	10	.82
Factor 3	Commitment	INV	8	.81
Factor 4	Effort/Initiative	ENG/SRL	5	.71
Factor 5	Conscientiousness/Value	ENG	5	.64
Factor 6	Self-Concept	INV/SRL	7	.71
Factor 7	School/Learning Importance (General)	INV	6	.66
Factor 8	Seeks Assistance/Reviews Tests	SRL	4	.65
Factor 9	School/Learning Importance (Relevance)	INV	5	.68
Factor 10	Feedback (of Performance)	SRL	3	.51
Factor 11	Absorption (Time Distortion)	ENG	3	.45
Factor 12	Ownership in Assessment	INV	2	.64
Factor 13	Commitment (Identity with School Activities)	INV	2	.85

Note. ENG=Engagement, INV=Involvement, SRL=Self-Regulated Learning

Table 2

Correlations between the Scaled Scores and Academic Performance Measures.

	ACT	SAT	HSRank ^a	F96	F96Cum	S97	S97cum
Factor 1	.09	.09	-.24***	.26	.27***	.27**	.28**
Factor 2	-.11*	-.04	-.08	-.01	.08	.08	.09
Factor 3	-.06	-.07	-.06	.33*	.18	.09	.12
Factor 4	.03	.02	-.23***	.20	.13*	.21	.19*
Factor 5	.05	.01	-.29***	.44**	.37***	.37***	.40***
Factor 6	.10	.15	-.05	.19	.20*	.29**	.29**
Factor 7	-.02	.06	-.14*	.09	.06	.25**	.19*
Factor 8	-.11	-.14	-.06	-.11	-.01	.01	.01
Factor 9	.18**	.15	-.09	.15	.07	.20*	.14
Factor 10	.09	.01	-.18**	.18	.06	.35***	.24**
Factor 11	.06	.12	.00	.35*	.22**	.11	.16
Factor 12	-.07	-.13	-.02	-.06	-.04	-.01	-.02
Factor 13	-.00	-.16*	-.20***	.12	.06	.04	-.00

Note: The sample size varied for each measure: ACT 296-302, SAT 149-152, HSRank 262-267, F96 36-38, F96cum 148-152, S97 and S97cum 111-113.

^a The lower the class rank, the higher the class standing (1=top)

* p<.05, ** p<.01, *** p<.001

CHARACTERIZATION OF HUMAN HEAD/NECK RESPONSE IN Z-DIRECTION IN TERMS OF
SIGNIFICANT ANTHROPOMORPHIC PARAMETERS, GENDER, HELMET WEIGHT AND HELMET
CENTER OF GRAVITY IN A +GZ ACCELERATION

Mariusz Ziejewski, Ph.D.
Associate Professor
Department of Mechanical Engineering

North Dakota State University
Dolve 111
Fargo, ND 58105

Final Report for:
Summer Research Extension Program

Sponsored by:
Air Force Office of Scientific Research
Bolling Air Force Base, DC

and

North Dakota State University

December 1997

CHARACTERIZATION OF HUMAN HEAD/NECK RESPONSE IN Z-DIRECTION IN TERMS OF
SIGNIFICANT ANTHROPOMORPHIC PARAMETERS, GENDER, HELMET WEIGHT AND HELMET
CENTER OF GRAVITY IN A +GZ ACCELERATION

Mariusz Ziejewski, Ph.D.
Associate Professor
Department of Mechanical Engineering
North Dakota State University

Abstract

During the ejection phase of escape from an aircraft, crew members are susceptible to neck related injuries. The objective of this study was to assess the head/neck response for accelerations in the z-direction for different body sizes, gender, helmet weight and helmet center of gravity. The experimental data used in this investigation was a selected group consisting of over 600 tests from the Vertical Drop Tower (VDT) studies, namely, VWI 199101, VCSI 199002 and Female Impact Program (FIP) study.

Several test variables were used, including fifteen anthropometric parameters, gender, helmet weight and helmet center of gravity expressed in terms of SIW and acceleration level. Throughout the analysis statistical methods were employed, namely, regression model fitting, cluster analysis, and principal component analysis. In this study, the head/neck response was defined by the x and z acceleration of the head.

The results from the analysis show that the utilized statistical methodology was adequate for the test data. The head acceleration in the x and z directions follow a non-linear five parameter model of a form $y = (b_0 + b_1 \bullet x + b_2 \bullet x^2) / (1 + c_1 \bullet x + c_2 \bullet x^2)$. Based on the results from the stepwise regression analysis, on average, sitting height, head length, chest circumference and body weight are the most significant parameters influencing the head/neck response. The preliminary regression equations for estimation of the parameters for the non-linear model predicting head z-acceleration in terms of the subject's anthropometry are given. The regression equations still can not be recommended for predictions, further refinement in regression parameters must be performed.

The subject's anthropometry itself does not dominate the response output, other factors as body position and helmet properties for given level of acceleration also influential parameters. The inclusion of the helmet properties and level of acceleration were not statistically feasible due to limited data involved in the analysis. The broad range of anthropometric and test parameters in the investigation, necessitates more data to be included in the analysis.

CHARACTERIZATION OF HUMAN HEAD/NECK RESPONSE IN Z-DIRECTION IN TERMS OF SIGNIFICANT ANTHROPOMORPHIC PARAMETERS, GENDER, HELMET WEIGHT AND HELMET CENTER OF GRAVITY IN A +GZ ACCELERATION

Mariusz Ziejewski, Ph.D.

Introduction

During the ejection phase of escape from an aircraft, crew members are susceptible to neck related injuries. Helmet-mounted systems, such as night vision goggles and helmet-mounted displays, have come into increased demand in recent years. Though these devices enhance the pilot's performance, they may also increase the chance of neck injury during ejection. The helmet-mounted systems change the helmet's mass properties such as weight, moment of inertia, and center of gravity location, which may alter the head/neck response and possibly change the pattern of neck loading.

There are two mechanisms of neck injury, direct impact to the neck and inertial loading of the head. During the ejection phase of escape, a direct impact to the pilot's neck is unlikely. However, the pilots are subjected to inertial loading of the head. During inertial loading of the head, forces are transmitted by the neck structure to the torso. The magnitude of the transmitted load is dependent on the inertia of the head/helmet system, the initial orientation of the cervical spine, and the direction of head motion.

The United States Air Force initiated testing to evaluate the effect of acceleration levels to human neck response during ejection procedures. The main objective of their study was to define neck response during the catapult or impact acceleration phase of the ejection. High-speed film footage clearly showed that for identical test conditions, some subjects responded with neck flexion, while others responded with neck extension. The difference in neck responses becomes a critical issue considering the different tolerance values for flexion and extension. Mertz and Patrick found that the resultant bending moment is an excellent indicator of neck strength [1]. For extension, a resultant bending moment of 42 ft-lbs (57 N-m) was proposed as the lower boundary for an injury tolerance level. For flexion, a resultant bending moment of 140 ft-lbs (190 N-m) was suggested as the injury tolerance level. Based on these bending moment tolerance levels, the neck appears to be at least three times stronger in resisting flexion than extension.

To accomplish the ultimate objective of defining the specifications or criteria for allowable head mounted mass and center of gravity location that is safe for the crew members, identification of the head/neck responses and the factors influencing those responses is necessary.

Objectives

To assess the head/neck response in z-direction for different body sizes, gender, helmet characteristics for a +Gz acceleration.

Specific Objectives

1. To determine the regression models adequately representing the head/neck response.
2. To assess the effect of the anthropometric parameters including gender, helmet characteristics and acceleration level on the head/neck response.
3. To identify significantly similar head/neck responses and to assess the parameters responsible for the similarities.

Experimental Data

In this study, the head/neck response was defined by the x and z acceleration of the head. The experimental data used in this investigation was a selected group consisting of over 600 tests from the Vertical Drop Tower (VDT) studies, namely, VWI 199101, VCSI 199002 and Female Impact Program (FIP) study. The VDT is composed of an impact carriage mounted on two vertical guide rails. The test assembly, including a generic ejection seat, as restraint harness, and the instrumentation, is mounted to the impact carriage is guided into the reservoir where the displacement of water around the position decelerates the carriage and produces an upward (+Gz) acceleration. The subjects are positioned in the VDT seat and restrained with a standard double shoulder strap-lap belt combination. Principle measured parameters include tri-axial linear accelerations at the head (mouthpiece or bitebar) and chest, angular acceleration about the lateral axis at the head and chest, seat and carriage vertical (z-axis) accelerations, and sat pan loads. Body displacements are measured by motion analysis using the SELSPOT infrared detection system. The helmet characteristics are defined in terms of Standard Inertial Weight [2].

Test Variables

For this study, several test variables were used. Fifteen variables are selected anthropometric parameters. The remaining parameters are gender, helmet weight, helmet center of gravity and acceleration level.

Out of the thirty-one (31) anthropomorphic parameters listed in the Generator of Body Data (GEBOD) manual [3], only the parameters defining the head, neck, upper torso, mid torso and lower torso was used. The parameters defining the upper and lower extremities were excluded. The following parameters have been selected for the analysis:

1. weight
2. standing height
3. shoulder height
4. armpit height

5. waist height
6. seated height
7. head length
8. head breadth
9. head to chin height
10. neck circumference
11. shoulder breadth
12. chest depth
13. chest breadth
14. waist depth
15. waist breadth

Procedure for Analysis

- Step 1. Collection of seat z acceleration data and linear and angular head acceleration data for the VDT tests from the biodynamic databank.
- Step 2. Collection of anthropomorphic data for the subjects involved in the tests.
- Step 3. Determination of the mathematical model representing the x and z acceleration of the head for all selected VDT tests.
- Step 4. Performance of principal component analysis on head x and z acceleration model parameters.
- Step 5. Performance of analysis of variance and parameter estimates for head x and z acceleration to assess the significance of the selected test parameters.

Methodology

Biomechanical consequences of impact depend not only on the maximum values of the response parameters, but also on the rate of increase and decrease of the response parameters. This calls for the evaluation of the entire response curve rather than just selected characteristics as maximum, minimum and duration. This investigation involved the following statistical methods:

- 1) Regression model fitting
- 2) Cluster analysis
- 3) Principal component analysis.

Model Fitting

Prior to the analysis, the variables were scaled to avoid overshadowing the influence of one variable by another. All relevant non-linear models were included in the analysis. Comparison between the proposed model and the actual

data was used to choose the appropriate model. The regression equation was in the form $Y = f(X, \beta_0, \dots, \beta_n) + \text{error}$. Where Y is the response, X is the time, and β_0 through β_n are parameters [4,5].

The method of least squares was utilized to estimate the parameter values by minimizing $\sum (Y - f(X, \beta_0, \dots, \beta_n))^2$ and hence the estimated model is $\hat{Y} = f(X, \hat{\beta}_0, \dots, \hat{\beta}_n)$.

Hypothesis Tested -

- 1) Model Adequacy (to see if the model is acceptable or statistically significant, at 5% level of significance)
- 2) $H_0: \beta_0 = 0$ vs. $H_1: \beta_0 \neq 0$ (to determine the significance of β_0 in the model)
- 3) ...
- 4) $H_0: \beta_n = 0$ vs. $H_1: \beta_n \neq 0$ (to determine the significance of β_n in the model)

Statistical Analysis System (SAS) computer program was used to perform these tests [6]. Nonlinear regression models differ from linear regressions models in two important ways. One major difference is that nonlinear regression models have a curved, rather than a straight, solution locus, which is the set of all possible values the parameters may assume, the least-squares solution being the one that is closest to the observed vector of Y values. The consequences of this curved solution locus, the extent of the curvature being a measure of the intrinsic nonlinearity, is that the fitted Y values and the residual sum of squares are biased. However, the extent of these bias is generally trivial as most models in practical use have very small intrinsic nonlinearities. The second major way in which nonlinear regression models differ from linear regression models has to do with the particular parameterization of the nonlinear regression model, from which the name "parameter effects" nonlinearity derives. This aspect of nonlinearity is a consequence of the lack of uniformity of the coordinate system on the solution locus (or the tangent plane to the solution locus). For a linear model, they are neither straight nor parallel, the greater the nonlinearity, the greater the curvature of the lines and the departure from parallelism [7].

Cluster Analysis

The purpose of the cluster analysis was to group tests with similar characteristics. Grouping was done with an adapted complete linkage method [8, 9, 10, 11]. This method insures that all the members of a cluster are similar and the members of different clusters are different. The grouping was based on the similarities or Euclidean distances between the β 's estimated in the analysis of variance.

To find the Euclidean distance between two points with n coordinates (β_0, \dots, β_n), the following equation is used (where p_1 is point 1 and p_2 is point 2):

$$d(p_1, p_2) = \sqrt{(\Delta\beta_0)^2 + \dots + (\Delta\beta_n)^2},$$

where

$\Delta\beta_0$ = difference between the β_0 's of point 1 and point 2,

$\Delta\beta_n$ = difference between the β_n 's of point 1 and point 2.

The cluster analysis began with each observation in a separate cluster. In the first step, the distances between clusters were determined. The distance between two clusters is defined to be the maximum of distances between each member of one cluster and each member of the other cluster. In the second step, the two clusters with the least distance in between them were merged to form a single cluster. These two steps were repeated until the appropriate number of clusters are formed.

Principal Component Analysis

The principal component method was used to reduce the number of test parameters (m) to a lower number of principal component variables. The principal components were found using the general equation below [8].

$$y_i = e_{1i} \left(\frac{x_1 - \bar{x}_1}{s_1} \right) + \dots + e_{mi} \left(\frac{x_m - \bar{x}_m}{s_m} \right)$$

The x values ($\bar{x}_1, \dots, \bar{x}_m$) represent the database average values for the test parameters. The s values (s_1, \dots, s_m) represent the standard deviations of the corresponding x values for the database. The x values are the test parameters of the current subject.

Analysis of the data for the m test parameters, x_1, \dots, x_m , of each of the observations, yielded the values for the eigenvectors (e_{ij}) in the above equations. The percent of variation accounted for by the principal components was used to choose the number of necessary principal components.

Results

Regression Models for Head/Neck Response

Initial visual analysis of the X and Z head acceleration data response curves indicates that all curves have similar pattern with one maximum/minimum value and a pair of inflection points. As an example for head z -acceleration see Figure 1.

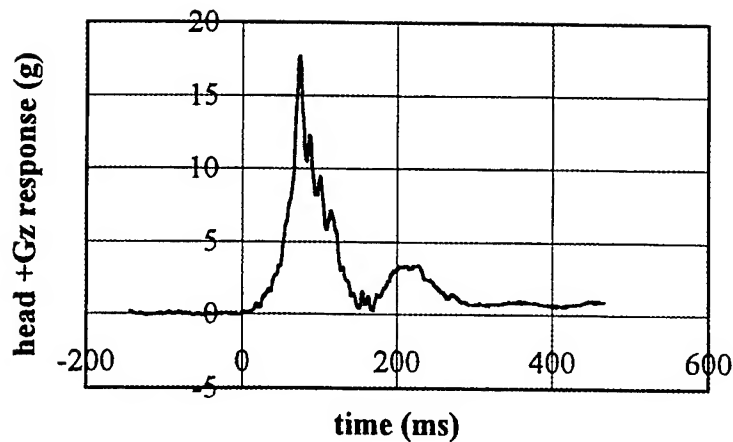


Figure 1 Example head z-acceleration for vertical drop test 1922.

Seven possible models with a maximum (and/or minimum) and two inflection points commonly used in data analysis are listed below [7]:

Model A.
$$y = \frac{b0 + b1 * x}{1 + c1 * x + c2 * x^2}$$

Note: This model is known as a rational function model.

Model B.
$$y = \frac{x}{b0 + b1 * x + b2 * \sqrt{x}}$$

Note: The model can have a maximum at $x = 4 * b0^2 / b2^2$ and a pair of inflection points. The three parameters, b0, b1, and b2 are all reasonably close-to-linear in estimation behavior.

Model C.
$$y = \frac{b0 + b1 * x + b2 * x^2}{1 + c1 * x + c2 * x^2}$$

Note: This model is known as an extended rational function model

Model D.
$$y = b1 * X^{b2 * X^{-b3}} \quad (b0, b1 > 0)$$

Note: The model is capable of having a maximum value at $x = \exp(1/b3)$ (when b1, b2 > 0) and a pair of inflection points. The statistical properties in estimation of all parameters are very good when the data contain sufficiently large x values so that b1 can be determined accurately.

Model E.
$$y = \exp(b0 + b1 * x + b2 * x^2) \quad b2 < 0$$

Note: This model can have a maximum at $x = -\frac{b_1}{2} * b_2$ (when $b_2 < 0$) and a pair of inflection points. All three parameters b_0 , b_1 , and b_2 have similar behavior in estimation, and all are close to linear.

Model F. $y = b_1 * X^{b_2} * e^{-b_3 * X}$

Note: The model can have a maximum (or minimum) and a pair of inflection points. The statistical properties of estimation are close-to-linear.

Model G. $y = b_1 * X^{b_2} * (b_3 - X)^{b_4} \quad (0 < X < b_3)$

Note: The maximum occurs at $x = \frac{b_2 * b_3}{b_2 + b_4}$. However, the model tends to have very poor estimation behavior and must be used with caution, as several parameters may simultaneously be far-from-linear.

Non-linear (Nlin) procedure with SAS program was employed to try all above models. Sample code for evaluating extended rational function is shown in Figure 2.

The parameters for each non-linear model for over 600 head z-acceleration curves and over 600 head x-acceleration curves were determined. The accuracy of each non-linear model was assessed using the midpoint value of the curve. A lower midpoint value corresponds to a better fit of the mathematical model to the experimental data. Frequency distribution charts provide the occurrence of midpoint values in a set of tests used in the analysis. The frequency distribution charts for the four models that provided the best results for head z-acceleration are given in Figures 3 through 6. Model A (rational function) and Model C (extended rational function) provide the most accurate representations of the experimental data. In comparing the standard deviations for Models A and C, it was found that all five parameters were significantly contributing to the model. On average, the Model C provided better estimation as judged based on the Mean Square Error (MSE). Model C was used in the remaining analyses.

```

Option ls=80;

filename pan '~/ashcan.pan/';

Data raw;
  input nowread $char12.;
  infile pan filevar=nowread firstobs=2 delimiter='09'x end=done;
  do until(done);
    Input time crgz headz chestz;
    x=time/100;
    xsq=x*x;
    sample=scan(nowread,1);
    If (time<=162) and (time>=1) then output;
  end;
  cards;
v1922.txt
v2063.txt
v2145.txt
v2208.txt
v2300.txt
v2361.txt
v2502.txt
v2607.txt
v3140.txt
v3183.txt
;;;
proc sort;
  by sample;
*proc print;

Proc Nlin data=raw method=gauss;
  Title ' model :  $y = (b_0 + b_1*x + b_2*x*x) / (1 + c_1*x + c_2*x*x)$  code 3 ';
  By sample;
  Params b0=2.7 b1=1.0 b2=1.2 c1=-2.4 c2=1.7;
  nom=b0+b1*x+b2*xsq;
  den=1.0+c1*x+c2*xsq;
  model headz = nom/den;
  der.b0=1/den;
  der.b1=x/den;
  der.b2=xsq/den;
  der.c1=-nom*x/(den*den);
  der.c2=-nom*xsq/(den*den);
  output out=new3 p=pre3 r=res3;
Run;

filename gsasfile 'meta3.gsf';
goption device=ps noprompt gprolog='25210D0A'X
gaccess=gsasfile gsfmode=append;

Proc gplot data=new3;
  By sample;
  Plot headz*time pre3*time / frame overlay vaxis=axis1 haxis=axis2;
  symbol1 c=black l=1 v=none i=j;
  symbol2 c=black l=2 v=none i=j;
  axis1 order= (-2 to 26 by 2)
    value=(c=black)
    minor=none
    label= (c=black f=none h=1.1 a=90 'head z response');
  axis2 value=(c=black)
    minor=none
    label = (c=black h=1.1 'time msec');
  title1 f=centbu j=c h=1.5 'gplot for model code #3';
Run;

```

Figure 2 Sample code for non-linear modeling using SAS.

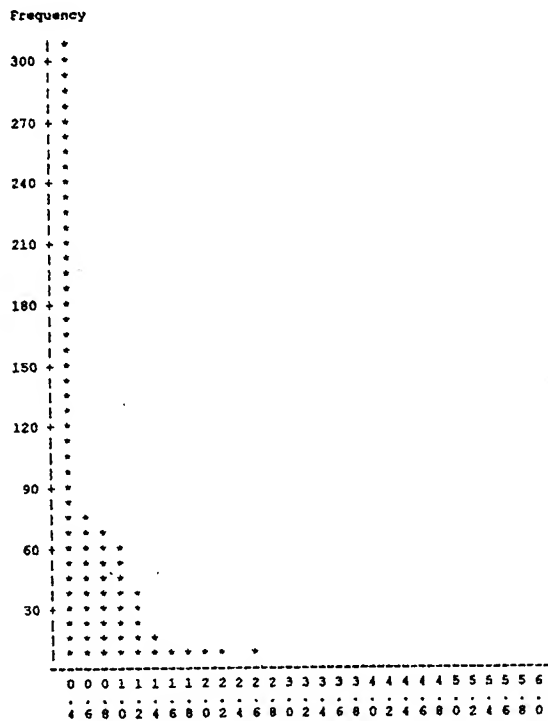


Figure 3 Frequency chart for Model A.

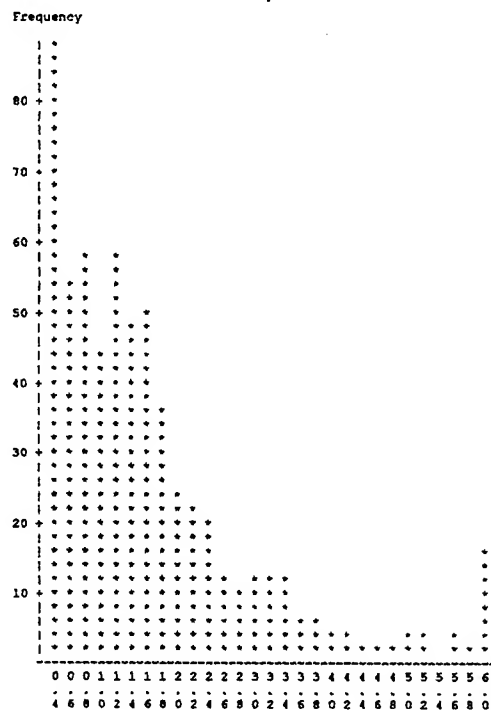


Figure 4 Frequency chart for Model B.

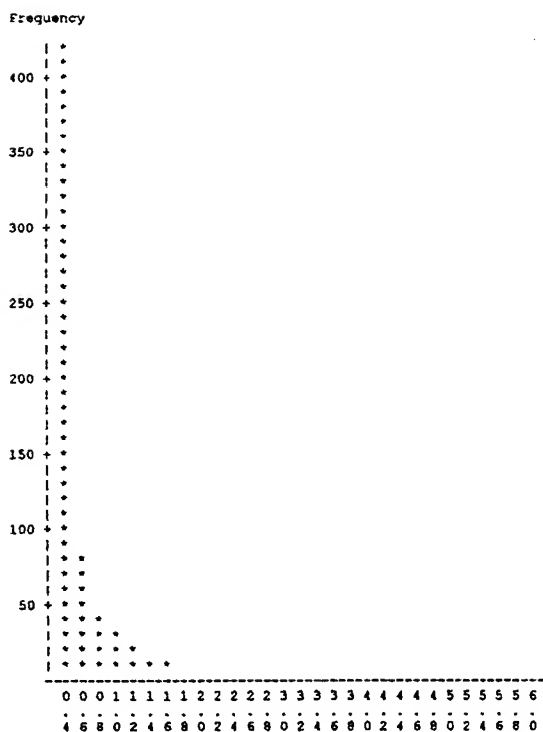


Figure 5 Frequency chart for Model C.

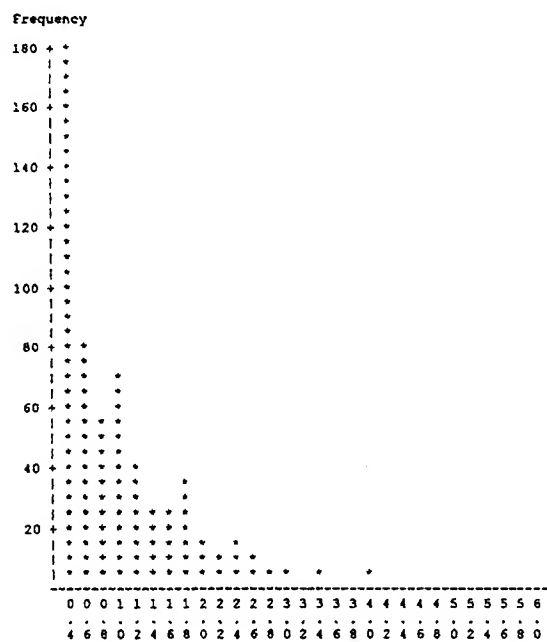


Figure 6 Frequency chart for Model D.

Several example graphs depicting the superimposed experimental head response and the extended rational function model are given in Figures 7 through 14.

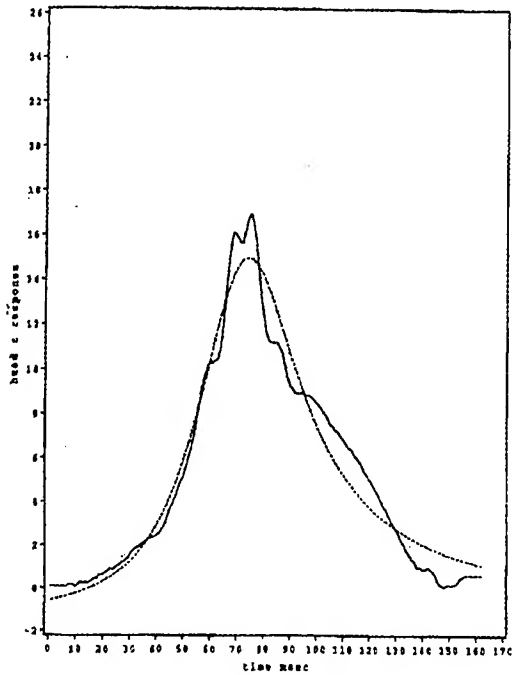


Figure 7 Simulated and Experimental Head z-acceleration for v1922

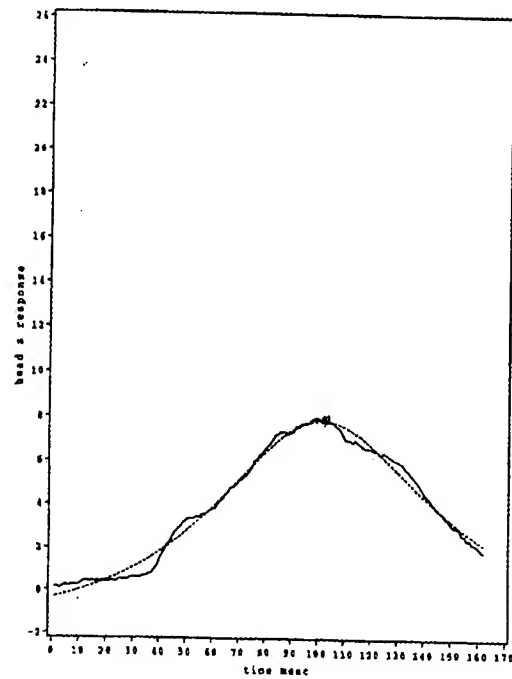


Figure 8 Simulated and Experimental Head z-acceleration for v2208

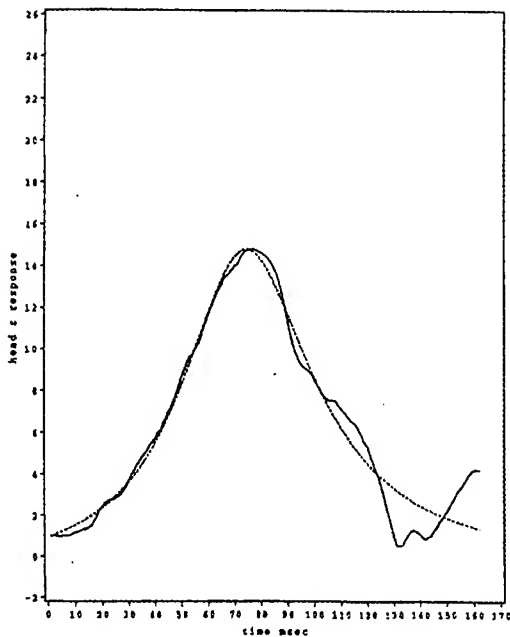


Figure 9 Simulated and Experimental Head z-acceleration for v2300

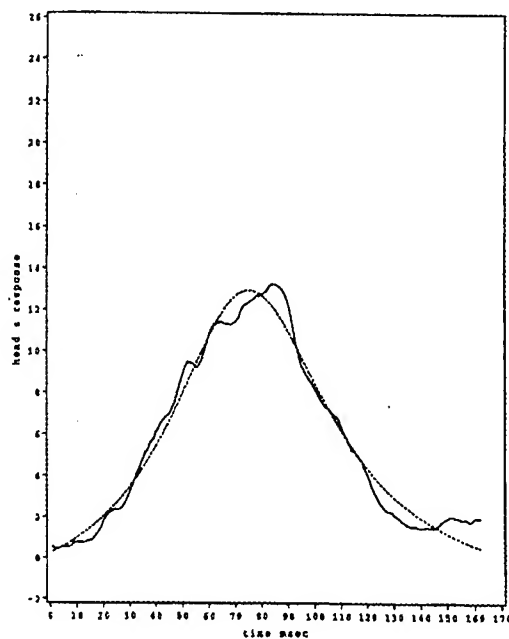


Figure 10 Simulated and Experimental Head z-acceleration for v2361

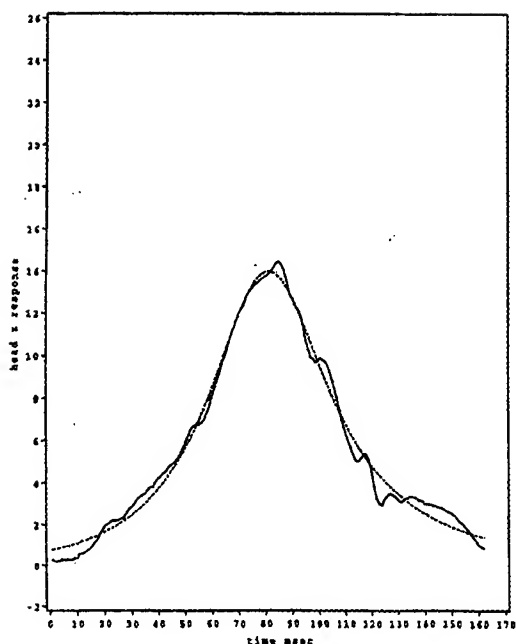


Figure 11 Simulated and Experimental Head z-acceleration for v2502

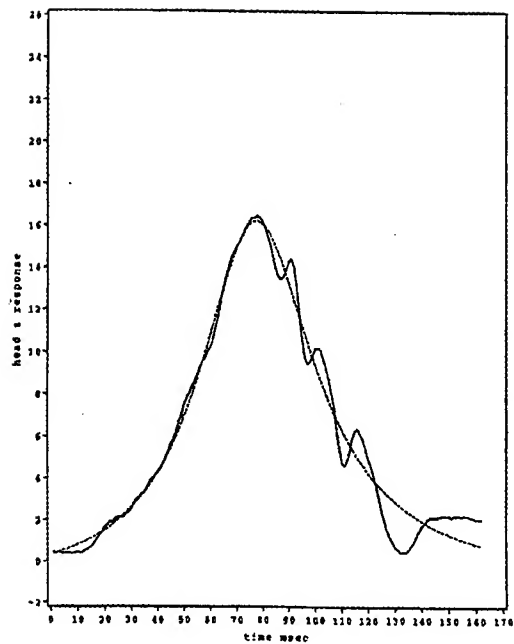


Figure 12 Simulated and Experimental Head z-acceleration for v2607

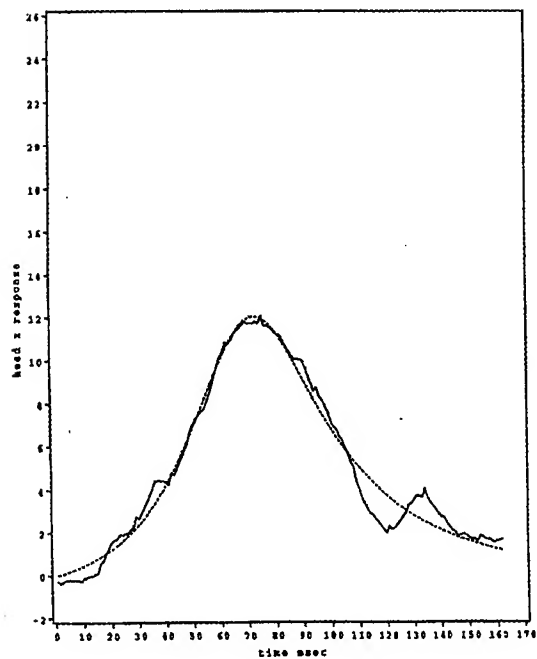


Figure 13 Simulated and Experimental Head z-acceleration for v3140

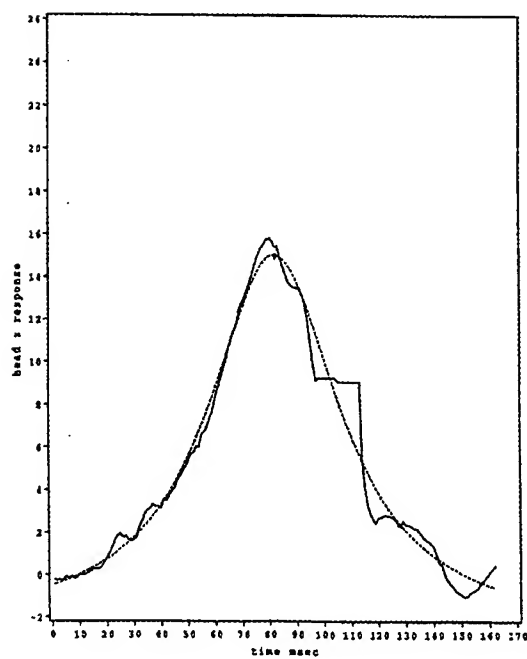


Figure 14 Simulated and Experimental Head z-acceleration for v3183

To better understand the behavior of the extended rational function model, a systematic evaluation of the model was performed. This was performed by changing a selected parameter and holding the remaining parameters constant. An increase in b_0 resulted in a parallel upward shifting of the entire response curve. An increase in b_1 resulted in mainly peak upward shifting with some upward shifting of the post maximum portion of the curve. An increase in b_2 resulted in an increase in peak and post-maximum regions of the response curve. An increase in c_1 resulted in peak upward and right shifting. An increase in c_2 resulted in peak downward and left shifting in addition to a downward shifting of the post maximum portion of the curve. The summary of the results are given in Table 1. The graphs indicating the sensitivity of different parameters of the extended rational function model are shown in Figures 15 through 19.

Table 1 Parameter Sensitivity Study for the Extended Rational Function Model

$$y = (b_0 + b_1 \cdot x + b_2 \cdot x^2) / (1 + c_1 \cdot x + c_2 \cdot x^2)$$

Parameters	Value	Response (shape change)
b_0	\uparrow (means increase)	\uparrow (parallel upward shifting)
b_1	\uparrow	\uparrow (peak upward shifting)
b_2	\uparrow	\uparrow (peak and post-max upward shifting)
c_1	\uparrow (normally negative value)	\uparrow (peak upward and right shifting)
c_2	\uparrow	\downarrow (peak downward and left shifting, post-max downward shifting)

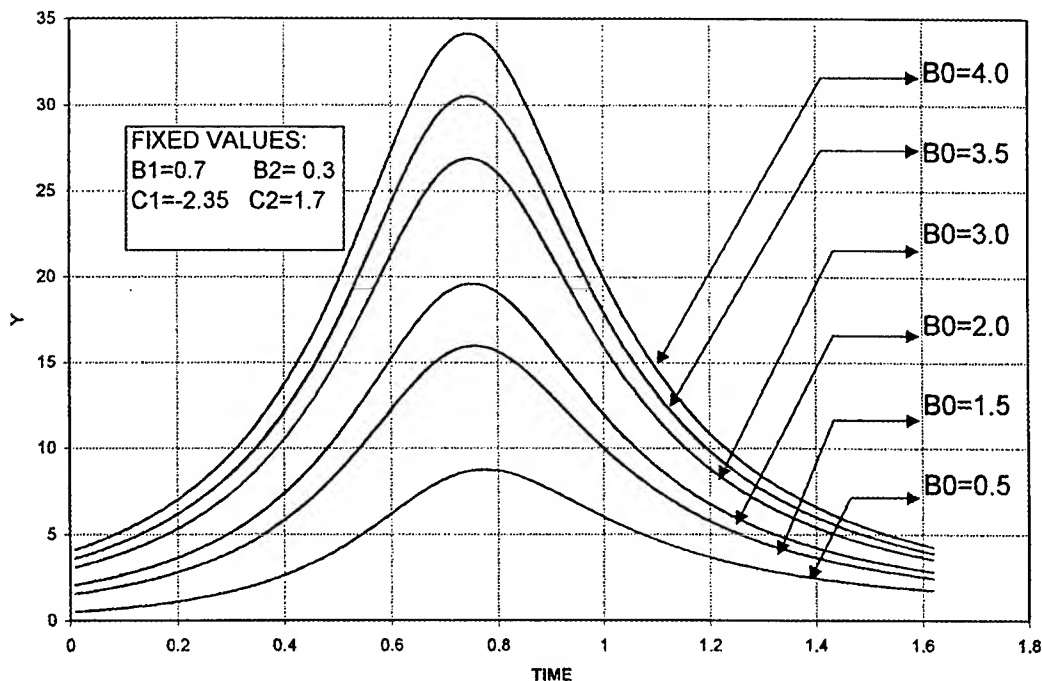


Figure 15 Sensitivity of extended rational function model to changes in b_0 .

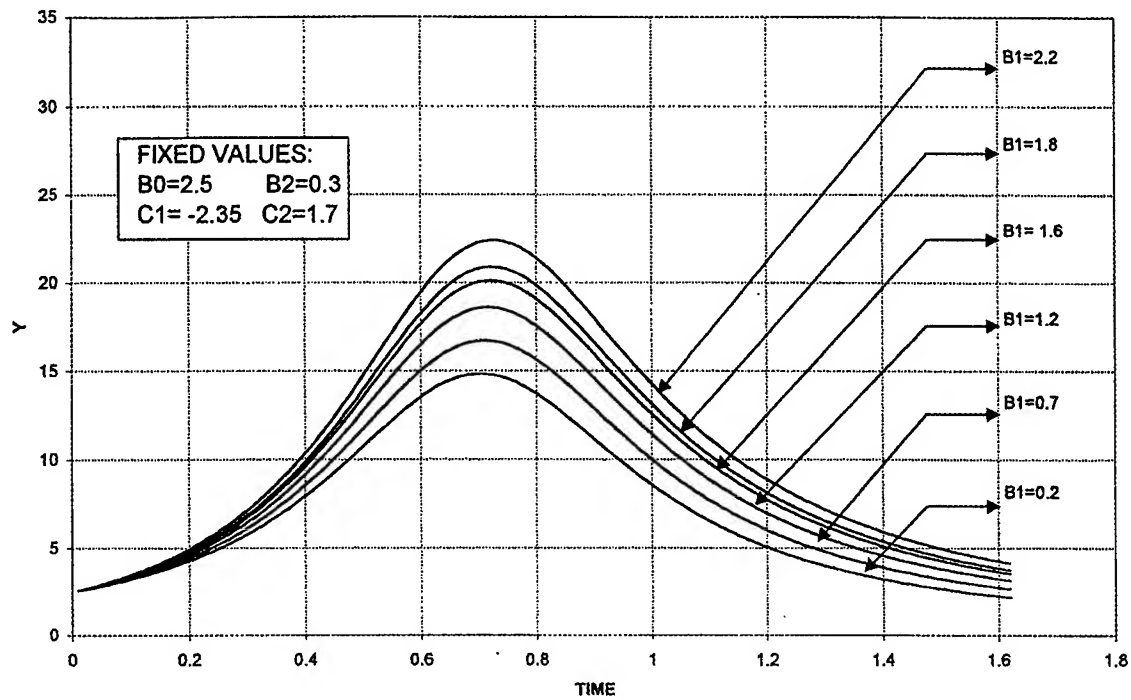


Figure 16 Sensitivity of extended rational function model to changes in b_1 .

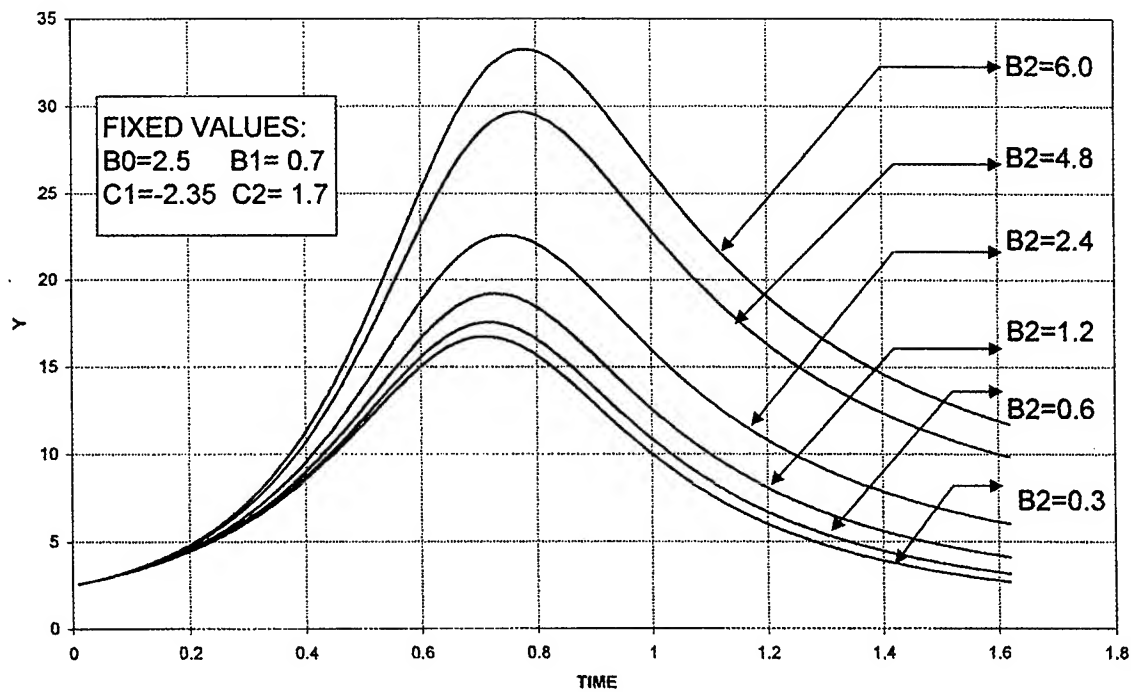


Figure 17 Sensitivity of extended rational function model to changes in b_2 .

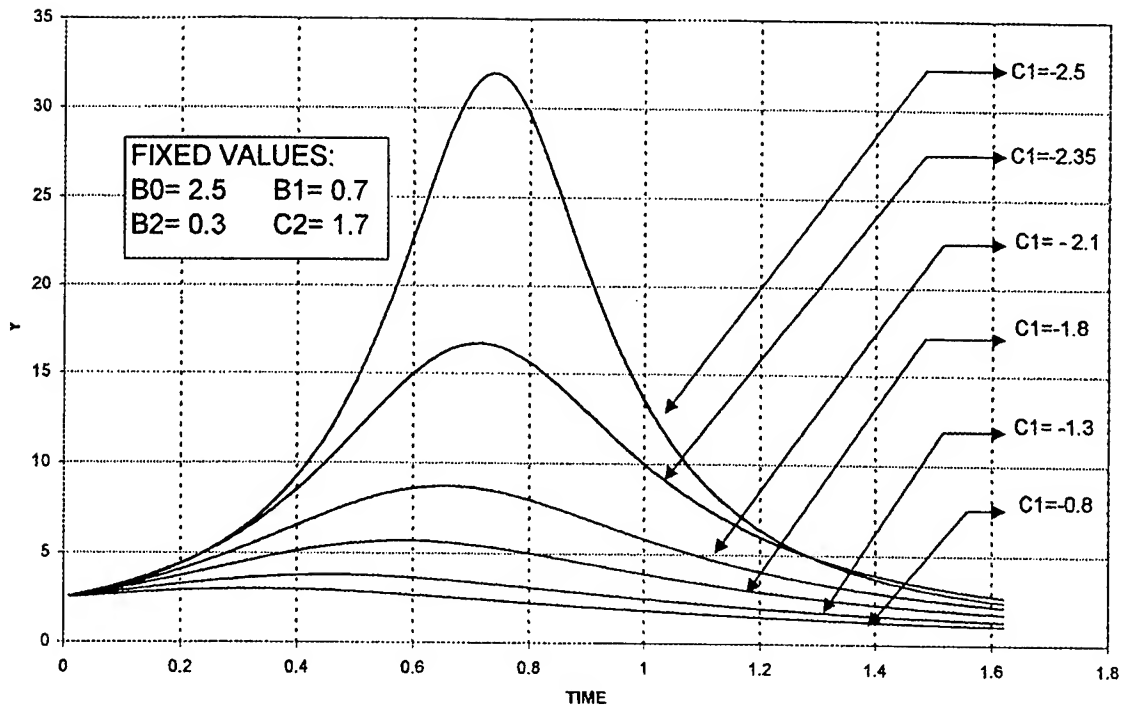


Figure 18 Sensitivity of extended rational function model to changes in c_1 .

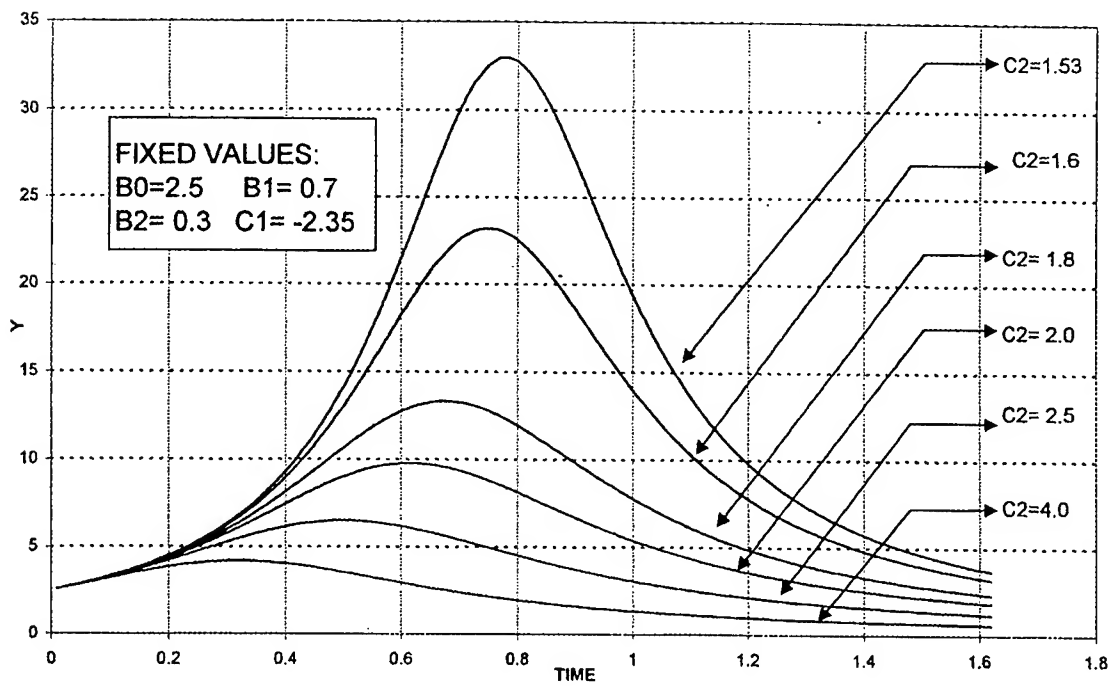


Figure 19 Sensitivity of extended rational function model to changes in c_2 .

Anthropometric parameters, helmet properties and acceleration level effect on head/neck response

Since high-speed film footage of VDT tests showed that for identical test conditions, some subjects responded with neck flexion, while others responded with neck extension, an effort was made to determine whether or not the regression model parameters could be used to determine a particular test subject's mode of head/neck response.

Clustering analyses of the extended rational function model parameters (b_0 , b_1 , b_2 , c_1 , c_2) for the x and z head acceleration data from the VCSI 199002 and VWI 199101 studies were conducted to see whether there were grouping trends. Several testing methods, such as, average linkage, Ward's method, and Cubic Clustering Criterion, etc., were evaluated. This portion of the analysis was done with JMP software [12]. Due to the broad range of anthropometric and test parameters in the study, the results of the cluster analysis do not suggest any obvious clustering tendencies, although arbitrary cluster number selection was possible.

In order to enhance the understanding of the influential parameters effecting head/neck response, the smaller FIP study was included in the investigation. About 125 observations were available for modeling. In the data sets, 27 subjects are represented, 20 subjects were involved in the 5 different helmet configuration tests. For this preliminary analysis the maximum and minimum values of the response parameters were used.

The FIP data sets include continuous variables as anthropometric variables, response variables and several categorical variables such as gender and the helmet SIW. The selected anthropometric parameters were:

1. weight
2. standing height
3. seated height
4. chest circumference
5. head breadth
6. head circumference
7. head length
8. neck circumference

The selected response parameters were:

1. head z acceleration
2. head resultant
3. head y acceleration
4. chest z acceleration
5. chest resultant

The neck calculated load was:

1. neck x force
2. neck y force

3. neck z force
4. neck x torque
5. neck y torque
6. neck z torque

An average linkage cluster analysis was carried out on the standardized anthropometric variables to help identify the homogeneous subgroups. The Ward's method on the standardized data was also carried out, but did not produce substantially different results than the average linkage analysis. The Cubic Clustering Criterion (CCC) method for identifying the number of clusters was used, but the size of the data set was not large enough to produce reliable results from the CCC. Consequently, an arbitrary number of clusters was chosen. From an engineering point of view, five clusters provided meaningful groupings.

In addition to the cluster analysis based on the anthropometric parameters, cluster analyses were also performed for:

- Maximum values of the five response variables for test cells D, E, F, G, and J
- Maximum values of the six calculated neck loads for test cells D, E, F, G, and J
- Minimum values of the five response variables for test cells D, E, F, G, and J
- Minimum values of the six calculated neck loads for test cells D, E, F, G, and J

A summary of the clustering results on are given in Table 2.

Based on the results presented in Table 2 it appears that for the FIP study, the female subjects anthropometric data is more linear than the male subjects data. This is shown by all the female subjects falling into Cluster 1. Even for a different number of clusters, the females all tend to remain in a cluster together. There are a few male subjects that also fall into the predominantly female cluster.

To minimize the number of parameters characterizing a subject's anthropometry, the principal component method was utilized. The results of the analysis showed that the first principal component accounts for 76% of the variation in anthropometry. The first and second principal components account for 86% of the variation. While the first three principal components account for 92% of the variability in anthropometry. This indicates that the several anthropometric parameters can be represented by two or three parameters (principal components) with minimal penalty.

Stepwise regressions using the mixed approach built into the JMP software on a variety of subsets of the FIP data including males alone, females alone, males in test cells D and E alone (since the helmets used in these tests had similar characteristics), females in test cells F, G and J alone, et cetera were carried out. The mixed approach

Table 2 Cluster Analysis Results for FIP Study

Analysis condition	anthropometric data (based on D cell)	Min D 5 measured	Min D neck load	Min E 5 measured	Min E neck load	Min F 5 measured	Min F neck load	Min G 5 measured	Min G neck load	Min J 5 measured	Min J neck load
cluster 1	B-16(F)	B-11	B-11	B-11	B-11	B-11	B-11	B-11	B-11	B-11	B-11
	B-17(F)	B-16(F)	B-17(F)	B-16(F)	B-18(F)	B-16(F)	B-16(F)	B-16(F)	B-17(F)	C-12	C-12
	B-18(F)	B-17(F)	C-12	B-18(F)	C-12	B-17(F)	B-17(F)	B-17(F)	B-18(F)	E-4	E-4
	B-9	B-18(F)	C-15(F)	C-12	C-15(F)	B-18(F)	B-18(F)	C-12	C-12	G-11	G-11
	C-15(F)	C-12	C-17	C-15(F)	C-17	B-9	B-9	C-17	C-17	J-10	J-10
	J-11(F)	C-15(F)	E-4	C-17	E-4	C-17	C-12	E-4	E-4	J-11(F)	J-11(F)
	J-9(F)	C-17	G-11	E-4	H-15	E-4	E-4	H-15	J-11(F)	J-7	J-7
	K-9(F)	G-11	H-15	G-11	J-10	J-7	G-11	J-11(F)	J-7	K-9(F)	M-21
	M-21	H-15	J-11(F)	H-15	J-11(F)	J-9(F)	H-15	J-7	M-21	M-30	M-30
	O-3	J-11(F)	J-7	J-11(F)	J-7	K-9(F)	J-9(F)	J-9(F)	O-3	O-3	O-3
	O-5(F)	J-7	M-21	J-7	M-21	M-21	M-21	M-21	S-20(F)	R-20(F)	R-21
	R-20(F)	J-9(F)	M-30	K-9(F)	O-3	M-30	O-3	O-3	V-3(F)	R-21	S-11
	S-20(F)	K-9(F)	O-3	M-21	R-21	O-3	O-5(F)	O-5(F)		S-20(F)	S-20(F)
	V-3(F)	M-21	R-20(F)	M-30	S-20(F)	O-5(F)	P-11	R-20(F)		V-3(F)	V-3(F)
	W-8(F)	M-30	R-21	O-3	V-3(F)	P-11	R-20(F)	R-21		W-8(F)	
		O-3	S-20(F)	P-11		R-20(F)	R-21	S-20(F)			
		P-11	V-3(F)	R-21		R-21	S-11	V-3(F)			
		R-20(F)		S-11		S-11	S-20(F)	W-8(F)			
		R-21		S-20(F)		V-3(F)	V-3(F)				
		S-20(F)		V-3(F)		W-8(F)	W-8(F)				
		W-8(F)									
cluster 2	B-11	B-9	B-18(F)	B-17(F)	B-16(F)	H-15	C-17	P-11	B-16(F)	M-21	B-16(F)
	E-4	O-5(F)	J-10	J-9(F)	B-17(F)	J-10	J-10	S-11	J-10	S-11	K-9(F)
	R-21		K-9(F)		G-11	S-20(F)	J-11(F)		J-9(F)		R-20(F)
	S-11		P-11		J-9(F)				K-9(F)		
			W-8(F)		P-11				O-5(F)		
cluster 3	G-11	E-4	B-9	B-9	K-9(F)	C-12	K-9(F)	J-10	G-11	B-17(F)	B-17(F)
	H-15	V-3(F)	J-9(F)	O-5(F)	M-30			M-30	P-11		
	J-10		S-11	W-8(F)	R-20(F)				S-11		
	P-11										
cluster 4	C-12	S-11	B-16(F)	R-20(F)	O-5(F)	J-11(F)	J-7	B-18(F)	H-15	B-16(F)	W-8(F)
	C-17				W-8(F)			G-11	R-21		
	J-7										
cluster 5	M-30	J-10	O-5(F)	J-10	B-9	G-11	M-30	K-9(F)	M-30	P-11	P-11
	PC1	0.76372	0.30102	0.57508	0.33652	0.51385	0.31246	0.38479	0.31343	0.49833	0.71854
	PC2	0.85356	0.58312	0.76333	0.59161	0.75288	0.56407	0.63522	0.5783	0.66241	0.89285
	PC3	0.91846	0.80937	0.88433	0.76196	0.89124	0.78741	0.79512	0.76888	0.81406	0.95246

Table 2 (Part 2) Cluster Analysis Results for FIP Study

Analysis condition	anthropo- metric data (based on D cell)	Max D 5 measured	Max D neck load	Max E 5 measured	Max E neck load	Max F 5 measured	Max F neck load	Max G 5 measured	Max G neck load	Max J 5 measured	Max J neck load
cluster 1	B-16(F)	B-11	B-11	B-11	B-11	B-11	B-16(F)	B-11	B-11	B-11	B-11
	B-17(F)	B-16(F)	B-17(F)	B-16(F)	B-16(F)	B-16(F)	B-18(F)	B-16(F)	B-16(F)	B-16(F)	E-4
	B-18(F)	B-17(F)	B-18(F)	B-17(F)	B-18(F)	B-17(F)	C-12	B-17(F)	B-17(F)	B-17(F)	J-11(F)
	B-9	C-15(F)	C-15(F)	C-15(F)	J-11(F)	B-18(F)	C-17	C-17	B-18(F)	E-4	J-7
	C-15(F)	C-17	C-17	C-17	K-9(F)	B-9	G-11	E-4	C-12	G-11	K-9(F)
	J-11(F)	E-4	H-15	E-4	M-30	C-17	P-11	H-15	C-17	J-10	O-3
	J-9(F)	G-11	J-11(F)	G-11	R-20(F)	E-4	R-21	J-11(F)	E-4	J-7	R-20(F)
	K-9(F)	H-15	J-9(F)	H-15	S-11	G-11		K-9(F)	G-11	M-21	V-3(F)
	M-21	J-10	K-9(F)	J-10		H-15		P-11	J-11(F)	M-30	
	O-3	J-11(F)	M-21	J-7		J-7		R-20(F)	J-7	P-11	
	O-5(F)	J-7	M-30	K-9(F)		J-9(F)		R-21	J-9(F)	S-11	
	R-20(F)	K-9(F)	R-21	R-20(F)		K-9(F)		S-11	K-9(F)	S-20(F)	
	S-20(F)	P-11	S-20(F)	S-11		M-21		S-20(F)	M-21	W-8(F)	
	V-3(F)	R-20(F)	V-3(F)	S-20(F)		M-30		W-8(F)	O-3		
	W-8(F)	R-21	W-8(F)	W-8(F)		O-5(F)			R-20(F)		
		S-20(F)				P-11			S-11		
		V-3(F)				R-20(F)			S-20(F)		
		W-8(F)				R-21			V-3(F)		
						S-11			W-8(F)		
						S-20(F)					
						V-3(F)					
						W-8(F)					
cluster 2	B-11	B-18(F)	C-12	B-18(F)	B-17(F)	J-10	B-11	B-18(F)	J-10	K-9(F)	B-16(F)
	E-4	C-12	E-4	C-12	C-12		B-17(F)	C-12	M-30	R-20(F)	B-17(F)
	R-21	M-21	J-7	M-21	C-17		E-4	M-21		V-3(F)	J-10
	S-11	M-30	P-11	M-30	E-4		J-7	O-5(F)			M-21
				P-11	G-11		R-20(F)				M-30
				R-21	H-15		V-3(F)				W-8(F)
					J-7		W-8(F)				
					O-3						
					P-11						
					R-21						
cluster 3	G-11	B-9	B-9	B-9	B-9	C-12	B-9	G-11	P-11	J-11(F)	C-12
	H-15	J-9(F)	G-11	J-9(F)	C-15(F)		J-11(F)	J-7	R-21	O-3	R-21
	J-10	S-11	O-3		J-9(F)		J-9(F)	J-9(F)			S-11
	P-11				M-21		K-9(F)				S-20(F)
cluster 4					W-8(F)		M-21				
	C-12	O-5(F)	B-16(F)	J-11(F)	O-5(F)	O-3	H-15	J-10	H-15	R-21	G-11
	C-17		J-10	O-3			J-10	O-3			
	J-7		R-20(F)	V-3(F)			M-30	V-3(F)			
			S-11				O-3				
							S-11				
cluster 5							S-20(F)				
PC1	0.76372	0.61475	0.45922	0.56212	0.40804	0.6405	0.50552	0.41261	0.5832	0.57755	0.5968
PC2	0.85356	0.86159	0.64577	0.836	0.70227	0.83369	0.70603	0.81693	0.76	0.8271	0.79828
PC3	0.91846	0.99736	0.81453	0.99568	0.84009	0.99705	0.86362	0.99253	0.8912	0.99457	0.89805

alternates the forward and backward selection methods in the regression. It first includes all variables that meet the probability to enter the model, then removes all terms that meet the probability for removal (.25 is the default used in both cases). It then switches back to forward selection and adds variables again if needed. The intent was to model all of the data at one time and incorporate terms such as gender and helmet properties into the model, however, the relatively small number of observations available for modeling prevents this from being an effective strategy. One can incorporate gender as a dummy variable and test its effect on the intercept for the model using only one degree of freedom, but attempts to check gender's affect on the "slope" parameter estimates requires one additional degree of freedom for each of the other explanatory variables. This quickly uses up the available degrees of freedom and is really not feasible to run in a consistent fashion. Incorporating the helmet properties used in the model is even more vexing since there are five different helmets used in the tests rather than just two levels as seen with gender. The results of a stepwise regression of the head z-acceleration data are shown in Table 3. The highest R-square value for the performed tests was only 55%, indicating a need for more data to be used in the analysis or to perform stepwise regression analysis for individual parameters. Using the individual stepwise regression analysis with the subsets of data as described above, in some cases the R-square values reached 88% as indicated in Table 4.

Based on the results from the stepwise regression analysis, on average, sitting height, head length, chest circumference and body weight are the most significant parameters influencing the head/neck response.

Table 3 Stepwise Regression using the Mixed Approach for the FIP Study

Runs	R square (including 9 variables)	R square after stepwise selection. The significant level : 0.15	R square (including 3 principal components)
D cell head z (max)	0.5514	0.4271 (sitht, headlen chestcir, weight)	0.1708
E cell head z (max)	0.4245	0.2731(sitht, headcir)	0.1199
F cell head z (max)	0.4041	no	0.0295
G cell head z (max)	0.1833	no	0.0124
J cell head z (max)	0.4546	0.3913(weight)	0.3319
D cell head z (min)	0.3424	no	0.0840

Table 4 provides the predictive regression equations for all of the extended rational function model parameters for head z-acceleration based on the evaluation of the entire response curves from test cells D, E, F, and G (Note that the nominal acceleration for these test cells was 10 G). Only headz-acceleration was used in the analysis since it showed more consistent trend than the head x-acceleration. Due to the limited number of observations, the independent variables used to generate the predictive regression equations were: height, sitting height (sitht), weight, chest circumference (chestcir), head breadth (headb), head circumference (headcir), head length (headl), and neck circumference (neckcir). The results from the analysis could be used to predict a particular subjects head

z-acceleration based on selected anthropometric parameters. The regression equations still can not be recommended for predictions, further refinement in regression parameters must be performed.

Table 4 Individual Stepwise Regression for the FIP Study

Responses	In-variables	R ²	adjust R ²	Regression equations
head z (also include J cell)	headb, headcir, headl	0.25	0.20	* R ² is too low
b0	headb, headcir, weight, headl, neckcir, sitht	0.627	0.56	b0 = -4.3221 + 0.0066*sitht - 0.0172 * weight - 0.0738 * headb + 0.0324 * headcir - 0.0559 * headl + 0.0139 * neckcir
b1	headb, headcir, headl	0.713	0.689	b1 = 6.2192 + 0.4736 * headb - 0.2098 * headcir + 0.2243 * headl
b2	headb, headl, headcir, neckcir, height, sitht	0.81	0.77	b2 = 47.5183 - 0.0264 * height + 0.0149 * sitht - 0.3644 * headb + 0.1165 * headcir - 0.2589 * headl + 0.0631 * neckcir
c1	headb, headl, headcir, neckcir, height, sitht, chestcir	0.88	0.85	c1 = -7.5391 + 0.0032 * height - 0.0021 * sitht - 0.0009 * chestcir + 0.0494 * headb - 0.0166 * headcir + 0.0365 * headl - 0.0077 * neckcir
c2	headb, headl, height, headcir, sitht, weight	0.85	0.81	c2 = 9.2335 - 0.0055 * height + 0.0048 * sitht + 0.0084 * weight - 0.0524 * headb + 0.0161 * headcir - 0.0352 * headl

The next step of the analysis included the mode of head/neck response as an additional exploratory variable as described in the author's 1997 Summer Faculty Research Report [13]. Sample ANOVA results using traditional split-plot analysis are given in Table 5. In some cases, mode appears to be significant but also causes helmet type to become non-significant. Additional stepwise regression analysis was performed where the mode of response was the grouping parameter. The partial ANOVA results for stepwise regression by mode are shown in Table 6. In Table 6, the variables in parenthesis are the significant parameters. Based on this analysis, it also can be concluded that Modes 1 and 2 tend to cluster, and Modes 3 and 4 also tend to cluster. This is expected since Modes 1 and 2 are flexion responses while Modes 3 and 4 are extension responses.

Table 5 ANOVA Results for Traditional Split-Plot Analysis

Response	Excluded mode (significant level 0.05)	Included mode (significant level 0.05)
head z(max)	no	no
b0	gender	gender
b1	gender, SIW(helmet)	gender, mode
b2	gender (0.0541), SIW(helmet)	gender, mode
c1, c2	no	no

Table 6 ANOVA Results for Stepwise Regression by Mode of Response

Response	Mode 1 R square	Mode 2 R square	Mode 3 R square	Mode 4 R square	Mode 5 R square
head z	no	0.2293 (sitht, neckcir)	0.6230 (headb, headcir)	no	0.4339 (sitht, neckcir)
b0	no	0.4206 (chestcir)	0.7504 (headb, headcir, height)	0.1284 (chestcir)	no
b1	no	0.3930 (chestcir)	0.9052 (headb, headcir, weight)	no	0.1605 (chestcir)
b2	0.7088 (height, sitht)	0.2723 (height)	0.8555 (headb, headcir)	0.1245 (headb)	no
c1	0.9154 (height, headb, headcir, sitht)	0.0752 (sitht)	0.7655 (headb, headl)	0.8056 (sitht, headb, height, headcir)	no
c2	0.8259 (height, headb, neckcir)	no	0.6974 (headb, neckcir)	0.8073 (sitht, neckcir, headcir, headb)	no

Finally, the Friedman's test (a type of non-parametric ANOVA) was carried out attempting to determine the importance of helmet type on each of the nonlinear parameters. In this case, the responses of an individual to each of the helmet types are ranked within that individual (this method allows to incorporate individual as a blocking factor in the model). The effects of helmet are determined using the sums of the rank for each helmet type. For some of the nonlinear parameters, it can be shown that after accounting for the effect of the subject, helmet properties are significant as given in Table 7. A non-parametric multiple comparisons test can be used subsequently to differentiate helmet types. However, before meaningful results can be obtained, increase in data set size is necessary.

Despite the fact that over 600 Vertical Drop Tower (VDT) tests from two studies, VWI (199101), VCSI(199002), and FIP study were used in a statistical analysis, the results were inconclusive. This was due to the variability in the test data. One of the significant sources of the variability came from the subjects modes of response. To continue with the overall research investigation, identification of the modes of head/neck response had to be performed.

Table 7 Friedman Two-Way Analysis of Variance by Ranks

Response	Rank		Friendchp
	set:	sum:	
headz	1 (Cell D) 2 (Cell E) 3 (Cell F) 4 (Cell G) 5 (Cell J)	54.0 72.0 48.0 50.0 61.0	0.0916
b0	1 2 3 4	60.0 47.0 58.0 65.0	0.2111
b1	1 2 3 4	59.0 70.0 54.0 47.0	0.0621
b2	1 2 3 4	54.0 43.0 62.0 71.0	0.0113 (note: it shows that helmet is significantly affect b2)
c1	1 2 3 4	54.5 59.0 60.0 56.5	0.9227
c2	1 2 3 4	64.0 55.0 56.0 55.0	0.6853

research program are summarized in Table 9. The results of this investigation including the description of five modes of head/neck response are defined in the final report from the author's Summer Faculty Research Program submitted to RDL[13].

"The first two modes, Modes A and B, represent forward neck and forward head rotation. Mode A differs from Mode B by the relative angular velocity of the neck in comparison to the head. Mode A has greater initial neck angular velocity than head angular velocity, while Mode B has greater initial head angular velocity than neck angular velocity. The second two modes, Modes C and D, represent forward neck rotation and rearward head rotation. Mode C differs from Mode D by the relative angular velocity of the neck in comparison to the head. Mode C has greater initial neck angular velocity than head angular velocity. Mode D has greater initial head angular velocity than neck angular velocity. Mode E of head/neck response has no significant head or neck rotation. "

The schematic diagrams for Modes A, B, C and D are given in Figure 20. Three categories of parameters have been identified and suggested to be the determining factors in a given subject's mode of response for a given condition. The categories include initial position, anthropometry, and other factors such as helmet weight, helmet center of gravity location and impact acceleration level. When Table 1 is completed, it will allow one to predict how a given subject will respond to a given vertical impact condition. With this table, one can also classify the modes of response for the existing VDT tests. This information can be used to study several different areas of interest such as:

- a) Frequency of response mode
- b) Gender differences
- c) Effect of helmet configurations on head/neck response

To use the developed method as a predictive tool, one must determine the magnitude of the values of each parameter in the three categories identified as influential factors in determining head/neck response including initial position, anthropometry, and other factors such as helmet, weight, helmet center of gravity location and impact acceleration level.

In order to utilize the above procedure for prediction purposes, one must assess the effect of initial body position for different impact acceleration levels on modes of head/neck response to vertical impact, to establish a procedure to determine the initial head and neck position, to determine the initial position for selected VDT test, to determine the statistical significance of initial head and neck positions on modes of response, to complete the characterization and method of prediction of head/neck response to vertical impact, to apply the developed procedure to other VDT studies carried out for different impact acceleration levels, to assess the influence of impact acceleration level on head/neck response, and to assess the accuracy of the prediction method.

Table 9 Modes of Head/Neck Response for Vertical Impact.

		MODES				
		A	B	C	D	E
RESPONSE	Neck Rotation (β)	forward	forward	forward	forward	none
	Head Rotation (γ)	forward	forward	back	back	none
	Condition	$\omega_\beta > \omega_\gamma$	$\omega_\beta < \omega_\gamma$	$\omega_\beta > \omega_\gamma$	$\omega_\beta < \omega_\gamma$	none
DIAGNOSTIC PARAMETERS	X - Acceleration <i>(Initial at mouthpiece)</i>	+	-	+	-	0
	Head Pitch <i>(Mouthpiece wrt shoulder)</i>	- ($>10^\circ$)	- (3° - 10°)	+	+	0
CATEGORY 1 <i>(Initial Position)</i>	Neck Pitch	*	*	*	*	*
	Head Pitch	*	*	*	*	*
CATEGORY 2 <i>(Anthropometry)</i>	Sitting Height (mm)	*	*	*	*	*
	Head Length (mm)	*	*	*	*	*
	Chest Circ. (mm)	*	*	*	*	*
	Weight (kg)	*	*	*	*	*
CATEGORY 3 <i>(Other Factors)</i>	Helmet Weight (kg)	*	*	*	*	*
	Helmet C. G.	*	*	*	*	*
	Acceleration Level (G)	*	*	*	*	*

Φ_β = angular velocity of the neck

Φ_γ = angular velocity of the head

* Indicates the values not available at this time. Values to be determined in the follow up research.

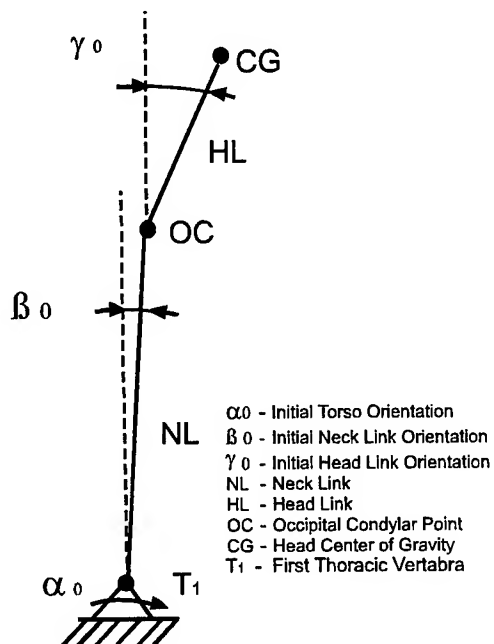


Figure 20. Two-pivot linkage mechanism representing head/neck structure.

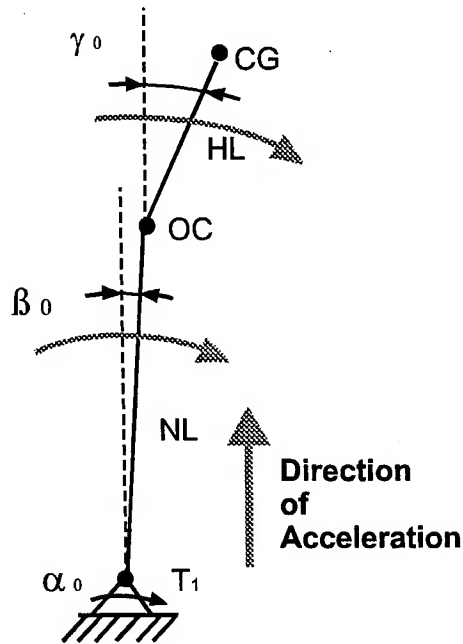


Figure 21. Schematic diagram showing direction of head/neck rotation for Modes A and B.

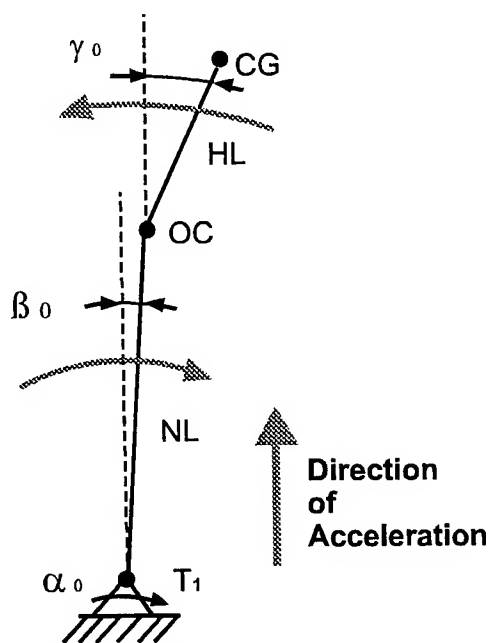


Figure 22. Schematic diagram showing direction of head/neck rotation for Modes C and D.

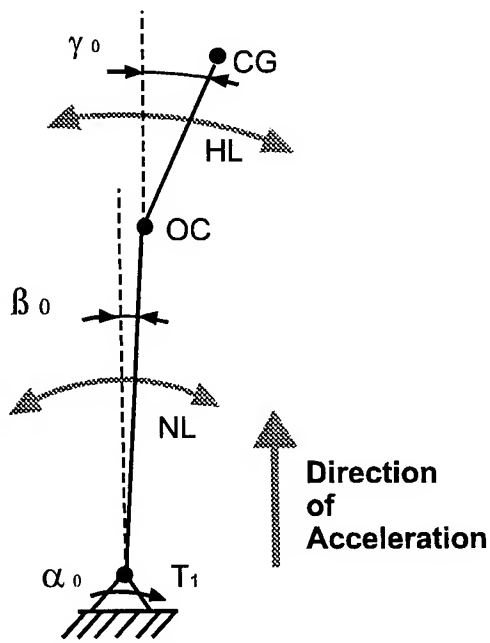


Figure 23. Schematic diagram showing direction of head/neck rotation for Mode E.

Conclusions

1. Utilized statistical methodology including regression model fitting, cluster analysis and principal component analysis, is adequate for the test data.
2. Broad range of physical characteristics represented by the individuals in the study combined with the relatively small number of individuals available for modeling necessitates more data to be included in the study and to identify more uniform subgroups of individuals within the data set that could effectively be modeled using regression and provide reliable results in a follow-up analysis.
3. The head acceleration in the x and z-direction follows a non-linear five parameter extended rational function model of a form $y = (b_0 + b_1 \bullet x + b_2 \bullet x^2) / (1 + c_1 \bullet x + c_2 \bullet x^2)$.
4. Female subjects anthropometric data fall into one cluster, there are a few male subjects as well, that also fall into the predominantly female cluster.
5. Based on the results from the stepwise regression analysis, on average, sitting height, head length, chest circumference and body weight are the most significant parameters influencing the head/neck response.
6. Regression equations for estimation of parameters to be used with the extended rational function non-linear model for head z-acceleration have been defined. The regression equations still can not be recommended for predictions, further refinement in regression parameters must be performed.
7. The fifteen selected anthropometric parameters can be successfully reduced to three principal components while maintaining 92% of the variability in anthropometry.
8. Gender and mode of head/neck response are significant variables in determining the mathematical model representing the head/neck response.
9. The results of the clustering analysis for different test cell maximum and minimum response values were not consistent. Each test cell has its own grouping pattern, which indicates that the subjects anthropometry itself does not dominate the response output. Other factors as body position, level of acceleration, helmet properties are influential parameters.

Reference

1. H. J. Mertz and L. M. Patrick, "Strength and Response of the Human Neck." SAE Paper No. 710855, Fifteenth Stapp Car Crash Conference, Nov. 17-19, 1971, Coronado, CA.
2. Perry, C. E., J. R. Buhrman, and F.S. Knox III, "The Effect of Head Mounted Mass on Males and Females Under +Gz Impact Acceleration, " Aviation, Space, and Environmental Medicine (ASEMCG 69 {5}:216), Presentation at Annual AsMA Meeting, May 1997.
3. Cheng, H., Obergefell, L., Rizer, A. "Generator of Body Data (GEBOD) Manual", AL/CF-TR-1994-0051, Air Force Materiel Command, Wright-Patterson Air Force Base, OH.
4. Neter, Wasserman, Kutner *Applied Linear Regression Models*. Richard D. Irwin, Inc.; 1983.
5. Draper and Smith. *Applied Regression Analysis*. 2nd ed. New York: John Wiley & Sons, 1981.
6. "SAS User's Guide", SAS Institute, Statistical Analysis System, 1982.

7. Ratkowsky, David, "Handbook of Nonlinear Regression Models," Marcel Dekker, Inc., 1990.
8. Johnson and Wichern. *Applied Multivariate Statistical Analysis*. 2nd ed. Prentice Hall, 1988.
9. Anderberg. *Handbook of Mathematical Functions*, U.S. Dept. Of Commerce, National Bureau of Standards Applied Mathematical Series. 55, 1964.
10. Gnanadesikan. *Methods for Statistical Data Analysis of Multivariate Observations*, New York: John Wiley, 1977.
11. Hartigan. *Clustering Algorithms*, New York: John Wiley, 1975.
12. "JMP Statistics and Graphics Guide", SAS Institute, Cary, North Carolina, 1994.
13. Ziejewski, M., "Modes of Human Head/Neck Response to Vertical Impact," Final Report for Summer Faculty Research Program, Office of Scientific Research, 1997.

EFFECTS OF DYNAMIC MAGNETIC TREATMENT ON
CALCIUM CARBONATE BEARING WATERS

Kevin M. Lambert
Graduate Student
Department of Civil and Environmental Engineering, 368 CB

Brigham Young University
Provo, UT 84602

Final Report for:
Summer Research Extension Program

Sponsored by:
Air Force Office of Scientific Research
Bolling Air Force Base, DC

and

Air Force Research Laboratory
Materials and Manufacturing Directorate
Airbase and Environmental Technology Branch
Tyndall Air Force Base, FL

and

Brigham Young University

March 1998

EFFECTS OF DYNAMIC MAGNETIC TREATMENT ON CALCIUM CARBONATE BEARING WATERS

Kevin M. Lambert
Graduate Student
Department of Civil and Environmental Engineering
Brigham Young University

Abstract

The magnetic treatment of water to reduce scale formation in industrial heat transfer equipment has been both supported and shown to have no effect in both field trials and laboratory studies. More recent laboratory research has shown many promising results for proven effects on magnetic treatment on calcium carbonate crystals and other effects. If the effective area of applicability, if indeed it is proven, can be defined, then this technology would yield significant economic and environmental benefits.

The research reported here summarizes the design and operation of a test system to produce calcium carbonate crystals for analysis after treatment with or without magnetic fields applied. Aqueous sampling was also performed. System test parameters varied during testing include water temperature, flow rate, test duration, magnetic exposure and the number of devices attached. Solid crystal residue was examined by XRD for relative proportions of calcite and aragonite. Filter residue was also examined by XRF for the presence of transition metals and elements known to substitute for calcium in known carbonate scale formers. Aqueous samples were tested for water chemistry, zeta potential of charged particles and by flame ionization AA for iron concentrations.

The percent of calcite in the sample residues showed very little change relative to the estimated error of the method, and the change was not consistent with any one system test parameter. Visual examination of filter residues did show effects of magnetic treatment versus non-magnetic treatment for certain test parameters. XRF analysis showed a consistent decreasing trend in iron content in the solid filter residue with increasing number of magnetic devices attached. The results for the zeta potential measurements are somewhat mixed, but imply there may be a consistent change with the number of magnets installed. One set of test data will need to be regenerated as the original samples were destroyed during concentration for AA analysis. Recommendations are given for further investigation.

EFFECTS OF DYNAMIC MAGNETIC TREATMENT ON CALCIUM CARBONATE BEARING WATERS

Kevin M. Lambert

1.0 INTRODUCTION

While chemical additives usually control the scaling of heat transfer surfaces, this imposes significant costs and maintenance. Where the chemicals do not completely solve the problem, acid cleaning, physical scraping or replacement of equipment is required; at additional financial and environmental costs and logistical support. A number of benefits accrue from the non-chemical suppression of scaling: decreased chemical purchasing, handling, use and disposal; reduced energy consumption due to scale-free heat transfer surfaces; lower labor requirements to perform chemical-based prevention and cleaning treatment; lower atmospheric emissions due to lower fuel consumption; reduced water use due to lowered system drainage requirements to remove scale-forming constituents; and extended service lifetimes of equipment. These environmental and economic benefits are not reliably predicted because the factors determining success or failure of non-chemical means such as magnetic treatment have either not been identified or are poorly defined.

A small sampling of the literature on the subject shows examples of successful field applications (MacGarva, 1993; Simpson, 1980; Raisen 1984) and measured effects due to magnetic treatment in the laboratory (Duncan, 1995; Busch and Busch, 1996). Other researchers have shown no effect or inconclusive evidence for the commercial magnetic devices tested (Lawrence, 1984; Limpert and Raber, 1985; Hasson and Bramson, 1985). For a larger discussion of the literature see Baker and Judd (1996) and Lambert (1998). Broad conclusions that may be drawn from reading a lot of the literature is that it is probable that the commercial devices do not work equally well and that there may be numerous situations where none will work due to inappropriate conditions for use. This is no different than looking at the success of other processes or equipment where improperly applied. Several problems exist with the use of magnetic treatment devices (MTDs) for anti-scale magnetic treatment (AMT) including lack of: successful replication of many experiments, good field trial controls, definitive causal mechanisms and clear cut success in all claimed applications. However, there is sufficient evidence that there are well defined changes in laboratory experiments and successful applications to merit further research. The second international symposium held in England in 1996 addressed principally by university researchers is ample evidence of the respectable attention afforded the subject by some in the international community.

2.0 PROBLEM DEFINITION

The two goals of the present research were: 1) demonstrating measurable changes in water or crystal parameters potentially tied to hard water scaling and the use of MTDs; 2) conducting testing and analysis to define selection of probable mechanisms or further areas of research. This was a rather broad approach. These goals were supported by objectives focusing on changes in two measurement criteria: 1) the relative proportion of calcite and aragonite (chemically identical forms of calcium carbonate, but different polymorphic crystalline forms - also called crystal habit) and 2) changes in the zeta potential (a measure of surface potential). The change in zeta potential (which affects colloid coagulation) was to be backed up with particle size distribution measurements to look for verification of colloid agglomeration. These objectives required completion of three major tasks: 1) design and construction of a test system that would mimic a circulatory system passing CaCO_3 laden water through MTDs, allowing for aqueous and crystalline sampling, 2) selection of the evaluation criteria, technologies and analytical approach and 3) development of sample preparation techniques. To look for changes in the noted measurement criteria seven factors were selected for examination. These factors were selected based on both an extensive literature review and consideration of the test capabilities. These seven factors are briefly described below.

- 1) Number of magnets - This impacts the number (or total time) of magnetic exposures that the circulating solution is exposed to.
- 2) Water temperature - This factor significantly impacts chemical solubility, reaction rates and crystal initiation and growth.
- 3) Calcium carbonate concentration at initial mixing time - The saturation level of CaCO_3 in the tested solution has been implicated by a number of researchers as to whether any positive results are seen or not. It is generally believed that the solution must be supersaturated in CaCO_3 .
- 4) Total circulating test time prior to sampling - This affects the total exposure time to the magnetic field.
- 5) Pumping rate - This factor affects the solution flow velocity which several researchers have implied as having an impact on the magnetic effect. The flow velocity potentially comes into play in two different areas: a) the Lorentz force on charged particles flowing through a magnetic field is proportional to the particle velocity, b) the flow regime (ie. laminar vs. turbulent) may have an impact on crystal nucleation in bulk solution and on solid surfaces.

- 6) Time between removal of the magnetic field and sampling - This factor may confirm what some researchers (Higashitani, 1996) call the memory effect" which shows that the measured impact persists some time after removal of the magnetic field.
- 7) Iron concentration - The iron concentration certainly may help explain why a magnetic field impacts MTD testing and why there is a difference in test results between natural waters (frequently containing moderate to low levels of iron) and pure waters containing little or no iron.

A few significant occurrences during test system operation modified some of the above factor manipulations during testing. Originally, lab filtered pure water (16 M Ω -cm resistivity) was to be used with appropriate amounts of CaCO₃ and iron added. System tests were run with this water but great difficulty was experienced in getting reliable zeta potential readings and producing sufficient residue for crystal examination. Examination of several different source waters with CaCO₃ added led to the use of tap water.

The original intent was to test using pump rates that allowed for laminar as well as mixed or turbulent flow. Unsteady operation at higher flow rates and pump freeze ups at low rates prevented system testing beyond a fairly narrow range - limiting the usefulness of this factor for interpretative purposes.

Fairly low concentrations of iron are known to greatly affect CaCO₃ crystal nucleation (Meyer, 1984). To look at the effect of iron it was decided to look at iron accumulation in the solid residue filtered from solution. It was anticipated that if the iron in the solid samples could be shown to significantly change in a consistent pattern tied to AMT application then this would point a direction for plausible mechanism development and further research.

The selection of the measurement criteria were based on reported changes in zeta potential and particle sizes (Parsons, et. al., 1997; Busch and Busch, 1996) or in the crystal habit (Deren, 1985; Donaldson and Grimes, 1988) among others.

3.0 DESIGN OF TEST SYSTEM

A test system to perform the desired functions was designed to meet the following requirements:

- a) Allow equilibration of CaCO₃ in solution at different concentrations.
- b) Allow heating of the solution to 105° F and maintaining a relatively constant temperature during the test. 105° F was suggested to represent average cooling tower temperatures. A heat exchanger with removeable pipe sections was beyond the scope of the current project

- c) Allow flow rate variation from laminar to mixed laminar/turbulent flow through the piping system.
- d) Include temperature, pressure and flow measurement and control.
- e) Allow pH measurement and aqueous sampling for alkalinity, hardness and Zeta-Meter measurements.
- f) Physical scale and construction to simulate a piping circulatory system.
- g) Include the ability to capture CaCO_3 crystals in the size range of 2 μm up to about 35 μm (the expected size range estimated from the literature) from the solution stream without plugging the line during tests.
- h) Have multiple, identical systems to allow side by side testing of parameters.
- i) No continuous water-metal contact was to be allowed in the entire system. This was to prevent the possibility of contamination with common metals used in piping system components: iron, copper, zinc.
- j) The pump should not risk crushing agglomerated crystal groups circulating through the system..
- k) The system should be a recirculating system, mimicking cooling tower recirculation.
- l) Pressure fluctuations should be kept to a minimum (desired to be less than four psi).
- m) Provide flow split flexibility between the main pipe line and the bypass tubing line.

Non-technical requirements also had major impacts on the design:

- 1) Budgeted costs. The entire system was designed and parts ordered prior to submittal of the final proposals for research grants. Additional funds availability was in no way certain at design and ordering time. The original budget was far more limited. The biggest impact the original equipment budget had on system design and operation was the elimination of automatic controls, principally for temperature control.
- 2) Timing of equipment orders. The original orders were placed prior to returning to the University where location and equipment questions had yet to be fully resolved, requiring additional design flexibility.
- 3) Regulations governing which companies could be ordered from and whether a specific item was currently in stock (and therefore could be ordered) affected many component decisions and in a few cases forced design changes to allow for available components.

Design specifics and drawings can be found in the author's thesis (Lambert, 1998). A schematic of the test system is illustrated in Figure 1 while photographs of the test systems are reproduced in Figures 2 and 3. The arrangement of the magnets in the commercial device and how they are mounted to the pipe is illustrated in Figure 4. The south poles of the magnet are oriented radially inward. Sets of magnetic devices were spaced about one half inch apart when multiple sets were installed. According to some manufacturers, the particular arrangement of the magnets, and their spacing can be important. The research literature does distinguish between externally mounted magnets and in-line (internally mounted) magnets. The internally mounted magnets influence flow properties locally and in some cases affect the release of iron to the water.

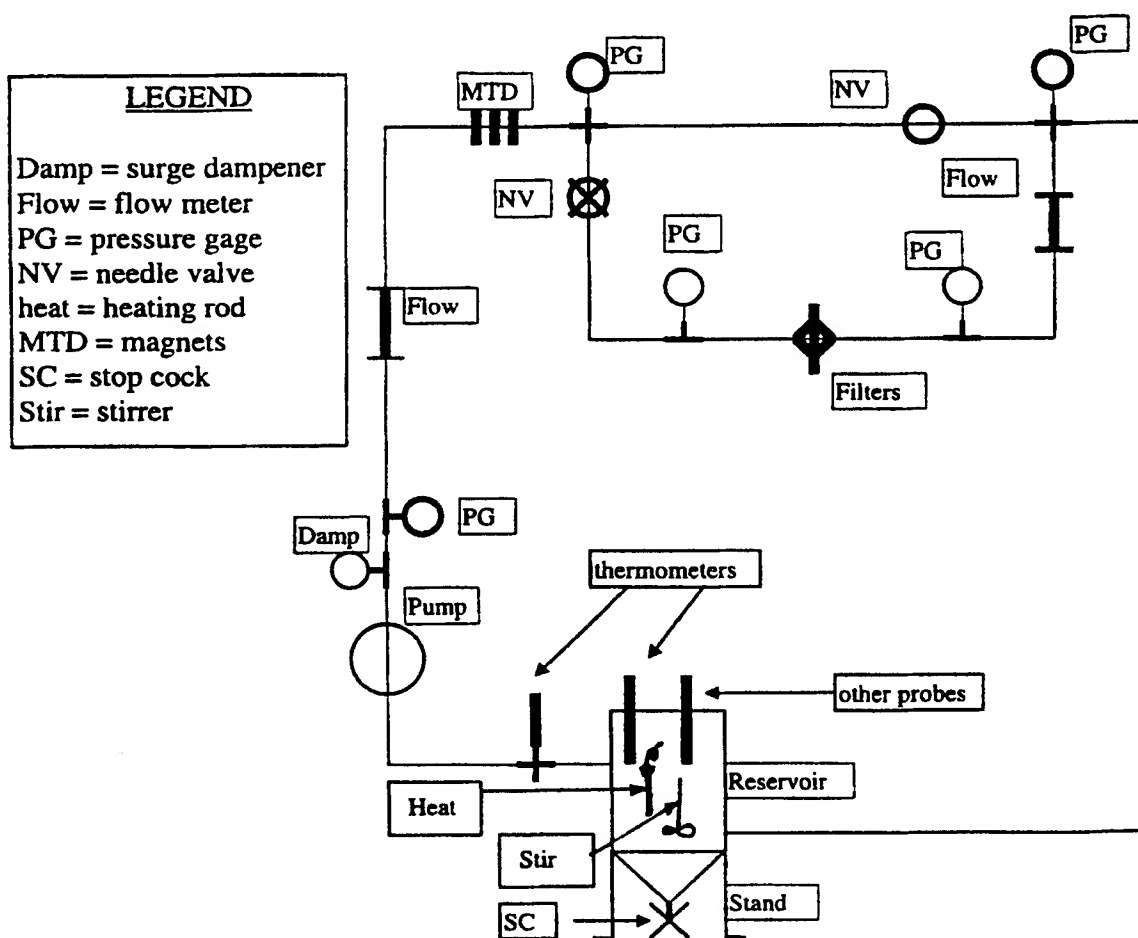


Figure 1 **Test System Schematic**

4.0 MATERIALS, EQUIPMENT AND METHODOLOGY

4.1 Materials

calcium carbonate, CaCO_3 , chelometric standard, assay 99.97% pure, Certified Lot Analysis

calcium nitrate tetrahydrate, $\text{Ca}(\text{NO}_3)_2 \cdot 4 \text{H}_2\text{O}$, reagent grade, assay minimum 99.0% pure

hydrogen peroxide (H_2O_2), 50% solution

sodium carbonate monohydrate, $\text{Na}_2\text{CO}_3 \cdot \text{H}_2\text{O}$, reagent grade

trichloroacetic acid (TCA)

R601 Min-U-Sil Test Colloid, Zeta-Meter, Inc. (used to verify equipment and technique for zeta potential)

NBS Traceable Polymer Microspheres, diameters: 29.9 +/- 0.20, 20.49 +/- 0.20, 7.040 +/- 0.051, 3.004 +/- 0.029 microns (used for particle counter operation and technique verification)

Hach Alkalinity test kit

Hach Hardness, Total and Calcium test kit

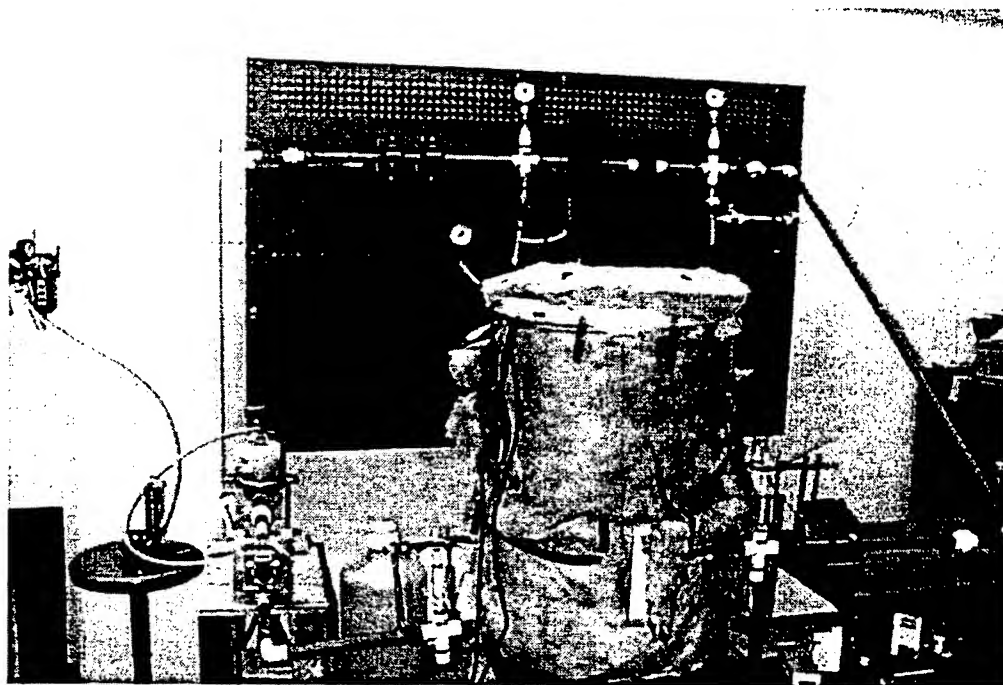


Figure 2 Overall view of test system 1. Insulation covers the tank. Digital thermometer on right.

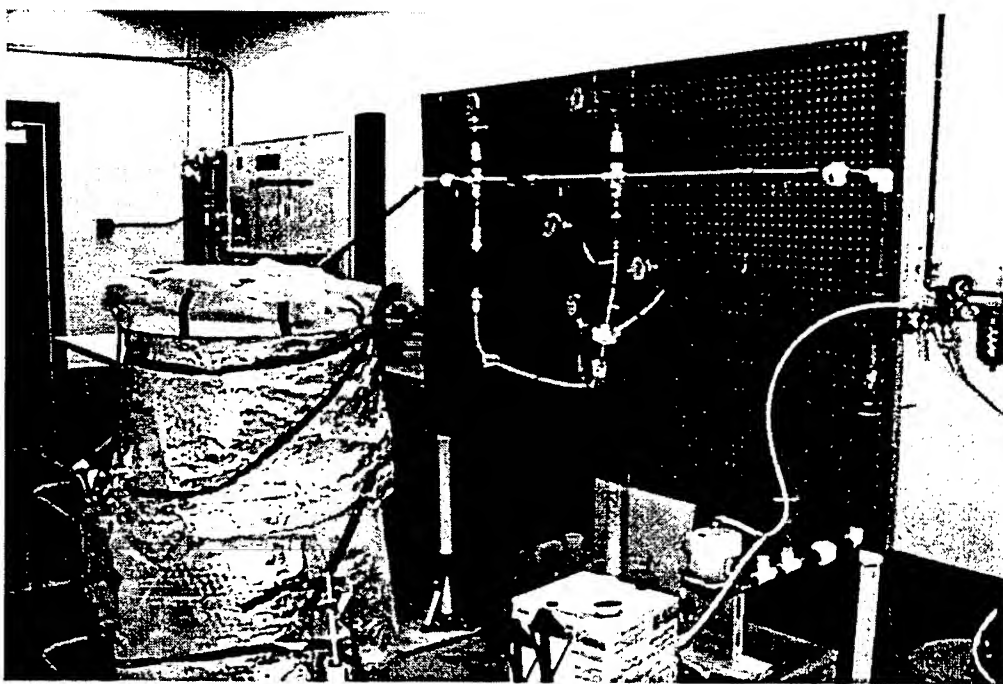
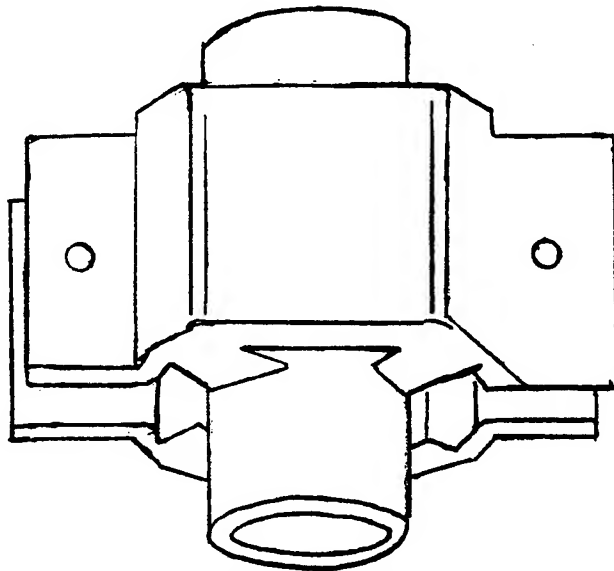
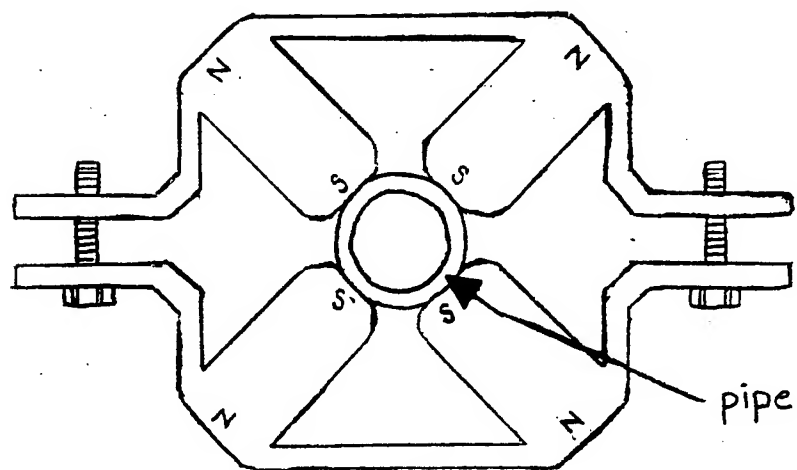


Figure 3 Overall view of test system 2. Insulated box over pump for noise attenuation.



a) Side view of magnetic device mounted on pipe



b) Cross-sectional view of magnetic device mounted on pipe

Figure 4 Views of magnetic device attached to section of pipe.

4.2 Test System Equipment (significant components only)

Wilden air operated, double diaphragm pump: designation: M.025/PPPD/WF/WF/PWF

The Equalizer (TM), Wilden automatic surge dampener, Wilden Pump & Engineering Co.

Mini-Trol Model 500 shock suppressor, Amtrol, Inc.

filter membrane: Nuclepore polycarbonate, 10.0 μm pore, track etched, 47 mm diameter

depth filter (for upstream pre-screening): Osmonics polyester drain disc, 42 mm diameter

fused quartz, Red Hot Immersion Heater, 300 and 400 watt BD series, Electrothermal Engineering Ltd.

Robotemp – heat controller Model No. 315, George Ulanet Co.

Barnant Series 10 variable speed mixer motor

Magnetic device model number M1-C, The Magnetizer Group, Inc.

4.3 Analytical Test Equipment

Scanning Electron Microscope (SEM): Zeiss DSM 960 (Tyndall AFB, FL)

Scanning Electron Microscope (SEM): Japanese Electron Optics Laboratory (JEOL) JSM-840A (BYU)

X-ray Diffraction (XRD): XDS 2000, Scintag Inc., USA

X-ray Fluorescence (XRF): Siemens SRS 303

Zeta Meter 3.0, Zeta-Meter, Inc.

Hiac/Royco ABS2 sampler, 8000A controller/counter, particle counter (BYU)

Hiac Royco Particle Size Analyzer Model PC-320 (Orem treatment plant)

Hach DR/4000U Spectrophotometer

Atomic Absorption (AA): Thermo Jarrell Ash model number 11

Modulab, Laboratory Research Grade Water (filter/purifier) System, Continental Water Systems Corp.

4.4 Operation Of Sample Production And Filtration Test System

The mixers and immersion heaters provided a thorough chemical and thermal mix of the 15 gallons of water in each of the two tanks. Two levels of CaCO_3 supersaturation were selected for testing: 25 and 75mg/L of CaCO_3 added to the existing tap water content. Supersaturation is used here as it is frequently used in the literature on magnetic descaling. Strictly speaking, the aqueous solutions are not supersaturated but only contain an excess amount of CaCO_3 above saturation levels which are circulated throughout the system as precipitated crystals or powder. As the filters remove CaCO_3 the excess maintains the system saturated. Hydrogen peroxide, 10 mg/L, was added to each fresh batch of water to minimize bacterial growth. Bacterial growth interferes with particle counting in the smaller size range of interest. Hydrogen peroxide was selected as the disinfectant least likely to interfere with the CaCO_3 . The immersion heaters were operated with and without the heat controllers depending on heat rate requirements. The immersion heaters required occasionally cleaning to prevent the hard film (scale) build

up from significantly reducing heat transfer. Filter membrane holders were checked and cleaned as necessary between tests. The fine pore downstream filter was replaced each test while the coarser prefilter could be cleaned and reused several times.

Hydrodynamic properties: flow rate, pressure and temperature were recorded to monitor system operation and watch for filter plugging. Water chemistry (pH, alkalinity, calcium and total hardness) were tested near the beginning and end of each test. As the alkalinity and hardness patterns developed (there was no reason to suspect that they should change significantly during the test), the alkalinity and hardness titrations were only performed near the end of each test. The titrations were performed using the portable Hach test kits. Generally the heater controllers had to be adjusted a number of times during each test. A few times near the end of testing, pump #1 began sticking if the flow rate dropped below 1 gpm so the last test conducted at this flow rate was run at 1.1 gpm for system 1. Water samples were also collected for use with the zeta meter, AA and the particle counter. These water samples were allowed to cool (sometimes refrigerated briefly) to near room temperature because of the thermal effects on the zeta potential measurement. After the titrations were performed, aqueous sampling completed and final system variables recorded, the systems were shut down. The filter membranes were removed (and in some cases the filter housings) and placed in dessicators for drying. The dried residue was removed from the membranes and housings, examined visually and weighed. The residue weights were used to prepare more CaCO_3 to mix back into the tanks to maintain approximately the same supersaturation level. The dissolved CaCO_3 removed during aqueous sampling (250 – 550 ml, depending on the titration) was not calculated and replaced in the tanks for subsequent test runs. The CaCO_3 lost during aqueous sampling was minimal compared to the total amount in the reservoir.

When a series of tests were completed the system was drained, the CaCO_3 residue was rinsed from the tank, then wiped out. New water was placed in the system and circulated (without filter membranes installed) to flush out the entire system. This was then drained. Depending on the situation, the tanks were then wiped down with a mild hydrogen peroxide solution and re-rinsed. Fresh water was added, then new CaCO_3 and hydrogen peroxide added to prepare for the next round of tests.

Due to the logistics involved of cleaning the circulatory system, preparing the new solution and reheating the water in the 30 gallon tank (the entire process could take eight hours for the two systems), this process was not performed between every individual test. It was performed between series of tests. Between each individual test, fresh CaCO_3 was mixed in to replace that which had been removed from the bypass filters, fresh makeup water was added as necessary and the temperature was brought back up (for those tests run at 105°F). Generally 12 hours up to several days passed between tests to allow the memory effect to dissipate. Unfortunately, no one currently knows how long the memory effect lasts or whether it's effects diminish exponentially, linearly or in some other fashion. For those tests run without

magnetic devices, there is no memory effect, and so the waiting time was not important, except to allow equilibration of any newly added CaCO_3 and thermal equilibrium to be reached.

4.5 Sample Evaluation Techniques

Aqueous samples were held in glass stoppered, glass bottles with dust caps at room temperature. These bottles had been washed and sterilized in an autoclave prior to use. Aqueous samples were removed from the tanks using plastic sampler bottles lowered 1 – 3 inches below the water surface at two separate locations. The plastic samplers were lowered into the tank with a heavy gauge metal wire handle. This handle had been painted and spray coated three times with an organic art coating to prevent metal particles (from the metal bending) from entering the tank. These samples were immediately transferred to the glass sample bottles. Thus each glass bottle held water sampled from two or three locations within the tank. After the solid filter residue was removed from filter holders it was held in tight fitting, lidded, plastic petri dishes. The residue was dried in dessicator chambers prior to weighing.

4.5.1 Scanning Electron Microscope (SEM): Two different SEM (at different laboratories, operated by experienced personnel) provided pictures and dimensional analysis of CaCO_3 crystals prepared at different times by different techniques. This analysis provided some very beneficial information for two purposes: filter membrane selection and crystal powder preparation for XRD calibration. The first SEM work showed the longer crystal dimension to vary from about 2 to 12 microns. This drove original attempts to use filter membranes with pore sizes in the 1 to 2 micron range (which plugged rapidly). The later SEM work showed crystal lengths in excess of 100 microns in some cases. These crystals were prepared by the method of Rao and Yoganarasimhan (1965) indicated that crystals of much larger dimensions might be present than shown by the original SEM work. This information coupled with the early filter plugging problem drove the decision to use 10.0 micron pore size filters. The range in crystal sizes seen in the two SEM efforts likely explains the problems originally encountered in packing powder samples in XRD sample holders. The second SEM analysis included some hand ground specimens as well as the original unground samples. This revealed the need for machine grinding to reduce the crystal aspect ratio which was causing preferred orientation problems in the early XRD work.

4.5.2 Spectrophotometer and Flame Ionization Atomic Absorption (AA): Standard Method 3500 D (Eaton, 1995) was followed with a spectrophotometer to first measure the ferrous (Fe^{++}) and total iron content of two water sources considered for use in the test system. Regular and deionized tap water were both measured against a blank of ultra-pure water (resistivity 16 $\text{M}\Omega\text{-cm}$) obtained from the MODULAB lab filter unit. Later system testing led to the decision to use tap water in the test system. Additional tap water analysis provided by the City of Provo implicated lower iron concentrations than measured by the

spectrophotometer method so additional iron concentration analysis was performed by flame ionization atomic absorption. The AA was expected to provide more accurate total iron concentrations at the expected lower levels. The minimum, reliable detection level for Fe for this machine and method were about 40 ppb. The AA analyses were conducted by an experienced operator.

4.5.3 Particle counters: The purpose of the particle counters was to provide particle size distributions in aqueous samples taken at the end of system tests. For example: an increase in the size distribution of particles would serve as confirmation that crystal agglomeration was taking place. This would back up a decrease in zeta potential which would indicate the increased potential for particle agglomeration. Two particle counters were used at different times, as both malfunctioned at different times with different problems. As both counters were not functioning properly, most planned comparisons were not made.

4.5.4 Zeta-Meter: The Zeta-Meter measures charged particle velocities. This information coupled with specific conductivity is used to calculate the zeta potential which comprises the majority of the surface potential of the charged particles in the sample. These values are then ratioed to a normalized value at a standard 22.5° C temperature. Measurements were taken as soon as the aqueous sample temperature approached room temperature. While temperature correction ratios are provided by the manufacturer, a problem occurs when temperatures differ very much from room temperature, in that the sample approaches room temperature during preparation and measurement (which can take up to 12 minutes). No current capability exists for monitoring the sample temperature during this time. If the sample started at a temperature much above ambient, the measured temperature (used to select a correction factor) may differ markedly from the actual test temperature and introduce an error of as much as 20%. Min-U-Sil test colloids were used to prepare standard dilutions (used similar to calibration standards) to develop operating experience with the equipment. No zeta meter operators were found in locally with experience in the types of waters (and hence test problems) encountered on this project. Use of the test colloid standard dilutions showed that the measured zeta potential of waters maintained in glass bottles declined noticeably within 24 hours after standard preparation. This was confirmed with the manufacturer. The situation was worse if the sample were stored in plastic containers. This led to the consistent measurement of aqueous samples as soon as they neared room temperature.

Considerable difficulty was experienced in measuring the zeta potential of laboratory filtered pure water that had been used in early system tests. There appeared to be insufficient particles to yield statistically significant results. This was a major part of the reason for the change to the use of tap water for the test systems.

4.5.5 X-ray Diffraction (XRD): The XRD was used to perform quantitative analysis to determine the relative proportions of calcite and aragonite in the powdered crystals obtained after drying the filter residue from the system tests. Appropriate techniques for producing relatively pure calcite and aragonite "standards" (which were not available commercially) were found and verified. The method of Wray and Daniels (1957) was selected to produce calcite while Rao's method (1965) was selected as producing the purest batch of aragonite. Wray and Daniels method uses calcium nitrate with sodium carbonate to precipitate calcite and aragonite (different procedures produce various mixes of the two polymorphic forms). Rao's method used calcium carbonate and trichloroacetic acid (TCA) to precipitate aragonite. Then powder preparation methods and a technique for creating a reasonably high quality calibration curve were found and tested that were suitable to this particular application.

The calibration standards (calcite and aragonite preparations) were machine ground in a Micronizing grinder for 60 – 90 seconds prior to XRD evaluation. After further SEM work it was decided that a slightly longer grinding time would provide a more consistent powder while avoiding the problem of converting aragonite to calcite by excessive grinding (Criado and Trillo, 1975 and Gammage and Glasston, 1975). So the test system residues were ground for about three minutes. The potential aragonite/calcite conversion problem was also minimized by the use of isopropyl alcohol to buffer the CaCO_3 powder during grinding.

The X-ray diffraction pattern provides signal peaks corresponding to compounds within the sample powder. The example shown in Figure 5 shows different peaks corresponding to the four most prominent angular positions for both calcite and aragonite. The intensity of the diffracted X-ray is proportional to the compound concentration in the sample. The intensity is related to the peak area which is approximated by the associated computer software algorithm. Among other factors, the peak area is a function of the amount of a given substance in the sample. The relationship between peak heights or individual peak areas is not necessarily linearly related to the concentration of calcite or aragonite. The particular calibration function selected for this analysis yielded close to a linear relationship for calcite as shown in Figure 6. A very flattened "S" curve fits the data better than the straight line, with defense for a little curvature coming from an understanding of the actual process of obtaining the peak areas. The "calcite proportion by XRD peak area ratio" = $(\sum A_{ci}) / ((\sum A_{ci}) + (\sum A_{ai}))$ where $i = 1$ to 4 and A_c and A_a are the areas of the calcite and aragonite peaks respectively. The "% Calcite" then becomes the estimated calcite percent in the diffracted sample. The form of the particular calibration function selected came from Milliman (1974) while the rationale for selecting the four most prominent peaks from known standards came from Bisch (1989). Additional details regarding the development of this calibration curve are found in Lambert (1998).

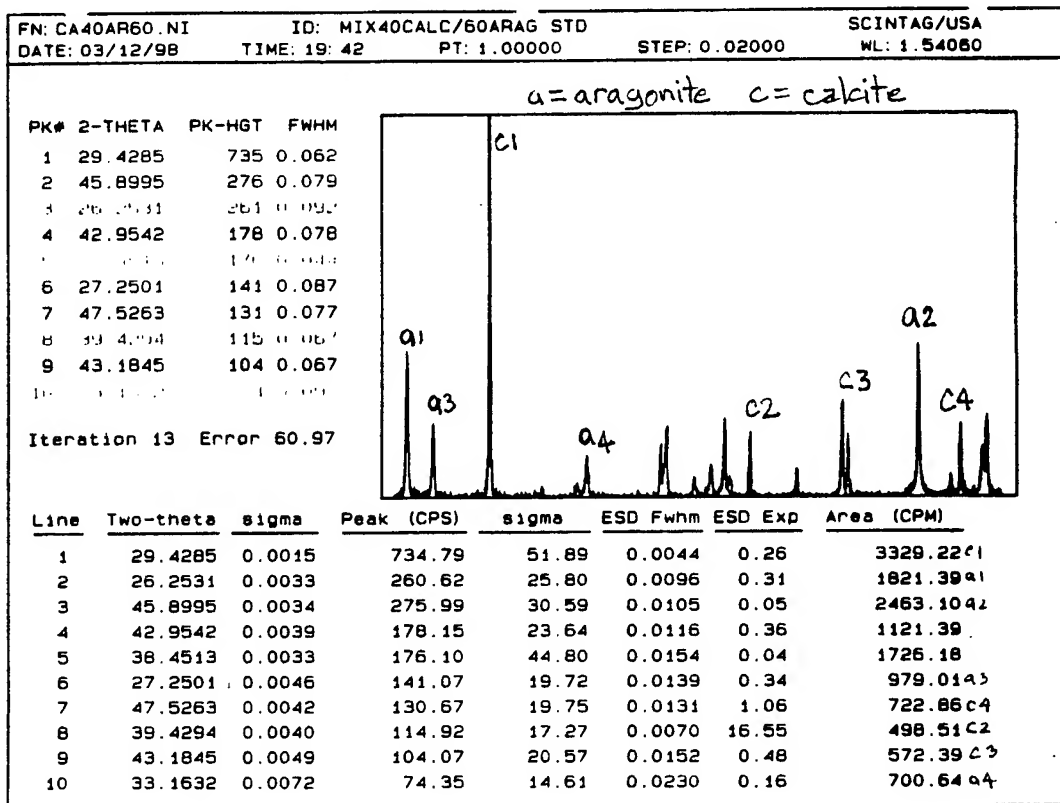


Figure 5 X-ray diffraction peaks for calcite and aragonite

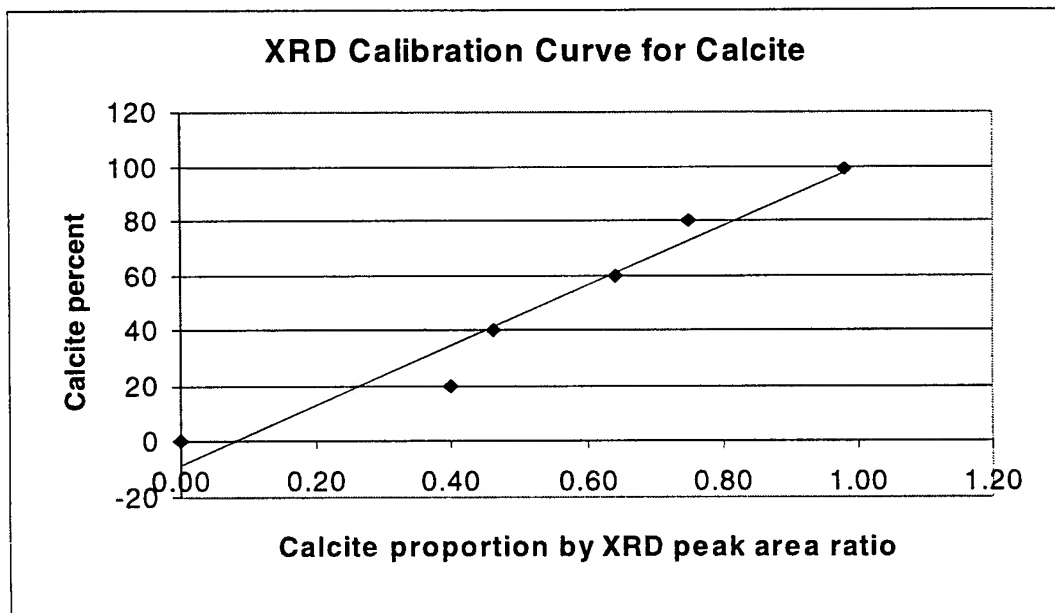


Figure 6 XRD calibration curve for calcite

4.5.6 Energy Dispersive X-ray (EDX): As EDX was available when the first CaCO_3 solid powder samples were prepared, this technique was used to verify good calibration standard preparation technique. For this purpose the EDX analysis provided an advantage of scanning for many substances (unknown beforehand), whereas the XRD is set up to look for given compounds.

4.5.7 X-ray Fluorescence (XRF): Color differences in solid residue removed from the test system bypass filters implicated the probable presence of transition metals in the CaCO_3 residue. This occurred only for certain test conditions where magnetic devices were not used. XRF was used to look at 15 solid residue samples to pinpoint significant changes in any transition metals tied to any particular system test parameter changes. The metals looked for included ones known to form carbonates (Sr, Mg, Pb) and those commonly found in natural or industrial water systems (Zn, Pb, Fe, Cu). The scans also covered the following elements (picked up within the range of interest): Si. As XRF counts individual atoms of the elements encountered, each sample contained the same total mass of powder ($\pm 1\%$) to provide results that would imply relative concentrations. The XRF operation was conducted by an experienced operator.

5.0 RESULTS

5.1 Test System

The principal parameters of the final round of system tests (using tap water) are summarized in Table I (see Appendix). Earlier system testing used to confirm and refine system design are not summarized. System testing with laboratory filtered water is also not summarized as they were not used in any of the final results and conclusions. Most of the solution temperatures were kept within about a six degree range near 105°F . However, without automatic temperature control, some of the longer tests (overnight or long memory-effect tests) exhibited larger temperature variations.

5.2 Solid Residue - Visual Examination

Figure 7 shows sample containers with dried powder that had been removed from the filter holders in the test systems. Although the original shapes were not preserved, nor can the photos show the consistency of the residues personally observed by this researcher, they do show some color distinctions. (Black and white reproductions only show light and dark shades). The powders with the light tan or yellow color (on the right of the figure) were taken from filters in the test system running without magnets. The white powders (on the left side of the figure) are from the system that was operating at the time with magnets attached to the system piping. These changes were only noted for the series of testing with the maximum flow rate (3 gpm), at 105°F bulk water temperature, with generally longer run times (10 hours). The test in this series run for four plus hours showed some similar tendencies, although to a

lesser extent. The magnets were swapped back and forth between systems and the tests repeated, with similar results. The residues removed from systems without the magnets had a cohesiveness to them that required more work to remove them and which had formed a solid disk in the filter holder. The residue removed from the systems with the magnets attached had a pasty consistency, like wet powder and had the same color as the CaCO_3 crystals added to the systems. This same phenomenon was not observed (at least in this pronounced manner) in other series of tests that ran at lower flow rates (1 gpm), at room temperature bulk water temperature or for shorter time periods (four to five hours). The coloration was attributed to the presence of a transition metal in the CaCO_3 residue. Especially the cohesive nature of the residue from the non-magnetic bearing systems indicated the onset of scale formation.

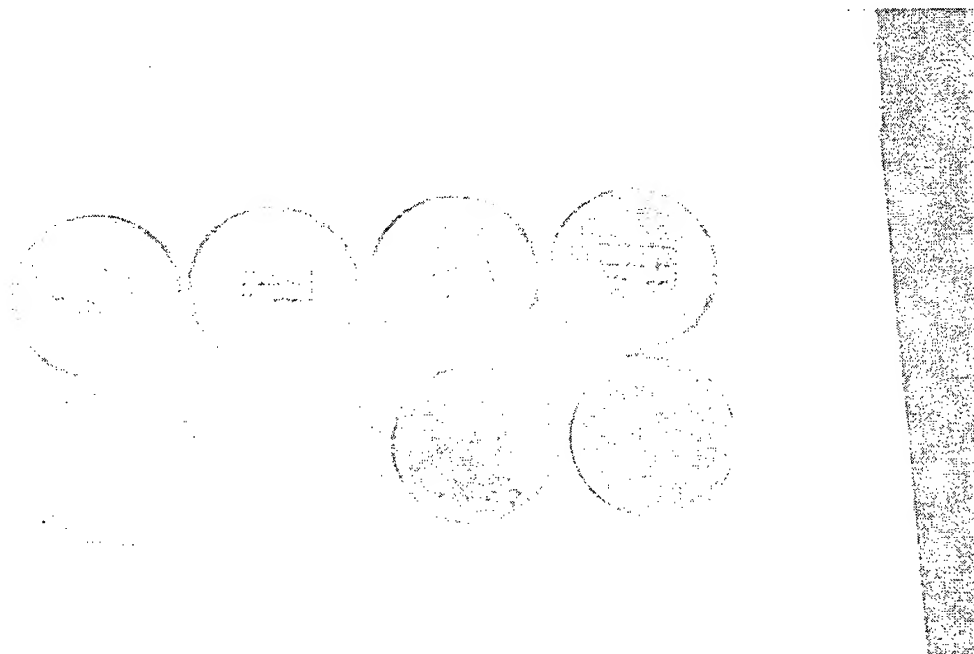


Figure 7 Filter residues from tests with and without magnets. Two samples on left from system with magnets installed. Two samples on right from system without magnets.

5.3 System Water Chemistry: pH, Alkalinity and Hardness

Typical chemistry for the tap water was provided by the City of Provo. Total iron concentrations don't normally exceed 25 ppb. The complete water analysis can be found in Lambert, 1998. The pH, alkalinity, calcium and total hardness values are included in Table II in the Appendix. The pH rarely varied more than 0.1 units from beginning to end of a test. The average pH change between magnetically and non-magnetically treated water was less than 0.1 and was considered insignificant. Alkalinity measurements were more consistent than the hardness values. The known sources of error in the alkalinity measurements account for about ± 5 mg/L as CaCO_3 . Calcium hardness data showed the greatest variation, possibly due to the more difficult nature of its titration. The titration color change for

calcium hardness was the least pronounced of the three titrations performed. Total hardness generally ran 25-100% higher than the calcium hardness. There are a few data among these chemical measures that seem unreasonably different from comparable data at say the beginning or end of the same test or when compared to the same piece of data for a similar test. For these cases the data were noted but not considered valid for data evaluation. In a few cases no definitive value is given as the color change was passed too quickly during titration. This was due to reaching the color change point much quicker than anticipated when compared to similar tests.

5.4 Purity Of CaCO_3 Powder Calibration Standard: EDX

EDX results indicated that the preparation techniques used to yield "pure" calcite or aragonite were successful in minimizing undesired elements. These crystal preparations were necessary as part of the function of developing a calibration curve of relative ratios of calcite and aragonite powder mixtures (from known mixtures) to be used in interpreting unknown mixtures run on the X-ray powder diffractometer.

5.5 Crystal Size And Habit (Aragonite, Calcite): SEM

SEM work showed significant differences between different crystal preparation techniques (for XRD calibration). Figure 8 shows calcite crystals. The calcite preparations utilizing precipitation (Wray and Daniels, 1957) showed consistent crystal production with very little aragonite found in batch 2 which was used for the calibration standard. Figure 9 shows calcite ground from a solid, pure crystal used in an attempt to provide 100% pure calcite for calibration. The distinct nature of the calcite ground from a solid crystal provided different diffraction patterns from the precipitated powders and so was abandoned as a standard. Aragonite preparations showed quite different results between methods. The aragonite crystal lengths varied a lot based on preparation technique. Generally, the shorter crystals were produced by the method of Wray and Daniels, 1957 (Figure 10). The longer crystals were produced by the method of Rao and Yoganarasimhan, 1965 (Figure 11). While they both produced a similar needle or cigar shape, the crystals prepared by the second method had a greater aspect ratio and a cleaner, smoother appearance. Very few calcite crystals were found by SEM in the powders produced by Rao's method, while a small, but very noticeable percentage of the crystals produced by Wray and Daniel's method were calcite, besides the desired aragonite. The SEM findings were important in selecting filters, in selecting Rao's method to produce aragonite powder for the calibration curve and in governing the crystal powder preparation technique. It was found that even the filtered and dried crystal powders required machine grinding. SEM work on the hand ground powders showed considerable variation in size, leading to powder packing inconsistencies. This leads to preferred orientation problems in the quantitative XRD work.



Figure 8 Calcite crystals prepared by method of Wray and Daniels. Larger crystal dimensions range from 5 to 16 microns. SEM image, 1200 X magnification.



Figure 9 Calcite after hand and machine grinding of a single, naturally occurring calcite crystal. Largest fragment dimensions about 54 x 17 microns. SEM image, 500 X magnification.



Figure 10 Aragonite crystals prepared by method of Wray and Daniels. Dimensions: widths vary 0.8 – 2, lengths vary 5.4 – 22 microns. SEM image, 1200? X magnification.



Figure 11 Aragonite crystals prepared by Rao's method. Dimensions: widths vary 0.4 – 4.6 microns, longest length about 100 microns. SEM image, 1200? X magnification.

5.6 Zeta Potential

Table III (in Appendix) lists all the zeta potential values measured, the standard deviation, and the mean values corrected for temperature for comparison purposes. Table III data shows a variation of zeta potential with the number of magnets attached to the systems. There is a decreasing trend in zeta potential with zero to three magnets. The data for six magnets does not agree with this trend. The standard deviation typically ran 20-30% of the mean value and occasionally as high as 40%. This imprecision lends difficulty to reliable data interpretation for changes in zeta potential on the order of 5-7% of the mean value. With the exception of the six vs. zero magnet data there were approximately 50 particles tracked for each test value recorded. This large number provides a sizeable statistical base for comparing averages. Unfortunately the six magnet data had far fewer particles tracked. Table IV shows the average change in zeta potential with changes in system operating parameters. The greatest variation in zeta potential due to change in any system test parameter was found tied to the number of magnets installed. Table IV also lists the number of test results examined to make delta zeta potential comparisons. The delta zeta potential tied to the number of magnets comes from the largest data set, and is likely the most reliable. Other system test parameters influencing the delta zeta potential values were test duration, bulk water temperature, pump rate and the amount of added CaCO_3 added. This last effect is not unexpected as the ion concentration level can impact zeta potential (Zeta Meter, Inc., 1993).

TABLE IV Zeta Potential Changes vs. System Test Parameters

Test parameter varied	Test parameter value for:		Average change in zeta potential	Number of test results evaluated
	larger	smaller		
No. of magnets	0	3	1.4	38
CaCO_3 added (mg/L)	75	25	1.1	23
Test duration (hrs)	9-10.5	4-5.0	1.1	19
Water Temp (F)	75	105	1.1	12
Pump rate (gpm)	3	1	1.0	12
Memory effect (hrs)	40	20	0.6	4

5.7 Particle Size Distribution

Table V summarizes some of the particle count data for system tests run for 0 and 6 magnetic devices installed. Generally this data is the average of two runs on the particle counter with the same water sample. Figure 12 plots this data with the exception of the counts for threshold sizes of 2 and 3 microns. It is believed that the large majority of the counts in these two lower sizes are due to bacterial and air bubble counts. Particle counts are higher for all three pairs of data for the system having the magnets attached. Particle counts for the pure water system tests also showed higher counts for samples from systems operated with magnets.

TABLE V Particle Size Distribution, System Test, Tap Water, 0 vs. 6 Magnets

Threshold Size (um)	1/23/98 System 1 0 magnets	1/23/98 System 2 6 magnets	1/27/98 System 1 6 magnets	1/27/98 System 2 0 magnets	1/29/98 System 1 6 magnets	1/29/98 System 2 0 magnets
	1/23,S1,M0	1/23,S2,M6	1/27,S1,M6	1/27,S2,M0	1/29,S1,M6	1/29,S2,M0
2	464	914	1099	309	1477	549
3	562	1032	2268	616	3462	893
6	95	126	473	150	1076	179
10	41	60	155	98	494	119
15	15.2	27	58	43	187	62
20	5	10.2	38	33	135	43
30	3.4	8.7	17.8	26	82	19.7
45	1	1	8	17.4	31	6.1

NOTES: BYU Counter, DI flush water not subtracted from counts, All system runs used tap water, 75 mg/L added CaCO₃, 3 gpm flow, hot water. Test hours varied from 4 to 10 1/2. Last 2 data pts for 1/23 Sys 1 & 2 estimated from original data. 3/19/98, Labdata, sht 4

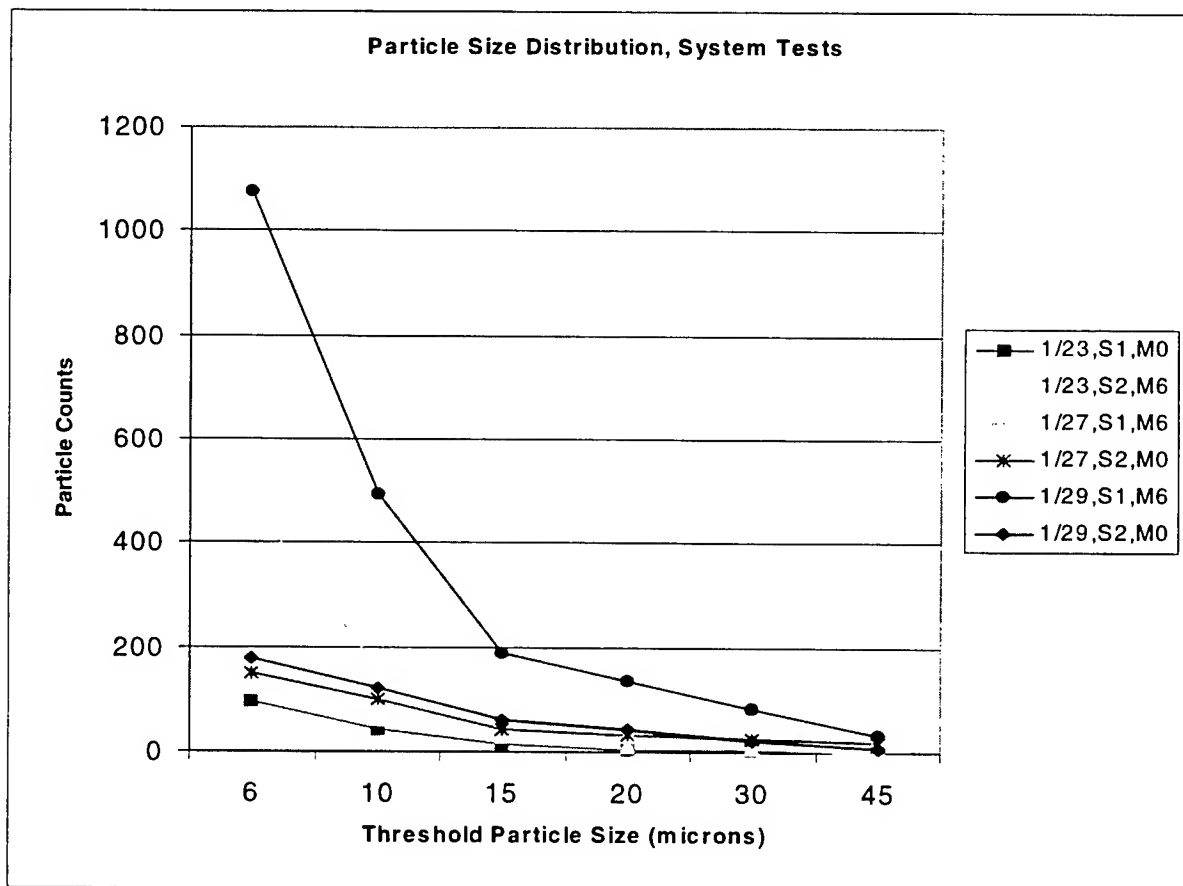


Figure 12 Particle size distributions for 6 and 0 magnets attached

5.8 Calcite/Aragonite Relative Proportions: XRD

Figure 5 shows an example of one of the diffraction patterns with the peak areas estimated by the software algorithm. Table VI (in Appendix) lists the estimated percent of calcite in the given sample residue, with the remaining being aragonite. Evidence of a small concentration of an unknown substance in many of the XRD patterns were ignored for this analysis. All but one test condition yielded calcite percentages in the 80-100% range. Comparison of changes in the calcite percentage between different sets of test conditions yielded very small changes on average (usually less than 5% change). The longer test times favored calcite (7% greater calcite content on average). There was no consistent trend of calcite proportion versus number of magnets installed. The best estimate for potential error in these readings is about 20% (+/- 10%).

5.9 Iron Content In Solid Residue: XRF

The only element to show a consistent pattern with any of the system test parameters was iron (Fe), which changed with the presence of magnets. Figure 13 (Table VII data) illustrates the change in Fe content in the samples with a change in the number of magnets attached to. It shows a consistent drop of iron in the filter residue with the presence of an increasing number of magnets used. Table VIII in the Appendix lists the counts, indicative of the relative amount of Fe, Zn, Sr, Cu, Pb and Mg in the filter residue. Other elements tested are not listed in Table VIII as they only showed non-detect or trace levels in all the samples tested.

TABLE VII Average Iron Content in Filter Residue: XRF Results

No. of magnets	No. of data pts.	Average Fe counts (cps)	Comments
0	7	1372	Theses residues were taken from system tests run at 3 gpm with 75 mg/L CaCO ₃ added. Test duration and system number varies.
1	2	687	
3	4	551	
6	2	544	

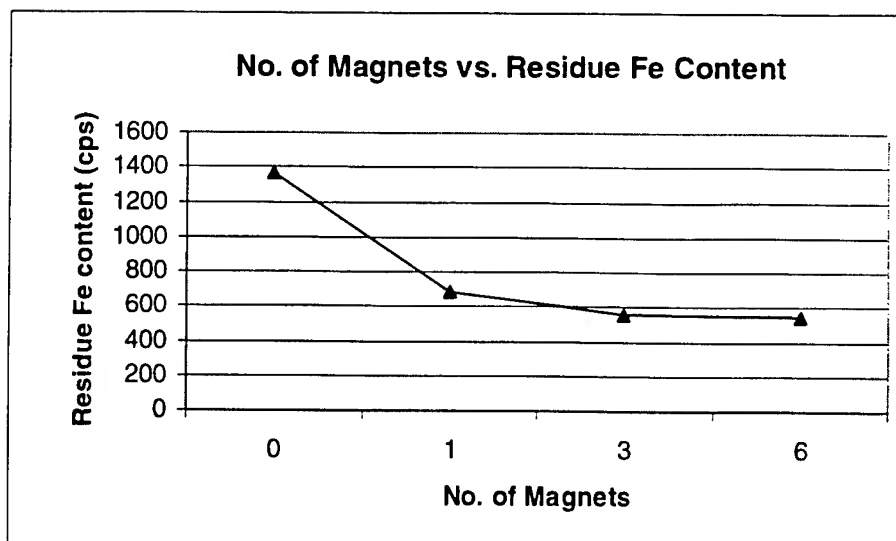


Figure 13 Residue iron content versus number of magnets

6.0 DISCUSSION OF RESULTS

6.1 Solid Residue and Iron

Although not part of the original evaluation plan, examination of the solid residue provided the most intriguing of clues as to whether the magnetic devices perform any useful function. This led to the XRF analysis which showed a consistent drop in iron content in the residue (for certain tests). This has potential implications from two perspectives. First, iron concentrations in aqueous solutions can have a large inhibitory effect on CaCO_3 crystal nucleation (Meyer, 1984) and growth. The removal of iron was cited by Belova (1972) as contributing significantly to the effectiveness of scale reduction in combination with AMT. One of the authors reviewed by O'Brien (1979) claims that iron oxides must be present for AMT to work successfully. Secondly, Fe substitutes for Ca and forms iron carbonate (siderite) a known scale component. Whether this affects scale formation on heat transfer surfaces is as yet unknown. These combined results (colored, cohesive residue plus XRF) may implicate iron as a significant component of the magnetic treatment effect. It is possible that the magnets simply retain the colloidal iron along the pipe, preventing it from entering the residue. The colored residue implies not only the presence of a transition metal but the formation of chemical bonds, apparently tied to iron.

Since the total iron in the water as determined by AA was usually in excess of the maximum expected from the source water (plus a minimal contribution of Fe impurity in the CaCO_3 powder) the additional iron may be attributable to iron piping or components.

6.2 Zeta Potential

The value of any conclusions based on zeta potential measurements is tied to the reliability of the data for six magnets installed. This particular data is far less reliable than the remaining data for several reasons. There were far fewer system tests run with six magnets installed. Far fewer particles were tracked for these first two sets of tap water tests run than for subsequent aqueous samples. This came as a result of continued conversations with the meter manufacturer that produced an evaluation procedure different than that suggested in the manual. The aqueous samples were not all remeasured for two reasons. Most of the samples in question were destroyed in the process of concentrating them for AA analysis. Secondly, it was found that the zeta potential readings change with time. It is hoped that at least a partial answer to this question can be found and included in the thesis currently being completed on this subject (Lambert, 1998). The drop in zeta potential of 7% from untreated samples to those treated with three magnets compares with an average drop of 16% measured by Parsons (1996).

6.3 Particle Size Distribution.

Unfortunately, breakdowns and malfunctions of the two particle counters used prevented gathering much data on size distributions. This reduces confidence in the data presented. For the three pairs of comparisons plotted in Figure 12 there was a consistent trend of higher particle counts for magnetically treated samples. Data evaluation could not attribute this trend to the system used or the amount of CaCO_3 residue deposited in the filters. The shape of the particle size distribution curves were nearly identical for treated and untreated samples. I would have more confidence in the data if it showed a change in the size distribution curve rather than just a larger number of particles for the tests with magnets attached. However, there was no other explanation found, other than the magnetic presence, to explain the higher counts.

6.4 Calcite vs. Aragonite: XRD.

The XRD results found in this research imply little variation in the calcite/aragonite composition when analyzed against the number of magnets used (including none). This is in stark contrast with some researcher's reported results (Deren, 1985 and Donaldson, 1988) that show an 80/20 mix of calcite and aragonite can nearly reverse itself after magnetic treatment. However, this phenomenon has only been observed by a very few researchers. Several have said that they have not seen this crystal change.

6.5 Magnesium content.

No water analysis was performed for Mg concentration and so no independent confirmation can be made regarding the Mg content implied by the significant difference between total and calcium hardness values. The Mg content in the source water analysis implies a lower Mg content than the

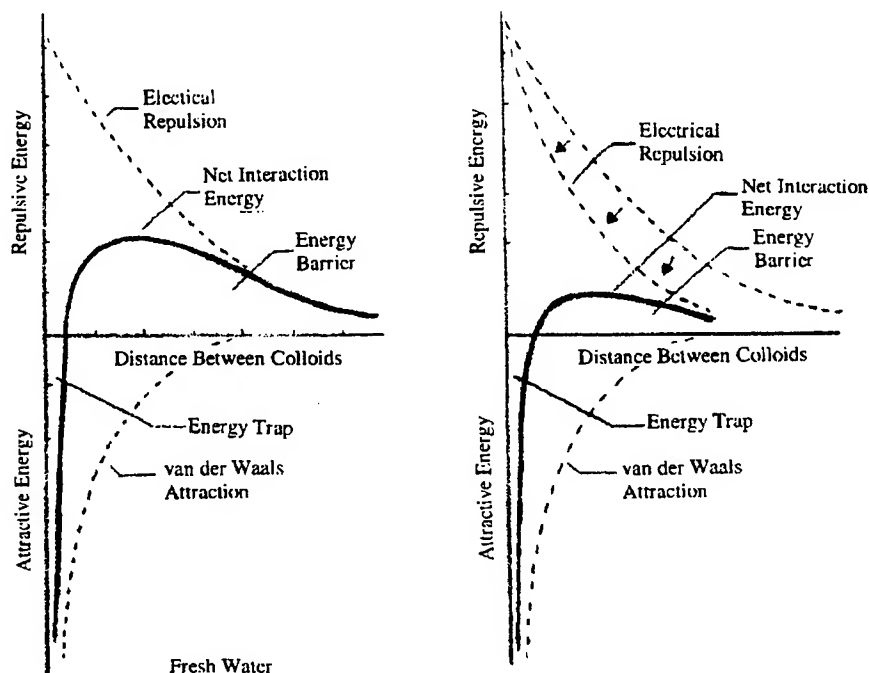
hardness values indicate. If one of the hardness values is to be doubted, it is the calcium hardness. The calcium titration endpoint was less distinct and data evaluation suggests unexplained variations in the calcium hardness. Magnesium can be important in this research as it substitutes for Ca and forms scale forming carbonates. Magnesium can also inhibit CaCO_3 crystal growth.

7.0 INTRODUCTION TO POSSIBLE MECHANISMS

There are many possible mechanisms suggested in the literature, from unbelievable to potentially defensible. Those papers and articles that propose mechanisms generally only briefly introduce them. The solid theoretical and microscopic test verification is lacking to date. The Lorentz Force is an accepted principal that applies to charged particles and is proportional to the flow velocity through a magnetic field. It would seem that the minimal forces generated by the low flow velocities encountered in a typical industrial facility would be insufficient to overcome repulsive forces of charged particles. However, it is the only force proposed to date that is known to tie velocity, particle charge and magnetic field together. It has not been well explained how this force would influence crystal nucleation except through forcing additional particle collisions.

The reduction of zeta potential lowers the energy barrier (see Figure 14) fostering coagulation in the bulk fluid which may provide the nucleus around which crystal growth begins. This may provide competitive sites for calcium carbonate crystal growth as opposed to heat transfer surfaces. Further information on zeta potential may be found in Sawyer, et al. (1994) or Zeta Meter, Inc. (1993).

Many impurities reduce calcium carbonate crystal nucleation and growth (Meyer, 1984). One of the most effective is iron. It has been suggested by several authors that iron must be present for AMT to be effective. It may be that the magnetic field affects the colloidal iron that may then affect crystal nucleation and growth. It is not necessary that this effect eliminates calcium carbonate formation but that it provides competing nucleation sites in the bulk fluid so that the crystals are carried to a slow flow point in the system to drop out rather than form scale on the heat transfer surfaces. If this happens, system design changes, such as side stream filtration (with cyclone separation of heavier particles) can be incorporated to clean out the system. With a recirculating system the calcium carbonate can then be gradually removed, leaving an undersaturated solution. This may then lead to gradual removal of built up scale. This in fact has been reported in a number of field trials. Crystal surface energy, effect of impurities, solubility and the effect of alkalinity and carbon dioxide on calcite and aragonite crystals is discussed by Fyfe and Bischoff (1964). Homogeneous and heterogeneous crystal nucleation are discussed by Reimers et al. (1986). While these sources provide some useful thoughts to get started on this line of research, it will require a very different experimental approach to delve into crystal nucleation because of the physical scale, equipment and processes used.



Interaction
The net interaction curve is formed by subtracting the attraction curve from the repulsion curve.

Compression
Double layer compression squeezes the repulsive Energy curve reducing its influence. Further compression would completely eliminate the energy barrier.

Figure 14 The energy barrier to colloidal flocculation.

a) Net interaction curve

b) Compression reduces the energy barrier

(From Zeta-Meter, Inc., 1993. Used by permission.)

8.0 CONCLUSIONS AND RECOMMENDATIONS

The principal goals have been met in that some effects of magnetic treatment have been demonstrated and some lines of reasoning, for causal mechanisms, have received support, while others have not. The reliability of much of the results are not as strong as desired, principally due to the broad based approach taken. This level of effort minimized the depth of analysis achievable in a more narrowly focused study. The crystal habit (aragonite vs. calcite) line of examination was not significantly supported by this research. Zeta potential coupled with particle size distribution was weakly supported by this research. This may be useful to pursue pending the resolution of equipment problems and one evaluation

question. The presence of iron in filter-retained residue provided good evidence of a line of research worth pursuing.

The impact of flow rate was not effectively examined due to pump operating limitations (different from the pump operating curves). However, flow rate, test duration and water temperature all played a part in determining residue collection. Insufficient residue for XRD examination was collected from tests involving low flow rates, room temperature or short test times. Generally any two of these parameters in combination were sufficient to cause insufficient residue retention. Minor influences were noted due to test length and water temperature. Significant influences were noted due to the presence of magnets and iron. More in depth comments follow, coupled with recommendations.

The current research study implies that pursuit of the relative proportions of calcite and aragonite versus magnetic treatment as determined by XRD quantitative analysis is unproductive, especially in light of the great amount of time involved in the overall process.

The results obtained in this study leave an open question as to whether surface potential (as represented by the zeta potential) could represent a worthwhile source of future study as an indicator of the mechanism for magnetic water treatment. I believe that with some procedural refinements, that this line of research merits continued examination. The interested reader is referred to the thesis (Lambert, 1998) for a possible update on this matter. Functional particle counting would provide a supportive background for this line of research. Particle size increases due to flocculation could easily be tied to reduced zeta potential.

The solid residue removed from the filters for the hot water, longer term tests with higher levels of CaCO_3 present (all factors known to favor scaling) indicate that at least in a number of repeated tests that these particular magnetic devices did indeed make a difference in the accumulated solid. This was mainly evidenced by the very cohesive residue in the non-magnetically treated system versus the soft paste accumulated in the system with magnetic treatment. Although no long term tests were run to confirm scale reduction - there is strong evidence that this might be possible. The color in the residue pointed to the presence of a transition metal which XRF analysis evidenced as being tied to iron in this instance. The amount of iron in the residue was tied to the number of magnets attached to the system.

This line of research (regarding iron) is well worth pursuing in my estimation. It could be pursued by using XRD to determine if the iron was in the form of siderite or iron oxides. AA analysis could be used to determine before and after iron contents in the water. The XRF analysis of solid residue could be compared with a mass balance of the AA results on the liquid samples to confirm iron transition from the colloidal state to potentially scale forming compounds. Additional literature review on crystallography and the effects of impurities on crystal nucleation and growth would be beneficial in this line of study.

It would be very beneficial to locate field studies where the participants feel that magnetic treatment has successfully removed scale and produced a soft, easily removable sludge at a slow flow point in the boiler or cooling tower system. Scale formed on heat transfer surfaces or piping should be sampled, along with the softened sludge and analyzed chemically to characterize the scale (i.e. Sr, Mg, Fe or other scale components) from the two sources. They should especially be evaluated for iron content form (i.e. oxides or carbonates) and concentration. The best source I am aware of for background on real scale composition is Cowan and Weintritt, 1974.

I believe a test system should be used to test these MTDs for somewhat longer time periods to look for effects on the solid residue. This likely requires larger pore size filters (or intermittent changing) to prevent premature plugging and would greatly benefit from the addition of automatic temperature control.

9.0 LITERATURE CITED

- Baker, J. S. and S. J. Judd, (1996). "Magnetic amelioration of scale formation." *Water Research*. 30(2) 247-260.
- Belova, V., (1972). "Magnetic treatment of water." *Soviet Science Review*. (May), 150-156.
- Bisch, D.L. (1989). "Modern Powder Diffraction" Reviews in Mineralogy, J.E. Post, ed., Volume 20. Bookcrafters, Inc., Chelsea, MI.
- Busch, Kenneth Walter and Busch, Marianna A. (1996). "Laboratory studies on magnetic water treatment and their relationship to a possible mechanism for scale reduction." Proc., Second International Meeting on Antiscale Magnetic Treatment, Department of Chemistry, Baylor University, Waco, TX.
- Cowan, J. C. and D. J. Weintritt. (1976). *Water-Formed Scale Deposits*. Gulf Publishing Co., Houston, 93-132.
- Criado, J.M. and Trillo, J.M.. (1975). "Effects of mechanical grinding on the texture and structure of calcium carbonate." *Journal of the Chemical Society*, Faraday Transactions I, London, 71(No. 4), 961-966.
- Deren, E., (1985). "Le traitement des depots calcaires dans l'eau par le procede CEPI." *L'eau, L'industrie, Les nuisances*. 91 (Avril), 49-52.
- Donaldson, J. D., and Grimes, S. (1988). "Lifting the scales from our pipes." *New Scientist*. 117(February), 20-24.
- Duncan, S. L. (1995). "Phase and morphological control of calcium carbonate," Master's thesis, Pennsylvania State University.

- Eaton, Andrew D. (1995). "Standard Methods" for the Examination of Water and Wastewater. 19th Edition. Leanore S. Clesceri and Arnold E. Greenberg, eds., American Public Health Association, Washington DC, 3-69-3-70.
- Fyfe, W.S. and Bischoff, J.L. (1964). "The Calcite-Aragonite Problem." *Symposium, Dolomitization and limestone diagenesis*, University of California. Berkeley, CA.
- Gammage, R. B. and Glasson, D. R. (1975). "The effect of grinding on the polymorphs of calcium carbonate." *Journal of Colloid and Interface Science*, Volume 55, Academic Press Inc., New York, 396.
- Hasson, D. and Bramson, D. (1985). "Effectiveness of magnetic water treatment in suppressing CaCO₃ scale deposition." *Ind. Eng. Chem. Process Des. Dev.* 24(3)588-592.
- Higashitani, K., A. Kage, S. Katamura, K. Hatade, Imai and S. (1993). "Effects of a magnetic field on the formation of CaCO₃ particles." *Journal of Colloid and Interface Science*. 156: 90-95.
- Lambert, K.L. (1998). "Study of factors related to magnetic treatment of calcium carbonate saturated water," Master's Thesis, Department of Civil and Environmental Engineering, Brigham Young University.
- Lawrence, D. J. (1984). "Evaluation of commercial magnetic descalers." *CERL Technical Report M-342*, US Army Corp of Engineers. May.
- Limpert, G. J. C. and Raber, J. L. (1985). "Tests of nonchemical scale control devices in a once-through system." *Materials Performance*. (October)40-45.
- MacGarva, G. J. (1993). "Naval engineers evaluate magnetic boiler feedwater treatment as an alternative to chemicals." *The Coast Guard Engineer's Digest*. 31(253, Spring)29-36.
- Meyer, H. J. (1984). "The influence of impurities on the growth rate of calcite." *Journal of Crystal Growth*. 66: 639-646.
- Milliman, J.D., Muller, G., and Forstner, U. (1974). "Recent Sedimentary Carbonates—Part 1 Marine Carbonates," Springer-Verlag, New York.
- O'Brien, W. P. (1979). "On the use of magnetic (and electric and ultrasonic) fields for controlling the deposition of scale in water systems" - A review of several (22) papers translated from Russian. October. Civil Engineering Laboratory of Port Hueneme, CA, 93108.
- Parsons, S.A., Judd, S.J., Stephenson, T., Udol, S., and Wang, B-L. (1997). "Magnetically augmented water treatment." *Process Safety and Environmental Protection*. 75(B2 May), 98-104.
- Parsons, Simon A. (1996). "Magnetically augmented water treatment." Proc., Second International Meeting on Antiscale Magnetic Treatment, School of Water Sciences, Cranfield University, Shrivenham, Wilts, England.
- Raisen, E. (1984). "The control of scale and corrosion in water systems using magnetic fields." Paper No.117, Corrosion 84 - N.A.C.E. Conference, April 2-6, New Orleans, LA., 1-20.

- Rao, M. Subba, and Yoganasimhan, S.R.. (1965). "Preparation of pure aragonite and its transformation to calcite." *The American Mineralogist*, 50(September), 1489-1493.
- Reimers, Robert S., Bock, Sharon F., and White, LuAnn E. (1986). "Applied fields for energy conservation, water treatment, and industrial applications." Final Report No. DE-FG01-82(CE40568), School of Public Health and Tropical Medicine, Tulane University, New Orleans, Louisiana.
- Sawyer, C. N., McCarty, P. L., and Parkin, G. F. (1994). *Chemistry For Environmental Engineering*. Fourth Edition. McGraw-Hill, Inc., New York, 332-339.
- Simpson, L.G. (1980). "Control scale and save energy." *The Coast Guard Engineer's Digest*. 20(No. 205; Winter), 32-34.
- Wray, J.L. and Daniels, F. (1957). "Precipitation of Calcite and Aragonite." *Journal of the American Chemical Society*. 79(No. 9 May 7).
- Zeta Meter, Inc. (1993) *Everything you want to know about Coagulation and Flocculation....* Fourth Edition. Staunton, Virginia.

APPENDIX

System Test And Analysis Data Tables

TABLE I System Test Summary

Test date	Syst. No.	Test Time (hrs)	Number of Magnet s	Added CaCO ₃ (mg/L)	Water Temp. (F)	Pump Rate (gpm)	Comments
1/23/98	1	10	0	75	103-105	3.0	colored residue
1/23/98	2	10	6	75	104-106	3.0	white paste residue
1/27/98	1	10 1/2	6	75	96-110	3.0	white paste residue
1/27/98	2	10 1/2	0	75	94-105	3.0	cohesive, colored residue
1/29/98	1	4	6	75	103-105	3.0	
1/29/98	2	4	0	75	104-112	3.0	
1/30/98	1	4	3	75	100-112	3.0	
1/30/98	2	4	3	75	99-105	3.0	
1/31/98	1	4	1	75	103-106	3.0	
1/31/98	2	4	1	75	105-115	3.0	
2/2/98	1	4	1	75	104-107	3.0	
2/2/98	2	4	1	75	94-113	3.0	tubing separated, water lost
2/6/98	1	4 1/4	3	75	103-104	1.0	
2/6/98	2	4 1/4	3	75	104-106	1.0	
2/7/98	1	5	0	75	102-107	1.0	
2/7/98	2	5	0	75	103-109	1.0	
2/9/98	1	9 1/4	0	75	76-77	3.0	
2/9/98	2	9 1/4	0	75	76-77	3.0	
2/10/98	1	9	3	75	74-76	3.0	
2/10/98	2	9	3	75	75-76	3.0	
2/11/98	1	5	3	75	73-74	1.0	
2/11/98	2	5	3	75	73-74	1.0	
2/13/98	1	4 1/4	3	25	100-107	3.0	
2/13/98	2	4 1/4	3	25	103-105	3.0	
2/13/98	1	20	0	25	86-112	2.15	memory effect
2/13/98	2	19 3/4	0	25	97-113	2.14	memory effect
2/14/98	1	9	3	25	103-109	3.0	
2/14/98	2	9	3	25	106-107	3.0	
2/15/98	1	41	0	25	103-115	3.0	memory effect
2/15/98	2	41	0	25	104-108	3.0	memory effect
2/16/98	1	mem. effect test 2/15/98 to 2/16/98					memory effect
2/16/98	2						memory effect
2/17/98	1	9 1/4	0	25	104-106	3.0	
2/17/98	2	9 1/4	0	25	102-109	3.0	
2/18/98	1	3 3/4	1	25	102-103	3.0	
2/18/98	2	3 3/4	1	25	104-107	3.0	
2/19/98	1	4 1/4	1	25	101-106	1.1	
2/19/98	2	4 1/4	1	25	101-109	1.0	
2/20/98	1	10 1/4	3	75	102-105	3.0	
2/19/98	2	23	0	75	101-112	3.0	
2/20/98	2	this test begun 2/19/98 ended on 2/20/98					
			Note: All tests in this table used regular hose tap water				FN=systest3a.xls

TABLE II Water Chemistry - Hardness, Alkalinity and pH

sheet 1

Test date	Syst. No.	No. of Magnet s	Type Water	Time since Mag.(hrs)	Alkalinity (mg/L as CaCO3)	Calcium Hardness s	Total Hardness	pH	Comment s
11/21/97	1		filter	0	25	19	19	-	
11/21/97	2		filter	0	25	19.7	20.3	-	
12/11/97	1		filter	0	35	26.2	26.7	-	
12/11/97	2		filter	0	30	26.1	26.6	-	
1/23/98	1	0	tap	0	38	30.5	-	-	start
1/23/98	2	6	tap	0	38	98	-	-	start
1/23/98	1	0	tap	0	152	29	160	-	end
1/23/98	2	6	tap	0	168	114	184	-	end
1/27/98	1	6	tap	0	145	82	137	8.8	start
1/27/98	2	0	tap	0	160	100	157	9.1	start
1/27/98	1	6	tap	0	118	77	160	8.8	end
1/27/98	2	0	tap	0	138	116	144	8.8	end
1/29/98	1	6	tap	0	115	<50	163	8.95	start
1/29/98	2	0	tap	0	102	64	119	9	start
1/29/98	1	6	tap	0	102	47	108	8.95	end
1/29/98	2	0	tap	0	105	62	117	9	end
1/30/98	1	3	tap	0	95	83	106	9.1	start
1/30/98	2	3	tap	0	100	50	117	8.9	start
1/30/98	1	3	tap	0	95	<=40	103	9	end
1/30/98	2	3	tap	0	100	62	114	8.9	end
1/31/98	1	1	tap	0	90	63	102	9.15	start
1/31/98	2	1	tap	0	100	52	107	9.3	start
1/31/98	1	1	tap	0	80	44	101	9.1	end
1/31/98	2	1	tap	0	92	46	111	9.2	end
2/2/98	1	1	tap	0	85	74	104	9.1	start
2/2/98	2	1	tap	0	110	48	111	9.2	start
2/2/98	1	1	tap	0	92	69	101	-	end
2/2/98	2	1	tap	0	110	73	131	9.1	end
2/6/98	1	3	tap	0	-	-	-	8.9	start
2/6/98	2	3	tap	0	-	-	-	8.95	start
2/6/98	1	3	tap	0	95	44	108	9.1	start
2/6/98	2	3	tap	0	125	78	133	-	start
2/7/98	1	0	tap	0	-	-	-	9.2	start
2/7/98	2	0	tap	0	-	-	-	9.1	start
2/7/98	1	0	tap	0	90	59	105	9	end
2/7/98	2	0	tap	0	105	58	131	9	end
2/9/98	1	0	tap	0	-	-	-	9	start
2/9/98	2	0	tap	0	-	-	-	9	start
2/9/98	1	0	tap	0	88	51	106	8.85	end
2/9/98	2	0	tap	0	102	61	119	8.85	end
2/10/98	1	3	tap	0	-	-	-	8.8	start
2/10/98	2	3	tap	0	-	-	-	8.8	start

TABLE II Water Chemistry - Hardness, Alkalinity and pH

sheet 2

Test	Syst.	No. of	Type	Tim since	Alkalinity	Calcium Hardnes s	Total Hardness	pH	Comment s
date	No.	Magnet s	Water	Mag.(hrs)	(mg/L as CaCO3)				
2/10/98	1	3	tap	0	95	42	136	8.6	end
2/10/98	2	3	tap	0	110	71	129	8.8	end
2/11/98	1	3	tap	0	-	-	-	8.6	start
2/11/98	2	3	tap	0	-	-	-	8.75	start
2/11/98	1	3	tap	0	90	<=35	107	8.55	end
2/11/98	2	3	tap	0	110	71	126	8.7	end
2/13/98	1	3	tap	0	-	-	-	8.5	start
2/13/98	2	3	tap	0	-	-	-	8.6	start
2/13/98	1	3	tap	0	162	116	170	8.7	start
2/13/98	2	3	tap	0	160	117	176	8.55	start
2/14/98	taken from hose			-	155	122	178	-	-
2/14/98	1	0	tap	20	-	-	-	8.7	start
2/14/98	2	0	tap	20	-	-	-	8.3	start
2/14/98	1	0	tap	20	150	108	169	9.0	end
2/14/98	2	0	tap	20	155	100	177	9.0	end
2/15/98	1	3	tap	-	-	-	-	8.85	start
2/15/98	2	3	tap	-	-	-	-	9.0	start
2/15/98	1	3	tap	-	130	74	145	8.55	end
2/15/98	2	3	tap	-	135	96	148	8.5	end
2/16/98	1	0	tap	41	-	-	-	8.9	start
2/16/98	2	0	tap	41	-	-	-	8.8	start
2/16/98	1	0	tap	41	85	<=39	110	8.7	end
2/16/98	2	0	tap	41	100	57	114	8.55	end
2/17/98	1	0	tap	-	-	-	-	8.9	start
2/17/98	2	0	tap	-	-	-	-	8.8	start
2/17/98	1	0	tap	-	75	72	103	9.0	end
2/17/98	2	0	tap	-	90	43	107	8.85	end
2/18/98	1	1	tap	-	-	-	-	9.0	start
2/18/98	2	1	tap	-	-	-	-	9.0	start
2/18/98	1	1	tap	-	85	39	105	9.0	end
2/18/98	2	1	tap	-	90	50	110	9.0	end
2/19/98								9.0	
2/19/98								9.0	
2/19/98								9.0	
2/19/98								9.0	
2/20/98	1	3	tap	-	-	-	-	8.8	start
2/20/98	2	0	tap	-	-	-	-	8.5	start
2/20/98	1	3	tap	-	135	93	161	8.5	end
2/20/98	2	0	tap	-	132	100	151	8.5	end

KML, 3/5/98, FN=chemistr2.xls

TABLE III Zeta Potential Results For System Tests

Test date	Sys No.	# of Mag- nets	Zeta Potent. ave.(mV)	Zeta Pot.- std. dev.(m V)	sample temp. (F)	Ct	Zeta Potential 22.5 C (mv)	Comments
1/27/98	1	6	-22.0	>5.84	73.4	0.99	-21.8	2 sets of 12 counts
1/27/98	2	0	-22.4	>5.34	73.4	0.99	-22.2	2 sets of 11 counts
1/29/98	1	6	-20.2	5.56	78.8	0.94	-19.0	42 counts
1/29/98	2	0	-20.1	5.19	76.1	0.965	-19.4	45 counts
1/30/98	1	3	-21.8	5.12	82	0.904	-19.7	rest are >= 48 counts
1/30/98	2	3	-22.2	5.12	81	0.918	-20.4	
1/31/98	1	1	-20.7	5.31	76	0.966	-20.0	
1/31/98	2	1	-19.8	3.95	76	0.966	-19.1	
2/2/98	1	1	-22.7	5.34	78	0.948	-21.5	
2/2/98	2	1	-21.2	4.59	77.5	0.954	-20.2	
2/6/98	1	3	-22.3	5.59	87	0.864	-19.3	
2/6/98	2	3	-20.7	7.09	85	0.882	-18.3	35 counts
2/7/98	1	0	-19.5	4.81	75	0.972	-19.0	
2/7/98	2	0	-20.4	4.81	75.5	0.968	-19.7	
2/9/98	1	0	-23.0	7.75	75.5	0.968	-22.3	
2/9/98	2	0	-23.1	11.43	75.5	0.968	-22.4	
2/10/98	1	3	-22.3	3.89	75.5	0.968	-21.6	
2/10/98	2	3	-20.0	6.66	75.5	0.968	-19.4	
2/11/98	1	3	-20.2	5.31	73	0.994	-20.1	
2/11/98	2	3	-20.3	4.72	73	0.994	-20.2	
2/13/98	1	3	-18.8	4	72	1.008	-19.0	
2/13/98	2	3	-18.5	8.06	71.5	1.012	-18.7	
2/14/98	1	0	-20.8	5.44	76	0.966	-20.1	memory effect
2/14/98	2	0	-18.6	8.37	76	0.966	-18.0	memory effect
2/14/98	1	3	-19.1	12.31	79.5	0.932	-17.8	
2/14/98	2	3	-18.1	15.37	78	0.948	-17.2	
2/16/98	1	0	-20.9	5.84	81	0.916	-19.1	memory effect
2/16/98	2	0	-21.6	10.12	79.5	0.932	-20.1	memory effect
2/17/98	1	0	-21.8	7.41	78	0.948	-20.7	
2/17/98	2	0	-22.7	15.43	77.5	0.954	-21.7	
2/18/98	1	1	-19.2	5.59	81	0.918	-17.6	
2/18/98	2	1	-19.0	10	78	0.948	-18.0	
2/19/98	1	1	-19.0	5.16	78	0.948	-18.0	
2/19/98	2	1	-23.1	4.91	77.5	0.954	-22.0	
2/20/98	1	3	-18.5	4.12	79	0.937	-17.3	
2/20/98	2	0	-23.2	>13.4	79	0.937	-21.7	

Notes: 1) The 6x scale used on the ocular (eyepiece) scale.

2) Kfactor tests at 66-67

3) Tracking time for good results should be > or = 2.5 sec

4) Water source for all these tests was the hose in the fluids lab.

5) Zeta potential corrected to 22.5 degree C

6) Ct= temperature correction factor interpolated from Zeta-Meter manual.

TABLE VI XRD Peak Areas (cpm)

2-Theta-->	29.49	39.43	43.18	47.53	26.24	45.9	27.25	33.18	sum c	sum a	calcite ratio	corrected calcite %	date	Sys No.	No. Mags
File	c1	c2	c3	c4	a1	a2	a3	a4							
kcalwd23.ni	15120	1986	1730	2615	0	369	0	0	21451	369	0.98	99	-	-	-
ca80ar20.ni	7806	1232	1279	1457	796	910	506	1720	11774	3932	0.75	80	-	-	-
ca60ar40.ni	5432	935	959	1163	1414	1581	1005	720	8489	4720	0.64	60	-	-	-
ca40ar60.ni	3329	499	572	723	1821	2463	979	701	5123	5964	0.46	40	-	-	-
ca20ar80.ni	1643	172	336	1691	1840	2389	915	667	3842	5811	0.40	20	-	-	-
klra03b2.ni	0	0	0	0	2661	3975	1640	1068	0	9344	0.00	0	-	-	-
klaast.ni	8430	1562	1259	1805	124	758	430	278	13056	1590	0.89	90	1/27	1	6
klbbst.ni	6563	1568	1481	2021	95	0	105	0	11633	200	0.98	98	1/27	2	0
klccst.ni	6200	1481	1294	1546	81	545	432	250	10521	1308	0.89	90	1/29	2	0
klldst.ni	10331	1247	1177	1802	140	590	197	0	14557	927	0.94	95	1/30	1	3
kleest.ni	7977	1238	1435	1783	200	0	550	250	12433	1000	0.93	94	1/29	1	6
klffst.ni	365	596	555	678	46	173	168	0	2194	387	0.85	86	1/30	2	3
klggst.ni	11257	1909	1549	2461	0	0	0	0	17176	0	1.00	100	1/23	1	0
klhhst.ni	11717	1434	1534	2047	0	0	0	0	16732	0	1.00	100	2/2	2	1
kljjst.ni	9969	1198	1465	1975	901	231	144	0	14607	1276	0.92	93	2/9	1	0
klkkst.ni	10435	1613	1439	2295	0	0	0	0	15782	0	1.00	100	2/13	1	0
klilst.ni	10777	1806	1574	1715	198	0	148	0	15872	346	0.98	98	2/10	1	3
klmmst.ni	10338	1642	1455	1666	195	0	0	0	15101	195	0.99	99	2/2	1	1
klloost.ni	8501	1447	1162	1257	179	391	363	177	12367	1110	0.92	93	2/20	2	0
klppst1.ni	7517	1462	1453	1656	25	346	124	1100	12088	1595	0.88	89	2/17	1	0
klqqst1.ni	7402	833	1000	1152	74	993	415	1570	10387	3052	0.77	79	1/31	1	1
klqqst2.ni	7265	1035	1260	1291	129	959	427	1295	10851	2810	0.79	81	1/31	1	1
klrrst2.ni	5105	699	501	774	764	1143	514	441	7079	2862	0.71	71	1/31	2	1

Notes:

File

Description

kcalwd23.ni calcite prepared by Wray and Daniel method. Nearly 100% calcite

ca80ar20.ni calcite 80% prepared by weight, aragonite 20% by weight

ca60ar40.ni calcite 60% prepared by weight, aragonite 40% by weight

ca40ar60.ni calcite 40% prepared by weight, aragonite 60% by weight

ca20ar80.ni calcite 20% prepared by weight, aragonite 80% by weight

klra03b2.ni calcite used in previous 4 samples are from batch 2, Wray & Daniel method. Aragonite used from Rao Method

klra03b2.ni Aragonite prepared by Rao method, batch 2

TABLE VIII XRF Results For Filter Residues

Sample	Test date	Syst. No.	Number of Magnets	Added CaCO3 (mg/L)	gpm	hrs	Fe (cps)	Zn (cps)	Sr (cps)	Cu (cps)	Pb (cps)	Mg (cps)
Batch 1 XRF Analysis Date 2/5/98												
1~1	chelometric std						280	ND	839	373	309	Tr
1~2	1/23/98	1	0	75	3	10	1010	13768	826	Tr	551	319
1~3	1/27/98	2	0	75	3	10.5	3645	13738	2056	654	654	805
1~4	1/27/98	1	6	75	3	10.5	595	2082	7336	397	Tr	Tr
1~5	1/29/98	2	0	75	3	4	970	2716	7953	Tr	388	685
1~6	1/29/98	1	6	75	3	4	494	1086	6515	Tr	Tr	Tr
1~7	1/30/98	2	3	75	3	4	749	1310	6550	374	Tr	446
1~8	1/30/98	1	3	75	3	4	387	678	5034	Tr	Tr	Tr
1~9	2/2/98	1	1	75	3	4	463	556	1668	Tr	Tr	Tr
1~10	2/2/98	2	1	75	3	4	911	1731	2824	364	Tr	328
Batch 2 XRF Analysis Date 3/4/98												
2~1	chelometric std						315	302	610	<300	ND	ND
2~2	2/20/98	1	3	75	3	10	613	4931	3766	<600	ND	150
2~3	2/20/98	2	0	75	3	23	1381	7954	5242	<700	Tr	242
2~4	2/17/98	1	0	25	3	9.25	341	1117	3530	<400	Tr	144
2~5	2/13/98	1	0	25	3	20	1738	3125	1489	Tr	Tr	190
2~6	2/10/98	1	3	75	3	9	456	744	1455	400-500	Tr	166
2~7	2/9/98	1	0	75	3	9	516	1021	2783	~500	ND	141
Notes: 1) ND=non-detect 2) Tr=trace (barely above background noise, generally 100-300 cps) 4) Batch 2 data for Cu was only noted roughly relative to Fe as Cu presence was mainly attributed to the XRF machine. 3) cps= counts per second FN= xrfcomp.xls (3/5/98)												

TABLE IX Flame Ionization AA Total Iron Results For The Unconcentrated Samples

Sample ID	Mean Concentration (ppb)	Standard Deviation (ppb)	Relative (%)	Description/Comments
AO	69	59	85.5	2/13/98 hose tap H2O, 0 mag, 0 gpm, 0 hrs
BO	13	37	28.5	2/25/98 hose tap H2O+75mg/L, 0 mag, 0 gpm, 0 hrs
EO	69	50	72.8	2/20/98 sys 2, tap+75mg/L, 0 mag, 3 gpm, 23 hrs
FO	44	48	109	2/20/98 sys 1, tap+75mg/L, 3 mag, 3 gpm, 10.25 hrs
GO	87	49	56.1	1/27/98 sys 2, tap+75mg/L, 0 mag, 3 gpm, 10.5 hrs
HO	78	56	71.2	1/23/98 sys 2, tpa+75mg/L, 6 mag, 3 gpm, 10 hrs
FN= orempint.xls				

Jacqueline C. Shin
Report not available at time of publication.

THE DEVELOPMENT OF A GENERAL
MEASURE OF PERFORMANCE

Travis C. Tubre
Graduate Student
Department of Psychology

Winfred Arthur, Jr., Ph.D.
Associate Professor
Department of Psychology

Texas A&M University
College Station, TX 77843-4235

Final Report for:
Summer Research Extension Program

Sponsored by:
Air Force Office of Scientific Research
Bolling Air Force Base, DC

Armstrong Laboratory
Brooks AFB, TX

and

Texas A&M University
College Station, TX

December 1997

THE DEVELOPMENT OF A GENERAL MEASURE OF PERFORMANCE

Travis C. Tubre
Graduate Student
Department of Psychology

Winfred Arthur, Jr., Ph.D.
Associate Professor
Department of Psychology

Texas A&M University

Abstract

The U.S. military has invested considerable resources in developing and validating approaches to measuring individual and workgroup performance. However, these approaches have typically been expensive to develop and time consuming to administer. In addition, considerable information about specific job content is often required to develop performance measures using these approaches. This paper presents the results of a pilot study, the first of a series of studies intended to develop a general measure of performance based on recent conceptualizations (e.g., Campbell, 1990a; Borman & Motowidlo, 1993; Viswesvaran, 1993) of the structure of performance which assert that aspects of performance generalize across different jobs. One appealing aspect of such models rests in the ability to develop approaches to measuring and predicting performance which are useful across a broad range of jobs. To date, however, these models have generally been examined at only the conceptual level and have rarely been empirically tested. The present paper describes the development of a core set of items which could be used to (1) empirically test various latent factor models of performance and (2) form the basis for a measure that could be used to obtain general job performance criterion data for a variety of uses (e.g., test validation, program evaluation). Results from the work to date and plans for future activities are highlighted and discussed.

THE DEVELOPMENT OF A GENERAL MEASURE OF PERFORMANCE

Travis C. Tubre and Winfred Arthur, Jr., Ph.D.

Introduction

Job performance is, perhaps, the most important construct in industrial and organizational (I/O) psychology and human resource management (HRM). Selection systems attempt to predict performance, while the majority of other organizational interventions (e.g., training, performance appraisal) focus on measuring or improving performance in some way. However, despite its importance, relatively little is known about the latent structure of performance. Indeed, many authors (e.g., Binning & Barrett, 1989; Campbell, 1990a; 1990c) have noted that of the parameters in the classic prediction model, performance has been the most ignored. Any number of predictors (e.g., cognitive ability, conscientiousness) have received a great deal more attention than has been devoted to criteria in general, and/or any specific criterion in particular. As noted by Viswesvaran (1993), very few efforts have been directed toward developing generalizable models of performance. It has typically been assumed that what constitutes performance differs from job to job. As a result, researchers have used countless numbers of measures as indicators of performance.

More recently, however, researchers (e.g., Borman & Motowidlo, 1993; Campbell, 1990a; Campbell, McCloy, Oppler, & Sager, 1993) have developed theories of job performance which posit that some latent performance dimensions generalize across a broad range of jobs. For instance, Campbell (1990a) asserts that core task proficiency, demonstrating effort, and the maintenance of personal discipline are components of every job. Models that posit the existence of core sets of performance dimensions which exist across a broad range of jobs are appealing for a number of reasons. First, as noted by Campbell (1990c), theory building is becoming an increasingly important facet of research in I/O psychology. Since job performance is arguably the most important construct in our domain, a more complete understanding of its structure is a necessity (Viswesvaran, 1993). Second, these theories are consistent with recent models (e.g., Schmidt & Hunter, 1992) describing common causal antecedents of performance (e.g., conscientiousness, general cognitive ability) across jobs of widely varying content. That is, one plausible explanation for the position that a relatively small subset of variables (e.g., general cognitive ability, conscientiousness) predict performance in virtually every job is that there are a number of core job performance dimensions that generalize across all jobs. For example, cognitive ability has been shown to predict performance using a variety of criteria across a wide

range of jobs. Thus, components of job performance which are strongly related to cognitive ability (e.g., core task proficiency) might be expected to be important components of performance across a broad range of jobs. Finally, if substantiated, such models could provide the basis for developing approaches to measuring and predicting performance which are useful across a variety of jobs. The development of such an approach or measure is one of the primary goals of our research program.

The pilot study presented here is the first in series of studies intended to develop a general measure of job performance and to also empirically test competing conceptualizations of the latent structure of performance. To date, these models have generally been examined at only the conceptual level and have rarely been empirically tested (Campbell, 1990a; Campbell et al., 1993). This paper describes the development of and conceptual basis for a measure which will be used for this purpose. If performance components which generalize across jobs can be identified, the measure could also form the basis for a system that could be used to obtain general job performance criterion data for a variety of uses (e.g., test validation, program evaluation) across a broad range of jobs. Such an instrument could have tremendous utility by reducing the resource demands associated with gathering criterion data.

The Latent Structure of Performance

Viswesvaran (1993) provides an excellent comprehensive review of historical developments in the conceptualization of job performance. As he notes, the literature examining the structure of job performance is fragmented and incomplete. This sentiment has been echoed by scores of researchers (e.g., Arthur & Bennett, 1995, 1997; Campbell, 1990a, 1990c) examining aspects of the criterion domain. Early conceptualizations (e.g., Brogden & Taylor, 1950) focused largely on the economic value of individual behaviors to the organization. Measures such as wages, work quality, and supervisory ability were identified (Toops, 1944) and related to the value of an individual to the organization. With the emergence of the literature on expectancy theory, many researchers began to focus on measures that reflected the effort expenditure and productivity of workers (Viswesvaran, 1993). This movement saw the use of criterion measures such as unit production and absenteeism. In the 1970s and 1980s research on prosocial and organizational citizenship behaviors proliferated (e.g., Bateman & Organ, 1983; Smith, Organ, & Near, 1983). This resulted in the introduction of a variety of criterion measures including teamwork, compliance, and altruism. Finally, in recent years, the impact of counterproductive behavior in the workplace has been studied extensively (e.g.,

Ones, Viswesvaran, & Schmidt, 1993; Sackett, 1994). This literature has yielded a number of criterion measures (e.g., substance abuse, theft, vandalism) related to honesty and integrity in the workplace.

Campbell (1990a; Campbell et al., 1993) provided one of the first large scale attempts to integrate the numerous dimensions of performance into a comprehensive model. According to Campbell, the latent structure of job performance can be modeled using the following eight general factors: (1) job-specific task proficiency, (2) non-job-specific task proficiency, (3) written and oral communication, (4) demonstrating effort, (5) maintaining personal discipline, (6) facilitating peer and team performance, (7) supervision/leadership, and (8) management/administration.

Job-specific task proficiency refers to the degree to which the individual can perform the core substantive or technical tasks that are central to the job and distinguish one job from another. Non-job-specific task proficiency refers to the extent to which the individual performs tasks or executes performance behaviors that are not specific to their particular job but are required of all members of the organization. Written and oral communication is defined as the proficiency with which an individual can communicate (through writing or speech) independent of the correctness of the subject matter. Demonstrating effort reflects the extent to which the individual displays perseverance and intensity in the completion of job tasks. Maintaining personal discipline captures the tendency of the individual to avoid negative behaviors including excessive absenteeism, substance abuse, and rule violations. Facilitating team performance refers to the extent to which the individual performs such behaviors as helping peers, being a good model, and reinforcing the participation of peers. The supervision/leadership dimension focuses on behaviors directed at influencing and maintaining the performance of subordinates. Finally, management/administration includes all of the elements of management that are distinct from direct supervision (e.g., monitoring progress, controlling expenditures).

According to Campbell (1990a; Campbell et al., 1993), these eight factors represent the highest-order factors that can be useful for describing performance in every job in the occupational domain, although some factors may not be relevant for all jobs. However, Campbell contends that core task proficiency, demonstrating effort, and maintaining personal discipline are important components of performance in every job. Campbell's model was largely influenced by the long-term Selection and Classification Project (Project A) sponsored by the U.S. Army (Campbell, 1990b; Campbell & Zook, 1990). While this model represents one of the most comprehensive treatments of the latent structure of job performance currently available, it has rarely been empirically tested. In fact, Campbell et al. (1993, p.

49) admit that direct evidence in support of the model is sparse. In response, they call for future construct validation efforts to test the adequacy of the eight-factor model.

In a similar vein, Borman and Motowidlo (1993) outlined the conceptual and theoretical basis for expanding the criterion domain beyond task (i.e., job-specific) performance to include elements of contextual performance. Drawing heavily from the literature on organizational citizenship behavior (Barnard, 1938; Bateman & Organ, 1983; Smith et al., 1983), prosocial organizational behavior (Brief & Motowidlo, 1986; Graham, 1986; Organ, 1988), and findings from Project A (Campbell, 1990b), Borman and Motowidlo (1993) described the structure of the contextual performance domain (Viswesvaran, 1993). Within this framework, contextual performance is principally defined in terms of behaviors that support the broad organizational, social, and psychological environment of the organization in contrast to behaviors that support the organization's technical core (Borman & Motowidlo, 1993; Motowidlo & Van Scotter, 1994). Contextual performance is further distinguished from task performance in that it is typically more discretionary as opposed to role prescribed. The authors describe five categories of contextual performance as follows: (1) volunteering to carry out task activities that are not formally part of the job, (2) persisting with extra enthusiasm when necessary to successfully complete task activities, (3) helping and cooperating with others, (4) following organizational rules and procedures even when it is personally inconvenient, and (5) endorsing, supporting, and defending organizational objectives.

As with Campbell's (1990a) model of performance, much remains to be accomplished with regard to providing empirical evidence for the adequacy of the task versus contextual performance distinctions. However, the model proposed by Borman and Motowidlo (1993) has recently received empirical support. Motowidlo and Van Scotter (1994) demonstrated that task and contextual performance contributed independently to overall performance in a sample of 421 U.S. Air Force mechanics. Further, their findings suggested that job experience was more highly correlated with task performance than with contextual performance, and personality variables (e.g., dependability) were more predictive of contextual performance than of task performance. These findings are logically consistent with Borman and Motowidlo's (1993) description of task and contextual performance dimensions. That is, within their framework, variation in task performance is posited to reflect individual differences in the proficiency with which task activities are carried out. Thus, individual differences in the knowledge, skills, and abilities associated with a given task should be more predictive of task performance than personality characteristics. Additionally, experience and training

performance should be more highly correlated with task performance (Borman & Motowidlo, 1997; Motowidlo & Van Scotter, 1994). Conversely, behaviors such as cooperation, persistence, and compliance would likely be more strongly related to personality variables than to experience, training performance, or ability.

In general, there is substantial overlap between the performance models proposed by Campbell (1990a; Campbell et al., 1993) and Borman and Motowidlo (1993). Campbell's (1990a) job-specific and non-job-specific task proficiency factors are captured in Borman and Motowidlo's (1993) task performance domain. Moreover, the majority of behaviors that Borman and Motowidlo describe as contextual performance would fit into Campbell's (1990a) demonstrating effort, maintaining personal discipline, and facilitating peer and team performance factors. However, it should be noted that Campbell's (1990a) model does not seem to adequately capture the contextual performance dimension associated with endorsing, supporting, and defending organizational objectives.

While somewhat different in their treatment of the criterion domain, neither the model proposed by Campbell (1990a), nor that proposed by Borman and Motowidlo (1993) fully examines the possibility of a general performance factor at the highest level of a hierarchical structure. In fact, as noted previously, Campbell (1990a) explicitly argues that his eight factors describe the highest order latent variables that can usefully describe performance. In contrast, a model proposed by Viswesvaran (1993) posits the existence of a strong general performance factor which explains substantial variation in virtually all measures of job performance that have appeared in the literature.

Using meta-analytic techniques, Viswesvaran (1993) cumulated studies reporting correlations between various measures of job performance. Next, he grouped the large number of measures into 25 conceptually distinct categories (e.g., quality of performance, communication skills, compliance and acceptance of authority). Based on an extensive literature review, he identified five themes which captured the vast number of performance measures utilized in the literature and sorted the 25 measures into these groups. The groups he utilized are as follows: (1) productivity, (2) conscientiousness, (3) interpersonal skills, (4) withdrawal (e.g., absenteeism, turnover), and (5) measures of overall job performance. Finally, he tested the adequacy of a three-level hierarchical model of job performance with a general performance factor at the highest level, the five-group factors at the second level, and the 25 categories of performance measurements at the lowest level. His results indicated a positive manifold of true score correlations among the 25 performance dimensions (Viswesvaran, 1993). In addition, the three-level hierarchical model provided a better fit to the data than a two-level hierarchical model in which the 25 dimensions were posited to load on a general factor.

The review of the literature on the factor structure of performance provided in this paper indicates that no clear consensus exists concerning the structure of the criterion domain. However, models such as those provided by Campbell (1990a), Borman and Motowidlo (1993), and Viswesvaran (1993) represent a much needed foundation in the development of comprehensive theories of work performance. The next logical step in this process is to empirically test the adequacy of these competing conceptualizations. The first step in this process calls for the development of a performance measure consisting of items which adequately represent the various performance dimensions posited in the competing theories. This paper reports on the development of such a measure and the results of an initial psychometric assessment.

Method

Participants

The study sample consisted of 501 participants (51% female) from a large southwestern university. Participation was restricted to only individuals who work or were employed. Data collection efforts consisted of eight experimental sessions conducted over two semesters. Six sessions (with a total of 385 participants) were conducted during the first semester and two sessions (with a total of 116 participants) were conducted during the second semester. Between 50 and 100 participants attended each of the sessions which were held in large lecture rooms and lasted approximately 75 minutes. The mean age for the total sample was 19.24 years ($SD = 1.41$). Additional demographic characteristics of the study sample are presented in Table 1. All demographic data were obtained by means of the Demographic Worksheet which was the first section of the General Performance Measure.

Measures

General Performance Measure. The General Performance Measure is a 125-item measure which asks participants to rate the extent to which each item is relevant to measuring performance in their current or most recent job. Responses were on a 5-point scale. The low, mid, and high anchor points were 1 (item not at all relevant), 3 (item neither relevant nor irrelevant), and 5 (item very relevant). This measure, which was designed to capture all of the generalizable dimensions of performance specified in the previously mentioned theories of job performance, is based on an extensive review of such sources as published articles, books, and a variety of instruments designed to measure various dimensions of performance. To ensure the completeness of its dimensional representation, and subsequently, its content-representativeness of the job performance domain, each stage in the item development process involved the

collaborative efforts of the present authors, a graduate student enrolled in an I/O psychology Ph.D. program, and a senior research scientist from the U.S. Air Force. Approximately 500 items describing performance in a broad variety of jobs were extracted and modified from sources such as those listed above. Next, each item was examined within the framework of the competing models identified previously. This was done to ensure that every dimension presented in the models was represented by a subset of items. Next, items that were vague or unclear were removed from the pool. Following this, items whose content was extremely similar to other items were either collapsed or removed from the pool. This process was repeated several times to reach consensus among the participants in the process.

It is important to note that the General Performance Measure does not include items representing job-specific task proficiency or performance. By its very nature, this dimension (i.e., the performance of core substantive or technical tasks that are central to the job and distinguish one job from another) is expected to be job-specific. Thus this precludes its inclusion in a performance measure designed to cut across all jobs. The final outcome of the item development process is presented in Appendix A.

As part of the initial psychometric evaluation of the general performance measure, we sought to investigate whether item endorsement would be related to participants' work ethic and their level of job performance as rated by their supervisor. Because participants responded to the General Performance Measure items in terms of the extent to which they were relevant to measuring performance in their job, it did not seem unreasonable to speculate that individuals high in work ethic may expand the criterion domain above and beyond the actual requirements of their job, while persons low in work ethic would narrow the criterion domain to make it more consistent with their value system. The same conceptual reasoning would serve as the basis for an observed relationship between actual job performance and endorsement of the relevance of the General Performance Measure items. The presence of these relationships would call the results of the present study into question since it would indicate that the observed representation of the criterion domain is influenced by the respondents' level of work ethic and job performance.

Work ethic was operationalized using Woehr and Miller's (1997) Multidimensional Work Ethic Profile. The Multidimensional Work Ethic Profile is a 65-item measure that provides scores on 7 dimensions of work ethic namely (1) centrality of work, (2) self-reliance, (3) hard work, (4) leisure, (5) morality/ethics, (6) delay of gratification, and (7) wasted time. For the purposes of the present study, the dimension scores were aggregated to obtain a composite work ethic score.

Table 1

Demographic Characteristics of Study Sample

VARIABLES	Frequency
Sex	Female = 51% Male = 49%
Currently Employed	Yes = 35% No = 65%
Employment Status	Full-time (year-round) = 5% Full-time (summer-only) = 28% Part-time (year-round) = 44% Part-time (summer-only) = 19% Other = 4%

Descriptive Statistics					
	Mean	SD	Min	Max	Range
Age	19.24	1.41	17.00	30.00	13.00
Number of college semesters completed	3.13	2.20	1.00	12.00	11.00
Hours worked per week (current or most recent job)	28.52	12.38	1.00	90.00	89.00
Tenure in current or most recent job (years)	1.05	1.16	0.08	9.00	8.92
Total tenure (across all jobs [years])	2.58	1.82	0.08	10.83	10.75

Job performance data was obtained from supervisors using the Performance Appraisal Research Form. This measure was a revised version of that developed by Douglas, McDaniel, and Snell (1996). The Performance Appraisal Research Form is an 11-item performance appraisal form which was completed by participants' supervisors and returned by mail in a stamped addressed return envelop to the second author. The measure focuses on various aspects of the ratee's job performance, specifically, including work quality, quantity, accuracy, job knowledge, efficiency, dependability, loyalty, and motivation. These dimensions were aggregated to obtain a total job performance score.

Supervisors were also asked to rate participants' "all-round ability" in terms of their job performance. This item was used as a second measure of overall job performance.

Procedure

After reporting to the experimental sessions, participants received a packet containing (1) an informed consent form, (2) the Demographic Worksheet, and (3) the General Performance Measure. Next, the experimenters presented some background information and a brief description of the purpose of the experiment. Following this, participants were instructed to sign their informed consent forms and return them to the researchers. Once these forms were collected, participants were instructed to complete the remaining forms in the order presented above. Participants returned their packets to the experimenters after completing them. At this point, participants were given the option of taking the Performance Appraisal Research Form to their work supervisor, who would be instructed to complete the form and return it by mail to the experimenters (a stamped, addressed envelope was provided). Participation in this phase of the study was also voluntary. Of the 501 participants, approximately 200 (40%) agreed to take the form and give it to their supervisor. Of the approximately 200 forms which were distributed to participants, 49 were returned for a response rate of approximately 25%. Upon completion of the experimental session, participants were provided with debriefing forms which more completely described the purpose of the study and listed contact information for the experimenters.

Results

Although attention was given to the representation of the other performance models in designing the General Performance Measure, the 125 items were specifically classified into the dimensions of Campbell's (1990a) performance model. Campbell's model was used as the primary guiding framework because it has the largest number of dimensions (i.e., 8 compared to 5 and 1 for Borman and Motowidlo [1993] and Viswesvaran [1993], respectively) and also because of the substantial degree of overlap between this model and Borman and Motowidlo (1993)'s. Consequently, using Campbell's model as the guiding framework ensured that the dimensions of the other models would be adequately represented. An initial test of the appropriateness of the rational classification of items into the specified dimensions was accomplished by assessing the internal consistencies of the 7 factors. The results of these analysis, which are presented in Table 2, indicate that the Cronbach alphas for the 7 factors were very high, ranging from 0.82 to 0.92 (mean = 0.89; SD = 0.03).

Table 2

Descriptive Statistics (for Factor Relevance) and Cronbach Alpha for the General Performance Measure (Rational)Factors

FACTORS	# of Items	Mean*	SD	Min	Max	Range	d	Cronbach Alpha
2. Non-job-specific task proficiency	20	4.05	0.55	1.30	5.00	3.70	0.14	0.87
3. Written and oral communication	13	3.42	0.86	1.15	5.00	3.85	0.98	0.90
4. Demonstrating effort	17	4.09	0.58	1.12	5.00	3.88	0.07	0.87
5. Maintaining personal discipline	13	4.13	0.59	1.38	5.00	3.62	--	0.82
6. Facilitating peer and team performance	23	3.75	0.64	1.39	5.00	3.61	0.62	0.92
7. Supervision/ leadership	21	3.67	0.72	1.29	5.00	3.71	0.70	0.92
8. Management/ administration	18	3.55	0.74	1.29	5.00	3.71	0.87	0.90

Note: The General Performance Measure does not include items representing job-specific task proficiency or performance (factor 1). In computing d , all factors are compared to factor 5 (maintaining personal discipline). Thus the d statistic reflects the difference in relevance between factor 5 and the specified factor. *All means are significantly different from one another ($p < .01$; two-tailed).

Although not presented here, additional future tests of the adequacy of the rational classification are planned. These tests will also entail a comparative evaluation of the fit of the competing models of performance. Specifically, the General Performance Measure items will first be resorted on the basis of Borman and Motowidlo's (1993) five-factor model. After this, the data will then be fit to an 8-factor (Campbell, 1990a), 5-factor (Borman & Motowidlo, 1993) and single, general factor model (Viswesvaran, 1993) to determine which provides the best fit to the data.

Campbell (1990a; Campbell et al., 1993), presents his eight factors as representing the highest-order factors that can be useful for describing performance in every job in the occupational domain. However, although Campbell contends that core task proficiency, demonstrating effort, and maintaining personal discipline are important components of performance in every job, he also recognizes that the eight factors do not have the same form for all jobs and further, that a particular job might not incorporate all eight factors. Various jobs may have different factor

patterns, along with variations in factor content. In summary, the tenets of the theory would suggest that the specific job performance components and their relative relevance would vary from one job to another. Consequently, the next set of analyses assessed the extent to which the performance factors were relevant across all the jobs represented in the sample. Participants had been requested to list their job titles on the demographic worksheet; there were a total number of 123 titles listed (although some of these may have been synonyms of the same title or word). A list of the job titles, along with frequencies is presented in Appendix B.

As previously noted, in completing the General Performance Measure, participants were asked to rate the extent to which each item was relevant to measuring performance in their current or most recent job. Responses were on a 5-point scale. The low, mid, and high anchor points were 1 (item not at all relevant), 3 (item neither relevant nor irrelevant), and 5 (item very relevant). As indicated in Table 2, the most relevant factor across all jobs was maintaining personal discipline (factor 5) and the least relevant was written and oral communication (factor 3). The magnitude of the differences in relevance are further demonstrated in the ds presented in Table 2. The factors that had the largest relevance difference from the most relevant factor (maintaining personal discipline) were written and oral communication (factor 3), management/administration (factor 8), supervision/leadership (factor 7), and facilitating peer and team performance (factor 6).

To test for the effect of job-type on the relevance of the factors in measuring performance across jobs, a multivariate analysis of variance (MANOVA) was run to test for the overall effect of job-type on factor relevance. To accomplish, the 123 job titles listed in Appendix B were classified into clerical, management, production, professional, and sales/service. Table 3 presents the frequency distribution of the job types. The type into which each job title was classified is also designated in Appendix B. The results of the MANOVA were significant ($F[28, 1874] = 2.62, p < .0001$). The results of subsequent analyses of variance (ANOVA) for the effect of job-type on the relevance of the specified factors are reported in Table 4. These results indicate that generally speaking participants in management type jobs considered factors like supervision/leadership (factor 7) and management/administration (factor 8) to be more relevant for measuring performance in their jobs. Campbell (1990a) asserts that demonstrating effort and maintaining personal discipline are core components of every job. Although the data presented in Table 4 provide some support for this assertion, it is interesting to note that compared to all other job types, individuals in production jobs considered maintaining personal discipline (factor 5) to be somewhat less relevant for measuring performance in their jobs.

Table 3

Frequency Distribution of Job Type Classification

Job Type Classification	Frequency	Percentage
Clerical	74	15%
Management	48	10%
Production	30	4%
Professional	39	8%
Sales/service	303	63%

Note: Seventeen participants did not report their job title.

As noted in the Method section, as part of the initial psychometric evaluation of the General Performance Measure, we sought to investigate whether item endorsement would be related to participants' work ethic and their level of job performance as rated by their supervisor. Because participants responded to the General Performance Measure items in terms of the extent to which they were relevant to measuring performance on their job, it did not seem unreasonable to speculate that individuals high in work ethic may expand the criterion domain above and beyond the actual requirements of their job, while persons low in work ethic would narrow the criterion domain to make it more consistent with their value system. The same conceptual reasoning would serve as the basis for an observed relationship between actual job performance and endorsement of the General Performance Measure items. The presence of these relationships would call the results of the present study into question since it would indicate that the observed representation of the criterion domain is influenced by the respondents' level of work ethic and job performance. Correlations between work ethic, job performance, and the General Performance Measure factor relevance scores are presented in Table 5. These results indicate that participants' ratings of factor relevance for measuring performance in their jobs were not related to either their work ethic or job performance level.

Table 4

Factor Relevance Means, Standard Deviations, and ANOVA Results for Job Type

FACTORS		JOB TYPE										F
		Clerical		Management		Production		Professional		Sales/Service		
		Mean	SD	Mean	SD	Mean	SD	Mean	SD	Mean	SD	
2.	Non-job-specific proficiency	4.30 acde	0.60	4.32 bcd	0.43	3.94 abcde	0.72	4.17 abcde	0.46	4.04 acde	0.52	3.60**
3.	Written and oral communication	3.45 acde	0.91	3.78 ab	0.67	3.12 ab	1.10	3.80 ac	0.73	3.36 b	0.86	4.47**
4.	Demonstrating effort	4.04	0.69	4.32	0.43	4.05	0.79	4.25	0.57	4.08	0.53	2.81*
5.	Maintaining personal discipline	4.16 a	0.59	4.23 a	0.55	3.76	0.90	4.19 a	0.64	4.14 a	0.54	2.59*
6.	Facilitating peer and team performance	3.67	0.66	3.97	0.55	3.57	0.92	3.95	0.59	3.73	0.62	3.05*
7.	Supervision/ leadership	3.51 a	0.83	4.00 b	0.59	3.60 ab	0.99	3.89 ab	0.69	3.65 a	0.68	4.38**
8.	Management/ administration	3.45 a	0.81	3.97 b	0.58	3.51 ab	1.00	3.70 ab	0.71	3.51 a	0.71	4.99***

Note: Means with different letters (within rows) differ significantly at the .05 level.

Table 5

Correlations Between General Performance Measure Factor Relevance Score, Work Ethic, and Job Performance

VARIABLES	2	3	4	5	6	7	8	9	10	11
2. Non job-specific task proficiency	--									
3. Written and oral communication	.66	--								
4. Demonstrating effort	.84	.55	--							
5. Maintaining personal discipline	.72	.55	.69	--						
6. Facilitating peer and team performance	.78	.65	.75	.71	--					
7. Supervision/ leadership	.78	.71	.75	.67	.85	--				
8. Management/ administration	.76	.72	.70	.65	.83	.90	--			
9. Work ethic	-.15	-.07	-.19	-.16	-.16	-.19	-.14	--		
10. Overall job performance	.09	-.19	.16	-.04	-.12	-.09	-.11	-.03	--	
11. Total job performance	.19	-.19	.11	.04	-.02	.07	-.02	-.06	.73	--
N	501	501	501	501	501	501	501	501	49	49
Mean	4.05	3.42	4.09	4.13	3.75	3.67	3.55	16.83	3.94	4.05
SD	0.55	0.86	0.58	0.59	0.64	0.72	0.74	3.16	0.69	0.53
Min	1.30	1.15	1.12	1.38	1.39	1.29	1.29	8.10	2.00	2.25
Max	5.00	5.00	5.00	5.00	5.00	5.00	5.00	31.06	5.00	4.75
Range	3.70	3.85	3.88	3.62	3.61	3.71	3.71	22.96	3.00	2.50

Note: All General Performance Measure factor intercorrelations are significant at the .001 level. All work ethic correlations larger than or equal to -.14 are significant at the .01 level. Total job performance represents the aggregate of the 8 performance dimensions noted in the Method section. Overall job performance is a single item rating obtained from the participants' supervisors. With the exception of the correlation between overall and total job performance which was significant at the .001 level, none of the job performance correlations are significant. All significance tests are two-tailed.

The final set of analyses assessed the user-friendliness of the General Performance Measure. This was accomplished by the inclusion of a number of questions to that effect. The data from these questions, which are presented in Table 6, are generally very favorable. It took the participants, on average, about 30 mins. to complete the measure. They found the items to be easy to read and understand. Finally, the participants also appeared to have no problems with either the readability or understanding of the instructions for completing the measure.

Table 6

General Performance Measure User-Friendliness Results

QUESTIONS	Mean	SD	Min	Max	Range
How well did you understand the instructions for this questionnaire?	1.71	0.85	1.00	5.00	4.00
How would you rate the readability of the instructions for this questionnaire?	1.82	0.81	1.00	5.00	4.00
How well did you understand the items in this questionnaire?	1.95	0.81	1.00	4.00	3.00
How would you rate the readability of the items in this questionnaire?	1.83	0.81	1.00	5.00	4.00

Note: Questions were responded to on a 5-point scale. The low, mid, and high anchor points were 1 (very easy to understand/read), 3 (neither easy nor difficult to understand/read), and 5 (very difficult to understand/read).

Discussion

The goal of this paper was to report on a pilot study which involved the development and preliminary evaluation of a general measure of performance. The measure was first evaluated in terms of the appropriateness of the rational classification of items into the seven specified dimensions of Campbell's (1990a) performance model. This was accomplished by an assessment of the internal consistency of the factors which were found to be very high, ranging from 0.82 to 0.92 (mean = 0.89; SD = 0.03). Future analyses, already in progress, will use more sophisticated confirmatory factor analytic techniques to not only further test the adequacy of the rational classification of items, but will also entail a comparative evaluation of the various models describing the latent structure of job performance. To accomplish this, the General Performance Measure items will first be resorted on the basis of Borman and Motowidlo's

(1993) five-factor model. After this, the data will then be fit to an 8-factor (Campbell, 1990a), 5-factor (Borman & Motowidlo, 1993) and single, general factor model (Viswesvaran, 1993) to determine which provides the best fit to the data. These analytic procedures will also be used for the purpose of scale refinement.

Next we assessed the generalizability and relevance of the dimensions for the measurement of performance across all jobs. To accomplish, the mean relevance scores, aggregated across all jobs, were computed. These results indicated that the highest relevance scores were obtained for maintaining personal discipline (factor 5), demonstrating effort (factor 4), and non-job-specific task proficiency (factor 2). These results provide some support for Campbell's (1990a; Campbell et al., 1993) contention that the latter two dimensions are important components of performance in every job. To further test whether job performance components and their relative relevance would vary from one job to another, the 123 job titles present in the sample were classified into five job types after which a MANOVA and series of ANOVAs were run. The results of these analyses indicated that factor relevance was not uniform across all jobs. For instance, as would be expected, participants in management type jobs considered factors like supervision/leadership (factor 7) and management/administration (factor 8) to be more relevant for measuring performance for their jobs. On the other hand, consistent with Campbell's assertion, demonstrating effort (factor 4) and maintaining personal discipline (factor 5) were found to be equally relevant across all jobs, with the exception of production jobs on the latter dimension.

Future studies will, again, employ more sophisticated tests of factor patterns across jobs. For instance both exploratory and confirmatory factor analysis procedures will be used to test the commonality and fit of factor patterns across different jobs. Preliminary analyses using these techniques to explore these issues in the current data are currently in progress.

The final set of analyses presented in this paper assessed the user-friendliness of the General Performance Measure. The results of these analyses were very favorable.

In summary, the results of the pilot study presented here are very encouraging and clearly demonstrate that the development of a general measure of job performance is not only feasible and practical, but that it could also be scientifically meaningful. As discussed here, such a measure could be used to comparatively test current competing conceptualizations and models of performance. Furthermore, when finalized in subsequent field evaluations discussed below, such a measure could be used to obtain job performance criterion data for a variety of uses (e.g., test validation,

program evaluation) across a broad range of jobs. Depending on the nature of the criterion data of interest, the measure could be modified to include job-specific task content. The U.S. military has invested considerable resources in developing and validating approaches to measuring individual and workgroup performance which are largely based on specific job content. However, these approaches have typically been expensive to develop and time consuming to administer. Thus, a general measure of performance which could be modified to obtain general criterion data across a broad range of jobs would be of tremendous utility. The development of such an instrument is the long term goal of our research program. However, before moving on to the next stage, questions concerning the latent structure of performance must be addressed.

Planned Future Research

The next stage of our research program calls for a field replication of the current pilot study along with a field evaluation of the General Performance Measure. Thus future proposed studies call for the administration of an adaptive computer-based version of the revised measure to approximately 2000 Air Force personnel across a wide range of career fields and job categories. (A white paper proposal has been submitted to AFRL/HEJD, Brooks AFB; we are currently waiting to hear on the status of this proposal.) To increase generalizability, an attempt will be made to incorporate a large number of career fields that are analogous to jobs in the civilian sector. In addition, data will be collected from incumbents in jobs with varying degrees of technical content. As with the college sample, participants will be asked to rate each item according to the extent to which it would be an appropriate measure of performance for their job. In addition, data will be collected from supervisors who will rate the extent to which each of the scale items would be an appropriate measure of performance for their subordinates. Job performance data on the participants will also be collected.

Because the General Performance Measure does not include items representing job-specific task performance, for each occupational classification included in the sample, a number of items dealing with job-specific task proficiency will be added to the measure. These items will be drawn from existing performance measurement instruments and job analysis data. In cases where this type of data is nonexistent or outdated, job analytic techniques will be employed to gather data that will be used for constructing items which measure job-specific task performance for the job in question.

The analyses reported and discussed here will be repeated for the field sample. In addition, we propose to test hypotheses concerning the stability of the factor structure of performance across different levels of occupations and incumbent characteristics (e.g., tenure). Further, administering versions of the measure which incorporate or omit job-specific task content will allow for the testing of various research questions concerning the relative impact associated with the inclusion or exclusion of job-specific task content.

Conclusions

As many authors (e.g., Arthur & Bennett, 1995, 1997; Viswesvaran, 1993) have noted, the existing literature on the criterion domain is fragmented and incomplete. Our research program attempts to clarify some of the confusion concerning what constitutes successful or unsuccessful job performance. The theories presented by Campbell (1990a), Borman and Motowidlo (1993), and Viswesvaran (1993) are the groundwork upon which our work will build. The importance of a more complete understanding of the construct of job performance cannot be overstated. Job performance is in some way related to virtually every activity carried out within the context of I/O psychology and HRM. However, our understanding of its structure and composition lags behind our understanding of predictors and outcomes of successful job performance. In addition, efforts directed at identifying generalizable dimensions are particularly valuable. As noted by Viswesvaran (1993):

Developing theories of job performance for each task (or even job) will hinder the development of a general theoretical understanding of the construct of job performance. As the content generality of the dimensions increases, the value of the dimensions in developing prediction instruments and theories of work-behavior increases (p. 64).

It is our belief that the value of developing theories of job performance incorporating dimensions with increased content generality goes beyond the development of prediction instruments and theories of work-behavior. Empirically identifying dimensions of performance with generalizable content represents the first step in the development of instruments that could be used to obtain general criterion data across a broad range of jobs. Instruments of this type could substantially reduce the resource demands of criterion measurement. In addition, such instruments would expand the criterion domain to include elements of contextual performance which may be overlooked in more traditional job-specific approaches to criterion measurement.

Appendix A

General Performance Measure Items Sorted on the Basis of Campbell's Taxonomy of Job-Performance (Eight Factor Model)

NOTE: The following instruction set was used for the administration of the measure.

Using the scale below, please rate the following items on the extent to which they are **RELEVANT** to measuring performance in your current or most recent job. Your responses should **NOT** indicate the level at which you are currently performing the behavior associated with each item. Rather, you should indicate the appropriateness of each item as a measure of performance for employees in your current or most recent job. Please make marks **ONLY** on your scantron and **NOT** in this booklet.

Fill in **A** if the item is *not at all relevant* for measuring performance in your job.

Fill in **B** if the item is *somewhat irrelevant* for measuring performance in your job.

Fill in **C** if the item is *neither relevant nor irrelevant* for measuring performance in your job.

Fill in **D** if the item is *somewhat relevant* for measuring performance in your job.

Fill in **E** if the item is *very relevant* for measuring performance in your job.

Please note the time that you start and finish completing this questionnaire. When you have finished, you will be asked how long it took you to complete this questionnaire.

A = Not at all relevant

B = Somewhat irrelevant

C = Neither relevant nor irrelevant

D = Somewhat relevant

E = Very relevant

NOTE: The operation measure did **not** include the dimension definitions presented below.

1. Job Specific Task Proficiency

Factor 1 reflects the degree to which the individual can perform the core substantive or technical tasks that are central to the job. These are the job-specific performance behaviors that distinguish the substantive content of one job from another. Constructing custom kitchens, doing word processing, and directing air traffic are all categories of job-specific task content. Individual differences in how well such tasks are executed are the focus of this factor.

NOTE: There were no items representing this factor.

2. Non Job-Specific Task Proficiency

This factor reflects the reality that, in virtually every organization, individuals are required to perform tasks or execute performance behaviors that are not specific to the job. For example, in research universities faculty members must teach classes, advise students etc. These behaviors are common across all faculty members in contrast to the job-specific tasks of doing chemistry, psychology, or engineering. In the military services this factor is institutionalized as a set of common tasks (e.g., first aid, basic navigation) for which everyone is responsible.

- 2. Displays commitment to the job
- 16. Challenges conventional thinking

- 17. Accepts direction from supervisors
- 29. Works well under adverse or uncertain conditions
- 39. Deliberates before making important decisions
- 46. Delivers effective customer service
- 49. Maintains a positive attitude
- 50. Displays flexibility in work assignments
- 51. Requires minimal supervision
- 69. Responds well to feedback
- 73. Diagnoses problems
- 90. Makes effective and timely decisions
- 98. Contributes innovative ideas
- 100. Sets realistic goals
- 101. Determines appropriate courses of action
- 104. Shows a clear understanding of the job
- 109. Grasps new information/tasks quickly
- 115. Uses criticism constructively
- 116. Works well independently
- 120. Understands the needs of clients

3. Written and Oral Communication

Many jobs in the work force require the individual to make formal oral or written presentations to large or small audiences. For these jobs, the proficiency with which one can write or speak, independent of the correctness of the subject matter, is a critical component of performance.

- 10. Presents material in a logical order
- 32. Gets his/her point across
- 41. Delivers clear, well organized presentations
- 43. Clearly expresses ideas and concepts orally
- 56. Effectively presents complex information
- 58. Clearly expresses ideas and concepts in writing
- 64. Effectively leads discussions
- 66. Uses a convincing presentation style
- 68. Interacts well with others
- 70. Displays impressive communication skills
- 76. Efficiently prepares written materials
- 83. Speaks clearly and concisely
- 112. Speaks well in front of a group

4. Demonstrating Effort

The fourth factor is meant to be a direct reflection of the consistency of an individual's effort on a day to day basis, the frequency with which people will expend extra effort when necessary, and the willingness to keep working under adverse conditions. Thus, this factor reflects the degree to which individuals commit themselves to all job tasks, work at a high level of intensity, and keep working as long as is necessary to complete the tasks at hand.

- 1. Strives to meet goals of the unit
- 4. Shows a strong desire to excel
- 8. Responds to challenging circumstances
- 26. Works effectively under stressful conditions
- 31. Pursues all job functions with energy
- 36. Follows through consistently
- 44. Volunteers for extra duties

- 54. Meets agreed upon deadlines
- 59. Maintains a high level of output
- 61. Commits personal time to the job if necessary
- 72. Is highly motivated to accomplish tasks
- 79. Responds immediately when required
- 82. Readily accepts new responsibilities
- 87. Works extra hours when necessary
- 107. Gets work done quickly
- 108. Takes on additional responsibilities in emergencies
- 121. Displays determination when faced with difficult tasks

5. Maintaining Personal Discipline

The fifth factor is characterized by the degree to which negative behavior such as substance abuse, rule violations, legal infractions, and excessive absenteeism are avoided.

- 7. Reports instances of unethical behavior
- 13. Avoids excessive absenteeism
- 30. Maintains stable relationships
- 33. Shows discipline in the work place
- 35. Reports to work on time
- 40. Complies with company policies and procedures
- 60. Avoids substance abuse
- 71. Obeys rules and regulations
- 74. Has high standards of personal integrity
- 85. Meets financial obligations
- 111. Exhibits honesty in the work environment
- 114. Treats others with respect
- 117. Preserves confidentiality

6. Facilitating Peer and Team Performance

Factor six is defined as the degree to which the individual supports his or her peers, helps them with job related problems, and acts as a de facto trainer. It also encompasses how well an individual facilitates group functioning by being a good model, keeping the group goal-directed, and reinforcing participation by other group members. Obviously, if the individual works alone, this component will be of little importance. However, in many jobs, high performance on this factor would be a major contribution towards the goals of the organization.

- 3. Provides training to others
- 6. Inspires peers to excel
- 11. Provides constructive feedback
- 14. Identifies with the needs of co-workers
- 15. Shares expertise and experience with others
- 24. Assists co-workers in task completion
- 27. Presents a positive image of the organization to others
- 37. Acknowledges the contributions of peers
- 38. Resolves conflicts
- 42. Seeks out the opinions of others
- 47. Cooperates well with others
- 48. Supports the directives of the unit
- 52. Gathers the support of co-workers
- 53. Provides assistance to team members
- 55. Shows consideration for the feelings of fellow workers

- 67. Demonstrates interpersonal sensitivity
- 78. Addresses and resolves conflicts
- 84. Encourages participation among co-workers
- 91. Treats others fairly and consistently
- 94. Defends organizational objectives
- 113. Readily accepts the opinions/suggestions of others
- 119. Clarifies ambiguous roles
- 124. Provides encouragement/guidance to co-workers

7. Supervision/Leadership

Proficiency in the supervisory component includes all the behaviors directed at influencing the performance of subordinates. Supervisors set goals for subordinates, show them more effective methods, model appropriate behaviors, and reward or punish behaviors. This factor differs from the previous one in the distinction between peer leadership and supervisory leadership. Although modeling, goal setting, coaching, and providing reinforcement are elements in both factors, Campbell's model posits that peer versus supervisory leadership implies significantly different determinants.

- 9. Maintains discipline in the work place
- 12. Challenges workers to excel
- 18. Displays prudence in supervision
- 21. Provides useful and accurate feedback
- 22. Develops the skills of subordinates
- 25. Clearly conveys expectations for assignments
- 45. Demonstrates authority and knowledge
- 57. Conveys a sense of purpose and mission
- 62. Motivates subordinates to accomplish goals
- 63. Identifies strengths/development needs in others
- 77. Provides subordinates with a sense of job-security
- 81. Plays a leadership role
- 88. Exhibits a strong sense of capability
- 92. Generates a sense of personal involvement
- 93. Helps others to achieve their full potential
- 99. Promotes a positive image of the organization
- 103. Takes decisive action when warranted
- 105. Takes appropriate risks to achieve results
- 110. Generates a feeling of energy
- 122. Inspires others to take action
- 125. Uses effective leadership skills

8. Management/Administration

The eighth factor is intended to include the major elements in management that are distinct from direct supervision. This factor includes performance behaviors directed at articulating goals for the unit or enterprise, organizing people and/or resources, monitoring progress, helping to solve problems/crises, controlling expenditures, obtaining additional resources, representing the unit in dealing with others, and so on.

- 5. Exhibits effective administrative skills
- 19. Provides useful feedback
- 20. Understands causes of problems
- 23. Attracts and selects high caliber talent
- 28. Understands organizational priorities
- 34. Facilitates the discussion and resolution of different views

- 65. Effectively delegates responsibility
- 75. Manages resources effectively
- 80. Differentiates between good and poor job performance
- 86. Effectively manages organization-wide activities
- 89. Integrates diverse efforts
- 95. Represents the unit well
- 96. Accomplishes goals through cooperation
- 97. Clarifies roles and responsibilities
- 102. Translates strategies into objectives
- 106. Addresses conflict in the unit
- 118. Observes and evaluates other employees
- 123. Monitors efforts and takes corrective action

Appendix B

Job Titles Along With Frequencies Within and Across Job-Type Classifications

Clerical Job Titles	Frequency	Percent Within	Percent Across
Accounting clerk	3	4.1	0.6
Bank assistant	1	1.4	0.2
Bank clerk	1	1.4	0.2
Bank teller	1	1.4	0.2
Banking	1	1.4	0.2
Clerk	17	23.0	3.5
Data entry	2	2.7	0.4
Office aide	1	1.4	0.2
Office assistant	1	1.4	0.2
Office clerk	1	1.4	0.2
Receptionist	20	27.0	4.1
Student worker	25	33.8	5.2
Management Job Titles			
Administrative assistant	2	4.2	0.4
Administrator	1	2.1	0.2
Assistant	21	43.8	4.3
Assistant manager	6	12.5	1.2
Director	1	2.1	0.2
Manager	11	22.9	2.3
Office manager	1	2.1	0.2
Service manager	1	2.1	0.2
Supervisor	3	6.3	0.6
Technical director	1	2.1	0.2
Production Job Titles			
Construction	1	5.0	0.2
Construction foreman	1	5.0	0.2
Construction worker	2	10.0	0.4
Field worker	1	5.0	0.2
Labor	9	45.0	1.9
Laborer	3	15.0	0.6
Loader	2	10.0	0.4
Rancher	1	5.0	0.2

Professional Job Titles	Frequency	Percent Within	Percent Across
Accountant	1	2.6	0.2
Advisor	1	2.6	0.2
Computer programmer	1	2.6	0.2
Counselor	10	25.6	2.1
Dance teacher	1	2.6	0.2
EMT	1	2.6	0.2
Engineer	1	2.6	0.2
Inspector	1	2.6	0.2
Instructor	6	15.4	1.2
Intern	2	5.1	0.4
Internship	4	10.3	0.8
Interviewer	1	2.6	0.2
Lab assistant	2	5.1	0.4
Piano teacher	1	2.6	0.2
Public relations	1	2.6	0.2
Research assistant	1	2.6	0.2
Researcher	1	2.6	0.2
Surveyor	2	5.1	0.4
Teacher's assistant	1	2.6	0.2

**Sales/service
Job Titles**

Animal care	2	0.7	0.4
Animal caretaker	3	1.0	0.6
Announcer	1	0.3	0.2
Associate	2	0.7	0.4
Attendant	1	0.3	0.2
Bartender	6	2.0	1.2
Bus driver	2	0.7	0.4
Busboy	1	0.3	0.2
Buyer	1	0.3	0.2
Carpenter	2	0.7	0.4
Cashier	48	15.8	9.9
Checker	2	0.7	0.4
Child care	5	1.7	1.0
Computer operator	1	0.3	0.2
Computer tech	2	0.7	0.4
Computer technician	3	1.0	0.6
Cook	8	2.6	1.7
Counter sales	2	0.7	0.4
Crew member	1	0.3	0.2
Customer service	6	2.0	1.2
Delivery	2	0.7	0.4
Driver	2	0.7	0.4

Sales/service Job Titles - cntd.	Frequency	Percent Within	Percent Across
Food clerk	3	1.0	0.6
Food preparation	1	0.3	0.2
Food sales	2	0.7	0.4
Food service	5	1.7	1.0
Greeter	1	0.3	0.2
Ground keeper	1	0.3	0.2
Host	3	1.0	0.6
Hostess	9	3.0	1.9
Inventory control	1	0.3	0.2
Janitor	1	0.3	0.2
Landscaper	2	0.7	0.4
Lawn care	1	0.3	0.2
Lawn worker	1	0.3	0.2
Library assistant	1	0.3	0.2
Lifeguard	18	5.9	3.7
Maintenance	6	2.0	1.2
Maintenance worker	1	0.3	0.2
Mechanic	1	0.3	0.2
Medical assistant	2	0.7	0.4
Merchandiser	2	0.7	0.4
Military	2	0.7	0.4
Model	1	0.3	0.2
Nail technician	2	0.7	0.4
Official	1	0.3	0.2
Operator	1	0.3	0.2
Painter	2	0.7	0.4
Recreation	1	0.3	0.2
Referee	2	0.7	0.4
Reservationist	1	0.3	0.2
Reset crew	1	0.3	0.2
Retail	1	0.3	0.2
Sacker	2	0.7	0.4
Sales	33	10.9	6.8
Sales associate	1	0.3	0.2
Sales clerk	2	0.7	0.4
Sales representative	1	0.3	0.2
Salesperson	5	1.7	1.0
Secretary	13	4.3	2.7
Security	1	0.3	0.2
Stocker	3	1.0	0.6
Team leader	1	0.3	0.2
Technical	1	0.3	0.2
Technician	7	2.3	1.4
Telemarketer	4	1.3	0.8
Telemarketing	1	0.3	0.2

Sales/service Job Titles - cntd.	Frequency	Percent Within	Percent Across
Transit operator	1	0.3	0.2
Travel agent	1	0.3	0.2
Tutor	2	0.7	0.4
Waiter	7	2.3	1.4
Waitress	9	3.0	1.9
Waitstaff	27	8.9	5.6
Youth director	1	0.3	0.2

References

- Arthur, W., Jr., & Bennett, W., Jr. (1995). The international assignee: The relative importance of factors perceived to contribute to success. Personnel Psychology, 48, 99-114.
- Arthur, W., Jr., & Bennett, W., Jr. (1997). A comparative test of alternative models of international assignee job performance. In Z. Aycan (Ed.), New approaches to expatriate management (Vol. 2, pp. 141-172). Greenwich, CT: JAI Press.
- Barnard, C. (1938). The functions of the executive. Cambridge, MA: Harvard University Press.
- Bateman, T. S., & Organ, D. W. (1983). Job satisfaction and the good soldier: The relationship between affect and employee "citizenship". Academy of Management Journal, 26, 587-595.
- Binning, J. F., & Barrett, G. V. (1989). Validity of personnel decisions: A conceptual analysis of the inferential and evidential bases. Journal of Applied Psychology, 74, 478-494.
- Borman, W. C., & Motowidlo, S. J. (1993). Expanding the criterion domain to include elements of contextual performance. In N. Schmitt & W. C. Borman (Eds.), Personnel selection in organizations (pp. 71-98). San Francisco, CA: Jossey Bass.
- Borman, W. C., & Motowidlo, S. J. (1997). Task performance and contextual performance: The meaning for personnel selection. Human Performance, 10, 99-109.
- Brief, A. P., & Motowidlo, S. J. (1986). Prosocial organizational behaviors. Academy of Management Review, 11, 710-725.
- Brogden, H. E., & Taylor, E. K. (1950). The dollar criterion: Applying the cost accounting concept to criterion construction. Personnel Psychology, 3, 133-154.
- Campbell, J. P. (1990a). Modeling the performance prediction problem in industrial and organizational psychology. In M. D. Dunnette & L. M. Hough (Eds.), Handbook of Industrial and Organizational Psychology (2nd Ed., Vol. 1, pp. 687-732). Palo Alto, CA: Consulting Psychologists Press.
- Campbell, J. P. (1990b). The role of theory in industrial and organizational psychology. In M. D. Dunnette & L. M. Hough (Eds.), Handbook of Industrial and Organizational Psychology (2nd Ed., Vol. 1, pp. 39-73). Palo Alto, CA: Consulting Psychologists Press.
- Campbell, J. P. (1990c). An overview of the army selection and classification project. Personnel Psychology, 43, 231-239.
- Campbell, J. P., McCloy, R. A., Oppler, S. H., & Sager, C. E. (1993). A theory of performance. In N. Schmitt & W. C. Borman (Eds.), Personnel Selection in Organizations (pp. 35-70). San Francisco, CA: Jossey Bass.
- Campbell, J. P., & Zook, L. M. (Eds.). (1990). Improving the selection, classification, and utilization of army enlisted personnel: Final report on Project A. Alexandria, VA: U.S. Army Research Institute for the Behavioral and Social Sciences.
- Douglas, E. F., McDaniel, M. A., & Snell, A. (1996). The validity of non-cognitive measures decays when applicants fake. Academy of Management Proceedings, ##, ###-###??
- Graham, J. W. (1986, August). Organizational citizenship informed by political theory. Paper presented at the meeting of the Academy of Management, Chicago, IL.

- Ones, Viswesvaran, C., & Schmidt, F. L. (1993). Meta-analysis of integrity test validities. Journal of Applied Psychology, 78, 679-703.
- Organ, D. W. (1988). Organizational citizenship behavior: The good soldier syndrome. Lexington, MA: Lexington Books.
- Motowidlo, S. J., & Van Scotter, J. R. (1994). Evidence that task performance should be distinguished from contextual performance. Journal of Applied Psychology, 79, 475-480.
- Sackett, P. R. (1994). Integrity testing for personnel selection. Current Directions in Psychological Science, 3, 73-76.
- Schmidt, F. L., & Hunter, J. E. (1992). Development of a causal model of processes determining job performance. Current Directions in Psychological Science, 1, 89-92.
- Smith, C. A., Organ, D. W., & Near, J. P. (1983). Organizational citizenship behavior: Its nature and antecedents. Journal of Applied Psychology, 68, 653-663.
- Toops, H. A. (1944). The criterion. Educational and Psychological Measurement, 4, 271-297.
- Viswesvaran, C. (1993). Modeling job performance: Is there a general factor? Unpublished doctoral dissertation, University of Iowa.
- Woehr, D. J., & Miller, M. J. (1997). The meaning and measurement of work ethic. Paper presented at the annual Southeastern Industrial/Organizational Psychology Meeting, Atlanta, GA.

**DEVELOPMENT OF QUALITATIVE PROCESS MODELING SYSTEMS
FOR CYTOKINES, CELL ADHESION MOLECULES, AND GENE REGULATION**

Robert B. Trelease
Assistant Professor
Department of Neurobiology and Pathology

University of California, Los Angeles
63-167D Center for Health Sciences
Los Angeles, CA 90095

Final Report for:
Summer Research Extension Program
Wright Patterson Medical Center

Sponsored by:
Air Force Office of Scientific Research
Bolling Air Force Base, DC,

and

Wright-Patterson Medical Center

December 1997

DEVELOPMENT OF QUALITATIVE PROCESS MODELING SYSTEMS FOR CYTOKINES, CELL ADHESION MOLECULES, AND GENE REGULATION

Robert B. Trelease
Assistant Professor
Department of Neurobiology
University of California, Los Angeles

Abstract

A previously prototyped computer-based qualitative simulation system and biology knowledge base (KB) were extended for modeling various aspects of reactive oxygen species (ROS), cytokine- and growth factor-mediated activation of the ubiquitous regulatory genes (protooncogenes) AP-1 and NF-kB. Development of the KB and simulation experiments was conducted in 4 phases: 1) refinement of original KB generically modeling ROS-stimulated AP-1- and NF-KB-mediated gene promotion; 2) elaboration of specific AP-1 and NF-KB pathways process rule to stimulate specific gene regulation experiments involving HIV, TNF-alpha, hydrogen peroxide (H2O2) effects; 3) expansion of the basic pathways to include membrane receptor-mediated and mitogen-activate protein kinase (MAPK) activation of individual promotor systems; 4) investigation of the use of the NASA CLIPS knowledge-based programming system with translated rules for qualitative simulation of the original TSC gene regulation models; and 5) development of new process rules to represent the TNF-alpha elicited up-regulation of the endothelial tissue factor promoter gene by combined NF-kB and dual AP-1 promoter site activation. Simulation experiments successfully replicated the reported qualitative findings of several important published molecular genetics research studies, demonstrating the practicality of using computer-based qualitative process methodology for formal representation and testing of scientific research hypotheses and conclusions.

DEVELOPMENT OF QUALITATIVE PROCESS MODELING SYSTEMS FOR CYTOKINES, CELL ADHESION MOLECULES, AND GENE REGULATION

Robert B. Trelease

Introduction

Certain types of physical systems problems and their models must deal with incompletely understood processes and/or unquantifiable relationships, and the argument has been put forth that real dynamical physical systems cannot be completely described in quantitative terms (Oreskes et al., 1994). To handle such difficult tasks, researchers have developed new computer-based reasoning methods, such as qualitative process (QP) theory (Forbus, 1984), that employ symbolic programming and cognitive sciences techniques used in artificial intelligence (AI) research (Weld and DeKleer, 1992; Uckun, 1992; DeKleer and Forbus, 1993).

Qualitative reasoning methods have been used successfully to solve physical sciences problems that are insoluble when approached with accepted quantitative techniques (e.g., computer-based mathematical modeling) (DeKleer and Weld, 1992). Qualitative modeling and simulation have been used for testing systems theories, for diagnosing problems (Uckun, 1992), for controlling processes (LeClair and Abrams, 1989; LeClair, Abrams, and Matejka, 1989), and for developing "discovery systems" that evolve new process theories (Weld and DeKleer, 1992).

Although qualitative reasoning methods have been applied to the solution of a variety of problems in physical sciences, related approaches have not been widely used in biomedical research domains. The greatest experience has been with qualitative modeling of physiology, intelligent monitoring, clinical/therapeutic applications (Bylander et al., 1988; Gaglio et al, 1991; Uckun, 1992; Barahona, 1994) and with representing scientific discovery processes for gene regulation (Karp, 1990, 1993) and renal biochemistry (Kulkarni and Simon, 1990). During the last three years, with prior AFOSR support, we have developed a biological qualitative process modeling system upon which one can perform experiments exploring processes involved in cellular and humoral immunity. Because the system's broad-scope biological knowledge base includes cells, systems, and a range of organisms, including different viruses, bacteria, and other parasitic organisms, a variety experiments could be created, for example, for simulating the interactions of human immunodeficiency virus with other pathogens in modifying cellular responses to those infections. During the Summer Research Program of 1996, we expanded the basic modeling system to include the processes of immune response-related changes in cell adhesion molecules (CAMs) and fundamental gene regulation mechanisms. This latter effort was particularly relevant to a very active current quest in molecular biology research for the understanding of the functions of various genes.

Certain classes of evolutionarily conserved genes are transcribed when a wide variety of cellular processes occur, ranging from activation and cytokine release in immune system cells, through protein-synthesis and signal

transduction involved in tissue reconstruction/healing. By "evolutionarily conserved" is meant genes that control fundamental cellular processes across a wide range of phylogenetic Phylae and Classes (taxa) with very little change in structural (DNA) sequences. These regulatory sequences, originally identified as "protooncogenes" (due to their association with growth regulation in cancerous cells) are thus ubiquitous in biological systems and very important to the understanding of the control of many crucial life processes.

Much recent evidence indicates that two classes of such genes, regulated by NF- κ B (nuclear factor kappa B) and activation protein 1 (AP-1) proteins may be transcriptionally regulated by reactive oxygen species (ROS) at various steps in cellular proteolytic and signal transduction pathways. These gene regulatory processes may thus be particularly important to modeling and understanding immunologic, other antimicrobial, reconstructive and other healing mechanisms enhanced by high pressure oxygen administration in HBO. Shortly after the beginning of the 1996 Summer Research Program, Sen and Packer (1996) published a comprehensive paper describing an integrative conceptual model accounting for the complex effects of ROS at multiple steps in the AP-1 and NF- κ B regulatory pathways within cells and nuclei.

A principal objective of the original 1996 AFOSR Summer Faculty Research project was to implement a computer-based qualitative process model of this basic Sen and Packer conceptual model. The regulatory substances ontology and taxonomy were greatly expanded by adding new actors, states, relations, and predicates to the pre-existing immunology KB files as described above. Furthermore, process rule sets were created for representing ROS-related interactions with cell enzymes and other regulatory process steps involved in AP-1 and NF- κ B mediated transcription of several generic promoter/enhancer genes. Several experiments were designed to demonstrate different outcomes of these gene regulatory processes in the presence and absence of different factors (ROS and AP-1 and NF- κ B regulatory proteins). This "generic" model was intended to serve as the basis for an expanded modeling system capable of representing changes in gene regulatory processes associated with the production of specific cytokines, cell behaviors, and other outcomes characteristic of HBO and other tissue processes.

The main emphases of the research reported here has been on integrating gene transcription-level multi-pathway responses, cytokine signaling and release in the presence of reactive oxygen species (ROS) such as those known to be produced in response to infections and in hyperbaric oxygenation treatments. The original project was undertaken in collaboration with Dr. (Colonel) Richard Henderson, AFMC, at the Hyperbaric Medicine facility of the 74th Medical Group, Wright-Patterson AFB (SGPH).

Methods

Computer Hardware, Modeling, and Problem Domain Knowledge Representation

All KB development QP modeling work was performed on Apple Macintosh computers, including PowerBook 3400c and Power Macintosh 8500 models, using TSC (Brownsville, CA), a symbolic, object-oriented programming environment composed of nested, extensible multiple language interpreters/compiler, run-time utilities, and an envisionment builder. A subtask of the study was to experiment with implementing the Macintosh-specific TSC KB and qualitative models with CLIPS (C Language Integrated Production System), an AI development shell produced by NASA (see below) and supported on a variety of platforms (Macintosh, Windows/DOS, UNIX, VMS).

Comparable to a more conventional AI expert system, TSC allows the definition of actors (e.g., different types of cells), taxonomic and functional relationships, physical and biochemical processes, and predicated interactions and behaviors in hierarchical sets of symbolic production rules. TSC also compiles the description of initial conditions and functional designs for simulated experimental trials to be run using defined KB actors (cells, molecules, and pathogens) and process behaviors. As distinguished from an expert system that uses a logical inference engine to evaluate acquired data in the context of logical relationships defined by the KB, TSC employs an "envisionment builder" to record and to visualize the evolution of process behaviors and cell interactions resulting from initial experimental conditions given the defined actors, substances, processes, and functional relationships. An envisionment is thus the depiction of all possible behaviors that can be produced given the initial conditions of a simulation/experiment and the specific actors, states, relations, predicates, and process rules defined in the related KB. Envisionments are represented by the output of "log files" that record all the antecedents, consequent terms, and super-episodes for all episodes (discrete system states encountered) as well as by "browser" graphics depicting the order and ontological relationships between episodes (see Figures 4-10).

TSC performs its functions under the direction of TASK statements. FILLIN tasks, for example, set up the system behaviors necessary to perform a simulation based on actors, states, relations, predicates, and process rules defined in the KB. Other tasks can be created to set up system behaviors to study specific envisionments. STUDY tasks can result in the identification of the sequence of process rule firings necessary for achieving a desirable process outcome. Other study tasks can be created to compare real world data with "expectations" defined in envisionment (process simulation) episodes, a crucial behavior in setting up TSC to produce discovery about processes. Rule mutation behaviors can be employed following study tasks to produce new process rules that can be used in building new envisionments. Finally, control tasks can be set up to handle process control based on process simulation envisionments.

The work described in this report builds on immune system knowledge bases first developed for modeling cell-cell-cytokine interactions during infectious processes (AFOSR SFRP/SREP, 1994-1995) (Trelease, 1994b, 1996). That

specific formal immune system model was composed of three conceptual parts: 1) A core biological knowledge base (KB) describing actors, taxonomic relationships, process definitions and predicates, 2) sets of behavioral rules for immune system actors, pathogens, and processes, and 3) sets of rules and conditions for the execution of experimental simulations. All rules and concepts (actors, predicates, etc.) were defined as frames in a Scheme dialect of the LISP programming language, and model components were divided into a group of loadable text files. This modular approach was taken in order to support orderly expansion of the KB and problem domain with additional heuristics, for example, for molecular biology, additional histology, pathological processes and treatments.

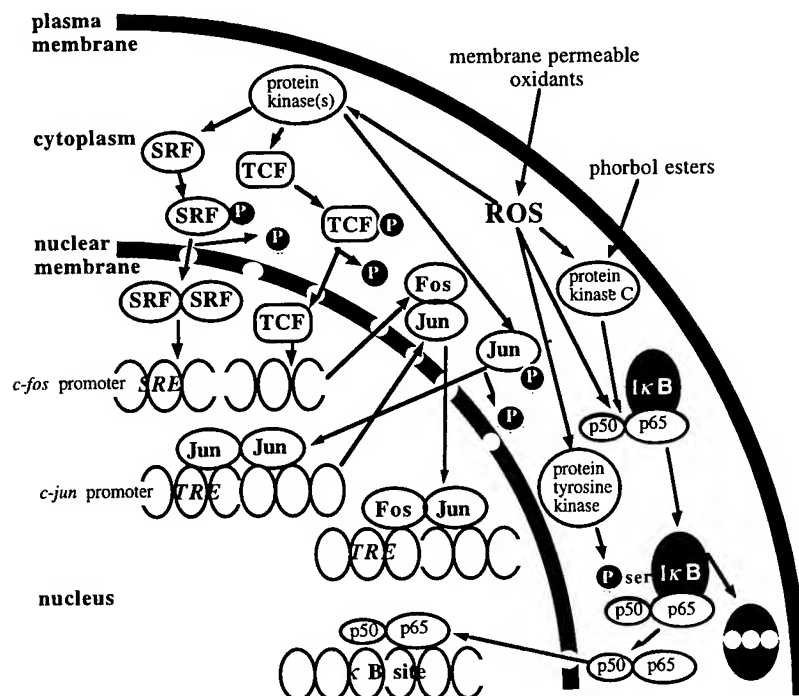
This core biological KB was composed of three incrementally compiled files. BIOPRIMITIVE.T included definitions of underlying physical, chemical, and biological actors (e.g., atoms, molecules, proteins, cells, organisms, endocytosis), taxonomic definitions and inheritance (e.g., class, order, family, genus, species), and some basic predicate relationships between various actors. CELL.T included fundamental definitions of biological structures (e.g., nuclei, membranes, mitochondria, etc.) substances and predicates central to cell biology. IMMUNE.T was comprised of definitions of immune system cells, receptors, cytokines and other actors, substances, organs, and predicates.

These specific heuristics for immune system cell processes, interactions, and behaviors were contained in IMMUNE.RBT. Different sets of initial conditions (specific actors, predicates and relationships) and specific experimental designs were maintained in separate files (e.g. IMMUNE.EXP1, IMMUNE.EXP2, etc.) allowing different experimental simulations to be run with the same underlying biological/immunological KB. All concepts and process rules were derived from current theories and objective information published in the current general biological (Purves et al., 1992), systematic (Fortuner, 1993), histological and cell biological (Junquiera et al., 1992; Weiss, 1993; Goodman, 1994) and specialized immunological (Abbas et al., 1991; Janeway and Travers, 1996) literatures.

Consistent with this modular approach and the principle of incremental KB expansion, the work for the 1996 SFRP project involved adding many new actors and process heuristics to the aforementioned files. Numerous new actors and predicates were added to BIOPRIMITIVE.T, CELL.T, and IMMUNE.T to support an expanded taxonomy and ontology of regulatory molecules, states, relationships and predicates for cytokines, cell adhesion molecules, enzyme regulation, and multiple gene transcription/regulation processes. Three different "subsets" of cellular/immune processes were modeled in order to yield discrete simulations of different functionalities: Cytokine interactions in differential gender-related innate immune responses to viral infection, cell adhesion molecule expression changes in innate immune responses, and gene regulation (protooncogene transcriptional control by antioxidants, cytokines and other bioactive molecules).

As previously noted, a major objective of the 1996 SFRP project was to implement a computer-based qualitative process model of this basic Sen and Packer conceptual model. Figure 1 graphically depicts many of the essential elements of their conceptual model. The regulatory substances ontology and taxonomy were greatly expanded by adding new actors, states, relations, and predicates to the pre-existing bioprimitives and immune system KB files as described above. Furthermore, process rule sets were created for representing ROS-related interactions with cell enzymes and other regulatory process steps involved in AP-1 and NF- κ B mediated transcription of several generic promoter/enhancer genes. The new gene regulation process rules were compiled in a new KB file, REGULATION.T, that was compiled following the BIOPRIMITIVE.T, CELL.T, and IMMUNE.T modules. Several experiments were designed to demonstrate different outcomes of these gene regulatory processes in the presence and absence of different factors (ROS and AP-1 and NF- κ B regulatory proteins). This "generic" model was intended to serve as the basis for an expanded modeling system capable of representing changes in gene regulatory processes associated with the production of specific cytokines, cell behaviors, and other outcomes characteristic of HBO and other tissue processes.

Figure 1: Graphic depiction of the hypothetical scheme for steps in cellular NF- κ B and AP-1 regulatory genes (protooncogene) activation that may be influenced by oxidants (ROS-reactive oxygen species) and antioxidants (after Sen and Packer, 1996)



Extension of this core KB and development of simulation experiments for the 1997 SREP follow-up project were conducted in 5 phases: 1) refinement of original KB generically modeling ROS stimulated AP-1- and NF- κ B-

mediated gene promotion; 2) elaboration of specific AP-1 and NF-KB pathways process rules to stimulate specific gene regulation experiments involving HIV, TNF-alpha, hydrogen peroxide (H2O2) effects; 3) expansion of the basic pathways process rules to include membrane receptor-mediated and mitogen-activated protein kinase (MAPK) "cascades" activating of individual gene promotor systems; 4) investigation of the use of the NASA CLIPS knowledge-based programming system with translated rules for qualitative simulation of the original TSC gene regulation models; and 5) development of new process rules to represent the TNF-alpha elicited up-regulation of the TF promoter gene by combined NF-kB and dual AP-1 promoter site activation. In general, Phases 1, 2, 3, and 5 of this research project conducted in serial order: Investigation of CLIPS as a QP modeling system began almost immediately, and ran parallel to the other phases, with translation of functioning TSC KBs to the CLIPS syntax.

Table 1 shows a list of a variety of different specific QP modeling experiments, simulations of research findings reported in the scientific literature, performed with the extended TSC KB.

Induction of specific immune responses in HIV infection (AIDS) stimulates expression of HIV proviral genes incorporated in the genome of infected cells, in a mechanism consistent with the ROS/oncogene regulation model of Sen and Packer (1996). Sappey et al. (1995) performed experiments in which hydrogen peroxide (H2O2; typically evolved during acute immune responses to infections) stimulated proviral gene expression in infected T-cells via AP-1 protooncogene promotion, with the radical scavenger deferoxamine (DFO) preventing gene expression. Experiments E6-E6B (Table 1) simulated the basic mechanisms of proviral gene expression, and the effects of H2O2 in the presence or absence of DFO.

Stimulation of AP-1 and NF-kB genes is evoked by different mitogen-activated protein kinase (MAPK) mechanisms in transduction of extracellular signals important to general immune responses, cell regulation by growth factors and cytokines, expression of CAMs, and neural transmission (Cooper, 1995). Again, these mechanisms are highly evolutionarily conserved, and specific MAPK-using signaling pathways are involved in many different types cellular processes in organisms ranging from the unicellular through humans. Experiment 8 (Table 1) simulated the basic MAPK "kinase cascade" evoked by growth hormone, leading to AP-1-mediated (fos-jun) gene promotion (Experiment 9).

A group of experiments focused on different aspects of the functionality of tumor necrosis factor alpha (TNF-alpha), a cytokine involve in a range of responses to a variety of pathogens, cancer cells, and inflammation. Lo et al. (1995) demonstrated that TNF-alpha evokes ROS production in chondrocytes (cartilage cells) and subsequent AP-1 upregulation in inflammation (related to arthritic mechanisms). This was simulated in Experiment E7 (Table 1). The cytokine IL-1 has been shown to evoke expression of the TNF-alpha gene via an AP-1 mechanism during immune responses to infection (Lieb et al., 1996), and this was simulated in Experiment E11 (Table 1). TNF-alpha

has been shown to induce the release of the clotting mediator Tissue Factor (TF) from endothelial (blood vessel lining) cells via a mechanism involving a single NF-kB and dual AP-1 enhancer sites on the ET promoter gene (Bierhaus et al., 1995). In contrast to other mechanisms simulated in this project, this model thus involved the functioning of three interacting gene promoter pathways, including separate, selective jun-jun and jun-fos AP-1 sites. The basic TNF-alpha-ET-promoter mechanism was modeled in Experiment E10 (Table 1).

Results

Gene Regulation: Protooncogene Transcriptional Control, Antioxidants, and Cytokines

The basic gene regulation model experiment environments (E1-E4) demonstrated the fundamental transcriptional promoter processes known to occur with ROS activation of phosphorylation (protein kinase) enzymes (Sen and Packer, 1996). Depending on initial conditions, such as the absence of a promoter promoter or the a full complement of necessary agents, the model would produce environments showing partial activation (Figures 2 and 3) or activation of a full complement of the appropriate genes (Figure 4). The fundamental conceptual model of Sen and Packer was full implemented at their chosen level of abstraction for the generic effects of ROS on intracellular enzymes catalyzing the activation of regulatory proteins.

The E6 series of experiments demonstrated the experimentally demonstrated effect of immune stimulation on expression of HIV proviral genes. In general, ROS would elicit proviral gene promotion via a protein kinase mediated production of AP-1 transcription factors (Figure 6; E6). Administration of H₂O₂ would produce hydroxyl radical, stimulating protein kinase to activate the AP-1 production pathway, also leading to expression of HIV proviral genes (Figure 8; E6B). Presence of the DFO prevented the production of hydroxyl radical, and thus, prevented AP-1 and proviral gene activation (yielding the abbreviated environment, E6A, shown in Figure 7).

In Experiment E7, presence of TNF-alpha caused chondrocyte production of ROS, inducing activation of protein kinase C and leading to the production of cfos via AP-1-mediated activation of the c-fos promoter gene (Figure 9).

In Experiment E8, we successfully simulated the process of coupling membrane receptor activation with upregulation of a nuclear gene via the MAPK kinase-phosphorylation cascade. The stimulatory molecule was growth hormone (GH), representing a class of regulatory signaling interactions between cells leading to the stimulation of genes for various metabolic and structural changes. Experiment E9 demonstrated the AP-1 promotion of a specific regulatory gene in the presence of cfos and cjun proteins.

Process rules for Experiment E10, simulating TNF-alpha-stimulated upregulation of complex NF-kB-dual-AP-1 regions on the Tissue Factor promoter gene, were still under development at the time of this report.

Table 1: Experiments Simulated with Current TSC Immunology/Gene Regulation Knowledge Base

Reg Exp	Prime Actors	Genes Activated	No. of Episodes	Scientific References
E1	cfos no cjun ROS	c-fos	20	Sen and Packer, 1996
E2	cfos cjun ROS	c-fos c-jun	139	Sen and Packer, 1996
E3	cfos cjun ROS NF-kB	c-jun	347	Sen and Packer, 1996
E4	ROS NF-kB	Gene A	97	Sen and Packer, 1996
E5	vacant	vacant		
E6	T-cell HIV ROS	HIV proviral	6	Sappey, et al., 1995
E6a	T-cell HIV DFO low H2O2	none: protein kinase C activation inhibited	2	Sappey, et al., 1995
E6b	T-cell HIV no DFO	Proviral	7	Sappey, et al., 1995
E7	Chondrocytes TNF-alpha cfos	c-fos	21	Lo et al., 1995
E8	Growth hormone Shc tyrosine kinase cRas cRaf MAPK MAPK kinase	MAPK	6	Cooper, G., 1995
E9	Same as E8 cfos cjun	Gene B	155	Cooper, G., 1995
E10	endothelial cell TF TNF-alpha NF-KB AP-1 (x2)	TF	—	Bierhaus et al., 1995
E11	IL-1 IL-1 Beta TNF-alpha	TNF-alpha	24	Lieb et al., 1996

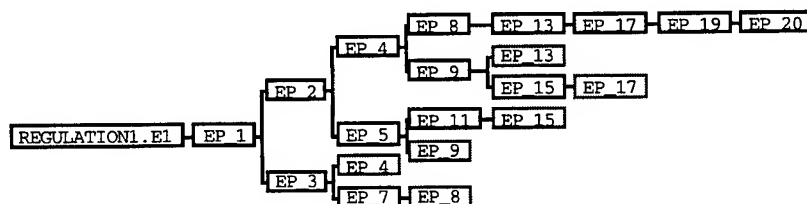


Figure 2: Graphic depiction of basic environment of Experiment E1: Promotion of transcription of a single gene by reactive oxygen species, with activation of protein kinase in the presence of only cjun promoter protein.

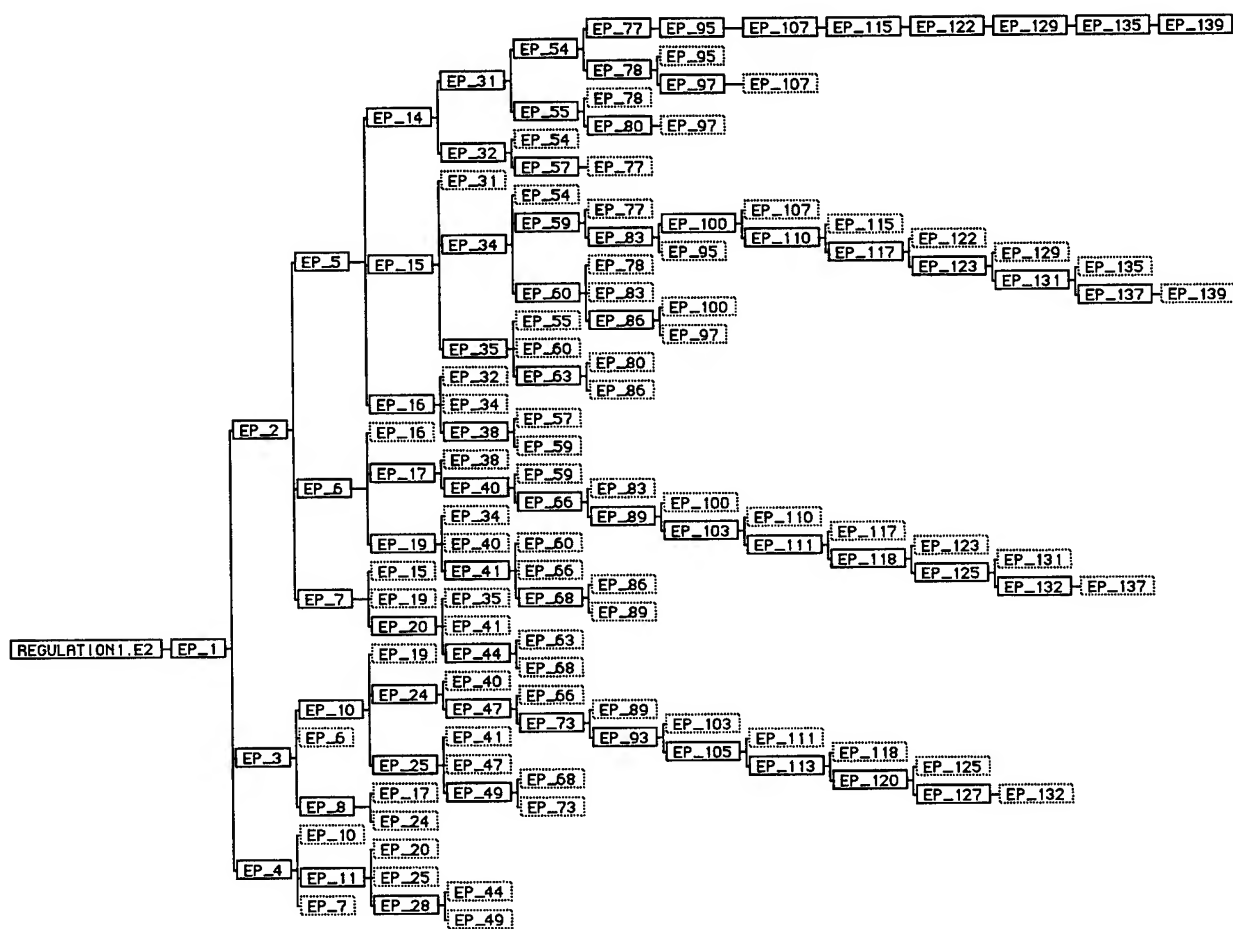


Figure 3: Graphic depiction of basic environment of Experiment E2: Promotion of transcription of a single gene by reactive oxygen species, with activation of protein kinase in the presence of only cjun promoter protein.

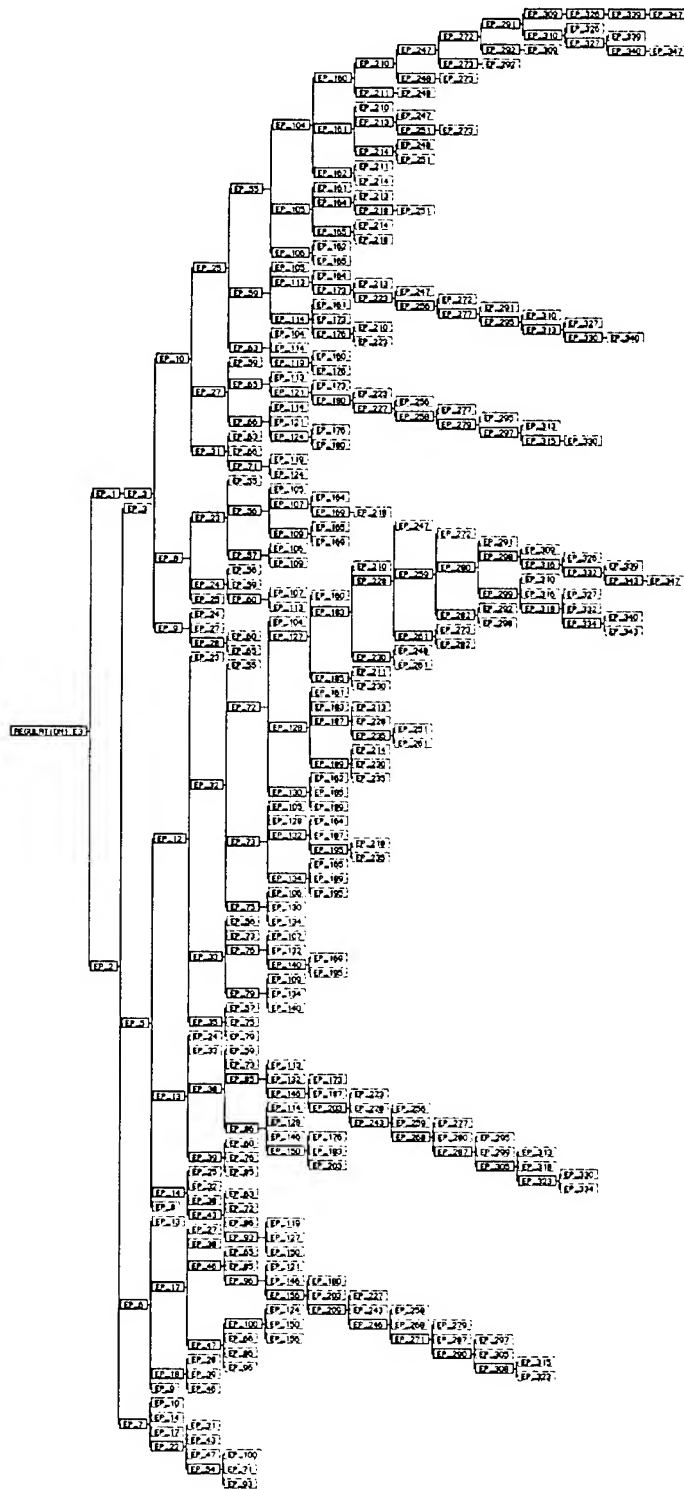


Figure 4: Graphic depiction of basic environment of Experiment E3: Promotion of transcription of 3 genes by reactive oxygen species, with activation of protein kinase in the presence of both cfos and cjun promoter proteins.

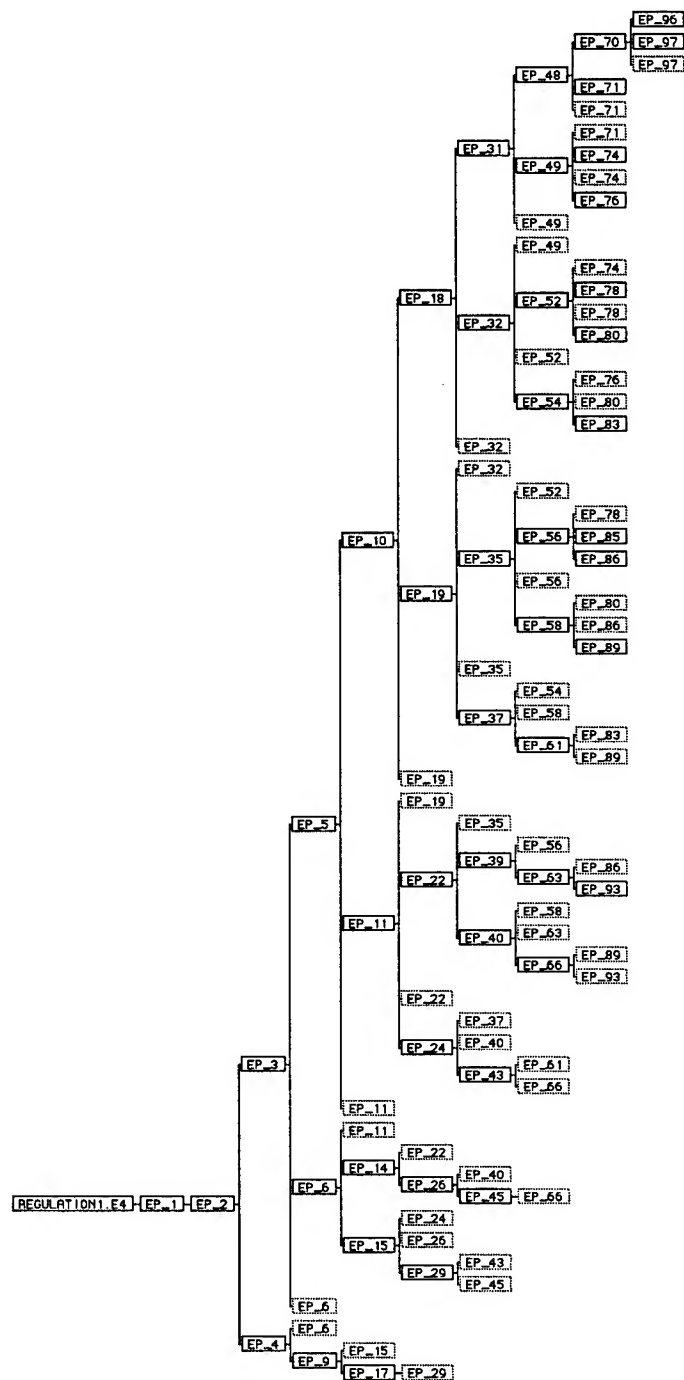


Figure 5: Graphic depiction of basic environment of Experiment E4: Promotion of transcription of 3 genes by reactive oxygen species, with activation of protein kinase in the presence of both cfos and cjun promoter proteins.

Figure 6: Graphic depiction of basic envisionment of Experiment E6: Induction of HIV proviral gene expression by ROS species stimulation of protooncogene systems.

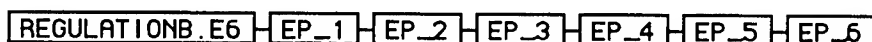


Figure 7: Graphic depiction of basic envisionment of Experiment E6A: Prevention of HIV proviral expression by DFO--a free radical scavenger that prevents conversion of H2O2.



Figure 8: Graphic depiction of basic envisionment of Experiment E6B: Activation of AP-1 production pathway by H2O2 evolution of hydroxyl radical, leading to promotion of HIV proviral gene expression



Figure 9: Graphic depiction of basic envisionment of Experiment E7: TNF-alpha upregulation

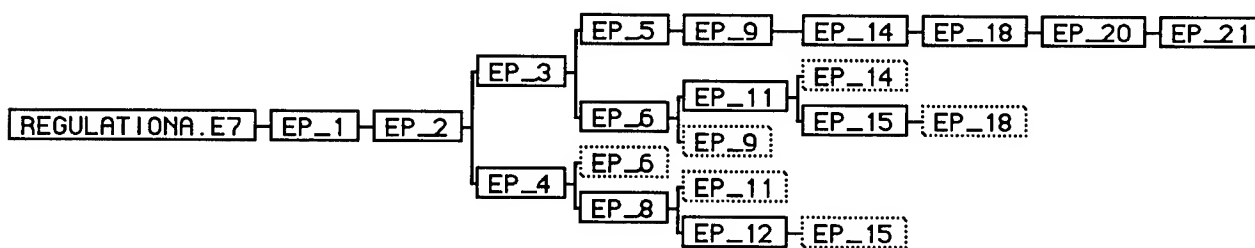


Figure 10: Graphic depiction of basic envisionment of Experiment E8: Initiation of MAPK cascade

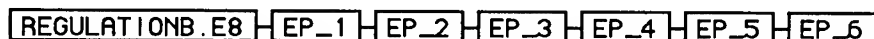


Figure 11: Graphic depiction of basic envisionment of Experiment E9: Initiation of MAPK kinase cascade by growth hormone, leading to AP-1 promoter production.

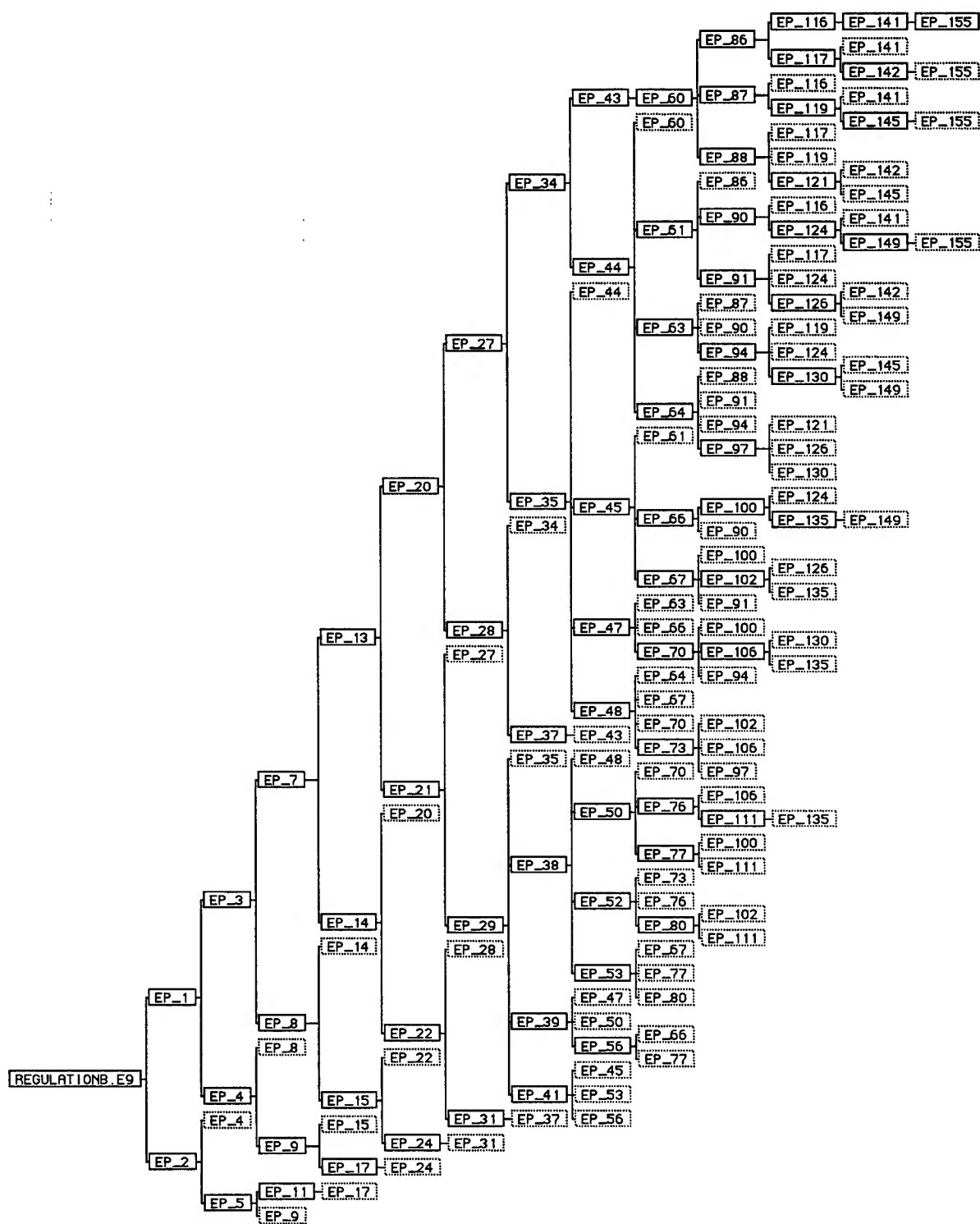


Figure 12: Graphic depiction of basic envisionment of Experiment E11: IL-1-beta receptor binding leads to AP-1 activation of the TNF-alpha promoter gene.

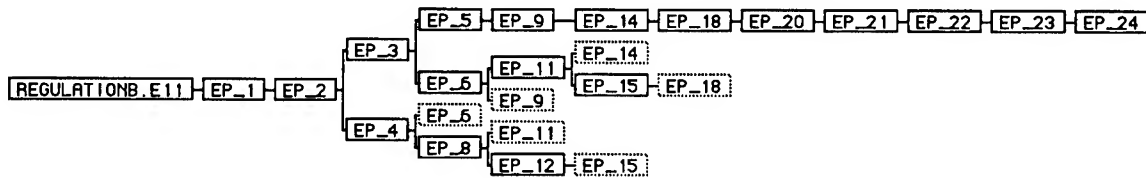


Figure 13: Comparison between the syntax of comparable TSC and CLIPS rules for NF-kB gene regulation

TSC

```
c:  Tyr.p.kin.IkB.phosphoryl
    level      basic
    sub.of     phys.process
    instance.of process.rule
    my.creator  rbt
    context    Gene.transcription.regulation
    if.actors  ( ( IkB-p50-p65 ( *IkB-p50-p65 ) true )
               ( IkB ( *IkB ) true )
               ( tyrosine.protein.kinase ( *tyrosine.protein.kinase ) true )
    if.states  ( ( activated ( *tyrosine.protein.kinase ) true ) )
    if.not.states ( ( phosphorylated ( *IkB ) true ) )
    then.states ( ( phosphorylated ( *IkB ) true ) )
    then.relates ( ( phosphorylates ( *tyrosine.protein.kinase *IkB ) true ) )
    then.say    " Tyrosine protein kinase phosphorylates IkB bound to p50-p65 Rel complex."
```

CLIPS

```
( defrule Tyr.p.kin.IkB.phosphoryl
  ( actor IkB-p50-p65 )
  ( actor IkB )
  ( actor protein.tyrosine.kinase )
  ( state ( condition activated ) ( actors_are protein.tyrosine.kinase ) )
  ( not ( state ( condition phosphorylated ) ( actors_are IkB ) ) )
=>
  ( assert ( state ( condition phosphorylated ) ( actors_are IkB ) )
    ( relate ( condition phosphorylates ) ( actors_are protein.tyrosine.kinase IkB ) )
    ( printout t " Protein tyrosine kinase phosphorylates IkB bound to p50-p65 Rel complex." )
  )
```

In Experiment E11, binding of the cytokine IL-1-beta to its membrane receptor lead to production of AP-1 (fos-jun heterodimer) and activation of the TNF-alpha promoter gene (Figure 12). It can be easily seen, by comparison with the envisionment for the GH pathway (Figure 10), that the IL-1/AP-1 gene regulation process is relatively simple.

TSC frame-based SCHEME dialect KB actors and REGULATION.T process rules were readily translated into the specific LISP notation and syntax supported by CLIPS (e.g., Figure 13). The individual TSC experimental conditions files (E1, E2, etc.) were also translated into individual CLIPS (text code) files. Individual simulation experiments run with the CLIPS versions of Experiments E1-4, E6-E9, and E11 successfully produced similar process state-transitions to those seen with the original TSC Experiments. However, CLIPS forward chaining inference engine preferentially executed depth-first search by default, resulting in faster execution of more compact rule expansions than seen with the breadth-first search method used by the TSC envisionment builder. Graphic depictions of the process transitions (like the TSC browser graphics) were not available for CLIPS experiments, although comparable rule-firing statements were produced.

Conclusions and Discussion

During the initial period of this Summer Research Extension Program project, robust fundamental simulation experiments were successfully run for each of the four different "subsets" of cell regulatory processes represented by the Sen and Packer (1995) model, demonstrating the practicality of QP methodology for characterizing functional interactions for fundamental aspects of molecular genetics. Results of these preliminary experiments were published and reported at the annual meeting of the Federation of American Societies of Experimental Biology (Trelease, 1997). This type of genetic process modeling has proven to be unique, and it may become a valuable tool for understanding gene function and regulation during a biomedical scientific epoch dominated by the Human Genome Project and widespread research in aspects of molecular genetics.

Although these simple discrete experiments simulated simple coexisting gene regulation processes, the same updated KB supported more complex, multi-modal simulations. Depending on initial experimental conditions, the KB produced different simulation of the experimentally demonstrated roles of AP-1/NF-kB regulatory protein pathways in mediating cellular responses to TNF α (receptor stimulation) and growth hormone, IL-1 stimulated upregulation of the TNF-alpha promoter gene, TNF-alpha-induced gene promotion via ROS intermediates. The fundamental NF-kB/AP-1 protooncogene pathways model was expanded to include an additional important signaling/regulatory reaction chain process--the MAPK kinase cascade.

In general, it was possible to set up the same fundamental TSC bioprimitive and gene regulation KB components using CLIPS. As shown in Figure 13, the specific syntaxes for representation of for right-hand-side (RHS; *if* predicates) and left-hand-side LHS (*then* predicates) were distinctively different, but clearly translatable. Successful

simulations were run for major TSC experiments (E1-4, 6, 7,8,9,11), although the base CLIPS system lacked one of the most important specific TSC enhancements for representing envisionments: The graphic Browser display of envisionments. Furthermore, because CLIPS by default implemented depth-first search of KB rule conditions, as opposed to TSC's breadth-first approach, basic CLIPS envisionments yielded fewer alternative execution paths (simpler decision trees) than those seen in comparable TSC experiments. Since CLIPS allows definition of breadth-first and other alternative inference methods, it could be set to build envisionments comparable to those generated by TSC.

The significance of this work is that it demonstrates the practicality of using knowledge-based (AI) methods for modeling complex biological processes that are virtually intractable to representation by conventional computer-based mathematical modeling methods. Furthermore, the QP simulations represented the outcomes of real, contemporary biomedical research experiments. Beyond providing a tool/methodology for formal representation and testing of crucial hypotheses in contemporary molecular genetics and biological sciences, this sets the stage for development of more advanced computational tools for advancing scientific discovery through research experiments. In particular, given the global approach taken to creating biological process heuristics, it should be possible to build complete intelligent systems that collect data from laboratory experiments, apply model-based reasoning to these data and automatically build new heuristics (refine model process rules) for the processes being observed.

This last aspect of scientific discovery process automation has important implications for the more generalized application of systems for basic experimental biology research. Typically, scientists formulate hypotheses based on cognitive (mental) models of systems under study, and then devise methods and experimental procedures to test those conjectures. If TSC or other QP hybrid programming environments are used for formalized modeling of those systems and hypotheses, the scientist will have a new computer-based testing tool for refining those models independently of and in conjunction with the performance of physical experiments. One consequence of such use could be experiment optimization, a valuable asset in an era of tight research funding. If the chosen experimental methodology is amenable to computer-based process control, it may be possible to "close the loop" in creating a discovery system that can iteratively evaluate hypotheses against experimental data, create new models/hypotheses, and devise new evaluative experiments.

References

- Abrams, F. L. Process Discovery: Automated Process Development for the Control of Polymer Curing. Doctoral Dissertation, School of Engineering, University of Dayton, 1995.
- Abbas, A.K., Lichtman, A.H., and Pober, J.S. Cellular and Molecular Immunology. W.B. Saunders Company: Philadelphia, 1991.
- Andersson, E.C., Christensen, J.P., Marker, O., and Thomsen, A.R. Changes in cell adhesion molecule expression on T cell associate with systemic virus infection. Journal of Immunology 152:1237-1245, 1994.
- Beiqing, L., Chen, M., and Whisler, R. Sublethal levels of oxidative stress stimulate transcriptional activation of c-jun and suppress IL-2 promoter activation in Jurkat T cells. Journal of Immunology 157:160-169, 1996.
- Bierhaus, A., Zhang, Y., Deng, Y., Mackman, N., Quehenberger, P., Haase, M., Luther, T., Muller, M., Bohrer, H., Greten, J., Martin, E., Bauerle, P., Waldherr, R., Kisiel, W., Ziegler, R., Stern, D., and Nawroth, P. Mechanism of the tumor necrosis factor alpha-mediated induction of endothelial tissue factor. Journal of Biological Chemistry 270(44):26419-26432, 1995.
- Cerutis, D., Bruner, R., Thomas, D., and Giron, D. Tropism and histopathology of the D, B, K, and MM variants of encephalomyocarditis virus. Journal of Medical Virology 29:63-69, 1989.
- Christensen, J.P., Andersson, E.C., Scheynius, A., Marker, O., and Thomsen, A.R. Alpha4 integrin directs virus-activated CD8-T cells to sites of infection. Journal of Immunology 154:5293-5301, 1995.
- Cooper, G.M. Oncogenes. Second Edition. James and Bartlett Publishers: Sudley, MA, 1996.
- Curiel, R.E. Cytokines Expressed By Cultured Splenocytes During The First 24 Hours Of Picorna Virus Infection Reflect The Disease Susceptibility Or Resistance Of The Spleen Cell Donors. Unpublished doctoral dissertation, Wright State University, Ohio, 1994.
- Curiel, R.E. , Miller, M., Ishikawa, R, Thomas, D. and Bigley, N.J. Does the gender difference in interferon production seen in picornavirus-infected spleen cell cultures from ICR Swiss mice have any in vivo significance? Journal of Interferon Research 13:387-395, 1993.

De Kleer J. and Forbus, K. D. Building Problem Solvers. MIT Press, Cambridge, MA, 1993.

De Kleer, J. and Weld, D.S. Qualitative Physics: A Personal View, *In*: D. S. Weld and J. De Kleer, Eds., Readings in Qualitative Reasoning about Physical Systems, pp. 1-8. Morgan Kaufmann, San Mateo, CA, 1992.

Forbus, K.D. Qualitative process theory. Artificial Intelligence 24:85-168, 1984.

Fortuner, Renaud (Editor). Advances in Computer Methods for Systematic Biology. The Johns Hopkins University Press: Baltimore, 1993.

Goodman, S.R. Medical Cell Biology. J.B. Lippincott Co.: Philadelphia, PA, 1994.

Hemler, M.E. and Mihich, E. (Eds.) Cell Adhesion Molecules: Cellular Recognition Mechanisms. Plenum Press, New York, 1993.

Imhof, B.A. and Dunon, D. Leukocyte migration and adhesion. Advances in Immunology (58):345-416, 1995.

Janeway, C.A., and Travers, P. Immunobiology. The Immune System in Health and Disease. Current Biology, Ltd./Garland Publishing, Inc: London, 1996.

Junqueira, L.C., Carneiro, J., And Kelly, R.O. Basic Histology. (7th Edition). Appleton and Lange: Norwalk, CT, 1992.

Karp, P.D. Frame representation and relational databases: Alternative information-management technologies for systematic biology, *In*: R. Fortuner, Ed., Advances in Computer Methods for Systematic Biology pp. 275-285 The Johns Hopkins University Press: Baltimore, MD, 1993.

Karp, P.D. Hypothesis formation as design, *In*: Computational Models of Scientific Discovery and Theory Formation, J. Shrager and P. Langley, Eds., pp. 276-317 Morgan Kaufman: San Mateo, CA, 1990.

Kopp, E.B., and Ghosh, S. NF- κ B and Rel proteins in innate immunity. Advances in Immunology 58:1-27, 1995.

Kulkarni, D. and Simon, H.A. Experimentation in machine discovery, *In*: J. Shrager and P. Langley, Eds., Computational Models of Scientific Discovery and Theory Formation, pp. 255-273 Morgan Kaufman: San Mateo, CA, 1990.

LeClair, S.R., Abrams, F.L., and Matejka, R.F. Qualitative process automation: Self-directed manufacture of composite materials. Artificial Intelligence for Engineering Design, Analysis and Manufacturing. 3(2):125-136, 1989.

LeClair, S.R., Abrams, F.L. Qualitative process automation. International Journal of Computer Integrated Manufacturing 2(4):205-211, 1989.

Lieb, K., Kaltschmidt, C., Kaltschmidt, B., Baeuerle, P., Berger, M., Bauer, J., and Fiebich, B. Interleukin-1 beta uses common and distinct pathways for induction of the Interleukin-6 and tumor necrosis factor alpha genes in the human astrocytoma cell line U373. Journal of Neurochemistry 66(4):1496-1503, 1996.

Lo, Y.Y.C. and Cruz, T.F. Involvement of reactive oxygen species in cytokine and growth factor induction of c-fos expression in chondrocytes. The Journal of Biological Chemistry 270(20):11727-11730, 1995.

Purves, W.K., Orians, G.H., Heller, H.C. Life, the Science of Biology, Third Edition. Sinauer Associates: New York, N.Y., 1992.

Sappey, C., Boelaert, J.R., Legrand-Poels, S., Forceille, C., Favier, A., and Piette, J. Iron chelation decreases NF-kB and HIV Type 1 activation due to oxidative stress. AIDS Research and Human Retroviruses 11(9):1049-1061, 1995.

Sen, C.K. and Packer L. Antioxidant and redox regulation of gene transcription. FASEB Journal 10: 709-720, 1996.

Trelease, R.B. Development of a feature-based knowledge base for biologically-based materials and processes. Contributed Research and Development 145:1-10, 1994.

Trelease, R.B. Developing qualitative process control discovery systems. Final Report, AFOSR Summer Faculty Research Program, 1994.

Trelease, R.B. and Park, J. Qualitative process modeling of cell-cell-pathogen interactions in the immune system. Computer Methods and Programs in Biomedicine 51:171-181, 1996.

Trelease, R.B. and Henderson, R.H. Computer-based qualitative process model of NF- κ B and AP-1 gene transcription regulation by reactive oxygen species. FASEB Journal 11(3):A4523, 1997.

Uckun, S. Model-based reasoning in biomedicine. Critical Reviews in Biomedical Engineering 19:261-292, 1992.

Weld, D.S. and De Kleer, J., Eds. Readings in Qualitative Reasoning About Physical Systems. Morgan Kaufmann, San Mateo, CA, 1992.